

P I E T E R L . D . A B R I E



DESIGN OF  
RF AND  
MICROWAVE  
AMPLIFIERS  
AND  
OSCILLATORS

DISK ENCLOSED

# CONTENTS

## PREFACE

## CHAPTER 1 CHARACTERIZATION AND ANALYSIS OF LINEAR CIRCUITS AT RF AND MICROWAVE FREQUENCIES

1.1	INTRODUCTION	1
1.2	Y-PARAMETERS	1
1.2.1	The Indefinite Admittance Matrix	7
1.3	Z-PARAMETERS	8
1.4	TRANSMISSION PARAMETERS	10
1.5	SCATTERING PARAMETERS	11
1.5.1	S-Parameter Definitions	12
1.5.2	The Physical Meanings of the Normalized Incident and Reflected Components of an $N$ -Port	18
1.5.3	The Physical Interpretations of the Scattering Parameters	20
1.5.4	Constraints Imposed on the Normalized Incident and Reflected Components by the Terminations of an $N$ -Port	23
1.5.5	Derivation of Expressions for the Gain Ratios and Reflection Parameters of a Two-Port	26
1.5.6	Signal Flow Graphs	31
1.5.7	The Indefinite $S$ -Matrix	35
1.5.8	Extension of the Single-Frequency $S$ -Parameter Definitions to the Complex Frequency Plane	37
1.5.9	Constraints on the Scattering Matrix of a Lossless $N$ -Port	40
1.5.10	Conversion of $S$ -parameters to Other Parameters	44
REFERENCES		46
SELECTED BIBLIOGRAPHY		46

**CHAPTER 2 CHARACTERIZATION AND ANALYSIS OF ACTIVE CIRCUITS AT RF AND MICROWAVE FREQUENCIES**

2.1	INTRODUCTION	47
2.2	NOISE PARAMETERS	48
2.2.1	Modeling the Noise Contribution of a Two-Port with Equivalent Circuits	48
2.2.2	Noise Correlation Matrices	55
2.2.3	Calculating the Noise Figure of a Cascade Network	58
2.3	THE OUTPUT POWER OF LINEAR AMPLIFIERS	60
2.3.1	Load-Line Considerations in Class A and Class B Amplifiers	61
2.3.2	Distortion in Linear Amplifiers	67
2.3.3	The Cripps Approach to Estimating the Maximum Output Power Obtainable from a Transistor	73
2.3.4	Estimation of the Maximum Output Power of a Linear Network by Using the Power Parameters	75
REFERENCES		92
SELECTED BIBLIOGRAPHY		92

**CHAPTER 3 RADIO-FREQUENCY COMPONENTS**

3.1	INTRODUCTION	93
3.2	CAPACITORS	94
3.3	INDUCTORS	97
3.3.1	The Influence of Parasitic Capacitance on an Inductor	98
3.3.2	Low-Frequency Losses in Inductors	100
3.3.3	The Skin Effect	100
3.3.4	The Proximity Effect	103
3.3.5	Magnetic Materials	104
3.3.6	The Design of Single-Layer Solenoidal Coils	107
3.3.7	The Design of Inductors with Magnetic Cores	113
3.4	TRANSMISSION LINES	117

3.4.1 Coaxial Cables	117
3.4.2 Microstrip Transmission Lines	118
3.4.3 Twisted Pairs	122
REFERENCES	123
SELECTED BIBLIOGRAPHY	124
<b>CHAPTER 4 NARROWBAND IMPEDANCE-MATCHING WITH LC NETWORKS</b>	
4.1 INTRODUCTION	125
4.2 PARALLEL RESONANCE	126
4.3 SERIES RESONANCE	131
4.4 L-SECTIONS	133
4.5 PI-SECTIONS AND T-SECTIONS	138
4.5.1 The PI-Section	139
4.5.2 The T-Section	142
4.6 THE DESIGN OF PI-SECTIONS AND T-SECTIONS WITH COMPLEX TERMINATIONS	143
4.7 FOUR-ELEMENT MATCHING NETWORKS	146
4.8 CALCULATION OF THE INSERTION LOSS OF AN LC IMPEDANCE-MATCHING NETWORK	147
4.9 CALCULATION OF THE BANDWIDTH OF CASCADED LC NETWORKS	149
SELECTED BIBLIOGRAPHY	150
<b>CHAPTER 5 COUPLED COILS AND TRANSFORMERS</b>	
5.1 INTRODUCTION	151
5.2 THE IDEAL TRANSFORMER	151

x	Design of RF and Microwave Amplifiers and Oscillators	
5.3	EQUIVALENT CIRCUITS FOR PRACTICAL TRANSFORMERS	153
5.4	WIDEBAND IMPEDANCE MATCHING WITH TRANSFORMERS	156
5.5	SINGLE-TUNED TRANSFORMERS	158
5.6	TAPPED COILS	159
5.7	PARALLEL DOUBLE-TUNED TRANSFORMERS	166
5.8	SERIES DOUBLE-TUNED TRANSFORMERS	172
5.9	MEASUREMENT OF THE COUPLING FACTOR OF A TRANSFORMER	175
5.9.1	Measurement of the Coupling Factor by Short-Circuiting the Secondary Winding	175
5.9.2	Measurement of the Coupling Factor by Measuring the Open-Circuit Voltage Gain	176
5.9.3	Deriving the Coupling Factor from S-Parameters Measurements	176
REFERENCES		177

## **CHAPTER 6 TRANSMISSION-LINE TRANSFORMERS**

6.1	INTRODUCTION	179
6.2	TRANSMISSION-LINE TRANSFORMER CONFIGURATIONS	181
6.3	ANALYSIS OF TRANSMISSION-LINE TRANSFORMERS	188
6.4	DESIGN OF TRANSMISSION-LINE TRANSFORMERS	196
6.4.1	Determining the Optimum Characteristic Impedance and Diameter of the Transmission Line to be Used	196
6.4.2	Determining the Minimum Value of the Magnetizing Inductance of the Transformer	197
6.4.3	Determining the Type and Size of the Magnetic Core to Be Used	201
6.4.4	Compensation of Transmission-Line Transformers for Nonoptimum Characteristic Impedances	203
6.4.5	The Design of High-Pass LC Networks to Extend the Bandwidth of a Transmission-Line Transformer	208

6.5	CONSIDERATIONS APPLYING TO RF POWER AMPLIFIERS	210
REFERENCES		215
SELECTED BIBLIOGRAPHY		216

## CHAPTER 7 FILM RESISTORS AND SINGLE-LAYER PARALLEL-PLATE CAPACITORS

7.1	INTRODUCTION	217
7.2	FILM RESISTORS	219
7.3	SINGLE-LAYER PARALLEL-PLATE CAPACITORS	220
7.3.1	Parallel-Plate Capacitors on a Ground Plane	223
7.3.2	Parallel-Plate Capacitors Used as Series Stubs	224
7.3.3	Series Connected Parallel-Plate Capacitors	226
REFERENCES		236

## CHAPTER 8 THE DESIGN OF WIDEBAND IMPEDANCE-MATCHING NETWORKS

8.1	INTRODUCTION	239
8.2	FITTING AN IMPEDANCE OR ADMITTANCE FUNCTION TO A SET OF IMPEDANCE VERSUS FREQUENCY COORDINATES	240
8.3	THE ANALYTICAL APPROACH TO IMPEDANCE MATCHING	246
8.3.1	Darlington Synthesis of Impedance-Matching Networks	248
8.3.2	LC Transformers	253
8.3.3	The Gain-Bandwidth Constraints Imposed by Simple RC and RL Loads	256
8.3.4	Direct Synthesis of Impedance-Matching Networks When the Load (or Source) Is Reactive	258
8.3.5	Synthesis of Networks for Matching a Reactive Load to a Purely Resistive or a Reactive Source by Using the Principle of Parasitic Absorption	263
8.3.6	The Analytical Approach to Designing Commensurate Distributed Impedance-Matching Networks	267

8.4	THE ITERATIVE DESIGN OF IMPEDANCE-MATCHING NETWORKS	273
8.4.1	The Line-Segment Approach to Matching a Complex Load to a Resistive Source	276
8.4.2	The Reflection Coefficient Approach to Solving Double-Matching Problems	284
8.4.3	The Transformation- <i>Q</i> Approach to the Design of Impedance-Matching Networks	291
8.5	THE DESIGN OF RLC IMPEDANCE-MATCHING NETWORKS	311
REFERENCES		317
SELECTED BIBLIOGRAPHY		318
<b>CHAPTER 9 MICROWAVE LUMPED ELEMENTS, DISTRIBUTED EQUIVALENTS, AND MICROSTRIP PARASITICS</b>		
9.1	INTRODUCTION	321
9.2	MICROWAVE RESISTORS	322
9.3	THE LIMITATIONS OF A SERIES TRANSMISSION LINE USED TO REPLACE A LUMPED ELEMENT	322
9.4	LUMPED MICROWAVE INDUCTORS	325
9.5	LUMPED MICROWAVE CAPACITORS	331
9.6	DISTRIBUTED EQUIVALENTS FOR SHUNT INDUCTORS AND CAPACITORS	333
9.7	A TRANSMISSION LINE EQUIVALENT FOR A SYMMETRIC LOW-PASS T-SECTION OR PI-SECTION	338
9.8	MICROSTRIP DISCONTINUITY EFFECTS AT THE LOWER MICROWAVE FREQUENCIES	345
9.9	A COMPENSATION TECHNIQUE FOR MICROSTRIP DISCONTINUITIES	353
REFERENCES		356

SELECTED BIBLIOGRAPHY	357
<b>CHAPTER 10 THE DESIGN OF RADIO-FREQUENCY AND MICROWAVE AMPLIFIERS AND OSCILLATORS</b>	
10.1 INTRODUCTION	359
10.2 STABILITY	362
10.2.1 Stability Circles on the Admittance Plane	364
10.2.2 Stability Circles on the Smith Chart	368
10.2.3 The Reflection Gain Approach	371
10.2.4 The Loop Gain Approach	374
10.2.5 Stabilization of a Two-Port with Shunt or Series Resistance	380
10.3 TUNABILITY	383
10.4 CONTROLLING THE GAIN OF AN AMPLIFIER	384
10.4.1 Circles of Constant Mismatch for a Passive Problem	387
10.4.2 Constant Operating Power Gain Circles	389
10.4.3 Constant Available Power Gain Circles	392
10.4.4 Constant Transducer Power Gain Circles	394
10.5 CONTROLLING THE NOISE FIGURE OF AN AMPLIFIER	396
10.6 CONTROLLING THE OUTPUT POWER OR THE EFFECTIVE OUTPUT POWER OF A TRANSISTOR	398
10.7 THE EQUIVALENT PASSIVE IMPEDANCE-MATCHING PROBLEM	399
10.7.1 Constant Operating Power Gain Case	401
10.7.2 Constant Available Power Gain Case	403
10.7.3 Constant Noise Figure Case	404
10.8 DEVICE-MODIFICATION	405
10.9 DESIGNING CASCADE AMPLIFIERS	417
10.10 LOSSLESS FEEDBACK AMPLIFIERS	431
10.11 REFLECTION AMPLIFIERS	436

10.12	BALANCED AMPLIFIERS	440
10.13	OSCILLATOR DESIGN	441
10.13.1	Estimation of the Compression Associated with the Maximum Effective Output Power	451
10.13.2	Derivation of the Equations for the T- and PI-Section Feedback Components Required	453
10.13.3	High <i>Q</i> Resonator Circuits	458
10.13.4	Transforming the Impedance Presented by a Resonator Network to That Required in the T- or PI-Section Feedback Network	460
10.13.5	Designing Varactor Circuits to Realize the Varactor-Type Reactance Required	462
10.13.6	Considerations Applying to Oscillators with Low Phase Noise	465
REFERENCES		465
SELECTED BIBLIOGRAPHY		467
<b>APPENDIX A</b>		469
<b>ABOUT THE AUTHOR</b>		473
<b>INDEX</b>		475

# CHAPTER 1

## CHARACTERIZATION AND ANALYSIS OF LINEAR CIRCUITS AT RF AND MICROWAVE FREQUENCIES

### 1.1 INTRODUCTION

Low-frequency circuits are usually analyzed in terms of transfer functions. This approach is seldom used at RF and microwave frequencies. Analysis at these frequencies is usually in terms of one of the many sets of single-frequency parameters.

The parameters most frequently used are the  $Y$ -,  $Z$ -,  $T$ -, and  $S$ -parameters. The first three sets of parameters relate the terminal voltages and currents in different ways, while the  $S$ -parameters are closely related to the power incident to and reflected from a network.

Because of the relative ease with which  $S$ -parameters can be measured and the useful information directly obtained from them, components are usually characterized by measuring their  $S$ -parameters, and circuits are analyzed by calculating their  $S$ -parameters. The other parameters are often used to simplify the computations necessary for circuit analysis and synthesis.

Each of these sets of parameters will be considered in detail in the following sections.

Any of the voltages, currents, or power levels in a linear  $N$ -port network can be calculated in terms of the external signals (independent variables) when one of these sets of parameters is known at the frequency of interest. Conversion between the different parameters is straightforward.

### 1.2 Y-PARAMETERS

The  $Y$ -parameters of an  $N$ -port network are defined by the expression

$$Y = \begin{bmatrix} Y_{11} & Y_{12} & \cdots & Y_{1N} \\ Y_{21} & Y_{22} & \cdots & Y_{2N} \\ \vdots & \vdots & \ddots & \vdots \\ Y_{N1} & Y_{N2} & \cdots & Y_{NN} \end{bmatrix} \quad (1.1)$$

where

$$\mathbf{I} = \begin{bmatrix} I_1 \\ I_2 \\ \vdots \\ I_N \end{bmatrix} \quad (1.2)$$

$$\mathbf{V} = \begin{bmatrix} V_1 \\ V_2 \\ \vdots \\ V_N \end{bmatrix} \quad (1.3)$$

$$\mathbf{Y} = \begin{bmatrix} y_{11} & y_{12} & \dots & y_{1N} \\ y_{21} & y_{22} & \dots & y_{2N} \\ \dots & \dots & \dots & \dots \\ y_{N1} & y_{N2} & \dots & y_{NN} \end{bmatrix} \quad (1.4)$$

$I_i$  is the current flowing into the  $i$ th terminal, and  $V_i$  is the voltage across the  $i$ th port of the network.

Each element of the  $Y$ -parameter matrix can be calculated or measured by using the relationship

$$y_{ij} = \frac{I_i}{V_j} \Big|_{V_h=0} \quad h \in [1, 2, 3, \dots, N] \quad h \neq j \quad (1.5)$$

that is,  $y_{ij}$  is given by the ratio of the current flowing into the  $i$ th terminal (output signal) and the voltage across the  $j$ th port (input signal), with all the other voltages set to zero.

By using (1.1), the terminal currents corresponding to any given set of terminal voltages can be determined. The linear response of the network is, therefore, completely characterized when the  $N^2$  elements of the  $Y$ -parameter matrix are known.

As with any other set of parameters, the  $Y$ -parameters can be used to calculate the impedances and gain ratios corresponding to any set of terminations. By using the equivalent circuit in Figure 1.1, it can be easily shown that the following expressions apply to a two-port network terminated as shown:

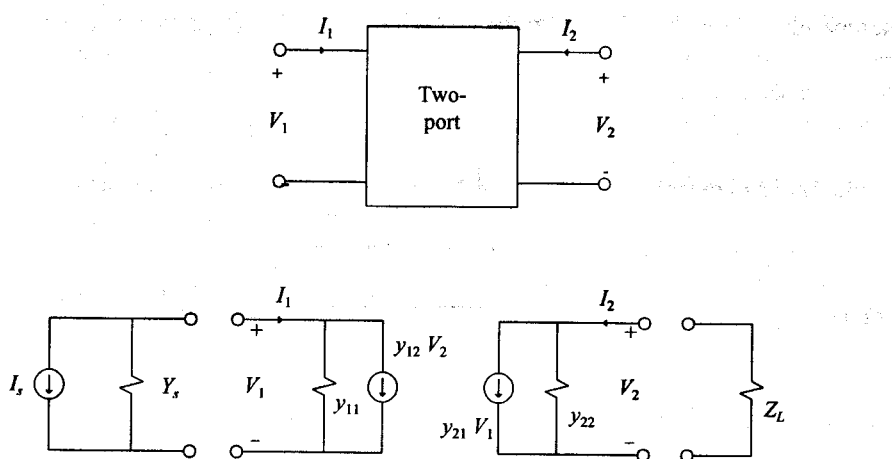


**Figure 1.1** An equivalent circuit for a two-port in terms of its  $Y$ -parameters.

$$Y_{\text{in}} = \frac{I_1}{V_1} = y_{11} - \frac{y_{12}y_{21}}{y_{22} + Y_L} \quad (1.6)$$

$$Y_{\text{out}} = \frac{I_2}{V_2} = y_{22} - \frac{y_{12}y_{21}}{y_{11} + Y_s} \quad (1.7)$$

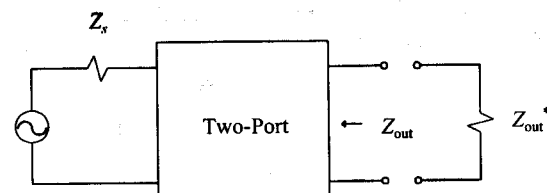
$$A_v = \frac{V_2}{V_1} = -\frac{y_{21}}{y_{22} + Y_L} \quad (1.8)$$

$$A_v = \frac{I_0}{I_1} = -\frac{I_2}{I_1} = A_v Y_L / Y_{\text{in}} \quad (1.9)$$

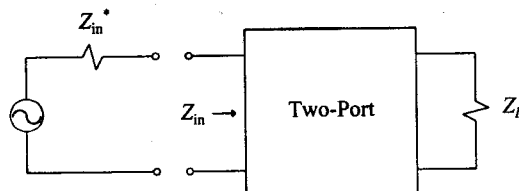
$$C = \frac{P_L}{P_{\text{in}}} = \left| \frac{y_{21}}{y_{22} + Y_L} \right|^2 \frac{G_L}{\text{Re}(Y_{\text{in}})} \quad (1.10)$$

$$= \frac{P_L}{P_{\text{av}-E}} = \left| \frac{y_{21}}{(y_{11} + Y_s)(y_{22} + Y_L) - y_{12}y_{21}} \right|^2 4 G_L G_s \quad (1.11)$$

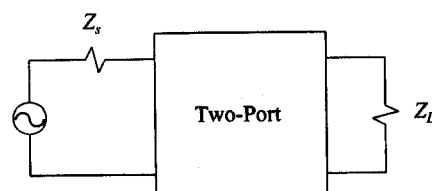
$$= \frac{P_{\text{av}-o}}{P_{\text{av}-E}} = \left| \frac{y_{21}}{y_{11} + Y_s} \right|^2 \frac{G_s}{\text{Re}(Y_{\text{out}})} \quad (1.12)$$



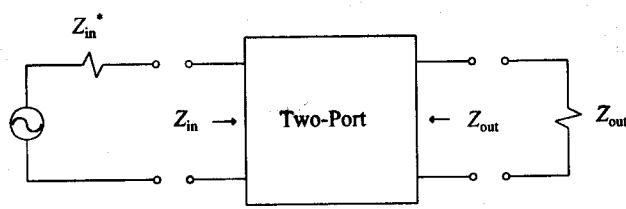
Available Power Gain



Operating Power Gain



Transducer Power Gain



MAG / MSG

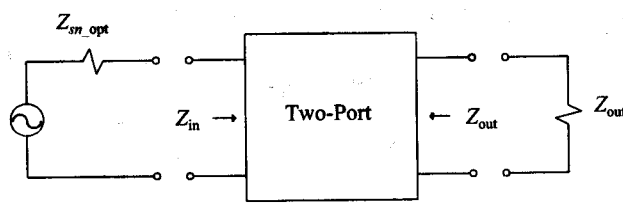
 $G_{an\_opt}$ 

Figure 1.2 The equivalent circuits relevant to the different power gain definitions.

In these equations,  $Y_L = G_L + jB_L$  is the load admittance,  $Y_s = G_s + jB_s$  is the source admittance,  $P_L$  is the power dissipated in the load,  $P_{in}$  is the power entering the input port of the network,  $P_{av-E}$  is the power available from the source,  $P_{av-o}$  is the available power at the output terminals of the two-port,  $Y_{in}$  is the input admittance, and  $Y_{out}$  is the output admittance.

The available power of a source is defined as the power dissipated in a load which conjugately matches the source, and is given by the expression

$$P_{av-E} = \frac{|E|^2}{4 R_s} = \frac{|I_s|^2}{4 G_s} \quad (1.13)$$

where  $E$  is the source voltage,  $I_s$  is the equivalent (Norton) source current, and  $R_s$  and  $G_s$  are defined by

$$Y_s = G_s + jB_s \quad (1.14)$$

$$Z_s = R_s + jX_s \quad (1.15)$$

where  $Z_s$  is the source impedance, and  $Y_s$  is its inverse.

Note that the operating power gain ( $G_o$ ) will be equal to the transducer power gain if the input is conjugately matched (see Figure 1.2). Similarly, the available power gain will be equal to the transducer power gain when the output is conjugately matched.

The maximum available gain (MAG) of a two-port is defined as the transducer power gain when both sides are conjugately matched (if possible). If the MAG cannot be calculated (negative resistance), the maximum stable gain (MSG) is of interest. The maximum stable gain (MSG) is the MAG associated with the device after adding the minimum shunt conductance or series resistance required for the MAG to exist.

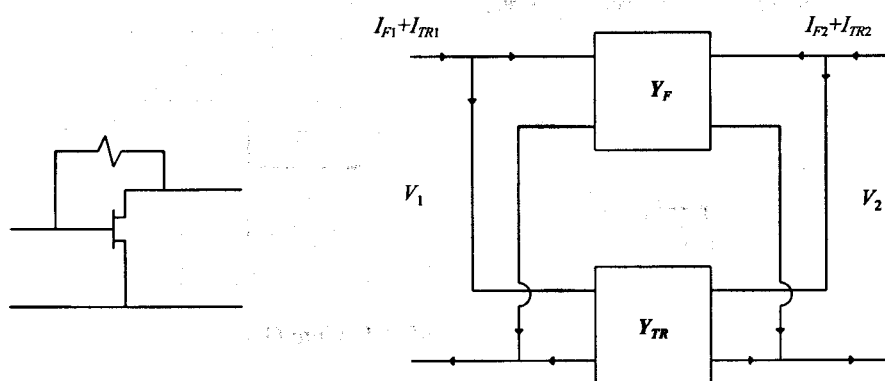


Figure 1.3 Two networks connected in parallel.

$G_{an, \text{opt}}$  is the available power gain associated with an optimum noise match on the input side (i.e.,  $Z_s$  is chosen to minimize the noise figure of the two-port).

When a circuit is analyzed, the  $Y$ -parameters are frequently used to find a single set of parameters characterizing two networks connected in parallel. This is illustrated in Figure 1.3. Note that the terminal voltages for the two networks are the same, while the currents add.

The  $Y$ -parameters of two networks connected in parallel simply equal the sum of the  $Y$ -parameters of each individual network:

$$Y_T = Y_A + Y_B \quad (1.16)$$

**EXAMPLE 1.1** Derivation of the equation for the input admittance of a two-port.

The input admittance is defined by (1.6):

$$Y_{\text{in}} = I_1 / V_1$$

To find the input admittance it is therefore necessary to find an expression for  $V_1$  in terms of  $I_1$ . Ohms law and Kirchhoff's current law applied to the input port yield

$$V_1 = [I_1 - y_{12} V_2] / y_{11} \quad (1.17)$$

The output voltage is given by

$$V_2 = -I_2 / Y_L = -[y_{21} V_1 + y_{22} V_2] / Y_L \quad (1.18)$$

that is,

$$V_2 = -\frac{y_{21}}{y_{22} + Y_L} V_1 \quad (1.19)$$

After some manipulation, substitution of (1.19) into (1.17) yields (1.6):

$$Y_{\text{in}} = y_{11} - \frac{y_{12} y_{21}}{y_{22} Y_L}$$

### 1.2.1 The Indefinite Admittance Matrix

The indefinite admittance matrix is a useful tool by which the  $Y$ -parameters of a network can be determined if they are known for the same network connected differently. For example, if the common-emitter parameters of a bipolar transistor are known, this matrix can be used to determine the common-base or common-collector parameters.

An admittance matrix is indefinite when none of the network terminals have been connected yet to ground, and the total current flowing into it is therefore equal to the sum of the currents flowing into each terminal.

It can easily be shown that the sum of the elements in each row or each column of an indefinite admittance matrix is equal to zero. Considering a three-port network, this implies that if four of the nine parameters are known, then all the parameters are known.

The proof that the sum of the elements of each row must equal zero follows by choosing the terminal voltages to be equal. Each of the currents will then be zero and extraction of each individual equation from (1.1) yields the desired result.

That the sum of the elements in each column should also equal zero follows by setting two of the voltages equal to zero and adding the three currents, the sum of which must be equal to zero.

#### EXAMPLE 1.2 Calculation of the common-base parameters in terms of the common-emitter parameters.

The common-base parameters of a transistor will be determined in terms of its common-emitter parameters, as an example of using the indefinite admittance matrix.

The indefinite admittance parameters, which correspond to the common-emitter parameters, can be identified by setting  $V_2$  in Figure 1.4 and in (1.20) equal to zero.

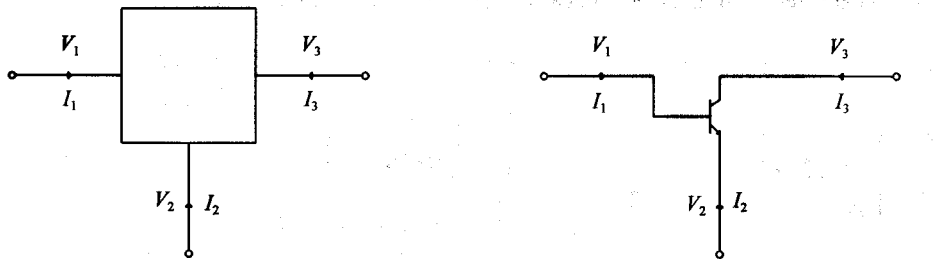


Figure 1.4 An indefinite three-port.

$$\begin{bmatrix} I_1 \\ I_2 \\ I_3 \end{bmatrix} = \begin{bmatrix} y_{11} & y_{12} & y_{13} \\ y_{21} & y_{22} & y_{23} \\ y_{31} & y_{32} & y_{33} \end{bmatrix} \begin{bmatrix} V_1 \\ V_2 \\ V_3 \end{bmatrix} \quad (1.20)$$

Because the current in the emitter ( $I_2$ ) is not of interest when the common-emitter configuration is considered, (1.20) then reduces to

$$\begin{bmatrix} I_1 \\ I_3 \end{bmatrix} = \begin{bmatrix} y_{11} & y_{13} \\ y_{31} & y_{33} \end{bmatrix} \begin{bmatrix} V_1 \\ V_3 \end{bmatrix} = \begin{bmatrix} y_{11e} & y_{12e} \\ y_{21e} & y_{22e} \end{bmatrix} \begin{bmatrix} V_1 \\ V_3 \end{bmatrix} \quad (1.21)$$

With the common-emitter parameters known,  $y_{11}$ ,  $y_{13}$ ,  $y_{31}$ , and  $y_{33}$  are also known, and the rule for the zero column and row can now be applied to determine the other parameters. The only remaining step is to identify the common-base parameters in (1.20). Similar to the common-emitter parameters, this is done by setting  $V_1$  in (1.20) equal to zero and eliminating the equation giving the base current ( $I_1$ ) as a function of the voltages. It follows that

$$\begin{bmatrix} y_{11b} & y_{12b} \\ y_{21b} & y_{22b} \end{bmatrix} = \begin{bmatrix} y_{22} & y_{23} \\ y_{32} & y_{33} \end{bmatrix} \quad (1.22)$$

The common-collector parameters are given by

$$\begin{bmatrix} y_{11c} & y_{12c} \\ y_{21c} & y_{22c} \end{bmatrix} = \begin{bmatrix} y_{11} & y_{12} \\ y_{21} & y_{22} \end{bmatrix} \quad (1.23)$$

### 1.3 Z-PARAMETERS

The Z-parameters of an  $N$ -port network are defined by the expression

$$\mathbf{V} = \mathbf{ZI} \quad (1.24)$$

where

$$\mathbf{Z} = \begin{bmatrix} z_{11} & z_{12} & \dots & z_{1N} \\ z_{21} & z_{22} & \dots & z_{2N} \\ \dots & \dots & \dots & \dots \\ z_{N1} & z_{N2} & \dots & z_{NN} \end{bmatrix} \quad (1.25)$$

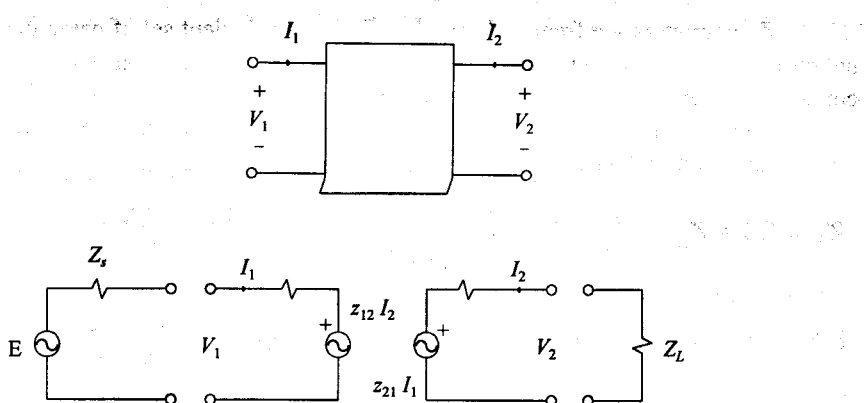


Figure 1.5 An equivalent circuit for a two-port network in terms of its Z-parameters.

$V$  and  $I$  are defined by (1.3) and (1.2), respectively. The equivalent circuit associated with the two-port case is shown in Figure 1.5.

Each element in (1.25) can be computed or measured by using the relationship

$$z_{ij} = \frac{V_i}{I_j} \Big|_{I_h=0} \quad h \in [1, 2, 3, \dots, N] \quad h \neq j \quad (1.26)$$

that is,  $z_{ij}$  is the ratio of the voltages across the  $j$ th port (output signal) and the current at the  $i$ th port (input signal) with all the other ports idle (open-circuited).

Equation (1.24) can be used to find the terminal voltages corresponding to any set of terminal currents.

Comparison of (1.24) and (1.1) reveals that the Z-parameters of a network are related to its Y-parameters in the following way:

$$Z = Y^{-1} \quad (1.27)$$

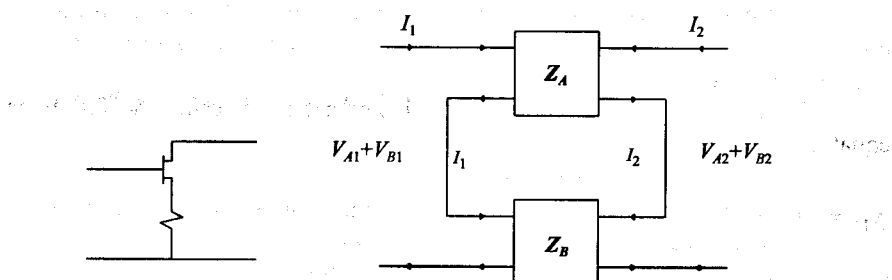


Figure 1.6 Two networks connected in series.

Z-parameters are frequently used to find an equivalent set of parameters for two networks connected in series, as illustrated in Figure 1.6. Note that when networks are connected in series, the terminal currents are the same, while the voltages add together.

The Z-parameters of two networks connected in series are given in terms of the individual Z-parameters by

$$\mathbf{Z}_T = \mathbf{Z}_A + \mathbf{Z}_B \quad (1.28)$$

## 1.4 TRANSMISSION PARAMETERS

The transmission parameters (*T*-parameters or ABCD parameters) of a two-port are defined by the equation

$$\begin{bmatrix} V_1 \\ I_1 \end{bmatrix} = \begin{bmatrix} A & B \\ C & D \end{bmatrix} \begin{bmatrix} V_2 \\ I_2 \end{bmatrix} \quad (1.29)$$

with the voltage and current as defined in Figure 1.7. Note that  $I_2$  is the output current and not the current entering the output terminal as in the case of the *Y*- and *Z*-parameters.

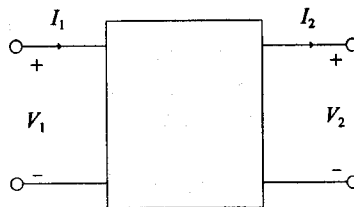


**Figure 1.7** The voltage and current relevant to the definition of the transmission parameters.

The expressions for the individual elements of the transmission matrix can be obtained by setting either  $V_2$  or  $I_2$  in (1.28) equal to zero after extracting the individual equations from the matrix equation.

*T*-parameters can be converted to *Y*-parameters by using the following set of equations:

$$y_{11} = D / B \quad (1.30)$$

$$y_{12} = C - AD / B \quad (1.31)$$

$$v_{21} = -1/B \quad (1.32)$$

$$v_{22} = A / B \quad (1.33)$$

The inverse expressions are

$$A = -y_{22} / y_{21} \quad (1.34)$$

$$B = -1 / y_{21} \quad (1.35)$$

$$C = y_{12} - y_{11}y_{22} / y_{21} \quad (1.36)$$

$$D = -y_{11} / y_{21} \quad (1.37)$$

Transmission parameters are frequently used to find an equivalent set of parameters for two cascaded networks. The transmission matrix for the equivalent network is given in terms of the matrices for the individual networks by

$$\mathbf{T} = \mathbf{T}_A \mathbf{T}_B \quad (1.38)$$

This is illustrated in Figure 1.8.

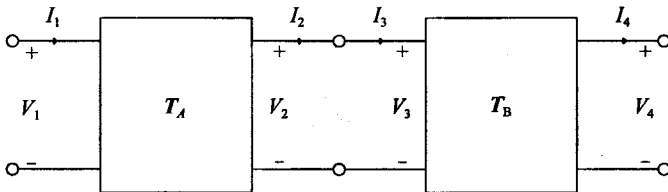


Figure 1.8 Two cascaded two-port networks.

## 1.5 SCATTERING PARAMETERS

Because of the ease with which scattering parameters (S-parameters) can be measured, as well as stability considerations and the physical meanings attached to them, S-parameters have been extensively used to characterize components and also to analyze circuits.

The definitions relevant to these parameters, their physical meanings, and their application in analyzing circuits will be considered in the following sections. Both single-frequency S-parameters and those in the complex frequency plane will be considered.

Because lossless networks are of considerable interest in this text, the constraints on the  $S$ -matrix of a lossless network will also be examined.

### 1.5.1 S-Parameter Definitions

Similar to the reflection coefficients in transmission-line theory,  $S$ -parameters are defined in terms of incident and reflected components. In  $S$ -parameter theory, however, an incident component is defined as that component which would exist if the port under consideration were conjugately matched to the normalizing impedance at that port. The normalizing impedances are the equivalents of the short-circuit and open-circuit terminations used to characterize a network in terms of its  $Y$ ,  $Z$ , or  $T$ -parameters. They can be defined to have any arbitrary value (as long as the resistive part is positive and not equal to zero), but  $50\Omega$  impedances are used in most cases.

In terms of the current and voltage at each terminal, the incident and reflected components are defined by the following set of matrix equations:

$$\mathbf{E}_0 = \mathbf{V} + Z_0 \mathbf{I} \quad (1.39)$$

$$\mathbf{I}_i = [\mathbf{Z}_0 + \mathbf{Z}_0^*]^{-1} \mathbf{E}_0 \quad (1.40)$$

$$\mathbf{I} = \mathbf{I}_i - \mathbf{I}_r \quad (1.41)$$

$$\mathbf{V}_i = \mathbf{Z}_0^* \mathbf{I}_i \quad (1.42)$$

$$\mathbf{V} = \mathbf{V}_i + \mathbf{V}_r \quad (1.43)$$

$$\mathbf{a} = \frac{1}{\sqrt{2}} [\mathbf{Z}_0 + \mathbf{Z}_0^*]^{1/2} \mathbf{I}_i \quad (1.44)$$

$$\mathbf{b} = \frac{1}{\sqrt{2}} [\mathbf{Z}_0 + \mathbf{Z}_0^*]^{1/2} \mathbf{I}_i \quad (1.45)$$

$$\mathbf{Z}_0 = \begin{bmatrix} Z_{01} & 0 & 0 & \dots & 0 \\ 0 & Z_{02} & 0 & \dots & 0 \\ 0 & 0 & Z_{03} & \dots & 0 \\ \dots & \dots & \dots & \dots & \dots \\ 0 & 0 & 0 & \dots & Z_{0N} \end{bmatrix} \quad (1.46)$$

$$\boxed{[\bar{Z}_0 + \bar{Z}_0^*]^{1/2} = \begin{bmatrix} \sqrt{R_{01}} & 0 & 0 & \dots & 0 \\ 0 & \sqrt{R_{02}} & 0 & \dots & 0 \\ 0 & 0 & \sqrt{R_{03}} & \dots & 0 \\ \dots & \dots & \dots & \dots & \dots \\ 0 & 0 & 0 & \dots & \sqrt{R_{0N}} \end{bmatrix}} \quad (1.47)$$

In  $Z_0$ , the normalizing impedance at port  $j$ ,  $Z_0^*$  the matrix with conjugate elements of  $Z_0$ ,  $I_{ji}$  and  $V_{ji}$  the incident current and voltage at port  $j$ ,  $I_{jr}$  and  $V_{jr}$  the reflected current and voltage,  $a_j$  the normalized incident component, and  $b_j$  the normalized reflected component at port  $j$ .

The voltage and current relationships are illustrated in Figure 1.9 for a two-port network.

Note that the incident voltage is equal to the product of the conjugate of the normalizing impedance and the incident current; that is,

$$= Z_0^* I_i$$

The equivalent relationship in transmission-line theory is

$$= Z_0 I_i$$

By using (1.40) to eliminate  $E_0$  in (1.39) and substituting (1.41) and (1.43) in the resulting equation, it can be shown easily that, similar to transmission-line theory, the relationship between the reflected currents and voltages is

$$= Z_0 I_r \quad (1.48)$$

There are three different types of  $S$ -parameters, which are defined in the following

$$= S^I I_i \quad (1.49)$$

$$= S^V V_i \quad (1.50)$$

$$= S \mathbf{a} \quad (1.51)$$

These parameter sets are the current, voltage, and normalized  $S$ -parameters, respectively.

For a two-port network, (1.51) reduces to

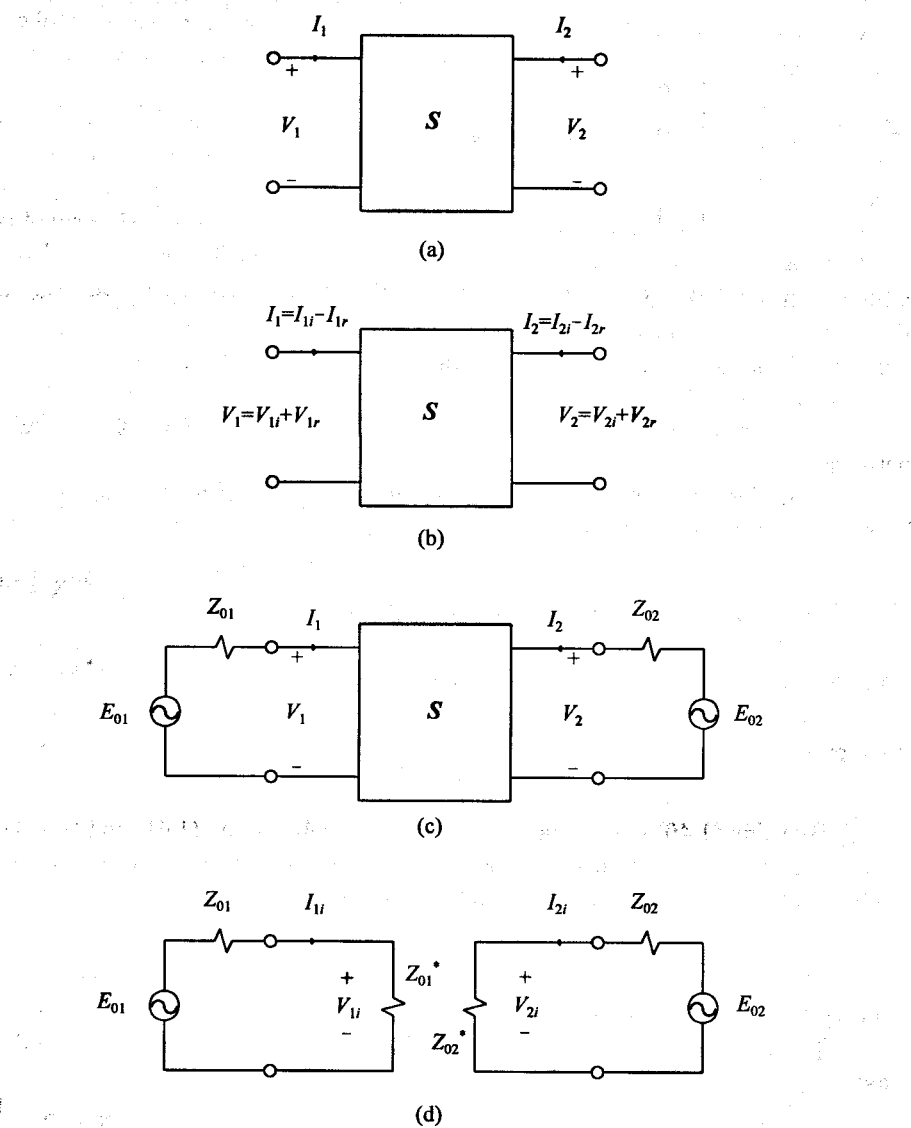


**Figure 1.9** (a), (b) The voltage and current relevant to the  $S$ -parameter definitions; (c) the two-port of (a) and (b) augmented by the normalizing impedances; (d) the equivalent circuit for calculating the incident current and voltage.

$$\begin{bmatrix} b_1 \\ b_2 \end{bmatrix} = \begin{bmatrix} s_{11} & s_{12} \\ s_{21} & s_{22} \end{bmatrix} \begin{bmatrix} a_1 \\ a_2 \end{bmatrix} \quad (1.52)$$

The definitions given above are summarized together with other useful relationships in

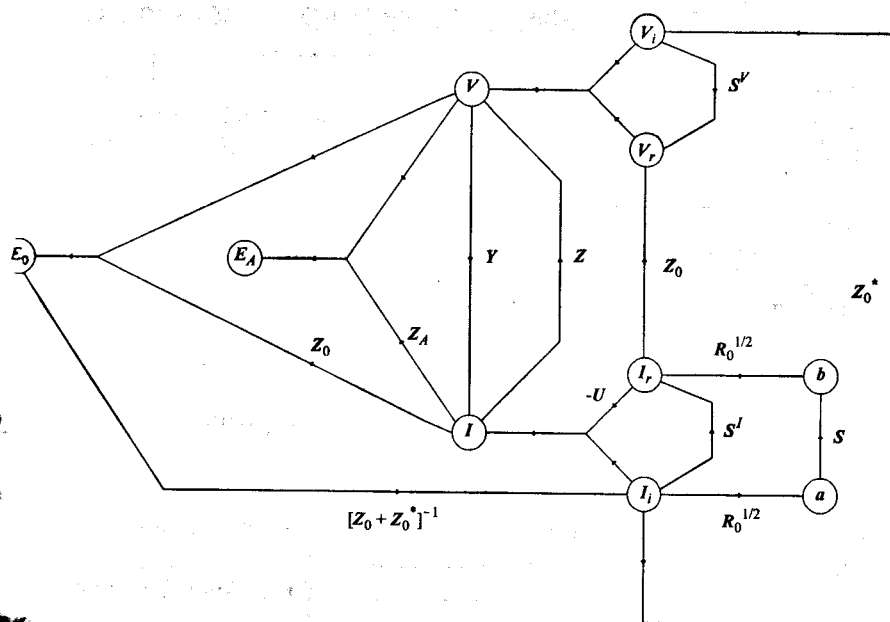


**Figure 1.10** A diagram of  $S$ -,  $Y$ -, and  $Z$ -parameter relationships.

**Figure 1.10.**

The impedance matrix  $Z_A$  in Figure 1.10 is defined by

$$Z = \begin{bmatrix} Z_{A1} & 0 & \dots & 0 \\ 0 & Z_{A2} & \dots & 0 \\ \vdots & \vdots & \ddots & \vdots \\ 0 & 0 & \dots & Z_{AN} \end{bmatrix} \quad (1.53)$$

the matrix  $E_A$  by

$$\begin{bmatrix} E_{A1} \\ E_{A2} \\ \vdots \\ E_{AN} \end{bmatrix} \quad (1.54)$$

$E_A$  refers to the source voltage at the  $j$ th port of the  $N$ -port augmented by the actual

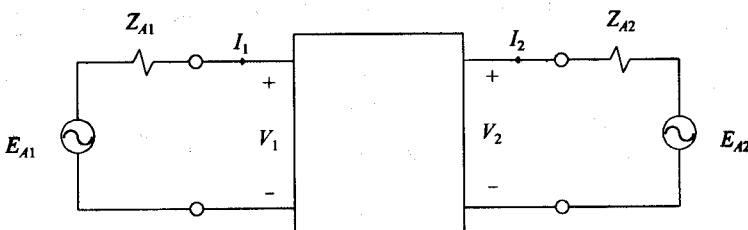


**Figure 1.11** The two-port augmented by the actual load and source terminations ( $E_{A2}$  is usually equal to zero).

source and load impedances of interest ( $Z_A$ ). These definitions are illustrated in Figure 1.11 for a two-port network.

Note that the vectors in Figure 1.10 flow into the dependent variables and emanate from the independent variables. The branch multipliers are shown next to each branch. If no multiplier is shown, the unit matrix ( $U$ ) should be used.

It can be shown that  $E_0$  (the source voltages of the  $N$ -port augmented by its normalizing impedances as illustrated in Figure 1.9) is given in terms of  $E_A$  (the source voltages of the  $N$ -port augmented by the actual impedances and source voltage of interest) by the expression

$$E_0 = [I_N - (Z_0 - Z_A)(I_N - S^T)(Z_0 + Z_0^*)^{-1}]^{-1} E_A \quad (1.55)$$

### EXAMPLE 1.3 Derivation of the relationship between the reflected current and voltage.

To use the diagram in Figure 1.10, consider the derivation of the equality (1.48):

$$V_r = Z_0 I_r$$

It follows by inspection of the diagram that in order to find a relationship between  $V_r$  and  $I_r$ , it is necessary to relate  $V$  to  $I$ . The easiest possible way would be to use the expression

$$E_0 = V + Z_0 I$$

$E_0$  can then be replaced in terms of  $I_i$ ,  $V$  in terms of  $V_i$  and  $V_r$ ,  $V_i$  in terms of  $Z_0^*$  and  $I_i$ , and  $I$  in terms of  $I_r$  and  $I_i$ .

After a few manipulations on the equation thus obtained, (1.48) follows.

**EXAMPLE 1.4** Calculation of the incident and reflected components for a two-port.

In order to make the definitions given above more real, consider finding the incident and reflected components when the terminal voltage and current of a two-port are given by

$$V_1 = 1.0\text{V}$$

$$V_2 = 0.5\text{V}$$

$$I_1 = 0.1\text{A}$$

$$I_2 = -0.2\text{A}$$

and the normalizing impedances are chosen to be

$$Z_{01} = 5\Omega$$

$$Z_{02} = 10\Omega$$

The first step is to find the source voltage in the equivalent circuit shown in Figure 1.9(d) in order to find the incident current and voltage. Inspection of the diagram yields (1.39):

$$E_0 = V + Z_0 I$$

$$= \begin{bmatrix} 1.0 \\ 0.5 \end{bmatrix} + \begin{bmatrix} 5 & 0 \\ 0 & 10 \end{bmatrix} \begin{bmatrix} 0.1 \\ -0.2 \end{bmatrix}$$

$$= \begin{bmatrix} 1.5 \\ -1.5 \end{bmatrix}$$

The incident components can now be obtained by using the equivalent circuit in Figure 1.9(d):

$$\begin{bmatrix} I_{1i} \\ I_{2i} \end{bmatrix} = \begin{bmatrix} 1/(2R_{01}) & 0 \\ 0 & 1/(2R_{02}) \end{bmatrix} \begin{bmatrix} E_{01} \\ E_{02} \end{bmatrix} = \begin{bmatrix} 0.150 \\ -0.075 \end{bmatrix}$$

$$\begin{bmatrix} V_{1i} \\ V_{2i} \end{bmatrix} = \begin{bmatrix} Z_{01}^* I_{1i} \\ Z_{02}^* I_{2i} \end{bmatrix} = \begin{bmatrix} 0.75 \\ -0.75 \end{bmatrix}$$

The normalized incident components follow by application of (1.44):

$$\begin{bmatrix} a_1 \\ a_2 \end{bmatrix} = \begin{bmatrix} \sqrt{R_{01}} I_{1i} \\ \sqrt{R_{02}} I_{2i} \end{bmatrix} = \begin{bmatrix} 0.3354 \\ -0.2372 \end{bmatrix}$$

The reflected components can be obtained by applying (1.41), (1.48), and (1.45):

$$\begin{bmatrix} I_{1r} \\ I_{2r} \end{bmatrix} = \begin{bmatrix} I_{1i} - I_1 \\ I_{2i} - I_2 \end{bmatrix} = \begin{bmatrix} 0.050 \\ 0.125 \end{bmatrix}$$

$$\begin{bmatrix} V_{1r} \\ V_{2r} \end{bmatrix} = \begin{bmatrix} Z_{01} I_{1r} \\ Z_{02} I_{2r} \end{bmatrix} = \begin{bmatrix} 0.25 \\ 1.25 \end{bmatrix}$$

$$\begin{bmatrix} b_1 \\ b_2 \end{bmatrix} = \begin{bmatrix} \sqrt{R_{01}} I_{1r} \\ \sqrt{R_{02}} I_{2r} \end{bmatrix} = \begin{bmatrix} 0.1118 \\ 0.3953 \end{bmatrix}$$

### 1.5.2 The Physical Meanings of the Normalized Incident and Reflected Components of an *N*-Port

The normalized incident and reflected components are defined in (1.44) and (1.45) in terms of the incident and reflected components of the terminal current. It is useful to have expressions for these components in terms of the terminal voltage and current. The inverse relationships are also of interest.

The required expression for  $a_j$  can be obtained easily by using the relationship between the incident current and  $E_0$ :

$$a_j = \sqrt{R_{0j}} I_{ji} \quad (1.56)$$

$$\begin{aligned} &= \sqrt{R_{0j}} E_{0j} / [R_{0j} + R_{0j}] \\ &= \frac{V_j + Z_{0j} I_j}{2\sqrt{R_{0j}}} \end{aligned} \quad (1.57)$$

The expression for the normalized reflected component can be derived by using this result in the following way:

$$b_j = \sqrt{R_{0j}} I_{jr} \quad (1.58)$$

$$\begin{aligned}
 &= \sqrt{R_{0j}} I_{ji} - \sqrt{R_{0j}} I_j \\
 &= \sqrt{R_{0j}} [I_{ji} - I_j] \\
 &= \frac{V_j + Z_{0j} I_j}{2\sqrt{R_{0j}}} - \sqrt{R_{0j}} I_j
 \end{aligned} \tag{1.59}$$

The inverse relationships follow easily by manipulating (1.57) and (1.59):

$$I = \frac{a_j - b_j}{\sqrt{R_{0j}}} \tag{1.60}$$

$$r = \frac{Z_{0j} a_j + Z_{0j} b_j}{\sqrt{R_{0j}}} \tag{1.61}$$

It follows from (1.60) that the normalized current at any point in the circuit can be defined as the difference between the normalized incident and reflected components at that point.

Note that, if squared, the units of the normalized current would be that of power. When

$$Z_0 = Z_{0j} = R_{0j}$$

simplifies to

$$I = \sqrt{R_{0j}} [a_j + b_j] \tag{1.62}$$

In this case, the normalized voltage at any point can be obtained as the sum of the normalized incident and reflected components. The units of the normalized voltage are that of power if it is squared.

An expression for the power entering any port can be derived in terms of the normalized components by using (1.60) and (1.61) in conjunction with the expression for input power:

$$= 0.5(V_j I_j^* + V_j^* I_j) \tag{1.63}$$

$$\begin{aligned}
 &= 0.5 \frac{Z_{0j}a_j^* + Z_{0j}b_j^*}{2\sqrt{R_{0j}}} \frac{a_j - b_j}{\sqrt{R_{0j}}} + \frac{Z_{0j}a_j + Z_{0j}b_j}{2\sqrt{R_{0j}}} \frac{a_j^* - b_j^*}{\sqrt{R_{0j}}} \\
 &= |a_j|^2 - |b_j|^2
 \end{aligned} \tag{1.64}$$

The power entering any port is, therefore, simply equal to the difference between the square of the normalized incident and reflected components at that port.

The last statement can be taken a step further. It can be shown easily that  $|a_j|^2$  is the available power at the  $j$ th port of the  $N$ -port augmented by its normalizing impedances (see Figures 1.9(c) and 1.9(d)). From this and from (1.64), it follows that  $|b_j|^2$  is the reflected power at the  $j$ th port of the augmented  $N$ -port, and, consequently, the power entering any port of a network is equal to the difference between the available and reflected power at the  $j$ th port of the  $N$ -port augmented by its reference impedances.

It is important to realize that the available power in the  $N$ -port augmented by the normalizing impedances is not equal to the available power in the  $N$ -port augmented by the actual source and load impedances, unless the two sets of impedances are identical.

The simple expressions for the voltage (1.61), current (1.60), and power (1.64) in terms of the normalized incident and reflected components are summarized below.

$$I_j = (a_j - b_j) / \sqrt{R_{0j}}$$

$$V_j = (Z_{0j}a_j + Z_{0j}b_j) / \sqrt{R_{0j}}$$

$$= \sqrt{R_{0j}}(a_j + b_j) \text{ if } Z_{0j} = Z_{0j}^*$$

$$P_j = |a_j|^2 - |b_j|^2$$

### 1.5.3 The Physical Interpretations of the Scattering Parameters

Consider the definitions of the elements of a two-port scattering matrix. The input reflection parameter  $s_{11}$  is defined by

$$s_{11} = \left. \frac{b_1}{a_1} \right|_{a_2 = 0} \tag{1.65}$$

and the forward transmission parameter  $s_{21}$  by

$$s_1 = \frac{b_2}{a_1} \Big|_{a_2=0} \quad (1.66)$$

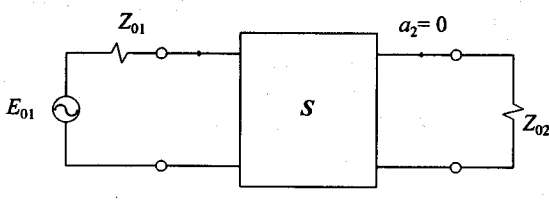
The constraints on the current and voltage at the output terminals, when  $a_2 = 0$ , can be determined by using (1.57):

$$s_2 = a_2 = \frac{V_2 + Z_{02}I_2}{2\sqrt{R_{02}}}$$

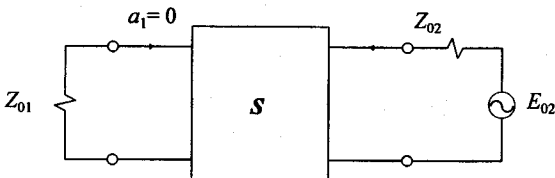
leading to

$$V_2 = Z_{02}[-I_2] \quad (1.67)$$

In order for  $a_2$  to be equal to zero, the load impedance across the output port must be equal to the normalizing impedance at that port, and the electromotive force must be equal to zero. This is illustrated in Figure 1.12(a).



(a)



(b)

- 12 The conditions under which (a)  $a_2 = 0$  and (b)  $a_1 = 0$ .

At this stage (1.57) and (1.59) can be substituted into (1.65) and (1.66) to find an equation for the parameters in terms of the terminal current and voltage:

$$s_{11} = \frac{V_1 - Z_{01}^* I_1}{V_1 + Z_{01} I_1} \Big|_{a_2=0} = \frac{Z_{in} - Z_{01}^*}{Z_{in} + Z_{01}} \Big|_{a_2=0} \quad (1.68)$$

$$s_{21} = \sqrt{\frac{R_{01}}{R_{02}}} \frac{V_2 - Z_{02}^* I_2}{V_1 + Z_{01} I_1} \Big|_{a_2=0} = \sqrt{\frac{R_{01}}{R_{02}}} \frac{Z_{02}(-I_2) - Z_{02}^* I_2}{E_{01}} \Big|_{a_2=0}$$

$$= -2\sqrt{R_{01} R_{02}} \frac{I_2}{E_{01}} \Big|_{a_2=0} \quad (1.69)$$

where  $Z_{in}$  is the input impedance of the two-port terminated, as shown in Figure 1.12(a).

The equivalence between (1.68) and the expression

$$\Gamma_{in} = \frac{Z_{in} - Z_{01}}{Z_{in} + Z_{01}} \quad (1.70)$$

for a reflection coefficient in transmission-line theory is obvious. When

$$Z_{01} = R_{01}$$

as is often the case, the two expressions will be identical.

When the normalizing resistance is equal, the forward transmission parameter  $s_{21}$  is simply the voltage gain  $V_L/(E_{01}/2)$  of the two-port augmented with its normalizing impedances and with  $E_{02}$  set equal to zero.

Because the S-parameters are defined in terms of the normalized incident and reflected components, and the square of these components was shown to be the incident and reflected power at the relevant port of the two-port augmented with its normalizing impedances, respectively, it follows that

$$\begin{aligned} |s_{11}|^2 &= \left| \frac{b_1}{a_1} \right|^2 \Big|_{a_2=0} \\ &= \frac{P_{lr}}{P_{av-E_{01}}} \Big|_{a_2=0} \end{aligned} \quad (1.71)$$

and

$$|s_{21}|^2 = \left| \frac{b_2}{a_1} \right|^2 \Big|_{a_2=0}$$

$$\begin{aligned}
 &= \frac{|b_2|^2 - |a_2|^2}{|a_1|^2} \Big|_{a_2=0} \\
 &= \frac{P_L}{P_{av-E}} \Big|_{a_2=0} \tag{1.72}
 \end{aligned}$$

where  $P_{av-E}$  is the power available from the source when the two-port is augmented by the normalizing impedances, and  $P_{1r}$  is the power reflected from the input port when it is augmented by the normalizing impedances and  $E_{02}$  is set equal to zero.

The meanings of  $|s_{11}|^2$  and  $|s_{21}|^2$  are illustrated in Figure 1.13.

Similar expressions apply to the output reflection parameter  $s_{22}$  and the reverse transmission parameter  $s_{12}$ .

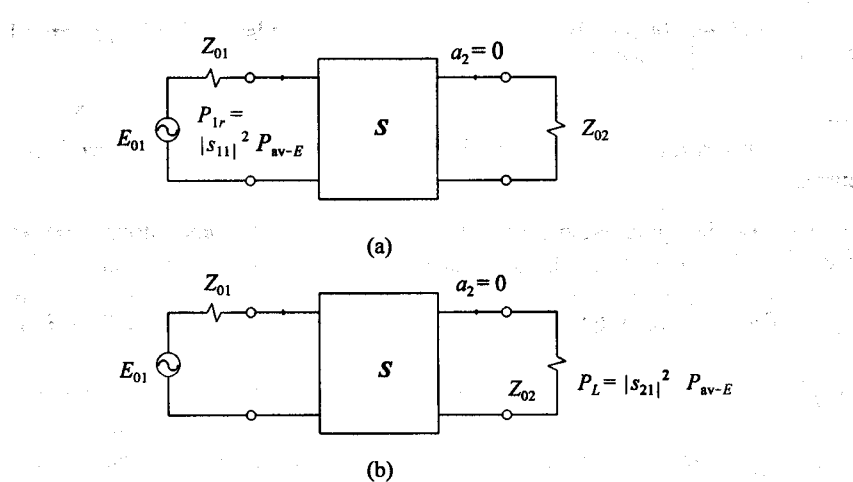


Figure 1.13 The physical meanings of the scattering parameters ( $s_{11}; s_{21}$ ) illustrated.

When the normalizing impedances are also the impedances in the actual network of interest, the transducer power gain and the ratio of the reflected power at the input to the available power from the source are given directly by  $s_{21}$  and  $s_{11}$ , respectively.

When the normalizing impedances are purely resistive, and  $s_{11}$  and  $s_{22}$  are displayed on a Smith Chart, the input and output impedances of the network can be read directly.

#### 1.5.4 Constraints Imposed on the Normalized Incident and Reflected Components by the Terminations of an $N$ -Port

In order to derive expressions for the gains and impedances of an  $N$ -port with arbitrary

terminations, it is necessary to derive expressions for the constraints imposed by the terminations on the normalized incident and reflected components.

Consider port  $n$  of the  $N$ -port terminated in an impedance  $Z_{An}$  in series with a voltage source  $E_{An}$  as shown in Figure 1.14.

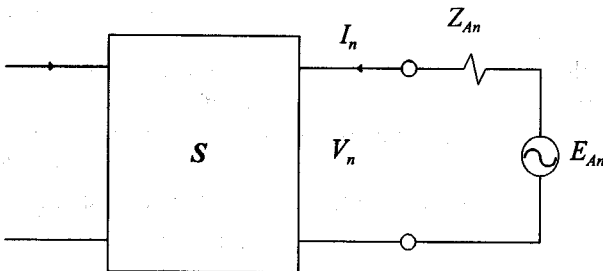


**Figure 1.14** The  $N$ -port under consideration.

The termination forces the following relationship between the terminal voltage and current:

$$E_{An} = V_n + Z_{An} I_n \quad (1.73)$$

By using this relationship in conjunction with (1.57) and (1.59), it follows that

$$2\sqrt{R_{0n}} a_n = V_n + Z_{0n} I_n = E_{An} - (Z_{An} - Z_{0n}) I_n$$

leading to

$$2\sqrt{R_{0n}} a_n - E_{An} = -(Z_{An} - Z_{0n}) I_n \quad (1.74)$$

and

$$2\sqrt{R_{0n}} b_n = V_n - Z_{0n}^* I_n = E_{An} - (Z_{An} - Z_{0n}^*) I_n$$

which leads to

$$2\sqrt{R_{0n}} b_n - E_{An} = -(Z_{An} + Z_{0n}^*) I_n \quad (1.75)$$

Dividing (1.74) by (1.75) yields

$$\frac{2\sqrt{R_{0n}}a_n - E_{An}}{2\sqrt{R_{0n}}b_n - E_{An}} = \frac{-(Z_{An} - Z_{0n})I_n}{-[Z_{An} + Z_{0n}^*]I_n}$$

which leads to

$$a_n = \frac{Z_{An} - (Z_{0n}^{**})}{Z_{An} + (Z_{0n}^*)} b_n + \frac{\sqrt{R_{0n}}}{Z_{An} + (Z_{0n}^*)} E_{An} \quad (1.76)$$

With

$$E_{An} = 0$$

the second term in (1.76) is equal to zero, and the following relationship applies:

$$= a_n / b_n = \frac{Z_{An} - (Z_{0n}^{**})}{Z_{An} + (Z_{0n}^*)} \quad (1.77)$$

This expression clearly has the form of a reflection parameter with normalizing impedance  $Z_{0n}^*$ . The termination can therefore be considered to be the interconnection of a one-port network with a port of the two-port. The normalizing impedance of the one-port must be the conjugate of that at the corresponding port of the two-port. This is illustrated in Figure 1.15.

One would expect that the normalized component incident on the one-port ( $a_L$ ) would be equal to the component reflected from the two-port ( $b_2$ ) and that the component reflected from the one-port ( $b_L$ ) should be equal to that incident on the two-port ( $a_2$ ), that is

$$= b_2 \text{ and } b_L = a_2$$

The proof follows easily from the fact that the voltage across the one-port is the same as that at the corresponding port of the two-port ( $V_L = V_2$ ) and that the currents are identical except for a difference in sign ( $I_L = -I_2$ ). It follows from (1.57) and (1.59)

$$\frac{V_2 + Z_{02} I_2}{2 \sqrt{R_{02}}} = \frac{V_L - (Z_{02}^*)^* I_L}{2 \sqrt{R_{02}}} = b_L \quad (1.78)$$

$$\frac{V_2 - Z_{02}^* I_2}{2 \sqrt{R_{02}}} = \frac{V_L + (Z_{02}^*) I_L}{2 \sqrt{R_{02}}} = a_L \quad (1.79)$$

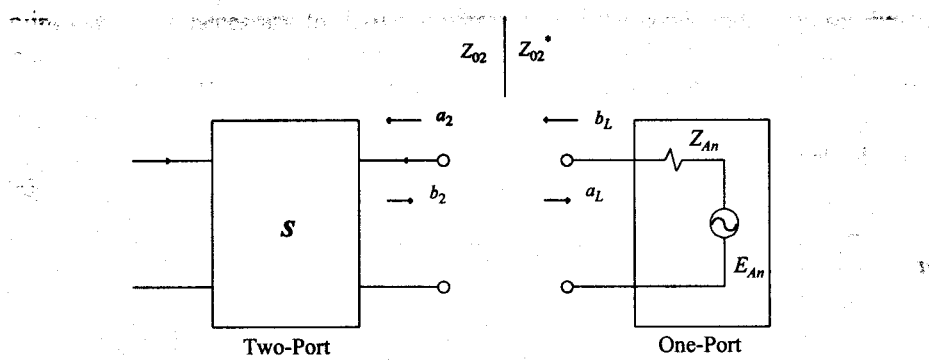


**Figure 1.15** Cascading a one-port with a two-port network.

The component incident on the  $N$ -port ( $a_n$ ) is, therefore, reflected from the one-port, and the component reflected from the  $N$ -port ( $b_n$ ) is incident on the one-port.

The normalizing impedance for the single-port is the conjugate of that for the  $N$ -port.

### 1.5.5 Derivation of Expressions for the Gain Ratios and Reflection Parameters of a Two-Port

Consider the two-port with terminations as shown in Figure 1.16 and the associated  $S$ -parameter expression:

$$\begin{bmatrix} b_1 \\ b_2 \end{bmatrix} = \begin{bmatrix} s_{11} & s_{12} \\ s_{21} & s_{22} \end{bmatrix} = \begin{bmatrix} a_1 \\ a_2 \end{bmatrix} \quad (1.80)$$

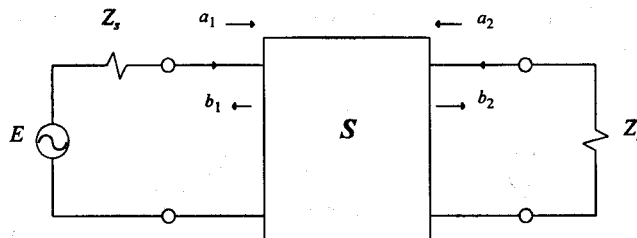


**Figure 1.16** The two-port under consideration.

In (1.80)  $a_1$  is an independent variable, the magnitude and phase of which are determined by the source voltage  $E$  and the fixed normalizing impedance  $Z_{01}$ .

According to (1.77),  $b_2$  is constrained to

$$\begin{aligned} &= a_2 / \frac{Z_L - (Z_{02}^{**})}{Z_L + (Z_{02}^*)} \\ &= a_2 / S_L \end{aligned} \quad (1.81)$$

With  $a_1$  the independent variable and  $b_2$  known in terms of  $a_2$ , (1.80) amounts to two equations with two unknowns and values for  $a_2$ ,  $b_1$ , and  $b_2$  can be determined in terms of the scattering parameters and  $a_1$ . The results are as follows:

$$= 1 \quad (1.82)$$

$$= s_{11} + \frac{s_{12}s_{21}S_L}{1 - s_{22}S_L} \quad (1.83)$$

$$= \frac{s_{21}S_L}{1 - s_{22}S_L} \quad (1.84)$$

$$= a_2 / S_L \quad (1.85)$$

At this stage, the reflection parameters and the gain ratios of interest can be determined. The expressions most frequently used are repeated below.

$$= \frac{Z_{in} - Z_{01}^*}{Z_{in} + Z_{01}} = \frac{V_1 - Z_{01}^* I_1}{V_1 + Z_{01} I_1} = \frac{b_1}{a_1} = s'_{11} = s_{11} + \frac{s_{12}s_{21}S_L}{1 - s_{22}S_L} \quad (1.86)$$

$$= \frac{Z_{out} - Z_{02}^*}{Z_{out} + Z_{02}} = \frac{V_2 - Z_{02}^* I_2}{V_2 + Z_{02} I_2} = \frac{b_2}{a_2} = s'_{22} = s_{22} + \frac{s_{12}s_{21}S_s}{1 - s_{11}S_s} \quad (1.87)$$

$$= \frac{Z_s - (Z_{01}^{**})}{Z_s + (Z_{01}^*)} \quad (1.88)$$

$$G_o = \frac{|b_2|^2 - |a_2|^2}{|a_1|^2 - |b_1|^2}$$

$$= \frac{|s_{21}|^2 [1 - |S_L|^2]}{|1 - s_{22}S_L|^2 - |s_{22}(1 - s_{22}S_L) + s_{12}s_{21}S_L|^2} \quad (1.89)$$

$$G_T = \frac{|b_2|^2 - |a_2|^2}{P_{av-E}}$$

$$= \frac{|s_{21}|^2 [1 - |S_L|^2] [1 - |S_s|^2]}{[1 - s_{11}S_s][1 - s_{22}S_L] - s_{12}s_{21}S_sS_L} \quad (1.90)$$

$$G_{T_{s_{12}=0}} = G_{T,u}$$

$$= \frac{1 - |S_s|^2}{|1 - s_{11}S_s|^2} |s_{21}|^2 \frac{1 - |S_L|^2}{|1 - s_{22}S_L|^2} \quad (1.91)$$

where  $G_{T,u}$  is the unilateral transducer power gain

$$G_A = \frac{P_{av-O}}{P_{av-E}} \quad (1.92)$$

$$= \frac{|s_{21}|^2 [1 - |S_s|^2]}{|1 - |s_{22}|^2 + |S_s|^2 [|s_{11}|^2 - |\Delta|^2] - 2 \operatorname{Re}(C_1 S_s)} \quad (1.93)$$

where  $P_{av-O}$  is the maximum available power at the output terminals of the transistor

$$\Delta = s_{11}s_{22} - s_{12}s_{21} \quad (1.94)$$

and

$$C_1 = s_{11} - \Delta s_{22} \quad (1.95)$$

$$= \frac{\sqrt{R_{02}}}{\sqrt{R_{01}}} \frac{a_2 + b_2}{a_1 + b_1} = \sqrt{\frac{R_{02}}{R_{01}}} \frac{s_{21}[1 + S_L]}{1 + s_{11} - s_{22}S_L - s_{11}s_{22}S_L + s_{12}s_{21}S_L} \quad (1.96)$$

In order for (1.96) to apply, the normalizing impedances must be purely resistive.

In (1.86),  $s_{11\omega}$  is defined to be the input reflection parameter with the two-port terminated in the actual load of interest (normalizing impedance on the input side:  $Z_{01}$ ), while  $s_{22\omega}$  is defined in (1.87) as the output reflection parameter with the two-port terminated in the source impedance of interest (normalizing impedance on the output side,

Similarly,  $s_{21\omega}$  is defined here as  $s_{21}$  when the output normalizing impedance is the actual load impedance of interest ( $Z_{02} = Z_L$ ) and the input normalizing impedance is taken to be the conjugate of the input impedance of the two-port ( $Z_{01} = Z_{in}^*$ ). It follows from this definition that

$$|s_{21}|^2 = G_\omega \quad (1.97)$$

Similarly,  $s_{21a}$  is defined as  $s_{21}$  when the input normalizing impedance is the actual source impedance of interest ( $Z_{01} = Z_s$ ) and the output normalizing impedance is taken to be the conjugate of the output impedance of the two-port ( $Z_{02} = Z_{out}^*$ ). It follows that

$$|s_{21a}|^2 = G_A \quad (1.98)$$

$s_{21T}$  is defined as  $s_{21}$  when the normalizing impedance on the load side is the actual load of interest ( $Z_{02} = Z_L$ ) and that on the input side the actual source impedance of interest ( $Z_{01} = Z_s$ ). This implies that

$$|s_{21T}|^2 = G_T \quad (1.99)$$

These definitions are relevant during circuit synthesis.

### EXAMPLE 1.5 Derivation of the expression for the transducer power gain.

As an example of the application of (1.82) to (1.85), consider the derivation of (1.90).

An expression for the power dissipated in the load follows directly from (1.84) and (1.85):

$$\begin{aligned} P_L &= |b_2|^2 - |a_2|^2 \\ &= \left| \frac{s_{21}}{1 - s_{22}S_L} \right|^2 [1 - |S_L|^2] |a_1|^2 \end{aligned} \quad (1.100)$$

In order to derive an expression for  $P_{av-E}$ , it is necessary to use (1.76). Application of (1.76) to port 1 yields

$$a_1 = \frac{Z_s - (Z_{01}^{**})}{Z_s + (Z_{01}^{*})} b_1 + \frac{\sqrt{R_{01}}}{Z_s + Z_{01}} E_1$$

from which it follows that

$$E_1 = \frac{a_1 - S_s b_1}{\sqrt{R_{01}}} (Z_s + Z_{01}) \quad (1.101)$$

Substitution of (1.101) in the expression for the available power gain yields

$$P_{av-E} = E_1^2 / [4R_s] = \frac{|Z_s + Z_{01}^*|^2}{4R_{01}R_s} |a_1 - S_s b_1|^2 = \frac{|a_1 - S_s b_1|^2}{1 - |S_s|^2} \quad (1.102)$$

After substitution of  $b_1$  in terms of  $a_1$  (see (1.83)) in this equation, it follows that

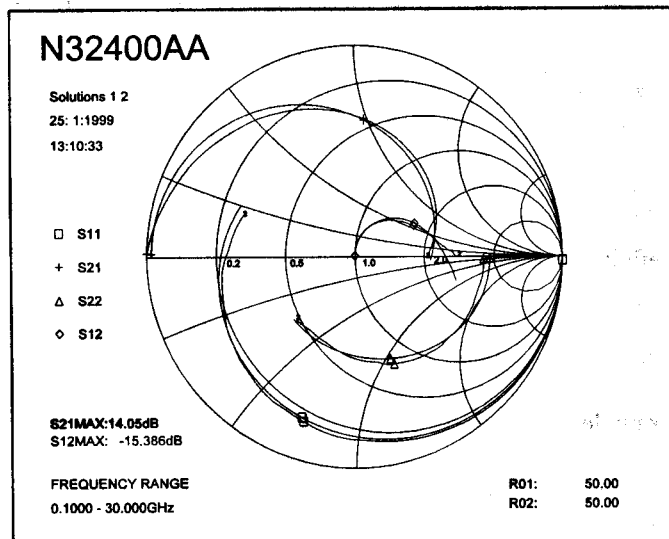


**Figure 1.17** The  $S$ -parameters (50Ω normalization) of a transistor displayed on a polar plot (the constant resistance and constant reactance circles only apply to  $s_{11}$  and  $s_{22}$ ;  $s_{12}$  and  $s_{21}$  were normalized as shown). The one set of traces is used for the parameters as supplied by the manufacturer (traces marked with a "2"), while the other set is used for the  $S$ -parameters of the small-signal model fitted [2]. Note that the highest frequency point on each curve is not marked.

$$P_{av-E} = \frac{[1 - s_{11}S_s][1 - s_{22}S_L] - s_{21}s_{12}S_sS_L}{[1 - |S_s|^2][1 - s_{22}S_L]^2} \quad (1.103)$$

Combination of (1.103) and (1.100) yields the desired expression.

The S-parameters ( $50\Omega$  normalization) for a typical microwave transistor are displayed in Figure 1.17. The performance with different terminations can be obtained by using the equations provided in this section.

## 1.5.6 Signal Flow Graphs

S-parameter equations shown above can also be derived by using signal flow graphs. Additional insight into the different relationships are also gained from the flow graphs.

The following rules apply when a signal flow graph is created:

1. Each variable is designated with a node (in the case of the two-port, nodes will be used for  $a_1$ ,  $a_2$ ,  $b_1$ ,  $b_2$ , and  $b_s$ ).
2. A multiplier is associated with each branch.
3. Branches emanate from independent variable nodes and terminate on dependent variable nodes (dependence and independence are established by the associated equation). The direction of the flow is indicated with an arrow on each branch. The branch multipliers are applied to the independent variable nodes.
4. The value of each dependent variable is determined by the multipliers and independent variables associated with the branches entering the relevant node.

These rules are illustrated below by building a signal flow graph for the normalized incident and reflected components of a two-port (Figure 1.18).

Apart from representing the relationships of interest graphically, flow graphs can be used to calculate the value of any of the dependent variables in the graph in terms of the independent variable of the graph ( $b_s$  in this case). This is done by applying Mason's rule to the graph. The following terms are required before the rule can be formulated:

1. A first-order loop product is defined as the product of the branch multipliers encountered in a journey starting from any specific node and moving back to the same node in the direction of the arrows. The first-order loop products in Figure 1.18 are  $s_{11}\Gamma_s$ ,  $s_{22}\Gamma_L$ , and  $s_{21}\Gamma_L s_{12}\Gamma_s$ .

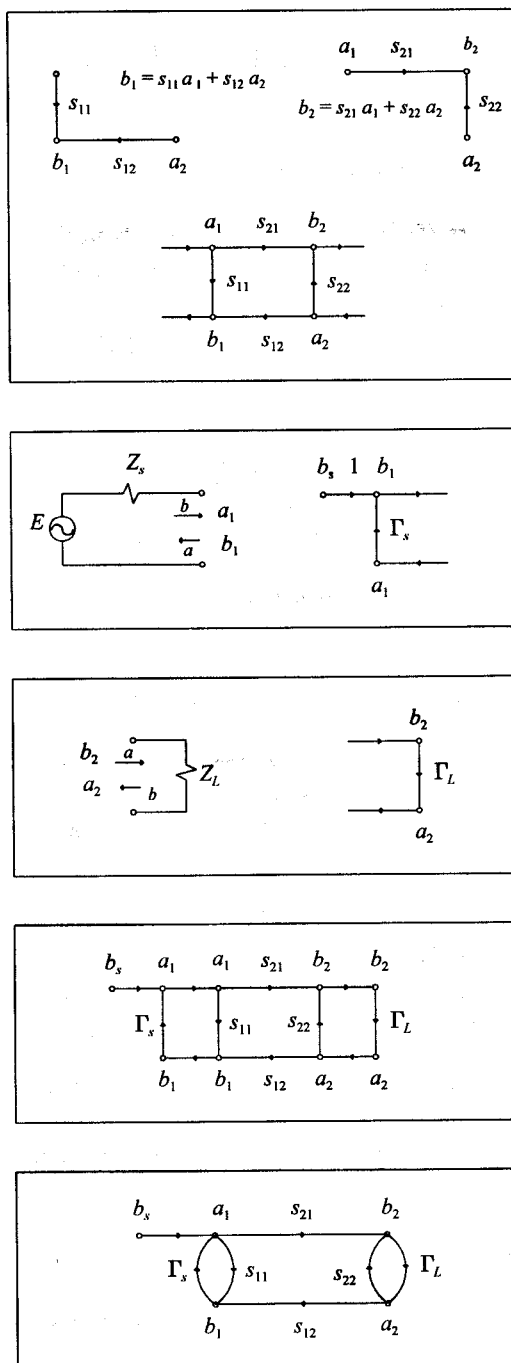


**Figure 1.18** A flow graph for the incident and reflected components of a two-port.

2. Loops are nontouching when they have no nodes or branches in common.
3. A second-order loop product is the product formed by combining the loop products of any two non-touching first-order loops.
4. A third-order loop product is the product associated with any three non-touching first-order loops.
5. An  $n$ th-order loop product is the product associated with any  $n$  non-touching first-order loops.
6. A path is any forward route (route in the direction of the arrows) emanating from the independent variable of the graph and terminating on the dependent variable of interest.

Mason's rule can be formulated at this point:

$$\frac{P_1[1 - \sum L_{NT P_1}^1 + \sum L_{NT P_1}^2 - ] + P_2[1 - \sum L_{NT P_2}^1 + \dots]}{1 - \sum L^1 + \sum L^2 - \sum L^3 + \dots} \quad (1.104)$$

$L^n$  is the sum of all the  $n$ th order loop products,  $\sum L_{NT P_m}^n$  is the sum of all the  $n$ th order products associated with the loops not touching path  $m$ , and  $P_m$  is the product of the branch terms along the path  $m$ .

Note that the denominator of (1.104) is only a function of the graph topology and is the same for all the dependent variables. It follows that this term will be cancelled if the value of any of the dependent variables is taken.

**EXAMPLE 1.6** Calculation of  $a_1$  in terms of  $b_s$ , and  $b_1$ ,  $b_2$ , and  $a_2$  in terms of  $a_1$ .

To demonstrate application of (1.104),  $a_1$  in Figure 1.18 will be calculated as a function of  $b_s$ .

The sum of all the first-order loop products is

$$s_{11} \Gamma_s + s_{22} \Gamma_L + s_{21} \Gamma_s s_{12} \Gamma_L$$

There is only one second-order loop (loop factor  $s_{11} s_{22} \Gamma_s \Gamma_L$ ).

The only loop that does not touch the path leading to  $a_1$  is the loop on the right-hand side of the flow graph (loop factor  $s_{22} \Gamma_L$ ).

This leads to

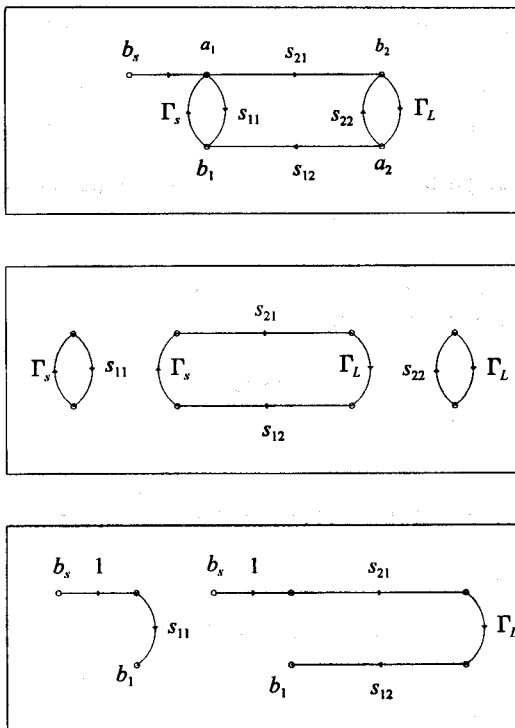


**Figure 1.19** The first-order loops and the forward paths relevant to calculation of the ratio  $b_1/b_s$ .

$$\frac{a_1}{b_s} = \frac{1 - s_{22} \Gamma_L}{1 - [s_{11} \Gamma_s + s_{22} \Gamma_L + s_{21} \Gamma_s s_{12} \Gamma_L] + s_{11} s_{22} \Gamma_s \Gamma_L} \quad (1.105)$$

In the previous section  $a_1$  was taken to be unity, which leads to

$$b_s = \frac{1 - [s_{11} \Gamma_s + s_{22} \Gamma_L + s_{21} \Gamma_s s_{12} \Gamma_L] + s_{11} s_{22} \Gamma_s \Gamma_L}{1 - s_{22} \Gamma_L} \quad (1.106)$$

$b_1$ ,  $b_2$ , and  $a_2$  can now be derived in terms of  $a_1$  by applying Mason's rule in each case. The results obtained will be the same as those in the previous section. To illustrate this, consider the derivation for  $b_1$ :

$$\frac{b_1}{b_s} = \frac{s_{11} (1 - s_{22} \Gamma_L) + s_{21} \Gamma_L s_{12} (1)}{1 - [s_{11} \Gamma_s + s_{22} \Gamma_L + s_{21} \Gamma_s s_{12} \Gamma_L] + s_{11} s_{22} \Gamma_s \Gamma_L} \quad (1.107)$$

Note that there are no nontouching loops associated with the second path term in the numerator of (1.105) ( $s_{21}\Gamma_L s_{12}(1)$ ).

Substituting  $b_s$  in this equation produces the same result as (1.83).

### 1.5.7 The Indefinite S-Matrix

Similar to the indefinite admittance matrix, the sum of the elements in each row or column of the indefinite S-matrix is equal to a constant. In this case the constant is unity.

In order to prove that the sum of the elements in each row must equal 1, consider the three-port shown in Figure 1.20.

Under the conditions shown, all the incident components are equal, and

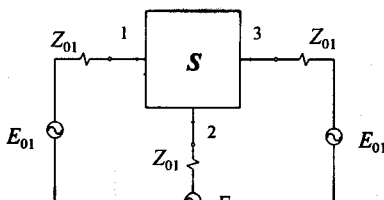
$$b_j = s_{j1}a_1 + s_{j2}a_2 + s_{j3}a_3$$

which simplifies to

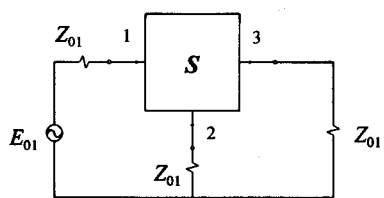
$$b_j = [s_{j1} + s_{j2} + s_{j3}]a_1$$

Substitution of  $b_j$  and  $a_1$  in terms of the reflected and incident currents yields

$$I_{j1} = [s_{j1} + s_{j2} + s_{j3}]I_{11}$$



(a)



(b)

Figure 1.20

Circuits used to prove that the sum of the elements in (a) any row or (b) any column of an indefinite S-matrix is equal to 1.

and because the terminal currents must equal zero when all the source voltages are equal,  $I_{jr}$  must equal  $I_{1r}$ . It follows that

$$s_{j1} + s_{j2} + s_{j3} = 1 \quad (1.108)$$

The circuit in Figure 1.20(b) can be used to prove that the sum of the elements of the first column of the indefinite matrix is equal to 1. Because the incident components at terminals two and three are equal to zero, the necessary condition

$$I_1 + I_2 + I_3 = 0$$

simplifies to

$$I_{1i} = I_{1r} + I_{2r} + I_{3r} \quad (1.109)$$

With

$$a_2 = 0 = a_3$$

$$b_1 = s_{11}a_1 + s_{12}a_2 + s_{13}a_3$$

$$b_2 = s_{21}a_1 + s_{22}a_2 + s_{23}a_3$$

$$b_3 = s_{31}a_1 + s_{32}a_2 + s_{33}a_3$$

simplifies to

$$b_1 = s_{11}a_1$$

$$b_2 = s_{21}a_1$$

$$b_3 = s_{31}a_1$$

and, therefore,

$$I_{1r} = s_{11}I_{1i} \quad (1.110a)$$

$$I_{2r} = s_{21}I_{1i} \quad (1.110b)$$

$$I_{3r} = s_{31}I_{1i} \quad (1.110c)$$

Equation (1.109) combined with (1.110) yields

$$s_{11} + s_{21} + s_{31} = 1 \quad (1.111)$$

By moving the voltage source in Figure 1.20(b) to the other two ports and follow-

the same procedure, it can also be shown that the sum of the elements in each of the two columns of the indefinite  $S$ -matrix is equal to 1.

### 1.8 Extension of the Single-Frequency S-Parameter Definitions to the Complex Frequency Plane

A necessary condition for a matrix to be the  $S$ -parameter matrix of a linear, lumped, passive network normalized to  $N$  minimum reactance functions (i.e., impedance functions with no poles on the real-frequency axis) is that none of its elements may have any poles in the right-hand side (RHS) of the complex frequency plane [3].

The definitions given for  $a$  and  $b$  in Section 1.5.1 are adequate for any single-frequency application, as well as in the complex plane when the normalizing impedance functions ( $Z_0(s)$ ) do not have any finite poles (i.e., purely resistive normalizing impedances, impedances of the form  $R_0 + sL_0$ ). However, when these impedance functions are more complex, it is necessary to extend the definitions of the normalized incident and reflected coefficients. The following definitions are relevant to the more general case:

$$= \begin{bmatrix} Z_{01}(s) & 0 & \dots & 0 \\ 0 & Z_{02}(s) & \dots & 0 \\ \dots & \dots & \dots & 0 \\ 0 & 0 & \dots & Z_{0N}(s) \end{bmatrix} \quad (1.112)$$

$Z_j(s)$  is the normalizing impedance at port  $j$ ,

$$= \begin{bmatrix} r_{01}(s) & 0 & \dots & 0 \\ 0 & r_{02}(s) & \dots & 0 \\ \dots & \dots & \dots & 0 \\ 0 & 0 & \dots & r_{0N}(s) \end{bmatrix} \quad (1.113)$$

$$= H(s)h(-s) \quad (1.114)$$

$$= 0.5 [Z_{0j}(s) + Z_{0j}(-s)] \quad (1.115)$$

$$\mathbf{h}(s) = \begin{bmatrix} m_1(s)/n_1(s) & 0 & \dots & 0 \\ 0 & m_2(s)/n_2(s) & \dots & 0 \\ \dots & \dots & \dots & \dots \\ 0 & 0 & \dots & m_N(s)/n_N(s) \end{bmatrix} \quad (1.116)$$

where  $m_j(s)$  and  $n_j(s)$  are polynomials and the zeros of  $n_j(s)$  (poles of  $h_j(s)$ ) are constrained to the open left-hand plane (LHP) and the zeros of  $m_j(s)$  (zeros of  $h_j(s)$ ) are constrained to the closed right-hand plane (RHP).

$$\mathbf{a}(s) = \mathbf{h}(-s)\mathbf{I}_i(s) \quad (1.117)$$

$$\mathbf{b}(s) = \mathbf{h}(s)\mathbf{I}_r(s) \quad (1.118)$$

Where  $\mathbf{a}(s)$  is the matrix of normalized incident components,  $\mathbf{b}(s)$  the normalized reflected components, and with  $\mathbf{I}_i$  and  $\mathbf{I}_r$  as defined in Section 1.5.1.

Note that the elements of  $\mathbf{r}(s)$  are even functions (i.e.,  $r_{0i}(s) = r_{0i}(-s)$ ) and are the effective series resistance parts of the corresponding normalizing impedances.

With these definitions for the normalized and reflected components, it follows that

$$a_j(s) = \frac{V_j(s) + Z_{0j}(s)I_j(s)}{2h_j(s)} \quad (1.119)$$

$$b_j(s) = \frac{V_j(s) - Z_{0j}(-s)I_j(s)}{2h_j(-s)} \quad (1.120)$$

$$S_{jj}(s) = \frac{h_j(s)}{h_j(-s)} \frac{Z_{inj}(s) - Z_{0j}(-s)}{Z_{inj}(s) + Z_{0j}(s)} \quad (1.121)$$

$$s_{jk}(s) = -2h_j(s)h_k(s) \frac{I_j(s)}{E_{0k}} \quad (1.122)$$

These relationships are identical to those derived previously for single-frequency applications as long as

$$h_j(s) = \sqrt{R_{0j}} = h_j(-s) \quad (1.123)$$

This relationship will apply in all cases where the normalizing impedances are purely resistive or of the form  $R_{0j} + sL_{0j}$ .

Independent of the complexity of the normalizing impedances, the incident and reflected power are still given by  $|a_j|^2$  and  $|b_j|^2$ , respectively.

### EXAMPLE 1.7 Calculating $h(s)$ for a two-port.

As an example,  $h(s)$  will be calculated for the normalizing impedances shown in Figure 1.21.

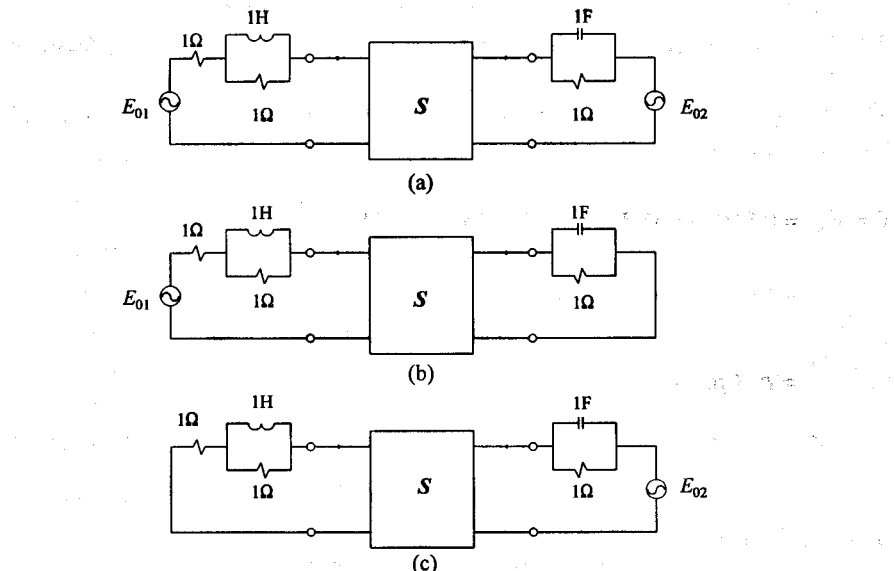


**Figure 1.21** (a) The normalizing impedances under consideration; (b) the equivalent circuit used to determine  $s_{11}(s)$  and  $s_{21}(s)$ ; (c) the equivalent circuit used to determine  $s_{22}(s)$  and  $s_{12}(s)$ .

Because

$$Z_{01}(s) = 1 + s / [1 + s]$$

it follows that

$$r_{01}(s) = 0.5 [Z_{01}(s) + Z_{01}(-s)]$$

$$\begin{aligned} &= \frac{1 - 2s^2}{1 - s^2} \\ &= \frac{1 - \sqrt{2}s}{1 + s} \frac{1 + \sqrt{2}s}{1 - s} \end{aligned}$$

and, therefore,

$$h_1(s) = (1 - \sqrt{2}s) / (1 + s)$$

Similarly,

$$h_2(s) = s / (1 + s)$$

### 1.5.9 Constraints on the Scattering Matrix of a Lossless N-Port

The average power entering a passive lossless device must be equal to zero. This imposes the following constraints on the scattering matrix:

$$\begin{aligned} 0 &= P_{\text{ave}} = 0.5 [V^{**}(j\omega) I(j\omega) + I^{**}(j\omega) V(j\omega)] \\ &= [\mathbf{a}^{**}(j\omega) \mathbf{a}(j\omega) - \mathbf{b}^{**}(j\omega) \mathbf{b}(j\omega)] \\ &= \mathbf{a}^{**}(j\omega) [\mathbf{I}_n - \mathbf{S}^{**}(j\omega) \mathbf{S}(j\omega)] \mathbf{a}(j\omega) \end{aligned} \quad (1.124)$$

leading to

$$\mathbf{S}^{**}(j\omega) \mathbf{S}(j\omega) = \mathbf{I}_n \quad (1.125)$$

In these equations the superscript  $^{**}$  indicates the transposed conjugate of the relevant matrix.

It is clear from (1.125) that the inverse of the scattering matrix of a lossless network is constrained to be equal to its transposed conjugate, that is,

$$\mathbf{S}^{-1}(j\omega) = \mathbf{S}^{**}(j\omega) \quad (1.126)$$

A matrix whose inverse is equal to its transposed conjugate is called a **unitary matrix**. A necessary and sufficient condition for a matrix to be unitary is that its columns (or rows) should be mutually orthogonal unit vectors [3]. In terms of the elements of the scattering matrix, this implies that the following equations must be satisfied:

$$\sum_{j=1}^N s_{ij}(j\omega) s_{kj}^*(j\omega) = \delta_{ik} \quad (1.127)$$

$$\sum_{j=1}^N s_{ij}(j\omega) s_{jk}^*(j\omega) = \delta_{ik} \quad (1.128)$$

where  $\delta_{ik}$  is the Kronecker delta ( $\delta_{ik} = 0$ , if  $i \neq k$ ;  $\delta_{ik} = 1$ , if  $i = k$ ).

The unitary constraint on the magnitude of each row or column vector of the scattering matrix forces the following two relationships on the elements of each row and column, respectively:

$$\sum_{j=1}^N |s_{ij}(j\omega)|^2 = 1 \quad (1.129)$$

$$\sum_{j=1}^N |s_{ji}(j\omega)|^2 = 1 \quad (1.130)$$

The magnitude of each element of the  $S$ -matrix of a lossless (and also passive) network is bounded by unity; that is,

$$|s_{ij}(j\omega)| \leq 1 \quad (1.131)$$

By applying (1.129) and (1.130) to a two-port network, it follows that

$$|s_{11}(j\omega)|^2 = 1 - |s_{12}(j\omega)|^2 \quad (1.132)$$

$$|s_{21}(j\omega)|^2 = 1 - |s_{22}(j\omega)|^2 \quad (1.133)$$

$$|s_{12}(j\omega)|^2 = 1 - |s_{21}(j\omega)|^2 \quad (1.134)$$

$$|s_{22}(j\omega)|^2 = 1 - |s_{12}(j\omega)|^2 \quad (1.135)$$

$$s_{12}(j\omega)s_{12}^*(j\omega) = -s_{21}(j\omega)s_{22}^*(j\omega) \quad (1.136)$$

$$s_{21}(j\omega)s_{21}^*(j\omega) = -s_{12}(j\omega)s_{22}^*(j\omega) \quad (1.137)$$

Moving (1.133) and (1.134) yields

$$|s_{11}(j\omega)| = |s_{22}(j\omega)| \quad (1.138)$$

while (1.134) and (1.135) can be combined to show that

$$|s_{12}(j\omega)| = |s_{21}(j\omega)| \quad (1.139)$$

Equation (1.138) can be extended to

$$s_{12}(j\omega) = s_{21}(j\omega) \quad (1.140)$$

whenever the network considered is passive and reciprocal. This can be proved easily by using the reciprocity theorem.

By combining (1.137) and (1.140), it can be shown that

$$s_{22}(j\omega) = - \frac{s_{21}(j\omega)}{s_{21}^*(j\omega)} s_{11}^*(j\omega) \quad (1.141)$$

These relationships will prove useful in later chapters.

### EXAMPLE 1.8 Calculation of the S-parameters of a lossless two-port.

As an example, the S-parameters of the lossless two-port in Figure 1.22 will be derived, and some of the relationships given above will be illustrated.

Because the normalizing impedances in Figure 1.22 are purely resistive, it follows that

$$h_j(s) = \sqrt{R_{0j}} = h_j(-s)$$

and the input reflection and forward transmission parameters can, therefore, be determined by using (1.68) and (1.69), respectively.

The equivalent circuit corresponding to  $a_2 = 0$  and the chosen normalizing impedances are shown in Figure 1.22.

The input impedance necessary for determining  $s_{11}(j\omega)$  is given by

$$Z_{in}(s) = \frac{1}{G_{02} + sC} + sL$$

and  $s_{11}(j\omega)$  is therefore given by

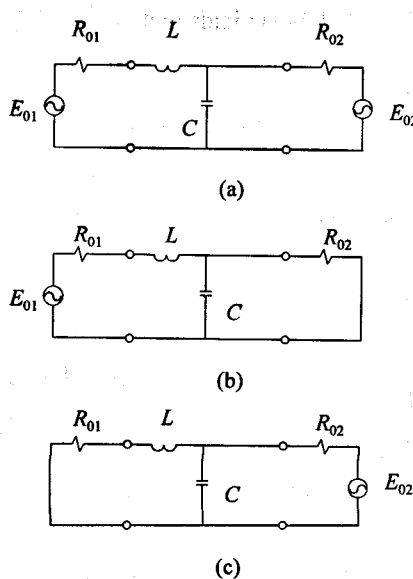


**Figure 1.22** (a) The lossless two-port under consideration; (b) the equivalent circuit used to determine  $s_{11}(j\omega)$  and  $s_{21}(j\omega)$ ; (c) the equivalent circuit used to determine  $s_{22}(j\omega)$  and  $s_{12}(j\omega)$ .

$$\begin{aligned}
 s_{11}(j\omega) &= \frac{Z_{in}(j\omega) - Z_{01}^*}{Z_{in}(j\omega) - Z_{01}} \Big|_{a_2 = 0} \\
 &= \frac{\frac{1}{G_{02} + j\omega C} + j\omega L - R_{01}}{\frac{1}{G_{02} + j\omega C} + j\omega L + R_{01}}
 \end{aligned} \tag{1.142}$$

Similarly, the output reflection parameter is given by

$$\begin{aligned}
 s_{22}(j\omega) &= \frac{\frac{R_{01} + j\omega L}{1 + (R_{01} + j\omega L)j\omega C} - R_{02}}{\frac{R_{01} + j\omega L}{1 + (R_{01} + j\omega L)j\omega C} - R_{02}} \\
 &= \frac{(R_{02} - R_{01} - \omega^2 L C R_{02}) + j\omega(L - R_{01} R_{02} C)}{R_{02} + R_{01} - \omega^2 L C R_{02} + j\omega(L + R_{01} R_{02} C)}
 \end{aligned} \tag{1.143}$$

Comparison of (1.142) and (1.143) yields that

$$|s_{11}(j\omega)| = |s_{22}(j\omega)|$$

as expected.

The forward transmission parameter is given by

$$\begin{aligned} s_{21}(j\omega) &= -2\sqrt{R_{01}R_{02}} \frac{I_{02}}{E_{01}} \Big|_{a_2=0} \\ &= 2 \frac{\sqrt{R_{01}R_{02}}}{R_{01} + R_{02}} \frac{R_{02}}{R_{02} - \omega^2 L C R_{02} + j\omega(L + C R_{01} R_{02})} \end{aligned} \quad (1.144)$$

$$\begin{aligned} s_{12}(j\omega) &= -2\sqrt{R_{01}R_{02}} \frac{I_{01}}{E_{02}} \Big|_{a_1=0} \\ &= 2 \frac{\sqrt{R_{01}R_{02}}}{R_{01} + R_{02}} \frac{R_{02}}{R_{02} - \omega^2 L C R_{02} + j\omega(L + C R_{01} R_{02})} \end{aligned} \quad (1.145)$$

Equations (1.144) and (1.145) are clearly identical and, therefore,

$$s_{21}(j\omega) = s_{12}(j\omega)$$

as expected. The same result can be obtained directly by application of the reciprocity theorem. It is a simple matter to show that

$$|s_{21}|^2 = 1 - |s_{11}|^2$$

and that

$$|s_{12}|^2 = 1 - |s_{22}|^2$$

### 1.5.10 Conversion of S-parameters to Other Parameters

The schematic representation of the S-parameter and related relationships in Figure 1.10 can be used to derive expressions for the conversion of the normalized S-parameters to the other S-parameters as well as to Z- or Y-parameters. The results are

$$\boldsymbol{\varsigma} = \mathbf{R}_0^{1/2} \mathbf{S}^I \mathbf{R}_0^{-1/2} \quad (1.146)$$

$$\boldsymbol{\varsigma}' = \mathbf{Z}_0^{-1} \mathbf{S}^V \mathbf{Z}_0^* \quad (1.147)$$

$$\boldsymbol{\varsigma}' = [\mathbf{Z} + \mathbf{Z}_0]^{-1} [\mathbf{Z} - \mathbf{Z}_0^*] \quad (1.148)$$

$$\boldsymbol{\varsigma}^V = -[\mathbf{Y} + \mathbf{Y}_0]^{-1} [\mathbf{Y} - \mathbf{Y}_0^*] \quad (1.149)$$

$$\mathbf{I} = \mathbf{Y}_0 [\mathbf{I}_n - \mathbf{S}^V] [\mathbf{I}_n + \mathbf{S}^V]^{-1} \quad (1.150)$$

with

$$\mathbf{I} = \mathbf{Z}_0^{-1} \quad (1.151)$$

When the normalizing impedances are all purely resistive and equal

$$\mathbf{S} - \mathbf{S}' = \mathbf{S}^V \quad (1.152)$$

**EXAMPLE 1.9** Derivation of the expression for the reflected voltages of an  $N$ -port in terms of the incident voltages.

It follows by inspection of the diagram in Figure 1.10 that

$$\mathbf{I} = \mathbf{Y}\mathbf{V}$$

is equivalent to

$$\mathbf{I}_i - \mathbf{I}_r = \mathbf{Y}(\mathbf{V}_i + \mathbf{V}_r)$$

which is equivalent to

$$\mathbf{Z}_0^{*-1} \mathbf{V}_i - \mathbf{Z}_0^{-1} \mathbf{V}_r = \mathbf{Y} \mathbf{V}_i + \mathbf{Y} \mathbf{V}_r$$

This equation can be manipulated to

$$\mathbf{V}_r = -(\mathbf{Y} + \mathbf{Y}_0)^{-1} (\mathbf{Y} - \mathbf{Y}_0^*) \mathbf{V}_i$$

which yields the required expression.

## REFERENCES

1. *S-parameter Design*, Application Note 154, Palo Alto: Hewlett Packard, April 1972.
2. *MultiMatch RF and Microwave Impedance-Matching, Amplifier and Oscillator Synthesis Software*, Somerset West, RSA: Ampsa (Pty) Ltd; <http://www.ampsacom>, 1998.
3. Chen, W. K., *Theory and Design of Broadband Matching Networks*, Oxford: Pergamon Press, 1976.

## SELECTED BIBLIOGRAPHY

Carson, R. S., *High Frequency Amplifiers*, New York: John Wiley and Sons, 1975.

## CHAPTER 2

# CHARACTERIZATION AND ANALYSIS OF ACTIVE CIRCUITS AT RF AND MICROWAVE FREQUENCIES

### 2.1 INTRODUCTION

Characterization and analysis of linear circuits in terms of  $Y$ -,  $Z$ -,  $T$ -, and  $S$ -parameters were considered in Chapter 1. When active circuits are designed, the noise performance and the input power are also of interest.

Noise parameters are used to characterize the noise behavior of linear circuits at RF and microwave frequencies. These parameters will be considered in Section 2.2. The noise figure of a linear circuit follows easily from the noise parameters. The relevant equations will also be derived in Section 2.2.

Noise characterization and analysis in terms of equivalent circuits and correlation matrices will also be considered in this section. The effect of feedback and loading on the noise parameters of a transistor can be established easily by using noise correlation matrices. Calculation of these effects will be considered in Section 2.2.2.

The power obtainable from a linear circuit (class A and class B) is a strong function of the bias point and the intrinsic voltage and current associated with each of the transistors used. The power level at which the intrinsic output current and/or voltage starts to clip usually provides a close estimate of the 1-dB compression point of a linear circuit [1]. The steps approach to calculating the maximum output power will be considered in Section 2.3, and a new set of parameters (power parameters) will be introduced [2]; these can be used to simplify calculation of the expected output power. The power parameters map the intrinsic voltages in each transistor to the external voltages and also map the intrinsic output current to the intrinsic voltages.

The relationship between the intrinsic load and the external load of each transistor follows easily from the power parameters. The derivation will be considered in Section 2.4. The power parameters can also be adjusted easily to incorporate the effect of feedback or loading or any change in the configuration (common-source, common-gate, etc.). These aspects will also be considered in Section 2.3.

A set of power parameters is associated with each transistor used in the circuit. The influence of each transistor is considered with the other transistors in the circuit assumed

to be ideal. The output power is mainly determined by the stage in which voltage and/or current clipping first occurs. The general case can follow an approach similar to when the output power of a cascade of power amplifiers is calculated. The intercept point and the 1-dB compression point of a cascade are considered in Section 2.3.2.

A model is required for each transistor used in the circuit in order to calculate the power parameters. The model used should provide a good fit over the complete frequency range over which data are available and should accurately represent the intrinsic part and the parasitics of the actual transistor. Conventional small-signal models were found to be adequate for this purpose.

## 2.2 NOISE PARAMETERS

Instead of considering the noise contribution of each physical noise source in a linear network, its noise contribution can be modeled in terms of equivalent noise sources at its input and/or output ports or by using correlation matrices. Both approaches will be considered here. The relationship between the equivalent noise sources or the correlation matrices and the noise parameters typically supplied for a transistor ( $F_{\min}$ ,  $\Gamma_{n\_opt}$ , and  $R_n$ ) will also be established.

The noise figure of a transistor is a function of its noise parameters at the bias point of interest and the source impedance presented to its input terminals by the circuit. The dependence of the noise figure on the source impedance will also be considered.

The equivalent noise sources or the correlation matrices can be used to find the noise parameters for parallel networks, series networks, or cascaded networks in terms of the noise parameters of the individual networks. The influence of matching networks or filters or of adding series and parallel feedback on the noise parameters of a transistor can be established easily by using the results.

The noise figure of cascaded networks will also be considered.

### 2.2.1 Modeling the Noise Contribution of a Two-Port with Equivalent Circuits

The noise generated by any two-port device can be modeled with two equivalent partially correlated noise sources [3]. The cascade, current, and voltage representations are shown in Figure 2.1. These representations are equivalent to the  $T$ -parameter,  $Y$ -parameter, and  $Z$ -parameter approaches, respectively.

The two sources used in each representation are partially correlated. The correlated and uncorrelated parts in each case are defined by the following set of equations:

$$I_n(t) = I_{nn}(t) + Y_{cor}V_n(t) \quad (2.1)$$

$$I_{2n}(t) = I_{2nn}(t) + X_i I_{1n}(t) \quad (2.2)$$

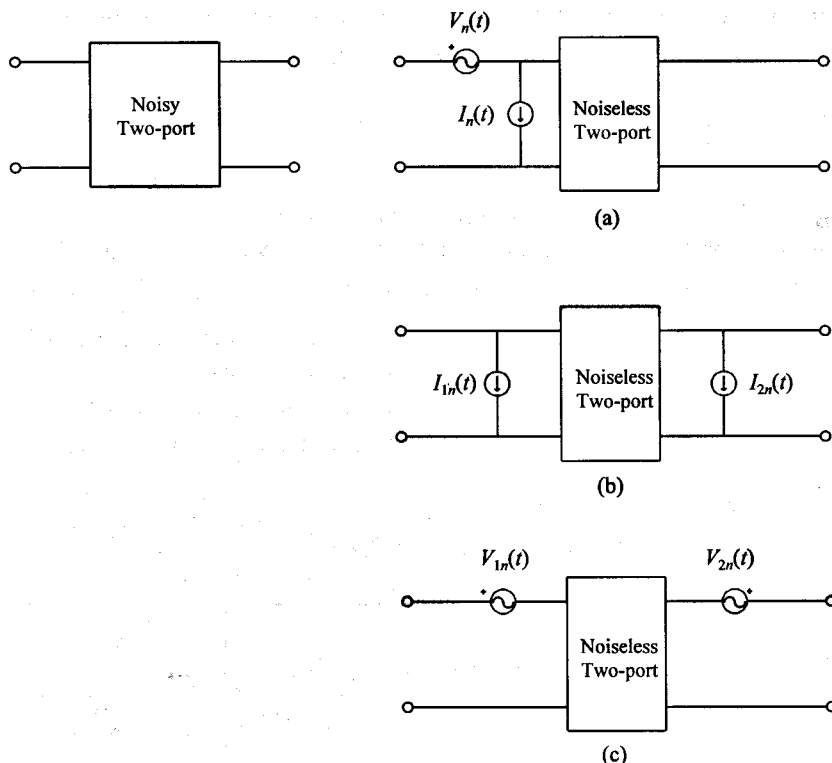


**Figure 2.1** Equivalent circuits for the noise contributed by a two-port device: (a) cascade, (b) current, and (c) voltage representation.

$$V_{2n}(t) = V_{2m}(t) + X_V V_{1n}(t) \quad (2.3)$$

By using the definition of the noise figure and these equivalent circuits, expressions for the noise figure in terms of the equivalent noise sources and the correlation factors can be derived. This will be done here for the cascade representation.

The noise figure of a device is defined as the ratio of the total noise power at the output to that which would have been delivered to the load if the device was noiseless, that is,

$$\frac{P_{no}}{P_{no-ide}} \quad (2.4)$$

If the spot noise figure (narrow band noise figure at a particular frequency) is considered, the noise power at the output in the ideal case is given by

$$P_{no-ide}(f) = kTBG_T(f) \quad (2.5)$$

where  $k$  is Boltzman's constant ( $1.38 \times 10^{-23}$  J/K),  $T$  is the absolute temperature (in Kelvin),  $B$  is the bandwidth (in Hertz), and  $G_T(f)$  is the transducer power gain of the two-port at frequency  $f$ . A noise reference temperature of 290 K (room temperature) is typically used.

When the spot noise figure is considered, the output power can be referenced easily to the input side, in which case (2.5) becomes

$$F = \frac{P_{ni\_av}}{P_{ni\_av\_ide}} \quad (2.6)$$

where  $P_{ni\_av}$  is the effective noise power available at the input side, and  $P_{ni\_av\_ide}$  is the noise power which would have been available at the input side if the device was noiseless.

The available power at the input terminals can be obtained by terminating the noise source(s) in the conjugate of the source admittance, as is illustrated in Figure 2.2.

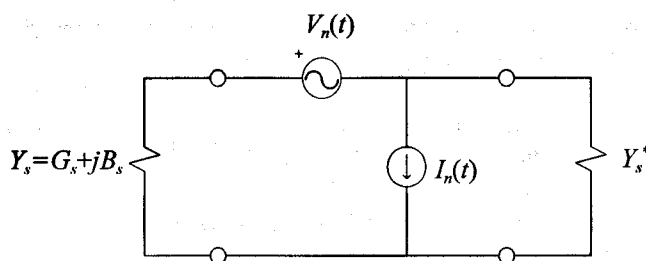


**Figure 2.2** The equivalent circuit used to calculate the available noise power at the input of a two-port (cascade representation).

It should be noted that superposition can be applied to the uncorrelated components of the noise power. In general, superposition only applies to the voltage and current in a circuit.

Because of the above, the noise power resulting from  $I_n(t)$  can simply be added to that resulting from  $V_n(t)$  and the correlated part of  $I_n(t)$  ( $Y_{cor} V_n(t)$ ).

The correlated fraction of the available power can be calculated in the following way:

$$\begin{aligned} V_{oc} &= V_n Y_s / (Y_s + Y_s^*) + V_n Y_{cor} / (2G_s) \\ &= V_n (Y_s + Y_{cor}) / (2G_s) \end{aligned} \quad (2.7)$$

$$\frac{P_{o\_cor}}{G_s} = \frac{1}{T} \int_0^T V_{oc}(t) V_{oc}^*(t) dt$$

$$\begin{aligned}
 &= V_{oc} V_{oc}^* \\
 &= \overline{V_n V_n^*} (Y_s + Y_{cor})(Y_s + Y_{cor})^* / (4G_s^2) \quad (2.8)
 \end{aligned}$$

where  $T$  is the period over which the noise power is averaged.

The uncorrelated fraction of the output power can be calculated in terms of  $I_n$  and by using (2.1):

$$\overline{I_n^*} = \overline{I_{nu} I_{nu}^*} + Y_{cor} Y_{cor}^* \overline{V_n V_n^*} \quad (2.9)$$

$$= I_n - Y_{cor} V_n \quad (2.10)$$

$$= I_{nu} / (2G_s) \quad (2.11)$$

Therefore,

$$\begin{aligned}
 G_s &= \overline{V_{ou} V_{ou}^*} = \overline{I_{nu} I_{nu}^*} / (4G_s^2) \\
 &= \overline{I_n I_n^*} / (4G_s^2) - \overline{V_n V_n^*} Y_{cor} Y_{cor}^* / (4G_s^2) \quad (2.12)
 \end{aligned}$$

Equation (2.9) follows from (2.1) because  $I_{nu}$  and  $V_n$  are uncorrelated.

The total available noise power at the input terminals can now be calculated:

$$\begin{aligned}
 \overline{I_n^*} &= \frac{\overline{I_n I_n^*}}{4G_s^2} - \frac{Y_{cor} Y_{cor}^* \overline{V_n V_n^*}}{4G_s^2} + \frac{(Y_s + Y_{cor})(Y_s + Y_{cor})^* \overline{V_n V_n^*}}{4G_s^2} \\
 &= \frac{\overline{I_n I_n^*}}{4G_s^2} + \frac{Y_s Y_s^* + 2 \Re(Y_{cor} Y_s^*)}{4G_s^2} \overline{V_n V_n^*} \quad (2.13)
 \end{aligned}$$

Because the available noise power in the ideal case is simply

$$= V_{o\text{-thermal}}^2 = kTB / G_s \quad (2.14)$$

it follows that

$$F = \frac{\frac{kTB}{G_s} + \frac{\overline{I_n I_n^*}}{4G_s^2} + \frac{Y_s Y_s^* + 2 \Re(Y_{\text{cor}} Y_s^*)}{4G_s^2} \overline{V_n V_n^*}}{kTB / G_s}$$

$$= 1 + G_{ni}/G_s + R_{nv} [(G_s + G_{\text{cor}})^2 + (B_s + B_{\text{cor}})^2 - (G_{\text{cor}}^2 + B_{\text{cor}}^2)] / G_s \quad (2.15)$$

where

$$\overline{I_n I_n^*} = 4kTBG_{ni} \quad (2.16)$$

$$\overline{V_n V_n^*} = 4kTBR_{nv} \quad (2.17)$$

$$Y_{\text{cor}} = G_{\text{cor}} + jB_{\text{cor}} \quad (2.18)$$

and

$$Y_s = G_s + jB_s \quad (2.19)$$

For any given value of  $G_s$ , there exists an optimum value for  $B_s$  that will minimize the noise figure. Taking the derivative of (2.15) and setting it equal to zero yields

$$\partial F / \partial B_s = 0 = 0 + 0 + 0 + 2R_{nv}(B_s + B_{\text{cor}}) / G_s \quad (2.20)$$

from which it follows that

$$B_{s-\text{opt}} = -B_{\text{cor}} \quad (2.21)$$

Note that the optimum value of  $B_s$  is the same for all values of  $G_s$ .

The value of  $G_s$  that will minimize the noise figure can now be obtained from (2.15), after replacing  $B_s$  with its optimum value. Taking the derivative yields

$$\begin{aligned} \partial F / \partial G_s &= 0 = 0 - G_{ni} / G_s^2 + 2R_{nv}(G_s + G_{\text{cor}}) / G_s \\ &\quad - R_{nv} [(G_s + G_{\text{cor}})^2 + (B_{s-\text{opt}} + B_{\text{cor}})^2 - (G_{\text{cor}}^2 + B_{\text{cor}}^2)] / \end{aligned} \quad (2.22)$$

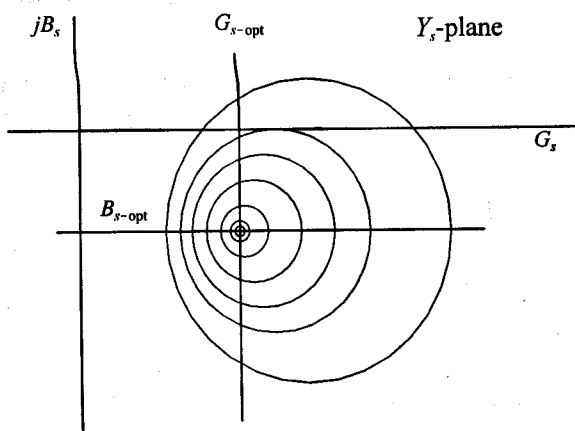


Figure 2.3 An example of the constant noise figure circles associated with a linear two-port device.

at is,

$$G_{s-opt} = \sqrt{G_{ni} / R_{nv} - B_{cor}^2} \quad (2.23)$$

Substituting (2.21) and (2.23) into (2.15) yields

$$F_{min} = 1 + 2R_{nv} (G_{s-opt} + G_{cor}) \quad (2.24)$$

The inverse relationships and an expression for the noise figure in terms of  $F_{min}$ ,  $G_{s-opt}$ ,  $B_{s-opt}$  and  $R_n$  can be derived easily by using (2.21), (2.23), and (2.24) and making the necessary substitutions in (2.15):

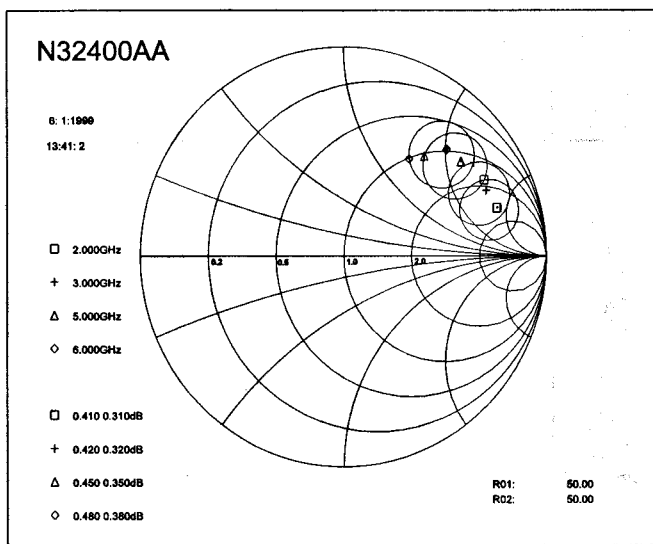
$$G_{cor} = (F_{min} - 1) / (2R_{nv}) - G_{s-opt} \quad (2.25)$$

$$B_{cor} = -B_{s-opt} \quad (2.26)$$

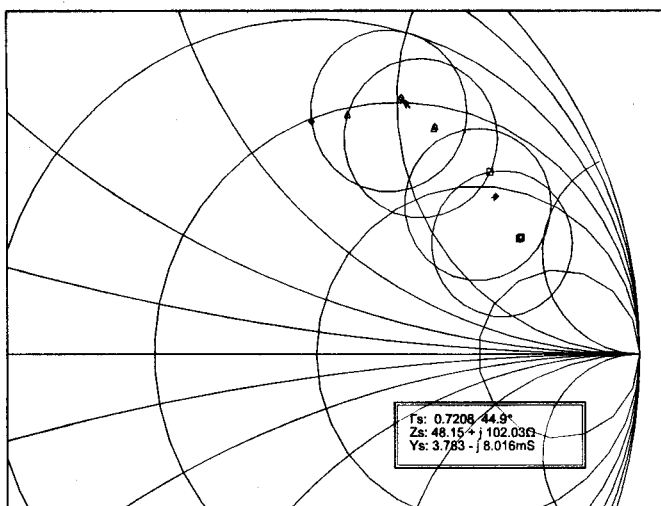
$$F = F_{min} + R_{nv} [ (G_s - G_{s-opt})^2 + (B_s - B_{s-opt})^2 ] / G_s \quad (2.27)$$

$$= F_{min} + \frac{R_{nv}}{G_s} |Y_s - Y_{s-opt}|^2 \quad (2.28)$$

By inspecting (2.27) it is clear that the loci of constant noise figures are circles in the linear admittance plane, as is illustrated in Figure 2.3.



(a)



(b)

**Figure 2.4** An example of constant noise figure circles displayed on a Smith Chart.

It will be shown in Chapter 10 that the constant noise figure contours are also circles on the Smith Chart. Some of the constant noise figure circles for a low-noise transistor are displayed in Figure 2.4.

## 2.2.2 Noise Correlation Matrices

A correlation matrix is defined for each of the three representations considered in the previous section [4]:

### Voltage Representation

$$\begin{aligned} C_v &= \overline{\begin{bmatrix} V_n(t) \\ I_n(t) \end{bmatrix}} \begin{bmatrix} V_n^*(t) & I_n^*(t) \end{bmatrix} / (2B) \\ &= \begin{bmatrix} \overline{V_n(t) V_n^*(t)} & \overline{V_n(t) I_n^*(t)} \\ \overline{V_n^*(t) I_n(t)} & \overline{I_n(t) I_n^*(t)} \end{bmatrix} / (2B) \end{aligned} \quad (2.29)$$

### Current Representation

$$\begin{aligned} C_i &= \overline{\begin{bmatrix} I_{n1}(t) \\ I_{n2}(t) \end{bmatrix}} \begin{bmatrix} I_{n1}^*(t) & I_{n2}^*(t) \end{bmatrix} / (2B) \\ &= \begin{bmatrix} \overline{I_{n1}(t) I_{n1}^*(t)} & \overline{I_{n1}(t) I_{n2}^*(t)} \\ \overline{I_{n1}^*(t) I_{n2}(t)} & \overline{I_{n2}(t) I_{n2}^*(t)} \end{bmatrix} / (2B) \end{aligned} \quad (2.30)$$

### Voltage Representation

$$\begin{aligned} C_v &= \overline{\begin{bmatrix} V_{n1}(t) \\ V_{n2}(t) \end{bmatrix}} \begin{bmatrix} V_{n1}^*(t) & V_{n2}^*(t) \end{bmatrix} / (2B) \\ &= \begin{bmatrix} \overline{V_{n1}(t) V_{n1}^*(t)} & \overline{V_{n1}(t) V_{n2}^*(t)} \\ \overline{V_{n1}^*(t) V_{n2}(t)} & \overline{V_{n2}(t) V_{n2}^*(t)} \end{bmatrix} / (2B) \end{aligned} \quad (2.31)$$

By using definitions (2.4), (2.16), and (2.17) it follows that

$$\mathbf{C}_a = 2kT R_{nv} \begin{bmatrix} 1 & Y_{cor}^* \\ Y_{cor} & G_{ni}/R_{nv} \end{bmatrix} \quad (2.32)$$

The second term of (2.32) is derived as follows:

$$I_n(t) = I_{nu}(t) + Y_{cor} V_n(t)$$

implies that

$$\begin{aligned} \frac{1}{T} \int_0^T I_n(t) V_n^* dt &= \frac{1}{T} \int_0^T I_u(t) V_n^*(t) + Y_{cor} V_n(t) dt \\ &= 0 + \frac{1}{T} Y_{cor} \int_0^T V_n(t) V_n^*(t) dt \\ &= 4kTBR_{nv} Y_{cor} \end{aligned} \quad (2.33)$$

It is a simple matter to show that (2.32) is also equivalent to

$$C_a = 2kT R_{nv} \begin{bmatrix} 1 & \frac{F_{min}-1}{2R_{nv}} - Y_{s-opt}^* \\ \frac{F_{min}-1}{2R_{nv}} - Y_{s-opt} & |Y_{s-opt}|^2 \end{bmatrix} \quad (2.34)$$

It is possible to transform any of the correlation matrices defined above to any other types. The transformation matrices required for this purpose are summarized in Table 2.1 [4]. In this table  $Y$ ,  $Z$ , and  $T$  are the  $Y$ -parameter,  $Z$ -parameter, and transmission parameter matrices, respectively, of the network under consideration. The transformation required is done by using the equation

$$C_{new} = X C_{ori} X^* \quad (2.35)$$

where  $*$  indicates the transposed conjugate of  $X$ .

The equations summarized in Table 2.1 can be derived easily by using the relationship between the noise voltages and currents in the different representations. Because of the principle of superposition, the equivalence can be derived by assuming the noise generators to be the only excitations present.

**EXAMPLE 2.1** Derivation of expressions for the equivalent noise sources  $I_{1n}(t)$  and  $I_{2n}(t)$  in terms of  $V_n(t)$  and  $I_n(t)$ .

Consider deriving expressions for the equivalent noise sources  $I_{1n}(t)$  and  $I_{2n}(t)$  (current representation) in terms of  $V_n(t)$  and  $I_n(t)$  in the cascade representation.

$I_n(t)$  is clearly part of  $I_{1n}(t)$  and, therefore, only the equivalent current sources for  $V_n(t)$  are required. Because of superposition and because there is no noise source on the output in the cascade representation, the load can be shorted and the currents resulting from  $V_n(t)$  can be calculated by using the  $Y$ -parameters:

$$I_1 = -y_{11} V_n(t) \quad I_2 = -y_{21} V_n(t)$$

Adding  $I_n(t)$  yields

$$I_{1n}(t) = -y_{11} V_n(t) + I_n(t)$$

$$I_{2n}(t) = -y_{21} V_n(t)$$

leading to

$$\begin{bmatrix} I_{1n}(t) \\ I_{2n}(t) \end{bmatrix} = \begin{bmatrix} -y_{11} & 1 \\ -y_{21} & 0 \end{bmatrix} \begin{bmatrix} V_n(t) \\ I_n(t) \end{bmatrix} \quad (2.36)$$

Equations (2.37) through (2.39) are generally used to calculate the equivalent correlation matrices of two networks connected in cascade, parallel, and series, respectively. The relevant equations [4] are

$$C_{zz} = C_{a1} + T C_{a2} T^* \quad (2.37)$$

$$C_{zz} = C_{y1} + C_{y2} \quad (2.38)$$

$$C_{zz} = C_{z1} + C_{z2} \quad (2.39)$$

$T$  in (2.37) is the transmission matrix of the network closest to the generator (i.e., network on the input side). The superscript used indicates the transposed conjugate of transmission matrix.

When the noise parameters for a network are calculated, it is useful to know that

$$C = 2 kT \Re(Z) \quad (2.40)$$

and

$$C_y = 2 kT \Re(Y) \quad (2.41)$$

for any passive network [4].

**Table 2.1**

The matrix ( $X$ ) required to transform any of the noise correlation matrices to another ( $C_{\text{new}} = X C_{\text{ori}} X'$ )

Original New \ \diagdown	$Y$	$Z$	$T$
$Y$	$\begin{pmatrix} 1 & 0 \\ 0 & 1 \end{pmatrix}$	$Y$	$\begin{pmatrix} -y_{11} & 1 \\ -y_{21} & 0 \end{pmatrix}$
$Z$	$Z$	$\begin{pmatrix} 1 & 0 \\ 0 & 1 \end{pmatrix}$	$\begin{pmatrix} 1 & -z_{11} \\ 0 & -z_{21} \end{pmatrix}$
$T$	$\begin{pmatrix} 0 & B \\ 1 & D \end{pmatrix}$	$\begin{pmatrix} 1 & -A \\ 0 & -C \end{pmatrix}$	$\begin{pmatrix} 1 & 0 \\ 0 & 1 \end{pmatrix}$

### 2.2.3 Calculating the Noise Figure of a Cascade Network

The noise figure of a cascade network (see Figure 2.5) is often of interest. Given the definition of the noise figure in terms of the available noise power at the input side of the network, it is a simple matter to prove that

$$F_T = F_1 + \frac{F_2 - 1}{G_{a1}} + \frac{F_3 - 1}{G_{a1}G_{a2}} + \dots \quad (2.42)$$

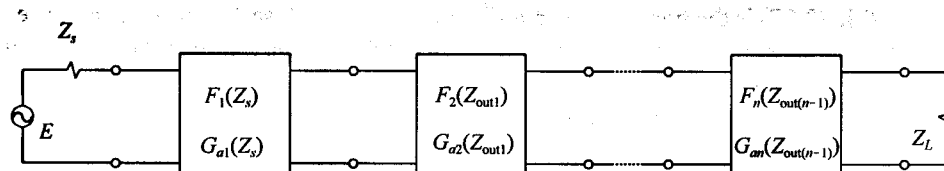


**Figure 2.5** The circuit used to calculate the noise figure of a cascade network.

where  $F_1$  is the noise figure of the first stage (input stage) and  $G_{a1}$  is its available power gain. Similarly,  $F_n$  is the noise figure of the  $n$ th stage when terminated on its input side with the output impedance of the previous stage, and  $G_{an}$  is its available power gain.

Equation (2.42) is known as Friiss' formula.

It is clear from Friiss' formula that the product of the gain of the stages preceding any given stage must be high in order for it to have a negligible contribution to the overall noise figure of the cascade.

It is also clear that any stage added will have a degrading effect on the noise figure. The contribution of any stage to the overall noise figure is a function of both its noise figure and its available power gain. The noise measure ( $M$ ) of a network is a figure of merit for this effect and is defined as

$$M = F_\infty - 1 \quad (2.43)$$

where  $F_\infty$  is the noise figure of an infinite chain of identical stages each with noise figure and available power gain  $G_a$ .

By using the identity

$$\frac{1}{1-X} = 1 + X + X^2 + \dots \quad (2.44)$$

can be shown that the noise measure,  $M$ , is given by

$$M = \frac{F - 1}{1 - 1/G_a} \quad (2.45)$$

where  $F$  is the noise figure of the stage of interest and  $G_a$  is its available power gain.

The associated noise figure is of greater interest and is given by substituting (2.43) into (2.45):

$$F = \frac{F - 1/G_a}{1 - 1/G_a} \quad (2.46)$$

### EXAMPLE 2.2 Calculation of the effect of the losses of a passive cascade on the noise figure of a transistor.

The effect of the insertion loss of a lossy passive network on the noise figure of an active stage will be calculated by using Friiss' formula.

The noise figure of a passive network is given by

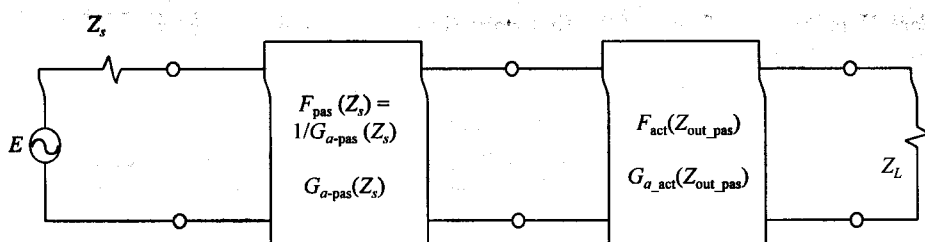


Figure 2.6 The effect of insertion loss on the noise figure of an amplifier stage.

$$F_{\text{pas}}(f) = P_{\text{no}}/P_{\text{no-ide}} = \frac{kTB}{kTB G_{a-\text{pas}}(f)} = 1/G_{a-\text{pas}}(f) \quad (2.47)$$

that is, if the passband is narrow enough for the available power gain and the mismatch from the output of the network to its load to be considered constant.

Entering this into Friiss' formula for the cascade combination (see Figure 2.6) yields

$$\begin{aligned} F_T &= F_{\text{pas}} + \frac{F_{\text{act}} - 1}{G_{a-\text{pas}}} = 1/G_{a-\text{pas}} + \frac{F_{\text{act}} - 1}{G_{a-\text{pas}}} \\ &= \frac{1 + F_{\text{act}} - 1}{G_{a-\text{pas}}} \\ &= F_{\text{act}} / G_{a-\text{pas}} \end{aligned} \quad (2.48)$$

Expressed in decibels, (2.48) becomes

$$F_T = F_{\text{act}} - G_{a-\text{pas}} \quad (\text{dB}) \quad (2.49)$$

It follows from (2.49) that the noise figure of any stage is degraded proportionately with any losses directly preceding it ( $G_{a-\text{pas}}$  in (2.49) will be negative for any passive network). This is illustrated in Figure 2.6.

## 2.3 THE OUTPUT POWER OF LINEAR AMPLIFIERS

The maximum output power obtainable from a linear amplifier (1-dB compression point)

will be considered in this section.

The transistors used in a linear amplifier are usually biased in class A ( $360^\circ$  conduction angle), class B ( $180^\circ$  conduction angle), or class AB mode. Class AB is often used at microwave frequencies instead of class B, mostly because the gain obtainable in class B mode is usually too low at these frequencies. The voltage and current waveforms and the load lines associated with class A and B stages will be considered in Section 2.3.1.

The 1-dB compression point and the third-order two-tone intercept point are usually used as measures of the linearity of an amplifier. The relevant definitions and the definition of the dynamic range of an amplifier will be considered in Section 2.3.2.

The 1-dB compression point and the third-order intercept point of an amplifier will be reduced by any driver stages added. This effect will also be considered in Section 2.3.2.

The maximum output power obtainable from a class A amplifier can be estimated at RF, as well as at microwave frequencies, by using the approach introduced by Cripps [1]. The Cripps approach will be considered in Section 2.3.3.

The Cripps approach can be generalized and many of the inherent inaccuracies can be removed by using the power parameter approach introduced in [2]. This approach is outlined in Section 2.3.4.

The Cripps approach and the power parameter approach are based on the assumption that the maximum power obtainable from a linear amplifier is determined by the power level at which the intrinsic output current and/or voltage of the transistor(s) used starts to clip; that is, the power is limited mainly by the limited swing in the intrinsic output current and voltage.

The power parameter approach is sufficiently general to handle any loading effects, feedback, changes in the transistor configuration, cascade networks, and/or multistage amplifiers. All of these aspects will also be considered in Section 2.3.4.

The power parameter approach can also be used to initialize the fundamental tone quantities in a full harmonic balance nonlinear simulation of the amplifier.

### 2.3.1 Load-Line Considerations in Class A and Class B Amplifiers

When a transistor is biased for class A operation, the average voltage across its output terminals (drain-source or collector-emitter) must be equal to the dc voltage ( $V_{DS}$  or  $V_{CE}$ ; usually the supply voltage,  $V_s$ , if power is important), and the average current must be equal to the dc current ( $I_{DS}$  or  $I_{CE}$ ) (the dc current may change as the drive level is increased). If the distortion in the waveforms is negligible, the voltage and current will swing symmetrically around the average values.

The maximum possible voltage swing ( $V_{DS}$  or  $V_{CE}$ ) is decreased in practice by the saturation voltage of the transistor ( $V_{sat}$ ) and any saturation resistance ( $R_{sat}$ ). The effect of the saturation resistance can be lumped with the load resistance presented at the transistor terminals.

The maximum output power obtainable from a class A or a class B amplifier at RF frequencies is given by [6]

$$P_{\max} = \frac{(V_s - V_{sat})^2}{2(R_L + \alpha R_{sat})} \frac{R_L}{R_L + \alpha R_{sat}} \quad (2.50)$$

where  $V_s$  is the supply voltage (assuming that no drain or collector resistor is used) and  $R_L$  is the parallel resistance presented to the output terminals of the transistor.  $\alpha$  is equal to 2 for class A amplifiers and equal to 1 for class B amplifiers. It follows from this equation that the effective supply voltage is decreased by the saturation voltage and that the effective intrinsic load resistance is increased by the saturation resistance.

In deriving (2.50), it was assumed that any susceptance present at the output terminals of the transistor was removed.

### 2.3.1.1 Class A Load Line

The output current and voltage and the associated load line in a class A stage will be considered next.

In general, if

$$V_{2i}(t) = |V_{2i}| e^{j\omega t} \quad (2.51)$$

and

$$Y_{L_{intr}} = -I_{2i} / V_{2i} = |Y_{L_{intr}}| e^{j\theta} \quad (2.52)$$

the drain voltage and current (dc and ac components) are given by

$$I_d(t) = I_{DS} - Y_{L_{intr}} V_{2i}(t) \quad (2.53)$$

$$V_d(t) = V_{DS} + V_{2i}(t) \quad (2.54)$$

With  $V_{2i}(t)$  replaced in terms of (2.51), it follows that

$$I_d(t) = I_{DS} - |V_{2i}| e^{j\omega t} |Y_{L_{intr}}| e^{j\theta} = I_{DS} - |Y_{L_{intr}} V_{2i}| e^{j(\omega t + \theta)} \quad (2.55)$$

$$V_d(t) = V_{DS} + |V_{2i}| e^{j\omega t} \quad (2.56)$$

It follows from the last two equations that the dynamic load line is defined by

$$I_{2i}(t) = I_d(t) - I_{DS} = -|Y_{L_{intr}} V_{2i}| e^{j(\omega t + \theta)} \quad (2.57)$$

$$V_{2i}(t) = V_d(t) - V_{DS} = |V_{2i}| e^{j\omega t} \quad (2.58)$$

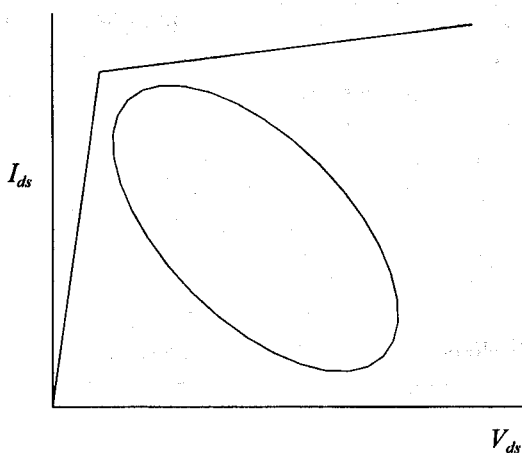


Figure 2.7 The dynamic load line of a transistor biased for class A operation (reactive load line).

If the load is reactive, the load line will be similar to that shown in Figure 2.7.

The dc power dissipated in a class A stage is constant and is given by

$$P_{dc} = V_{DS} I_{DS} \quad (2.59)$$

The power dissipated in the intrinsic load is given by

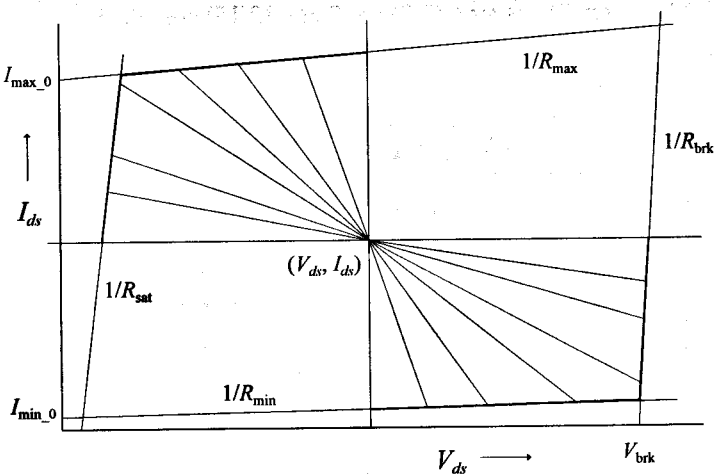


Figure 2.8 Clipping in a class A amplifier can occur on any of the four line segments shown (resistive load lines shown).

$$P_o = |V_{2i}|^2 G_{L_{\text{intr}}} / 2 \quad (2.60)$$

$$\leq P_{dc} / 2$$

or by

$$P_o = |I_{2i}|^2 R_{L_{\text{intr}}} / 2 \quad (2.61)$$

$$\leq P_{dc} / 2$$

If the voltage is clipped first, the maximum output power will be given by (2.60). If the current is clipped first, (2.61) will apply. In general, clipping can occur on any of the four line segments shown in Figure 2.8 (resistive load lines shown).

### 2.3.1.2 Class B Load Line

The conduction angle in a class B amplifier is  $180^\circ$ . A parallel-tuned circuit or a push-pull configuration is usually used to suppress the harmonics in the voltage waveform. When this is done, the output voltage can be assumed to be sinusoidal and can therefore be represented by using the same equations as in the class A case.

The intrinsic transistor current ( $I_T(t)$ ) is a half-sinusoid. The peak amplitude of the fundamental tone (which determines the ac power) can be obtained from the Fourier series expansion for the half-sinusoid (refer to Figure 2.9).

The Fourier series expansion of a half-sinusoid is given by

$$I_T(t) = (I_{T_{\text{peak}}} / \pi) [1 + (\pi / 2) \cos \omega t + (2/3) \cos 2\omega t - (2/15) \cos 4\omega t + \dots] \quad (2.62)$$

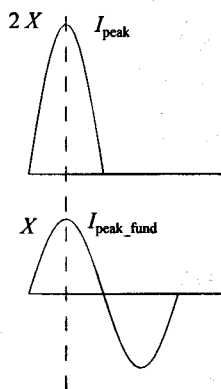


**Figure 2.9** The relationship between the actual (intrinsic) output current and its fundamental tone component.

Note that the half-sinusoid output current and its fundamental tone are in phase. This implies that if the amplitude of the fundamental tone output current is  $I_{\text{fund}}(t)$  at any given moment in time, then the amplitude of the actual output current is  $2 I_{\text{fund}}(t)$ . This can be used to translate the left-side boundary and the upper boundary for the transistor current on the  $I/V$ -plane to equivalent boundary lines for the fundamental tone component [2].

It follows from (2.62) that the peak amplitude of the fundamental tone is equal to half of the peak amplitude of the half-sinusoid ( $I_{T,\text{peak}}$ ):

$$|I_{2i}| = I_{T,\text{peak}} / 2 \quad (2.63)$$

The average value (dc component) of the transistor current ( $I_T(t)$ ) is given by

$$I_{\text{dc}} = I_{T,\text{peak}} / \pi \quad (2.64)$$

It follows that the dc dissipation in the transistor is given by

$$P_{\text{dc}} = V_{ds} I_{T,\text{peak}} / \pi \quad (2.65)$$

While the output power is given by

$$P_o = |V_{2i}|^2 G_{L,\text{intr}} / 2 = |I_{2i} / Y_{L,\text{intr}}|^2 G_{L,\text{intr}} / 2 \quad (2.66)$$

$$= |I_{T,\text{peak}} / (2 Y_{L,\text{intr}})|^2 G_{L,\text{intr}} / 2$$

$$= |I_{T,\text{peak}} / Y_{L,\text{intr}}|^2 G_{L,\text{intr}} / 8 \quad (2.66)$$

$$= |I_{T,\text{peak}}|^2 R_{L,\text{intr}} / 8 \quad (2.67)$$

The efficiency is calculated as the ratio of the output power ( $P_o$ ) or the effective output power ( $P_o - P_{\text{in}}$ ) to the dc power ( $P_{\text{dc}}$ ):

$$\eta = P_o / P_{\text{dc}} \quad (2.68)$$

$$\eta = (P_o - P_{\text{in}}) / P_{\text{dc}} \quad (2.69)$$

If (2.68) is used, the efficiency is given by

$$\eta = (V_{\text{peak,fund}} / V_{ds}) (\pi / 4) \quad (2.70)$$

The efficiency ( $\eta$ ) of a class B amplifier increases linearly with increasing output voltage up to a maximum of 78.5%. If the intrinsic load termination is reactive, the efficiency will drop.

When the output power is lower than the maximum possible, the efficiency of a class B stage will be observed to vary with the angular position around the constant output

power contours. The efficiency of a class A amplifier is constant around a constant output power contour.

The dynamic load line for a class B amplifier is shown in Figure 2.10. When the effective load line is purely resistive, the output current of the transistor and the voltage across it are constrained as shown in Figure 2.10(a). When the effective load line is reactive, the current and voltage are constrained as shown in Figure 2.10(b). Note that the current is zero during half of the cycle.

The  $I/V$ -constraints of a class B stage apply to the total current through the transistor (half sinusoid) and the voltage across the transistor. The constraints on the fundamental tone quantities are, however, of greater interest. Because the voltage waveform was assumed to be a pure sinusoid and because of the fixed relationship between the total current and its fundamental tone (see Figure 2.9), the constraints on the fundamental tone quantities can be taken to be as illustrated in Figure 2.11. Note that the new origin ( $V_{ds}'$ ,  $I_{ds}'$ ) should be moved down far enough to allow the fundamental tone current to swing symmetrically without clipping when the instantaneous voltage is higher than  $V_{dc}$ .

Under the transformation illustrated in Figure 2.11, a class B stage can be treated as a class A stage when its output power is calculated. This can also be done when a set of load-pull contours is generated for the transistor.

The dc  $I/V$ -constraints for a power transistor are often supplied by the manufacturer. These constraints can be taken to be the RF constraints of the intrinsic device too, if the current is interpreted as the sum of the current of the voltage-controlled current source and the intrinsic output resistance in the equivalent circuit.

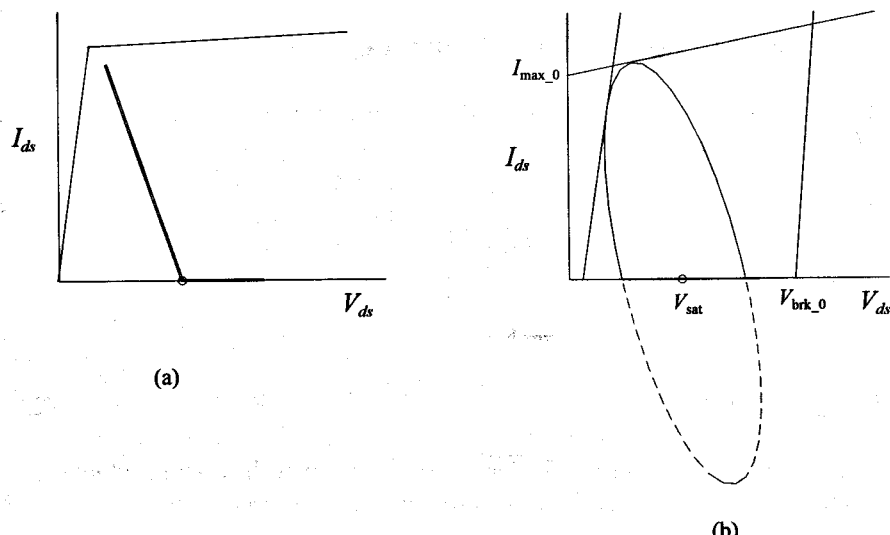


**Figure 2.10** The dynamic load line of a transistor biased for class B operation: (a) resistive load line and (b) reactive load line.

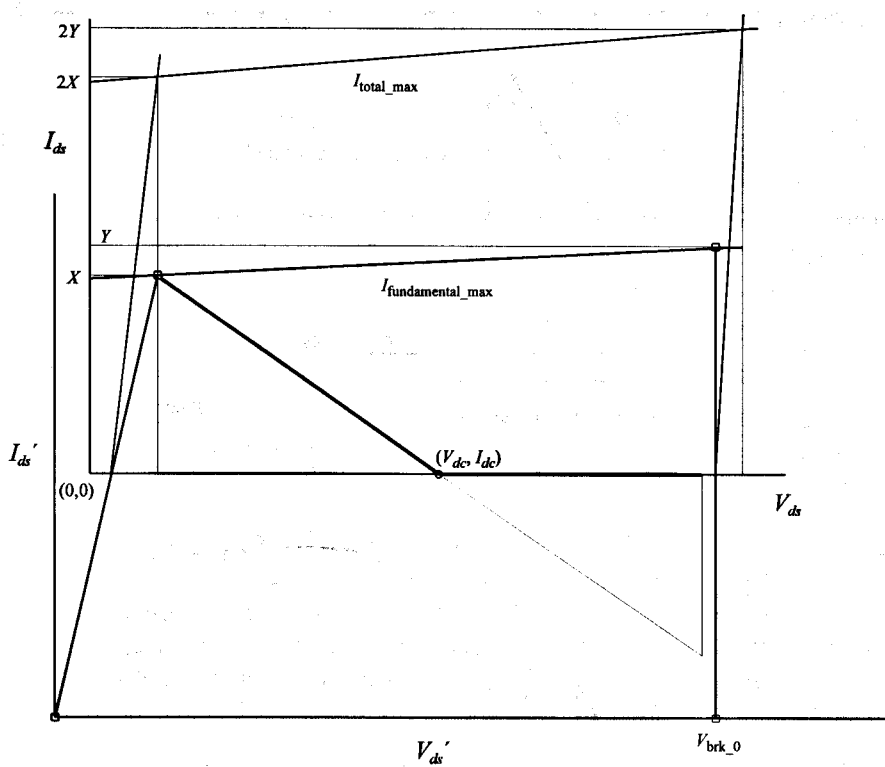


**Figure 2.11** Illustration of the conversion of the  $I/V$  constraints on the total output current and the output voltage of a class B amplifier to those applying to the fundamental tone quantities.

### 2.3.2 Distortion in Linear Amplifiers

The 1-dB compression point (single tone) and the third-order intercept point for two-tone products are usually used as measures of the linearity of an amplifier.

The 1-dB compression point is defined as the level (usually expressed in terms of ~~the~~ output power) at which the operating power gain ( $G_o$ ) is 1 dB down from its small-signal level. The third-order two-tone intercept point (TOI) is defined as the power level at which each extrapolated third order product ( $2f_1 - f_2$  and  $2f_2 - f_1$  components) is equal in magnitude to the extrapolated fundamental tone component.

At low signal levels the slope of the fundamental tone component ( $P_{out}$  in decibels versus  $P_{in}$  in decibels) is 1:1, and that for the third order products is 3:1.

The definitions are illustrated in Figure 2.12.

The third-order intercept point of a linear amplifier is usually about 10 dB higher than the 1-dB compression point [7].

The dynamic range of an amplifier is usually defined as the difference between the 1-dB compression level and that of the minimum detectable signal, referenced to the output

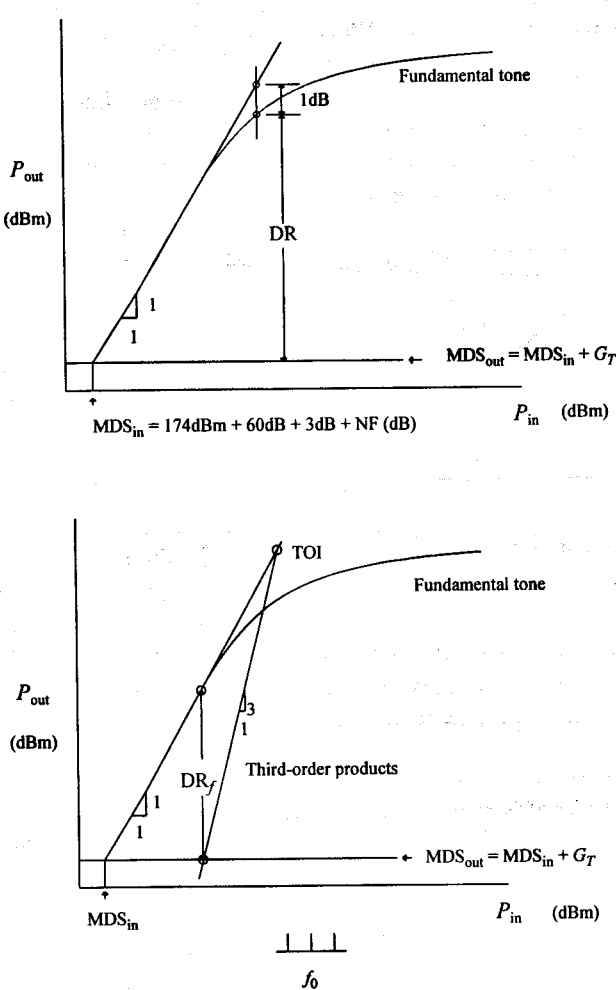


Figure 2.12 The dynamic range (DR) and the spurious free dynamic range ( $DR_f$ ) of an amplifier.

of the amplifier [5]:

$$DR = P_{1dB} - MDS_{out} \quad (2.71)$$

The minimum detectable signal could be defined as 3 dB above the noise floor of the amplifier, that is,

$$MDS_{out} = kTB + F + G_T + 3 \text{ (dB)} \quad (2.72)$$

where  $F$  is the noise figure of the amplifier and  $G_T$  is its transducer power gain.

The spurious free dynamic range ( $DR_f$ ) is often also of interest. The definition is illustrated in the lower panel of Figure 2.12.

### 2.3.2.1 The Third-Order Intercept Point of a Cascade

Gain compression and any additional frequency components generated are the result of the weak) nonlinear transfer function of the amplifier [7]. At a given bias point ( $V_i, V_o$ ), the output signal ( $v_o = \delta V_o; v_i = \delta V_i$ ) can be calculated by using Taylor's theorem:

$$v_o = \frac{\partial V_o}{\partial V_i} v_i + \frac{\partial^2 V_o}{\partial^2 V_i} \frac{v_i^2}{2} + \frac{\partial^3 V_o}{\partial^3 V_i} \frac{v_i^3}{6} + \dots \quad (2.73)$$

This can be simplified to

$$v_o = a_1 v_i + a_2 v_i^2 + a_3 v_i^3 + \dots \quad (2.74)$$

The coefficients in (2.74) are usually taken to be real, but they could be complex in general. If the coefficients are real, any distortion products generated will have a fixed phase relationship with the input signal.

If

$$v_i = a \cos \omega t \quad (2.75)$$

Substituted in (2.74), it can be shown that:

- Odd order harmonic components ( $3f, 5f, \dots$ ) are generated by the odd order terms. In addition, each odd order term will also generate a component at the fundamental frequency ( $f$ ). These fundamental tone components are responsible for the gain compression observed in amplifiers.
- Even order components will generate even order harmonics ( $2f, 4f, \dots$ ). In addition, each even order term will also generate a dc component. These components cause the shift in bias point observed when an amplifier is driven strongly.

The distortion created by the third-order term in (2.75) is usually of most interest:

$$\begin{aligned} a_3(a \cos \omega t)^3 &= a_3 a^3 \cos^3 \omega t = a_3 a^3 \cos \omega t \cdot 0.5(1 + \cos 2\omega t) \\ &= a_3 a^3 \cdot 0.5 \cos \omega t + 0.5(\cos \omega t \cos 2\omega t) \\ &= a_3 a^3 \cdot 0.5 \cos \omega t + 0.5(0.5(\cos \omega t + \cos 3\omega t)) \end{aligned}$$

$$= a_3 a^3 \left[ \frac{3}{4} \cos \omega t + \frac{1}{4} \cos 3\omega t \right] \quad (2.76)$$

Note that if  $a_3$  in (2.76) is negative, the third-order contribution at the fundamental frequency will decrease the signal level; that is, the gain will be compressed. It is also clear that the third-order terms will be very small when the signal level is low ( $a^3$ -term in (2.76)).

If the contribution of the higher order terms is ignored, the 1-dB gain compression point can be estimated by setting

$$a_1 v_{ic} - \frac{3}{4} a_3 v_{ic}^3 = a_1 v_{ic} 10^{-1/20}$$

from which it follows that

$$v_{ic}^2 = \frac{4 a_1 (1 - 10^{-1/20})}{3 a_3} \quad (2.77)$$

When a two-tone signal is used, the input signal is given by

$$v_i = a [\cos \omega_1 t + \cos \omega_2 t] \quad (2.78)$$

In this case, fundamental tone components ( $f_1; f_2$ ) with amplitude ( $2.25 a_3 a^3$ ) are generated. The third harmonic components generated at each frequency are of the same amplitude as in the single tone case ( $0.25 a_3 a^3$ ).

Apart from these components, additional components are generated at ( $2f_2 - f_1$ ) and ( $2f_1 - f_2$ ) in the two-tone case. The amplitude of these components is ( $0.75 a_3 a^3$ ).

If displayed logarithmically, the two-tone products will increase at a 3:1 rate with increasing signal level, that is as long as the contribution of any higher order terms can be neglected. The fundamental tone will increase at a 1:1 rate as long as the compression can be neglected.

The two-tone intercept point can be estimated by using the results obtained:

$$a_1 v_{ip3} = \frac{3}{4} a_3 v_{ip3}^3$$

$\Rightarrow$

$$v_{ip3}^2 = \frac{4}{3} \frac{a_1}{a_3} \quad (2.79)$$

Equations (2.79) and (2.77) can be used at this point to find the relationship between the third-order intercept point and the 1-dB compression point:

$$\frac{v_{o3}^2}{v_{ic}^2} = \frac{1}{1 - 10^{-1/20}} = 9.195 = 9.6 \quad (2.80)$$

Note that the contribution of the higher order terms ( $5f$ ,  $7f$ , ...) was ignored in this derivation. The estimation, however, is good enough to be of practical use.

Note that because of the fixed slopes (at least at lower signal levels), the level of third-order components associated with any signal level can be calculated easily from the third-order intercept specification:

$$\begin{aligned} P_{o1}(X) &= P_{o1}(X_{IP3}) - (P_{o1}(X_{IP3}) - G - X) \\ &\Rightarrow \\ P_{o1}(X) &= G + X \end{aligned} \quad (2.81)$$

$$\begin{aligned} P_{o3}(X) &= P_{o3}(X_{IP3}) - 3(P_{o3}(X_{IP3}) - G - X) \\ &= -2P_{o3}(X_{IP3}) + 3(X + G) \\ &= -2P_{o3}(X_{IP3}) + 3P_{o1}(X) \quad (\text{dBm}) \end{aligned} \quad (2.82)$$

where  $P_{o1}(X)$  is the fundamental tone output power at signal level  $X$ , and  $P_{o3}(X)$  is the power at  $(2f_1 - f_3)$  or  $(2f_2 - f_1)$  at the same signal level  $(X)$ .

If the power is expressed as a number and not in dBm, (2.82) becomes

$$P_{o3}(X) = \frac{P_{o1}^3(X)}{P_{o3}^2(X_{IP3})} \quad (2.83)$$

An interesting result follows directly from (2.83):

$$X_{IP3} = \sqrt{\frac{P_{o1}^3(X)}{P_{o3}(X)}} \quad (2.84)$$

That is, the third-order intercept point can be calculated from the fundamental tone and the third-order power level at any signal level. This result can be applied to calculate the third-order intercept point of a cascade. In this case  $P_{o1}$  would be the fundamental tone power at the load, and  $P_{o3}$  the total third-order contribution associated with that signal level, at the load.

Before deriving the result, it is useful to consider the effect of adding an ideal amplifier stage on the intercept point. If the operating power gain of the ideal stage is  $G_I$ , it follows from (2.84) that

$$P_{o3-A}(X_{IP3}) = \sqrt{\frac{(G_I P_{o1}(X))^3}{G_I P_{o3}(X)}} = G_I P_{o3}(X_{IP3}) \quad (2.85)$$

that is, the third-order intercept point is simply increased with the gain, as would be expected.

At this point the third-order intercept point of a cascade can be calculated easily. Consider the amplifier chain in Figure 2.13. It follows from (2.85) that the intercept point of each stage as calculated at the load is increased with the gain of the stages following it. The distortion component (power) contributed by stage  $j$  at the load is given by (2.82)

$$P_{o3-jA}(X) = \frac{P_{o1-jA}^3(X)}{P_{o3-jA}^2(X_{IP3})} \quad (2.86)$$

where all the power levels and the intercept point are referenced to the load. The normalized voltage contributed by stage  $j$  can be obtained by taking the square root of (2.86); that is,

$$v_{o3-jA}(X) = \frac{P_{o1-jA}^{3/2}(X)}{P_{o3-jA}(X_{IP3})} \quad (2.87)$$

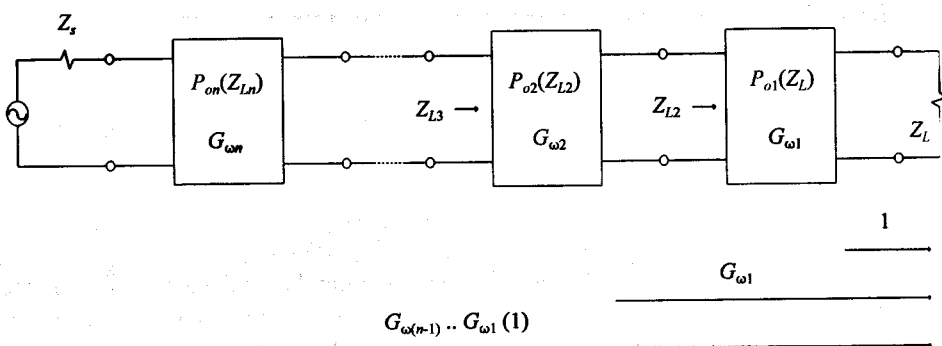


**Figure 2.13** The circuit used to calculate the third-order two-tone intercept point of a cascade.

The fundamental tone power level at the load,  $P_{o1-jA}(X)$ , is the same for each stage and, therefore, it follows from (2.87) that the voltage contribution from each stage at the load (superposition) is inversely proportional to the modified (amplified) intercept point for that stage. By using (2.87) and assuming the worst case where all the third-order terms add in-phase, it follows that the intercept point for the cascade is given by

$$\begin{aligned} P_T^2(X_{IP3}) &= \frac{P_{o1-jA}^3(X)}{\left[ \frac{P_{o1-jA}^{3/2}(X)}{P_{o3-1A}(X_{IP3})} + \dots + \frac{P_{o1-jA}^{3/2}(X)}{P_{o3-nA}(X_{IP3})} \right]^2} \\ &= \frac{1}{\left[ \frac{1}{P_{o3-1A}(X_{IP3})} + \dots + \frac{1}{P_{o3-nA}(X_{IP3})} \right]^2} \end{aligned} \quad (2.88)$$

that is,

$$\frac{1}{(X_{IP3})} = \frac{1}{P_{o3-1A}(X_{IP3})} + \dots + \frac{1}{P_{o3-nA}(X_{IP3})} \quad (2.89)$$

If the assumption is made that the ratios of the 1-dB compression points and the corresponding third-order intercept points will remain invariant, (2.89) leads to

$$\frac{1}{P_{o3-T}} = \frac{1}{P_{1dB-1A}} + \frac{1}{P_{1dB-2A}} + \dots + \frac{1}{P_{1dB-nA}} \quad (2.90)$$

where  $P_{1dB-iA}$  is the 1-dB compression point of stage  $i$  referenced to the load (that is, increased with the operating power gain of the stages following it).

If an infinite chain of identical stages is considered, (2.89) becomes

$$P_{o3}(X_{IP3}) = P_{o3}(X_{IP3}) (1 - 1/G_p) \quad (2.91)$$

(2.91) is a figure of merit similar to the noise measure [5].

### The Cripps Approach to Estimating the Maximum Output Power Obtainable from a Transistor

constant output power contours for a transistor are usually closer to ellipses than circles. This leads to the assumption that even the linear power generated by a transistor (up to the 1-dB compression point) is strongly influenced by the nonlinear components in the equivalent circuit. Cripps [1] demonstrated that the maximum linear

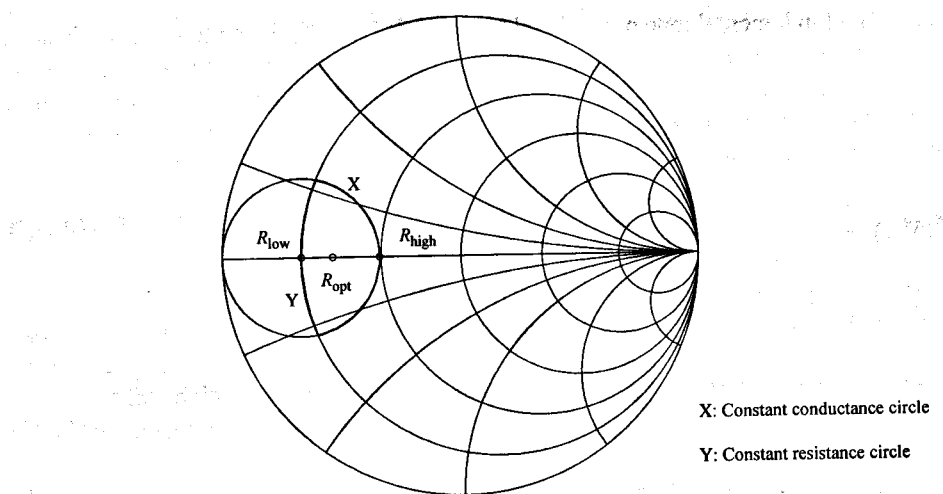


**Figure 2.14** The elliptical power contours obtained for linear amplifiers can be approximated as the intersection of circles when the intrinsic load line is considered [1].

output power obtainable from a transistor is mainly determined by clipping of the intrinsic output voltage and current and that the elliptic form of the contours can be approximated as the intersection of two circles. This is illustrated in Figure 2.14.

In the Cripps approach the intrinsic output voltage is assumed to be bounded to a maximum  $V_{\max}$ , while the current is bounded by  $I_{\max}$ . Under these assumptions, the optimum intrinsic load-line is given by

$$Y_{L_{\text{opt},i}} = G_{L_{\text{opt},i}} = I_{\max} / V_{\max} \quad (2.92)$$

If  $R_{L,i}$  is smaller than  $R_{L_{\text{opt},i}}$ , the current will be clipped and the voltage swing will be smaller than the maximum allowed. Relative to the maximum possible output power, the power ( $P_{oi}$ ) is then given by

$$P_{oi} = (I_{\max}^2 R_L) / (I_{\max}^2 R_{L_{\text{opt}}}) = R_L / R_{L_{\text{opt}}} \quad (2.93)$$

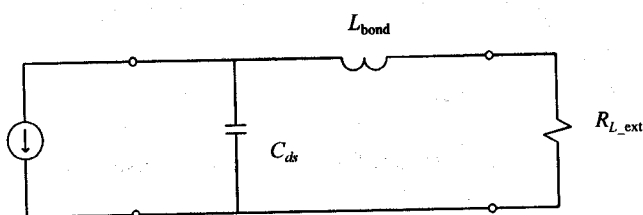


**Figure 2.15** The equivalent circuit used in the Cripps approach.

In this case, reactance can be added in series with the resistance without changing the maximum output power obtainable until the magnitude of the load impedance is equal to  $R_{L_{\text{opt}}}$ , at which point the current and the voltage are both clipped.

When the intrinsic load resistance is higher than the optimum, the voltage will be clipped and the current will be lower than the maximum allowed. The output power relative to the maximum ( $P_{\text{ov}}$ ) is given in this case by

$$P_{\text{ov}} = (V_{\text{max}}^2 G_L) / (V_{\text{max}}^2 G_{L_{\text{opt}}}) = G_L / G_{L_{\text{opt}}} \quad (2.94)$$

Susceptance can be added in parallel with this resistance without changing the output power obtainable until the magnitude of the load admittance is equal to  $G_{L_{\text{opt}}}$ , at which point the voltage and the current are both clipped.

Equations (2.92) through (2.94) can be used to calculate the intrinsic power generated or to find the contours of constant output power as a function of the intrinsic load. If the  $-X$  dB output power contour is of interest, the two resistance values are given by

$$R_{L_{\text{low}}} / R_{L_{\text{opt}}} = 10.0^{-0.1X} \quad (2.95)$$

and

$$R_{L_{\text{high}}} / R_{L_{\text{opt}}} = 10.0^{0.1X} \quad (2.96)$$

In order to find the constant output power contours in terms of the actual load impedance, the transforming effect of the transistor parasitics must be taken into account. If the simple equivalent circuit shown in Figure 2.15 is used, the load admittance corresponding to any given intrinsic load admittance can be calculated easily and the constant output power contours for the actual load can be obtained by adjusting the intrinsic line contours appropriately.

Calculation of the external load associated with a given intrinsic termination can be a major task if feedback (parasitic or otherwise) is applied to the transistor. Any losses in the output circuit or a feedback loop will also be a problem.

### 2.3.4 Estimation of the Maximum Output Power of a Linear Network by Using the Power Parameters

Because of the simplifications in the equivalent circuit used for the transistor in the Cripps approach, the intrinsic load termination corresponding to any given external load could be calculated easily. With the intrinsic termination and the  $I/V$  constraints known, the output power could be estimated. The implicit assumption that all the intrinsic power generated ends up in the external load is made in the process.

The Cripps approach can be generalized by introducing a new set of parameters to

map the intrinsic voltages to the external voltages and to the intrinsic output current [2]. Any reduction in the power caused by losses in the output circuit or in any feedback circuit is automatically tracked when this approach is followed.

The assumption that the intrinsic output current and voltage are constrained to a rectangular area on the  $I/V$ -plane can also be lifted. The allowable area on the  $I/V$ -plane can be restricted to the area defined by four boundary lines instead, as shown in Figure 2.16. If the goal is maximum power, the lines can be set to prevent voltage breakdown, operation in the resistive area, and forward conduction (field-effect transistors (FETs)). The current limit can usually be set slightly above  $I_{ds}$ .

If the goal is linearity, the lines can be set to bound the area where the  $I/V$  curves are evenly spaced.

Because the purpose of these mapping parameters is to calculate the output power, they will be referred to as power parameters. The power parameters are defined by the following equations:

$$V_1 = MV_{1i} + NV_{2i} \quad (2.97)$$

$$V_2 = OV_{1i} + PV_{2i} \quad (2.98)$$

$$I_{2i} = RV_{1i} + SV_{2i} \quad (2.99)$$

In these equations,  $V_{1i}$  and  $V_{2i}$  are the intrinsic input and output voltages, respectively, while  $I_{2i}$  is the intrinsic output current, as shown in Figure 2.16 for an FET.  $V_1$  and  $V_2$  are the input and output voltages, respectively.

The power parameters can be used to calculate the intrinsic load associated with a given external load directly, as will be shown in Section 2.3.4.1. The external voltage and current associated with the maximum intrinsic voltage or current and the associated power at the load can then be calculated easily by using (2.97) through (2.99).

Similarly, the external load associated with a given intrinsic load can also be calculated easily by using the power parameters. This is useful when contours of constant output power are generated.

The main assumptions in this approach are linearity and hard clipping of the intrinsic output current and voltage at the boundary lines. The power parameter approach has proven to be useful up to at least the 1-dB compression point of class A amplifiers.

The power parameters are quite general and can be manipulated to include the effect of any passive network in which the transistor may be imbedded. A set of power parameters should be calculated for each transistor used in the network. This is required because, in general, the output power may be limited by clipping in any of the transistors used in the circuit.

When the power parameters for any given two-port are calculated, it is assumed that no clipping will occur in any of the other active two-ports that may be present. The maximum (linear) output power is determined by the two-port in which clipping first occurs, that is, if the other stages are not close to clipping too.

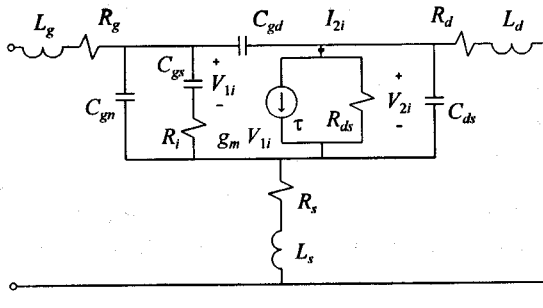
2. The behavior of the transistor is essentially linear up to (Class A) or around (Class B) the 1-dB compression point.
3. The output voltage of the transistor is sinusoidal.

The last condition can be approximated in class B stages by using a push-pull stage or by short-circuiting the harmonic currents of each transistor by using a resonant or low-pass circuit.

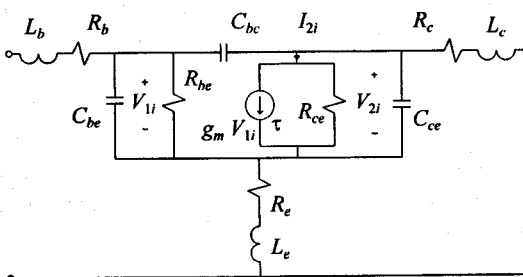
In order to calculate the linear behavior of the transistor with the load termination of interest, a linear model of the transistor is required. This is a simple matter in the class A case (conventional small-signal models have been found to be adequate), but not necessarily so in the class B case.

Acceptable results are usually obtained for the class B case by using the class A small-signal parameters at the rated class B output current and reducing the  $g_m$  of the associated small-signal model by a factor of two.

Typical small-signal models are shown in Figure 2.17.



(a)



(b)

**Figure 2.17** Typical small-signal models used for (a) FETs and (b) bipolar transistors.

### 2.3.4.1 Calculating the Intrinsic Load Associated with a Given External Load

The intrinsic load ( $Y_{Li} = -I_{2i} / V_{2i}$ ) associated with any given external load can be calculated by using the  $Y$ -parameter expression for the voltage gain in terms of  $Y_L$  [2]:

$$\frac{V_2}{V_1} = \frac{V_2}{V_1} = - \frac{y_{21}}{y_{22} + Y_L} \quad (2.100)$$

Equations (2.97) and (2.98) can be used to replace  $V_2$  and  $V_1$  above, leading to

$$\frac{V_2}{V_1} = \frac{O V_{1i} + P V_{2i}}{M V_{1i} + N V_{2i}} = - \frac{y_{21}}{y_{22} + Y_L} = A_v \quad (2.101)$$

in (2.101) can now be replaced in terms of  $V_{2i}$  and  $I_{2i}$  by using (2.99):

$$\frac{O \left( \frac{1}{R} I_{2i} - \frac{S}{R} V_{2i} \right) + P V_{2i}}{U \left( \frac{1}{R} I_{2i} - \frac{S}{R} V_{2i} \right) + N V_{2i}} = A_v \quad (2.102)$$

The next step is to eliminate  $V_{2i}$  and  $I_{2i}$  in this expression in terms of the intrinsic load admittance ( $Y_{Li} = -I_{2i} / V_{2i}$ ):

$$\frac{\frac{O}{R} I_{2i} + \left( P - \frac{S O}{R} \right) V_{2i}}{\frac{U}{R} I_{2i} + \left( N - \frac{M S}{R} \right) V_{2i}} = \frac{-\frac{O}{R} Y_{Li} + \left( P - \frac{S O}{R} \right)}{-\frac{M}{R} Y_{Li} + \left( N - \frac{M S}{R} \right)} = A_v \quad (2.103)$$

The required expression for  $Y_{Li}$  follows after rearranging this equation:

$$Y_L = \frac{\frac{R}{O} \left( P - \frac{S O}{R} \right) - \frac{X R}{M} \left( N - \frac{M S}{R} \right)}{1 - X} \quad (2.104)$$

Here  $X$  is given by

$$X = A_v \frac{M}{R} \frac{R}{O} \quad (2.105)$$

Equation (2.104) can be used to find the intrinsic load associated with any external load,

at which point the maximum output power can be calculated by finding the power level at which (hard) clipping will occur.

Equation (2.103) can also be used to find  $A_v$  in terms of  $Y_{L_i}$ . With  $A_v$  known, the external load ( $Y_L$ ) follows directly from (2.100).

Similar to the Cripps approach, these equations can be used to generate contours of constant output power or constant effective output power. The latter is of interest when an oscillator is designed.

An important difference between the Cripps approach and the power parameter approach is that the assumption that the output power will be a maximum when the intrinsic power generated is a maximum is inherent to the Cripps approach, while no such assumption is made when the power parameters are used. This assumption may lead to errors if the output circuit is loaded with the optimum power termination for the lossless case. If the external load impedance is a short-circuit, the power generated will still be a maximum but no power will be delivered to the load.

The power contours generated for a transistor (Texas Instruments Foundry FET) by using the power parameters [2] are shown in Figure 2.19. The optimum load line (maximum power) is also shown. The predicted contours at 10 GHz closely correspond with the measured load-pull contours provided by the manufacturer (the location and orientation of the contours are the same, but the measured contours are rounder). The  $S$ -parameters of the model used to calculate the power parameters are compared with the measured parameters in Figure 2.18.

Note that  $s_{11\omega}$  in Figure 2.19 is the input reflection coefficient (referenced to  $Z_{01} = 50\Omega$ ) associated with the optimum power load ( $S_L$ );  $s_{22\omega}^*$  is the conjugate of the output reflection coefficient when the input side is conjugately matched (if possible).

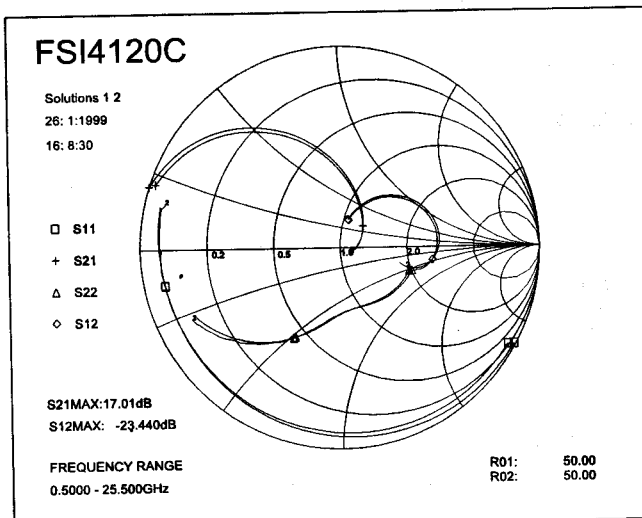


Figure 2.18 Comparison of the measured  $S$ -parameters of the transistor used in Figure 2.19 with the parameters associated with the small-signal model.

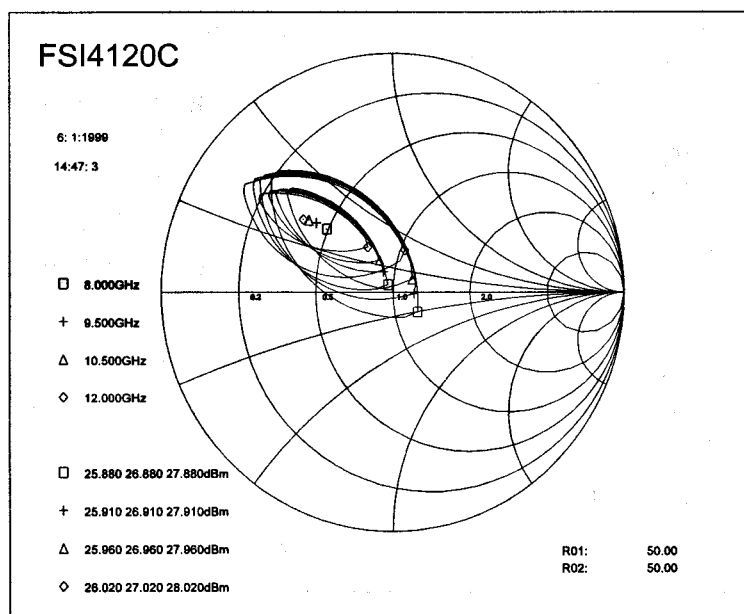
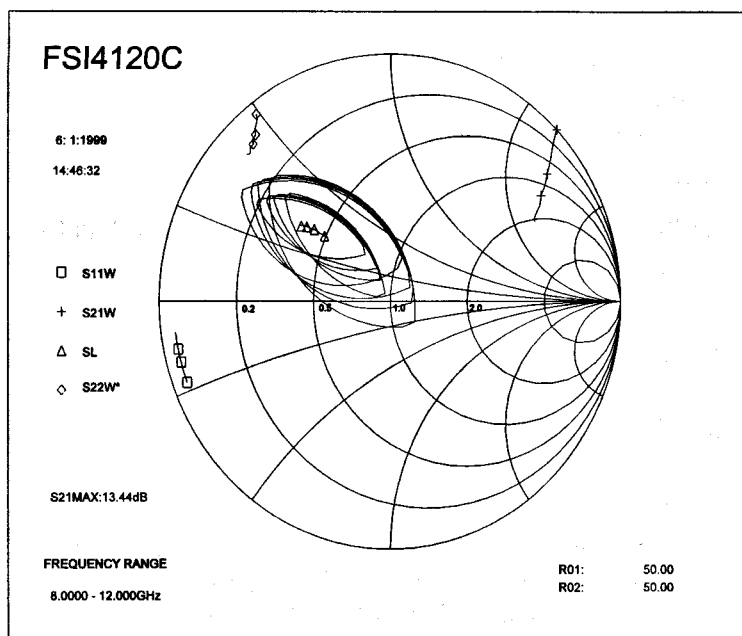


Figure 2.19

The load-pull contours (-1 dB; -2 dB) and the optimum load termination ( $S_L$ ) for a transistor as predicted by using the power parameters [2].

If  $S_L$  and  $s_{22\omega}$  were on top of each other, the optimum power and optimum output match ( $VSWR_{out} = 1$ ) points would have been the same.

Voltage-shunt feedback can be added to this transistor to improve the output match associated with maximum power without losing too much power (around 1 dBm).

### 2.3.4.2 Modification of the Power Parameters of a Two-Port by Adding a Cascade Network on Its Output Side

When a passive network (two-port) is added in cascade on the output side of an active two-port, as shown in Figure 2.20, its power parameters are modified. The derivation for the new parameters is shown below.

The intrinsic voltages of the original network are mapped to the external voltages by

$$V_1 = M V_{1i} + N V_{2i} \quad (2.106)$$

$$V_2 = O V_{1i} + P V_{2i} \quad (2.107)$$

$V_1$  is also the input voltage of the combination, but the new output voltage is  $V_3$  instead of  $V_2$ . It is therefore necessary to find  $V_2$  as a function of  $V_3$ .

The input current and voltage of the cascade network are given in terms of the output quantities by

$$\begin{bmatrix} V_2 \\ I_2 \end{bmatrix} = \begin{bmatrix} A_2 & B_2 \\ C_2 & D_2 \end{bmatrix} \begin{bmatrix} V_3 \\ I_3 \end{bmatrix} \quad (2.108)$$

that is,

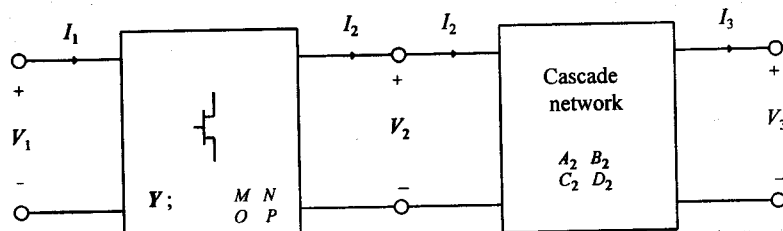


Figure 2.20 Adding a cascade network to the right of an active network.

$$V_2 = A_2 V_3 + B_2 I_3 \quad (2.109)$$

$$I_2 = C_2 V_3 + D_2 I_3 \quad (2.110)$$

Eliminating  $I_3$  from the last two equations gives

$$V_2 = A_2 V_3 + B_2 \left( \frac{I_2}{D_2} - \frac{C_2}{D_2} \right) V_3$$

$$= A_2 V_3 + \frac{B_2}{D_2} I_2 - \frac{B_2 C_2}{D_2} V_3$$

leading to

$$= (A_2 - \frac{B_2 C_2}{D_2}) V_3 + \frac{B_2}{D_2} I_2 \quad (2.111)$$

can be eliminated from this equation in terms of  $V_1$  and  $V_2$  by using the  $Y$ -parameters of the original network:

$$= y_{21} V_1 + y_{22} V_2 \quad (2.112)$$

leading to

$$= (A_2 - \frac{B_2 C_2}{D_2}) V_3 + \frac{B_2}{D_2} [-y_{21} V_1 - y_{22} V_2]$$

Rearranging this equation yields

$$\begin{aligned} &= V_2 + \frac{B_2}{D_2} y_{21} V_1 + \frac{B_2}{D_2} y_{22} V_2 \\ &= \frac{B_2}{D_2} y_{21} V_1 + (1 + \frac{B_2}{D_2} y_{22}) V_2 \\ &= \frac{\frac{B_2}{D_2} y_{21}}{A_2 - \frac{B_2 C_2}{D_2}} V_1 + \frac{1 + \frac{B_2}{D_2} y_{22}}{A_2 - \frac{B_2 C_2}{D_2}} V_2 \\ &= \frac{y_{21} B_2}{A_2 D_2 - B_2 C_2} V_1 + \frac{D_2 + y_{22} B_2}{A_2 D_2 - B_2 C_2} V_2 \end{aligned} \quad (2.113)$$

**After setting**

$$\alpha_1 = \frac{y_{21}B_2}{A_2D_2 - B_2C_2} \quad (2.114)$$

and

$$\alpha_2 = \frac{D_2 + y_{22}B_2}{A_2D_2 - B_2C_2} V_2 \quad (2.115)$$

it follows that

$$\begin{aligned} V_3 &= \alpha_1 V_1 + \alpha_2 V_2 \\ &= \alpha_1(MV_{1i} + NV_{2i}) + \alpha_2(OV_{1i} + PV_{2i}) \\ &= (\alpha_1 M + \alpha_2 O)V_{1i} + (\alpha_1 N + \alpha_2 P)V_{2i} \end{aligned} \quad (2.116)$$

The new power parameters of the two-port are therefore given in terms of the original power parameters by (2.106):

$$V_1 = M V_{1i} + N V_{2i}$$

and

$$V_3 = (\alpha_1 M + \alpha_2 O)V_{1i} + (\alpha_1 N + \alpha_2 P)V_{2i} \quad (2.117)$$

### 2.3.4.3 Modification of the Power Parameters of a Two-Port by Adding a Cascade Network on Its Input Side

When a cascade network is added to the input side of a two-port, the input voltage for the combination is different from that of the original network, and the power parameters are therefore also changed. The effect of the cascade network is derived below.

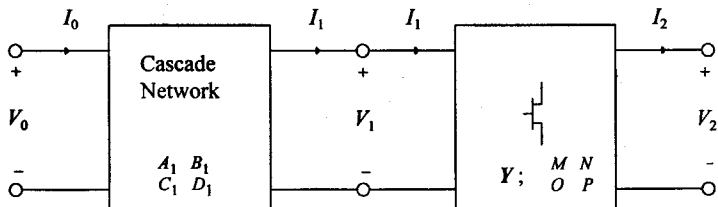


Figure 2.21 Adding a cascade network on the input side of a network.

The new input voltage and current ( $V_0$  and  $I_0$ ) are given in terms of the previous input voltage and current:

$$\begin{bmatrix} V_0 \\ I_0 \end{bmatrix} = \begin{bmatrix} A_1 & B_1 \\ C_1 & D_1 \end{bmatrix} \begin{bmatrix} V_1 \\ I_1 \end{bmatrix} \quad (2.118)$$

Therefore,

$$V_0 = A_1 V_1 + B_1 I_1$$

$I_1$  in this equation can be replaced in terms of  $V_1$  and  $V_2$  in this equation by using the  $Y$ -parameters of the original two-port:

$$I_1 = y_{11} V_1 + y_{12} V_2 \quad (2.119)$$

Therefore,

$$\begin{aligned} V_0 &= A_1 V_1 + B (y_{11} V_1 + y_{12} V_2) \\ &= (A + B y_{11}) V_1 + B y_{12} V_2 \end{aligned} \quad (2.120)$$

With

$$z = A + B y_{11} \quad (2.121)$$

and

$$c = B y_{12} \quad (2.122)$$

allows that

$$\begin{aligned} z &= \alpha_{1L} V_1 + \alpha_{2L} V_2 \\ &= \alpha_{1L} (M V_{1i} + N V_{2i}) + \alpha_{2L} (O V_{1i} + P V_{2i}) \\ &= (\alpha_{1L} M + \alpha_{2L} O) V_{1i} + (\alpha_{1L} N + \alpha_{2L} P) V_{2i} \end{aligned} \quad (2.123)$$

The modified power parameters are, therefore, given by (2.123) and (2.107):

$$= (\alpha_{1L} M + \alpha_{2L} O) V_{1i} + (\alpha_{1L} N + \alpha_{2L} P) V_{2i}$$

$$= O V_{1i} + P V_{2i}$$

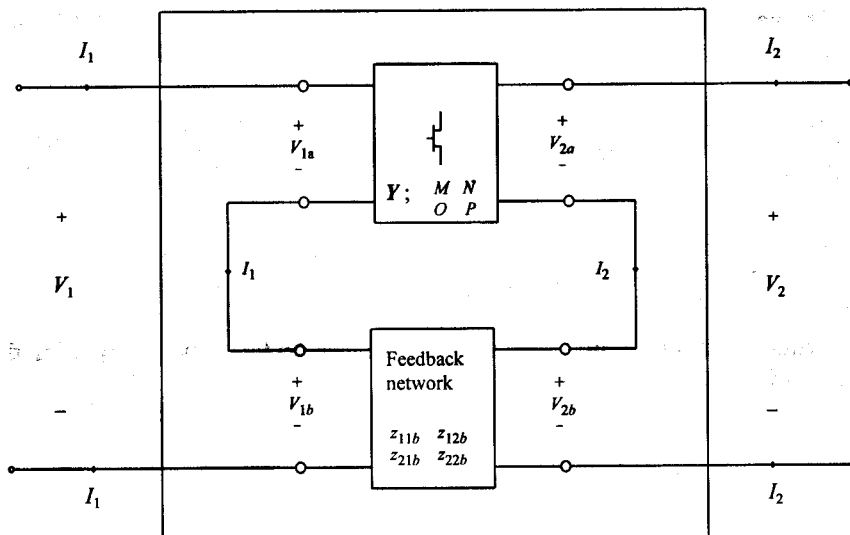


Figure 2.22 A network with series feedback.

### 2.3.4.4 The Influence of Series Feedback on the Power Parameters of a Two-Port

The influence of series feedback (see Figure 2.22) on the power parameters of a two-port will be derived here.

Before adding the series feedback network, assume that the power parameters are given by

$$V_{1a} = MV_{1i} + NV_{2i} \quad (2.124)$$

$$V_{2a} = OV_{1i} + PV_{2i} \quad (2.125)$$

The new input and output voltages are given by

$$V_1 = V_{1a} + V_{1b} \quad (2.126)$$

$$V_2 = V_{2a} + V_{2b} \quad (2.127)$$

From

$$V_{1b} = z_{11b} I_1 + z_{12b} I_2 \quad (2.128)$$

$$V_{2b} = z_{21b} I_1 + z_{22b} I_2 \quad (2.129)$$

and

$$I_1 = y_{11} V_{1a} + y_{12} V_{2a} \quad (2.130)$$

$$I_2 = y_{21} V_{1a} + y_{22} V_{2a} \quad (2.131)$$

it follows that

$$\begin{aligned} V_{1b} &= z_{11b} (y_{11} V_{1a} + y_{12} V_{2a}) + z_{12b} (y_{21} V_{1a} + y_{22} V_{2a}) \\ &= (z_{11b} y_{11} + z_{12b} y_{21}) V_{1a} + (z_{11b} y_{12} + z_{12b} y_{22}) V_{2a} \end{aligned} \quad (2.132)$$

and

$$\begin{aligned} V_{2b} &= z_{21b} (y_{11} V_{1a} + y_{12} V_{2a}) + z_{22b} (y_{21} V_{1a} + y_{22} V_{2a}) \\ &= (z_{21b} y_{11} + z_{22b} y_{21}) V_{1a} + (z_{21b} y_{12} + z_{22b} y_{22}) V_{2a} \end{aligned} \quad (2.133)$$

With

$$z_{1s} = z_{11b} y_{11} + z_{12b} y_{21} \quad (2.134)$$

$$z_{2s} = z_{11b} y_{12} + z_{12b} y_{22} \quad (2.135)$$

$$z_{11s} = z_{21b} y_{11} + z_{22b} y_{21} \quad (2.136)$$

$$z_{12s} = z_{21b} y_{12} + z_{22b} y_{22} \quad (2.137)$$

(2.132) and (2.133) reduce to

$$V_{1b} = \alpha_{11s} V_{1a} + \alpha_{12s} V_{2a} \quad (2.138)$$

$$V_{2b} = \alpha_{21s} V_{1a} + \alpha_{22s} V_{2a} \quad (2.139)$$

With  $V_{1b}$  and  $V_{2b}$  known in terms of the original power parameters, the modified power parameters can be calculated:

$$\begin{aligned}
 V_1 &= V_{1a} + V_{1b} \\
 &= V_{1a} + \alpha_{11s} V_{1a} + \alpha_{12s} V_{2a} \\
 &= (1 + \alpha_{11s}) V_{1a} + \alpha_{12s} V_{2a} \\
 &= (1 + \alpha_{11s}) (M V_{1i} + N V_{2i}) + \alpha_{12s} (O V_{1i} + P V_{2i}) \\
 &= [(1 + \alpha_{11s}) M + \alpha_{12s} O] V_{1i} + [(1 + \alpha_{11s}) N + \alpha_{12s} P] V_{2i}
 \end{aligned} \tag{2.140}$$

and

$$\begin{aligned}
 V_2 &= V_{2a} + V_{2b} \\
 &= V_{2a} + \alpha_{21s} V_{1a} + \alpha_{22s} V_{2a} \\
 &= [\alpha_{21s} M + (1 + \alpha_{22s}) O] V_{1i} + [\alpha_{21s} N + (1 + \alpha_{22s}) P] V_{2i}
 \end{aligned} \tag{2.141}$$

### 2.3.4.5 The Effect of Changing the Configuration on the Power Parameters

As was the case with the two-port parameters, the power parameters change when the configuration is changed. The change in the parameters is established below.

#### Common-Source to Common-Gate Case

If the power parameters for the common-source configuration (see Figure 2.23) are given by

$$V_{1s} = M_s V_{1i} + N_s V_{2i} \tag{2.142}$$

$$V_{2s} = O_s V_{1i} + P_s V_{2i} \tag{2.143}$$

the parameters for the common-gate configuration can be calculated from the voltage relationships:

$$V_{1g} = -V_{1s} \tag{2.144}$$

$$V_{2g} = V_{2s} - V_{1s} \tag{2.145}$$

$\Rightarrow$

$$V_{2g} = V_{2s} + V_{1g} \tag{2.146}$$

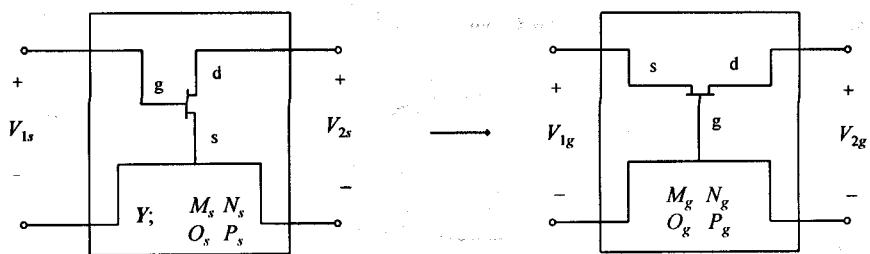


Figure 2.23 The effect of changing the configuration from common-source to common-gate on the power parameters.

The first two parameters follow easily from (2.144) and (2.142):

$$V_{1s} = M_s V_{1i} + N_s V_{2i}$$

becomes

$$-V_{1g} = M_s V_{1i} + N_s V_{2i} \quad (2.147)$$

which implies

$$V_{1i} = -M_s V_{1i} - N_s V_{2i} \quad (2.148)$$

substituting this result in (2.146), it follows that

$$V_{1s} = V_{1g} = V_{2s} = O_s V_{1i} + P_s V_{2i}$$

$$= O_s V_{1i} + P_s V_{2i} + V_{1g}$$

$$= O_s V_{1i} + P_s V_{2i} + [-M_s V_{1i} - N_s V_{2i}]$$

therefore, that

$$\begin{aligned} V_{1s} &= (O_s - M_s)V_{1i} + (P_s - N_s)V_{2i} \\ &= (O_s + M_g)V_{1i} + (P_s + N_g)V_{2i} \end{aligned} \quad (2.149)$$

Power parameters for the common-gate configuration are given by (2.148) and (2.149).

### Common-Gate to Common-Drain Case

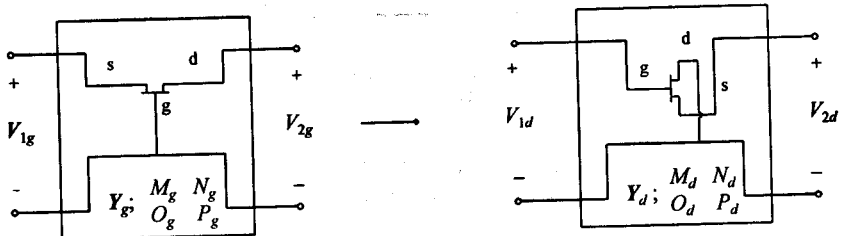


**Figure 2.24** The effect of changing the configuration from common-gate to common-drain on the power parameters.

The common-drain power parameters (see Figure 2.24) can be calculated from the common-gate parameters as follows.

Starting with

$$V_{1g} = M_g V_{1i} + N_g V_{2i} \quad (2.150)$$

$$V_{2g} = O_g V_{1i} + P_g V_{2i} \quad (2.151)$$

and the voltage relationships

$$V_{1d} = -V_{2g} \quad (2.152)$$

$$V_{2d} = V_{1g} - V_{2g} \quad (2.153)$$

it follows that

$$\begin{aligned} -V_{1d} &= V_{2g} \\ &= O_g V_{1i} + P_g V_{2i} \end{aligned}$$

and, therefore, that

$$V_{1d} = -O_g V_{1i} - P_g V_{2i} \quad (2.154)$$

and

$$\begin{aligned} V_{2d} &= V_{1g} - V_{2g} \\ &= M_g V_{1i} + N_g V_{2i} - O_g V_{1i} - P_g V_{2i} \end{aligned}$$

$$= (M_g - O_g) V_{1i} + (N_g - P_g) V_{2i} \quad (2.155)$$

### Common-Drain to Common-Source Case

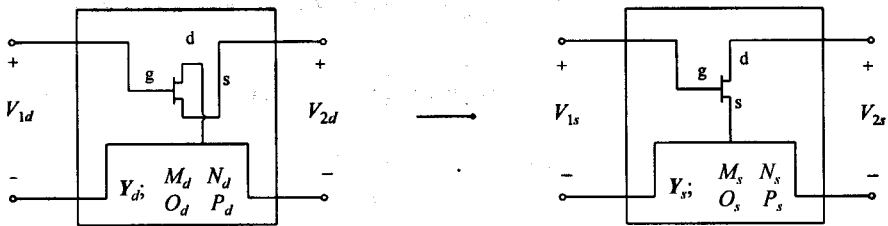


**Figure 2.25** The effect of changing the configuration from common-drain to common-source on the power parameters.

The common-source power parameters can be calculated from the common-drain parameters (see Figure 2.25) as follows.

Starting with

$$V_{1d} = M_d V_{1i} + N_d V_{2i} \quad (2.156)$$

$$V_{2d} = O_d V_{1i} + P_d V_{2i} \quad (2.157)$$

and the voltage relationships

$$V_{2s} = -V_{2d} \quad (2.158)$$

$$V_{1s} = V_{1d} - V_{2d} \quad (2.159)$$

it follows that

$$\begin{aligned} I_{1s} &= V_{1d} - V_{2d} \\ &= M_d V_{1i} + N_d V_{2i} - O_d V_{1i} - P_d V_{2i} \\ &= (M_d - O_d) V_{1i} + (N_d - P_d) V_{2i} \end{aligned} \quad (2.160)$$

$$\begin{aligned}
 V_{2s} &= -V_{2d} = -O_d V_{1i} - P_d V_{2i} \\
 &= -O_d V_{1i} - P_d V_{2i}
 \end{aligned} \tag{2.161}$$

## REFERENCES

1. Cripps, S. C., "GaAs Power Amplifier Design," Technical Notes 3.2, Palo Alto, CA: Matcom Inc.
2. *MultiMatch RF and Microwave Impedance-Matching, Amplifier and Oscillator Synthesis Software*, Somerset West: Ampsa (Pty) Ltd.; <http://www.ampsap.com>.
3. Haus, H. A., and R. B. Adler, *Circuit Theory of Linear Noisy Networks*, New York: Wiley, 1959.
4. Hillbrand, H., and P. H. Russer, "An Efficient Method for Computer Aided Noise Analysis of Linear Amplifier Networks," *IEEE Trans. Circuits and Systems*, Vol. CAS-23, No. 4, April 1976.
5. Vendelin, G. D., A. M. Pavio, and U. L. Rohde, *Microwave Circuit Design Using Linear and NonLinear Techniques*, New York: John Wiley, 1990.
6. Kraus, H. L., C. W. Bostian, and F. H. Raab, *Solid State Radio Engineering*, New York: John Wiley, 1980.
7. Cripps, S. C., "Harmonic and Intermodulation Distortion in GaAsFET Amplifiers," Technical Notes 2.1, Palo Alto, CA: Matcom Inc.

## SELECTED BIBLIOGRAPHY

- Roddy, D., and J. Coolen, *Electronic Communications*, Reston, VA: Reston Publishing Company, Inc., 1981, pp. 103–136.

## CHAPTER 3

# RADIO-FREQUENCY COMPONENTS

### 3.1 INTRODUCTION

In order to design realizable radio-frequency and microwave circuits, some knowledge of the limitations of and the parasitics associated with practical components is essential. The characteristics of practical capacitors, inductors, magnetic materials, and microstrip transmission-lines will be considered in this chapter.

The capacitors used in an RF circuit (impedance-matching networks, filters, coupling and de-coupling networks) can usually be obtained from one of the many manufacturers of these components. Unfortunately, this does not always apply to inductors. The design of inductors will, therefore, also be considered in this chapter. Single-layer air-cored inductors and inductors with magnetic cores will be considered.

In order to get the circuit manufactured to perform as expected, care should be taken to ensure that the circuit realized is the same as the one designed. Apart from the parasitic effects of the components used, care should also be taken with any connections made between components. The effect of all the connections made should be included in the simulation.

Connections to the ground plane should also be made with care. Ground loops (unnecessary ground connections) should be avoided and connections cannot be made arbitrarily to the ground plane on the (false) assumption that all points on the ground plane are at the same potential (as would be the case on the circuit diagram). When any uncertainty arises as to exactly where a connection should be made to the ground plane, it is useful to realize that the electric signal is traveling as a wave through the circuit and is at any point is where the wave is.

When an active circuit is manufactured, RF and microwave decoupling of the dc circuit is essential (introducing an RF ground). Parasitic resonances can easily be introduced inadvertently when this is done. It is often possible to eliminate such resonances by using small resistors in the decoupling circuit (the voltage across these resistors can also be used to check the dc current). A number of capacitors can also be used in parallel. The capacitance of the different capacitors is usually chosen to differ by a factor of 10 when this is done.

When different capacitors are used in parallel, the series resonating frequencies of the different capacitors should be taken into account when the values are chosen (the smaller

## CHAPTER 3

# RADIO-FREQUENCY COMPONENTS

### 3.1 INTRODUCTION

In order to design realizable radio-frequency and microwave circuits, some knowledge of the limitations of and the parasitics associated with practical components is essential. The characteristics of practical capacitors, inductors, magnetic materials, and microstrip transmission-lines will be considered in this chapter.

The capacitors used in an RF circuit (impedance-matching networks, filters, coupling and de-coupling networks) can usually be obtained from one of the many manufacturers of these components. Unfortunately, this does not always apply to inductors. The design of inductors will, therefore, also be considered in this chapter. Single-layer air-cored inductors and inductors with magnetic cores will be considered.

In order to get the circuit manufactured to perform as expected, care should be taken to ensure that the circuit realized is the same as the one designed. Apart from the parasitic effects of the components used, care should also be taken with any connections made between components. The effect of all the connections made should be included in the simulation.

Connections to the ground plane should also be made with care. Ground loops (unnecessary ground connections) should be avoided and connections cannot be made arbitrarily to the ground plane on the (false) assumption that all points on the ground plane are at the same potential (as would be the case on the circuit diagram). When any uncertainty arises as to exactly where a connection should be made to the ground plane, it is useful to realize that the electric signal is traveling as a wave through the circuit and ground at any point is where the wave is.

When an active circuit is manufactured, RF and microwave decoupling of the dc circuit is essential (introducing an RF ground). Parasitic resonances can easily be introduced inadvertently when this is done. It is often possible to eliminate such resonances by using small resistors in the decoupling circuit (the voltage across these resistors can also be used to check the dc current). A number of capacitors can also be used in parallel. The capacitance of the different capacitors is usually chosen to differ by a factor of 10 when this is done.

When different capacitors are used in parallel, the series resonating frequencies of the different capacitors should be taken into account when the values are chosen (the smaller

the capacitance value, the higher the resonating frequency will be) and care should be taken to avoid parallel resonances between the components used.

The thin-film resistors and parallel plate (single-layer) capacitors used at microwave frequencies cannot be accurately simulated as lumped components. The distributed nature of these components must be taken into account in the design. These components will be considered in Chapter 7.

Additional complications are introduced by the steps, T-junctions, and crosses associated with planar transmission lines. The ideal connection is a point junction, but these junctions are not point junctions. These effects will be considered in Chapter 9.

## 3.2 CAPACITORS

Capacitors differ in capacitance, resonant frequency, losses, temperature stability tolerances, packaging, and size. Most of these characteristics are determined by the dielectric material used. The parasitic inductance is, however, also a function of the packaging and the lead lengths of the capacitor.

The equivalent circuit for a practical capacitor is shown in Figure 3.1.

The parasitic inductance causes the impedance of the capacitor to be lower than expected. The impedance at the series resonant frequency is equal to the series resistance of the capacitor. Above this frequency the impedance becomes inductive.

The effective capacitance below the resonant frequency is given by

$$C_{\text{eff}} = C_0 / [1 - (f / f_r)^2] \quad (3)$$

where  $C_0$  is the capacitance at low frequencies and

$$f_r = \frac{1}{2\pi\sqrt{LC_0}}$$

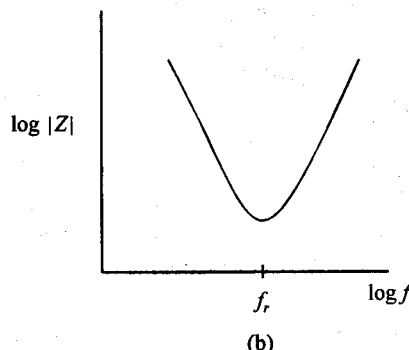
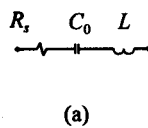


**Figure 3.1** (a) An equivalent circuit for a capacitor; (b) the effect of the parasitic inductance resistance on the impedance of a capacitor.

**Table 3.1**  
The resonant frequencies for some capacitors [1–4]

Capacitance	1 pF	10 pF	100 pF	1 nF	10 nF
Mica; Disk Ceramic	—	—	170 MHz	60 MHz	20 MHz
Porcelain chip capacitors	7–10 GHz	2–3 GHz	1 GHz	230 MHz	—
Parallel-plate capacitors	20 GHz	7 GHz	2 GHz	600 MHz	—

where  $f_r$  is the resonant frequency of the capacitor.

The resonant frequencies for some capacitors (with very short lead lengths or no leads) are shown in Table 3.1 [1–4].

As can be seen from Table 3.1, even chip capacitors have some parasitic inductance. There are two reasons for this: First, the finite dimensions (and therefore the inductance) of the capacitor plates, and second, the finite distance across the plates.

That there must be some inductance associated with the finite separation of the capacitor plates is obvious if Maxwell's law

$$\nabla \times \mathbf{H} = i + \partial \mathbf{D} / \partial t$$

is inspected. According to this equation, even a displacement current generates magnetic flux and, therefore, has inductance associated with it. The inductance can be minimized by choosing the smallest capacitor available (with voltage and power ratings taken into account).

The losses in a capacitor are usually specified by the quality factor ( $Q$ ), where

$$Q = X_s / R_s \quad (3.2)$$

$R_s$  is the series resistance of the capacitor, and  $X_s$  is the effective reactance of the capacitor.

The quality factor ( $Q$ -factor) is frequency- and temperature-dependent. It is, therefore, important to specify the measuring frequency and the power level at which the measurement was made.

While the losses of the component are specified in terms of the  $Q$ -factor, the losses of dielectric materials are specified in terms of the dissipation factor ( $DF$ ) or the loss tangent ( $\tan \delta$ ).

**Table 3.2**  
The dielectric constants ( $\epsilon_r$ ) and dissipation factors for some commonly used materials

Material	$\epsilon_r$	$DF$ (low frequencies)	$DF$ (@ 100 MHz)
BaTiO <sub>3</sub>	1200	0.01	0.03
NPO	30	0.0001	0.002
Porcelain	15	—	0.00007

The dissipation factor specifies the ratio of the power dissipated to the power stored in the material:

$$DF = P_{\text{diss}} / P_{\text{stored}} \quad (3.3)$$

The relative power dissipation of dielectric materials is directly proportional to the dissipation factor. High losses are associated with high dielectric constants.

The dissipation factors for three commonly used materials are given in Table 3.2 [2]. Note the decrease in losses as the relative dielectric constant drops, as well as the increase in dissipation at higher frequencies.

It can be easily shown that if the parasitic inductance of a capacitor can be ignored, the dissipation factor and the *Q*-factor are related in the following way:

$$DF = 1 / Q \quad (3.4)$$

The losses of the dielectric materials and capacitors are sometimes specified in terms of the loss tangent ( $\tan \delta$ ). The definition of the loss tangent is the same as that of the dissipation factor.

Dissipation factors are not only frequency dependent, but increase with temperature and, therefore, with power level. The power dissipation inside a typical chip capacitor only needs to be on the order of 40 mW to increase the temperature to that of commonly used soldering irons [2]. At high temperatures the dissipation factor can be an order of magnitude higher than at room temperature. As the temperature inside a capacitor increases, the dissipation factor increases, which causes a further increase in temperature with more losses. This thermal runaway phenomenon is particularly important at low impedance and high power level points in a circuit.

The series resistance and *Q*-factors of two high-quality capacitors at room temperature are given at two different frequencies in Table 3.3 [2]. Even for good capacitors, the *Q*-factor is surprisingly low at high frequencies.

**Table 3.3**  
The quality factor and resistance of two capacitors at high frequencies

Frequency	100 MHz	500 MHz
10 pF	2200 (0.055Ω)	180 (0.169Ω)
100 pF	700 (0.018Ω)	60 (0.055Ω)

Not only the dissipation factor, but also the capacitance of a capacitor, are affected by a change in temperature. The change in capacitance can be very small (NPO) and linear (class 1 ceramics), or large and nonlinear (class 2 ceramics). Class 1 ceramics with positive (up to 150 ppm/°C) and negative (up to -5500 ppm/°C) temperature coefficients are available [5].

As a final remark on capacitors, it should be noted that the capacitance of capacitors with high dielectric constants is usually also voltage-sensitive. The capacitance of Class 2 ceramics can change by more than 20% if the voltage is varied from 0% to 150% of the rated value [5].

### Summary

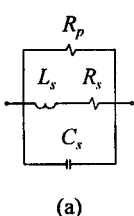
The following points are important when choosing a capacitor for a particular purpose:

1. The parasitic inductance;
2. The tolerance of the capacitor;
3. The *Q*-factor at the desired frequency and power level;
4. The influence of voltage on the capacitor (capacitance changes, as well as the breakdown voltage);
5. The influence of temperature on the capacitor (ambient as well as increases due to the power dissipation in the capacitor);
6. The size and packaging of the capacitor.

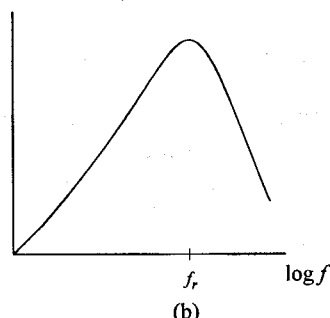
## 3.3 INDUCTORS

The performance of practical inductors are degraded by parasitic capacitance and resistive losses.

The parasitic capacitance (see Figure 3.2) causes the resistance of the inductor to be higher than expected. This effect is very pronounced near the resonant frequency ( $f_r$ ).



(a)



(b)

(a) The equivalent circuit of a practical inductor; (b) the effect of parasitic capacitance and losses on its impedance.

Inductor losses consist of copper losses ( $R_s$ ) and, if magnetic material is used, hysteresis and eddy current losses ( $R_p$ ). All of these losses are frequency dependent. The copper losses increase above its dc value because of the skin and proximity effects.

By using magnetic material, the size of the inductor can be reduced drastically and the parasitic capacitance will, therefore, also be considerably lower. Unfortunately, there will also be some losses in the material. These losses are mainly hysteresis losses in the case of ferrite materials.

The effect of parasitic capacitance on the  $Q$ -factor and the inductance of inductors, the skin and proximity effects, the design of air-cored solenoidal coils, the properties of magnetic materials, and the design of inductors with ferrite cores will be discussed in the following sections.

### 3.3.1 The Influence of Parasitic Capacitance on an Inductor

By using the equivalent circuit shown in Figure 3.2, it can be easily shown that the effective inductance ( $L_{\text{eff}}$ ) of an inductor is given by

$$L_{\text{eff}} = L_s / [1 - (f / f_r)^2] \quad (3.5)$$

where  $f_r$  is the parallel resonant frequency of the inductor.

This equation applies only if the approximation

$$1 + 1/Q_s^2 \approx 1 \quad (3.6)$$

where

$$Q_s = \omega L_s / R_s$$

can be made.

As can be seen from (3.5), the inductance increases rapidly as the resonant frequency ( $f_r$ ) is approached.

Under the same conditions, the effective resistance ( $R_p$  ignored) is given by

$$R_{\text{eff}} = R_s / [1 - (f / f_r)^2] \quad (3.7)$$

Because the effective resistance has increased because of the parasitic capacitance present, the losses in the coil are higher if the input current to the inductor is considered to be the same. This happens because the current in the parasitic capacitor is out of phase with that in the inductive part of the inductor.

The effective  $Q$ -factor of the coil will therefore be lower than without parasitic capacitance. The effective  $Q$ -factor is given by

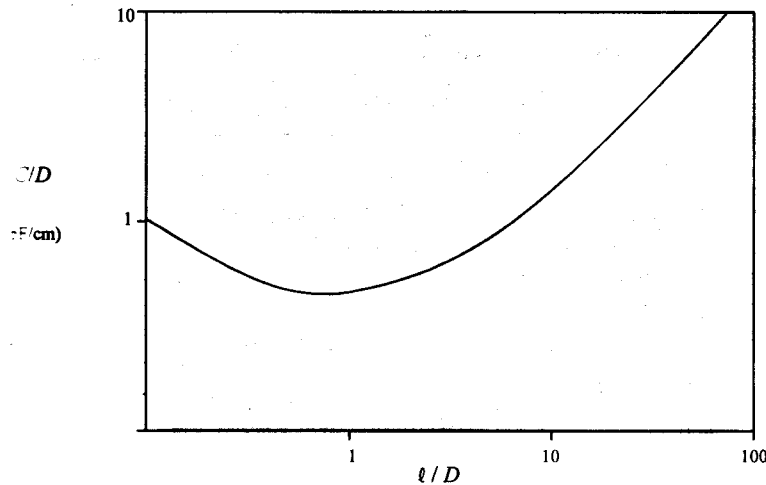
$$Q_{\text{eff}} = Q_s [1 - (f / f_r)^2] \quad (3.8)$$

When  $f = 0.707 f_r$ , the effective  $Q$ -factor will be half that of the inductive part of the inductor.

These effects can be minimized by keeping the parasitic capacitance as low as possible.

The capacitance of an air-cored solenoidal coil is given in Figure 3.3 as a function of the length-to-diameter ratio and the mean radius of the coil [6].

The capacitance of the coil is not a function of the number of turns as might be expected; it is a strong function of the coil size (radius) and a weak function of the coil shape (length-to-diameter ratio,  $\ell/D$ ). The capacitance can therefore be minimized by making the coil as small as possible. An initial value of 2 can be used for the length-to-diameter ratio.



3.3 The self-capacitance of a single-layer solenoidal coil (Source: [6]).

For high inductance, the turns of a coil should be spaced as closely as possible. It will be shown later that this distance is determined by the desired  $Q$ -factor of the coil.

When the coil capacitance is known, the resonant frequency can be found by using equation

$$\frac{1}{2\pi\sqrt{L_s C_s}} \quad (3.9)$$

Typical resonant frequencies for some inductance values are given here as a guide and can be achieved easily [1]:

100 nH:	400–800 MHz
1 $\mu$ H:	100–200 MHz
10 $\mu$ H:	25–60 MHz

**Table 3.4**

The wire diameter and resistance for wire gauges 12–32 (20°C; copper material)

Gauge	Bare diameter (mm)	Double enamel- coated diameter (mm)	Resistance (Ω/km)
	AWG (SWG)	AWG (SWG)	AWG (SWG)
12	2.052 (2.64)	2.13 (2.73)	5.5 (3.1)
14	1.628 (2.03)	1.71 (2.12)	8.6 (5.2)
16	1.291 (1.63)	1.37 (1.71)	15.2 (8.2)
18	1.024 (1.22)	1.10 (1.29)	22.0 (14.5)
20	0.812 (0.914)	0.879 (0.984)	34.3 (25.8)
22	0.644 (0.711)	0.701 (0.774)	61.0 (42.6)
24	0.511 (0.559)	0.564 (0.617)	87.8 (69.1)
26	0.405 (0.457)	0.452 (0.512)	133.9 (103.2)
28	0.321 (0.376)	0.366 (0.424)	212.9 (152.6)
30	0.255 (0.315)	0.295 (0.361)	338.5 (217.4)
32	0.202 (0.274)	0.241 (0.316)	538.5 (286.6)

Miniature chip coils (0805, 1008, ...) with self-resonant frequencies ranging from 250 MHz to above 6 GHz for values ranging from 1500 nH to 2.2 nH are commercially available. The resonance frequency claimed for a 100 nH (22 nH) miniature chip inductor is 1.5 GHz (3.2 GHz) for a chip size of 0805 (8mils × 5mils) and 1 GHz (2.4 GHz) for a chip size of 1008 [7]. The minimum *Q*-values quoted at 150 MHz (250 MHz) and 100 MHz are 40 and 50, respectively [7].

### 3.3.2 Low-Frequency Losses in Inductors

The resistive losses in a conductor are approximately constant at low frequencies. The resistance is a function of the material used and the wire diameter. The diameters and the resistance of copper wire with wire gauges ranging from 12 to 32 are given in Table 3.4. The American wire gauge (AWG) values are listed with the corresponding standard wire gauge (SWG) values. Note that the wire diameter doubles whenever the wire gauge decreases by a factor of 6.

It can be seen from the table that the diameter of AWG No. 12 wire is approximately 2 mm and that of AWG No. 22 is 0.2 mm. The resistance of No. 12 wire is 5.5 Ω/km and that of No. 32 wire is 538 Ω/km. The increase of approximately 100 in resistance correlates well with the decrease in the diameter by a factor of 10 ( $R \propto 1/A$ , where  $A$  is the cross-section area of the wire).

### 3.3.3 The Skin Effect

A conductor can be viewed as a guide for the electrical and magnetic fields around it, as

is shown in Figure 3.4. The current flowing in the conductor is caused by the changing magnetic flux that penetrates into the conductor. This current opposes the magnetic field that causes it. The result is that the magnetic field decreases in strength (exponentially) as it penetrates the conductor.

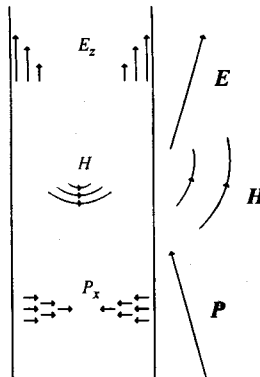


**Figure 3.4** The electric, magnetic, and Poynting fields around and inside a circular conductor (after [9]).

The induced electrical field within the conductor is given as a function of the penetration depth  $x$  by

$$E_z = E_{z0} e^{-\Gamma x} \quad (3.10)$$

where  $E_{z0}$  is the electric field strength at the surface of the conductor (in the direction of the conductor).

The propagation constant of the electrical field in the wire is

$$\begin{aligned} \Gamma &= \sqrt{j \omega \mu \gamma} \\ &= (1 + j) \sqrt{\pi f \mu \gamma} \\ &= \alpha + j\beta \end{aligned} \quad (3.11)$$

where  $\gamma$  is the resistivity of the conductor.

The inverse of the attenuation constant  $\alpha$  is defined as the skin depth  $\delta$ :

$$\delta = 1 / \alpha = 1 / \sqrt{\pi f \mu \gamma} \quad (3.12)$$

Therefore, the amplitude of the electrical field at a distance  $x$  inside the conductor is

**Table 3.5**  
The skin depth of some materials as a function of frequency

Material	Skin Depth (cm)
Brass	$12.7/f^{1/2}$
Aluminum	$8.3/f^{1/2}$
Gold	$7.7/f^{1/2}$
Copper	$6.6/f^{1/2}$
Silver	$6.2/f^{1/2}$
Mu-metal	$0.4/f^{1/2}$

$$E(x) = E(0)e^{-x/\delta} \quad (3.13)$$

Because of the decrease in the field strength, the current density will be higher closer to the surface of the conductor. When the conductor is at least six skin-depths (or depths of penetration) in diameter, all the current can be considered to flow uniformly in a layer one skin-depth deep along the surface of the conductor.

The resistance of the conductor can then be calculated within 10% by using the following equations [9]:

$$R_{ac} = \{\pi r^2 / [\pi r^2 - \pi(r - \delta)^2]\} R_{dc} \quad (3.14)$$

$$= \{\pi r^2 / [\pi r^2 - \pi(r^2 - 2\delta r + \delta^2)]\} R_{dc}$$

$$= \{\pi r^2 / [2\pi\delta r - \pi\delta^2]\} R_{dc} \quad (3.15)$$

where  $2r$  is the outside diameter of the conductor.

At high frequencies, where  $\delta \ll 2r$ , this equation simplifies to

$$R_{ac} = [r / (2\delta)] R_{dc} \quad (3.16)$$

Because the skin depth is inversely proportional to the square root of the frequency, the resistance  $R_{ac}$  will increase proportionally to the root of the frequency, that is, if  $\delta \ll d$  (where  $d$  is the diameter of the conductor).

The skin depths for some materials are given in Table 3.5 as a function of the frequency.

As an illustration of the change in skin depth with frequency, consider the skin depth for copper at various frequencies:

$$\delta = 0.66 \text{ mm at } 10 \text{ kHz}$$

$$\delta = 66 \mu\text{m at } 1 \text{ MHz}$$

$$\delta = 6.6 \mu\text{m at } 100 \text{ MHz}$$

Because the skin depth is very small at high frequencies, it is important to ensure

that conductor surfaces are smooth if the lowest possible resistance with a specific material is required. When materials with low conductivities are used (usually to ensure temperature stability), it becomes worthwhile to plate the conductors with silver above 100 MHz.

To get an idea of the increase in resistance with frequency caused by the skin effect, consider the resistance of 1 m of AWG No. 22 wire as a function of frequency:

$$R = 0.06 \Omega \text{ at dc}$$

$$R = 0.60 \Omega \text{ at } 1 \text{ MHz}$$

$$R = 5.95 \Omega \text{ at } 100 \text{ MHz}$$

Note that the resistance at 100 MHz is approximately  $100^{1/2}$  times that at 1 MHz.

It is obvious from these numbers that the increase in resistance caused by the skin effect cannot be ignored at high frequencies.

### 3.3.4 The Proximity Effect

A conductor carrying alternating current has a changing magnetic field around it. If another conductor is brought close to it (see Figure 3.5), the changing magnetic field through or around it will cause eddy current losses in it (when  $d > 5\delta$ , the penetration depth of the field is small compared to the diameter). These losses are reflected in the first conductor as increased resistance.

Similar to the skin effect, the increase in resistance is proportional to the root of the frequency at high frequencies ( $d > 5\delta$ ).

When only two conductors are in close proximity, the influence of the proximity effect is relatively small compared to that of the skin effect, but when more conductors are used it should be taken into account. Because a solenoidal coil consists of many conductors close to one another, the proximity effect can significantly affect its resistance at high frequencies. As an example of this, the resistance of a single-layer solenoidal coil with its touching and a length-to-diameter ratio of 0.7 is almost six times that of the same coil when straightened out (that is, if more than 10 turns are used).

When the turns of a coil are spaced well apart, the proximity effect can be ignored.

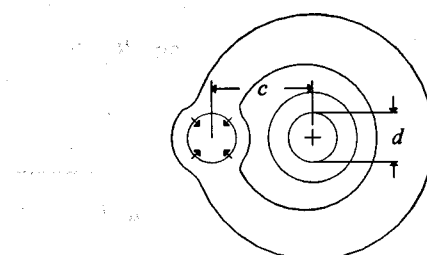


Figure 3.5 The proximity effect.

### 3.3.5 Magnetic Materials

The inductance of an air-cored coil can be increased significantly by using a magnetic material as the core. The reason for this is that the magnetic flux density increases substantially when the relative permeability of the material is high.

Typical values for the relative permeability ( $\mu_r$ ) of ferrite materials at radio frequencies are 10–150. The higher value is associated with cut-off frequencies on the order of 20 MHz, while lower value is associated with cut-off frequencies of around 1 GHz. Above the cut-off frequency, the relative permeability decreases sharply.

Apart from the relative permeability and its frequency dependence, losses in magnetic materials must also be taken into account, especially at high voltage points.

When ferrite materials are used, these losses are mainly hysteresis losses. When materials with higher conductivities are used, the eddy-current losses in the material also become significant.

Losses in a ferrite core are proportional to the energy stored in it. The energy stored is proportional to the energy density and the volume of the core. The volume is approximately equal to the product of the cross-sectional area and the mean path length. Therefore, losses in a ferrite core are given by an equation of the form

$$P_{\text{loss}} = k(\mu_r, f, B_{\text{max}}) B_{\text{max}}^2 Al \quad (3.17)$$

where  $A$  is the average cross-sectional area of the core,  $l$  the mean path length of the core,  $B_{\text{max}}$  the maximum root mean square (rms) flux density in the core, and  $k$  a constant dependent on the frequency, relative permeability, flux density, and material used.

The power losses in a ferrite core are best specified in terms of the ratio  $\mu_r R_p / L$  and not by (3.17).  $R_p$  is the loss resistance in parallel with the inductance ( $L$ ) of the magnetic-cored inductor.

This ratio is independent of the core dimensions and is only a function of the material used and the maximum flux density. That the ratio  $\mu_r R_p / L$  should be independent of the core size can be established as follows.

Because  $R_p$  represents the losses in the core, the power loss in the core is given by

$$P_{\text{loss}} = V_p^2 / R_p \quad (3.18)$$

where  $V_p$  is the rms voltage across the inductor.

This voltage is related to the maximum flux density  $B_{\text{max}}$  by

$$V_p = j\omega(N\Phi) = j\omega NAB_{\text{max}} \quad (3.19)$$

where  $N$  is the number of turns.

By using these two equations, the resistance  $R_p$  is found to be

$$R_p = V_p^2 / P_{\text{loss}}$$

$$\begin{aligned}
 &= \frac{\omega^2 N^2 A^2 B_{\max}^2}{P_{\text{loss}}} = \frac{\omega^2 N^2 A^2 B_{\max}^2}{k A l B_{\max}^2} \\
 &= [\omega^2 / k] N^2 A / l
 \end{aligned} \tag{3.20}$$

The resistance  $R_p$  is, therefore, proportional to the square of the number of turns and the cross-sectional area of the coil. It is inversely proportional to the mean path length.

This is also true for the inductance, which is given by

$$L = \frac{\Lambda}{I} = \frac{N\Phi}{I} = \mu_0 \mu_r N^2 \frac{A}{l} \tag{3.21}$$

The ratio  $\mu_r R_p / L$  is, therefore, independent of the core dimensions.

By using (3.20) and (3.21), it follows that

$$\mu_r R_p / L = \omega^2 / (k \mu_0) \tag{3.22}$$

Because  $k$  is a function of the flux density and the frequency, the ratio  $\mu_r R_p / L$  is so a function of the flux density and the frequency.

Curves for this ratio as a function of frequency are shown in Figure 3.6 [8]. These curves apply at small-signal conditions (that is, when  $B_{\max}$  is small).

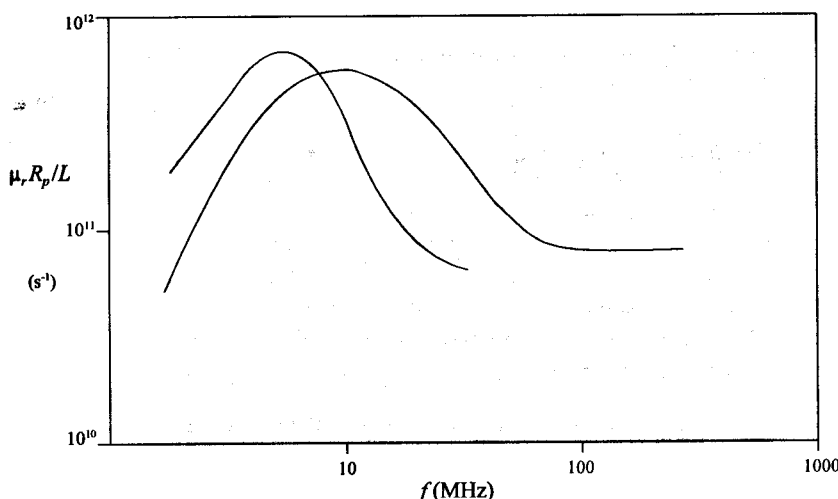
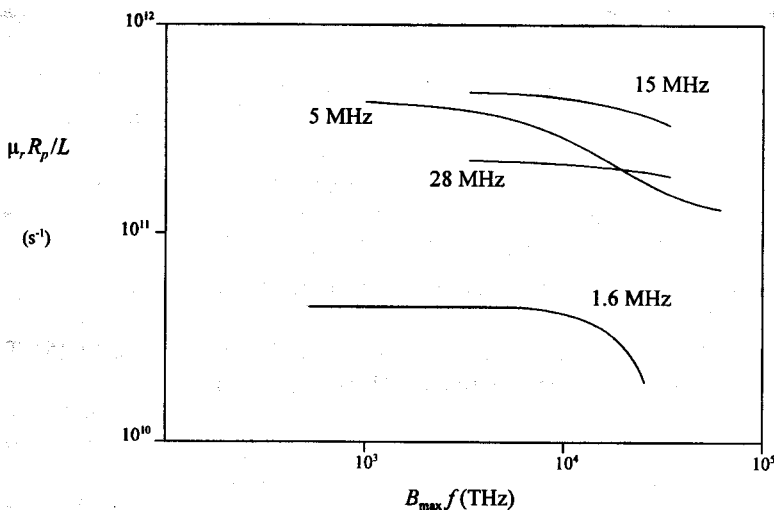


Figure 3.6 Curves of the ratio  $\mu_r R_p / L (\omega \mu_r / \tan \delta)$  plotted against frequency for two ferrite materials ( $B_{\max} = 0$ ) (Source: [8]).

By using these curves and a value of 120 for the relative permeability, it can be shown easily that the highest unloaded  $Q$  ( $Q_u = R_p / (\omega L)$ ) that can be expected at 6 MHz by using 4C6 material is approximately 125.

When the flux density increases, the losses in the core increase as well. Curves for the ratio  $\mu_r R_p / L$  as a function of the product  $B_{\max} f$  are shown for 4C4 material at different frequencies in Figure 3.7.

The product  $B_{\max} f$  is used because it is independent of the frequency if the maximum voltage across the inductor ( $V_p$ ) is assumed to be constant.



**Figure 3.7** Curves of  $\mu_r R_p / L$  ( $\omega \mu_r / \tan \delta$ ) plotted against the product  $(B_{\max} f)$  for 4C4 material at various frequencies (Source: [8]).

By using the curve for 1.6 MHz, it follows that the losses double from their small-signal value when the flux density is approximately 14 mT (140 Gauss).

As a final remark on magnetic materials, it should be noted that the relative permeability of magnetic materials is temperature-dependent. Materials with higher permeabilities are influenced more by temperature changes.

Because the temperature of the material changes when heat is dissipated in it, the relative permeability will also change when more power is dissipated in it.

## Summary

The following points should be taken into account when a magnetic material is selected for a particular purpose:

1. The highest frequency of operation;
2. The maximum allowable amount of losses;
3. The size of the inductor and, therefore, the relative permeability;
4. The temperature dependence of the magnetic material.

### 3.3.6 The Design of Single-Layer Solenoidal Coils

Single-layer solenoidal coils are often used at radio frequencies. Their use is limited by the inductance values and unloaded  $Q$ -factors obtainable, as well as by the associated parasitic capacitance.

The inductance of a single-layer solenoidal coil is given approximately by

$$L = N^2 r / [22.91/r + 25.4] \quad (\mu\text{H}) \quad (3.23)$$

where  $r$  is the mean radius of the coil (in centimeter),  $l$  the length of the coil (in centimeter), and  $N$  the number of turns.

The parasitic capacitance of these coils is given in Figure 3.3 as a function of the length-to-diameter ratio ( $l/D$ ) and the radius of the coil. The capacitance is small when the coil radius is small.

The unloaded  $Q$  of air-cored coils is a function of the frequency, inductance, dc resistance, skin effect, proximity effect, and self-capacitance of the coil.

At frequencies where the self-capacitance can be neglected, the unloaded  $Q$  is given by [6]

$$Q_u = kr \sqrt{f} \quad (3.24)$$

where the radius must be specified in centimeters and the frequency in Hertz.

The factor  $k$  depends on the length-to-diameter ratio of the coil and the relative spacing of the turns. Its value is plotted in Figure 3.8 for various coil shapes and wire spacing ratios ( $d/c$ ), where  $c$  is the distance between the centers of two adjacent turns and  $d$  the diameter of the wire used.

The following facts can be deduced from the curves in Figure 3.8 and (3.24):

1. Higher unloaded  $Q$ -factors can be obtained by using coils with larger diameters and length-to-diameter ratios ( $l/D$ ).
2. The turns of an air-cored solenoidal coil should be spaced close enough to ensure that the  $d/c$  ratio is larger than  $0.4 d$ , and in shorter coils ( $l/D \approx 1$ ) they should be spaced far enough apart to ensure that the  $d/c$  ratio is smaller than  $0.8 d$ .

When larger coils are used the turns can touch without any significant reduction in the unloaded  $Q$  (less than 25%).

By using the curves in Figure 3.8 and the equations given, solenoidal coils can be designed to have a specified inductance and unloaded  $Q$ . The parasitic capacitance can be determined by using the curve in Figure 3.3. The design can be done as summarized below.

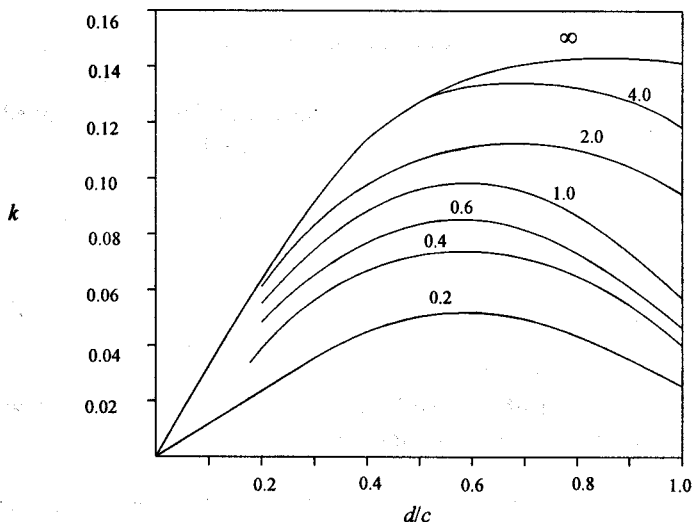


**Figure 3.8** Curves for calculating the unloaded  $Q$  of single-layer solenoidal coils at high frequencies. (Source: [6]).

### A Design Procedure for Controlling the Inductance and Quality Factor of an Air-Cored Solenoidal Coil

1. Choose the length-to-diameter ratio ( $l/D$ ) equal to 1.
2. Calculate the radius ( $r$ ) of the coil (in centimeter) by using the equation

$$r = Q_u / (k \sqrt{f}) \quad (3.25)$$

where  $Q_u$  is the unloaded  $Q$  required, and  $k = 0.1$  for  $l/D = 1.0$  (see Figure 3.8).

3. Find the parasitic capacitance of the coil by using Figure 3.3. Calculate the resonant frequency by using the equation

$$f_r = 1 / \sqrt{LC} / (2\pi) \quad (3.26)$$

where  $C/D = 0.45 \text{ pF/cm}$  for  $I/D = 1$ .

4. If the resonant frequency is too low, the specifications cannot be reached and it will have to be changed.
5. Calculate the required number of turns by using the equation

$$N = [L(22.9(l/r) + 25.4)/r]^{1/2} \quad (3.27)$$

6. Calculate the required wire thickness by using the  $d/c$  ratio used in step 2:

$$d = (d/c)[l/(N-1)] = (l/D)(d/c)[2r/(N-1)] \quad (3.28)$$

where  $d$  is the wire diameter to be used, and  $d/c = 0.55$  for  $I/D = 1$  (see Figure 3.8).

7. If the required wire thickness is small, a coil former will be needed. If the coil is to be self-supporting, it can be redesigned.

In order to increase the wire diameter, it will be necessary to increase the size of the coil. When the resonant frequency is a potential problem, the  $I/D$  ratio can be increased. The resonant frequency will decrease if the radius is increased.

Where the resonant frequency is not a problem, the radius of the coil can be increased in order to increase the wire diameter. The maximum value of the radius is

$$r_{\max} = C_m / (2C) \quad (3.29)$$

where  $C_m$  is the maximum self-capacitance allowable, and  $C$  is the capacitance per centimeter as given by Figure 3.3.

With  $I/D = 1$ ,  $C = 0.45 \text{ pF/cm}$ .

### **EXAMPLE 3.1** Designing a single-layer air-cored solenoidal coil to have a specified $Q$ and resonant frequency.

As an example of the application of the procedure outlined, a  $1 \mu\text{H}$  coil was designed to have a minimum unloaded  $Q$  of 300 at 50 MHz and resonant frequency above 250 MHz. The results of the different steps are as follows:

1.  $I/D = 1$
2.  $r = 0.42 \text{ cm}$

3.  $f_r = 256 \text{ MHz}$
4. —
5.  $N = 13$
6.  $d = 0.36 \text{ mm}$
7. Because the wire diameter is small, it will be necessary to use a coil former.

It is not possible to increase the wire diameter by increasing the coil radius in this case ( $f_r = 250 \text{ MHz}$ ). It is possible, however, to increase it by increasing the  $I/D$  ratio of the coil.

Unfortunately, it is not possible to increase sufficiently the wire thickness to make the coil self-supporting.

The results for different  $I/D$  ratios are compared in Table 3.6. Note that the wire diameter can be doubled if the length-to-diameter ratio is chosen to be equal to 4.

Although the wire thickness is a strong function of the length-to-diameter ratio, the resonant frequency of coils with length-to-diameter ratios from 0.6 to 4 does not vary significantly if they are designed to have the same unloaded  $Q$ -factor.

The volumes of the coils in Table 3.6 increase with increasing  $I/D$  ratio. When a small coil is required, the length-to-diameter ratio can therefore be chosen to be equal to 0.6.

**Table 3.6**

The dimensions, unloaded  $Q$ , and resonant frequency for a  $1 \mu\text{H}$  coil as a function of the  $I/D$  ratio

$I/D$	$r$ (cm)	$N$	$d$ (mm)	$d/c$	$f_r$ (MHz)	$Q_u$
0.6	0.48	10	0.31	0.55	252	300
1.0	0.42	13	0.36	0.55	256	300
2.0	0.37	18	0.52	0.63	255	300
4.0	0.32	26	0.63	0.63	242	300

The capacitance,  $k$ -factor, and optimum  $d/c$  ratio for coils with the  $I/D$  ratios used in Table 3.6 are tabulated in Table 3.7 for convenience.

When resonant circuits with high  $Q$ -factors are designed, the unloaded  $Q$ -factors of the coils and capacitors used must be as high as possible. In order to determine the maximum realizable unloaded  $Q$  possible for a single-layer air-cored coil, it is necessary

to determine the optimum  $I/D$  ratio. Because, in (3.24),

$$Q = k r \sqrt{f}$$

(see (3.24)) the length-to-diameter ratio influences the unloaded  $Q$  directly through the associated value of the constant,  $k$ , and indirectly (through  $r$ ) because of the limit that exists on the self-capacitance of the coil.

The maximum radius corresponding to a particular  $I/D$  ratio can be determined by using (3.29).

**Table 3.7**

The self-capacitance,  $d/c$  ratio, optimum value of  $k$  ( $k_{\text{opt}}$ ), and the ratio of the  $k$  and the self-capacitance per centimeter for coils with different  $I/D$  ratios

$I/D$	$C$ (pF/cm)	$d/c$	$k_{\text{opt}}$ (Hz/cm)	$k/C$ (pF/Hz)
0.6	0.44	0.55	0.088	0.200
1.0	0.45	0.55	0.100	0.222
2.0	0.53	0.63	0.115	0.216
4.0	0.68	0.63	0.133	0.196

By substituting the value for  $r$  as given by (3.29) into (3.24), the maximum  $Q$  corresponding to a particular  $I/D$  ratio is found to be

$$Q_{\text{max}} = (k_m / C) \sqrt{f} C_{\text{max}} \quad (3.30)$$

where  $k_m$  is the maximum value of  $k$  corresponding to the particular  $I/D$  ratio,  $C$  is the capacitance per centimeter as given by the curve in Figure 3.3, and  $C_{\text{max}}$  is the maximum value of the self-capacitance as determined from the specified resonant frequency.

The influence of the  $I/D$  ratio on the unloaded  $Q$  is clearly limited to the first term in (3.30). The  $k/C$  ratios for different  $I/D$  ratios are compared in the last column of Table 7. It follows from this comparison that the highest  $Q$  will be obtained when the length-to-diameter ratio of the coil is equal to 1.

At this stage, the highest  $Q$  realizable with a single-layer solenoidal air-cored coil can be determined for any particular inductance value if the operating frequency and the self-resonant frequency are specified. The following procedure can be followed in order to determine the  $Q$ .

### Design Procedure for Maximum $Q$ and Specified Inductance

1. Choose  $I/D = 1$ .

2. Determine the maximum value of the self-capacitance ( $C_{\max}$ ). If the coil is to be used in a parallel resonant circuit, the self-resonant frequency can be chosen close to the resonant frequency of the circuit.

Calculate the maximum allowable radius of the coil by using the equation

$$r_{\max} = C_{\max} / (2C) = C_{\max} / 0.9 \quad (\text{cm}) \quad (3.31)$$

with  $C_{\max}$  specified in picofarads (pF).

If the value of the radius is unrealistically high, reduce it to an acceptable value.

3. Determine the maximum realizable unloaded  $Q$  by using (3.24):

$$Q_{\max} = 0.10 r_{\max} \sqrt{f} \quad (3.32)$$

4. Calculate the required thickness of the wire:

$$N^2 = 71.2 L / r_{\max} \quad (3.33)$$

where the inductance ( $L$ ) is specified in  $\mu\text{H}$  and  $r_{\max}$  in centimeter.

$$c = l / (N - 1) = 2r_{\max} / (N - 1) \quad (3.34)$$

$$d = 0.55 c \quad (\text{cm}) \quad (3.35)$$

If the wire thickness turns out to be unrealistic, change the radius.

### EXAMPLE 3.2 Designing a single-layer solenoidal coil for maximum $Q$ .

The highest possible  $Q$  will be determined for a coil of  $10\mu\text{H}$  at  $5 \text{ MHz}$  with self-resonant frequency at  $10 \text{ MHz}$  by following the procedure outlined above.

1.  $I/D = 1$

2.  $C_{\max} = 1 / [(2\pi \times 10 \times 10^6)^2 10 \times 10^{-6}]$   
 $= 25.3 \text{ pF}$

$$r_{\max} = 25.3 / 0.9 \\ = 28.1 \text{ cm}$$

3.  $Q_{\max} = 0.10 r_{\max} (f)^{1/2}$   
 $= 6286!$

$$4. \quad N^2 = 71.2 \times 10 / 28.1 = 25.3$$

$$N = 5.0$$

$$c = 2 \times 28.1 / (5-1) \\ = 14.1 \text{ cm}$$

$$d = 0.55 c \\ = 7.73 \text{ cm!}$$

If the coil size is limited to 3 cm by 3 cm by 3 cm, the maximum realizable  $Q$  will be 335.

### 3.3.7 The Design of Inductors with Magnetic Cores

Smaller inductors with less parasitic capacitance can be designed by using magnetic materials.

The core can be a rod, a toroid, a balun, or stacked toroids (see Figure 3.9).

Rods are often used if the inductor is to be tuned, while toroids and baluns are used for fixed-value inductors. Stacked cores can be used as an alternative to a balun.

The type of material used is a function of the frequency range over which the inductor is to be used, the desired unloaded  $Q$ , the available space, and the temperature range.

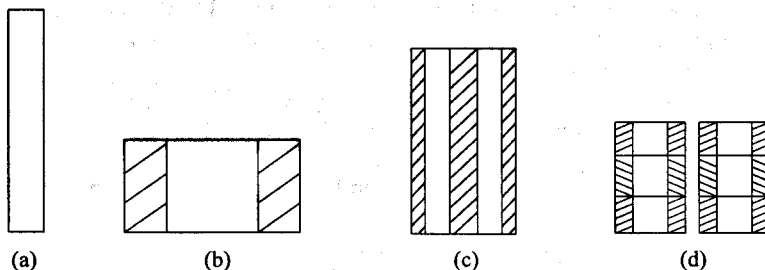


Figure 3.9 Different types of magnetic cores: (a) rod core, (b) toroid, (c) balun core, and (d) stacked toroids.

The unloaded  $Q$  is determined by the flux density in the core and, therefore, by the maximum voltage across the inductor, the number of turns, and the frequency.

Materials with a high relative permeability are usually very sensitive to changes in temperature.

With the material and type of core selected, the size of the core must be determined.

The core must be large enough for the flux density to be sufficiently low to ensure that the desired unloaded  $Q$  is realized and that the required number of turns can be accommodated.

The selection of the minimum core size for toroidal (single and stacked) inductors will be discussed in the next two sections. If a balun is to be used, the results for stacked cores can be applied to get an idea of the size required.

### 3.3.7.1 The Design of an Inductor with a Single Toroidal Core

The inductance of a toroidal core inductor is given by

$$L = \partial\phi / \partial i = \mu_0 \mu_r N^2 A / l \quad (3.36)$$

The value of the product  $\mu_r R_p / L$  can be determined from the unloaded  $Q$  ( $Q_u$ ) by using the following equation:

$$\mu_r R_p / L = \mu_r \omega R_p / (\omega L) = 2\pi \mu_r f Q_u \quad (3.37)$$

The flux density corresponding to this ratio ( $B_{maxA}$ ) can be determined, where given, from the manufacturer's specifications (see Figure 3.7 for an example).

The flux density in the core is given by

$$B_{max} = V_{max} / (\omega AN) \quad (3.38)$$

The flux density in the core must be less than or equal to the maximum allowable value  $B_{maxA}$ .

If the number of turns in (3.36) is replaced by using (3.38), the product of the cross-section area of the core ( $A$ ) and the mean path length ( $l$ ) is found to be

$$Al = [\mu_r \mu_0 / (\omega B_{maxA}^2)] V_{max}^2 / (\omega L) \quad (3.39)$$

The required core size can now be found by comparing this product with that of available cores.

If a core with the required  $Al$ -product is not available, a core with a larger  $Al$ -product can be chosen. The number of turns required must then be calculated by using (3.36). The alternative is to use more than one core (smaller) to obtain the required  $Al$ -product.

With the core dimensions known, the number of the turns required can be found by using (3.38).

The following procedure can be followed to design an inductor with a toroidal core.

#### A Design Procedure for an Inductor with a Toroidal Core

1. Select a suitable material. Take the frequency range, temperature range

required unloaded  $Q_u$  and inductor size into account.

2. Calculate the  $\mu_r R_p / L$  ratio at the lowest frequency by using (3.37):

$$\mu_r R_p / L = 2\pi \mu_r f Q_u$$

where  $Q_u$  is the desired value of the unloaded  $Q$ .

3. Find the flux density corresponding to the calculated  $\mu_r R_p / L$  ratio from the manufacturer's specifications.
4. Calculate the required  $Al$ -product by using (3.39):

$$Al = \mu_r \mu_0 / (\omega B_{\max}^2 A) V_{\max}^2 / (\omega L)$$

5. Compare this product to that of available cores. Select a core with an  $Al$ -product equal or close to it. If the difference in  $Al$ -product is significant, choose the core with an  $Al$ -product greater than that required.  
Alternatively, smaller cores can be combined to obtain the required  $Al$ -product (see Section 3.3.7.2).
  6. Calculate the required number of turns by using (3.36):
- $$L = \mu_r \mu_0 N^2 A / l$$
7. Check if there is enough space to accommodate the required number of turns of the conductor with the required thickness. If the core is too small, a larger toroid must be used.

**Table 3.8**  
A list of typical magnetic core sizes

Core	$A$ ( $\mu\text{m}^2$ )	$l$ (mm)	$Al$ ( $\mu\text{m}^3$ )	Size (mm $^3$ )
1	12.5	36	0.44	14×9×5
2	31.5	57	1.80	23×14×7
3	37.5	75	2.81	29×19×7.5
4	65.0	92	5.98	36×23×10
5	97.5	92	8.97	36×23×15

### EXAMPLE 3.3 Finding the core size required for an inductor.

As an example of the application of the procedure outlined here, the core size for a magnetic-cored inductor with  $31.4\Omega$  reactance at 2 MHz, and loss resistance

equal to  $392\Omega$ , will be determined. The maximum rms voltage across the inductor will be 20V and 4C4 material is available. Note that  $\mu_r = 120$ .

The  $\mu_r R_p / L$  ratio for the inductor is

$$\frac{\mu_r R_p}{L} = \frac{120 \times 392}{31.4 / (2\pi \times 2 \times 10^6)} = 1.88 \times 10^{10} \text{ s}^{-1}$$

By using the 1.6 MHz curve given for 4C4 material in Figure 3.7, the  $(B_{\max} f)$  product corresponding to a  $\mu_r R_p / L$  ratio of  $1.8 \times 10^{10} \text{ s}^{-1}$  is found to be  $2 \times 10^4 \text{ THz}$ . The maximum allowable flux density in the core is, therefore, 0.01 T.

The  $Al$ -product of the required core can be found by using (3.39). The required  $Al$ -product is  $1.53 \times 10^{-6} \text{ m}^3$ .

By comparing this value to those in the list of some  $Al$ -products given in Table 3.8, it can be seen that the core with  $Al$ -product equal to  $1.8 \mu\text{m}^3$  ( $A = 31.5 \mu\text{m}^2$ ;  $l = 57\text{mm}$ ;  $23 \times 14 \times 7 \text{ mm}^3$ ) can be used.

The number of turns required is

$$N = \sqrt{L l / (\mu_0 \mu_r A)} = 5.5$$

The selected core can accommodate the required number of turns with ease.

### 3.3.7.2 The Design of an Inductor with a Stacked Toroidal Core

The design of an inductor with a stacked toroidal core is similar to that of an inductor with a single core, except for the fact that the cross-sectional area ( $A$ ) used in the previous section must now be taken as  $N_c A$ , where  $N_c$  is the number of toroids used (an even number) and  $A$  is the cross-sectional area of a single toroid. The mean path length is that of a single toroid.

The inductance of a stacked core inductor is given by the equation

$$L = \mu_r \mu_0 N^2 (N_c A / l) \quad (3.40)$$

The maximum flux density is

$$B_{\max} = V_{\max} / [\omega (N_c A) N] \quad (3.41)$$

and the required  $Al$ -product is obtained from

$$N_c Al = [\mu_r \mu_0 / (\omega B_{\max}^2)] V_{\max}^2 / (\omega L) \quad (3.42)$$

## 3.4 TRANSMISSION LINES

The transmission lines used at radio frequencies are usually coaxial cables (flexible (F) or semi-rigid (SR)), microstrip lines, or twisted pairs. The important characteristics of these lines are the characteristic impedance, the insertion loss, and the power-handling capability.

The characteristics of coaxial cables, microstrip lines, and twisted pairs will be discussed briefly.

### 3.4.1 Coaxial Cables

The characteristic impedance of a coaxial cable is given by

$$Z_0 = (138 / \sqrt{\epsilon_r}) \log_{10}(b/a) \quad (3.43)$$

where  $a$  is the outer diameter of the inner conductor (centimeter) and  $b$  is the inner diameter of the outer conductor (in centimeter).

The attenuation of the cable is given by [10]

$$\alpha = (3.615 / Z_0) (K_1 / a + K_2 / b) T \sqrt{f} + 9.121 f \sqrt{\epsilon_r} \tan \delta \quad (3.44)$$

where

$\alpha$  is the attenuation in decibels/100m;

$K$  is the square root of the ratio of the resistivity of copper to that of the particular conductor;

$f$  is the operating frequency in megahertz;

$T = [1 + 0.0039(t - 20)]^{1/2}$ , where  $t$  is the operating temperature in degrees Celsius;

$a$  is the inner conductor outer diameter in centimeter;

$b$  is the outer conductor inner diameter in centimeter;

$\tan \delta$  is the loss tangent of the inner conductor insulation.

The attenuation is increasing with frequency because of the skin effect and the losses in the dielectric material.

The power-handling capability of a coaxial cable is limited by the maximum allowable temperature. This is a function of the insulation used (200°C for polytetrafluoroethylene), the diameter of the cable, and the environmental temperature.

The power-handling capability and attenuation along some coaxial cables are given in Table 3.9 [11]. Note the decrease in power-handling capability with increasing frequency.

Semi-rigid coaxial cable is often used for transmission-line transformers in the VHF and UHF ranges.

Coaxial lines with characteristic impedances of  $50\Omega$  and  $25\Omega$  are freely available. Lower impedances can be obtained by connecting cables in parallel, while higher imped-

**Table 3.9**

The attenuation and average power-handling capabilities of some coaxial cables (F:Flexible cable; SR:Semi-rigid cable) at different frequencies

Cable Type	$\alpha$ (dB/m) ( $P$ (W))			
	@ 1 MHz	@ 10 MHz	@ 100 MHz	@ 500 MHz
50Ω; 1.7 mm (F)	0.04 (1k)	0.14 (300)	0.44 (90)	—
50Ω; 2.8 mm (F)	0.03 (1k)	0.08 (800)	0.27 (250)	—
50Ω; 1.1 mm (SR)	—	—	0.35 (68)	0.75 (32)
50Ω; 2.2 mm (SR)	—	—	0.18 (330)	0.43 (140)
50Ω; 6.4 mm (SR)	—	—	0.11 (1.17k)	0.25 (515)

ances can be obtained by connecting lines with lower impedances in series (using semi-rigid cable). By doing the latter, the effective capacitance is decreased. The series connection is shown in Figure 3.10.

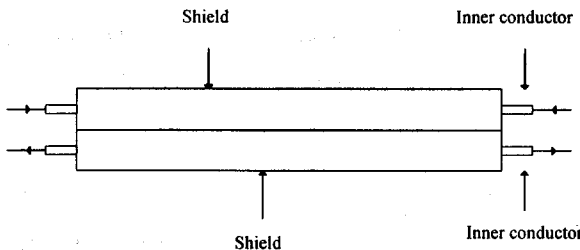


**Figure 3.10** Increasing the characteristic impedance of a coaxial cable by connecting two cables in series.

### 3.4.2 Microstrip Transmission Lines

The characteristic impedance ( $Z_0(f)$ ) and the effective relative dielectric constant ( $\epsilon_{r,\text{eff}}(f)$ ) of a microstrip line is a function of the width-to-height ratio ( $W/h$ ), the conductor thickness ( $t$ ), cover height ( $H_2$ ), and frequency ( $f$ ). The characteristic impedance is also a function of the effective dielectric constant.

The characteristic impedance ( $Z_0(f)$ ) and effective relative dielectric constant ( $\epsilon_{r,\text{eff}}(f)$ ) can be computed by using the following set of equations [12, 13]:

$$W_{\text{eff}} = W + \frac{t}{\pi} \left\{ 1 + \ln 4 - 0.5 \ln \left[ \left( \frac{t}{h} \right)^2 + \left( \frac{t}{\pi W} \right)^2 \right] \right\} \quad (3.45)$$

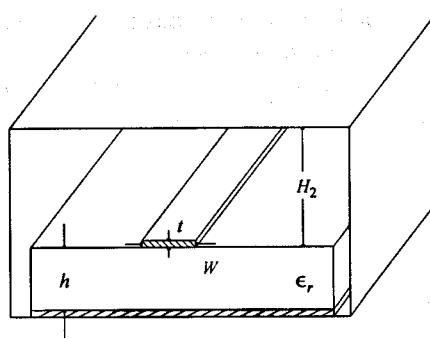


Figure 3.11 The geometry of a microstrip line.

$$f(W/h) = 6 + (2\pi - 6) \text{EXP} \left[ - \left( \frac{30.666}{W/h} \right)^{0.7528} \right] \quad (3.46)$$

$$Z_{0,\infty} = 60 \ln \left[ \frac{f(W/h)}{W/h} + \left[ 1 + \left( \frac{2h}{W} \right)^2 \right]^{1/2} \right] \quad (3.47)$$

$$P = 270 \left\{ 1 - \tanh \left[ 1.192 + 0.706 (1 + H_2/h)^{1/2} - \frac{1.389}{1 + H_2/h} \right] \right\} \quad (3.48)$$

$$\begin{aligned} Q &= 1.0109 - \tanh^{-1} \{ [0.012 W/h + 0.177 (W/h)^2 - 0.027 (W/h)^3] \\ &/ [1 + H_2/h]^2 \} \end{aligned} \quad (3.49)$$

$$Z_{\gamma_d} = Z_{0,\infty} - PQ \quad (3.50)$$

$$b = -0.564 \left( \frac{\epsilon_r - 0.9}{\epsilon_r + 3.0} \right)^{0.053} \quad (3.51)$$

$$\begin{aligned} a &= 1 + (1/49) \ln \{ (W/h)^2 [(W/h)^2 + 1/52^2] / [(W/h)^4 + 0.432] \} \\ &+ (1/18.7) \ln \{ 1 + [W/(18.1h)]^3 \} \end{aligned} \quad (3.52)$$

$$\gamma = ab \quad (3.53)$$

$$\begin{aligned} &\{ [1 + 10h/W]^j - 2[(\ln 2)/\pi] (t/h)/(W/h)^{1/2} \} \\ &\tanh [1.043 + 0.121(H_2/h) - 1.164/(H_2/h)] \end{aligned} \quad (3.54)$$

$$\epsilon_{\text{eff}} = \frac{\epsilon_r + 1}{2} + q \frac{\epsilon_r - 1}{2} \quad (3.55)$$

$$Z_0 = Z_{0a} / \sqrt{\epsilon_{\text{eff}}} \quad (3.56)$$

$$v_p = c / \sqrt{\epsilon_{\text{eff}}} \quad (3.57)$$

where  $v_p$  is the phase velocity in the microstrip,

$$f_p = Z_0 / [2\mu_0 h] \quad (3.58)$$

$$G = (\pi^2 / 12)[(\epsilon_r - 1) / \epsilon_{\text{eff}}](Z_0 / 60)^{1/2} \quad (3.59)$$

$$\epsilon_{r-\text{eff}}(f) = \epsilon_r - \frac{\epsilon_r - \epsilon_{\text{eff}}}{1 + G(f/f_p)^2} \quad (3.60)$$

$$s = \frac{c^2}{4f^2[\epsilon_{r-\text{eff}}(f) - 1]} \quad (3.61)$$

$$y = s/3 - (W/3)^2 \quad (3.62)$$

$$W_{\text{eff}}(0) = 120\pi h / [Z_0 \sqrt{\epsilon_{\text{eff}}}] \quad (3.63)$$

$$P = (W/3)^3 + (s/2)[W_{\text{eff}}(0) - W/3] \quad (3.64)$$

$$r = (P^2 + y^3)^{1/2} \quad (3.65)$$

$$W_{\text{eff}}(f) = W/3 + [r + p]^{1/3} - [r - p]^{1/3} \quad (3.66)$$

$$Z_0(f) = \frac{120\pi h}{W_{\text{eff}}(f) \sqrt{\epsilon_{r-\text{eff}}(f)}} \quad (3.67)$$

The frequency dependence (dispersion) of the characteristic impedance and the effective dielectric constant of a microstrip line result from the non-TEM nature (inhomogeneity) of the mode of propagation along the microstrip.

As an example of the application of (3.45) to (3.67), the width-to-height ratios and the effective dielectric constants of a  $50\Omega$  line on an alumina ( $\epsilon_r = 10.2$ ) and a Teflon ( $\epsilon_r = 2.5$ ) substrate at 2 GHz with  $H_2/h = 20.0$  were calculated. The results, respectively, are as follows:

$$W/h = 0.85 \text{ with } \epsilon_{r,\text{eff}} = 6.6945$$

and

$$W/h = 2.75 \text{ with } \epsilon_{r,\text{eff}} = 2.0775$$

At microwave frequencies it also becomes necessary to take into account the losses (conductor and dielectric) in microstrip lines. The main source of these losses is usually conductor loss. The conductor loss attenuation constant  $\alpha_c$  is given by the following set of equations [14, 15]:

$$\alpha_c = \frac{8.68 R_s M}{2\pi Z_0 h} \left[ 1 + \frac{h}{W_{\text{eff}}} + \frac{h}{\pi W_{\text{eff}}} \left( \ln \frac{4\pi W}{t} + \frac{t}{W} \right) \right] \quad (W/h < 1/(2\pi))$$

$$\alpha_c = \frac{8.68 R_s M N}{2\pi Z_0 h} \quad 1/(2\pi) < (W/h) < 2$$

$$\alpha_c = \frac{8.68 R_s N}{Z_0 h} \left\{ \frac{W_{\text{eff}}}{h} + \frac{2}{\pi} \ln \left[ 2\pi \text{EXP} \left( \frac{W_{\text{eff}}}{2h} + 0.94 \right) \right] \right\}^{-2} \\ \left[ \frac{W_{\text{eff}}}{h} + \frac{W_{\text{eff}} / (\pi h)}{W_{\text{eff}} / (2h) + 0.94} \right] \quad (W/h) > 2 \quad (3.68)$$

$\alpha_c$  in decibels per centimeter.

$$\alpha_c = 1 - \left[ \frac{W_{\text{eff}}}{4h} \right]^2 \quad (3.69)$$

$$\alpha_c = h/W_{\text{eff}} + \frac{h}{\pi W_{\text{eff}}} \left[ \ln \frac{2h}{t} - t/h \right] \quad (3.70)$$

$$R_s = \sqrt{\pi f \mu_0 / \sigma} \quad (3.71)$$

where  $\sigma$  is the conductivity of the strip conductor.

At high frequencies, the copper losses are higher than those predicted by the equations above. This is due to the coarse interface between the dielectric material and the conductor. These losses are included in the dielectric losses by some manufacturers.

With the loss tangent ( $\tan \delta$ ) known, the attenuation constant corresponding to the dielectric losses in a microstrip line can be calculated by using the following equation [14, 16]:

$$\alpha_d = 27.3 \frac{\epsilon_r [\epsilon_{r-\text{eff}} - 1] \tan \delta}{\lambda_0 \sqrt{\epsilon_{r-\text{eff}} [\epsilon_r - 1]}} \quad (\text{dB/cm}) \quad (3.72)$$

where  $\lambda_0$  is the operating wavelength.

Materials with dissipation factors of 0.00085 at 1 MHz and 0.0018 at 10 GHz are available. With such low values for the dissipative factor, the dielectric losses are usually small compared to the conductor losses. Silicon is an example of a material where the dielectric losses cannot be neglected.

As an example of the dissipative losses in a microstrip line, the insertion loss of an 8-in  $50\Omega$  line on an Epsilam-10® substrate is specified by the manufacturer to be approximately 0.1 dB at 100 MHz and 0.21 dB at 500 MHz (0.19 dB/wavelength).

The power-handling capability of a microstrip line is a function of the insertion loss, the breakdown voltage of the dielectric material, and the maximum allowable temperature of the line. If the thermal resistance of the substrate is known as a function of the line width, the maximum power-handling capability can be computed easily.

### 3.4.3 Twisted Pairs

Transmission lines with a wide range of characteristic impedances can be realized by twisting lengths of wire together.

The characteristic impedances of these twisted-pair lines decrease when thicker wire is used. For example, the characteristic impedance is  $35\Omega$  when No. 20 (AWG) enamel-insulated wire with three twists per centimeter is used and is  $120\Omega$  when No. 30 vinyl-coated wire (0.05 cm outside diameter) with 3.6 twists per centimeter is used [17].

Increasing the number of twists per centimeter also decreases the characteristic impedance of these transmission lines. For example, the characteristic impedance obtained by twisting two No. 20 enamel-insulated wires together decreases from approximately  $42\Omega$  to  $30\Omega$  when the number of twists is doubled from two to four [17].

A line with  $50\Omega$  characteristic impedance can be obtained by twisting two No. 22 enamel-insulated wires together to have 2.5 twists per centimeter.

Characteristic impedances lower than  $10\Omega$  are often required in the HF range. These

impedances can be realized by twisting together many wires (using two-wire lines) with smaller diameters.

It is difficult to calculate the losses in these transmission lines because the dielectric losses, skin effect, proximity effect, and the fact that the current is flowing in both directions along the line must be taken into account. It is, therefore, easier to determine the attenuation of these lines practically.

The losses in twisted-wire transmission lines are usually not a problem below 100 MHz.

## REFERENCES

1. Krauss, H. L., W. B. Bostian, and F. H. Raab, *Solid State Radio Engineering*, New York: John Wiley and Sons, 1980.
2. *The RF Capacitor Handbook*, American Technical Ceramics, 1979.
3. "RF & Microwave Porcelain Capacitors," Cazenovia, NY: Dielectric Laboratories, Inc., 1998.
4. "Di-Cap Microwave Ceramic Capacitors," Cazenovia, NY: Dielectric Laboratories, Inc., 1998.
5. Hardy, K. H., *High Frequency Circuit Design*, Reston, VA: Preston Publishing Company, 1979.
6. Medhurst, R. G., "High Frequency Resistance and Capacity of Single-Layer Solenoids," *Wireless Engineer*, March 1947, p. 35.
7. "High-Performance Chip Coils for the Wireless Communication Industry," Franklin Park, IL: Stetco, Inc., 1998.
8. Hilbers, A. H., "On the Design of H. F. Wideband Power Transformers (ECO 6907)," Eindhoven: Philips C.A.B. Group, 1969.
9. Skilling, H. H., *Fundamentals of Electric Waves*, New York: John Wiley and Sons, 1948.
10. Coaxitube Semi-Rigid Coaxial Cable, North Wales, UK: Precision Tube Company, Inc., (n.d.).
11. Welsby, V. G., *The Theory and Design of Inductance Coils*, London: MacDonald and Co. Ltd., 1960.

12. March, S., "Microstrip Packaging: Watch The Last Step," *Microwaves*, December 1981.
13. Pues, H. F., and A. R. van de Capelle, *Electron. Letters*, Vol. 16, November 6, 1980, pp. 870-872.
14. Bahl, I. J., and D. K. Trevedi, "A Designer's Guide to Microstrip Line," *Microwaves*, May, 1977.
15. Pucel, R. A., D. J. Masse, and C. P. Hartwig, "Losses in Microstrip," *IEEE Trans. Microwave Theory Tech.*, Vol. MTT-16, June 1968, pp.342-350; "Correction to Losses in Microstrip," *Ibid.*, (Corresp.), Vol. MTT-16, December 1968, p. 1064.
16. Welsh, J. D., and H. J. Pratt, "Losses in Microstrip Transmission Systems for Integrated Microwave Circuits," *NEREM Rec.*, Vol. 8, 1966, pp. 100-101.
17. Krauss, H. L., and C. W. Allen, "Designing Toroidal Transformers to Optimize Wideband Performance," *Electronics*, August 16, 1973.

## SELECTED BIBLIOGRAPHY

- Snelling, E. C., *Soft Ferrites: Properties and Applications*, London: Iliffe Books Ltd., 1969.
- Howe, H. *Stripline Circuit Design*, Dedham, MA: Artech House, 1974.

## CHAPTER 4

# NARROWBAND IMPEDANCE-MATCHING WITH LC NETWORKS

### 4.1 INTRODUCTION

Impedance-matching networks are used for transforming impedances to certain required values, which may or may not be the conjugate of the source or the load impedance. When a source is conjugately matched to a load (i.e.,  $Z_L = Z_s^*$ ), maximum power is transferred between them. This is important when the power gain of a transistor is low, as is the case with most transistors at higher frequencies.

Apart from matching, impedance-matching networks are also often used to control the gain, the noise figure, or the output power of the different stages in an amplifier. These networks are more accurately referred to as control networks (gain, noise figure, or power control), but they are also generally referred to as impedance-matching networks.

When a matching network is designed for maximum power transfer, the terminations are usually known. The terminations to be used when a control network is designed are determined by the parameter to be controlled. This aspect will be considered in Chapter 10.

Independent of how the terminations are established, the design procedure for the matching network remains the same. The design of narrowband impedance-matching networks, mostly for maximum power transfer, will be considered in this chapter.

Narrowband impedance matching is done with two or more components. Where two components are used to bring about an impedance transformation, the matching network is called an L-section. Three-element matching networks are usually T- or PI-sections. The names are descriptive of the configuration formed by the reactive elements.

The design of L-, T-, and PI-sections will be discussed in this chapter. Transformation of real and reactive loads will be considered.

When T- and PI-sections are used, it is possible to bring about the required transformation and to control the bandwidth of the network. Although the 3-dB bandwidth of an L-section can be determined easily, it is not a design parameter.

It is sometimes necessary to know the bandwidth resulting from a transformation more accurately than is possible with the approximation method that is usually used. In these cases, as well as in instances where a bandwidth other than the 3-dB bandwidth is of interest, the procedure outlined in Section 4.9 can be used.

It was shown in Chapter 3 that lossless reactive components do not exist. For this reason, all impedance-matching networks will have some insertion loss. These losses can be quite pronounced when the bandwidth of a circuit is very narrow. A simple procedure for calculating the insertion loss caused by a cascaded LC network will be outlined in Section 4.8.

Apart from matching and transforming impedances, impedance-matching networks are sometimes also used to reject unwanted signals outside the pass band (this practice is not recommended when wideband impedance-matching networks are designed). The rejection required can often be obtained by using impedance-matching networks with high  $Q$ -factors, that is, if the rejection required is not too great.

The rejection obtainable by using parallel and series resonant circuits will be considered in Section 4.2.

When the required rejection becomes very high, the  $Q$  of the components, their temperature stability, and any tuning required can become a problem. If the associated insertion loss can be tolerated and the filtering occurs at low power levels, the required rejection can often be obtained by using surface acoustic wave (SAW) devices, ceramic filters, or crystal filters. These components are very stable and can provide extremely sharp rejection. Because of the impedances presented by these devices, some (low  $Q$ ) impedance matching is usually also required.

## 4.2 PARALLEL RESONANCE

A parallel resonant circuit is shown in Figure 4.1. Although it is not an impedance-matching network, it is of interest here because of its frequency response.

The frequency response of this circuit is determined by the zero at the origin, the zero at infinity, and the two poles. That is,

$$V_o(s) = Z(s) I$$

$$= I / [1 / R_L + sC + 1 / (sL)]$$

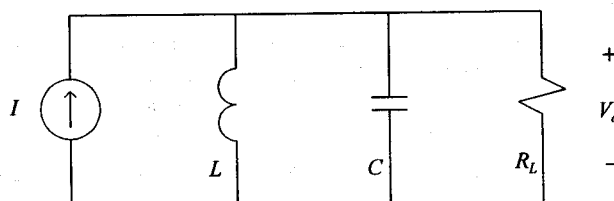


Figure 4.1 A parallel resonant circuit.

$$= \frac{sL I}{s^2 LC + sL / R_L + 1} \quad (4.1)$$

From Figure 4.1 it is obvious that the highest possible output voltage will occur where

$$\omega L = 1 / (\omega C)$$

that is, when

$$\omega_0 = 1 / \sqrt{LC} \quad (4.2)$$

The 3-dB frequencies of the circuit can be determined by using (4.1) and (4.2). These frequencies occur where

$$\begin{aligned} |1 / R_L + j\omega C + 1 / (j\omega L)| &= \sqrt{2} |1 / R_L + j\omega_0 C + 1 / (j\omega_0 L)| \\ &= \sqrt{2} / R_L \end{aligned} \quad (4.3)$$

After some manipulation, the solutions of this equation are found to be

$$\omega_{3dB} = \omega_0 \sqrt{1 + 1 / (4Q^2)} \pm 1 / (2RC) \quad (4.4)$$

Therefore, the bandwidth of the circuit is

$$B = \omega_{3dB\_2} - \omega_{3dB\_1} = 1 / (RC) \quad (\text{rad/s}) \quad (4.5)$$

It can be seen from (4.4) that the circuit response is not symmetrical around the resonant frequency  $\omega_0$ . It can be proved easily, however, that the resonant frequency is the geometric mean of the two cut-off frequencies by multiplying the two solutions given by (4.4), that is,

$$\omega_0 = \sqrt{\omega_{3dB\_1} \cdot \omega_{3dB\_2}} \quad (4.6)$$

The  $Q$ -factor of the circuit is defined as the ratio of the center frequency to the bandwidth; that is,

$$Q = \omega_0 / B \quad (4.7)$$

$$= \omega_0 CR \quad (4.8)$$

$$= R / (\omega_0 L) \quad (4.9)$$

A high  $Q$ , therefore, implies a very small relative bandwidth and, in the case of parallel resonance, reactances with low impedance compared to that of the load resistance. The reactances are shown in Figure 4.2 for a  $Q$  of 10.

When the  $Q$  of the circuit is high, the arithmetic and the geometric mean of the cut-off frequencies are approximately the same (see (4.4)).

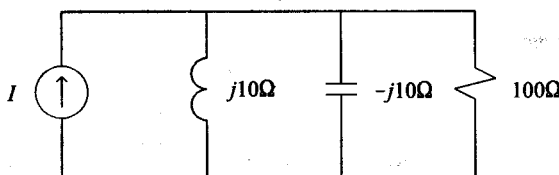


**Figure 4.2** A parallel resonant circuit with  $Q = 10$ .

Extremely sharp rejection can be obtained by using a parallel or series resonant circuit. When the components can be considered to be ideal, it can be shown that the ratio of the power transmitted to the load at resonance ( $P_{o\text{-max}}$ ) and that at any other frequency ( $P_o(f)$ ) can be calculated by using the following equation:

$$\frac{P_{o\text{-max}}}{P_o(f)} = (1 - 2Q^2) + Q^2[(\omega / \omega_0)^2 + (\omega_0 / \omega)^2] \quad (4.10)$$

As an illustration of the rejection characteristics of the circuit, the attenuation is given in Table 4.1 as a function of the normalized frequency ( $f/f_0$ ) for different values of the circuit  $Q$ . Only the frequencies above resonance are considered, because the response is close to symmetrical when the  $Q$  is high. Where the response curve levels off to a single-pole response, no more entries were made into the table.

In order to appreciate the rate of rejection, a -30-dB quality factor ( $Q_{-30}$ ) is defined here as

$$Q_{-30} = f_0 / B_{-30} \quad (4.11)$$

where  $B_{-30}$  is the -30-dB "bandwidth" of the circuit (in Hertz).

The -30-dB  $Q$ -factors for the three  $Q$ -factors used in Table 4.1 are 0.315 ( $Q = 10$ ), 3.15 ( $Q = 100$ ), and 7.90 ( $Q = 250$ ), respectively.

It follows by observation of the results obtained that the -30-dB  $Q$ -factor of a resonant circuit is related to the 3-dB  $Q$ -factor in a simple way when the 3-dB  $Q$ -factor is greater than 10:

$$Q_{-30} \cong 0.0315 Q \quad (4.12)$$

The normalized -30-dB bandwidth of the circuit is therefore given to good approximation by the following equation:

$$B_{-30} = 31.75 / Q \quad (4.13)$$

It can be shown that the two normalized -30-dB rejection frequencies are given to good approximation by the following equation:

$$f_{-30} = \pm 15.875 / Q + \sqrt{\left(\frac{15.875}{Q}\right)^2 + 1}. \quad (4.14)$$

By using (4.13), the  $Q$ -factor required for a specified -30-dB bandwidth can be calculated easily.

**Table 4.1**

The frequencies at which the output signal of an ideal parallel or series resonant circuit is attenuated as listed for some values of the circuit quality factor

Attenuation (dB)	Normalized frequencies ( $f/f_0$ )		
	$Q = 10$	$Q = 100$	$Q = 250$
0	1.0000	1.000	1.000
-3	1.0512	1.005	1.002
-10	1.1615	1.015	1.006
-20	1.615	1.051	1.020
-30	3.46	1.171	1.065
-40	—	1.620	1.22
-50	—	3.46	1.82
-60	—	4.24	—
-70	—	—	—

**EXAMPLE 4.1** Establishing the  $Q$ -factor required for -30-dB rejection at two specified frequencies.

As an example of the application of (4.13), the  $Q$ -factor necessary to provide -30-dB rejection at 40 and 60 MHz with a parallel resonant circuit will be determined.

The resonant frequency of the circuit is

$$f_0 = \sqrt{40 \times 60} = 48.99 \text{ MHz}$$

The normalized -30-dB bandwidth is

$$B_{-30} = (60 - 40) / 48.99 = 0.4082$$

The required  $Q$  is obtained by using (4.13):

$$Q = 31.75 / B_{-30} = 77.76 \quad (4.15)$$

Up to this point the losses in the components of the parallel resonant circuit have been ignored. When the required  $Q$  of the circuit becomes of the same order as the unloaded  $Q$ s of the components used, this cannot be done.

When the losses are taken into account, the effective load resistance ( $R_T$ ) at the resonant frequency is then given by

$$1/R_T = 1/R_L + 1/(Q_L X_L) + 1/(Q_C X_C) \quad (4.16)$$

where  $X_L$  and  $X_C$  are the reactance of the inductor and capacitor, respectively, at the resonant frequency (see Figure 4.3).  $Q_L$  and  $Q_C$  are the unloaded  $Q$ -factors of the inductor and capacitor, respectively.

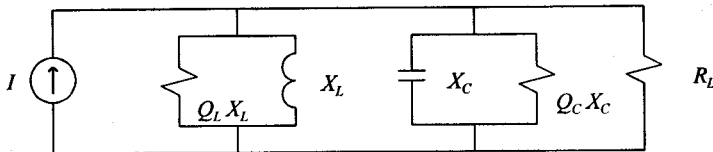


**Figure 4.3** A parallel resonant circuit with lossy components.

At resonance the capacitive and inductive reactances are equal, and (4.16) can be simplified to

$$X_L / R_T = X_L / R_L + [1/Q_L + 1/Q_C] \quad (4.17)$$

The last term in this equation is defined as the unloaded  $Q$  ( $Q_u$ ) of the circuit:

$$1/Q_u = 1/Q_L + 1/Q_C \quad (4.18)$$

The effective  $Q$  of the circuit ( $Q_{\text{eff}}$ ) is therefore given by

$$1/Q_{\text{eff}} = 1/Q_I + 1/Q_u \quad (4.19)$$

where  $Q_I$  is the  $Q$  when the components are assumed to be lossless.

The highest  $Q$  obtainable with a parallel resonant circuit is limited by component losses and the temperature stability of the components.

### 4.3 SERIES RESONANCE

The results obtained for a parallel resonant circuit can be applied directly to a series resonant circuit by using the principle of dualism.

According to this principle, for every circuit there is another circuit for which whatever applies to the current of one circuit, also applies to the voltage of the other circuit, and vice versa.

This equivalent can be obtained by following the procedure illustrated in Figure 4.4. A node is placed in every loop of the first circuit, as well as in the space outside it. These nodes are then connected by passing from one loop to another through the components of the different loops. Inductors are replaced with capacitors, capacitors with inductors, resistors with conductors, and conductors with resistors. The values assigned to the new components ( $H$ ,  $F$ ,  $\Omega$ ,  $S$ ) are numerically equal to those of the original components.

The output voltage of the parallel resonant circuit in Figure 4.4 is given by the following equation:

$$V_o = I / [1 / R + sC + 1 / (sL)] = 0.2 / [0.5 + 3s + 1 / (5s)] \quad (4.20)$$

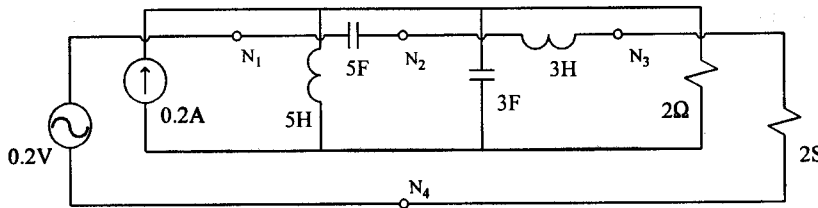


**Figure 4.4** The principle of dualism applied to a parallel resonant circuit.

The output of the series resonant circuit is obtained by replacing  $V_o$  with  $I_o$ ,  $I$  with  $E$ ,  $R$  with  $G$ ,  $C$  with  $L$ , and  $L$  with  $C$ .

Thus,

$$I_o = E / [1 / G + sL + 1 / (sC)] = 0.2 / [0.5 + 3s + 1 / (5s)] \quad (4.21)$$

It follows from Figure 4.4 that the output current of the series resonant circuit is indeed given by this equation.

By applying the principle of dualism to the results deduced in the previous section,

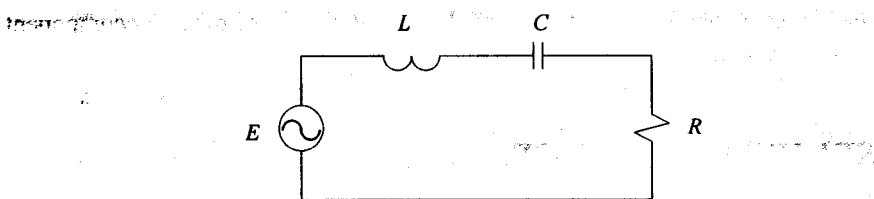


**Figure 4.5** The series resonant circuit.

the following equations are found to apply to the series resonant circuit of Figure 4.5:

$$Q = \omega_0 L / R = 1 / (\omega_0 C R) \quad (4.22)$$

$$\omega_{3\text{dB}} = \omega_0 \sqrt{1 + 1/(4Q^2)} \pm R / (2L) \quad (4.23)$$

$$B = R / L \text{ (rad/s)} \quad (4.24)$$

$$R_T = R_L + X_L / Q_L + X_C / Q_C \quad (4.25)$$

$$1/Q_{\text{eff}} = R_L / X_L + (1/Q_L + 1/Q_C) \quad (4.26)$$

It follows from (4.26) that similar to the parallel resonant circuit, the unloaded  $Q$  for the series resonant circuit is given by

$$1/Q_u = 1/Q_L + 1/Q_C \quad (4.27)$$

The reactance for a series resonant circuit with  $Q = 10$  are shown in Figure 4.6 at the resonant frequency. Note that the reactance values are high compared to the load resistance.

With the same loaded  $Q$ , the frequency response of the series resonant circuit is identical to that of the parallel resonant circuit.

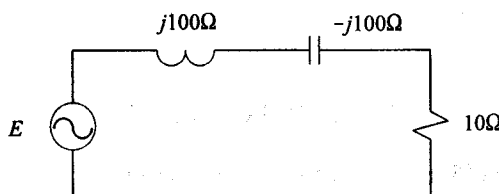


**Figure 4.6** A series resonant circuit with  $Q = 10$ .

## 4.4 L-SECTIONS

An L-section is a two-element matching network. The four possible configurations are shown in Figure 4.7.

Depending on the position of the first component (as viewed from the load), the load resistance can be transformed upwards or downwards with an L-section.

When the first reactive component is a series component, the transformation is upward; and when it is a parallel element, the transformation is downward.

The second element in the L-section is used to remove the residual reactance caused by the transformation element (i.e., the first element). This second element is therefore the compensating element.

The basic principle used in narrowband impedance matching is that the resistance of a complex load is not the same when viewed in impedance or admittance form. This is illustrated in Figure 4.8.

When a reactive element ( $X_1$ ) is added in series with a resistor ( $R$ ) and the equivalent parallel combination is considered (series to shunt transformation), the resistance increases with a factor

$$D_1 = 1 + Q_1^2 \quad (4.28)$$

where

$$Q_1 = X_1 / R \quad (4.29)$$

When a reactive element ( $X_1$ ) is added in parallel with a resistor ( $R$ ) and the equivalent series combination is considered (parallel to series transformation), the resistance decreases with the same factor ( $D_1$ ). In this case, however, the  $Q$ -factor in (4.28) is defined by

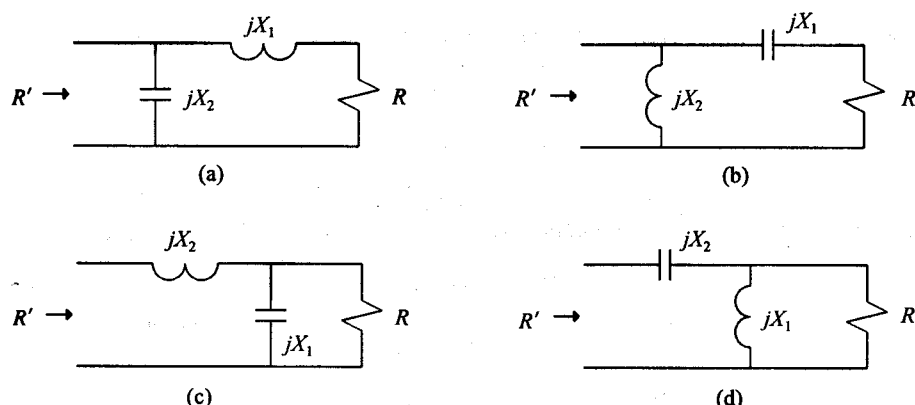


**Figure 4.7** The four possible configurations for an L-section.



**Figure 4.8** A complex impedance displayed in impedance and admittance form.

$$Q_1 = -R / X_1 = B_1 / G \quad (4.30)$$

The ratios defined in (4.29) and (4.30) are similar in form to the  $Q$ -factors of the series or parallel resonant circuits, respectively. These ratios are referred to as transformation  $Q$ s.

The sign of the reactance or susceptance is carried over to the transformation  $Q$ . It follows that the transformation  $Q$  is positive when the effective series reactance is inductive (impedance format) or when the effective shunt susceptance is capacitive (admittance format).

The reactance changes by a factor

$$E_1 = 1 + 1/Q_1^2 \quad (4.31)$$

in the transformation step.

As is the case with the resistance, the reactance increases after a series to shunt transformation and decreases when a shunt to series transformation is considered.

The reactance of the first element used in an L-section is determined by the transformation  $Q$  required to transform the load resistance ( $R$ ) to the value required ( $R'$ ). The  $Q$  value can be calculated by using the relationship

$$R' = D_1 R = (1 + Q_1^2) R \quad (4.32)$$

A positive or a negative sign can be assigned to the transformation  $Q$ .

The second element in the L-section is used to achieve the desired reactance level. If a purely resistive input impedance is required, the reactance of this element is given by

$$X_2 = -X_1(1 + 1/Q_1^2) = R'/Q_1 \quad (4.33)$$

if the first element is a shunt element, and by

$$X_2 = -X_1 / (1 + 1/Q_1^2) = -R'Q_1 \quad (4.34)$$

if the first element is a shunt element.

Equations (4.33) and (4.34) can be verified easily by using the relationships  $Z = 1/Y$  and  $Y = 1/Z$ , respectively.

The formulas relevant to the design of an L-section are summarized in Table 4.2. When the transformation  $Q$  is high, the frequency response of an L-section near the resonant frequency will be similar to that of a simple series or parallel resonant circuit.

The circuit  $Q$  of the L-section is approximately equal to half the transformation  $Q$ . If a more accurate value for the  $Q$  of the circuit is required, the procedure outlined in Section 4.9 can be followed.

### EXAMPLE 4.2 Illustration of the transformation properties of an L-section.

The transformation and compensation properties of an L-section will be illustrated here by using the L-section shown in Figure 4.7(a) as an example. In this example,

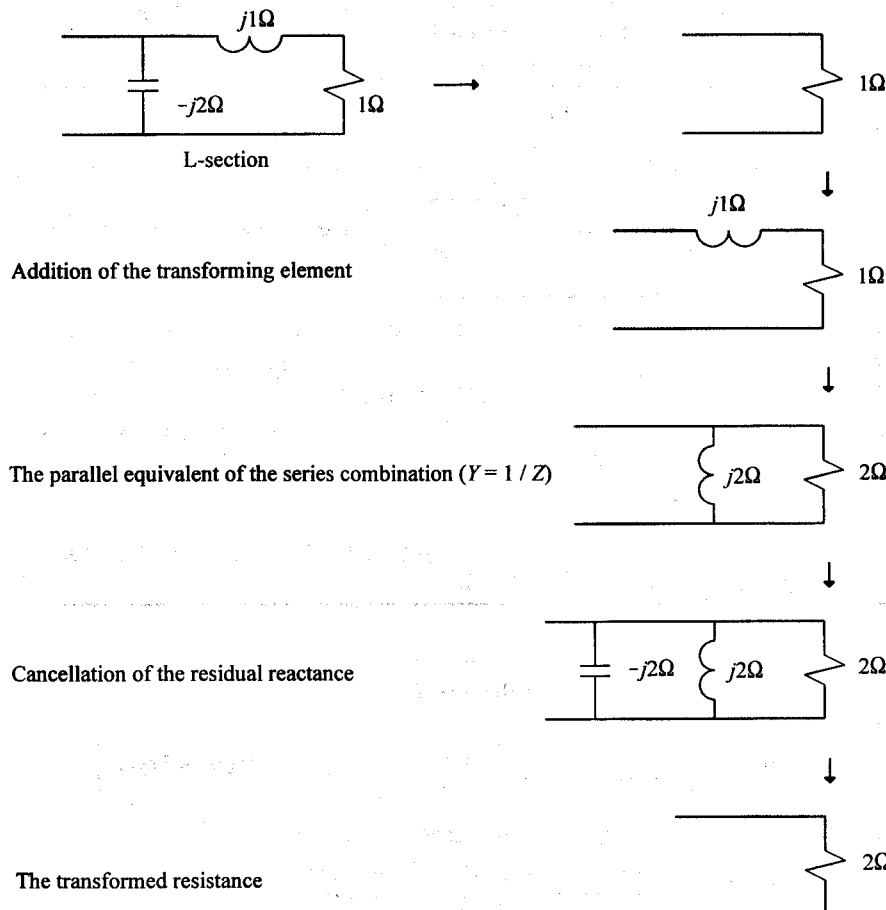
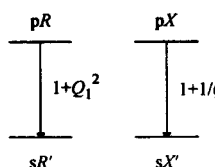
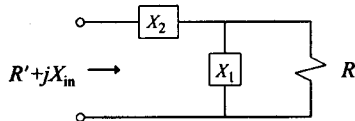


Figure 4.9 Illustration of the transformation and compensation properties of an L-section.

**Table 4.2**  
Formulas Relevant to the Design of L-Sections

**Downward transformations**

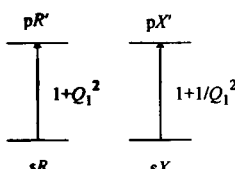
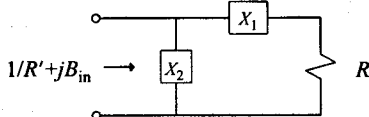


$$R' = R / (1 + Q_1^2) \quad (4.35)$$

$$X' = X_1 / (1 + 1/Q_1^2) \quad (4.36)$$

$$X_2 = X_{in} + Q_1 R' \quad (4.37)$$

**Upward transformations**



$$R' = R(1 + Q_1^2) \quad (4.38)$$

$$X' = X(1 + 1/Q_1^2) \quad (4.39)$$

$$B_2 = B_{in} + Q_1 / R' \quad (4.40)$$

the resistance and reactance at the transformation frequency are taken to be

$$R = 1\Omega$$

$$\omega L = 1\Omega$$

$$1/\omega C = 2\Omega$$

The first element in the matching network (see Figure 4.9) is a series inductor of  $j1\Omega$ . Because the load resistance is also equal to  $1\Omega$ , the transformation  $Q$  is equal

to +1, and the  $1\Omega$  load resistance is transformed upwards with a factor  $1 + 1^2 = 2$  to a value of  $2\Omega$ . The transformation  $Q$  has the same magnitude before and after the transformation (the sign of the  $Q$  changes in the process), and the reactance in parallel with the transformed resistance is therefore  $+j2\Omega$  (still inductive). This reactance is removed by resonating it off with a capacitor ( $-j2\Omega$  reactance), after which the original  $1\Omega$  resistor has been transformed to  $2\Omega$  at the frequency of interest.

Note that the series inductor is a transformation element, while the capacitor is a compensation element.

#### EXAMPLE 4.3 Designing an L-section.

An L-section will be designed to transform a load of  $50\Omega$  to  $250\Omega$  at 50 MHz as an example of the application of the theory discussed above.

Because the transformation is upwards, the first element of the L-section must be a series element. The diagram in Figure 4.10(a) applies.

It follows from the diagram that the transformation  $Q$  must be equal to 2; it follows that a series inductor or capacitor with reactance equal to

$$X = Q R = 2 \times 50 = 100\Omega$$

is required.

If the first element is chosen to be an inductor, the required inductance is

$$L = 100 / (2 \pi \times 50 \times 10^6) = 0.318 \mu\text{H}$$

The parallel equivalent of the transforming section is the required  $250\Omega$  in parallel with a reactance

$$X' = R' / Q_1 = 250 / 2 = 125\Omega$$

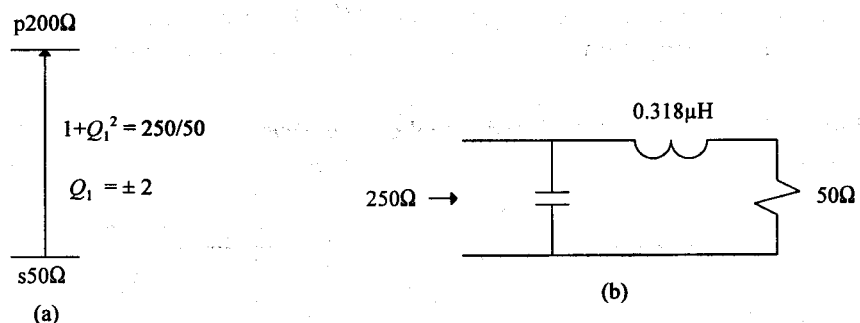


Figure 4.10 (a) The transformation diagram and (b) the L-section relevant to Example 4.3.

Note that the  $Q$ -factors of the series combination and its parallel equivalent must be equal in magnitude (the sign of the  $Q$  changes when the transformation is done).

The capacitance required to remove the reactive part of the input admittance of the resistor and inductor combination is

$$C = 1 / [125(2\pi \times 50 \times 10^6)] = 125 \text{ pF}$$

The designed network is shown in Figure 4.10(b).

## 4.5 PI-SECTIONS AND T-SECTIONS

PI-sections and T-sections are three-element matching networks. A PI-section has two parallel elements, and the T-section has two series elements, as shown in Figure 4.11.

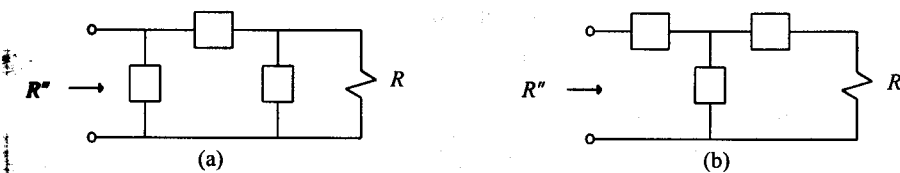


**Figure 4.11** Topology for (a) a PI-section and (b) a T-section.

The first two elements in these sections are transforming elements. One of these elements causes the resistance to increase, while the other causes it to decrease.

The reactance level is set by the last element in the section (the compensating element).

Because the resistance is transformed twice, there are two transformation  $Q$ s in these sections. The highest transformation  $Q$  can be chosen to have any value higher than that required in an equivalent L-section.

As in the case of L-sections, the bandwidth of PI-sections and T-sections are also determined by the transformation  $Q$ s. Where the two  $Q$ -factors are different, the  $Q$  of the

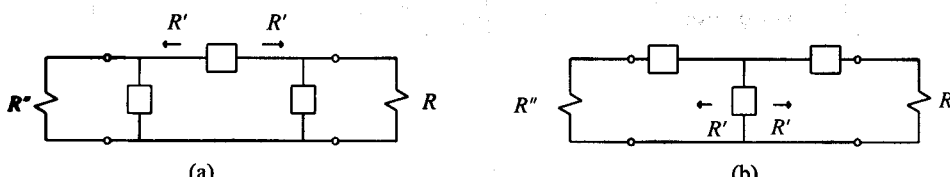


**Figure 4.12** An alternative view of the transformation process in (a) a PI- or (b) a T-section.

network will be approximately equal to half of the highest transformation  $Q$ .

Because the highest transformation  $Q$  is adjustable, the bandwidth of a PI-section or a T-section can be controlled.

The transformation properties of a PI-section or a T-section can also be considered, as illustrated in Figure 4.12. The fact that the source termination ( $R''$ ) and the load termination ( $R$ ) must be transformed to the same intermediate value ( $R'$ ) is considered in this case. Both terminations are transformed downwards in a PI-section and upwards in a T-section. The second element (as counted from the load side) is the compensation element in this case. The bandwidth is determined by the side with the highest transformation  $Q$ .

#### 4.5.1 The PI-Section

The resistance transformations caused by a PI-section (cascade approach) are illustrated in Figure 4.13. The resistance is first transformed downwards by a factor  $1 + Q_1^2$  and then upwards with a factor  $1 + Q_2^2$ .

$Q_1$  is the first transformation  $Q$  and is associated with the load resistance and the first element of the network.  $Q_2$  is the second transformation  $Q$ .

The second transformation  $Q$  is equal to the ratio of the effective reactance in series with the transformed resistance ( $R'$ ) and the transformed resistance itself.

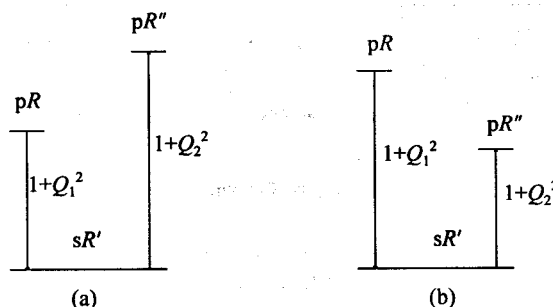
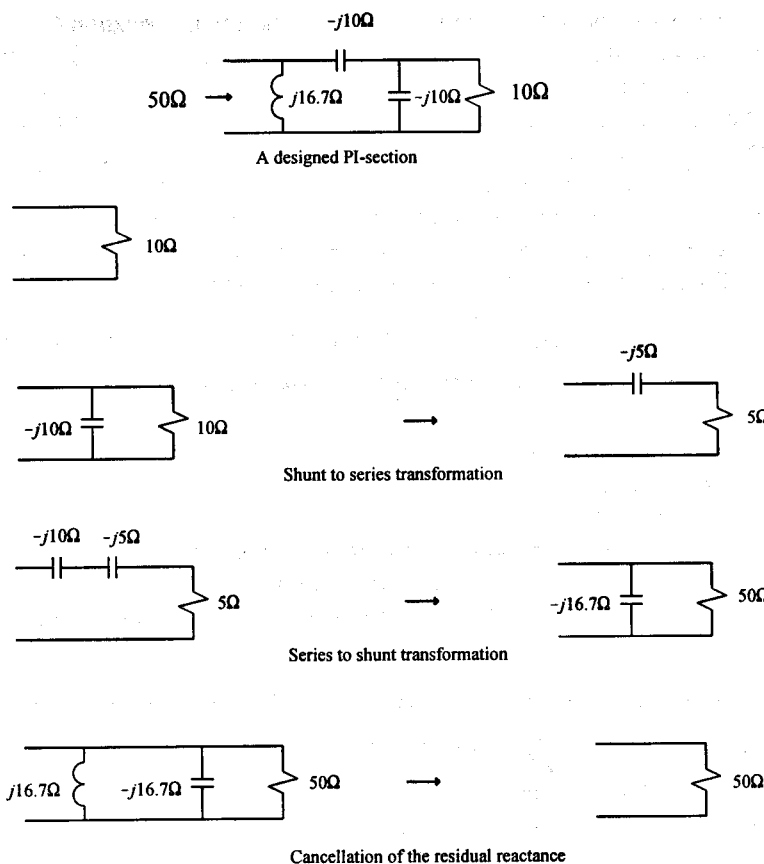


Figure 4.13 (a) Upward transformation of the load resistance with a PI-section and (b) downward transformation of the load resistance with a PI-section.

The transformed resistance will be lower than the load resistance when the first transformation  $Q$  is higher than the second. An upward transformation requires the second transformation  $Q$  to be higher than the first.

The value of the highest transformation  $Q$  is determined by the required bandwidth of the network. The  $Q$  of the network is approximately equal to one-half of the highest transformation  $Q$  when the transformation  $Q$  factors are sufficiently different.

The transformation of a  $10\Omega$  load to  $50\Omega$  by using a PI-section is illustrated in detail in Figure 4.14.



**Figure 4.14** The transformation of a  $10\Omega$  load to  $50\Omega$  with a PI-section.

The formulas relevant to the design of a PI-section are summarized in Table 4.3.

#### EXAMPLE 4.4 A PI-section example.

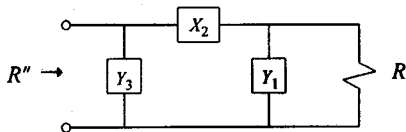
A matching network for transforming  $50\Omega$  to  $12.5\Omega$  will be designed. The maximum transformation  $Q$  will be taken to be 5.

Because the transformation is downwards, the first transformation  $Q$  will be the highest.

The next step is to choose the network topology to be used. The network is arbitrarily assumed to have an inductor as the first element, while the other components are chosen to be capacitors. (It is not possible to choose both of the first two components to be inductors or capacitors. If this is done, the second transformation  $Q$  will be the highest.)

**Table 4.3**  
Formulas for designing a PI-section

**Decreasing the load resistance**



$$Q_1 = Q_{\max} = 2Q \quad (4.41)$$

$$R' = R / (1 + Q_1^2) \quad (4.42)$$

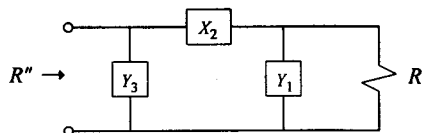
$$1 + Q_2^2 = R'' / R' \quad (4.43)$$

$$Y_1 = Q_1 / R \quad (4.44)$$

$$X_2 = R' (Q_1 + Q_2) \quad (4.45)$$

$$Y_3 = Q_2 / R'' \quad (4.46)$$

**Increasing the load resistance**



$$Q_2 = Q_{\max} = 2Q \quad (4.47)$$

$$R' = R'' / (1 + Q_2^2) \quad (4.48)$$

$$1 + Q_1^2 = R / R' \quad (4.49)$$

$$Y_1 = Q_1 / R \quad (4.44)$$

$$X_2 = R' (Q_1 + Q_2) \quad (4.45)$$

$$Y_3 = Q_2 / R'' \quad (4.46)$$

Because the first transformation  $Q$  is

$$Q_1 = -5$$

the reactance of the inductor must be

$$X_1 = 50/5 = 10\Omega$$

The second component must change the transformation  $Q$  to 2.35. The  $Q$  must be positive (inductive) if the last component is to be a capacitor:

$$X_2 = R'(Q_1 + Q_2) = 1.92(2.35 + (-5)) = -5.1\Omega$$

The reactance of the last component is

$$X_3 = -R'' / Q_2 = -12.5 / 2.35 = -5.3\Omega$$

The designed network is shown in Figure 4.15(b).

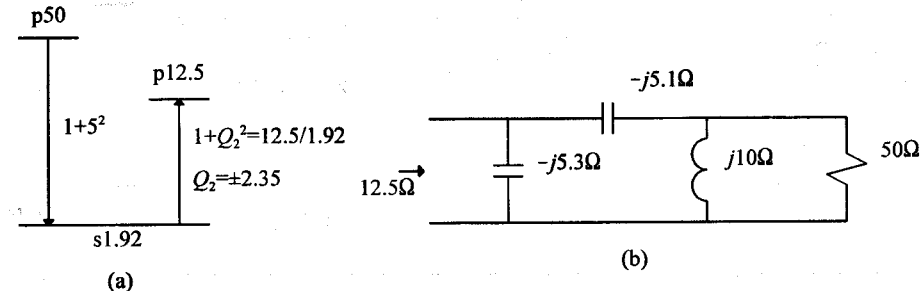


**Figure 4.15** (a) The transformation diagram corresponding to Example 4.4; (b) a PI-section for matching  $50\Omega$  to  $12.5\Omega$ .

### 4.5.2 The T-Section

The dual of a PI-section is a T-section. Therefore, the formulas for designing a PI-section can also be used to design a T-section. In order to do this, it is necessary to replace the resistance and reactance in these formulas with conductance and susceptances, respectively. The terminations used must also be inverted (i.e., if the actual terminations for the T-section are  $50\Omega$  terminations, the terminations for the equivalent PI-section should be  $1/50\Omega$ ).

The reactance results of the PI-section apply directly to the T-section if these are interpreted to be susceptances. To illustrate this, if the components required for a PI-section are  $j10\Omega$ ,  $-j5\Omega$  and  $j3\Omega$ , the components required in the T-section are  $j10S$ ,  $-j5S$ , and  $j3S$ .

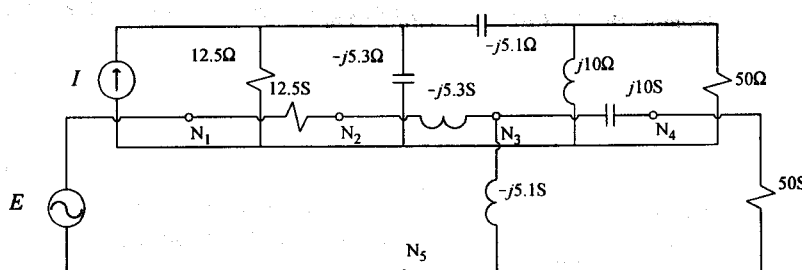


**Figure 4.16** An example of finding the dual of a PI-section.

**Table 4.4**  
Formulas for designing T-sections

<b>Decreasing the load resistance</b>	
	$Q_2 = Q_{max} = 2Q$ (4.50)
	$R = R''(1 + Q_1^2)$ (4.51)
	$1 + Q_1^2 = R'/R$ (4.52)
	$X_1 = Q_1 R$ (4.53)
	$Y_2 = (Q_1 + Q_2) / R'$ (4.54)
	$X_3 = Q_2 R''$ (4.55)
<b>Increasing the load resistance</b>	
	$Q_1 = Q_{max} = 2Q$ (4.56)
	$R' = R(1 + Q_1^2)$ (4.57)
	$1 + Q_2^2 = R'/R''$ (4.58)
	$X_1 = Q_1 R$ (4.53)
	$Y_2 = (Q_1 + Q_2) / R'$ (4.54)
	$X_3 = Q_2 R''$ (4.55)

This approach is useful when a program to design PI- and T-sections is developed. The program can be written to design PI-sections only, and by entering the specifications correctly it can also be used to design T-sections. When the design is not done by computer, it is better to follow the procedure outlined in Table 4.4.

## 4.6 THE DESIGN OF PI-SECTIONS AND T-SECTIONS WITH COMPLEX TERMINATIONS

The procedures outlined in the previous sections can be extended easily to the general case where the load and source impedances are complex. The approach is illustrated in Figure 4.17.

The reactive parts of the load and source impedance (T-section) or admittance (PI-section) are ignored initially, and the network is designed to match the load and source resistance to each other. The first and last components are then changed to take the imaginary parts of the load and source impedance or admittance into account.

Because a T-section transforms a series load resistance to a new series value, the load and the required input impedance must be specified in series form, that is, as impedances. The specifications for a PI-section must be of parallel form. The first step in designing a matching network when the terminations are complex, therefore, is to get the terminations in the right form.

The following equations apply to Figure 4.17:

$$X'_3 = Q_2 R'' \quad (4.59)$$

$$X_1 = Q_1 R_L - X_L \quad (4.60)$$

$$B'_3 = Q_2 / R'' \quad (4.61)$$

$$B_1 = Q_1 / R_L - B_L \quad (4.62)$$

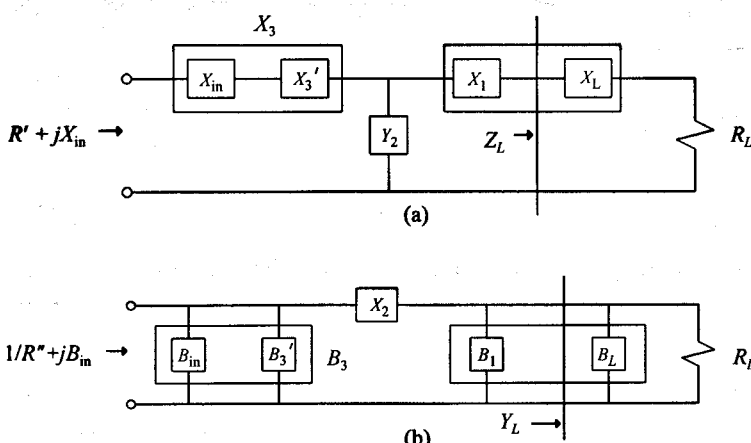
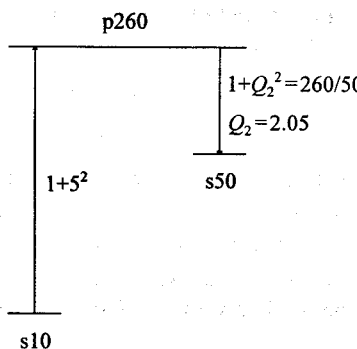


Figure 4.17 The design of (a) a T-section and (b) a PI-section when the terminations are complex.

#### EXAMPLE 4.5 Designing a T-section with complex terminations.

A T-section for matching a  $10 + j10\Omega$  load to  $50 + j40\Omega$  (see Figure 4.19) with a maximum transformation  $Q$  equal to 5 will be designed. These specifications are in impedance form, as required for a T-section.



**Figure 4.18** The transformation diagram for the T-section of Example 4.5.

The transformation diagram for this problem is shown in Figure 4.18. Because the transformation is upwards, the first transformation  $Q$  must be the highest in this case. The second transformation  $Q$  must be equal to 2.05.

With the  $Q$ -factors known, the next step is to choose a topology. If the network shown in Figure 4.19 is chosen, the bandwidth of the circuit can be calculated as was done before. Since the  $Q$ -factors of the load and source impedances are low compared to the maximum transformation  $Q$ , predictable results can also be obtained with other topologies. The only major difference will be in the rate at which the slope outside the pass band levels off because of the higher number of poles.

The component values of the chosen network can now be determined by using the values calculated for the transformation  $Q$ 's.

In order to have a transformation  $Q$  of 5 at the load, a reactance of  $+j40\Omega$  must be added to the existing  $+j10\Omega$ ; that is,

$$X_1 = (5 Q_1) - 10 = 40\Omega$$

After the first transformation, the transformation  $Q$  is still equal to 5. In order to change it to 2.05, a capacitor with susceptance

$$Y_2 = (Q_1 + Q_2) / R' = (5 + 2.05) / 260 = 27.1 \text{ mS}$$

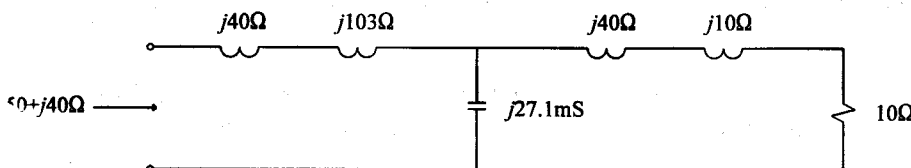


**Figure 4.19** A T-section for transforming a  $10 + j10\Omega$  load to  $50 + j40\Omega$ .

must be used; that is, both  $Q_1$  and  $Q_2$  must be positive.

It is not possible in this case to use a capacitor with susceptance

$$Y = (Q_1 - |Q_2|) / R'$$

since the last component of the network was chosen to be an inductor.

The last component of the T-section must remove the residual reactance and change it to the required level of  $+j40\Omega$ . In order to do this, a  $14.3\Omega$  inductor is required.

The designed network is shown in Figure 4.19.

## 4.7 FOUR-ELEMENT MATCHING NETWORKS

When four elements are used, the control over the frequency response of the impedance-matching network increases. The bandwidth can be lower or higher than that of an L-section.

One possible approach to designing a network to have a very high  $Q$  is shown in Figure 4.20.

The two low- $Q$  sections transform the load impedance and the source impedance to have the same resistance ( $R < R_1, R < R_2$  with the network, as shown in Figure 4.20), and the high- $Q$  section sets the reactance level and provides the required rejection.

Strictly speaking, only one downward transforming section is required in this network. When two downward transforming sections are used, however, it is often possible to decrease the insertion loss of the circuit. This follows because it is often possible to use higher  $Q$  components in the circuit when this is done.

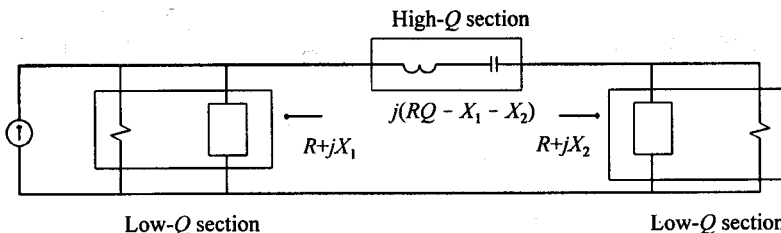


**Figure 4.20** A high- $Q$ , easily tunable, four-element impedance-matching network.

When the approach illustrated in Figure 4.21 is followed, the bandwidth can be wider than that obtainable with an L-section ( $R_2$  is assumed to be smaller than  $R_1$ ). In this case the source and the load resistance are transformed to their geometric mean by using two L-sections.

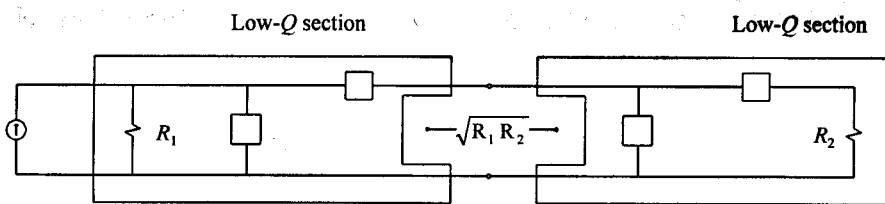


Figure 4.21 A wideband four-element impedance-matching network.

## 4.8 CALCULATION OF THE INSERTION LOSS OF AN LC IMPEDANCE-MATCHING NETWORK

It was shown in Chapter 3 that the ideal component does not exist. For this reason, all practical circuits will have some insertion loss. If the insertion loss is to be kept low, the unloaded  $Q$ -factors of the components must be significantly higher than the  $Q$  of the circuit.

The insertion loss of any cascaded LC network can be computed by following the procedure outlined below:

1. Model each reactive component in the network as an ideal component with a resistor in series or in parallel with it, depending on whether it is a series or shunt element, respectively.

The value of this resistance can be determined from the unloaded  $Q$ -factor estimated for the component.

Unloaded  $Q$ -factors for capacitors and magnetic-core inductors can usually be found by using the data given by the manufacturer, while those of air-cored solenoidal coils can be determined by following the procedure outlined in Section 3.3.6.

The unloaded  $Q$  of a component may be a strong function of the frequency.

2. Assume that the power dissipated in the load is equal to 1W.
3. If the first component of the network (as viewed from the load) is a series element, calculate the power dissipated in it by using the equation

$$P_D = (R_Q / R_L) P_L \quad (4.63)$$

where  $R_Q$  is the series resistance associated with the element and  $R_L$  is the (effective) load resistance.  $P_L$  is the power dissipated in the load (1W in this case).

If the first component is a parallel element, calculate the power dissipated in it by using the equation

$$P_D = (G_Q / G_L) P_L \quad (4.64)$$

where  $G_Q$  is the parallel conductance associated with the component, and  $G_L$  is the (effective) conductance of the load.  $P_L$  is the power dissipated in the load.

4. Add the power dissipated in the first component to that dissipated in the load:

$$P_T = P_L + P_D \quad (4.65)$$

5. Consider the first component to be part of the load and calculate the new (effective) load admittance or impedance.
6. Repeat steps 3 to 5 until the power entering the matching network ( $P_T$ ) and the effective input impedance of the network ( $Z_{in}$ ) are known.
7. Calculate the transducer power gain of the network ( $G_T$ ) by using the equation

$$G_T = (1 - |S_s|^2) \frac{P_L}{P_T} \quad (4.66)$$

$$= \left[ 1 - \left| \frac{Z_{in} - Z_s^*}{Z_{in} + Z_s} \right|^2 \right] P_L / P_T \quad (4.67)$$

$$= \frac{4R_{in}R_s}{(R_{in} + R_s)^2 + (X_{in} + X_s)^2} P_L / P_T \quad (4.68)$$

where  $S_s$  is the input reflection parameter with  $Z_s$  as normalizing impedance,

$$Z_{in} = R_{in} + jX_{in} \quad (4.69)$$

and

$$Z_s = R_s + jX_s \quad (4.70)$$

where  $Z_s$  is the internal impedance of the source driving the network.

#### EXAMPLE 4.6 Calculating the insertion loss of a PI-section.

As an example of the application of this procedure, the insertion loss of the PI-

section designed in Example 4.4 will be calculated at the center frequency. The unloaded  $Q$ -factors of the capacitors are assumed to be 500, while that of the inductor is taken as 100.

The conductance associated with the inductor is 1 mS, the series resistance associated with the first capacitor is 0.01Ω, and the conductance associated with the second capacitor is 0.38 mS.

The power dissipated in the inductor is 50 mW. The power entering the last section of the network is therefore 1.05W. The input impedance of this section is

$$Z = 2.0 + j9.6\Omega$$

The power dissipated in the first capacitor is 5 mW. The power entering the network at this point is therefore 1.055W. The input admittance at this point is

$$Y = (84 - j186) \text{ mS}$$

The power dissipated in the last capacitor is also 5 mW. The total power entering the network is therefore 1.06W. The input impedance is

$$Z_{in} = 11.9 - j0.45\Omega$$

The transducer power gain of the network was calculated to be 0.94, that is, an insertion loss of 0.3 dB.

## 4.9 CALCULATION OF THE BANDWIDTH OF CASCADED LC NETWORKS

The bandwidth of a network can be found iteratively if its transducer power gain is determined as a function of frequency. The transducer power gain of any cascaded LC network can be found by following the procedure outlined in the previous section.

Because the cut-off frequencies (3-dB) of L-, PI-, and T-sections are known to good approximation ( $f_{-3dB} = f_0 \pm f_0 / Q_{max}$ ), the exact bandwidth of these circuits can be determined quickly by following this procedure.

### EXAMPLE 4.7 The 3-dB bandwidth of a matching network.

By following the procedure described, the 3-dB cut-off frequencies of the network in Example 4.6 are found to be 83 and 130 MHz, that is, if the center frequency is selected as 100 MHz. The exact  $Q$  of the circuit is therefore 2.3 instead of the estimated 2.5.

If a bandwidth other than the 3-dB bandwidth is required, it can be found easily by following the same procedure.

## SELECTED BIBLIOGRAPHY

**RF Power Transistor Manual**, Somerville, NJ: RCA Corporation (Solid State Division), 1971.

## CHAPTER 5

# COUPLED COILS AND TRANSFORMERS

### 5.1 INTRODUCTION

When the parasitics can be ignored, transformers are ideally suited for impedance scaling. Ideal and practical transformers will be considered in this chapter.

A practical transformer differs from the ideal in that it has leakage flux, finite magnetizing inductance, losses, and parasitic capacitance, all of which degrade its performance. Several equivalent circuits for practical transformers will be presented here.

Transformers are often used when wideband transformation of resistance is required (when possible, this is usually a better option than using LC networks). It will be shown here that the wideband performance of a transformer is mainly determined by the coupling factor. This is also the reason why stacked toroids or balun cores are usually used to realize such a transformer.

Although the finite magnetizing inductance and the leakage inductance are undesirable in a wideband transformer, they can be put to good use in narrowband matching networks. Several narrowband matching networks using transformers will be covered in detail.

Because it is important to adjust the coupling factor of a transformer to the required value when narrowband matching networks are used, methods to measure the coupling factor will be also be considered in this chapter.

### 5.2 THE IDEAL TRANSFORMER

The equivalent circuit of the ideal transformer is shown in Figure 5.1. The number of turns on the primary and secondary sides of the transformer are, respectively,  $n_1$  and  $n_2$ .

The ideal transformer has the following characteristics:

1. The magnetic flux in the two windings is the same. Therefore, there is no leakage flux.

The voltage induced by the changing flux in each winding is given by Faraday's law:

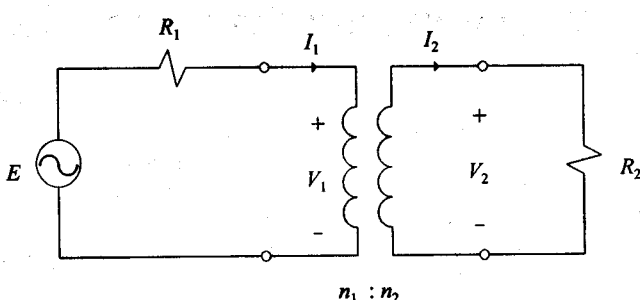


**Figure 5.1** The ideal transformer.

$$V = n_x \frac{\partial \Phi}{\partial t} \quad (5.1)$$

where  $n_x$  is the number of turns in the winding under consideration. Because the flux coupling each winding is the same, the ratio of the primary to secondary voltage of the transformer is

$$V_1 / V_2 = n_1 / n_2 \quad (5.2)$$

This relationship is more significant if it is written in the form

$$V_1 / n_1 = V_2 / n_2 \quad (5.3)$$

The voltage per turn, therefore, is the same for both sides of the transformer.

2. The primary current necessary to establish the flux in the ideal transformer is negligible. The input impedance of the transformer with the load open-circuited, therefore, is infinite.
3. There are no losses in the ideal transformer. The average power dissipated in the load, therefore, is exactly the same as the average power entering the transformer.

Because the ideal transformer has no reactive components, the instantaneous power dissipated in the load is also equal to the instantaneous power entering the transformer; that is,

$$v_1 i_1 = v_2 i_2 \quad (5.4)$$

By using (5.2) to replace the voltages in this equation, the relationship between the primary and secondary currents is found to be

$$n_1 I_1 = n_2 I_2 \quad (5.5)$$

The demagnetizing force (magnetomotive force) of the current in the secondary winding is, therefore, balanced by that of the current in the primary winding.

By using this equation and (5.3), the relationship between the primary and secondary impedances is found to be

$$Z_1 = V_1 / I_1 = [n_1 / n_2]^2 Z_2 \quad (5.6)$$

The impedance ratio is, therefore, only a function of the turns ratio of the transformer.

4. The permeability of the ideal transformer is independent of the flux density in the core. This implies that the ideal transformer is a perfectly linear device.

From an impedance-matching viewpoint, the ideal transformer is very useful in that it can be used to scale impedances by any factor.

### 5.3 EQUIVALENT CIRCUITS FOR PRACTICAL TRANSFORMERS

A practical transformer deviates from the ideal in the following ways:

1. There is some leakage flux and, therefore, leakage inductance.
2. The magnetizing inductance is finite.
3. There are losses in the windings of the transformer (copper losses), as well as in the core (hysteresis and eddy current losses).
4. The relative permeability of the magnetic material changes with signal level and dc current (saturation), as well as with frequency and temperature.
5. Apart from the effect of the leakage inductance, the high-frequency response is degraded by the presence of parasitic capacitance between the windings and turns of each winding.

A circuit model for the practical transformer, ignoring the capacitance and nonlinearities, is shown in Figure 5.2 [1]. The two dots indicate the sides of the two windings that have the same voltage polarity.

The two series inductances represent the leakage flux, the series inductance to the left together with the shunt inductance are the magnetizing inductances, the resistance  $r_1$

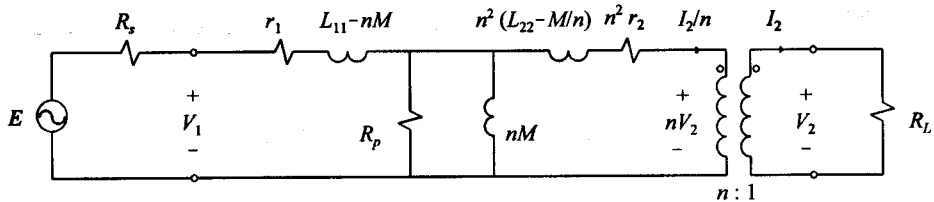


Figure 5.2 An equivalent circuit for a practical transformer.

and  $r_2$  represent the copper losses, and  $R_p$  represents the losses in the magnetic material.

The mutual inductance  $M$  can be determined as a function of the magnetizing inductances  $L_{11}$  and  $L_{22}$  by using the relationship

$$M = k(L_{11}L_{22})^{1/2} \quad (5.7)$$

where  $k$  is the coupling factor of the transformer.

The symbol  $n$  in Figure 5.2 can have any arbitrary value, but it is usually chosen to be equal to the turns ratio of the two windings of the transformer. However, a better choice for it is

$$n = \frac{1}{k} \sqrt{\frac{L_{11}}{L_{22}}} \quad (5.8)$$

If the losses in the magnetic material can be ignored, the equivalent circuit for two coupled coils (see Figure 5.3(a)) can be used for the transformer. The circuit shown in Figure 5.3(b) is equivalent to the coupled coil circuit [2]. This can be proven by setting up the Z-parameter matrices for the two circuits. The transformation ratio shown in Figure 5.3(b) is that for the impedances.

The following characteristics of the transformer are immediately evident from the equivalent circuit in Figure 5.3(b):

1. The load impedance is transformed to the primary side of the transformer as

$$Z'_L = [L_{11} / (k^2 L_{22})] [Z_L + r_2] \quad (5.9)$$

that is, as long as

$$[\omega L_{22}(1 - k^2)]^2 \ll |Z_L + r_2|^2 \quad (5.10)$$

This equation can be changed to a more useful form by substituting  $L_{22}$  by using (5.9):

$$[\omega L_{22}(1 - k^2) / k^2]^2 \ll |Z'_L|^2$$

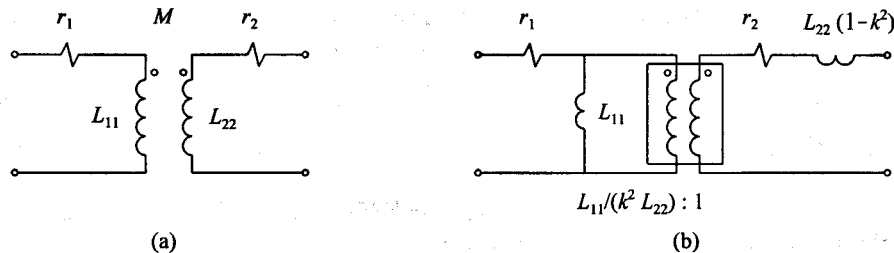


**Figure 5.3** Two equivalent circuits for a practical transformer ( $R_p$  neglected).

$$[\omega L_{22} (1 - k^2) / k^2]^2 \ll |Z'_L|^2$$

leading to

$$[1/k^2 - 1] \ll |Z'_L / (\omega L_{11})|^2 \quad (5.11)$$

This inequality will always apply at low frequencies, and, if the coupling between the windings is good, it will also apply at higher frequencies.

It follows from (5.9) that the impedance transformation factor at low frequencies is always

$$n^2 = L_{11} / (k^2 L_{22}) \quad (5.12)$$

2. The high frequency response of the transformer is limited by the leakage reactance  $\omega L_{22} (1 - k^2)$ .
3. The low-frequency response of the transformer is limited by the magnetizing inductance  $L_{11}$ .
4. The input inductance at low frequencies is equal to the magnetizing inductance  $L_{11}$ .

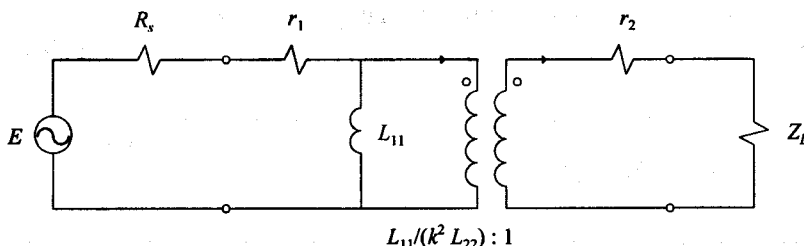


**Figure 5.4** An equivalent circuit for the practical transformer at low frequencies.

If the frequency is low enough for (5.11) to apply, the equivalent circuit of Figure 5.3(b) can be simplified to that shown in Figure 5.4.

By using this equivalent circuit, the low cut-off frequency is found to be

$$\omega_{L-3\text{dB}} = R_s / (2L_{11}) \quad (5.13)$$

This equation applies when  $r_1$  and  $r_2$  can be ignored and the load resistance  $R_L$  is transformed to be equal to the source resistance  $R_s$ .

It follows that, under these circumstances, the required primary inductance can be determined by using the specifications for the cut-off frequency and the source resistance. The required secondary inductance is given by the equation

$$L_{22} = \frac{R_L}{R_s} \frac{L_{11}}{k^2} \quad (5.14)$$

This inductance is clearly a function of the coupling factor, which is usually not known at the design stage.

The easiest way to overcome this problem is to ensure that the coupling factor is close to unity, if possible.

Very good coupling can usually be obtained by using materials with high relative permeabilities. The coupling between the windings of the transformer is also better if balun or stacked toroidal cores, instead of a single toroidal core, are used.

## 5.4 WIDEBAND IMPEDANCE MATCHING WITH TRANSFORMERS

Impedance matching over very wide bandwidths (decades) is possible with transformers when the coupling between the windings is good and when the parasitic capacitance between the windings and turns of each winding is small.

If the parasitic capacitance can be ignored, the 3-dB bandwidth of a transformer can be determined by finding the poles of the equivalent circuit in Figure 5.5. This equivalent circuit can be derived from the one in Figure 5.2 by setting  $n$  equal to 1.

The equivalent circuit has two poles, a zero at the origin and 1 at infinity. The poles

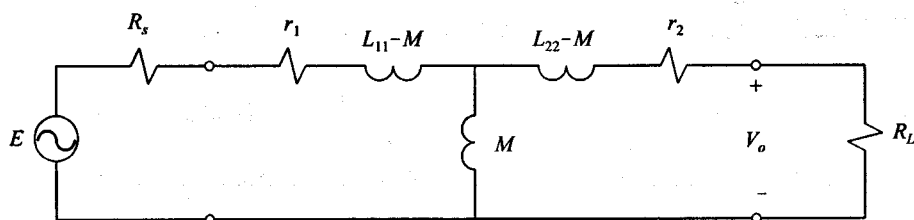


Figure 5.5 A T-section equivalent for the transformer.

can be found by setting the impedances in either of the two loops of the equivalent circuit equal to zero. If this is done for the first loop, the following equation is obtained:

$$(R_s + r_1) + s(L_{11} - M) + sM \{ [sL_{22} - sM + (R_L + r_2)] = 0 \quad (5.15)$$

This equation simplifies to

$$s^2 L_{11} L_{22} (1 - k^2) + s[L_{22} R'_s + L_{11} R'_L] + R'_s R'_L = 0 \quad (5.16)$$

The poles, and therefore the cut-off frequencies, can be obtained by solving this equation.

When the load resistance and the source resistance are matched, as is generally the case, the following equation applies:

$$R'_L = R_L + r_2 = (k^2 L_{22} / L_{11}) \cdot R'_s \quad (5.17)$$

Because the coupling factor is usually unknown at the outset of the problem and is usually close to unity at low frequencies, the transformer is normally designed for

$$R'_L = (L_{22} / L_{11}) \cdot R'_s \quad (5.18)$$

If this value for  $R'_L$  is substituted in (5.16), it simplifies to

$$s^2 L_{11} L_{22} (1 - k^2) + 2sL_{22} R'_s + (L_{22} / L_{11}) R'_s R'_s = 0 \quad (5.19)$$

This equation can be written as

$$[sL_{11}(1+k) + R'_s][sL_{11}(1-k) + R'_s] = 0 \quad (5.20)$$

The cut-off frequencies are, therefore, given by the following equations:

$$\omega_L = R'_s / [L_{11}(1+k)] \quad (5.21)$$

$$\omega_H = R'_s / [L_{11}(1-k)] \quad (5.22)$$

that is, when (5.18) applies.

It is clear from these equations that the low cut-off frequency of the transformer is determined by the effective resistance in parallel with the magnetizing inductance and that the high cut-off frequency is a strong function of the coupling factor.

The relative bandwidth of the transformer with the load and source impedances matched is given by

$$\omega_H / \omega_L = [1+k] / [1-k] \quad (5.23)$$

The relative bandwidth of the transformer, therefore, is only a function of the coupling

factor, that is, when the load and source impedances are matched and the parasitic capacitance can be ignored.

Because the coupling factor is frequency-dependent and close to unity at the lower frequencies, (5.23) can be simplified to

$$\omega_H / \omega_L = 2 / [1 - k] \quad (5.24)$$

### **EXAMPLE 5.1** Designing a transformer to transform a $50\Omega$ load to $300\Omega$ .

The primary inductance, secondary inductance, and coupling factor required to transform a load of  $50\Omega$  to  $300\Omega$  with 3-dB cut-off frequencies at 1 and 20 MHz will be determined as an example.

Assuming that the copper losses in the windings and the hysteresis losses in the magnetic core can be ignored, the required inductance ratio of the transformer can be obtained by using (5.18):

$$L_{11} / L_{22} = R_s / R_L = 50 / 300 = 0.1667$$

The required magnetizing inductance  $L_{11}$  can be obtained by using (5.21):

$$L_{11} = 300.0 / [2.0 \pi \times 1.0 \times 10^6 (1+1)] = 23.9 \mu\text{H}$$

The secondary inductance, therefore, is

$$L_{22} = L_{11} / 6 = 4.0 \mu\text{H}$$

The required coupling factor at 20 MHz can be obtained by using (5.24):

$$1 - k = 2 / [20 / 1] = 0.1$$

$$k = 0.9$$

The coupling factor required to obtain a relative bandwidth of 20, therefore, is 0.9.

## **5.5 SINGLE-TUNED TRANSFORMERS**

The single-tuned transformer shown in Figure 5.6 can be used to step the load impedance up or down and to obtain a frequency response identical to that of a parallel resonant circuit.

If the coupling between the windings of the transformer is good, the leakage inductance of the transformer can be ignored.

The required magnetizing inductance of the transformer can be found in terms of the  $Q$ -specification, and the source and load resistance, by using the equation

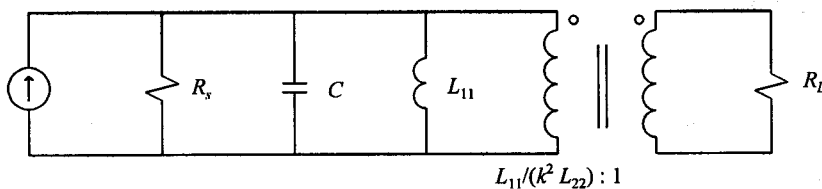


Figure 5.6 The single-tuned transformer.

$$\omega_0 L_{11} = (R_s \parallel R'_L) / Q = R_s / (2Q) \quad (5.25)$$

where  $R'_L$  is the load resistance referenced to the input side and  $Q$  the circuit  $Q$ .

The capacitance necessary to provide resonance is

$$C = 1 / (\omega_0^2 L_{11}) \quad (5.26)$$

Because the coupling is assumed to be good, the required secondary inductance is given by the equation

$$L_{22} = (R_L / R_s) L_{11} / k^2 \approx (R_L / R_s) L_{11} \quad (5.27)$$

The next step in the design of the single-tuned transformer is to select a suitable magnetic material and to determine the type and size of the core required (see Chapter 3).

If necessary, the required number of turns around the core can be found by measuring the inductance of a few turns of wire around the core to be used. Because the inductance is proportional to the square of the number of turns, the number of turns required can be found easily.

## 5.6 TAPPED COILS

The tapped coil (Figure 5.7) is a very useful narrowband matching network. Independent adjustment of the center frequency and the transformation ratio of the transformer is

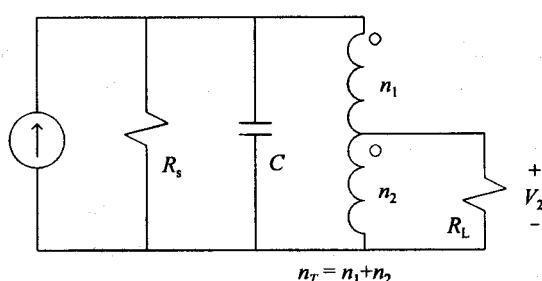


Figure 5.7 The tapped coil resonant circuit.

possible. It is also very easy to manufacture once it has been designed.

The frequency response of this transformer is usually similar to that of the single-tuned transformer.

Analysis of the tapped coil is possible by considering it to be two coupled coils.

It follows from (3.23) that the self-inductance of the upper section of the coil is given by

$$L_1 = r n_1^2 10^{-6} / \left[ 22.9 \frac{l_T}{r} \frac{n_1}{n_T} + 25.4 \right] \quad (5.28)$$

and that of the lower section by

$$L_2 = r n_2^2 10^{-6} / \left[ 22.9 \frac{l_T}{r} \frac{n_2}{n_T} + 25.4 \right] \quad (5.29)$$

where  $l_T$  is the total length of the coil,  $n_1$  the number of windings in the upper section,  $n_2$  the number in the lower section, and  $n_T$  the total number of turns ( $n_T = n_1 + n_2$ ).

The inductance of the coil as a whole is given by the equation

$$L_T = r n_T^2 10^{-6} / \left[ 22.9 \frac{l_T}{r} + 25.4 \right] \quad (5.30)$$

If viewed in terms of its component parts, the total inductance can also be written as

$$L_T = L_1 + L_2 + 2M \quad (5.31)$$

By using this equation together with (5.7),

$$M = k(L_1 L_2)^{1/2}$$

the coupling factor is found to be

$$k = [L_T - L_1 - L_2] / [2(L_1 L_2)^{1/2}] \quad (5.32)$$

By substituting (5.28) through (5.31) into (5.32), the following can be deduced:

1. The coupling factor is dependent on the length-to-radius ratio of the coil, as well as the relative position of the tap-point.
2. The coupling factor is independent of the total number of turns ( $n_T$ ).

The coupling factor of the tapped coil is given in Table 5.1 as a function of the relative position of the tap-point for a number of  $l_T/r$  ratios. The coupling factors are not shown for relative positions greater than 0.5, since they are the mirror image (arithmetic) of the lower values (0.8 corresponds to 0.2).

**Table 5.1**

The coupling factor of the tapped coil as a function of the  $l_T/r$  ratio of the coil and the relative position of the tap-point

$n_1/n_T$	$l_T/r = 1$	$l_T/r = 1.5$	$l_T/r = 2$	$l_T/r = 3$	$l_T/r = 4$	$l_T/r = 5$
0.1	0.543	0.449	0.386	0.304	0.253	0.218
0.2	0.535	0.438	0.372	0.288	0.235	0.200
0.3	0.530	0.431	0.363	0.277	0.225	0.189
0.4	0.529	0.426	0.358	0.272	0.219	0.183
0.5	0.526	0.425	0.357	0.270	0.217	0.182

It can be seen from Table 5.1 that the coupling factor is not a strong function of the relative position of the tap-point.

The input admittance of the coupled coil can be found by using the equation

$$\begin{bmatrix} j\omega L_{1+2+2M} & -j\omega L_{2+2M} \\ -j\omega L_{2+M} & j\omega L_2 + R_L \end{bmatrix} \begin{bmatrix} I_1 \\ I_2 \end{bmatrix} = \begin{bmatrix} E \\ 0 \end{bmatrix} \quad (5.33)$$

By applying Cramer's rule to this equation, it follows that

$$\begin{aligned} Y_{in} &= I_1 / E \\ &= \frac{\begin{vmatrix} 1 & -j\omega L_{2+M} \\ 0 & j\omega L_2 + R_L \end{vmatrix}}{\begin{vmatrix} j\omega L_{1+2+2M} & -j\omega L_{2+2M} \\ -j\omega L_{2+M} & j\omega L_2 + R_L \end{vmatrix}} / \Delta \\ &= (R_L + j\omega L_2) / [j\omega L_{1+2+2M}(R_L + j\omega L_2) - j\omega L_{2+M}j\omega L_{2+M}] \end{aligned}$$

After some manipulation, it follows that

$$= \frac{L_2 L_T R_L + L_1 L_2 (k^2 - 1) R_L}{\omega^2 L_1^2 L_2^2 (k^2 - 1)^2 + L_T^2 R_L^2} - j \frac{L_T R_L^2 - \omega^2 L_1 L_2 (k^2 - 1)}{\omega^3 L_1^2 L_2^2 (k^2 - 1)^2 + \omega L_T^2 R_L^2} \quad (5.34)$$

If the coupling is perfect, this equation reduces to

$$Y_{in} = \frac{L_2}{L_T} / R_L - j / (\omega L_T) \quad (5.35)$$

expected.

When the coupling is not perfect, the resistive part of the input admittance will be frequency-independent if

$$\omega^2 L_1^2 L_2^2 (k^2 - 1)^2 \ll L_T^2 R_L^2$$

that is, if

$$[\omega L_1 L_2 (1 - k^2)]^2 \ll (L_T R_L)^2 \quad (5.36)$$

When this is true, the input conductance will be

$$\begin{aligned} G'_L &= \frac{L_2 L_T R_L + L_1 L_2 (k^2 - 1) R_L}{L_T^2 R_L^2} \\ &= \frac{L_2}{L_T} G_L - \frac{L_1 L_2 (1 - k^2)}{L_T^2} G_L \end{aligned} \quad (5.37)$$

It can be seen from (5.34) that the actual conductance of the coil will be 10% higher than the value predicted by this equation if

$$[\omega L_1 L_2 (k^2 - 1)]^2 = 0.1 (L_T R_L)^2$$

For the parallel input inductance to be approximately  $L_T$ , it is necessary that both (5.36) and the following equation apply:

$$\omega^2 L_1 L_2 (1 - k^2) \ll L_T R_L^2 \quad (5.38)$$

It follows that the equivalent circuit of the tapped coil can be simplified to that shown in Figure 5.8 when these two equations apply.

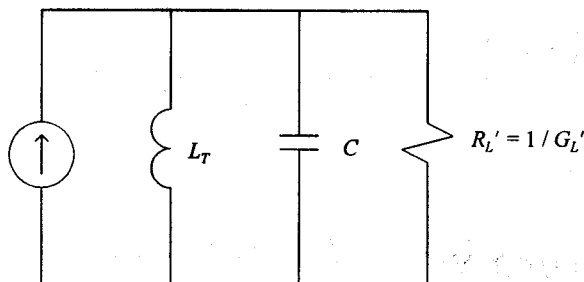


**Figure 5.8** A simplified equivalent circuit for a tapped coil resonant circuit.

**Table 5.2**

The transformation factor of the tapped coil as a function of the  $l/r$  ratio and the relative position of the tap-point from the upper end of the coil

$n_1/n_T$	$R'_L/R_L$		
	$l_T/r = 2$	$l_T/r = 4$	$l_T/r = 6$
0.10	1.18	1.18	1.18
0.20	1.46	1.46	1.48
0.30	1.92	1.92	1.94
0.40	2.66	2.68	2.70
0.50	4.00	4.00	4.00
0.55	5.08	5.07	5.05
0.60	6.64	6.62	6.56
0.65	9.04	8.99	8.86
0.70	12.90	12.80	12.60
0.75	19.70	19.60	19.10
0.80	33.00	33.00	32.10
0.85	64.00	64.70	62.80
0.90	160.00	166.00	162.00
0.95	732.00	505.00	808.00

It should be noted that, from a practical viewpoint, it is more important that (5.36) applies rather than (5.38). This is because the resonant frequency of the circuit can be adjusted easily to the desired frequency by stretching or compressing the coil slightly (the coupling factor is only a weak function of the  $l/r$  ratio of the coil).

The transformation factor of the load (as given by (5.37)) is a function of the inductance  $L_T$ , the ratios  $L_1/L_T$ ,  $L_2/L_T$  and the coupling factor  $k$ . The last three variables are determined by the relative position of the tap-point and the  $l_T/r$  ratio of the coil. The transformation factor itself is therefore only a function of the  $l/r$  ratio of the coil and the relative position of the tap-point.

The transformation factor for different  $l/r$  ratios and positions of the tap-point was determined and is tabulated in Table 5.2. This table can only be used when (5.36) applies. When it does not, the transformation factor can be calculated by using (5.28) to (5.30), and (5.34).

It can be seen from Table 5.2 that the transformation factor of the tapped coil is only a weak function of the  $l/r$  ratio of the coil. It is also evident that the transformation factor becomes very sensitive when the coil is tapped close to its ground point.

A tapped coil resonant circuit can be designed to match a source to a load with a fixed  $Q$  by following the procedure outlined below.

### Procedure for a Tapped-Coil Resonant Circuit

- Assume that the input inductance of the tapped coil will be equal to the inductance ( $L_T$ ) of the coil itself (refer to Figures 5.7 and 5.8). Find the required inductance by using (5.25):

$$\omega L_T = [R' \| R_s] / Q = R_s / [2Q]$$

This equation will only apply if the unloaded  $Q$ -factor of the inductor and capacitor used are high compared to the specified circuit  $Q$ .

2. Design the inductor ( $L_T$ ) to have the required unloaded  $Q$  as described in Chapter 3.

Check if the self-capacitance of the designed coil is lower than the capacitance required for resonance.

At this stage  $L_T$ ,  $l_T$ ,  $r$ , and  $n_T$  are known.

3. The next step is to determine the relative position of the tap-point. If the inequality (5.36)

$$[\omega L_1 L_2 (1 - k^2)]^2 \ll (L_T R_L)^2$$

applies, Table 5.2 can be used for this purpose. If it does not apply, then it will be easier to determine the tap-point practically.

#### **EXAMPLE 5.2** Designing a tapped coil resonant circuit to transform a $50\Omega$ load to $1000\Omega$ .

A tapped coil resonant circuit will be designed to meet the following specifications, if possible:  $f_0 = 10$  MHz,  $R_L = 50\Omega$ ,  $R_s = 1000\Omega$ ,  $Q = 20$ , and  $IL < 10\%$ .

In order to have less than 10% losses, the loss resistance must be higher than (approximately) ten times the transformed load resistance ( $P = V^2/R$ ); that is,

$$R_{\text{loss}} = 10.0 \times 1.0 \times 10^3 = 10k\Omega$$

This implies that the unloaded  $Q$  of the inductor must be at least

$$Q_u = R_{\text{loss}} / (\omega L) = 10k / 25 = 400$$

It is assumed here that the losses in the capacitor can be ignored. The required  $Q$ , however, is high in this design and it will be necessary to use a very good capacitor and even a parallel combination of smaller values to obtain a  $Q$  that is high compared to that of the inductor.

Assuming the  $l_T/r$  ratio of the coil to be equal to 2.0 and a  $d/c$  ratio of 0.55, the required radius of the coil is found to be (using (3.25))

$$r = Q_u / [k(f)^{1/2}] = 1.26 \text{ cm}$$

The required length of the coil is 2.53 cm ( $l_T/r = 2$ ). The number of turns

can be found by using (3.27):

$$n = [L (22.9 \cdot l/r + 25.4) / r]^{1/2} = 4.75$$

The required wire thickness is (using (3.28))

$$d = (l/D) \times (d/c) \times 2r / (N - 1) = 0.37 \text{ cm}$$

Because the thickness of No.12 SWG wire is 0.264 cm, the required wire thickness is unrealistic and a  $Q$  of 400 cannot be obtained with a standard value of the wire diameter.

If the radius of the coil is decreased to  $r_2 = 1.01$  cm, the required wire thickness will be 0.26 cm.

The ratio of the former radius ( $r_1$ ) to that of the required radius was obtained iteratively by using the equation

$$\frac{r_1}{r_2} \left[ \sqrt{\frac{r_1}{r_2}} - 1/N_1 \right] = \frac{d_1}{d_2} [1 - 1/N_1] \quad (5.39)$$

This equation can be derived easily from (3.27) and (3.28).

The number of turns required is

$$N_2 = [r_1 / r_2]^{1/2} N_1 = 5.3 \quad (5.40)$$

Because of the reduction in radius, the unloaded  $Q$  of the inductor will decrease to 317. The insertion loss will therefore increase to approximately 13%.

The parasitic capacitance of the coil (0.51 pF) is much smaller than the capacitance required to provide resonance (637 pF).

With the coil designed and realizable, the tap-point can be determined. This can be done by using Table 5.2, that is, if inequality (5.36) applies. It follows from the  $l/r = 2$  column that the coil must be tapped where

$$N_1 / N_T = 0.75$$

that is, where

$$N_1 = 40$$

In order to establish whether the inequality does apply, it is necessary to calculate the values of the inductances  $L_1$  and  $L_2$  and to determine the coupling factor of the tapped coil by using (5.28):

$$L_1 = r n_1^2 \cdot 10^{-6} / \left[ 22.9 \frac{l_T}{r} \frac{n_1}{n_T} + 25.4 \right]$$

$$= 0.269 \mu\text{H}$$

By using (5.29), the value of  $L_2$  is found to be  $L_2 = 46.6 \text{ nH}$ .

The value of the coupling factor can be determined from Table 4.1 (or by using (5.32)). Its approximate value is 0.37.

Because

$$[\omega L_1 L_2 (1 - k^2)]^2 = 462.1 \times 10^{-15}$$

and

$$[L_T R_L]^2 = 400.0 \times 10^{-12}$$

inequality (5.36) does apply, and the tap-point as determined from Table 5.2 will be accurate.

## 5.7 PARALLEL DOUBLE-TUNED TRANSFORMERS

The narrowband circuits discussed up to this point match the load conjugately to the source at a single frequency only. With the double-tuned transformer shown in Figure 5.9, it is possible to match the source to the load at two different frequencies. If these frequencies are close enough to each other, the ripple in the passband can be designed to be small.

The shape of the frequency response of the double-tuned transformer is shown in Figure 5.10 for different values of the coupling factor. When the coupling factor is smaller than a certain critical value ( $k_c$ ), the source cannot be matched to the load.

The rejection characteristics of the double-tuned transformer are superior to those of a simple parallel resonant circuit. The difference becomes very pronounced when the circuit  $Q$  becomes high.

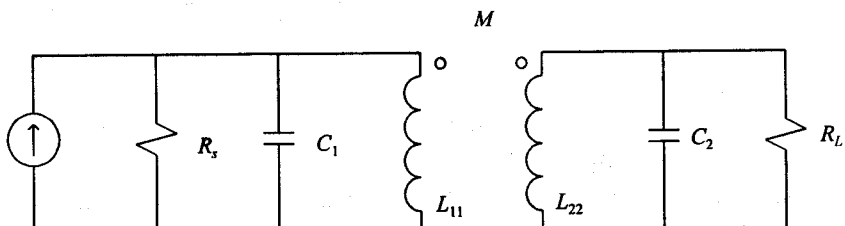


Figure 5.9 A parallel double-tuned transformer.

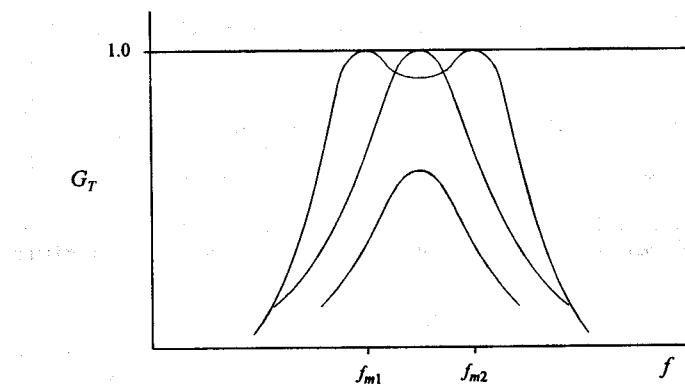


Figure 5.10 Three typical responses of the double-tuned transformer.

The transformer can be analyzed by using the equivalent circuits shown in Figure 5.11.

It is possible to match the load to the source at two different frequencies with the parallel double-tuned circuit by splitting the circuit up, as shown in Figure 5.12 (or Figure 5.13).

In Figure 5.12,  $L_2'$  and  $C_2'$  are transforming elements, while  $L_{11}$  and  $C_1$  are compensating elements. The two transforming elements can match the load resistance to  $R_L$  at two different frequencies, while the two compensating elements can be designed to cancel the residual reactance at these frequencies.

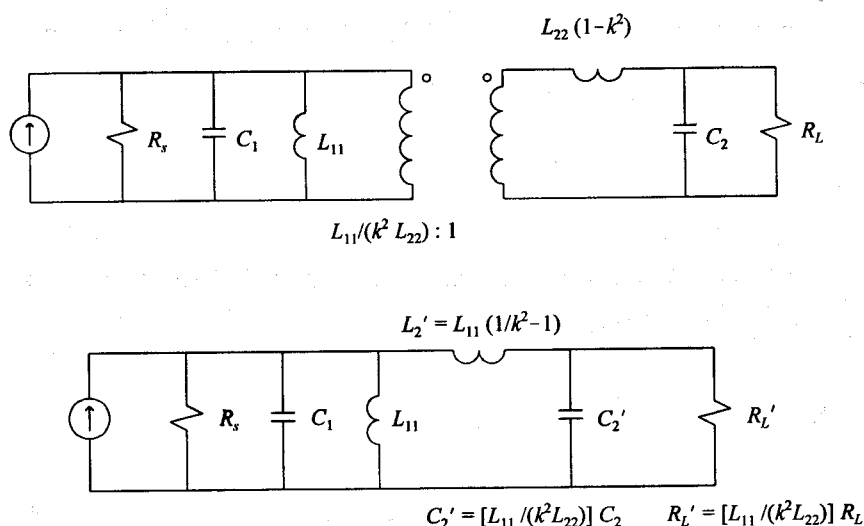
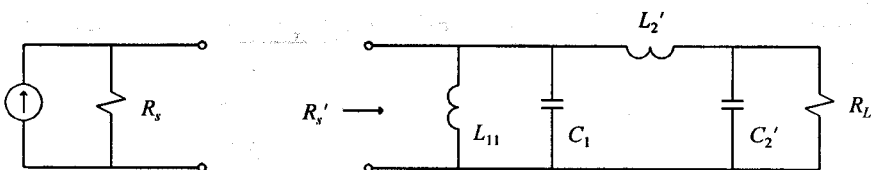


Figure 5.11 Two equivalent circuits for a parallel double-tuned transformer.



**Figure 5.12** An equivalent circuit for determining the frequencies where maximum power is transferred.

Equations for the ripple in the passband of the double-tuned transformer (see Figure 5.10) can be established by breaking up the equivalent circuit, as shown in Figure 5.13. The capacitor and inductor of the left-hand matching section cause the series resistance  $R_L'$  to decrease at high and low frequencies, respectively.  $R_L'$  is equal to the source resistance  $R_s$  at the resonant frequency of the inductor and capacitor. The capacitor in the right-hand section causes the series resistance  $R_s$  to decrease monotonically with increasing frequency. If  $R_L'$  is small enough, there will be two frequencies where the series resistance of the left-hand section is equal to that of the right-hand section.

Because the transformed resistance varies over the passband, there must inevitably be some ripple in the passband. The size of the ripple is a function of the ratio of the source resistance  $R_s$  to the series resistance of the right-hand section at the resonant frequency

$$\omega_0 = 1 / \sqrt{L_{11} C_1}$$

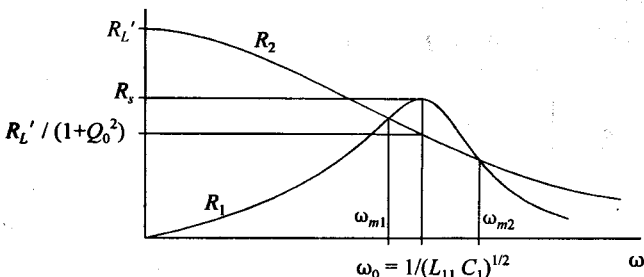
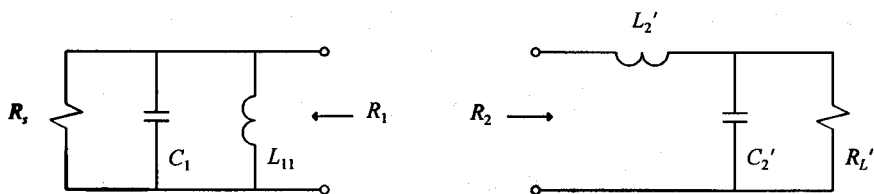


**Figure 5.13** The series resistance of the two impedance-matching sections as a function of frequency.

## A Design Procedure for a Double-Tuned Transformer

**Specifications:** The two maximum power transfer frequencies  $f_{m1}$  and  $f_{m2}$ , the load resistance  $R_L$ , the source resistance  $R_s$ , and the transducer power gain ( $G_T$ ) at the center frequency.

- As might be expected, the minimum ripple in the passband is a function of the bandwidth required. It can be shown that, for two given maximum power transfer frequencies,  $f_{m1}$  and  $f_{m2}$ , the minimum value of the transducer power gain in the passband will always be lower than

$$G_{T,\min} = \frac{4f_{m2}/f_{m1}}{(f_{m2}/f_{m1})^2 + 2f_{m2}/f_{m1} + 1} \quad (5.41)$$

The first step in the design process, therefore, is to establish whether the specified  $G_{T,\min}$  can be realized.

- Calculate the resistance ratio  $r$  ( $r = R_s/[R'_L(1+Q_0^2)]$ ) for the required passband ripple:

$$r = \frac{1 + |1 - G_T|^{1/2}}{1 - |1 - G_T|^{1/2}} \quad (5.42)$$

- Calculate the value of  $Q_2$  (i.e., the second transformation  $Q$  of the transforming section in Figure 5.12) at the two desired maximum power transfer frequencies:

$$Q_{2\_m1}^2 = r f_{m1} / f_{m2} - 1 \quad (5.43)$$

$$Q_{2\_m2}^2 = r f_{m2} / f_{m1} - 1 \quad (5.44)$$

- Solve the following two equations for the values of  $L'_2$  and  $C'_2$ :

$$-\omega_{m1} L'_2 + (1/C'_2)/\omega_{m1} = |Q_{2\_m1}| R_s / [1 + Q_{2\_m1}^2] \quad (5.45)$$

$$+\omega_{m2} L'_2 - (1/C'_2)/\omega_{m2} = |Q_{2\_m2}| R_s / [1 + Q_{2\_m2}^2] \quad (5.46)$$

- Calculate the value of  $R'_L$ :

$$R'_L = (1 + Q_{2\_m1}^2) / (\omega_{m1}^2 C'_2^2 R_s) \quad (5.47)$$

6. Calculate the value of the input susceptance ( $B_{m1}$ ,  $B_{m2}$ ) of the right-hand section in Figure 5.13 at the maximum power transfer frequencies  $f_{m1}$  and  $f_{m2}$ .

These susceptances are given by the equations

$$B_{m1} = \text{Imag} \frac{1}{j\omega_{m1}L'_2 + \frac{1}{G'_2 + j\omega_{m1}C'_2}} \quad (5.48)$$

$$B_{m2} = \text{Imag} \frac{1}{j\omega_{m2}L'_2 + \frac{1}{G'_2 + j\omega_{m2}C'_2}} \quad (5.49)$$

7. Solve the following two equations for the values of  $L_{11}$  and  $C_1$ :

$$(1/L_{11})/\omega_{m1} - \omega_{m1}C_1 = |B_{m1}| \quad (5.50)$$

$$(1/L_{11})/\omega_{m2} - \omega_{m2}C_1 = -|B_{m2}| \quad (5.51)$$

8. Calculate the values of  $k$ ,  $L_{22}$ , and  $C_2$  by using the following equations:

$$k = 1 / (1 + L'_2/L_{11})^{1/2} \quad (5.52)$$

$$L_{22} = (L_{11}/k^2) R_L / R'_L \quad (5.53)$$

$$C_2 = [L_{11}/(k^2 L_{22})] C'_2 \quad (5.54)$$

9. If the components of the transformer turn out to be unrealizable, it is often possible to obtain a practical circuit by impedance scaling of the results. L-sections can then be used to transform the load resistance and the source resistance as required. The alternative is to design a series double-tuned transformer.
10. Check the insertion loss and the frequency response by following the procedures outlined in Sections 4.8 and 4.9.

**EXAMPLE 5.3** Designing a parallel double-tuned transformer to have a passband ripple of less than 0.5 dB.

The procedure outlined above was followed to design a parallel double-tuned trans-

former with perfect matching at 9.0 and 11.0 MHz and a passband ripple of less than 0.5 dB ( $G_T = 10^{-0.5/10} = 0.89$ ). The load resistance is  $50\Omega$ , and the source resistance is  $500\Omega$ .

The results of the calculations in the different steps are repeated here:

$$1. \quad G_{T,\min} = 0.99$$

$$2. \quad r = 1.9925$$

$$3. \quad Q_{2\_9}^2 = 0.630 \quad (Q_{2\_9} = 0.739)$$

$$Q_{2\_11}^2 = 1.435 \quad (Q_{2\_11} = 1.198)$$

$$4. \quad L'_2 = 19.5 \mu\text{H}$$

$$C'_2 = 13.2 \text{ pF}$$

$$5. \quad R'_L = 5.9 \text{ k}\Omega$$

$$6. \quad B_{m1} = 1.49 \text{ mS}$$

$$B_{m2} = -2.36 \text{ mS}$$

$$7. \quad C_1 = 157 \text{ pF}$$

$$L_{11} = 1.71 \mu\text{H}$$

$$8. \quad k = 0.284$$

Table 5.3

The transducer power gain of the double-tuned transformer as a function of the frequency

Frequency (MHz)	$G_T$ (dB)
4.00	-23.00
5.00	-19.00
7.50	-5.50
8.00	-2.40
9.00	-0.06
9.95	-0.53
11.00	-0.05
12.00	-3.70
15.00	-19.00

$$L_{22} = 0.18 \mu\text{H}$$

$$C_2 = 1.55 \text{nF}$$

9. The transducer power gain of the double-tuned transformer is given in Table 5.3 as a function of the frequency (the components were assumed to be lossless).

**EXAMPLE 5.4** Illustration of the rejection obtainable with a parallel double-tuned transformer.

As an illustration of the good rejection characteristics of a double-tuned transformer, the -30-dB quality factor of a double-tuned transformer with maximum power transfer frequencies at 5.97 and 6.03 MHz (0.1-dB ripple) was calculated.

The -30-dB cut-off frequencies for the designed transformer are approximately 5.915 and 6.082 MHz. The resulting -30-dB  $Q$ -factor, therefore, is

$$Q_{-30} = 36$$

If the same results were to be obtained with a simple parallel resonant circuit, the required 3-dB  $Q$ -factor would have been 1026! The highest transformation  $Q$  in the double-tuned transformer is 60.

The -3dB  $Q$ -factor for the double-tuned transformer is approximately equal to 7. The ratio of the -3-dB and -30-dB  $Q$ -factors of the transformer, therefore, is

$$Q_{-30} / Q = 36 / 7 = 5.1$$

This ratio is 145 times that of the equivalent simple parallel resonant circuit.

## 5.8 SERIES DOUBLE-TUNED TRANSFORMERS

Although it is not the dual of the parallel double-tuned transformer, the response of the series double-tuned transformer shown in Figure 5.14 is similar to that of the parallel double-tuned transformer.

The insertion loss of the series circuit will be lower than that of the equivalent parallel circuit when the load resistance and source resistance are low.

Impedance transformation can be obtained with the circuit shown in Figure 5.14 by scaling the components on each side of the transformer to the required levels while the coupling factor remains unchanged.

The series tuned transformer can be designed to match the source conjugately to the

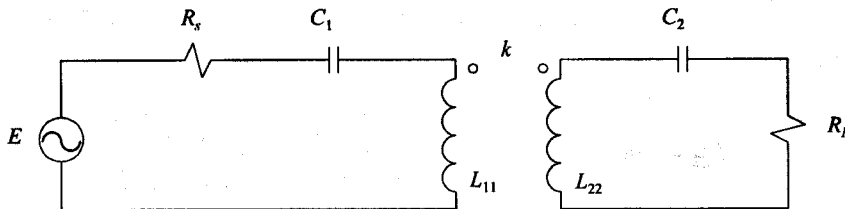


**Figure 5.14** A series double-tuned transformer.

load at two specified frequencies by following the procedure outlined below.

### A Design Procedure for a Series Double-Tuned Transformer

**Specifications:** The two maximum power transfer frequencies,  $f_{m1}$  and  $f_{m2}$ , the load resistance, the source resistance, and the transducer power gain ( $G_T$ ) at the center frequency.

1. Calculate the value of the product  $kQ$ :

$$kQ = 1 / \sqrt{G_T} + \sqrt{\frac{1}{G_T} - 1} \quad (5.55)$$

$k$  is the required coupling factor and  $Q$  is the quality factor of each of the two sides of the transformer when the coupling between them is equal to zero.

2. Determine the coupling factor required by solving the following equation:

$$k^4 + k^2[(kQ)^4 M^2 - 4(kQ)^2] + [4 - M^2](kQ)^4 = 0 \quad (5.56)$$

where

$$M = \frac{f_{m1}^2 + f_{m2}^2}{f_{m1} f_{m2}} \quad (5.57)$$

3. Determine the required uncoupled  $Q$ -factor and the circuit components:

$$Q = (kQ) / k \quad (5.58)$$

$$f_0 = [f_{m1} f_{m2} (1 - k^2)^{1/2}]^{1/2} \quad (5.59)$$

$$C_1 = 1 / [\omega_0 R_s Q] \quad (5.60)$$

$$L_{11} = Q R_s / \omega_0 \quad (5.61)$$

$$L_{22} = Q R_L / \omega_0 \quad (5.62)$$

$$C_2 = 1 / [\omega_0 R_L Q] \quad (5.63)$$

If some of these components are unrealizable, the specifications can be changed to be more realistic, or, in some cases, the components can be scaled to more realistic values. In the latter case, L-sections can be used to transform the source and load terminations to those required.

4. The insertion loss and frequency response of the transformer can be determined by following the procedure outlined in Sections 4.8 and 4.9. The 3-dB bandwidth of the series double-tuned transformer can be calculated by using the equation

$$B = \sqrt{b^2 + 2b - 1} f_0 / Q \quad (5.64)$$

where

$$b = k / k_c \quad (5.65)$$

and

$$k_c = 1 / Q \quad (5.66)$$

**EXAMPLE 5.5** Designing a series double-tuned transformer to transform a  $50\Omega$  load to  $20\Omega$ .

As an example of the application of the procedure outlined above, a transformer was designed to have maximum power transfer frequencies at 27 and 28MHz. The other specifications were  $G_T = 0.89$ ,  $R_s = 50\Omega$ , and  $R_L = 20\Omega$ .

The results obtained in the different steps are as follows:

$$1. \quad kQ = 1.41156$$

$$2. \quad M = 2.00132$$

$$k^4 + 7.93123 k^2 - 0.02101 = 0$$

$$k = 0.05246$$

3.  $Q = 27.43$   
 $f_0 = 27.48 \text{ MHz}$   
 $C_1 = 4.2 \text{ pF}$   
 $L_{11} = 7.94 \mu\text{H}$   
 $L_{22} = 3.18 \mu\text{H}$   
 $C_2 = 10.6 \text{ pF}$

4. If the transformer is assumed to be lossless, the 3-dB bandwidth is  
 $B = 1.97 \text{ MHz}$ .  
The -3-dB and -30-dB  $Q$ -factors of the transformer are

$$Q = 13.98$$

$$Q_{-30} = 2.81$$

The ratio of the two  $Q$ -factors is

$$Q_{-30}/Q = 0.2$$

## 5.9 MEASUREMENT OF THE COUPLING FACTOR OF A TRANSFORMER

Accurate measurement of the coupling factor of a transformer is sometimes required. Three ways to determine the coupling factor will be discussed here.

In the first method, the open-circuit and short-circuit input inductances of the transformer are measured, and the coupling factor is derived from these values. This method can only be used when the losses in the transformer are negligible.

In the second method, the coupling factor is estimated by measuring the open-circuit voltage gain of the transformer. An oscilloscope or voltmeter with a high input impedance (compared to the leakage reactance of the transformer at the measuring frequency) is required if reliable results are to be obtained with this method.

The Z-parameters of the transformer are used in the last method. It is usually more convenient to measure the S-parameters of the transformer. These parameters can be converted easily to Z-parameters by using (1.148).

### 5.9.1 Measurement of the Coupling Factor by Short-Circuiting the Secondary Winding

The influence of short-circuiting the secondary winding of two coupled coils can be established by using the equivalent circuit shown in Figure 5.3(b). The resistive losses will be assumed to be negligible.

The input admittance of the transformer, with the secondary winding short-circuited, is given by the equation

$$\begin{aligned} 1/(\omega L_T) &= 1/(\omega L_{11}) + 1/[(L_{11}/(k^2 L_{22})) \omega L_{22}(1 - k^2)] \\ &= 1/(\omega L_{11}) + 1/[\omega L_{11}(1/k^2 - 1)] \end{aligned} \quad (5.67)$$

This equation can be rewritten to obtain the value of the coupling factor as a function of the other variables:

$$k = [1 - L_T/L_{11}]^{1/2} \quad (5.68)$$

It is therefore possible to determine the coupling factor of the transformer by measuring the open-circuit and short-circuit impedances of the transformer (i.e., if the losses in the transformer can be ignored).

### 5.9.2 Measurement of the Coupling Factor by Measuring the Open-Circuit Voltage Gain

When the equivalent circuit of Figure 5.3(b) applies, the open-circuit voltage gain of the transformer is given by the equation

$$V_2 = \pm[j\omega k(L_{11}L_{22})^{1/2}]V_1 / (r_1 + j\omega L_{11}) \quad (5.69)$$

From this equation, the coupling factor can be obtained as

$$k = [(r_1^2 + \omega^2 L_{11}^2) / (\omega^2 L_{11}L_{22})]^{1/2} V_2 / V_1 \quad (5.70)$$

The coupling factor can, therefore, be determined by measuring the open-circuit voltage gain of the transformer  $r_1$  and the inductances  $L_{11}$  and  $L_{22}$  can be determined by measuring the open-circuited primary and secondary input impedances of the transformer.

It is important for the input impedance of the voltmeter or oscilloscope used to be much higher than the leakage reactance  $\omega L_{22}(1 - k^2)$ . Because of this, it is a good idea to define the low-impedance side of the transformer as the secondary side.

### 5.9.3 Deriving the Coupling Factor from S-Parameter Measurements

If the equipment is available, the S-parameters of the transformer can be measured. These parameters can be converted to Z-parameters by using standard conversion formulas.

If the equivalent circuit of Figure 5.3(b) applies, the transformer Z-parameters are given by the equation

$$\mathbf{Z} = \begin{bmatrix} r_1 + j\omega L_{11} & \pm j\omega M \\ \pm j\omega M & r_2 + j\omega L_{22} \end{bmatrix} \quad (5.71)$$

With the  $Z$ -parameters known, it is a simple matter to determine the copper losses, as well as the primary and secondary inductances.

The coupling factor can be determined from the mutual inductance  $M$  and the magnetizing inductances  $L_{11}$  and  $L_{22}$  by using (5.7).

## REFERENCES

1. Skilling, H. H., *Electrical Engineering Circuits*, New York: John Wiley and Sons, 1965.
2. Van der Walt, P. W., "A Simple Procedure for Designing Impedance-Matching Networks with Loosely Coupled Transformers," Research Note, University of Stellenbosch, South Africa.

# CHAPTER 6

## TRANSMISSION-LINE TRANSFORMERS

### 6.1 INTRODUCTION

The high-frequency response of a magnetically coupled transformer is limited by the leakage inductance and the parasitic capacitance of the transformer.

The leakage inductance can be decreased significantly if a balun or a stacked core (instead of a toroidal core) is used. It is more difficult, however, to decrease the parasitic capacitance between the two windings and the turns of each winding.

If the outer and center conductor of a coaxial cable are used as the primary and secondary windings of a 1:1 transformer and connected as shown in Figure 6.1(b), a 1:4 impedance transformation can be obtained (similar to that obtained with the auto-transformer shown) and the parasitic capacitance between the windings can be controlled.

One would expect the performance of this transmission-line transformer to be optimum when the capacitance between the windings is low, that is, when the characteristic impedance of the line is high. Fortunately, this is not true; rather, there is an optimum characteristic impedance for the line. The high-frequency performance of the transformer is therefore improved by the transmission-line effect.

At low frequencies the transmission-line transformer can be considered to be a conventional transformer with excellent coupling. Because of the transmission-line capacitance, however, this model is not valid at high frequencies. In fact, the magnetic coupling between the windings can be removed completely (by not using a magnetic core and straightening the line), and the high-frequency performance of the transformer will not be influenced at all (i.e., if the losses were negligible).

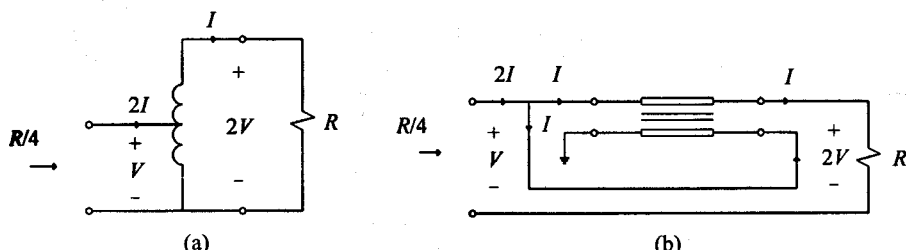
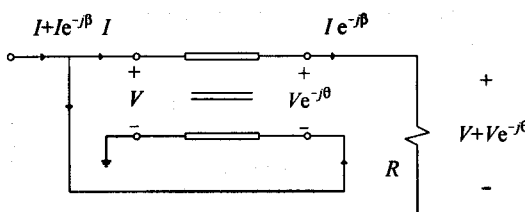


Figure 6.1 (a) A conventional auto-transformer and (b) a 1:4 transmission-line transformer.



**Figure 6.2** The voltages across and the currents in a transmission-line transformer at high frequencies.

That this is possible can be appreciated by assuming the currents in the transmission line to be balanced and the line to be short enough for the phase difference between the voltages across the line and the currents in the line to be small. This is illustrated in Figure 6.2.

It has been assumed in Figure 6.2 that the currents in the transmission line are balanced. If the currents were perfectly balanced, as shown in Figure 6.3(a), the output voltage would have been zero, which is not the case. The currents in the line must be unbalanced for the output voltage to be non-zero.

Because

$$V_o = 2sL_u \ell I_{1u} = 2j\omega L_u \ell I_{1u} \quad (6.1)$$

the unbalanced current is very small at high frequencies. In (6.1)  $L_u$  is the inductance per unit length for the unbalanced current,  $\ell$  the length of the line, and  $I_{1u}$  the unbalanced component of the current in each of the two conductors of the line.

Although the high-frequency performance of the transmission-line transformer is not affected by the removal of the magnetic core, the low-frequency response is seriously degraded when this is done. The reason for this is the increase in the unbalanced current. This current increases approximately inversely with frequency. When magnetic material is used, the inductance in (6.1) is increased and the unbalanced current is reduced. If the unbalanced current is small enough, the frequency response of the transformer will be very good at both high and low frequencies.

The bandwidth obtainable with a transmission-line transformer is significantly better than that obtainable with a conventional transformer.

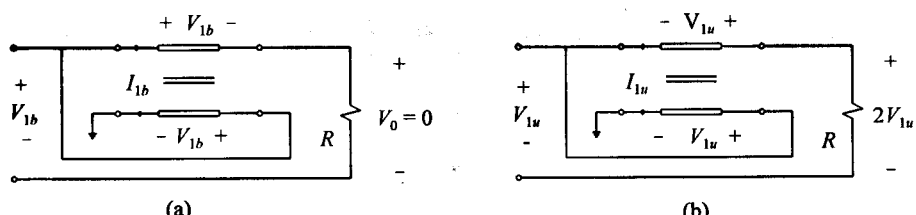


**Figure 6.3** The output voltage of the 1:4 transmission-line transformer as a function of (a) the balanced and (b) unbalanced currents in the line.

Because of the wide bandwidth, transmission-line transformers are often used to transform resistance. When only one transmission line is used, the only transformation ratios that can be obtained are 1:1 and 1:4. When more than one line is used, it is possible to realize transformers with other transformation ratios.

Apart from impedance matching, transmission-line transformers are also used to perform various combining and splitting functions.

The most commonly used configurations will be presented in the next section.

The analyses of the 1:4 transmission-line transformer and other transmission-line transformers will be discussed in detail in Section 6.3. It will be shown in this section that the basic component of any transmission-line transformer is an unbalanced transmission line with increased inductance for the unbalanced currents in the line. This simplifies to a balanced transmission line at high frequencies and a 1:1 transformer with magnetizing inductance at low frequencies.

The design of transmission-line transformers primarily requires that the transformer meets the low-frequency specifications. Compensation at low and/or high frequencies may also be required to extend the bandwidth. The various steps in designing these transformers will be considered in detail in Section 6.4.

Transmission-line transformers are used extensively in RF power amplifiers. The design of impedance-matching networks for these amplifiers will be considered in Section 6.5.

## 6.2 TRANSMISSION-LINE TRANSFORMER CONFIGURATIONS

Transmission-line transformers are used to change resistance levels in impedance-matching networks and amplifiers, as well as to perform certain splitting and combining functions.

The transformation ratios obtainable with these transformers are limited to those shown in Table 6.1, that is, if less than five transmission lines are used.

The number of lines used in a practical application is limited by the available space. To ensure a good low-frequency response, each line must be wound around a magnetic core.

More than one line can sometimes be wound around the same core. The polarity of the voltage induced by the flux in the core and the relative size of the voltage across each winding must be taken into account when this is done.

The configuration corresponding to a particular transformation ratio can be found by using the technique illustrated in Figure 6.4 [1]. When this technique is applied, the ratio of the input to output voltage changes from  $x / y$  to  $[x / (x + y)]$ . The impedance transformation ratio is changed from  $(x / y)^2$  to  $[x / (x + y)]^2$ .

In the simplest case,

$$x = 1 = y$$

and the application of this technique results in the configuration for the 1:4 transmission-line transformer.

Table 6.1

Transformation ratios obtainable with transmission-line transformers as a function of the number of lines used

Number of lines	1	2	3	4
Transformation ratios obtainable	1:1.00 $(1/1)^2$	1:2.25 $(2/3)^2$	1:1.78 $(3/4)^2$	1:1.56 $(4/5)^2$
	1:4.00 $(1/2)^2$	1:4.00 $(1/2)^2$	1:2.78 $(3/5)^2$	1:1.96 $(5/7)^2$
	—	1:9.00 $(1/3)^2$	1:6.25 $(2/5)^2$	1:2.56 $(5/8)^2$
	—	—	1:16.0 $(1/4)^2$	1:3.06 $(4/7)^2$
	—	—	—	1:5.44 $(3/7)^2$
	—	—	—	1:7.11 $(3/8)^2$
	—	—	—	1:12.3 $(2/7)^2$
		—	—	1:25.0 $(1/5)^2$

If the technique is applied to the 1:4 transformer, the 1:9 transformer shown in Figure 6.5(a) is obtained.

By considering the high impedance side of the 1:4 transformer to be the input, the 1:2.25 transformer shown in Figure 6.5(b) is obtained.

The configurations for the  $(3/4)^2$ ,  $(1/4)^2$  and the  $(2/5)^2$ ,  $(3/5)^2$  transformers can be found by applying the technique to the 1:9 and 9:1 and the 4:9 and 9:4 transformers, respectively. The configurations for the 1:16 and the 4:25 transformers are shown in Figure 6.6.

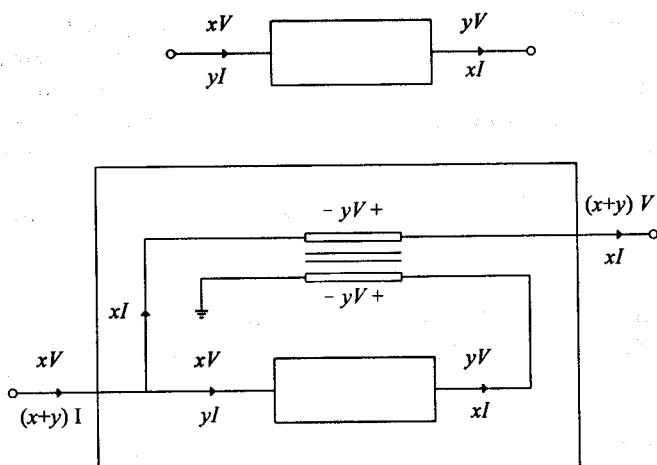


Figure 6.4 The influence of adding an extra line on the impedance transformation ratio of a transmission-line transformer.

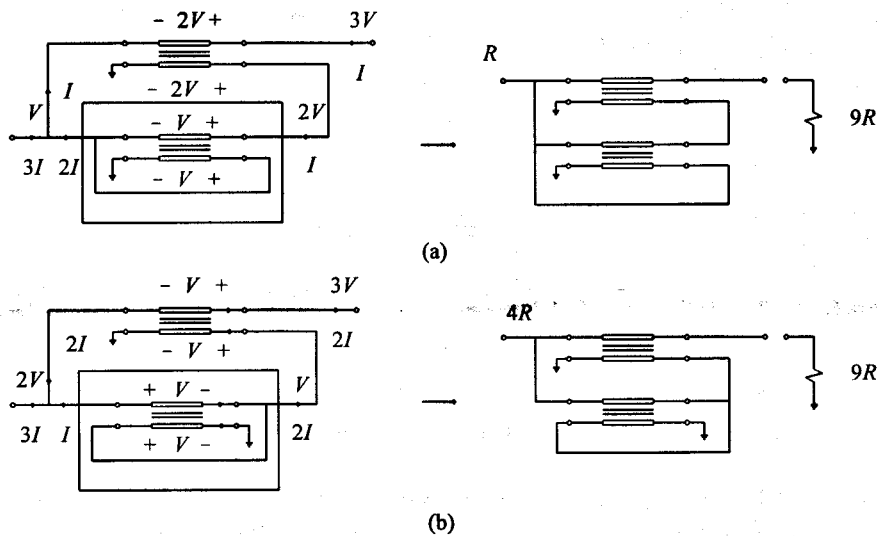


Figure 6.5 Derivation of the configurations for the (a) 1:9 and (b) 4:9 transmission-line transformers.

The transformers most often used in power amplifiers are the 1:4 and 1:9 transmission-line transformers. The high cut-off frequency of the 1:4 transformer can be increased considerably if two lines instead of only one are used, as shown in Figure 6.7 [2].

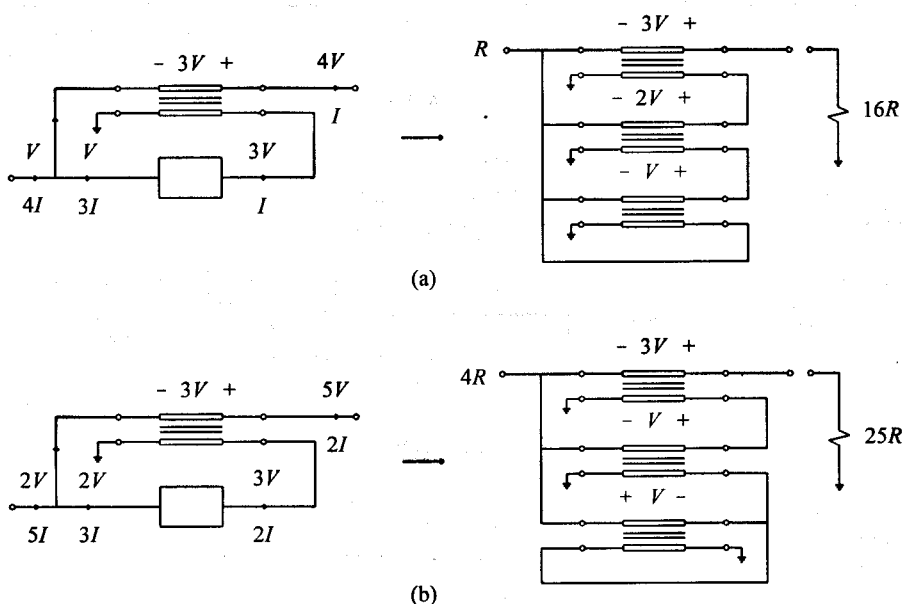
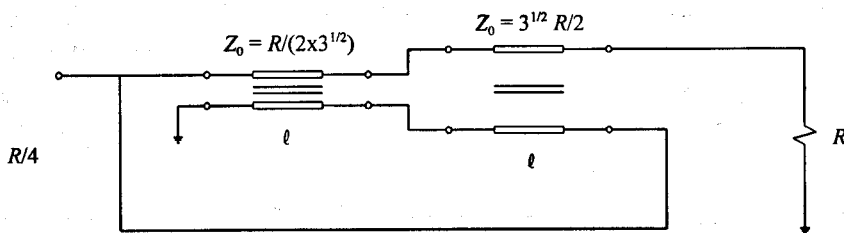
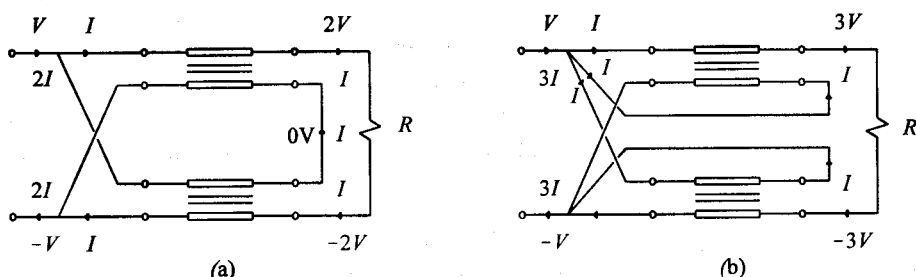


Figure 6.6 The configurations of the (a) 1:16 and (b) 4:25 transmission-line transformers.



**Figure 6.7** The configuration of a 1:4 transmission-line transformer that has no high cut-off frequency (theoretically).

Impedance transformation between a balanced source and a balanced load is often required. The configurations for the balanced 1:4 and 1:9 transmission-line transformers are shown in Figure 6.8(a) and (b), respectively.



**Figure 6.8** The configurations for the balanced (a) 1:4 and (b) 1:9 transmission-line transformers.

When either the load or the source is unbalanced, the 1:1 transformer shown in Figure 6.9 can be used to provide the required unbalanced-to-balanced transformation.

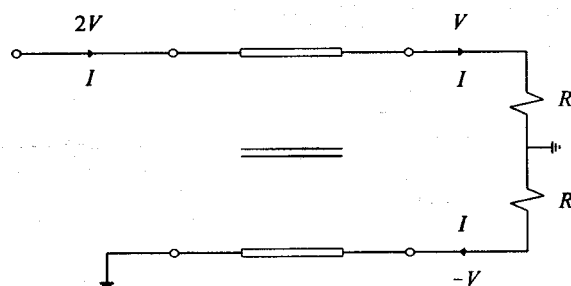


**Figure 6.9** The unbalanced-to-balanced 1:1 transmission-line transformer.

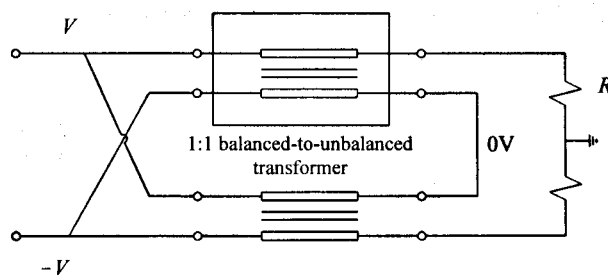


**Figure 6.10** Illustration of the equivalence between the 1:4 balanced and the 1:1 balanced-to-unbalanced transmission-line transformers.

At high frequencies, the frequency response of the 1:1 transformer is exactly the same as that of a transmission line terminated in the same load.

Because of the symmetry, the high-frequency response of the 1:4 balanced transformer is identical to that of the 1:1 transformer. The equivalence is illustrated in Figure 6.10.

A 4:1 unbalanced-to-balanced transformation can be obtained by combining the 1:1 and 1:4 balanced transformers, as shown in Figure 6.11(a), or by using the transformer shown in Figure 6.11(b). The latter transformer is less sensitive to nonoptimum characteristic impedances than the former, although it has a lower cut-off frequency when the optimum characteristic impedance is used.

The output currents of the two transistors in a push-pull class B amplifier are often

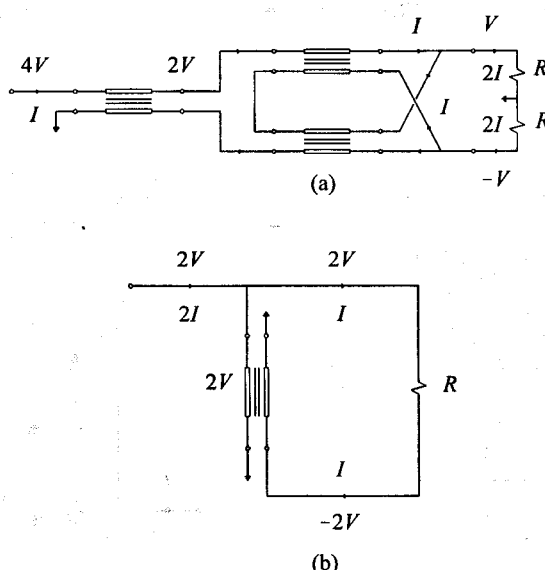


**Figure 6.11** (a) Combination of a 1:1 transformer and a 4:1 transformer to obtain an unbalanced-to-balanced transformation. (b) A 1:4 unbalanced transmission-line transformer.

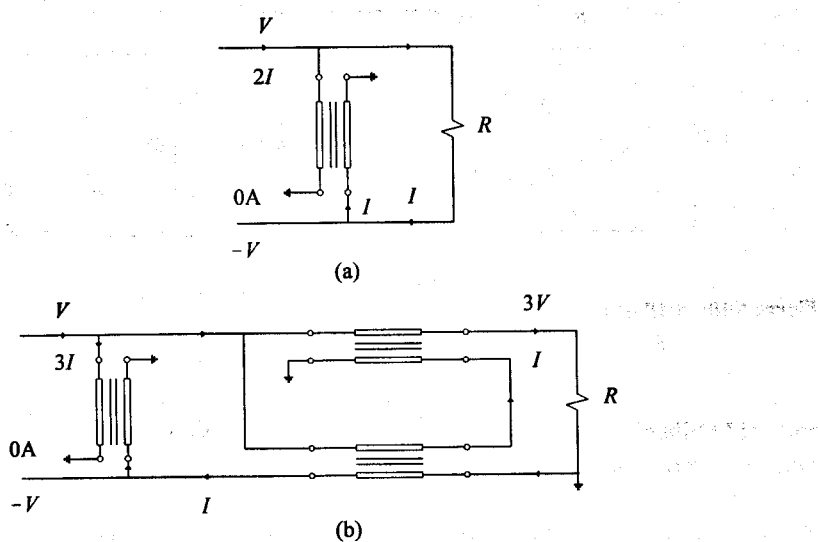


**Figure 6.12** (a) 1:4 and (b) 1:9 transformers for combining the currents of the transistors in a class B amplifier into a single load.

combined (at lower frequencies where the conduction angle is  $180^\circ$ ) by using either of the 1:4 or 1:9 transformers shown in Figure 6.12.

Although they are used for different purposes, it can be seen that the configurations of the 1:4 transformer shown in Figure 6.12 are similar to that of the 1:4 unbalanced-to-balanced transformer shown in Figure 6.11(b).

By redefining the reference plane of the 1:4 transformer in Figure 6.12(a) (as shown in Figure 6.13), it becomes clear that the frequency responses of both are identical.

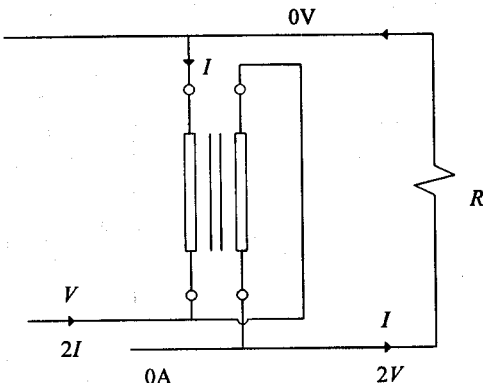


**Figure 6.13** The configuration of the 1:4 transformer from Figure 6.12 with a redefined reference plane (ground).

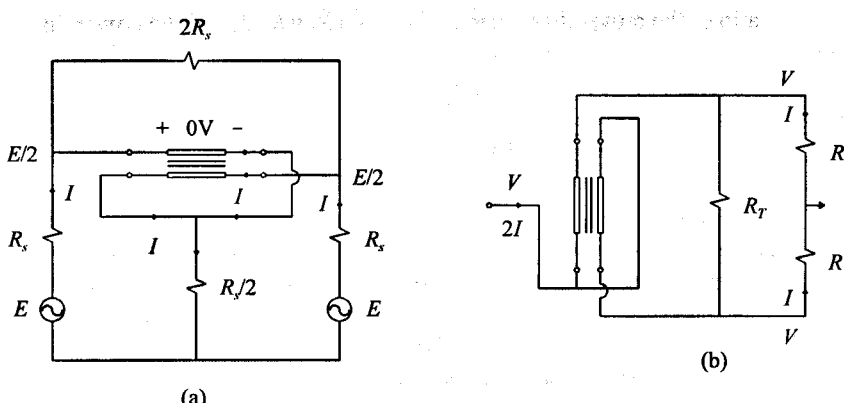


**Figure 6.14** (a) A transformer for combining two in-phase signals into the same load; (b) the same transformer used as an in-phase power splitter.

The combiner shown in Figure 6.14(a) is often used to combine two in-phase signals at radio frequencies.

As indicated in the figure, the voltage drop across the 1:1 transformer used in the combiner is equal to zero when the two input signals are equal in amplitude and are in-phase. When the signals are unbalanced, the two sources will be isolated from each other by the transformer. This is illustrated in Figure 6.15 for the case where  $E_2 = 0$ . If the transformer is assumed to be ideal, and  $R_T = 2R_s = 4R_L$ , no current will flow in the resistance  $R_{s2}$ .

At low frequencies, the isolation obtainable with this transformer is a function of the magnetizing inductance of the 1:1 transformer; that is,

$$S = [4\omega L_{11} / (R_s / 2)]^2 + 1 \quad (6.2)$$

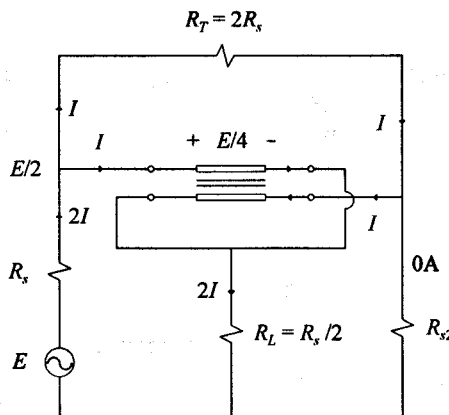


**Figure 6.15** Illustration of the isolating action of the hybrid transformer shown in Figure 6.14(a).

where  $S$  is the ratio of the power dissipated in the load ( $R_L = R_s/2$ ) and the power dissipated in the source resistance ( $R_{s2}$ ), when  $E_2 = 0$ .

The isolation at high frequencies is a function of the electrical length of the line and the characteristic impedance.

The combiner can be changed to a splitter by connecting it as shown in Figure 6.14(b).

As in the case of the combiner, the voltage drop across the 1:1 transformer will be zero as long as the loads are balanced. If not, the transformer will cause the power to be distributed more evenly between the two loads than would be the case with a direct connection.

### 6.3 ANALYSIS OF TRANSMISSION-LINE TRANSFORMERS

The basic building block of a transmission-line transformer is an unbalanced transmission line (see Figure 6.16). The line can be wound around magnetic material or can be shaped as a solenoidal coil. The latter can be done by using semi-rigid coaxial cable.

The currents in the two conductors of an unbalanced transmission-line are not equal, but are related by the equation

$$I_2(x) = I_1(x) + I_0(x) \quad (6.3)$$

Because the effective current entering the line at any point ( $I_{\text{eff}} = I_1(x) - I_2(x) = -I_0(x)$ ) must be equal to the current flowing out of the line at any other point further along the line (see Figure 6.17), the unbalanced current ( $I_0(x)$ ) is independent of the distance ( $x$ ) along the line. Therefore, (6.3) simplifies to

$$I_2(x) = I_1(x) + I_0 \quad (6.4)$$

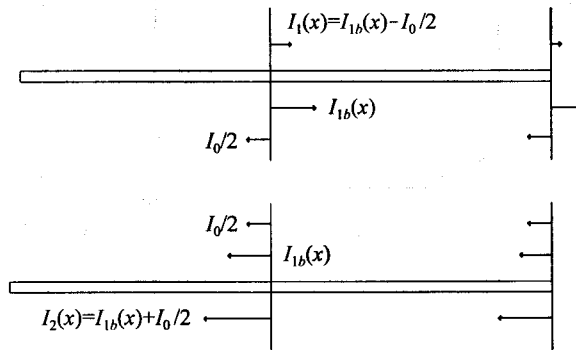


**Figure 6.16** The balanced and unbalanced components of the current in a transmission line.

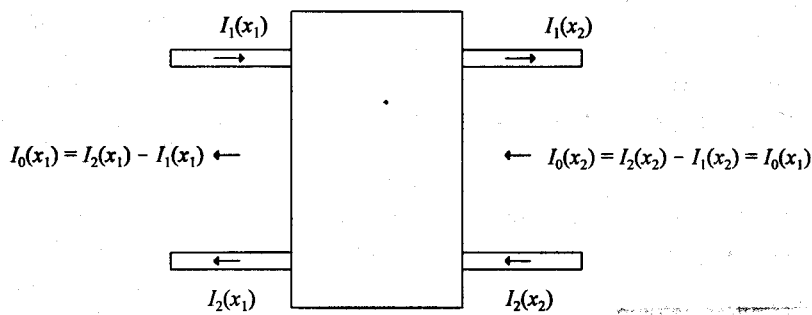


**Figure 6.17** The unbalanced current on a transmission line as a function of the distance along the line.

The effect of the magnetic material (or solenoidal shape) is to increase the impedance associated with the unbalanced currents in the line.

Because there is no external magnetic field associated with the balanced currents ( $\oint H dl = I_{lb} - I_{lb} = 0$ ), these currents are not influenced by the magnetic material used or by the form in which the line is wound.

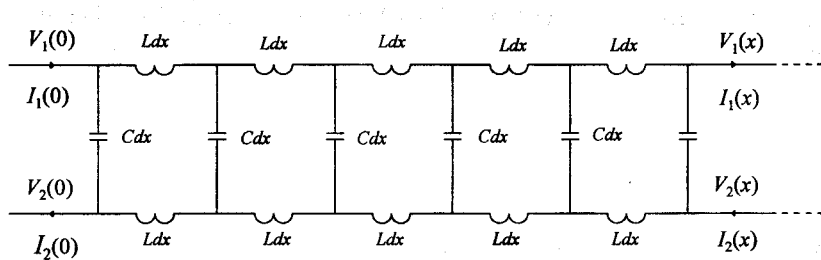


**Figure 6.18** The equivalent circuit of an unbalanced transmission-line.

If the influence of the magnetic core or the coil form on the unbalanced currents is ignored initially, the equivalent circuit shown in Figure 6.18 applies and equations for the voltage on and the current in the unbalanced transmission line can be derived in a way similar to the balanced transmission line case (refer to Appendix A). The results of the derivation are shown below:

$$I_1(x) = -I_0 / 2 + Ae^{-\Gamma x} + Be^{+\Gamma x} \quad (6.5)$$

$$I_2(x) = I_0 / 2 + Ae^{-\Gamma x} + Be^{+\Gamma x} \quad (6.6)$$

$$V_1(x) = V_1(0) - Z_0 / 2 \cdot (A - B) + Z_0 / 2 \cdot [Ae^{-\Gamma x} - Be^{\Gamma x}] + s L_u x I_0 / 2 \quad (6.7)$$

$$V_2(x) = V_2(0) + Z_0 / 2 \cdot (A - B) - Z_0 / 2 \cdot [Ae^{-\Gamma x} - Be^{\Gamma x}] + s L_u x I_0 / 2 \quad (6.8)$$

$$V_{12}(x) = V_1(x) - V_2(x) = Z_0 [Ae^{-\Gamma x} - Be^{\Gamma x}] \quad (6.9)$$

where

$$\Gamma = \sqrt{2LC} \quad s = j\omega \sqrt{2LC} \quad (6.10)$$

$$Z_0 = \sqrt{2L/C} \quad (6.11)$$

$L$  and  $C$  are the inductance and capacitance of the line per unit length, respectively, and  $x$  is the position of the point of interest on the line (relative to the LHS). Note that the inductance for the balanced currents ( $L$ ) and that for the unbalanced currents ( $L_u$ ) are not the same because of the magnetic coupling between the two conductors of the line.

When magnetic material is used or the line is shaped as a coil, the reactance associated with the unbalanced currents ( $I_0 / 2$ ) must be changed from  $sL_u l$  to

$$X_u = 2sL_{11} \quad (6.12)$$

where  $L_{11}$  is the inductance associated with each conductor of the line when the other conductor is open-circuited and  $l$  is the length of the transmission-line.

The inductance associated with the unbalanced current in each conductor is twice the expected value ( $L_{11}$ ) because of the excellent coupling between the two conductors of the transmission line. When current is flowing in only one conductor, the voltage across the length of the other conductor will be equal to that of the first, provided that there are no resistive losses in the conductors. The coupling factor, therefore, is very close to unity.

When magnetic material is used or the line is wound as a coil, (6.7) and (6.8) must be changed to

$$V_1(x) = V_1(0) - (Z_0 / 2)(A - B) + (Z_0 / 2)[Ae^{-\Gamma x} - Be^{\Gamma x}] + s(2L_{11})(x/l)I_0 / 2 \quad (6.7b)$$

and

$$V_2(x) = V_2(0) + (Z_0 / 2)(A - B) + (Z_0 / 2)[Ae^{-\Gamma x} - Be^{\Gamma x}] + s(2L_{11})(x/l)I_0 / 2 \quad (6.8b)$$

Before (6.5) through (6.9) can be used to determine the voltages on and the currents in any particular transmission-line transformer, the constants  $A$ ,  $B$ ,  $I_0$ ,  $V_1(0)$ , and  $V_2(0)$  must be determined.

These constants can be determined by using the boundary conditions for the transformer under consideration.

When the voltages and currents are known, the power gain and the input and output impedances of the transformer can be determined easily.

Because the transmission line can usually be considered lossless, it is sufficient that the input impedance of a transformer is known (in the lossless case, the magnitudes of the input and output reflection coefficients are equal, and the magnitude of the transducer power gain is only a function of the reflection coefficient). The input impedance of a transmission-line transformer is a function of the frequency, the load impedance, and the length and characteristic impedance of the transmission line used. The expression for the input impedance is therefore usually quite complex.

Although the complexity is not a problem when a computer program is used to analyze a transmission-line transformer, it is possible to simplify the equation for the input impedance at low and high frequencies by making appropriate assumptions. At high frequencies, the reactance associated with each conductor is high compared to the characteristic impedance of the line, and the approximation

$$sL_u l \gg Z_0 \quad (6.13)$$

can be made. Under this approximation, the input impedance of the transformer is only a function of the balanced currents in the line. As far as the impedance is concerned, the transmission line can then be considered balanced.

At low frequencies, the line is electrically very short and the approximation

$$z^{\Gamma I} = 1 \quad (6.14)$$

can be made and the input impedance of the transformer is independent of the length and the characteristic impedance of the transmission line. The transmission-line transformer can then be considered to be a conventional transformer.

It follows that the basic building block of a transmission-line transformer reduces to a balanced transmission line and a conventional 1:1 transformer with magnetizing inductance  $L_{11}$  at high and low frequencies, respectively. This is illustrated in Figure 6.19.

### EXAMPLE 6.1 The input impedance of a 1:4 transmission-line transformer.

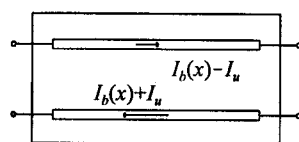
The input impedance of a 1:4 unbalanced transmission-line transformer (see Figure 6.20) will be determined as an example of the application of (6.5) to (6.11).

The boundary conditions for the transformer are as follows:

$$V_2(0) = 0 \quad (6.15)$$

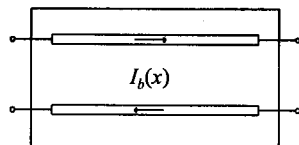
$$V_2(l) = V_1(0) \quad (6.16)$$

$$V_1(l) = Z_L I_1(l) \quad (6.17)$$



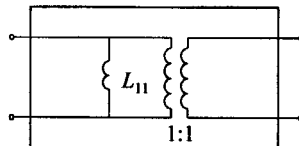
Unbalanced transmission line

(a)



Balanced transmission

(b)



Ideal 1:1 transformer with magnetizing inductance

(c)

**Figure 6.19** (a) The basic building block of a transmission-line transformer simplified at (b) high and (c) low frequencies.

These conditions will be used to find two independent equations for the unbalanced current  $I_0$  in terms of  $A$  and  $B$ . In this way, the relationship between  $A$  and  $B$  can be established and the input impedance can be found:

$$V_1(0) = V_{12}(0) = Z_0[Ae^{-\Gamma x} - Be^{\Gamma x}] = Z_0(A - B)$$

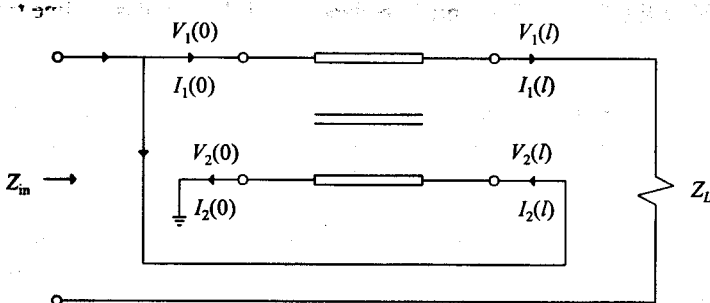


**Figure 6.20** The 1:4 unbalanced transmission-line transformer.

$$V_2(l) = 0 + 0.5 Z_0 [A - B] + s L_u l I_0 / 2 - 0.5 Z_0 [A e^{-\Gamma l} - B e^{\Gamma l}]$$

Because  $V_1(0)$  and  $V_2(l)$  are equal, these two equations can be used to obtain an equation for  $I_0$  in terms of  $A$  and  $B$ . After some manipulation, the following equation is obtained:

$$s L_u l I_0 = Z_0 / (s L_u l) \cdot [A - B] + Z_0 / (s L_u l) \cdot [A e^{-\Gamma l} - B e^{\Gamma l}] \quad (6.18)$$

The second equation is established by using the constraint imposed by the load:

$$V_1(l) = V_1(0) - 0.5 Z_0 [A - B] + s L_u l I_0 / 2 + 0.5 Z_0 [A e^{-\Gamma l} - B e^{\Gamma l}]$$

and

$$Z_L I_1(l) = Z_L [-I_0 / 2 + A e^{-\Gamma l} + B e^{\Gamma l}]$$

By equating these two equations, it follows that

$$\begin{aligned} [Z_L + s L_u l] I_0 &= 2A[Z_0 e^{-\Gamma l} - 0.5 Z_0 (e^{-\Gamma l} + 1)] \\ &\quad + 2B[Z_0 e^{\Gamma l} + 0.5 Z_0 (e^{\Gamma l} + 1)] \end{aligned} \quad (6.19)$$

The relationship between  $A$  and  $B$  can now be determined by using (6.18) and (6.19):

$$\frac{B}{A} = \frac{Z_0 E_2 [1 + Z_L / (s L_u l)] - 2[Z_L e^{-\Gamma l} - (Z_0 / 2) E_2]}{Z_0 E_1 [1 + Z_L / (s L_u l)] + 2[Z_L e^{\Gamma l} + (Z_0 / 2) E_1]} \quad (6.20)$$

where

$$E_1 = 1 + e^{\Gamma l}$$

and

$$E_2 = 1 + e^{-\Gamma l}$$

The input impedance of the transformer is given by the equation

$$Z_{in} = V_1(0) / [I_1(0) + I_2(l)]$$

$$= Z_0 \frac{1 - B/A}{E_2 + (B/A) \cdot E_1} \quad (6.21)$$

If the approximation

$$e^{\pm\Gamma l} \approx 1$$

is used, the equations for the ratio  $B/A$  and the input impedance of the transformer simplifies to

$$\frac{B}{A} = \frac{2Z_0 s L_u l + Z_L Z_0 - Z_L s L_u l}{2Z_0 s L_u l + Z_L Z_0 + Z_L s L_u l} \quad (6.22)$$

and

$$Z_{in} = (Z_0 / 2) \frac{1 - B/A}{1 + B/A} = \frac{(Z_L / 4) \cdot s L_u l / 2}{(Z_L / 4) + s L_u l / 2} \quad (6.23)$$

If magnetic material is used, the reactance  $sL_u l$  in these equations must be replaced with  $(2L_{11})s$ . The input impedance is then

$$Z_{in} = \frac{(Z_L / 4) \cdot sL_{11}}{(Z_L / 4) + sL_{11}} \quad (6.24)$$

At high frequencies, the approximation

$$sL_u l \gg Z_0$$

can be made, and the expression for the ratio  $B/A$  simplifies to

$$\frac{B}{A} = \frac{Z_0 [1 + e^{-\Gamma l}] - Z_L e^{-\Gamma l}}{Z_0 [1 + e^{+\Gamma l}] + Z_L e^{+\Gamma l}} \quad (6.25)$$

The impedance is still given by (6.21).

The transducer power gain for the transformer can be determined by using the equation

$$G_T = 1 - \left| \frac{Z_{in} - Z_s^*}{Z_{in} + Z_s} \right|^2 \quad (6.26)$$

where  $Z_s$  is the impedance of the source driving the transformer.

**EXAMPLE 6.2** The input impedance of a 1:1 balanced-to-unbalanced transformer.

The input impedance of a 1:1 balanced-to-unbalanced transmission-line transformer (see Figure 6.21) can be determined by using the following boundary conditions:

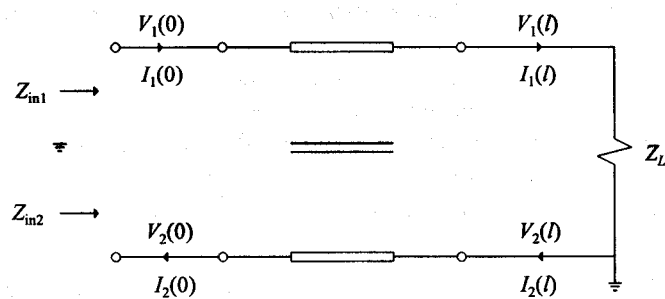


Figure 6.21 The 1:1 balanced-to-unbalanced transmission-line transformer.

$$V_1(l) = Z_L I_1(l) \quad (6.27)$$

$$V_2(l) = 0 \quad (6.28)$$

$$V_1(0) = -V_2(0) \quad (6.29)$$

By using (6.27), the unbalanced current is found to be

$$I_0 / 2 = Ae^{-\Gamma l} [1 - Z_0 / Z_L] + Be^{\Gamma l} [1 + Z_0 / Z_L] \quad (6.30)$$

When (6.28) and (6.29) used, the second equation necessary for determining the ratio  $B/A$  is found to be

$$s L_u l I_0 / 2 = (Z_0 / 2) \cdot [Ae^{-\Gamma l} - Be^{\Gamma l}] \quad (6.31)$$

The ratio  $B/A$  can now be obtained by using these two equations:

$$\frac{B}{A} = -\frac{e^{-\Gamma l} [1 - Z_0 / Z_L] - [Z_0 / (2s L_u l)] e^{-\Gamma l}}{e^{\Gamma l} [1 + Z_0 / Z_L] + [Z_0 / (2s L_u l)] e^{\Gamma l}} \quad (6.32)$$

When  $B/A$  is known, the input impedances  $Z_{in1}$  and  $Z_{in2}$  can be determined. These impedances are given by the equations.

$$Z_{in1} = \frac{Z_0 [1 - B/A]}{-[Z_0 / (s L_u l)] [e^{-\Gamma l} - (B/A) e^{\Gamma l}] + 2[1 + B/A]} \quad (6.33)$$

$$Z_{in2} = \frac{Z_0 [1 - B/A]}{+[Z_0 / (s L_u l)] [e^{-\Gamma l} - (B/A) e^{\Gamma l}] + 2[1 + B/A]} \quad (6.34)$$

It is clear from the different signs in the denominators of (6.33) and (6.34) that the two input impedances are not equal at low frequencies.

When  $sL_u l \gg Z_0$ , the two impedances are approximately equal, independently of the characteristic impedance value of the line.

Furthermore, the input impedance of the transformer is identical to that of a balanced transmission line terminated in the same load impedance ( $Z_L$ ).

By using this equivalence, it follows that the input impedance of the 1:1 balanced-to-unbalanced transmission-line transformer will be purely resistive at high frequencies if  $Z_0 = R_L$ .

Because of the symmetry, the same applies to the 1:4 balanced transmission-line transformer.

## 6.4 DESIGN OF TRANSMISSION LINE TRANSFORMERS

The design of transmission-line transformers consists of the following:

1. Determining the characteristic impedance and the diameter of the transmission line to be used;
2. Determining the minimum value of the magnetizing inductance of the transformer at the lowest passband frequency;
3. Selecting a suitable magnetic material (if needed);
4. Determining the type and size of the core to be used;
5. Calculating the line length and the corresponding high cut-off frequency of the transformer;
6. Compensating the transformer for nonoptimum characteristic impedance, if necessary;
7. Extending the bandwidth by using LC impedance-matching networks, if necessary.

Each of these points will be discussed in detail in the following sections.

### 6.4.1 Determining the Optimum Characteristic Impedance and Diameter of the Transmission Line to Be Used

At high frequencies, the input impedance of a transmission-line transformer is a function of the characteristic impedance of the transmission line.

The optimum characteristic impedance can be established by taking the ratio of the

voltage across one end of the transmission line and the current passing through it. The basic building block of the transformer is then considered to be an ideal 1:1 transformer.

The application of this rule to a 1:4 unbalanced transmission-line transformer is illustrated in Figure 6.22.

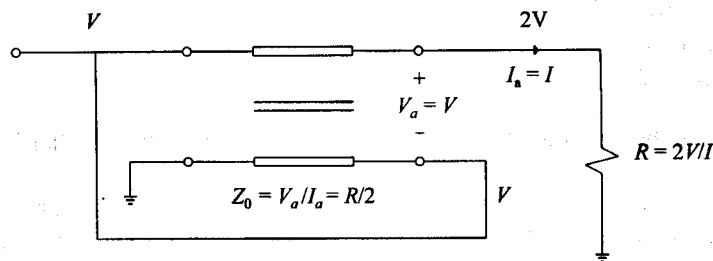


**Figure 6.22** Determining the optimum characteristic impedance of an 1:4 unbalanced transmission-line transformer.

If a line with any other characteristic impedance is used, the input reflection coefficient of the transformer will be affected adversely.

The effect of the characteristic impedance on the cut-off frequency of the transformer will be discussed later.

When the optimum characteristic impedance is known, the type of line to be used must be chosen.

Coaxial cables with  $25\Omega$  and  $50\Omega$  characteristic impedance are freely available. A line with a  $12.5\Omega$  characteristic impedance can be obtained by connecting two  $25\Omega$  lines in parallel, while  $100\Omega$  can be obtained by connecting two  $50\Omega$  lines in series.

A wide range of characteristic impedances can be obtained by twisting together pairs of conductors with various diameters. When very low impedances are required (less than  $10\Omega$ ), many conductors with smaller diameters can be twisted together.

The characteristic impedances of these twisted lines are influenced by the diameter of the wire used, as well as the number of twists per unit length.

Apart from the characteristic impedance, it is also necessary to decide on the diameter of the cable to be used where applicable. This is determined by the losses that can be tolerated and the power to be transmitted through the line.

The attenuation of bifilar or multifilar transmission lines can become a problem at high frequencies, as mentioned in Chapter 3.

#### 6.4.2 Determining the Minimum Value of the Magnetizing Inductance of the Transformer

At low frequencies the transmission-line transformer can be considered to be a conventional 1:1 transformer connected in a special way.

When this model is used, the input impedance and power gain versus frequency response at low frequencies can be determined by using Kirchhoff's voltage and current laws on the simplified equivalent circuit.

If the load consists of a single resistor, only the input impedance of the transformer needs to be determined. The power dissipated in the load (and therefore the power gain) can be found by using the equation

$$P_L = V_{cc}^2 G_{\text{eff}} / 2 \quad (6.35)$$

where  $V_{cc}$  is the maximum (peak) voltage across the effective parallel input resistance ( $R_{\text{eff}} = 1/G_{\text{eff}}$ ) of the transformer.

When the input impedance and the transfer function are known, the minimum inductance ( $L_{11}$ ) required to meet the low-frequency specifications can be determined.

The minimum value of the magnetizing inductance of the 1:4 unbalanced and 1:1 unbalanced-to-balanced transformers will be established as examples.

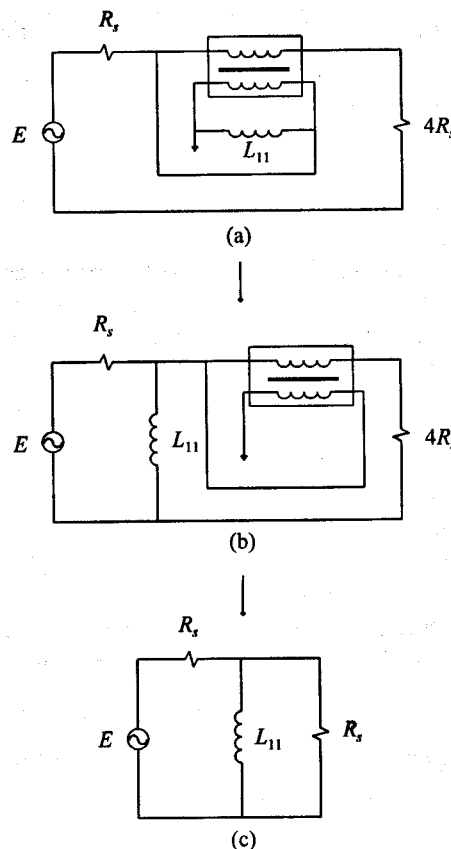


**Figure 6.23** Simplification of the equivalent circuit of the 1:4 unbalanced transformer at low frequencies.

**EXAMPLE 6.3**

The magnetizing inductance required in a 1:4 transmission-line transformer.

With the transmission line replaced by a 1:1 transformer with magnetizing inductance, the equivalent circuit of the 1:4 transmission-line transformer can be simplified as shown in Figure 6.23.

If the cut-off frequency is to be the 3-dB cut-off frequency, it is obvious from Figure 6.23(c) that the required magnetizing inductance  $L_{11}$  must be such that

$$\omega L_{11} = R_s / 2 \quad (6.36)$$

If this transformer is to be used in a power amplifier, the magnetizing inductance must be high enough for the specified minimum allowable ripple in the passband to be achieved.

Because the power dissipated in the load is given by (6.35), the output power is directly proportional to the effective parallel input resistance.

The efficiency of the amplifier is decreased if the effective load is reactive (refer to Section 2.3.3), that is, if the output impedance of the transistor is assumed to be purely resistive. Specifically, it is decreased by a factor

$$\eta_r = 1 / [1 + (R_{\text{eff}} / X_{\text{eff}})^2]^{1/2} \quad (6.37)$$

where  $X_{\text{eff}}$  is the effective parallel input reactance of the transformer.

Because  $R_{\text{eff}}$  is equal to the optimum value ( $R_s$ ) in this particular problem, the power transmitted through the 1:4 transformer is also equal to the optimum value, that is, at low frequencies.

The relative efficiency is given by

$$\eta_r = 1 / [1 + (R_s / (\omega L_{11}))^2]^{1/2}$$

If  $\eta_r = 0.95$  is acceptable, the magnetizing inductance must be such that

$$\omega L_{11} = 3R_s \quad (6.38)$$

( $\omega L_{11}$  is often chosen to be equal to  $4R_s$ ).

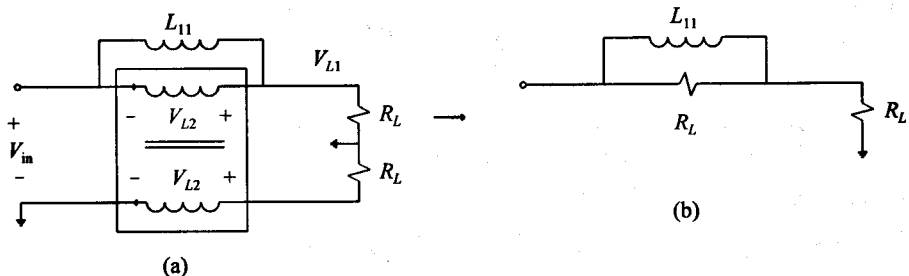


**Figure 6.24** The 1:1 unbalanced-to-balanced transmission-line transformer at low frequencies.

**EXAMPLE 6.4** The magnetizing inductance required in a 1:1 transmission-line transformer.

The equivalent circuit for the 1:1 unbalanced-to-balanced transformer is shown in Figure 6.24(a).

By transforming the load on the secondary side of the transformer to the primary side, the equivalent circuit of the 1:1 unbalanced-to-balanced transformer can be simplified to that shown in Figure 6.24(b).

By using this equivalent circuit, the input admittance is found to be

$$\begin{aligned}
 Y_{in} &= \frac{1}{R_L + sL_{11}R_L / [R_L + sL_{11}]} \\
 &= \frac{R_L + 2sL_{11}}{R_L^2 + 2sL_{11}R_L} \\
 &= \frac{1}{2R_L} \cdot \frac{1 + R_L / (sL_{11})}{1 + R_L / (2sL_{11})}
 \end{aligned} \tag{6.39}$$

It is clear from this equation that the input resistance will be equal to  $2R_L$  if the magnetizing reactance is relatively high.

The relative power dissipation in the two load resistances can be determined by transforming the parallel combination of  $\omega L_{11}$  and  $R_L$  in Figure 6.24(b) to the equivalent series impedance shown in Figure 6.25.

Because the same current flows through the two resistors, the ratio of the power dissipated in each load is equal to the ratio of the resistance of these resistors. If

$$\omega L_{11} = 4.4 R_L \tag{6.40}$$

the power dissipated in the two load resistors will differ by 5%. The input power to the transformer will then be 1% higher than the design value, and the relative efficiency will be 0.99.

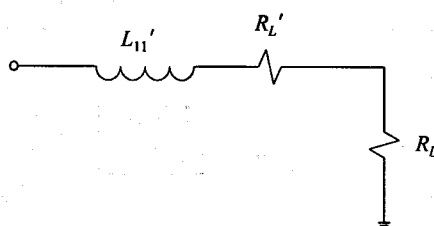


**Figure 6.25** The series equivalent of the impedance of the circuit from Figure 6.24(b).

### 6.4.3 Determining the Type and Size of the Magnetic Core to Be Used

Toroidal cores are often used in transmission-line transformers. The size of the toroidal core is determined by the inductance required, the maximum flux density in the core (and therefore the allowable losses), and the line length required to meet these specifications.

It was shown in Chapter 3 that if the inductance and flux density specifications are to be met simultaneously, a core with

$$Al = \frac{\mu_0 \mu_r}{\omega B_{\max}^2} \frac{V_{\max}^2}{\omega L_{11}} \quad (6.41)$$

should be used (see (3.33)).

It can be shown that the line length will always increase if a core with an  $Al$ -product larger than that given by this equation is used.

If the core size is decreased, it is possible that the line length might be shorter, at least initially.

Whether it will be shorter is a function of the extent to which the inductance must be increased to meet the loss specification (the flux density in the core will be too high if the inductance is not increased), as well as the dimensions of the core.

If the losses in the material increase sharply when the flux density is increased, the optimum core size will always be that given by (3.39).

It is sometimes possible to reduce the line length necessary to provide the required magnetizing inductance by using a number of smaller toroidal cores instead of only one larger core.

The ratio of the line length for a single core to that of  $N_c$  stacked cores is given approximately by the equation

$$\frac{l_{c1}}{l_{c2}} = \frac{2w_1 + 2h_1 + 4t}{(A_1 / A_2) \cdot h_2 + (l_2 / l_1) \cdot (4w_2 + 4t)} \quad (6.42)$$

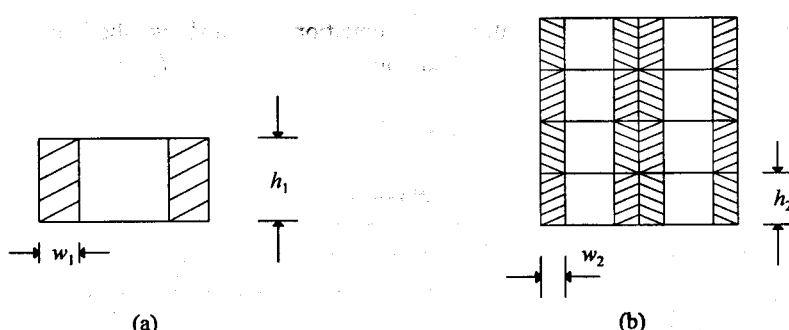


**Figure 6.26** The cross-section of (a) a single toroidal core and (b) a number of stacked toroidal cores.

where  $t$  is the outer diameter of the transmission line used,  $l_1$  the mean path length of the larger core,  $l_2$  the mean path length of each of the smaller cores,  $A_1$  the effective cross-sectional area of the larger core, and  $A_2$  the effective cross-sectional area of each of the smaller cores.  $w_1$ ,  $w_2$ ,  $h_1$ , and  $h_2$  are defined in Figure 6.26.

Equation (6.42) was derived by assuming the inductance and the flux densities of the two inductors to be equal.

In order to have the same flux density, it is necessary that

$$N_1 / l_1 = N_2 / l_2 \quad (6.43)$$

where  $N_1$  is the number of turns used with the single core and  $N_2$  the number of turns used with the stacked core.

The inductance of the two inductors will be the same if

$$N_1^2 A_1 / l_1 = N_c N_2^2 A_2 / l_2 \quad (6.44)$$

where  $N_c$  is the number of cores used in the stacked-core inductor.

By using (6.43), (6.44) can be changed to

$$A_1 l_1 = N_c \cdot A_2 l_2 \quad (6.45)$$

It follows from this equation that the effective  $Al$ -products of the single-cored and stacked-cored inductors must be the same.

Equations (6.45) and (6.43) can be used to determine the number of cores and the number of turns required, if using a transformer with stacked cores is worthwhile (i.e., if the core dimensions are known).

If a core with suitable dimensions (comparable to those of the stacked core) is available, a balun core can also be used to decrease the line length of the transformer.

### EXAMPLE 6.5 Comparison of the line lengths associated with a stacked core and a single core transmission-line transformer.

As an example of the application of the equations given above, the line lengths of a single toroidal core and a stacked core with  $A_2 = 0.5A_1$ ,  $l_2 = 0.5l_1$ ,  $w = h$ , and  $t = w_1 / 3$  will be compared.

With  $w = h$ , (6.41) becomes

$$\begin{aligned} \frac{l_{e1}}{l_{e2}} &= \frac{4w + 4t}{2(w/\sqrt{2}) + (1/2) \cdot [4(w_2/\sqrt{2}) + 4t]} \\ &= \frac{4w + 4t}{\sqrt{2} \cdot 2w + 2t} \end{aligned} \quad (6.46)$$

From this it follows that the ratio of the line length for the two different cores is

$$\frac{l_{e1}}{l_{e2}} \cong \frac{4 + 4/3}{2\sqrt{2} + 2/3} = 1/0.655 = 1.5$$

Because of the reduced line length, the bandwidth of the transformer, therefore, can be increased significantly by using a stacked core or a balun core.

#### 6.4.4 Compensation of Transmission-Line Transformers for Nonoptimum Characteristic Impedances

When a line with the optimum characteristic impedance is not available, it is possible to compensate for the degradation of the high-frequency response of the transformer by using compensating inductors and/or capacitors.

It is usually adequate to use two compensating elements. One element is used in parallel (capacitor) or in series (inductor) with the load to change the input resistance or conductance to the required value at some frequency below the cut-off frequency, while the other is used to remove the reactive part of the input impedance or admittance at the same frequency.

The compensation frequency can be chosen such that the ripple in the output power is equal to a specified value. The optimum compensation frequency can be found iteratively.

The compensation of some frequently used transformers will be considered here as examples.

##### EXAMPLE 6.6 Compensation of a 1:4 unbalanced transmission-line transformer.

The 1:4 unbalanced transmission-line transformer can be compensated as shown in Figure 6.27, that is, if  $Z_0 > 1.35 Z_{0,\text{opt}}$ .

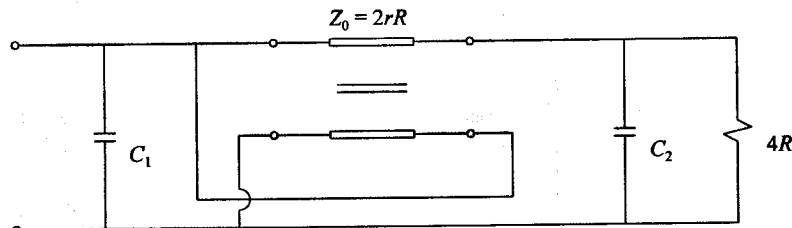


**Figure 6.27** Compensation of the unbalanced 1:4 transformer when  $Z_0 > 1.35 Z_{0,\text{opt}}$

The values of the two compensation capacitors are given by the equations [3]

$$C_1 = \frac{1 + \cos(\beta l) - \{[1 + \cos(\beta l)]^2 - \sin^2(\beta l) \cdot r^2\}^{1/2}}{\omega_{\max} r R \sin(\beta l)} \quad (6.47)$$

$$C_2 = \frac{2 \cos(\beta l) - \{[1 + \cos(\beta l)]^2 - \sin^2(\beta l) \cdot r^2\}^{1/2}}{4 \omega_{\max} r R \sin(\beta l)} \quad (6.48)$$

$$r = Z_0 / (2R) \quad (6.49)$$

Equations (6.47) and (6.48) can be derived by setting the real part of the input admittance of the transformer terminated in a resistor ( $4R$ ) in parallel with an unknown capacitor ( $C_2$ ) equal to  $1/R$ .  $C_1$  is used to cancel the reactive part of the input admittance.

The compensation frequency ( $f_{\max} = \omega_{\max} / (2\pi)$ ) is a function of the acceptable variation in the output power and the minimum efficiency required in the passband. It can be found iteratively.

The high-frequency response of the transformer can be improved considerably by using this compensation technique. This can be appreciated by comparing the electrical lengths of the line, with and without compensation, at the cut-off frequencies of the transformer.

The electrical lengths of the line at the cut-off frequency, with and without compensation, are compared in Table 6.2 for

$$\Delta P_L \leq 17\%$$

and

$$\eta_r \geq 95\%$$

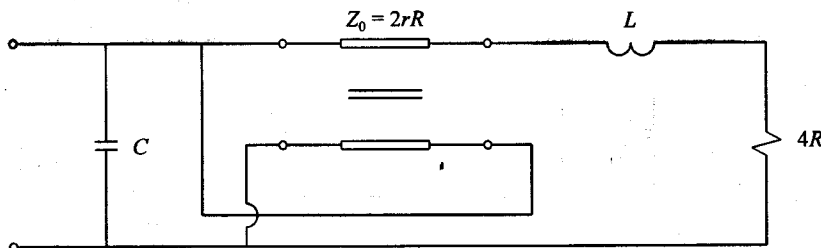


Figure 6.28 Compensation of the unbalanced 1:4 transmission-line transformer when  $Z_0 < 1.35Z_{0,\text{opt}}$

It can be seen from Table 6.2 that the high cut-off frequency can be increased by more than an octave above its uncompensated value, independently of the characteristic impedance.

The high-frequency response of the transformer can also be improved when

$$Z_0 < 1.35 Z_{0,\text{opt}}$$

This can be done by using an inductor and a capacitor as compensating elements. The inductor is used in series with the high-impedance end of the transformer, while the capacitor is connected in parallel with the low-impedance side, as shown in Figure 6.28.

When  $Z_0 = Z_{0,\text{opt}}$  the cut-off frequency can be increased by an octave. The required inductance and capacitance can be found by using the following equations:

$$\omega_H L = 0.7558 Z_0 \quad (6.50)$$

$$\omega_H C = 0.8961 Y_0 \quad (6.51)$$

$$\omega_H = \omega_{0.2474} \lambda \quad (6.52)$$

Exact equations for the values of the inductance and capacitance can be derived by following the same procedure as before.

**Table 6.2**

The electrical length of the transmission line used in an 1:4 unbalanced transmission-line transformer at the compensation and cut-off frequencies, with and without compensation

$r = Z_0 / (2R)$	Line length without compensation ( $\lambda$ )	Line length at the compensation frequency ( $\lambda$ )	Line length with compensation ( $\lambda$ )
2.0	0.070	0.144	0.160
2.5	0.050	0.116	0.130
3.0	0.036	0.099	0.110
3.5	0.032	0.085	0.095
4.0	0.027	0.075	0.084
4.5	0.024	0.068	0.075
5.0	0.021	0.061	0.068

#### EXAMPLE 6.7 Compensation of a 1:1 balanced-to-unbalanced transformer.

The 1:1 balanced-to-unbalanced (and 1:4 balanced) transmission-line transformer

can be compensated for characteristic impedances that are too high, as shown in Figure 6.29.

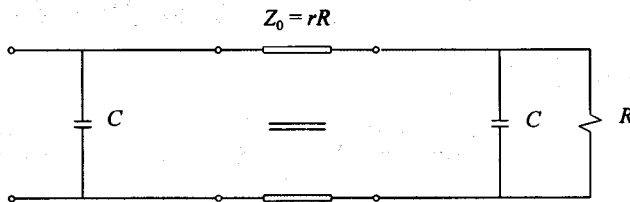


**Figure 6.29** Compensation of the 1:1 balanced-to-unbalanced transformer ( $r > 1$ ).

The capacitance of both capacitors is given by the equation

$$C = \frac{1 - [1 - (r^2 - 1) \tan^2(\beta l)]^{1/2}}{\omega_{\max} r R \tan(\beta l)} \quad (6.53)$$

where  $r = Z_0 / Z_{0,\text{opt}} = Z_0 / R$ , and  $\omega_{\max}$  is the compensation frequency.

**Table 6.3**

The electrical length of the transmission line used in the 1:1 balanced-to-unbalanced transmission-line transformer at the compensation and cutoff frequencies, with and without compensation

$r = Z_0 / R$	Line length without compensation ( $\lambda$ )	Line length at compensa- tion frequency ( $\lambda$ )	Line length with compensation ( $\lambda$ )
0.5	0.073	—	—
0.6	0.080	—	—
0.7	0.089	—	—
0.8	0.109	—	—
0.9	0.170	—	—
1.0	∞	—	—
1.1	∞	—	—
1.2	0.119	0.131	0.180
1.3	0.092	0.094	0.155
1.4	0.075	0.075	0.135
1.5	0.065	0.075	0.123
1.6	0.058	0.081	0.116
1.8	0.042	0.081	0.101
2.0	0.041	0.056	0.085
2.5	0.031	0.038	0.066
3.0	0.025	0.044	0.058
3.5	0.021	0.044	0.048
4.0	0.018	0.031	0.043
5.0	0.013	0.031	0.035

The allowable ripple in the output power and the minimum efficiency should be taken into account when the compensation frequency is calculated.

The cut-off frequency ( $\Delta P_L \geq 17\%$ ,  $\eta_r \geq 95\%$ ) of the 1:1 transformer, with and without compensation, is shown in Table 6.3 as a function of the characteristic impedance of the line. It can be seen by inspection of this table that the cut-off frequency of the 1:1 transmission-line transformer (and therefore the 1:4 balanced transformer) is more sensitive to deviations in the characteristic impedance than the unbalanced 1:4 transformer.

Compensation of the transformer has a significant effect on the cut-off frequency.

### EXAMPLE 6.8 Compensation of a hybrid coupler.

The optimum characteristic impedance of the hybrid transformer shown in Figure 6.30 cannot be determined by using the rule given in Section 6.4.1. The reason for this is that the voltage across the end of the line is equal to zero in the balanced case.

It can be shown (by deriving the exact equations for this transformer) that the optimum characteristic impedance for this transformer is the lowest available characteristic impedance.

The hybrid transformer can be compensated with an inductor and a capacitor as shown in Figure 6.30. The compensation frequency (as well as the cut-off frequency of the transformer, with and without compensation) is given in Table 6.3 as a function of the characteristic impedance.

The component values are given by the equations

$$\omega_H L = 0.3015 Z_{L1} / 2 \quad (6.54)$$

$$1 / (\omega_H C) = 1.8005 Z_{L1} / 2 \quad (6.55)$$

where the compensation frequency ( $f_H$ ) can be determined by using Table 6.4.

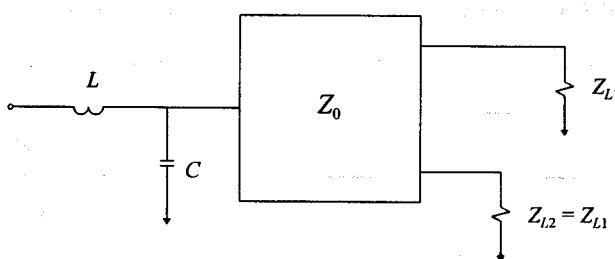


Figure 6.30 Compensation of the hybrid divider shown in Figure 6.14(b).

**Table 6.4**

The electrical length of the transmission line used in the hybrid divider (and combiner) at the compensation and cut-off frequencies, with and without compensation

$Z_0 / Z_{L1}$	Line length without compensation ( $\lambda$ )	Line length at the compensation frequency ( $\lambda$ )	Line length with compensation ( $\lambda$ )
0.25	0.212	0.283	0.367
0.50	0.121	0.173	0.303
1.00	0.066	0.093	0.139
2.00	0.029	0.048	0.075
3.00	0.020	0.034	0.057

#### 6.4.5 The Design of High-Pass LC Networks to Extend the Bandwidth of a Transmission-Line Transformer

The bandwidth of a transmission-line transformer can be extended considerably by using a high-pass matching network to compensate for the effect of the magnetizing inductance.

A network that can be used for this purpose is shown in Figure 6.31(a). It is sometimes also possible to use its dual, which is shown in Figure 6.31(b).

The optimum reactances of the components of the network are given in Table 6.5 as a function of the allowable ripple in the passband. The reactances are normalized for a load resistance of  $1\Omega$ .

When this compensation technique is used, the magnetizing reactance required to meet the low-frequency specifications decreases. Because this implies a shorter line, the high cut-off frequency of the transformer will increase.

The exact amount by which the bandwidth will increase is a function of the acceptable ripple in the output power, the magnetic material used, and the losses that can be tolerated.

The new line length can be determined by using the information in Section 6.4.3. It should be noted that the maximum voltage across the line is slightly more than that with-

**Table 6.5**

The normalized values of the reactance in Figure 6.31(a) at the lowest frequency in the passband as a function of the ripple in the output power

Ripple (%)	0.5	1.0	2.0	3.0	4.0	5.0
$X_C (\Omega)$	0.30	0.36	0.45	0.50	0.55	0.59
$X_L (\Omega)$	1.80	1.52	1.31	1.20	1.14	1.09
Increase in bandwidth	1.48	1.61	1.73	1.82	1.87	1.90

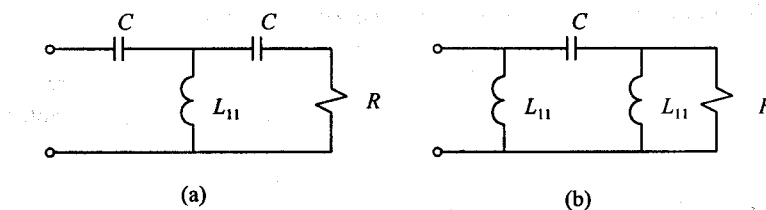


**Figure 6.31** Two low-frequency impedance-matching networks that can be used to extend the bandwidth of a transformer.

out compensation. The capacitor in series with the load resistance transforms the resistance slightly upward, and the voltage across the line must therefore be higher than that across the load resistance in order to deliver the same power in the effective resistance in parallel with the magnetizing inductance as in the load. This is illustrated in Figure 6.32.

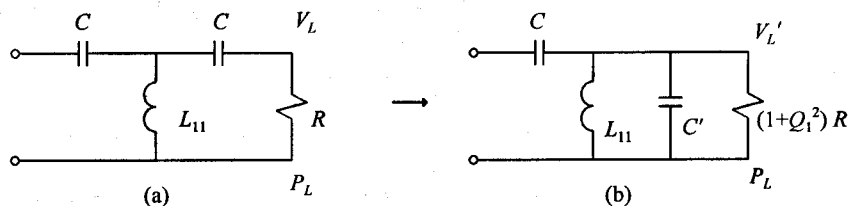


**Figure 6.32** Illustration of the increase in the voltage across the magnetizing inductance of the transmission-line transformer with low-frequency compensation.

Because of the decrease in the reactance of the magnetizing inductance and the increase in the effective resistance in parallel with it, the unloaded  $Q$  of the magnetizing inductance will also change if the losses are to remain the same as without compensation. The maximum allowable flux density in the core, therefore, will also change (it must be less than before).

Despite the increase in the voltage across the magnetizing inductance and the decrease in the maximum allowable flux density in the core, it is usually worthwhile to use this compensation technique.

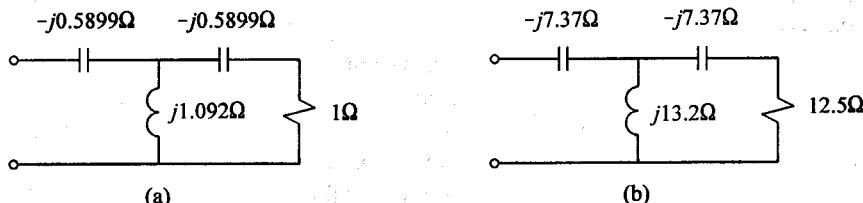


**Figure 6.33** The low-frequency impedance-matching network of Figure 6.31(a) if the passband ripple is 5% and (a)  $R_t = 1\Omega$  and (b)  $R_t = 12.5\Omega$ .

If the losses in the core can be ignored and the core size remains the same as before compensation, the improvement in the bandwidth will be that given in Table 6.5, as long as the transformer is designed to have the same low cut-off frequency as before.

Along with improving the bandwidth, this technique has the added advantage that the required frequency response might be obtained by using an air-cored solenoidal coil instead of magnetic material. If this can be done, the increase in the voltage per turn is not a problem and the flux density consideration does not apply.

**EXAMPLE 6.9** Low-frequency compensation of a 1:4 unbalanced transmission-line transformer.

As an example of the application of the low-frequency compensation technique, the required magnetizing inductance and capacitance for a 1:4 unbalanced transmission-line transformer with  $R_L = 12.5\Omega$  and  $f_L = 2$  MHz will be determined. The passband ripple is to be 5%.

The compensation networks for  $R_L = 1\Omega$  and  $R_L = 12.5\Omega$  are shown in Figure 6.33. The component values in Figure 6.33(a) were obtained from Table 6.5.

The positions of the compensating capacitors in the 1:4 transformer are shown in Figure 6.34(a). The input impedance of the transformer is the same as that of the equivalent circuit shown in Figure 6.34(b), which is of the same form as the matching network in Figure 6.33(a).

By using this equivalence, it follows that if the required high cut-off frequency of the transformer is low enough, the magnetizing inductance can be realized by using an air-cored solenoidal coil.

## 6.5 CONSIDERATIONS APPLYING TO RF POWER AMPLIFIERS

The design of RF and microwave power amplifiers differs from that of small-signal amplifiers in the design of the output circuit. While the output circuit in small-signal amplifiers is usually conjugately matched to the load or used to taper the gain response, the load impedance of a power amplifier must be chosen in such a way that the required power can be obtained and that the efficiency is as high as possible.

The output power obtainable from an amplifier stage is limited by the limitations of the transistor used and/or the output circuit designed. The device limitations stem from the finite voltage, current, and power ratings of the transistor and its saturation voltage or saturation resistance. The saturation voltage or resistance of a transistor determines the lowest value of the instantaneous voltage across it (ideally the voltage should go down to zero). Saturation voltages of a few volts for bipolar transistors, and saturation resistance of fractions of an ohm up to a few ohms are typical for FETs. It was shown in Section 2.3.1 that the maximum output power obtainable from a class A or a class B stage at RF frequencies is given by

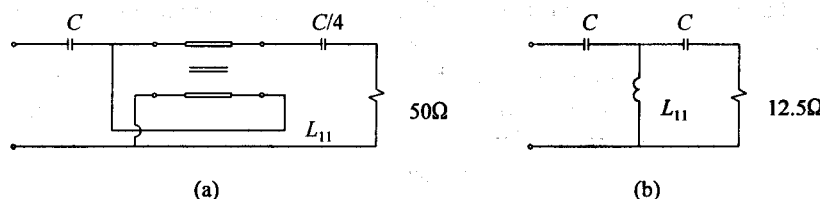


**Figure 6.34** (a) The positions of the compensating capacitors in the unbalanced 1:4 transmission-line transformer and (b) the equivalent circuit for the input impedance of the transformer.

$$P_{\max} = \frac{(V_s - V_{\text{sat}})^2}{2(R_L + \alpha R_{\text{sat}})} \cdot \frac{R_L}{R_L + \alpha R_{\text{sat}}} \quad (6.56)$$

where  $V_s$  is the supply voltage,  $V_{sat}$  the saturation voltage, and  $R_{sat}$  the saturation resistance.  $\alpha$  is equal to 2 for class A amplifiers and equal to 1 for class B amplifiers. In deriving this equation (see Figure 6.35), it was assumed that the output susceptance of the transistor was removed by the output matching network and that the output power is voltage limited (i.e., the output voltage clips before the output current).

The saturation resistance of bipolar transistors is usually negligibly small, while the saturation voltage for FETs can be neglected.

It follows from (6.56) that, in order to obtain the maximum possible output power from a transistor, it is necessary to use the highest supply voltage possible, and to choose the load resistance as small as possible (the saturation resistance is usually significantly smaller than the load resistance required). The minimum value of the load resistance is determined by the maximum dc and RF currents that can be tolerated through the transistor.

The optimum load for an RF power transistor is usually specified by the manufacturer. When this is not done, the optimum terminations can be determined practically at each frequency of interest by using stub tuners. The optimum terminations can also be estimated by using a large-signal model, if such a model is available. Alternatively, the small-signal  $S$ -parameters at the rated current and the dc  $I/V$ -curves can be measured, and the power parameter approach outlined in Section 2.3 can be used to generate load-pull contours for the transistor.

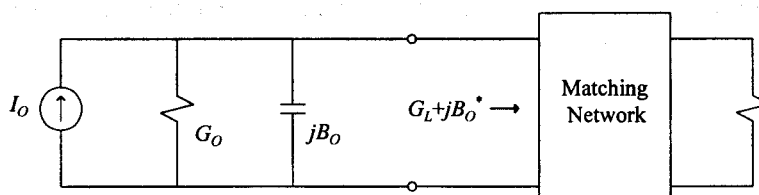


**Figure 6.35** The matching problem associated with the output circuit of a power amplifier.

The optimum load is often specified in terms of the equivalent output impedance of the device under the assumption of a conjugate output match. It is important to realize that this impedance is not the same as the actual output impedance of the transistor. The terminations required for the optimum power match are usually not the same as those required for a conjugate match (low output voltage standing wave ratio (VSWR)).

The efficiency of a power amplifier is a function of the class of operation and the effective shunt susceptance in the output circuit (the transistor susceptance included). When the voltage across the output terminals of the transistor is purely sinusoidal, the efficiency will always be less than 50% for class A amplifiers (the conduction angle of the current through the transistor is then 360°), while that for class B amplifiers (180° conduction angle) is constrained to below 78.5%. Higher efficiencies can be obtained with class C amplifiers, but because the same power must be concentrated in a narrower pulse, the peak current through the transistor increases as the efficiency increases. The device specifications for a class C amplifier, therefore, are more severe than those for class A or B amplifiers of the same output power with the same supply voltage. A class C amplifier also cannot be used directly for linear applications.

When the effective load (the output susceptance of the transistor is considered as part of the load) of a power stage is reactive, the efficiency decreases by a factor

$$\eta_r = \frac{1}{\sqrt{1 + (B_L / G_L)^2}} \quad (6.57)$$

because of the increase in the supply current caused by the effective shunt susceptance ( $B_L$ ). In optimizing the efficiency of an amplifier, it is therefore essential to remove the effect of the output susceptance of a transistor.

In order to obtain the required output power, the physical load of a power amplifier (usually  $50\Omega$ ) must be transformed to a lower value. It will be shown in Chapter 8 that this often cannot be done with LC networks (transformation to very low resistance values is usually required and the insertion loss may also be a problem). Consequently, transmission-line transformers are usually used for this purpose at RF frequencies. Combiners and splitters are also required in a balanced or a push-pull configuration or to connect transistors in parallel for higher output power. The cancellation of the output susceptance of a power transistor is carried out with an LC network between these transformers and the transistor.

The gain tapering required in a power amplifier is best done on the input side of each transistor with an RLC matching network. It will be shown in Chapter 8 that these networks can be used to level the gain (the operating power gain in this case) without reactive mismatching. Any reactive mismatching will increase the power required from the driver stages.

It should be noted that ferrites are usually not required in transmission-line transformers at the higher RF frequencies (typically 100 MHz and above).

This section concludes by considering two power amplifier examples. In the first example, designing the output matching network of a narrowband (225–260 MHz) television broadcast amplifier will be considered. The design of a broadband input

matching network (2–30MHz) for a push-pull class B amplifier will be considered in the second example.

**EXAMPLE 6.10** Designing an output matching network for a power amplifier.

As an example of the design of an RF power amplifier, an output matching network will be designed for the balanced amplifier shown in Figure 6.36 over the passband 225–260 MHz. The network will be designed for an output power of 165W. The supply voltage will be taken as 28V, and the output capacitance of each transistor as 130 pF.

An approximate value for the required load resistance for each transistor can be obtained from (6.56). The saturation voltage will be taken as 3V, and saturation resistance is assumed to be negligible. Application of (6.56) yields

$$165/2 = P_L = \frac{(28 - 3)^2}{2 R_L}$$

leading to

$$R_L = 3.79 \Omega$$

The quarter-wavelength transformers (baluns) in the output circuit and the input circuit are used to transform the load impedance and the source impedance to approximately  $6.25\Omega$  ( $12.5/2$ ) for each transistor, and also serves as a combiner for the output power and a splitter for the input power. The actual impedances can be obtained easily by the standard equation for the input impedance of a transmission line (the unbalanced current is very small in this case) and dividing the results by 2 to get the load for each transistor. The impedance thus obtained is the

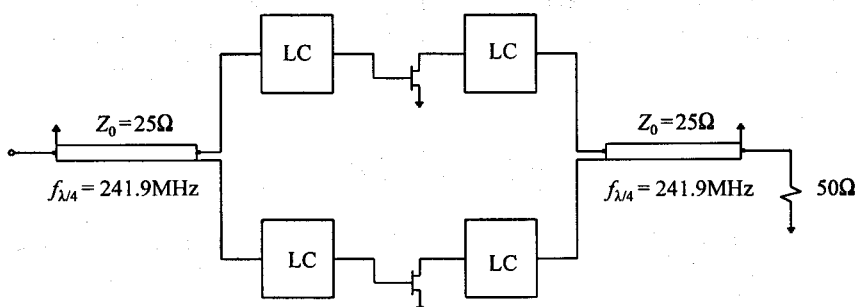


Figure 6.36 The configuration of the balanced power amplifier in Example 6.10.

Table 6.6

The specifications for the output matching network of the power amplifier of Example 6.10

Frequency (MHz)	Source impedance ( $\Omega$ )	Load impedance ( $\Omega$ )	Transducer power gain
225	$2.55 - j1.78$	$6.31 - j1.03$	1.0
230	$2.51 - j1.79$	$6.28 - j0.72$	1.0
235	$2.48 - j1.80$	$6.27 - j0.43$	1.0
240	$2.44 - j1.81$	$6.25 - j0.16$	1.0
245	$2.41 - j1.82$	$6.25 + j0.20$	1.0
250	$2.38 - j1.83$	$6.27 + j0.49$	1.0
255	$2.33 - j1.84$	$6.29 + j0.80$	1.0
260	$2.30 - j1.85$	$6.32 + j1.10$	1.0

load specification for the output impedance-matching network to be designed.

The source impedance for the output matching network is simply equal to the load resistance required to obtain the specified output power, in parallel with the output capacitance of each transistor. Because a conjugate match to this impedance is required, the transducer power gain required for this matching problem is equal to 1. The specifications for the matching network to be designed are summarized in Table 6.6. This matching problem can be solved by first designing an L-section to provide a conjugate match at the highest frequency, after which it can be optimized for the best performance over the passband. The solution shown in Figure 6.37 was synthesized by using the transformation-Q impedance-matching technique described in Section 8.4.3. The deviation from the specified performance is negligibly small.

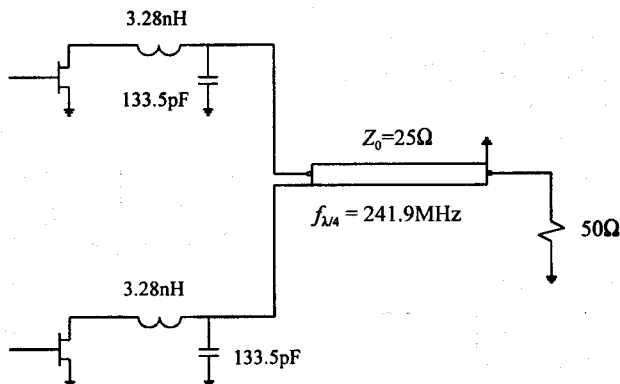
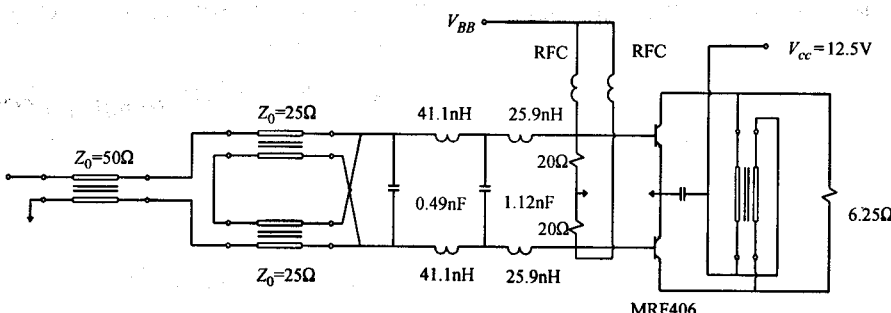


Figure 6.37 The output matching network designed for the power amplifier of Example 6.10.



**Figure 6.38** The input matching network designed for the push-pull power amplifier of Example 6.11.

### EXAMPLE 6.11 Designing a input matching network for a power transistor.

Designing a wideband (2–30 MHz) input matching network for a push-pull class B stage (40W peak envelope power (PEP)) will be considered in this example. No attempt was made to level the gain response in this case. The input impedance of the transistor used (MRF406) is listed in Table 8.1.

The matching network designed is shown in Figure 6.38. The  $50\Omega$  balun on the input side was used to obtain a balanced signal, after which the balanced 4:1 transformer was used to transform the  $50\Omega$  source resistance to  $12.5\Omega$ . The LC network was designed to match this resistance to the input impedance of the two transistors (the inputs are effectively connected in series) by using an earlier version of the program LSM FORTRAN provided on the diskette accompanying this book (refer to Section 8.4.1).

The balanced matching problem can be transformed to a single-ended problem by replacing each of the two capacitors used with two capacitors connected in series and by using the fact that the center points are virtual grounds. The single-ended matching network was designed to match half of the output impedance presented by the 1:4 transformer (approximately  $6.25\Omega$ ) to the input impedance of a single transistor. The gain ( $G_T$ ) of the LC network obtained varied between 0.85 and 0.95 over the passband.

With the output power higher than 6W, the input VSWR of the amplifier was measured to be better than 2.6 over the complete passband [4], which is close to the expected value of 2.3.

## REFERENCES

- Rotholtz, E., "Transmission-Line Transformers," *IEEE Trans. Microwave Theory Tech.*, Vol. MTT-29, No. 4, April 1981.
- Dutta Roy, S. C., "A Transmission-Line Transformer Having Frequency Independent Properties," *Int. J. Circuit Theory App.*, Vol. 8, January 1980, pp. 55–64.

3. Hilbers, A. H., "On the Design of HF Wideband Transformers (ECO 6907)," Eindhoven, Netherlands: Philips C.A.B. Group, 1969.
4. Abrie, P. L. D., *Impedance Matching Networks and Bandwidth Limitations of Class B Power Amplifiers in the HF and VHF Ranges*, Master's Thesis, University of Pretoria, 1982.

## SELECTED BIBLIOGRAPHY

- Krauss, H. L., and C. W. Allen, "Designing Toroidal Transformers to Optimize Wideband Performance," *Electronics*, August 16, 1973.
- Ruthroff, C. L., "Some Broad-Band Transformers," *Proc. IRE*, August 1959.
- Van Nierop, J. H., "Evolution of a 4:1 Impedance Transforming Balun," *IEEE Trans. Antennas Propag.*, Vol. AP-30, No. 4, July 1982.

# CHAPTER 7

## FILM RESISTORS AND SINGLE-LAYER PARALLEL-PLATE CAPACITORS

### 7.1 INTRODUCTION

The distributed nature of film resistors and parallel-plate capacitors cannot be ignored at microwave frequencies and will be considered in this chapter.

The behavior of film resistors can be accurately modeled by considering the resistor to be a lossy transmission line. Film resistors will be considered in Section 7.2.

Single-layer parallel-plate capacitors are often used at microwave frequencies. The configurations commonly used in hybrid circuits are shown in Figure 7.1. Metal-insulator-metal (MIM) capacitors (see Figure 7.2) are extensively used in MMICs (monolithic microwave integrated circuits).

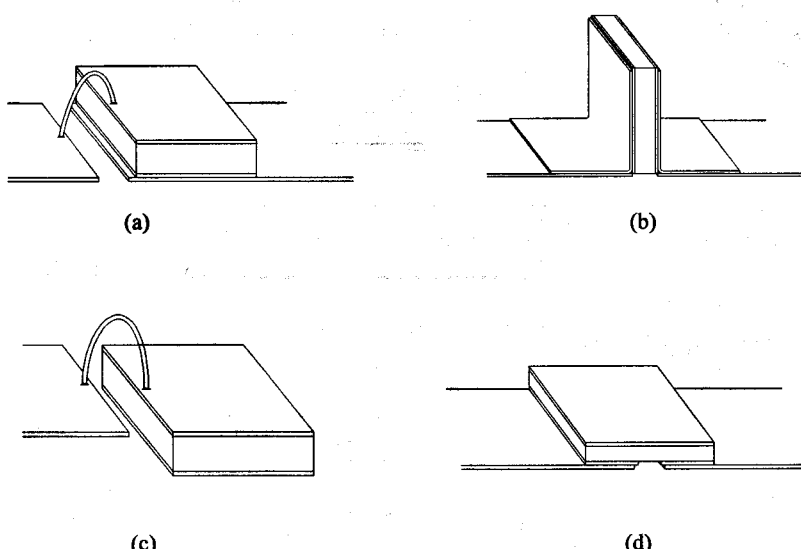


Figure 7.1 (a) A series connected parallel-plate capacitor, (b) a vertically mounted capacitor, (c) a parallel-plate capacitor mounted on a ground plane, and (d) a gap-capacitor.

At low frequencies these capacitors could be treated as ideal lumped capacitors, but their distributed nature must be taken into account at higher frequencies.

When the capacitor is mounted on a ground plane (bottom plate connected to ground; see Figure 7.1(c)) and the excitation can be taken to be uniform across the width of the capacitor (narrow width, ribbon or multiple bond wire cases), the parasitic behavior of the capacitor can be modeled fairly accurately by considering it to be an open-ended transmission line. This case will be considered in Section 7.3.1. The general case (microstrip capacitors) is considered in [1].

Analysis of the vertically mounted parallel-plate capacitor (Figure 7.1(b)) is also straightforward. This capacitor can be considered to be a series connected open-ended stub. The same resonances encountered in an open-ended stub are also encountered in this configuration. Fortunately, the resonant behavior is sharply reduced by any capacitor losses (this is important when a capacitor is used for wideband coupling or decoupling).

Analysis of the series configuration shown in Figure 7.1(a) proves to be more challenging. If the capacitance density of the capacitor is high compared to that of the associated microstrip line (which is usually the case) and the behavior at frequencies significantly lower than parallel resonance is considered, these capacitors can be accurately modeled as a lumped capacitor cascaded with a transmission line on both sides (line-capacitor-line model) [2]. In this case the transmission-line behavior of the capacitor is essentially that of the microstrip line.

The line-capacitor-line approach is very practical and is adequate in most cases. Modeling of parallel-plate capacitors in this way will be considered in detail in this chapter.

The general case can be handled as described in [2, 3]. The model used for the capacitor in [2] is instructive and is shown in Figure 7.2(b). Note that the magnetic coupling between the capacitor plates ( $L_{12}$ ) and capacitance to the ground plane ( $C_{10}, C_{20}$ ) are included in the model.

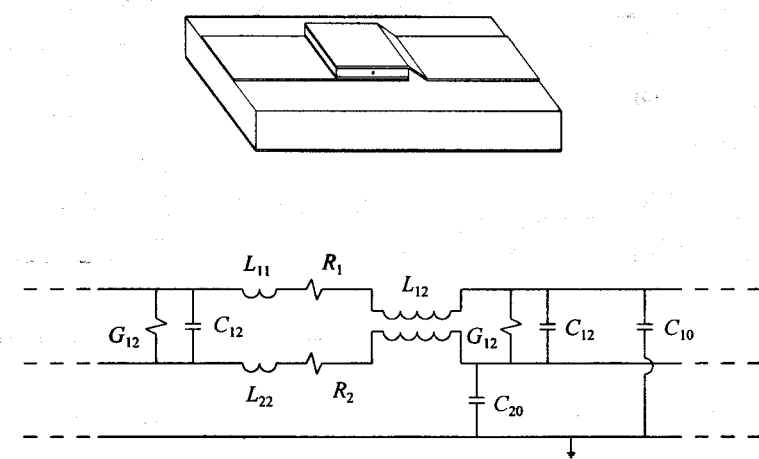


**Figure 7.2** The distributed model used for a parallel-plate capacitor in [2].

Parallel-plate capacitors exhibit series and parallel resonant behavior as the frequency is increased. These effects are very pronounced in high  $Q$  capacitors and are important when designing coupling or decoupling capacitors. The parallel-resonant behavior is not evident in the line-capacitor-line model.

The basic reason for the parallel resonance in overlay capacitors will be established by considering the parallel-plate capacitor in free space. It will be shown in Section 7.3.3 that a more accurate model for the capacitor would be to use the line-capacitor-line model with a frequency-dependent value for the capacitance. The analysis will be done by considering the series connected parallel-plate capacitor to be an unbalanced transmission line, as was done with transmission-line transformers in the previous chapter. This approach can be extended to handle the microstrip case, too [4].

## 7.2 FILM RESISTORS

Thin-film techniques are often used to manufacture resistors at microwave frequencies. By keeping the dimensions of the resistor small, the associated capacitance and inductance can be minimized. The capacitance can be reduced further by depositing the thin film on a substrate with a low dielectric constant.

A film resistor (see Figure 7.3) can be modeled as a lossy transmission line. The relevant equations are as follows

$$r = R_s / W \quad (7.1)$$

$$v_{ph} = c / \sqrt{\epsilon_{r\_eff}} \quad (7.2)$$

$$C = 1 / (v_{ph} \cdot Z_{0\_LC}) \quad (7.3)$$

$$L = Z_{0\_LC} / v_{ph} \quad (7.4)$$

$$\theta_1 = 0.5 \left[ \frac{\pi}{2} + \tan^{-1}(\omega L / r) \right] \quad (7.5)$$

$$z = \alpha + j\beta = \sqrt{\omega C \cdot (r + j\omega L)} = \sqrt{\omega C \sqrt{r^2 + (\omega L)^2}} \cdot [\cos \theta_1 + j \sin \theta_1] \quad (7.6)$$

$$\theta_2 = -0.5 \tan^{-1}[r / (\omega L)] \quad (7.7)$$

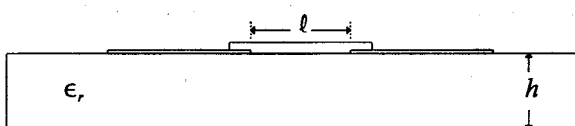


**Figure 7.3** A film resistor on microstrip.

$$Z_0 = \sqrt{\frac{r + j\omega L}{j\omega C}} = \sqrt{\frac{\sqrt{r^2 + (\omega L)^2}}{\omega C}} \cdot [\cos \theta_2 + j \sin \theta_2] \quad (7.8)$$

$$\begin{bmatrix} V_I \\ I_I \end{bmatrix} = \begin{bmatrix} \cosh(\zeta l) & Z_0 \sinh(\zeta l) \\ \sinh(\zeta l) / Z_0 & \cosh(\zeta l) \end{bmatrix} \begin{bmatrix} V_L \\ I_L \end{bmatrix} \quad (7.9)$$

where  $Z_{0,LC}$  is the characteristic impedance of a lossless line with identical dimensions,  $W$  the width (in meters) of the film resistor,  $l$  its length (in meters) and  $R_s$  the resistance per square. The angles  $\theta_1$  and  $\theta_2$  are specified in radians.

Films with resistances of  $10\Omega$  to  $1000\Omega$  per square are available.

The influence of the skin-effect on the resistance can be incorporated into the resistance per square,  $R_s$ . The skin effect can usually be ignored because of the high resistivity of the film material.

The transmission matrix equation for a series resistor is defined in (7.9).  $V_I$  and  $I_I$  in this equation are the input voltage and current, while  $V_L$  and  $I_L$  are the load voltage and the load current, respectively.

The impedance presented to the circuit by a film resistor (or any transmission line with series losses) connected in series (cascaded) with a load  $Z_L$  can be derived from (7.9) and is given by

$$\begin{aligned} Z_{in} &= \frac{Z_L \cosh \zeta l + Z_0 \sinh \zeta l}{Z_L \cdot Y_0 \cdot \sinh \zeta l + \cosh \zeta l} \\ &= Z_0 \cdot \frac{Z_L \cosh \zeta l + Z_0 \sinh \zeta l}{Z_L \sinh \zeta l + Z_0 \cosh \zeta l} \\ &= Z_0 \cdot \frac{Z_L + Z_0 \tanh \zeta l}{Z_0 + Z_L \tanh \zeta l} \end{aligned} \quad (7.10)$$

### 7.3 SINGLE-LAYER PARALLEL-PLATE CAPACITORS

The configurations of single-layer capacitors typically used were considered in Section 7.1. The capacitor can be mounted on the ground plane or on a microstrip line (conductive epoxy is used for this purpose). When mounted on microstrip, the series connection is usually used (see Figure 7.1(a)), but vertical mounting is also an option. Standing axial beam leads are usually used when vertical mounting is required. A gap-capacitor (Figure 7.1(d)) has the advantage that no bonding wires or ribbons are required when it is used. This capacitor consists basically of two parallel-plate capacitors connected in cascade.

Parallel-plate capacitors are used for filtering, impedance matching, coupling, and decoupling.

When decoupling to ground is required, the capacitor is usually mounted on the ground plane and connection to the circuit is made with bond wires or a ribbon. The parasitic inductance associated with a ribbon will usually be lower than that associated with bonding wires. Several bonding wires can (and should) be used in parallel, but the inductance will not decrease proportionally with the number of wires used because of the coupling between them.

Discrete parallel-plate capacitors are available in different sizes. Typical widths are 10 mil (D10), 15 mil (D15), 20 mil (D20), and so on.

The capacitance values obtainable from [5] are listed in Table 7.1 as a function of the width (50V breakdown voltage). Class I materials are used when high  $Q$  capacitors are required (filtering and impedance matching), while class II materials are usually used for resonance-free coupling and decoupling.

**Table 7.1**

The capacitance values (pF) obtainable as a function of the capacitor width

	Capacitor width					
	D10	D15	D20	D25	D30	D35
Class I	0.05–4.7	0.05–12	0.08–18	0.2–33	0.3–39	0.4–68
Class II	1.8–68	3.3–180	3.9–220	10–470	12–560	20–1000

The length of these capacitors is a function of the dielectric material used and the layer thickness. To provide an idea of the lengths, upper bounds on the lengths are provided in Table 7.2 for various dielectric materials [5] with a dielectric thickness of 4 mil (50V breakdown voltage). The values were calculated by considering only the plate capacitance and neglecting any fringing capacitance. The dissipation factors [5] for the different materials are also listed in the table. The second group of materials are class II materials.

Accurate information on the exact size of a capacitor can be obtained from the manufacturer.

With the physical dimensions of a capacitor known, the associated characteristic impedance and electrical line length can be determined (vertical mounting is assumed here; see Figure 7.1(b)). The electrical length can also be estimated by measuring the first parallel resonant frequency (open circuit) of the capacitor.

The first parallel resonant frequency and the characteristic impedance are not independent for a given capacitance value. This follows from the following equations:

$$C_T = (Y_0 / v_{ph}) \cdot \ell = Y_0 \cdot \frac{\sqrt{\epsilon_{r\_eff}}}{c} \cdot \ell = Y_0 \cdot \frac{\sqrt{\epsilon_{r\_eff} \cdot \ell}}{c} \quad (7.11)$$

$$Y_0 = C_T \cdot \frac{c}{\sqrt{\epsilon_{r\_eff} \cdot \ell}} \quad (7.12)$$

$$\Delta\theta = 2\pi \cdot \ell / \lambda = 2\pi \cdot \ell / (v_{ph} / f) = \omega \cdot \frac{\sqrt{\epsilon_{r\_eff}}}{c} \cdot \ell = \omega \cdot \frac{\sqrt{\epsilon_{r\_eff} \cdot \ell}}{c} \quad (7.13)$$

$$\pi = \omega_0 \frac{\sqrt{\epsilon_{r\_eff} \cdot \ell}}{c}$$

→

$$f_0 = \frac{1}{2} \cdot \frac{c}{\sqrt{\epsilon_{r\_eff} \cdot \ell}} = \frac{1}{2} \cdot \frac{Y_0}{C_T} \quad (7.14)$$

where  $C_T$  is the capacitance,  $Y_0$  the characteristic admittance ( $Y_0 = 1/Z_0$ ),  $\ell$  the capacitor length, and  $f_0$  the first parallel resonant frequency.

**Table 7.2**

Upper bounds on the length required per picofarad for different dielectric materials  
(dielectric layer thickness: 4 mil)

Material (DF)	Length per picofarad (mm)					
	D10	D15	D20	D25	D30	D35
CF (0.6%)	2.0616	1.3744	1.0308	0.8246	0.6872	0.5890
CG (0.7%)	0.6479	0.4320	0.3240	0.2592	0.2160	0.1851
NR (0.25%)	0.2926	0.1951	0.1463	0.1170	0.0975	0.0836
NS (0.5%)	0.1463	0.0975	0.0732	0.0585	0.0488	0.0418
NU (1.5%)	0.0756	0.0504	0.0378	0.0302	0.0252	0.0216
NV(1.2%)	0.0454	0.0302	0.0227	0.0181	0.0151	0.0130
<b>BG (2.0%)</b>	<b>0.1134</b>	<b>0.0756</b>	<b>0.0567</b>	<b>0.0454</b>	<b>0.0378</b>	<b>0.0324</b>
<b>BH (2.5%)</b>	<b>0.0181</b>	<b>0.0121</b>	<b>0.0091</b>	<b>0.0073</b>	<b>0.0060</b>	<b>0.0052</b>
<b>BU (2.5%)</b>	<b>0.0082</b>	<b>0.0055</b>	<b>0.0041</b>	<b>0.0033</b>	<b>0.0027</b>	<b>0.0024</b>

It follows from (7.12) and (7.14) that the first parallel resonant frequency and the characteristic impedance associated with a given capacitance value is completely determined by the product  $\sqrt{\epsilon_{r\_eff} \cdot \ell}$ .

If the  $\sqrt{\epsilon_{r\_eff} \cdot \ell}$  product is kept constant, the frequency-dependent behavior of different realizations (different values of  $\epsilon_r$ ) of the same capacitor value will be identical (i.e., if any difference in the dissipation factors is ignored).

Equations (7.11) and (7.14) can also be combined to give an expression for the capacitance in terms of the  $Y_0$  and  $f_0$ :

$$C_T = Y_0 / (2f_0) \quad (7.15)$$

The electrical performance of a parallel-plate capacitor depends on the way it is connected. The different cases will be considered next.

### 7.3.1 Parallel-Plate Capacitors on a Ground Plane

The equivalent circuit of a capacitor mounted on a ground plane is shown in Figure 7.4. This equivalent circuit is valid if the excitation can be considered to be uniform across the width of the capacitor. This can be ensured by using several bond wires in parallel or by using a ribbon instead of the bond wires.

The bond wire (or ribbon) inductance can and should be minimized by keeping its length as short as possible.

With the equivalent characteristic impedance and the resonant frequency of the parallel-plate capacitor known, the impedance presented by it to the circuit can be calculated. Note that because one side of the capacitor is directly connected to the ground plane, the transmission-line inductance could be reduced by up to one-half compared to the vertically mounted case (this effect will be reduced by coupling effects). A slight change in the capacitance should also be expected because of the difference in the fringing fields.

The equations derived in Section 7.2 for a thin-film resistor (transmission line with series losses) also apply to this case. If the parasitic edge capacitance in Figure 7.4 is ignored,  $Z_L$  in (7.10) is an open circuit and (7.10) simplifies to

$$Z_L = Y_0 \tanh \zeta \ell \quad (7.16)$$

$$\begin{aligned} &= Y_0 \frac{\tanh \alpha \ell + \tanh(j\beta \ell)}{1 + \tanh \alpha \ell \cdot \tanh(j\beta \ell)} \\ &= Y_0 \frac{\tanh \alpha \ell + j \tan \beta \ell}{1 + j \tanh \alpha \ell \cdot \tan \beta \ell} \end{aligned} \quad (7.17)$$

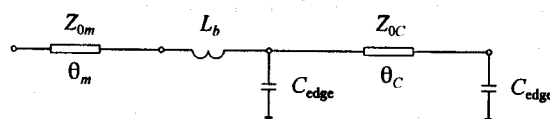
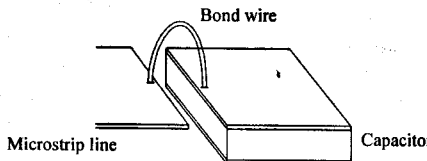


Figure 7.4 The equivalent circuit for a capacitor mounted directly on a ground plane.

The general case can be handled by using the following equation:

$$Y_{in} = j\omega C_{edge} + Y_0 \cdot \frac{j\omega C_{edge} \cdot \cosh \zeta \ell + Y_0 \sinh \zeta \ell}{j\omega C_{edge} \cdot \sinh \zeta \ell + Y_0 \cosh \zeta \ell} \quad (7.18)$$

where  $C_{edge}$  is the parasitic capacitance at each open end.

If the excitation is at the center of the capacitor instead of at the edge, the capacitor can be considered to consist of two transmission lines connected in parallel. The excitation must be uniform across the width for this to be the case.

### 7.3.2 Parallel-Plate Capacitors Used as Series Stubs

The equivalent circuit for a parallel-plate capacitor used as a series connected open-ended stub is shown in Figure 7.5. If the fringing capacitance at the open end is ignored, the series admittance presented to the circuit by the capacitor can be calculated by using (7.17).

The insertion loss associated with the capacitor can be calculated by using (7.17) and (1.11):

$$G_T = \left| \frac{y_{21}}{(y_{11} + Y_s)(y_{22} + Y_L) - y_{12}y_{21}} \right|^2 \cdot 4G_s G_L$$

$$= \left| \frac{-Y_{in}}{(Y_{in} + Y_s)(Y_{in} + Y_L) - (-Y_{in})(-Y_{in})} \right|^2 \cdot 4G_s G_L$$

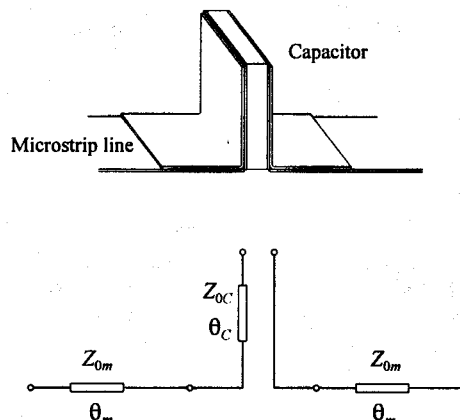


**Figure 7.5** The equivalent circuit for a parallel-plate capacitor used as a series stub.

$$= \left| \frac{1}{Y_s + Y_L + \frac{Y_s Y_L}{Y_{in}}} \right|^2 \cdot 4G_s G_L \quad (7.19)$$

where  $Y_s$  is the admittance to the left of the stub and  $Y_L$  is the admittance to the right.

With  $Y_s = Y_0 = Y_L$  and  $Y_s = G_s$  and  $Y_L = G_L$ , (7.19) simplifies to

$$G_T = \left| \frac{1}{1 + \frac{1}{2} \frac{Y_0}{Y_{in}}} \right|^2 \quad (7.20)$$

Expressed in decibels, this becomes

$$G_T (\text{dB}) = -10 \log_{10} \left| 1 + \frac{1}{2} \frac{Y_0}{Y_{in}} \right|^2 = -20 \log_{10} \left| 1 + \frac{1}{2} \frac{Y_0}{Y_{in}} \right| \quad (7.21)$$

Substitution of the expression for  $Y_{in}$  yields that the insertion loss of the capacitor is given by

$$IL = 20 \log_{10} \left| 1 + \frac{1}{2} \frac{Y_0}{Y_{0C}} \frac{1 + j \tanh \alpha \ell \cdot \tan \beta \ell}{\tanh \alpha \ell + j \tan \beta \ell} \right| \quad (7.22)$$

The insertion loss at the series ( $\beta \ell = (2n + 1) \cdot \pi/2$ ) and the parallel ( $\beta \ell = 2n \cdot \pi/2$ ) resonant frequencies are of interest. Substitution of the relevant values for  $\beta \ell$  in (7.22) yields that the insertion loss at the series resonant frequencies is given by

$$IL = 20 \log_{10} \left| 1 + \frac{1}{2} \frac{Y_0}{Y_{0C}} \cdot \tanh \alpha \ell \right| \quad (7.23)$$

while that at the parallel resonant frequencies is given by

$$IL = 20 \log_{10} \left| 1 + \frac{1}{2} \frac{Y_0}{Y_{0C}} \cdot \frac{1}{\tanh \alpha \ell} \right| \quad (7.24)$$

Because  $\tanh \alpha \ell$  is small when  $\alpha \ell$  is small, it follows from (7.23) that the insertion loss will be small at the series resonant frequencies when  $\alpha \ell$  is small, as expected. It follows from (7.24) that the insertion loss will be severe at the parallel resonant frequencies when  $\alpha \ell$  is small, again as expected.

The attenuation at the parallel resonant frequencies is decreased sharply with increasing  $\alpha\ell$ . In contrast with this, the attenuation at the series resonant frequencies increases slowly with increasing  $\alpha\ell$ . It follows that a resonance-free low-impedance connection can be obtained by using a capacitor with significant losses.

It is also clear from (7.23) and (7.24) that the insertion loss at the series and the parallel resonant frequencies will be decreased as the characteristic impedance of the capacitor is decreased. The ideal coupling capacitor, therefore, will have the lowest possible characteristic impedance with sufficient losses to remove any resonance effects.

The characteristic impedance values claimed for the capacitors considered in Section 7.3 [5] range from  $0.4\Omega$  to  $50\Omega$  (capacitance range: 800 to 0.05 pF;  $f_0$  range: 1.5–200 GHz; 50V breakdown voltage).

The ideal capacitor for a filter or an impedance-matching network would be one with negligible losses and with the series resonant frequency ( $f_0/2$ ) far outside the passband. When a coupling capacitor is required, the series resonant frequency ( $f_0/2$ ) should be chosen to be inside the passband, if possible.

### 7.3.3 Series Connected Parallel-Plate Capacitors

A series connected parallel-plate capacitor (see Figure 7.1(a)) can be considered to be a cascade connection of two transmission lines separated by a lumped capacitor, as explained in Section 7.1. The basic reason for this model will be illustrated in this section by deriving the  $Y$ -parameters and the associated model for the capacitor in free space (no ground plane; see Figure 7.6). The results obtained can also be used to refine the line-capacitor-line model

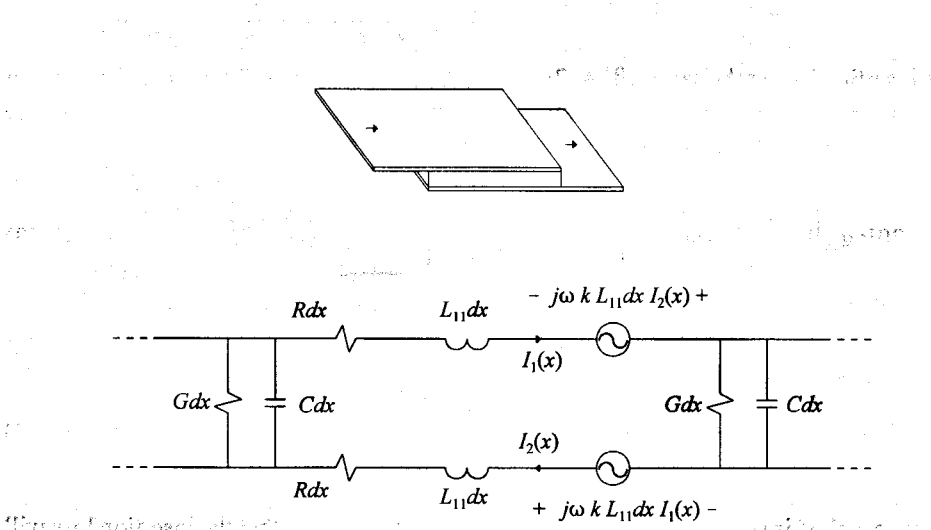


**Figure 7.6** An equivalent circuit for the free space capacitor based on [2].

by replacing the capacitance value with that obtained in this section for the free space capacitor. In doing so, the parallel resonant behavior expected is also obtained in the modified model.

An equivalent circuit for the capacitor based on [2] is shown in Figure 7.6. Instead of using this equivalent circuit, the analysis will be done in terms of the balanced and unbalanced currents on the line, as was done for transmission-line transformers in Chapter 5. The effective inductance presented to the balanced and the unbalanced currents will also be different in this case. The relationship can be established by using the equivalent circuit for two coupled coils (see Figure 5.3(a)).

The effective voltage drop across the inductance and the mutual inductance for an incremental section in the top plate is given by

$$\begin{aligned}
 \delta V_1(x) &= j\omega L_{11}dx \cdot I_1(x) - j\omega kL_{11}dx \cdot I_2(x) \\
 &= j\omega L_{11}dx \cdot (I_1(x) - kI_2(x)) \\
 &= j\omega L_{11}dx \cdot \{[I_b(x) - I_u(x)] - k[I_b(x) + I_u(x)]\} \\
 &= j\omega L_{11} \cdot (1 - k) \cdot dx \cdot [I_b(x) - \frac{1+k}{1-k} I_u(x)] \\
 &= j\omega [(1 - k)L_{11}]dx \cdot I_b(x) - j\omega [(1 + k)L_{11}]dx \cdot I_u(x)
 \end{aligned} \tag{7.25}$$

while that on the bottom plate is given by

$$\begin{aligned}
 \delta V_2(x) &= j\omega L_{11}dx \cdot I_2(x) - j\omega L_{11}dx \cdot I_1(x) \\
 &= j\omega [(1 - k)L_{11}]dx \cdot I_b(x) - j\omega [(1 + k)L_{11}]dx \cdot I_u(x)
 \end{aligned} \tag{7.26}$$

where

$$I_1(x) = I_b(x) - I_u(x) \tag{7.27}$$

$$I_2(x) = I_b(x) + I_u(x) \tag{7.28}$$

$L_{11}$  in these equations is the (magnetizing) inductance per unit length of one of the capacitor plates with the other plate open-circuited (zero current).

It follows from (7.25) and (7.26) that the inductance presented to the balanced currents is decreased by a factor  $(1 - k)$  because of the coupling between the lines, while the inductance presented to the unbalanced currents is increased with a factor  $(1 + k)$ .

The inductance used when the characteristic impedance of a transmission line is calculated is the inductance per unit length associated with the balanced currents

$(L_b = [1-k]L_{11})$ . The inductance presented to the unbalanced currents is given in terms of this value by

$$L_u = (1+k) L_{11} = \frac{1+k}{1-k} L_b \quad (7.29)$$

The equivalent circuit shown in Figure 7.6(b) can now be modified as required. The new equivalent circuits are shown in Figure 7.7.

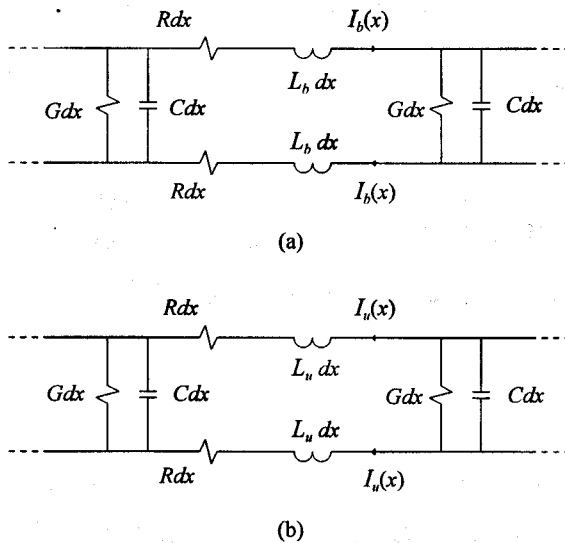


Figure 7.7 The equivalent circuits used to calculate the influence of (a) the balanced and (b) the unbalanced currents on a transmission line.

The final equivalent circuit is shown Figure 7.8(b).  $Ldx$  in this figure should be interpreted as explained above.

At this point the free space capacitor can be analyzed by considering it to be an unbalanced transmission line. The input and output current and voltage of the capacitor will first be established, after which the  $Y$ -parameters will be calculated.

It follows from Figure 7.8(b) that  $I_2(0) = 0$  and  $I_1(l) = 0$ . Since the capacitor is in free space and no other path is available for the current, it follows that

$$I_2(l) = -I_1(0) \quad (7.30)$$

The current entering the top plate of the capacitor on the left is therefore leaving it at the RHS of the bottom plate.

The currents on the two capacitor plates are given by

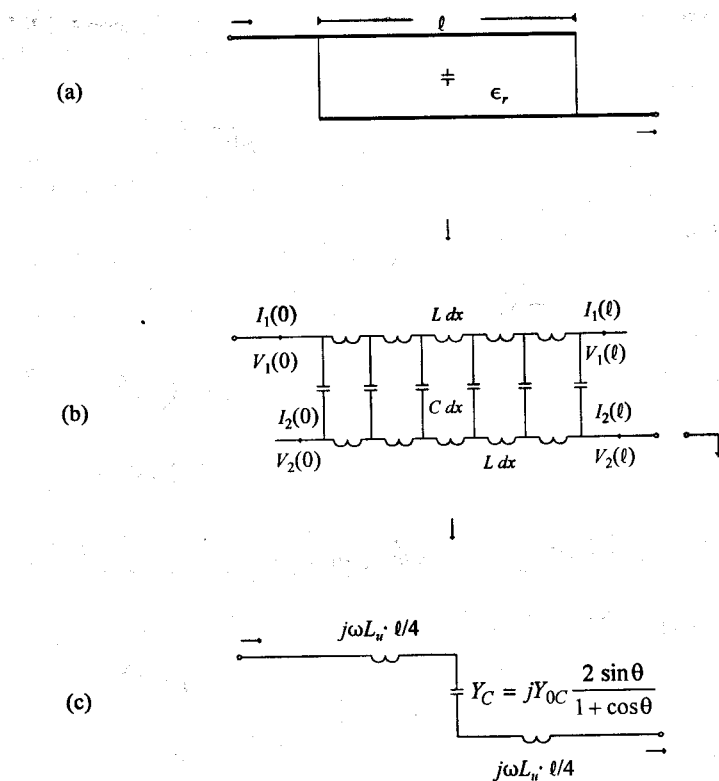


Figure 7.8 The equivalent circuit for a single-layer parallel-plate capacitor in free space.

$$I_1(x) = -\frac{I_0}{2} + Ae^{-\zeta x} + Be^{\zeta x} \quad (7.31)$$

and

$$I_2(x) = \frac{I_0}{2} + Ae^{-\zeta x} + Be^{\zeta x} \quad (7.32)$$

where  $I_1(x)$  is the current on the top plate,  $I_2(x)$  the current on the bottom plate, and  $I_0/2$  the unbalanced current on the line.

By applying (7.31) at  $x = l$  and considering that the current at this point is zero, an expression for the unbalanced current is obtained:

$$I_1(l) = 0 = -\frac{I_0}{2} + Ae^{-\zeta l} + Be^{\zeta l}$$

$$\frac{I_0}{2} = Ae^{-\zeta t} + Be^{\zeta t} \quad (7.33)$$

If (7.32) is applied at  $x = 0$ , a second expression for  $I_0$  is obtained:

$$I_2(0) = 0 = \frac{I_0}{2} + A + B$$

$$\Rightarrow \frac{I_0}{2} = -(A + B) \quad (7.34)$$

A relationship between  $A$  and  $B$  is obtained by combining (7.33) and (7.34):

$$-(A + B) = Ae^{-\zeta t} + Be^{\zeta t}$$

$$A(e^{-\zeta t} + 1) = -B(e^{\zeta t} + 1)$$

$$A = -B \frac{e^{\zeta t} + 1}{e^{-\zeta t} + 1} \quad (7.35)$$

The expression for the current entering the top plate of the capacitor can be simplified by using this expression:

$$I_1(0) = -\frac{I_0}{2} + A + B \quad (7.36)$$

$$= (A + B) + (A + B) = 2(A + B)$$

$$= 2B \frac{e^{-\zeta t} - e^{\zeta t}}{e^{-\zeta t} + 1} \quad (7.37)$$

Because of the relationship between  $I_1(0)$  and  $I_2(t)$ , the expression for  $I_2(t)$  follows immediately from (7.37):

$$I_2(t) = -I_1(0) = -2B \frac{e^{-\zeta t} - e^{\zeta t}}{e^{-\zeta t} + 1} \quad (7.38)$$

With  $B$  known, both the input and the output currents are known at this point.

The voltages on the two plates are given by (6.7) and (6.8), while the voltage difference between the two plates is given by (6.9). Since  $I_0$  is known in terms of  $A$  and  $B$ ,

and  $A$  is known in terms of  $B$ , all the voltages are also known in terms of  $B$  at this point.

The  $Y$ -parameters of the capacitor can now be calculated. In order to derive these parameters, only  $y_{11}$  must be calculated ( $y_{12} = -y_{11}$ ,  $y_{12} = y_{21}$ , and  $y_{22} = y_{11}$ ).

In order to calculate  $y_{11}$ , expressions for the input current and the input voltage are required. An expression for the input current has already been derived. Derivation of the expression for the input voltage follows:

$$V_1(\ell) = V_{12}(\ell) = Z_0(A e^{-\zeta \ell} - B e^{\zeta \ell}) \quad (7.39)$$

Substitution of  $V_1(\ell)$  in the expression by using (6.7) yields

$$0 = V_1(0) - \frac{Z_0}{2}(A - B) - \frac{Z_0}{2}(A e^{-\zeta \ell} - B e^{\zeta \ell}) + s\ell L_u[-(A + B)]$$

from which it follows that

$$\begin{aligned} V_1(0) &= \frac{Z_0}{2}(A - B) + sL_u \ell(A + B) + \frac{Z_0}{2}(A e^{-\zeta \ell} - B e^{\zeta \ell}) \\ &= A \left[ \frac{Z_0}{2}(1 + e^{-\zeta \ell}) + sL_u \ell \right] - B \left[ \frac{Z_0}{2}(1 + e^{\zeta \ell}) - sL_u \ell \right] \\ &= -B \frac{e^{\zeta \ell} + 1}{e^{-\zeta \ell} + 1} \left[ \frac{Z_0}{2}(1 + e^{-\zeta \ell}) + sL_u \ell \right] - B \left[ \frac{Z_0}{2}(1 + e^{\zeta \ell}) - sL_u \ell \right] \\ &= -B Z_0(e^{\zeta \ell} + 1) + sL_u \ell B \frac{e^{-\zeta \ell} - e^{\zeta \ell}}{e^{-\zeta \ell} + 1} \end{aligned} \quad (7.40)$$

With the input current and the input voltage known, the desired expression for  $y_{11}$  can now be derived:

$$\begin{aligned} y_{11} &= \frac{2 \cdot \frac{e^{-\zeta \ell} - e^{\zeta \ell}}{1 + e^{-\zeta \ell}}}{-Z_0(e^{\zeta \ell} + 1) + sL_u \ell \frac{e^{-\zeta \ell} - e^{\zeta \ell}}{1 + e^{-\zeta \ell}}} \\ &= \frac{1}{s \frac{L_u \ell}{2} + \frac{Z_0}{2} \frac{(1 + e^{\zeta \ell})(1 + e^{-\zeta \ell})}{e^{\zeta \ell} - e^{-\zeta \ell}}} \end{aligned} \quad (7.41)$$

If the capacitor is assumed to be lossless, the second term in the denominator of (7.41) can be simplified as follows:

$$\begin{aligned}
 X &= \frac{Z_0}{2} \frac{(1+e^{\zeta\ell})(1+e^{-\zeta\ell})}{e^{\zeta\ell}-e^{-\zeta\ell}} \\
 &= \frac{Z_0}{2} \frac{1+e^{-\zeta\ell}+e^{\zeta\ell}+1}{e^{\zeta\ell}-e^{-\zeta\ell}} \\
 &= \frac{Z_0}{2} \frac{e^{-j\beta\ell}+e^{j\beta\ell}+2}{e^{j\beta\ell}-e^{-j\beta\ell}} \\
 &= \frac{Z_0}{2} \frac{2 \cos \theta + 2}{\cos \theta + j \sin \theta - (\cos \theta - j \sin \theta)} \\
 &= \frac{(\cos \theta + 1)/2}{+jY_0 \sin \theta} \tag{7.42}
 \end{aligned}$$

Substitution of (7.42) in (7.41) yields

$$y_{11} = \frac{1}{\frac{sL_u \ell}{2} + \frac{1}{jY_0 C \cdot \frac{(1+\cos\theta)/2}{\sin\theta}}} \tag{7.43}$$

With  $y_{11}$  known, the other  $Y$ -parameters can be calculated and the  $Y$ -parameter matrix for the parallel-plate capacitor in free space is known.

In the lossless case, these  $Y$ -parameters lead directly to the equivalent circuit shown in Figure 7.8(c). It follows that the parallel-plate capacitor in free space can be considered to be purely lumped, with fixed inductance and variable capacitance. As expected, the capacitance at low frequencies reduces to  $C\ell$ :

$$Y_C = j2Y_{0C} \frac{\sin \beta \ell}{1 + \cos \beta \ell} \tag{7.44}$$

$$\begin{aligned}
 &\equiv j2Y_{0C} \frac{\beta \ell}{2} \\
 &= \sqrt{\frac{C}{2L_b}} \cdot \omega \sqrt{(2L_b) \cdot C} \cdot \ell \\
 &= \omega \cdot (\mathcal{A}) \tag{7.45}
 \end{aligned}$$

If the capacitor is assumed to be lossless, the second term in the denominator of (7.41) can be simplified as follows:

$$\begin{aligned}
 X &= \frac{Z_0}{2} \frac{(1+e^{\zeta\ell})(1+e^{-\zeta\ell})}{e^{\zeta\ell}-e^{-\zeta\ell}} \\
 &= \frac{Z_0}{2} \frac{1+e^{-\zeta\ell}+e^{\zeta\ell}+1}{e^{\zeta\ell}-e^{-\zeta\ell}} \\
 &= \frac{Z_0}{2} \frac{e^{-j\beta\ell}+e^{j\beta\ell}+2}{e^{j\beta\ell}-e^{-j\beta\ell}} \\
 &= \frac{Z_0}{2} \frac{2 \cos \theta + 2}{\cos \theta + j \sin \theta - (\cos \theta - j \sin \theta)} \\
 &= \frac{(\cos \theta + 1)/2}{+jY_0 \sin \theta} \tag{7.42}
 \end{aligned}$$

Substitution of (7.42) in (7.41) yields

$$y_{11} = \frac{1}{\frac{sL_u\ell}{2} + \frac{1}{jY_{0C} \cdot \frac{(\cos \theta + 1)/2}{\sin \theta}}} \tag{7.43}$$

With  $y_{11}$  known, the other  $Y$ -parameters can be calculated and the  $Y$ -parameter matrix for the parallel-plate capacitor in free space is known.

In the lossless case, these  $Y$ -parameters lead directly to the equivalent circuit shown in Figure 7.8(c). It follows that the parallel-plate capacitor in free space can be considered to be purely lumped, with fixed inductance and variable capacitance. As expected, the capacitance at low frequencies reduces to  $C\ell$ :

$$Y_C = j2Y_{0C} \frac{\sin \beta\ell}{1 + \cos \beta\ell} \tag{7.44}$$

$$\begin{aligned}
 &\cong j2Y_{0C} \frac{\beta\ell}{2} \\
 &= \sqrt{\frac{C}{2L_b}} \cdot \omega \sqrt{(2L_b) \cdot C \cdot \ell} \\
 &= \omega \cdot (\mathcal{C}) \tag{7.45}
 \end{aligned}$$

The series inductance obtained in (7.43) is also significant. Since  $\omega L_u = \omega L_{11} \cdot (1 + k)$ , it follows that

$$\frac{sL_u \ell}{2} = sL_{11} \frac{1+k}{2} \ell$$

from which it follows that, if the magnetic coupling between the two capacitor plates is tight (this is usually the case), the series inductance will be approximately the same as the uncoupled inductance (zero current in the other capacitor plate) of one of the capacitor plates. Instead of interpreting this inductance as the total inductance of one plate, it would be more accurate to see it as the sum of the inductance of the top plate from the LHS edge to the center and the inductance of the bottom plate from the center to the RHS edge (see Figure 7.8). Note that the inductance of a microstrip line identical to the bottom plate and with the top plate absent would also be  $L_{11} \cdot \ell$ . The significance of this will be appreciated when the microstrip case is considered.

In order to establish the influence of this inductance on the resonance frequencies of the free space capacitor, (7.43) must be simplified by replacing  $L_u$  in terms of  $Z_{0C}$ . This can be done by using (7.29) and (7.15):

$$Z_{0C} = \sqrt{\frac{2L_b}{C}} = \sqrt{\frac{2L_b \cdot \ell}{C \cdot \ell}} = \sqrt{\frac{2L_b \cdot \ell}{C_T}}$$

→

$$2L_b \cdot \ell = Z_0^2 \cdot C_T = Z_0^2 \cdot \frac{Y_0}{2f_0} = \frac{Z_0}{2f_0} \quad (7.46)$$

from which it follows (by using (7.15)) that

$$L_u \cdot \ell = \frac{1+k}{1-k} \cdot \frac{Z_0}{4f_0} \quad (7.47)$$

Substitution of this expression in (7.43) yields that

$$Y_{11} = \frac{1}{j\omega \frac{1+k}{1-k} \frac{Z_{0C}}{8f_0} + \frac{1}{jY_{0C} \frac{\sin \theta}{1+\cos \theta}}} \quad (7.48)$$

$$= jY_{0C} \frac{2 \sin \theta}{(1+\cos \theta) - \frac{1+k}{1-k} \cdot \frac{\theta}{2} \cdot \sin \theta} \quad (7.49)$$

The effective admittance presented by the free space capacitor can be calculated by using this expression. In interpreting this expression, it should be kept in mind that the characteristic impedance of the capacitor ( $Y_{0c}$ ) is not independent of the coupling factor and will approach infinity as the coupling factor approaches unity.

The effective capacitance of the capacitor in the equivalent circuit is determined by the  $\sin\theta / [(1 + \cos\theta) / 2]$  term in (7.43). This function is compared with the tangent function ( $\tan\theta$ ) in Figure 7.9. It is clearly much more linear than the tangent function, and series resonance only occurs when the electrical line length is  $180^\circ$ , not  $90^\circ$  as in the case of the tangent function. Series resonance in the actual capacitor will occur sooner because of the effect of the series inductance. Parallel resonance (open circuit) occurs when the line length is  $360^\circ$ . The parallel resonance frequency is not influenced by the series inductance.

The combined influence of the inductance and the capacitance on the total admittance of the free space capacitor (as calculated with (7.49)) is shown in Figure 7.10 for a coupling factor of zero and one-half. Series resonance is clearly accelerated drastically by any magnetic coupling between capacitor plates. Fortunately, this problem is eliminated when the capacitor is mounted on a microstrip line.

When the coupling is tight and the capacitor is mounted on a microstrip line, the inductance of the bottom plate becomes the inductance of the microstrip line (as was shown above), and this inductance combines with the microstrip capacitance to have a transmission-line effect up to the center of the parallel-plate capacitor. The characteristic impedance and phase response of this line section is essentially that of the microstrip line.

Similarly, the inductance of the top plate combines with the series combination of the capacitor capacitance and the microstrip capacitance to have a similar line effect (the

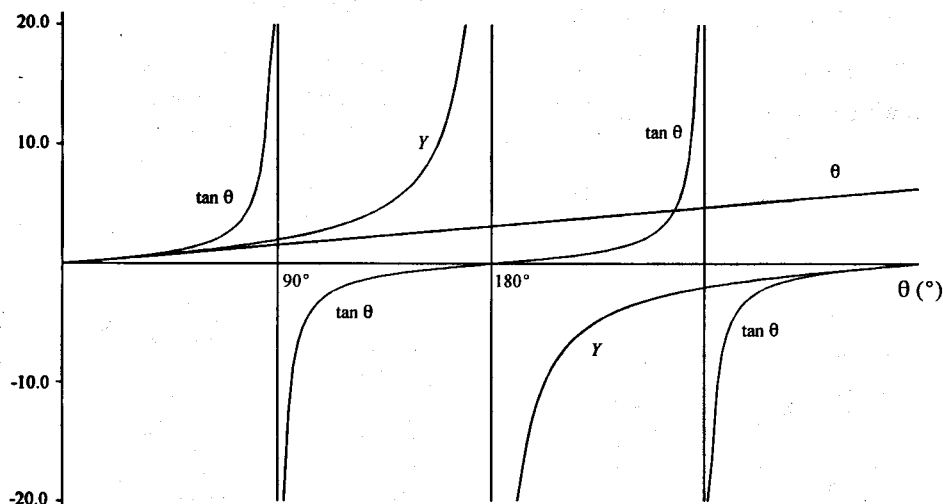


**Figure 7.9** Comparison of the tangent function ( $\tan\theta$ ) with the functions  $Y = \sin\theta / [(1 + \cos\theta)/2]$  and  $Y = \theta$  ( $\omega C$  case).

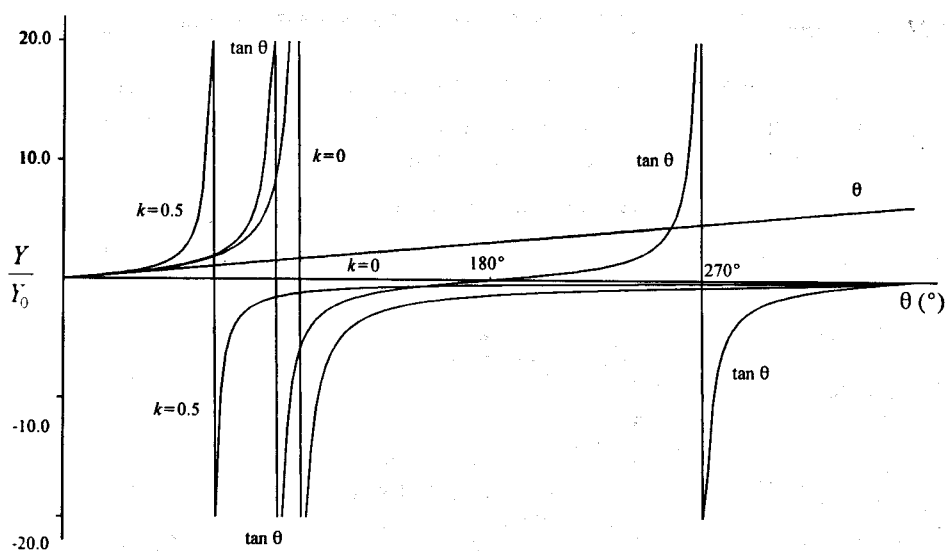


**Figure 7.10** Comparison of the tangent function ( $Y/Y_0 = \tan \theta$ ) and the linear case ( $\theta$ ) with the normalized admittance of the free space capacitor when  $k = 0$  and  $k = 0.5$  (lossless case).

capacitance of the capacitor usually acts as a short-circuit compared to the microstrip capacitance because of the relative difference in the dielectric constants and the thickness of the dielectric layers).

The free space analysis clearly supports the use of the line-capacitor-line model.

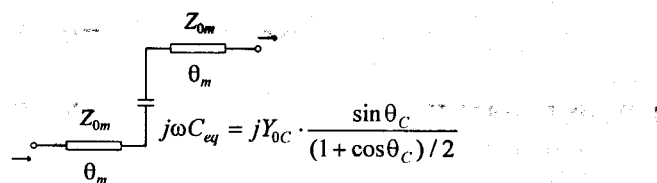
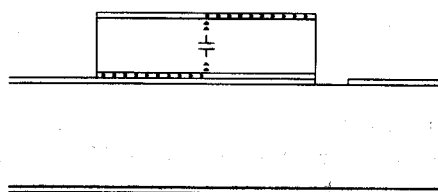


**Figure 7.11** A transmission-line model for a parallel-plate capacitor mounted on microstrip (the  $m$  and  $c$  subscripts denote microstrip and capacitor quantities, respectively).

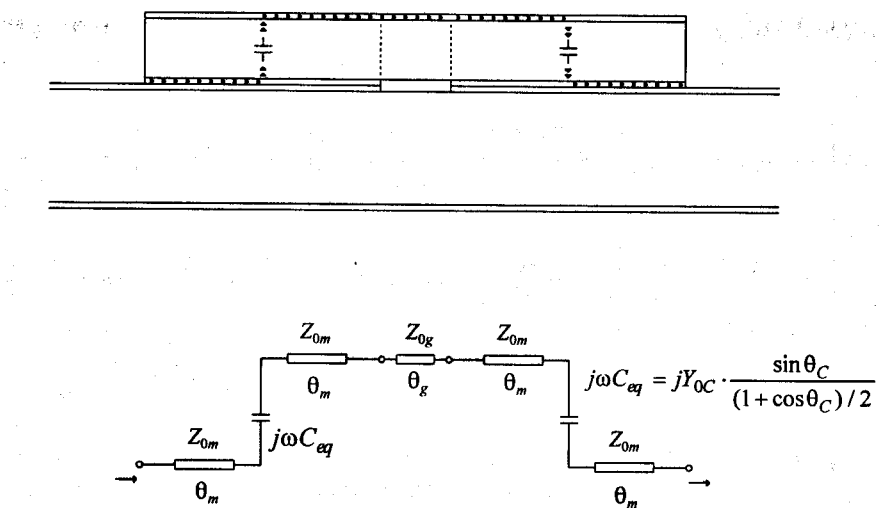


**Figure 7.12** A transmission-line model for a gap-capacitor on microstrip.

This model can be enhanced by replacing the fixed capacitance value with a frequency-dependent term based on (7.44). It should be noted that the difference in the models will be minor when the line length is short (the capacitance will differ by 10% when the electrical line length is 60°).

The proposed model is shown in Figure 7.11. Note that in an MIM capacitor the top plate is smaller than the bottom plate.

The model for a single parallel-plate capacitor can be extended easily to obtain a model for gap-capacitors too. The gap-capacitor model is shown in Figure 7.12.

If the dielectric constant of the capacitor dielectric is much higher than that of the microstrip and the capacitor is thin compared to the microstrip substrate height, the characteristic impedance of the line section associated with the gap can usually also be estimated to be that of the microstrip.

It should be noted that, when possible, the widths of a gap-capacitor and the microstrip line should be chosen to be the same. The main reason for this is the parasitic effect of the step discontinuities introduced at the gap when this is not the case.

## REFERENCES

1. Wolff, I., and N. Knoppik, "Rectangular and Circular Microstrip Disk Capacitors and Resonators," *IEEE Trans. Microwave Theory Tech.*, Vol. MTT-22, No. 10, October 1974.
2. Mondal, J. P., "An Experimental Verification of a Simple Distributed Model of MIM

- Capacitors for MMIC Applications," *IEEE Trans. Microwave Theory Tech.*, Vol. MTT-35, No. 4, April 1987.
3. Giancarlo, B., F. Giannini, E. Limit, and S. P. Marsh, "MIM Capacitor Modeling: A Planar Approach," *IEEE Trans. Microwave Theory Tech.*, Vol. MTT-43, No. 4, April 1995.
4. *MultiMatch RF and Microwave Impedance-Matching, Amplifier and Oscillator Synthesis Software*, Somerset West, RSA: Ampsa (PTY) Ltd; <http://www.amps.com>., 1998.
5. "Di-Cap Microwave Ceramic Capacitors," Cazenovia, NY: Dielectric Laboratories Inc., 1998.

# CHAPTER 8

## THE DESIGN OF WIDEBAND IMPEDANCE-MATCHING NETWORKS

### 8.1 INTRODUCTION

An impedance-matching network usually matches a load to a source inside the passband and may also be used to attenuate unwanted signals outside it.

When the load impedance and the source impedance are purely resistive, inductor-capacitor (LC) networks can be designed relatively easily to fulfill the filter specifications in wideband matching networks. It is difficult, however, if not impossible, to scale impedances over a wideband by using only a limited number of inductors and capacitors. This transformation function can only be done with transformers when the bandwidth-transformation product becomes large. If the required bandwidth is relatively small, however, it is possible to transform resistance over large distances with LC networks.

When the load impedance or the source impedance is reactive, part of the impedance transformation function of the matching network is to remove this reactivity. The extent to which this can be done is a function of the load impedance itself, as well as the transducer power gain versus the frequency response required.

The limitations of a specific load impedance for a specific frequency response can be determined in at least three ways. Fano's set of integral equations can be used to determine these constraints [1], while Youla formulated the constraints in terms of Laurent series expansions [2]. Carlin advanced an iterative procedure for this purpose [3].

Because of its relative simplicity, only the iterative technique developed by Carlin will be presented here.

While the underlying theory will not be considered here, the integral constraints on simple resistor-inductor (RL) and resistor-capacitor (RC) networks lead to simple and useful upper limits on the gain [4]. These gain limits will be considered in Section 8.3.3, along with the Youla gain-bandwidth constraints associated with a parallel RC or a series load (Chebyshev response).

With the limitations of a particular load (or source) known, a network that will provide the required power gain versus frequency response can be designed by using direct synthesis or iterative techniques. Both of these approaches will be discussed in this chapter.

Networks for matching a complex load to a complex source are often required. A theoretical approach to solving this class of problems was developed by Chen and Satyana-

rayana [5], and more recently an alternative and simplified theory was introduced by Carlin and Yarman [6]. Carlin and Yarman also developed iterative techniques for matching a complex load to a complex source [6, 7]. Because of its relative simplicity and its superior results [8], only iterative techniques for matching a complex load to a complex source will be considered.

It is often possible to design matching networks for complex terminations by initially assuming the terminations to be purely resistive. The reactances are then absorbed parasitically into the network when the design is completed. Because the effort required to design a network in this way is minimal when it can be done, this approach will also be considered in this chapter.

Impedance-matching networks are often required to provide a transducer power gain versus frequency response with a positive slope in the passband. LC networks can be designed either interactively or directly to fulfill this requirement. There is, however, the disadvantage that the source will inevitably be mismatched at the lower frequencies in the passband. LC networks with gain slopes also tend to be sensitive to changes in the component values. Because this does not necessarily apply to RLC impedance-matching networks, the design of these networks will also be examined in this chapter.

## 8.2 FITTING AN IMPEDANCE OR ADMITTANCE FUNCTION TO A SET OF IMPEDANCE VERSUS FREQUENCY COORDINATES

When impedance-matching networks are designed, impedance (or admittance) functions that will approximate a set of discrete impedance versus frequency coordinates are often required. The set of coordinates might be the measured input impedance of a transistor or antenna, or it could be the output or input impedance (admittance) of a network to be designed.

It is sometimes possible to approximate the measured impedance of a device with simple RC, RL, or RLC equivalent circuits. This can usually be done when the resistive part of the impedance or admittance is more or less constant over the frequency range of interest.

The components of such an equivalent circuit can be determined by setting up an equation for the input impedance or admittance of the network chosen, and equating its real and imaginary parts to the measured values. Although this technique can be used, more sophisticated techniques are often required.

A major problem in finding an impedance function that will fit a given set of coordinates is its realizability. The function obtained must be positive-real.

A technique that usually gives good results is based on the fact that the reactance (**susceptance**) of a minimum-impedance (admittance) function can be determined when the resistance (conductance) is known [9]. The equivalent circuit of a minimum-impedance function that has a parallel capacitor or inductor as the last element is shown in Figure 8.1.

Because the reactance can be determined when the resistance is known, it follows

that the impedance itself is known when its resistive part is known. In terms of equations, if

$$R(\omega) = \left[ \sum_{2n} C_j / (\omega - \omega_j) + R_0 / 2 \right] + \left[ \sum_{2n} \bar{C}_j / (\omega - \bar{\omega}_j) + R_0 / 2 \right] \quad (8.1)$$

then

$$Z(j\omega) = \sum_{2n} 2C_j / (\omega - \omega_j) + R_0 \quad (8.2)$$

The poles  $\omega_1, \omega_2, \dots, \omega_{2n}$  are the first and second quadrant poles of the resistance function (which is an even function), while  $C_1, C_2, \dots, C_{2n}$  are the residues of these poles. The poles  $\bar{\omega}_1, \bar{\omega}_2, \dots, \bar{\omega}_{2n}$  and the residues  $\bar{C}_1, \bar{C}_2, \dots, \bar{C}_{2n}$  are the conjugates of the first and second quadrant poles and the residues, respectively.  $R_0$  is a real-valued (positive) constant.

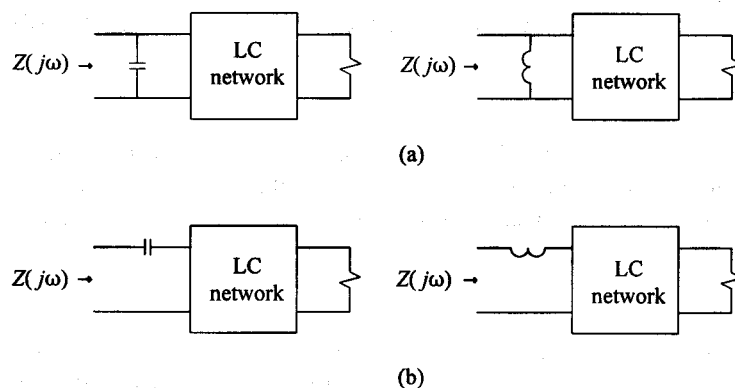


**Figure 8.1** Equivalent circuits for (a) minimum-impedance and (b) minimum-admittance functions.

If a rational function for the resistive part of the minimum impedance function can be found, the impedance function itself can be found by using (8.1) and (8.2).

If the resistance function is assumed to be of the form

$$R(\omega) = \omega^{2p} / (a_{2m}\omega^{2m} + a_{2m-2}\omega^{2m-2} + \dots + a_0) \quad (8.3)$$

The unknown coefficients in the function can be found by using the equations available for fitting a polynomial to a given set of coordinates with least-square error.

Equation (8.3) can be changed to have the following form

$$T(\omega) = \omega^{2p} / R(\omega)$$

$$= a_{2m}(\omega^2)^m + a_{2m-2}(\omega^2)^{m-1} + \dots + a_0$$

$$= b_m x^m + b_{m-1} x^{m-1} + \dots + b_0 \quad (8.4)$$

where  $x = \omega^2$ .

Because  $R(\omega)$  and the number of zeros at the origin are known (the designer must choose the number of zeros), the function  $T(\omega)$  is also known at discrete frequencies.

The coefficients  $b_0, b_1, \dots, b_m$  can now be determined by solving the following set of equations:

$$s_0 b_0 + s_1 b_1 + \dots + s_m b_m = t_0$$

$$s_1 b_0 + s_2 b_1 + \dots + s_{m+1} b_m = t_1$$

$$s_{m+1} b_0 + s_{m+2} b_1 + \dots + s_{2m} b_m = t_m \quad (8.5)$$

where

$$s_0 = h$$

$$s_1 = \sum x_i$$

$$s_{2m} = \sum x_i^{2m} \quad (8.6)$$

and

$$t_0 = \sum T(\omega_i)$$

$$t_1 = \sum T(\omega_i) x_i$$

$$t_m = \sum T(\omega_i) x_i^m \quad (8.7)$$

where  $h$  is the number of coordinates ( $x_i, T(\omega_i)$ ).

With these equations solved, the coefficients in (8.4) and, therefore, those in (8.3) are known.

The minimum-impedance function itself can now be determined by using (8.1) and (8.2). In order to use these equations, the poles of the resistance function must be determined.

The impedance function fitted will be positive-real if care is taken to ensure that the approximation function has no real zeros in the  $\omega$ -plane.

It is possible that the input impedance, as given by the synthesized minimum impedance function, will deviate slightly from the initial set of coordinates. This situation

can be improved by adding a pole at the origin or infinity to the impedance function.

Alternatively, either the minimum-admittance function corresponding to the set of impedance coordinates can be determined or a computer optimization program can be used to improve the match between the two sets of impedances.

An approximation function for the resistive part of an impedance function can be found by using the program PLNM FORTRAN (this program is provided on the diskette accompanying this book). With  $R(\omega)$  known, the minimum-impedance function associated with the resistance function will also be found by this program.

The program ZVR FORTRAN can also be used to find the minimum impedance or minimum-admittance function associated with a specified resistance or conductance function (the discrete target values for the resistance/conductance to be fitted are specified in PLNM).

It happens occasionally that the polynomial determined by the program PLNM is not positive-real. There are two reasons for this.

First, the number of coordinates specified in areas where  $T(\omega)$  approaches zero may be insufficient. This can be remedied easily by specifying more coordinates in these areas.

Second, the increase in  $T(\omega)$  may be too slow at high frequencies. In such a case the polynomial will have a zero on the real axis of the  $\omega$ -plane. This, in turn, implies a real pole in the resistance function  $R(\omega)$ , and therefore a pole on the  $j\omega$ -axis for the function  $R(s)$ , which is, of course, not allowable.

In order to overcome this problem, the option to add an extra data point at a frequency one and a half times the highest frequency specified is provided.

The initial value specified at this extra frequency should be incremented until the zero problem is resolved. The initial value must be specified relative to the value specified at the highest frequency.

The initial value specified at the extra frequency will be incremented for a specified number of times. If the zero problem still persists, more iterations and/or a larger initial value should be used.

### EXAMPLE 8.1 Fitting a function to a set of resistance coordinates.

As an example of the application of the programs PLNM FORTRAN and ZVR FORTRAN, an equivalent circuit for the input impedance of the Motorola MFR406 power transistor will be determined.

The input impedance of the MFR406, as specified by the manufacturer, is tabulated in Table 8.1. It can be seen from this data that the resistance approaches a constant at low frequencies. The approximation function for the resistance, therefore, should be of low-pass form; that is, the function must be of the form

$$R(\omega) = 1 / [a_{2m}\omega^{2m} + a_{2m-2}\omega^{2m-2} + \dots + a_0] \quad (8.8)$$

In polynomial form, this becomes

$$T(\omega) = 1/R(\omega) = b_m(\omega^2)^m + b_{m-1}(\omega^2)^{m-1} + \dots + b_0 \quad (8.9)$$

The resistance function and the associated minimum impedance function will be fitted by using the program PLNM.

The data for the program must be entered in a text file (only ASCII characters are allowed in the file). The default name of the data file is "plnm.dat", but any other name (DOS compatible) may be specified.

The data for this problem were specified in a file "MRF406.dat" which can be found in directory "plnm" on the diskette supplied with this book. The source code for this program can also be found in this directory with a WATCOM make file. An executable version of this program is provided in the main directory of the diskette as "PLNM.EXE". The DOS4GW DOS extender is required in order to run the programs provided, and a copy of this extender is provided in the main directory of the diskette.

The following data must be specified in the data file:

1. Any arbitrary title line (the length of this line can be up to 79 characters);
2. The degree of the polynomial ( $m$ );
3. The resistance or conductance to be fitted at the frequencies (Hz) of interest.

The data must be specified as shown in the example files. When a new problem is defined, the best approach is to make a copy of one of the data files provided (use a different name for the file) and edit the values in the new file.

If zeros on the real axis are required in the function fitted, the option to add an extra data point (as explained above) will be provided.

The resistances specified are shown in Table 8.1.

The user is prompted for the number of zeros required in the resistance function at the origin during execution of the program.

The polynomial obtained from the program is

**Table 8.1**  
The input impedance of the MRF406 as a function of the frequency

Frequency (MHz)	Input impedance ( $\Omega$ )
2	7.5 - j2.6
5	5.2 - j2.4
10	3.1 - j1.9
15	2.3 - j1.8
20	1.7 - j1.7
25	1.3 - j1.4
30	1.0 - j1.0

$$T(\omega) = 0.1448 + 0.4284 \times 10^{-4} \omega^2 - 0.1181 \times 10^{-8} \omega^4 + 0.1841 \times 10^{-13} \omega^6$$

The resistance function obtained is

$$R(\omega) = 1 / [0.1448 + 0.4284 \times 10^{-4} \omega^2 - 0.1181 \times 10^{-8} \omega^4 + 0.1841 \times 10^{-13} \omega^6]$$

The poles of this function are

$$\omega = \pm 204.92 \pm j91.483$$

$$000.000 \pm j55.704$$

There are four poles in the complex  $\omega$ -plane and two poles on the imaginary axis.

After multiplication of the numerator and the denominator by  $-j$ , the minimum-impedance function obtained from the program is

$$Z(j\omega) = \frac{-0.3969 \times 10^3 \omega^2 + 0.94728 \times 10^5 j\omega + 0.19368 \times 10^8}{-j\omega^3 - 0.238669 \times 10^3 \omega^2 + 0.605525 \times 10^5 j\omega + 0.28053 \times 10^7}$$

The impedance function is given as a function of  $s$  by the equation

$$Z(s) = \frac{0.3969 \times 10^3 s^2 + 0.9473 \times 10^5 s + 0.1937 \times 10^8}{s^3 + 0.2387 \times 10^3 s^2 + 0.6055 \times 10^5 s + 0.2805 \times 10^7} \quad (8.10)$$

The impedance as given by this equation is compared to the measured impedance in Table 8.2. The equivalent circuit associated with this impedance function is shown in Figure 8.2. The network (without the 6.6 nH series inductor) was extracted by continued fractionation from the impedance function (Cauer development).

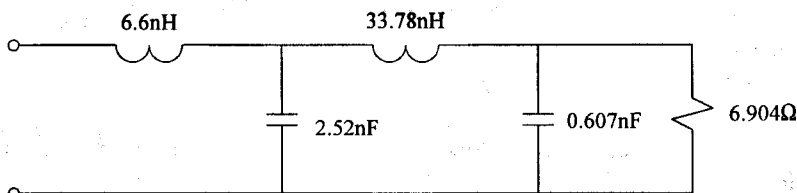


Figure 8.2 An equivalent circuit for the input impedance of the MRF406 transistor.

**Table 8.2**

The input impedance of the MRF406 compared to the impedance as given by (8.10), as well as the input impedance of the equivalent circuit shown in Figure 8.2

Frequency (MHz)	Input impedance of transistor (Ω)	Impedance as given by (8.10) (Ω)	Input impedance of the equivalent circuit shown in Figure 8.2 (Ω)
2.0	$7.5 - j2.6$	$6.6 - j1.4$	$6.6 - j1.3$
5.0	$5.2 - j2.4$	$5.4 - j2.8$	$5.4 - j2.6$
10.0	$2.6 - j1.8$	$3.4 - j3.2$	$3.4 - j2.8$
15.0	$2.3 - j1.8$	$2.2 - j2.9$	$2.3 - j2.3$
20.0	$1.7 - j1.7$	$1.7 - j2.6$	$1.7 - j1.8$
25.0	$1.3 - j1.4$	$1.3 - j2.4$	$1.3 - j1.4$
30.0	$1.0 - j1.0$	$1.0 - j2.3$	$1.0 - j1.1$

It can be seen from Table 8.2 that the impedance given by (8.10) correlates well with the input impedance of the transistor. The match can be improved, however, by adding a pole at infinity (series inductor) to the impedance function. The resulting network is shown in Figure 8.2.

If necessary, the correlation between the impedance of the transistor and that given by the new equation can be improved by entering the network into an optimization program. The alternative is to fit a minimum-admittance function to the measured data.

### 8.3 THE ANALYTICAL APPROACH TO IMPEDANCE MATCHING

Impedance-matching networks can be designed directly (analytically) or iteratively. The direct approach will be discussed in this section.

In its simplest form the load impedance and the source impedance of an impedance-matching problem are purely resistive and equal. In this case the matching network has only a filtering function.

When an explicit function for the required transducer power gain versus frequency response is specified, the network required to meet the filtering specifications can be designed easily with the well-known Darlington synthesis technique. Darlington synthesis will be discussed in Section 8.3.1.

When a band-pass network is designed by using Darlington synthesis, the source or load resistance of the network synthesized often does not have the required value. When the bandwidth is relatively narrow (less than two octaves) and the network contains L-sections consisting only of inductors or capacitors, it is sometimes possible to transform

the source or the load to have the required value by using LC transformers. The design of these networks will be discussed in Section 8.3.2.

The only solution possible when the required bandwidth is large is to use conventional or transmission-line transformers. Although transformation over a wide bandwidth is possible when a transmission-line transformer is used, the transformation ratios are limited (1/4, 1/9, ...).

At microwave frequencies, wideband transformation of resistance is possible when tapered or stepped-impedance lines are used.

It is often possible to eliminate the need for resistance transformation by designing a network with a semi-low-pass or semi-high-pass transducer power gain versus frequency response (i.e., matching networks without transmission zeros at the origin or infinity, respectively). This technique can also be used to provide matching between unequal load and source terminations when the transformation bandwidth is small enough.

It should be noted that the transformation distance obtainable over a given bandwidth with LC impedance-matching networks is limited. This follows from the fact that a high transformation  $Q$  is required when the transformation distance is large. A high transformation  $Q$ , in turn, implies a high network  $Q$  and therefore a narrow bandwidth.

The gain-bandwidth products of impedance-matching networks are also limited when the load or source impedance is reactive. The extent to which this reactivity can be removed is limited because negative inductors and capacitors do not exist.

When only the load (or source) impedance is reactive, the gain-bandwidth constraints imposed by the load (or source) on a particular transducer power gain versus frequency response can be determined by using the integral constraints formulated by Fano, the Laurent series constraints of Youla, or the iterative approach of Carlin.

The constraints on several types of loads, usually for Chebyshev responses, are available in the literature in explicit form. Only the limitations imposed by simple RC and RL loads will be considered here, in Section 8.3.3.

The constraints imposed by any other load can be determined by using Carlin's iterative approach, which will be discussed in Section 8.4.

The analytical design of networks for matching a complex load to a purely resistive source is discussed in Section 8.3.4. Two analytical approaches to solving impedance-matching problems belonging to this class will be considered.

When the technique discussed in Section 8.3.4.1 is used, the complexity of the load is immaterial. As long as the specified transducer power gain versus frequency response is realizable, any load can be matched to a resistive source.

The parasitic absorption approach discussed in Section 8.3.4.2 can only be used when the terminations can be modeled with simple equivalent circuits.

When the load is parasitically absorbed into an impedance-matching network, it is initially assumed to be purely resistive. A network with a suitable topology is then designed and, if the gain-bandwidth constraints imposed by the reactive load on the transducer power gain versus frequency response chosen were taken into account, it will be possible to absorb the reactive part of the load into the designed network.

Although it is limited to simpler problems, this technique has the advantage that less effort is required in designing the network. Parasitic absorption can also be used to

solve simple problems where both the source and the load terminations are reactive.

The principle of parasitic absorption is illustrated in Figure 8.3.

Although it is also possible to match a complex load to a complex source analytically [5, 6], the relevant theory will not be considered here, because much better results can be obtained with considerably less effort by using iterative techniques [8].

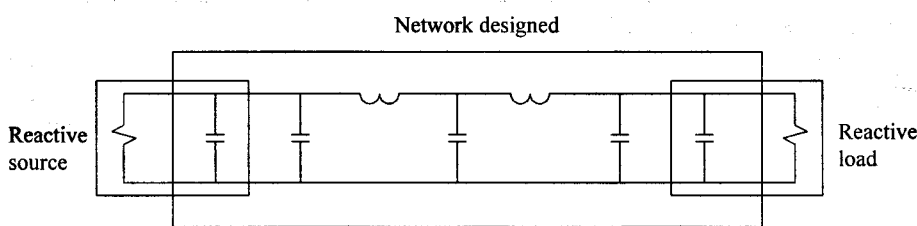


Figure 8.3 Illustration of the principle of parasitic absorption.

The additional theory necessary to design commensurate distributed networks will be covered in Section 8.3.6. Richards' transformation, Kuroda and Norton's identities, and unit elements and their extraction will be considered.

Under Richards' transformation all of the theory applicable to the design of lumped element networks also apply to commensurate distributed networks.

### 8.3.1 Darlington Synthesis of Impedance-Matching Networks

When a resistive load is matched to a resistive source (see Figure 8.4), a network that will provide the required transducer power gain versus frequency response can be designed by following the procedure outlined here.

It should be noted that the source (or load) resistance of the network designed by following this procedure will often not be equal to the specified value. When the network designed contains band-pass L-sections, it is sometimes possible to use LC transformers to adjust the resistance level. Transformers can be used to change the impedance levels in wideband designs.

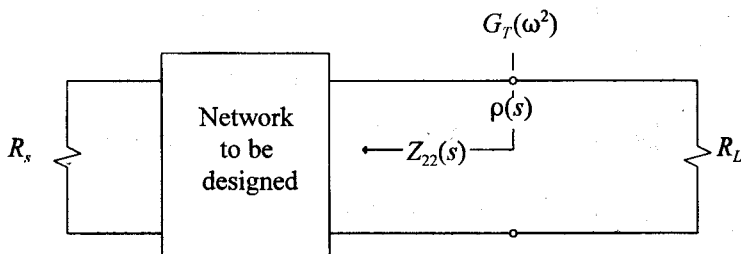


Figure 8.4 The design of an impedance-matching network when the terminations are purely resistive.

If a network without transmission zeros at  $\omega = 0$  or  $\omega \rightarrow \infty$  is designed and the gain-bandwidth limitations are not a problem, the source resistance will always have the required value.

## Darlington Synthesis

**Specifications:** The transducer power gain versus frequency response required and the values of the load resistance and the source resistance.

1. Replace all the  $\omega^2$  terms in the specified transducer power gain function  $G_T(\omega^2)$ , with  $-s^2$  terms.

Determine the product  $\rho(s)\rho(-s)$ , where  $\rho(s)$  is the reflection coefficient  $s_{22}(s)$  corresponding to the specified transducer power gain function:

$$\rho(s)\rho(-s) = 1 - G_T(-s^2) \quad (8.11)$$

2. The next step is to determine  $\rho(s)$ .

Assign all the left-hand plane (LHP) poles of  $\rho(s)\rho(-s)$  to  $\rho(s)$ . It is not necessary to assign only LHP zeros to  $\rho(s)$ . Any combination of zeros can be assigned to it, as long as they are assigned in conjugate pairs and the relationship between  $\rho(s)$  and  $\rho(-s)$  is kept in mind.

When a minimum phase network (i.e., a network with minimum phase variation in the passband) is required, all the LHP zeros must be assigned to  $\rho(s)$ .

When the parasitic absorption approach is followed, the right-hand plane (RHP) zeros must be assigned to  $\rho(s)$  if the source is reactive. When both the load and the source impedances are reactive, it is usually best to try all possible combinations.

The sign assigned to  $\rho(s)$  is often important. When low-pass networks are designed and the load and the effective source resistance, as viewed from the load terminals at  $\omega = 0$ , are not equal, the sign of  $\rho(s)$  is determined by its value at the origin. The sign must be such that

$$\rho(0) = \frac{Z_{22}(0) - R_L}{Z_{22}(0) + R_L} \quad (8.12)$$

When the two resistance values are equal, a plus or a minus sign may be assigned to  $\rho(s)$ .

When the value of  $\rho(s)$  is plus one (open-circuit) at infinity, the first element of the network (as viewed from the load terminals) will be a series inductor. When the sign is negative (short-circuit), the first element will be a parallel capacitor. The sign of  $\rho(s)$  must be such that

$$\rho(\infty) = \frac{Z_{22}(\infty) - R_L}{Z_{22}(\infty) + R_L} \quad (8.13)$$

Where the load resistance is equal to the source resistance and a network with a series capacitor as first element is required, the sign of  $\rho(s)$  must be such that

$$\rho(0) = +1$$

When

$$\rho(0) = -1$$

the first element will be a parallel inductor.

The relationship between the value of the reflection coefficient at zero or infinity and the topology of the network is summarized in Table 8.3 for low-pass, high-pass, and band-pass networks.

The information in this table is useful when networks are designed to absorb the reactive part of the load impedance parasitically.

3. Find the impedance function corresponding to the reflection coefficient  $\rho(s)$  by using the equation

$$\frac{Z_{22}(s)}{R_L} = \frac{1 + \rho(s)}{1 - \rho(s)} \quad (8.14)$$

4. Synthesize the required network by using standard filter theory. If the topology is important, the transmission zeros and the poles at the origin and infinity must be extracted in the proper sequence.
5. If the source resistance of the network does not have the required value, transformers or LC transformers can be used to change the impedance level as required.

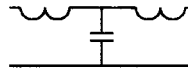
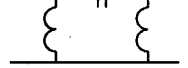
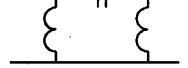
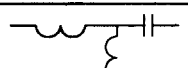
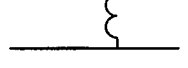
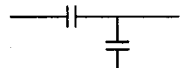
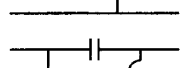
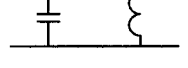
#### **EXAMPLE 8.2** Darlington synthesis of a Butterworth network.

A third-order Butterworth network will be synthesized as an example of the application of this procedure.  $R_L = 1\Omega = R_s$  and the required 3-dB cut-off frequency is 1 rad/s. A low-pass network with an inductor as the first element is required.

1. The transducer power gain function for the third-order Butterworth characteristic is

Table 8.3

The relationship between the reactive part of the output impedance of a network and the value of the corresponding reflection coefficient  $\rho_{22}(s)$  at the origin and infinity

Type of network	$\rho(s)$	$Z_{22}(s)$ at $\omega = 0$	$Z_{22}(s)$ at $\omega \rightarrow \infty$	Example
Low-pass	$\rho(0) = \frac{R_s - R_L}{R_s + R_L}$	Resistive		
	$\rho(\infty) = 1$		Inductive	
	$\rho(\infty) = -1$		Capacitive	
High-pass	$\rho(0) = 1$	Capacitive		
	$\rho(\infty) = \frac{R_s - R_L}{R_s + R_L}$		Resistive	
	$\rho(0) = -1$	Inductive		
Band-pass	$\rho(0) = \frac{R_s - R_L}{R_s + R_L}$		Resistive	
	$\rho(0) = 1$	Capacitive		
	$\rho(\infty) = 1$		Inductive	
	$\rho(0) = -1$	Inductive		
	$\rho(\infty) = 1$		Inductive	
	$\rho(0) = 1$	Capacitive		

$$G_T(\omega^2) = 1/[1 + \omega^2]$$

By substituting each  $\omega^2$  term with  $-s^2$ , this becomes

$$G_T(-s^2) = 1/[1 + (-s^2)^3] = 1/[1 - s^6]$$

The product  $\rho(s)\rho(-s)$  can now be determined:

$$\begin{aligned}\rho(s)\rho(-s) &= 1 - G_T(-s^2) \\ &= \frac{s^6}{s^6 - 1} \\ &= \frac{\pm s^3}{s^3 + 2s^2 + 2s + 1} \quad \frac{\pm s^3}{-s^3 + 2s^2 - 2s + 1}\end{aligned}$$

2. After calculation of the pole positions and the zero positions, all the LHP poles and half of the  $j\omega$ -axis zeros are assigned to  $\rho(s)$ . Because  $R_L = 1\Omega = R_s$ , a positive or a negative sign can be assigned to  $\rho(s)$  if the topology was not important. Because an inductor is required as the first element in this example, the output impedance of the network will be high at high frequencies and therefore a positive sign must be assigned to  $\rho(s)$ :

$$\rho(s) = s^3 / (s^3 + 2s^2 + 2s + 1)$$

3. The output impedance of the network to be designed is given by (8.14):

$$\begin{aligned}\frac{Z_{22}(s)}{R_L} &= \frac{1 + \rho(s)}{1 - \rho(s)} \\ &= \frac{2s^3 + 2s^2 + 2s + 1}{2s^2 + 2s + 1}\end{aligned}$$

4. The network can now be synthesized by continued fractionation (Cauer development) of the impedance function:

$$\frac{Z_{22}(s)}{R_L} = s + \frac{1}{2s + \frac{1}{s+1/1}} = sL_1 + \frac{1}{sC_2 + \frac{1}{sL_3 + 1/G_4}}$$

Because the source resistance has the required value, no transformers or LC transformers are required in this particular case.

The network designed by this example is shown in Figure 8.5.

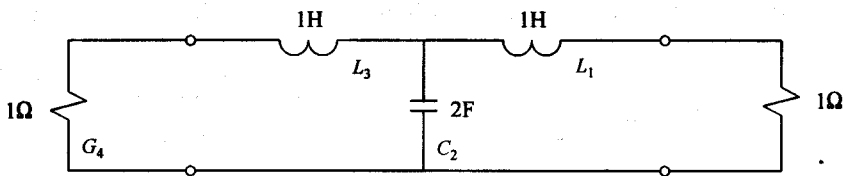


Figure 8.5 A network with a third-order Butterworth response.

### 8.3.2 LC Transformers

The impedance level in a band-pass network containing an L-section consisting of capacitors or inductors only can be changed by replacing the L-section with a suitable T- or PI-section.

Similar to the L-sections discussed in Chapter 4, the output impedance will be transformed downward when the element of the L-section to the left is a parallel element and will be transformed upward when it is a series element.

The T- and PI-section equivalents for the band-pass L-sections are shown in Figures 8.6 and 8.7.

The maximum transformation distance of these sections ( $n^2$ ) is limited by the ratio of the series reactance and the parallel reactance of the original section, as can be seen by inspection of (8.15) to (8.18).

The program LCTRANS FORTRAN, which is provided in directory “\lctrans” on the diskette, can be used to calculate the components required.

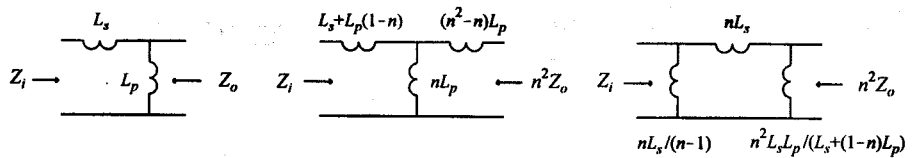
$$\begin{array}{c}
 \text{Left: } Z_i \xrightarrow{\left\{ \begin{array}{c} L_p \\ L_s \end{array} \right\}} Z_o \\
 \text{Right: } Z_i \xrightarrow{\left\{ \begin{array}{c} nL_p \\ (1-n)L_p \end{array} \right\}} n^2Z_o \quad Z_i \xrightarrow{\left\{ \begin{array}{c} nL_s \\ n^2L_s \end{array} \right\}} n^2Z_o
 \end{array}$$

$$\frac{nL_s L_p}{(nL_{s+p} - L_p)} < n^2 < \frac{n^2 L_s}{(1-n)} \quad (8.15)$$

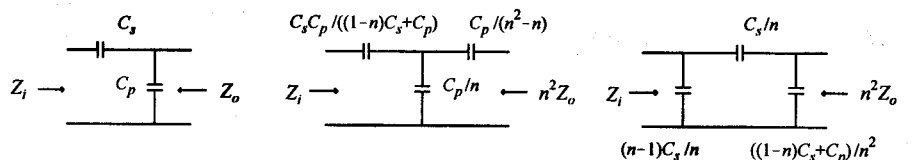
$$\begin{array}{c}
 \text{Left: } Z_i \xrightarrow{\left\{ \begin{array}{c} C_p \\ C_s \end{array} \right\}} Z_o \\
 \text{Right: } Z_i \xrightarrow{\left\{ \begin{array}{c} C_p/n \\ C_p/(1-n) \end{array} \right\}} n^2Z_o \quad Z_i \xrightarrow{\left\{ \begin{array}{c} C_s/n \\ C_{s+p}/(n^2 C_{s+p} - nC_s) \end{array} \right\}} n^2Z_o
 \end{array}$$

$$C_{p+s} - C_s/n < n^2 < (1-n)C_s/n^2 \quad (8.16)$$

Figure 8.6 LC transformers yielding a downward transformation.



$$1 < n < 1 + \frac{L_s}{L_p} \quad (8.17)$$



$$1 < n < 1 + \frac{C_p}{C_s} \quad (8.18)$$

**Figure 8.7** LC transformers yielding an upward transformation.

### EXAMPLE 8.3

The transformation properties of a second-order Chebyshev bandpass network.

A band-pass network with a second-order Chebyshev response is shown in Figure 8.8. The ripple in the passband is 0.5 dB, the center frequency is  $f_0$  and the bandwidth is  $B$ .

The input impedance of the network can be transformed downward (or the output impedance can be transformed upward) by replacing either of the two band-pass L-sections with an equivalent T- or PI-section (The second L-section is obtained by moving the series capacitor to the left and the shunt capacitor to the right).

The maximum transformation distance ( $n^2$ ) possible by replacing either of the two band-pass L-sections in Figure 8.8 with its equivalent T- or PI-section can be determined by using (8.15) to (8.18):

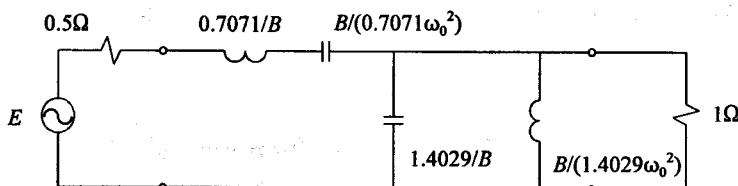


**Figure 8.8** A band-pass network with a second-order Chebyshev response (center frequency:  $\omega_0$  rad/s; bandwidth:  $B$  rad/s).

**Table 8.4**

The maximum transformation distance for an LC transformer in the network shown in Figure 8.8 as a function of the relative bandwidth ( $f_H/f_L$ )

Relative bandwidth	Transformation distance of the LC transformer
2	9.0
3	3.0
5	1.7
10	1.2

$$\begin{aligned}
 n_{\max}^2 &= 1 / \left[ 1 + \frac{1.4209}{B} / \frac{B}{0.7071 \omega_0^2} \right]^2 \\
 &= \left[ \frac{1}{1 + (\omega_0 / B)^2} \right]^2
 \end{aligned} \tag{8.19}$$

The transformation distance obtainable, therefore, is a function of the ratio of the center frequency and the bandwidth of the network. (This ratio can be defined as the  $Q$ -factor of the network.)

The maximum transformation distance for different values of the relative bandwidth ( $f_H/f_L$ ) is shown in Table 8.4. The transformation distance obtainable is large when the bandwidth is narrow and is small when the bandwidth is wide.

The transformed network for  $\omega_0 = 1.732$  rad/s,  $B = 3$  rad/s ( $f_H/f_L = 3$ ),  $R_L = 1\Omega$ , and  $R_s = 1/6\Omega$  is shown in Figure 8.9. Note that the inductor to the left of the replaced capacitive L-section is scaled by a factor of 3. This must be done because of the change in impedance level caused by the LC transformer.

Because of the difference in the load and source impedances imposed by the ripple specification and the order of the network, the transformation distance of the network in Figure 8.9 is twice that of the LC transformer.

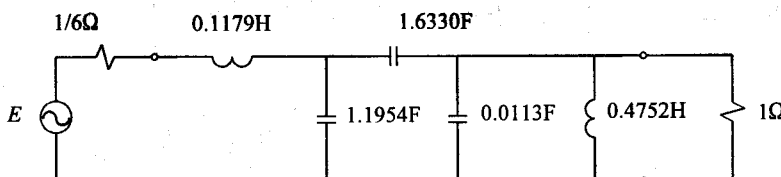


**Figure 8.9** A network for matching a  $1\Omega$  load to a source with  $1/6\Omega$  internal resistance (Chebyshev response,  $1/2$  dB ripple,  $\omega_0 = 1.732$  rad/s,  $B = 3$  rad/s).

### 8.3.3 The Gain-Bandwidth Constraints Imposed by Simple RC and RL Loads

The constraints imposed by a parallel RC load on the gain-bandwidth product of a lossless network with reflection coefficient  $\rho(s)$  can be expressed in the form [1]

$$\int_0^\infty \ln \frac{1}{|\rho(j\omega)|} d\omega \leq \frac{\pi}{RC} \quad (8.20)$$

If the  $RC$  time-constant in (8.20) is replaced with  $L/R$ , the gain-bandwidth constraints associated with a series RL load can also be determined by using (8.20).

The gain-bandwidth expression for a series RC load is [1]

$$\int_0^\infty \omega^{-2} \ln \frac{1}{|\rho(j\omega)|} d\omega \leq \pi RC \quad (8.21)$$

The constraints associated with a parallel RL load also follow from (8.21) by replacing  $RC$  with  $L/R$ .

Because the value of  $\ln(1/|\rho(j\omega)|)$  is normally high inside the passband and close to zero outside it, these integral equations clearly illustrate the trade-off possible between the gain and the bandwidth of the matching network. It follows that any increase in the bandwidth will bring about a decrease in the gain when the gain-bandwidth product exceeds the limit imposed by the load.

Assuming that the matching network has an ideal response ( $G_{T,\max}$  inside the passband and zero outside it), (8.20) and (8.21) can be manipulated to obtain the absolute maximum transducer power gain associated with a bandwidth  $B$  (Hz).

The upper limit resulting from (8.20) is

$$G_{T,\max} \leq 1 - e^{-1/(RCB)} \quad (8.22)$$

A similar expression can be derived for the series RC case. Because this derivation is more involved, the details are shown below:

$$\begin{aligned} \int_0^\infty \omega^{-2} \ln \left| \frac{1}{\rho(j\omega)} \right| d\omega &= \int_0^{\omega_L} \omega^{-2} \ln \left| \frac{1}{\rho(j\omega)} \right| d\omega + \int_{\omega_L}^{\omega_H} \omega^{-2} \ln \left| \frac{1}{\rho(j\omega)} \right| d\omega \\ &\quad + \int_{\omega_H}^\infty \omega^{-2} \ln \left| \frac{1}{\rho(j\omega)} \right| d\omega \\ &= \int_0^{\omega_L} \omega^{-2} \ln \left| \frac{1}{1} \right| d\omega + \int_{\omega_L}^{\omega_H} \omega^{-2} \ln \left| \frac{1}{\rho_{\min}(j\omega)} \right| d\omega + \int_{\omega_H}^\infty \omega^{-2} \cdot 0 d\omega \end{aligned}$$

$$= -\ln \left| \frac{1}{\rho_{\min}} \right| \omega^{-1} \Big|_{\omega_L}^{\omega_H} = \ln |\rho_{\min}| \left( \frac{1}{\omega_H} - \frac{1}{\omega_L} \right)$$

$$= \pi R C$$

It follows from this result that

$$|\rho_{\min}| = e^{-\frac{\pi R C \omega_L \omega_H}{\omega_H - \omega_L}} \quad (8.23)$$

Because  $G_T = 1 - |\rho|^2$ , the required expression for the gain can now be obtained:

$$G_{T,\min} = 1 - e^{-\frac{2\pi R C \omega_L \omega_H}{\omega_H - \omega_L}} \quad (8.24)$$

It has been shown in [4] that these gain expressions can be simplified to

$$G_{T,\min} = 1 - e^{-2\pi Q_c / Q_L} \quad (8.25)$$

in all four cases.

$Q_c$  in (8.25) is the circuit  $Q$  and is defined by

$$Q_c = \frac{\sqrt{\omega_H \omega_L}}{\omega_H - \omega_L} = \frac{\omega_0}{B} \quad (8.26)$$

(as usual), while  $Q_L$  is the  $Q$ -factor of the load at the center frequency ( $\omega_0 C/R$  in the parallel RC case,  $1/(\omega_0 CR)$  in the series RC case,  $\omega_0 L/R$  in the series RL case, and so on).

The expressions derived by using the gain-bandwidth theory developed by Youla [2] are generally more convenient when a specific transducer power gain versus frequency response is of interest. If the parallel RC load is considered and the transducer power gain function is a low-pass Chebyshev function with ripple factor  $\epsilon$  and cut-off frequency  $\omega_c$  rad/s), the maximum gain in the passband ( $K_n$ ) can be determined by using the equation [10]

$$[1 - K_n]^{1/2} = \epsilon \sinh \left\{ n \sinh^{-1} \left[ \sinh \left( \frac{1}{n} \sin^{-1} \frac{1}{\epsilon} \right) - \frac{2 \sin \frac{\pi}{2n}}{R C \omega_c} \right] \right\} \quad (8.27)$$

where  $n$  is the order of the network.

Curves illustrating the relationship between the maximum realizable gain ( $K_n$ ) as a function of the  $RCf_c$  product are given in Figure 8.10 for a Chebyshev response with 0.5-dB ripple in the passband [10].

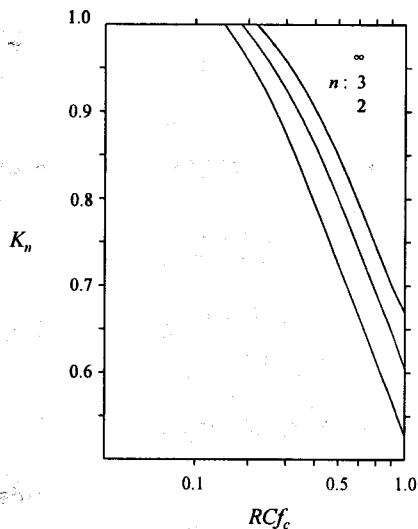


**Figure 8.10** The maximum realizable power gain ( $K_n$ ) of a parallel RC load as a function of the  $RCf_c$  product of the load (low-pass Chebyshev response with 0.5-dB ripple in the passband) (after [10]).

It can be seen from these curves that the maximum power gain will be less than 1 when the  $RCf_c$  product is greater than approximately 0.3. When the  $RCf_c$  product increases above this value, the maximum realizable gain drops rapidly.

If more elements ( $n$ ) are used in the impedance-matching network, the gain-bandwidth product increases. The improvement, however, is small when more than four elements are used.

### 8.3.4 Direct Synthesis of Impedance-Matching Networks When the Load (or Source) Is Reactive

If the specified transducer power gain can be realized, a network for matching a reactive load to a resistive source can be designed by following the procedure outlined here [10].

Similar to Darlington synthesis, the source resistance obtained will often not be equal to that specified. The required transformation can usually be obtained by using transformers or LC transformers.

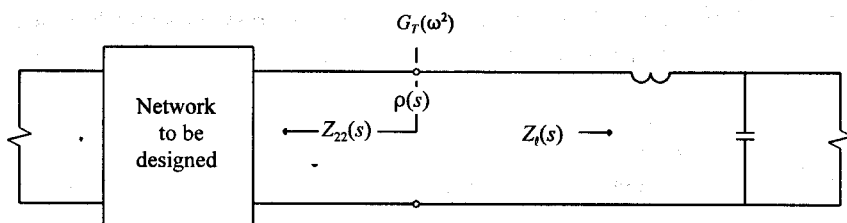


**Figure 8.11** Illustration of the design of impedance-matching networks between a resistive source and a reactive load.

## Design Procedure

Specifications: The source resistance, the load impedance ( $Z_l(s)$ ), and the transducer power gain versus frequency response required (see Figure 8.11).

6. Replace all  $\omega^2$  terms in the specified transducer power gain versus frequency function ( $G_T(\omega^2)$ ) with  $-s^2$  terms.

Determine the product  $\rho(s)\rho(-s)$  by using (8.11):

$$\rho(s)\rho(-s) = 1 - G_T(-s^2)$$

2. The next step is to determine  $\rho(s)$ . Assign all LHP poles to  $\rho(s)$ . If a minimum phase solution is required, assign all the LHP zeros to  $\rho(s)$ . If not, any combination of the zeros can be assigned to it, as long as they are assigned in conjugate pairs, and the relationship between  $\rho(s)$  and  $\rho(-s)$  is kept in mind.

When the load resistance differs from the source resistance and a low-pass or high-pass network is designed, the sign of  $\rho(s)$  can be determined by determining the value of  $\rho(s)$  as defined by (8.28) at  $\omega = 0$  and when  $\omega \rightarrow \infty$ , respectively.

$$\rho(s) = \frac{Z_{22}(s) - Z_l(-s)}{Z_{22}(s) + Z_l(s)} A(s) \quad (8.28)$$

$$A(s) = \prod_i [s - s_i] / [s + s_i] \quad (8.29)$$

where  $A(s)$  is an all-pass function with poles ( $s_i$ ) equal to the open LHP poles (LHP poles with the  $j\omega$ -axis poles excluded) of the load impedance function  $Z_l(s)$ .  $A(s)$  ensures that all the poles of the reflection coefficient,  $\rho(s)$ , will lie in the LHP by canceling the RHP poles caused by  $Z_l(-s)$  in (8.28).

$Z_{22}(s)$  is the output impedance of the network to be designed.

When the load and source impedances are purely resistive and band-pass networks are designed, the sign of  $\rho(s)$  is indeterminate and either sign can be used, that is, unless a specific topology is required. This does not always apply when the load impedance is reactive.

Whether there are any constraints on the sign of  $\rho(s)$  can be determined by considering (8.28) at  $\omega = 0$  and when  $\omega \rightarrow \infty$ .

3. Determine the output impedance of the impedance-matching network as seen from the load terminals. This can be done by using the following equations:

$$r_l(s) = 0.5 [Z_l(s) + Z_l(-s)] \quad (8.30)$$

where  $r_l(s)$  is the even (resistive) part of the load impedance function  $Z_l(s)$ .

$$F(s) = 2r_l(s)A(s) \quad (8.31)$$

$$Z_{22}(s) = \frac{F(s)}{A(s) - \rho(s)} - Z_l(s) \quad (8.32)$$

4. Synthesize the required network by using standard filter theory. When the topology is important, the elements of the network must be extracted in the proper sequence.

#### EXAMPLE 8.4 Darlington synthesis when the load is complex.

As an example of the application of this procedure, a network will be designed to match a load consisting of  $1\Omega$  resistor in parallel with a  $1.39\text{F}$  capacitor to a source with  $0.5\Omega$  internal resistance. The transducer power gain versus frequency function is to be a second-order low-pass Chebyshev function with 0.5-dB ripple in the passband.

$$\omega_c = 1 \text{ rad/s}; K_n = 1$$

The specified transducer power gain function is

$$G_T(\omega^2) = \frac{K_n}{1 + \varepsilon^2 C_n^2 (\omega / \omega_c)^2}$$

$$= \frac{1}{1 + 0.12202(4\omega^4 - 4\omega^2 + 1)}$$

(The ripple factor and the polynomial  $C_2(\omega)$  were obtained from standard filter tables.)

Because  $RCf_c = 0.221$ , it is clear from Figure 8.10 ( $n = 2$ ) that the gain function specified is realizable.

### Step 1

$$G_T(-s^2) = \frac{1}{1 + 0.12202(4s^4 + 4s^2 + 1)}$$

$$\rho(s)\rho(-s) = 1 - G_T(-s^2)$$

$$= \frac{s^4 + s^2 + 0.2500}{s^4 + s^2 + 2.2988}$$

### Step 2

By assigning the LHP poles of the product  $\rho(s)\rho(-s)$  to  $\rho(s)$ , its denominator is found to be

$$p(s) = s^2 + 1.4257s + 1.5126$$

By assigning the LHP zeros to  $\rho(s)$ , the numerator is found to be

$$q(s) = s^2 + 0.5000$$

The reflection coefficient  $\rho(s)$  is therefore

$$\rho(s) = \pm \frac{s^2 + 0.5000}{s^2 + 1.4256s + 1.5162}$$

Since, by using (8.29),

$$A(s) = \prod_i [s - s_i] / [s + s_i]$$

$$= \frac{s - 0.7914}{s + 0.7914}$$

and, by using (8.28),

$$\begin{aligned}\rho(0) &= \frac{Z_{22}(0) - Z_l(0)}{Z_{22}(0) + Z_l(0)} A(s) \\ &= \frac{0.5 - 1.0}{0.5 + 1.0} \frac{0 - 0.7194}{0 + 0.7194} \\ &= \frac{0.5}{1.5}\end{aligned}$$

it follows that a positive sign must be assigned to  $\rho(s)$ .

### Step 3

$$Z_l(s) = 1 / [1 + 1.39 s]$$

$$r_l(s) = 0.5 [Z_l(s) + Z_l(-s)]$$

$$= -0.5176 / [s^2 - 0.5175]$$

$$F(s) = -1.0351 / [s + 0.7194]^2$$

$$Z_{22}(s) = F(s) / [A(s) - \rho(s)] - Z_l(s)$$

$$= \frac{1.4297 s}{0.0185 s^2 + 0.0129 s + 2.0360}$$

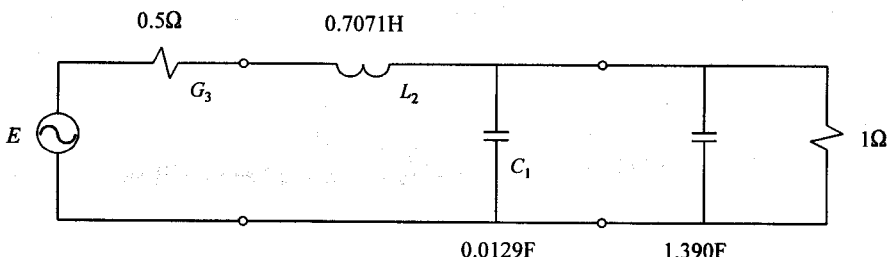


**Figure 8.12** A network for matching a capacitive load to a source with  $0.5\Omega$  internal resistance (0.5-dB ripple, second-order Chebyshev response).

**Step 4**

$$Z_{22}(s) = \frac{1}{0.0129s + \frac{1}{0.7071s + \frac{1}{2.0}}} = \frac{1}{sC_1 + \frac{1}{sL_2 + \frac{1}{G_3}}}$$

**Step 5**

The source resistance is equal to the specified value and, therefore, no transformer is required.

The designed network is shown in Figure 8.12.

### 8.3.5 Synthesis of Networks for Matching a Reactive Load to a Purely Resistive or a Reactive Source by Using the Principle of Parasitic Absorption

When the load impedance or the source impedance can be approximated with simple RC, RL, or RLC networks, impedance-matching networks for the reactive terminations can be designed by at first ignoring the reactivity. If the gain-bandwidth constraints are taken into account and a network with a suitable topology is designed, it will be possible to absorb the reactive parts of the terminations into the designed network.

The topology of the network is a function of the order of the gain function chosen, its transmission zeros, and the sign of  $\rho(s)$ , as was explained in Section 8.3.1.

When only the load or source impedance is reactive and it can be approximated with a parallel RC or series RL network, the maximum gain in the passband ( $K_n$ ) can be determined for a Chebyshev transducer power gain versus frequency response with a specified ripple factor  $\epsilon$ , by using (8.27).

Although this equation gives the optimum  $K_n$  corresponding to a specified ripple factor, it gives no indication as to which ripple factor will cause the lowest insertion loss in the passband; in other words, the optimum ripple factor is not known.

The optimum ripple factors corresponding to some values of the load or source quality factors at the highest frequency in the passband ( $2\pi RCf_c$ ) were determined iteratively by substituting various values for the ripple factor into (8.27). The corresponding values for the highest gain and the lowest gain in the passband ( $K_n$ ;  $K_n / (1 + \epsilon^2)$ ) are tabulated for different values of the  $Q$ -factor and the number of elements used in the network in Table 8.5.

It follows from the table that the insertion loss will be approximately 0.5 dB when  $Q = 2.25$  and four matching elements are used (an ideal transformer will also be required if the source or load resistance differs from that required).

When both the source impedance and the load impedance are reactive and can be approximated with parallel RC or series RL networks, the optimum values for the maxi-

**Table 8.5**

The values of the highest and the lowest transducer power gain in the passband ( $K_n; K_n/(1+\epsilon^2)$ ) of the optimum low-pass Chebyshev function as a function of the load or the source  $Q$ -factor at the highest frequency in the passband and the number of elements used

$Q$	$K_n; K_n/(1+\epsilon^2)$			
	$n = 2$	$n = 3$	$n = 4$	$n = 5$
0.25	1.0000	1.0000	1.0000	1.0000
	0.9998	1.0000	1.0000	1.0000
0.50	0.9997	0.9999	1.0000	1.0000
	0.9969	0.9994	0.9998	1.0000
0.75	0.9997	0.9989	0.9992	0.9994
	0.9876	0.9961	0.9981	0.9988
1.00	0.9929	0.9951	0.9962	0.9968
	0.9703	0.9876	0.9925	0.9946
1.25	0.9814	0.9875	0.9894	0.9905
	0.9459	0.9729	0.9816	0.9856
1.50	0.9685	0.9749	0.9789	0.9805
	0.9165	0.9527	0.9655	0.9715
1.75	0.9515	0.9589	0.9626	0.9665
	0.8839	0.9284	0.9451	0.9533
2.00	0.9319	0.9419	0.9453	0.9492
	0.8499	0.9016	0.9216	0.9319
2.25	0.9111	0.9206	0.9256	0.9294
	0.8157	0.8731	0.8963	0.9083
2.50	0.8877	0.9004	0.9046	0.9082
	0.7821	0.8442	0.8699	0.8834
2.75	0.8666	0.8776	0.8828	0.8861
	0.7496	0.8152	0.8431	0.8580
3.00	0.8440	0.8548	0.8609	0.8638
	0.7184	0.7868	0.8165	0.8325
3.25	0.8223	0.8344	0.8391	0.8415
	0.6887	0.7592	0.7903	0.8073
3.50	0.7997	0.8126	0.8177	0.8195
	0.6606	0.7326	0.7648	0.7827
3.75	0.7800	0.7915	0.7968	0.8000
	0.6340	0.7071	0.7402	0.7587
4.00	0.7597	0.7695	0.7749	0.7791
	0.6090	0.6827	0.7165	0.7355

imum gain in the passband ( $K_n$ ) and the ripple factor ( $\epsilon$ ) can be determined by using the following set of equations [11]:

$$X = [1/Q_2 + 1/Q_1] \sin \frac{\pi}{2n} \quad (8.33)$$

$$Y = [1/Q_2 - 1/Q_1] \sin \frac{\pi}{2n} \quad (8.34)$$

$$A = \sinh^{-1} X$$

$$= \ln[X + \sqrt{X^2 + 1}] \quad (8.35)$$

$$B = \ln[Y + \sqrt{Y^2 + 1}] \quad (8.36)$$

$$= 1/\sinh[nA] \quad (8.37)$$

$$C = 0.5 \frac{\sinh^2[nB]}{\sinh^2[nA]} + 0.5 \sqrt{\frac{\sinh^4[nB]}{\sinh^4[nA]} + \frac{4}{\sinh^2[nA]}} \quad (8.38)$$

$$K_n = 1/[C^2 \sinh^2(nA)] \quad (8.39)$$

$$G_T(\omega^2) = K_n / [1 + \epsilon^2 C_n^2(\omega)] \quad (8.40)$$

$Q_1$  and  $Q_2$  are, respectively, the source and load  $Q$ -factors at the highest frequency in the passband.

When the load or source impedance can be approximated with series or parallel RLC resonant circuits, the inductance or capacitance can be increased to cause resonance at the center frequency of the passband ( $\omega_0$ ), and the band-pass problem can be transformed to an equivalent low-pass problem ( $\omega_c = 1$  rad/s) by using the standard transformation formulas repeated in Figure 8.13. The optimum Chebyshev gain function can then be determined as described above.

The low-pass  $Q$ -factors corresponding to the band-pass  $Q$  (at the center frequency) can be determined by using the equation

$$Q_L = Q_B / (\omega_0 / B) \quad (8.41)$$

This equation can be derived easily by using (8.44) and (8.45).

### EXAMPLE 8.5 A gain-bandwidth example based on Table 8.5.

The optimum values of  $K_n$  and  $\epsilon$  (two-element Chebyshev matching network) will be determined for the load of Example 8.4 ( $1\Omega \parallel 1.39F$ ).

Since

$$Q_L = \omega_c R C = 1.39$$

it follows from the first column of Table 8.5 and linear interpolation of the data that

$$\begin{aligned} K_n &\approx 0.9814 - \frac{1.39 - 1.25}{1.50 - 1.25} [0.9814 - 0.9685] \\ &= 0.9742 \end{aligned}$$

and

$$\begin{aligned} \frac{K_n}{1 + \epsilon^2} &\approx 0.9459 - \frac{1.39 - 1.25}{1.50 - 1.25} [0.9459 - 0.9165] \\ &= 0.9294 \end{aligned}$$

It follows by manipulation of the last equation that the optimum value of the ripple factor is

$$\epsilon = 0.2196$$

Therefore, the optimum two-element gain function is

$$G_T(\omega^2) = \frac{0.97}{1 + 0.0482 C_2^2(\omega)}$$

The maximum value of the insertion loss is 0.32 dB.



$$L_{BL} = L / B \quad (8.42)$$



$$C_{BL} = 1 / (\omega_0^2 L_{BL}) \quad (8.43)$$

$$C_{BC} = C / B \quad (8.44)$$

$$L_{BL} = 1 / (\omega_0^2 C_{BC}) \quad (8.45)$$

**Figure 8.13** Formula for transforming a low-pass network ( $\omega_c = 1$  rad/s) to a band-pass network with center frequency  $\omega_0$  and bandwidth  $B$  (rad/s).

### 8.3.6 The Analytical Approach to Designing Commensurate Distributed Impedance-Matching Networks

By using Richards' transformation [12], the analytical theory applicable to the design of lumped-element networks also applies to commensurate distributed networks (i.e., distributed networks in which the line lengths are all equal). Open-ended lines are transformed to lumped capacitors, and short-circuited lines to lumped inductors under this transformation.

Unlike short-circuited and open-ended stubs, the series transmission lines used in distributed designs have no lumped equivalents under Richards' transformation. The influence of these series lines (unit elements) on the gain function and their extraction from an impedance function when a network is synthesized will be discussed in Section 8.3.6.1, together with Richards' transformation.

The series short-circuited stubs, which are often found in a network designed by the use of Richards' transformation, are not realizable in planar form. When the designed network is to be realized in planar form, these unwanted stubs can be removed by using Kuroda's low-pass identities.

As in the case of lumped networks, impedance scaling is often required for a designed impedance-matching network. This impedance scaling function can be performed by using Kuroda's high-pass identities and Norton's band-pass identities.

Kuroda's and Norton's identities will be discussed in Section 8.3.6.2.

#### 8.3.6.1 Richards' Transformation

By using Richards' transformation [12]

$$S = j\Omega = j \tan[\beta l] = j \tan \left[ \frac{\pi}{2} \frac{\omega}{\omega_0} \right] \quad (8.46)$$

open-ended and short-circuited stubs are mapped to capacitors and inductors in the S-plane.

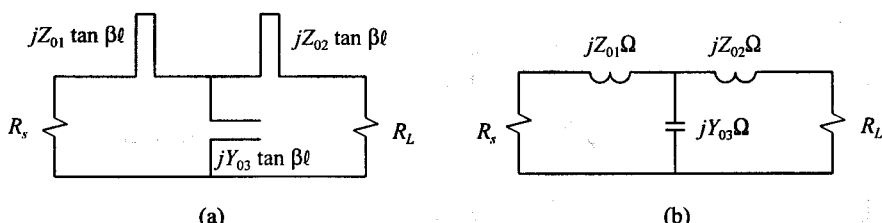


**Figure 8.14** (b) A lumped-element equivalent for the distributed network in (a) under Richards' transformation.

The inductance and capacitance of the lumped equivalents are respectively equal to the characteristic impedance and admittance of the short-circuited and open-ended lines in the distributed network. This is illustrated in Figure 8.14.

The frequency response of a commensurate distributed network is compared with that of its lumped equivalent in Figure 8.15. Note that the response of the distributed network is periodic ( $\beta l$  versus  $\tan \beta l$  characteristic) and that the gain at the even harmonics (including  $\omega = 0$ ) and the uneven harmonics of  $\omega_0$  is equal to that of the lumped equivalent at  $\omega = 0$  and  $\omega \rightarrow \infty$ , respectively. The distributed response is simply a compressed, periodic version of its lumped equivalent.

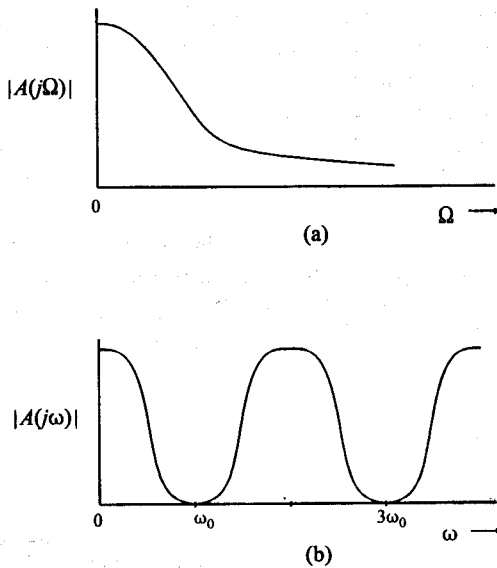


**Figure 8.15** (b) The change in the frequency response of (a) a low-pass network with Richards' transformation.

Series transmission lines are often used in distributed designs. The transmission matrix for a unit element (series transmission line in a commensurate distributed network) is

$$T = \begin{bmatrix} \cos\left(\frac{\pi}{2} \frac{\omega}{\omega_0}\right) & jZ_0 \sin\left(\frac{\pi}{2} \frac{\omega}{\omega_0}\right) \\ jY_0 \sin\left(\frac{\pi}{2} \frac{\omega}{\omega_0}\right) & \cos\left(\frac{\pi}{2} \frac{\omega}{\omega_0}\right) \end{bmatrix} \quad (8.47)$$

By using Richards' transformation, the transmission matrix becomes

$$T = \frac{1}{\sqrt{1-S^2}} \begin{bmatrix} 1 & Z_0 S \\ Y_0 S & 1 \end{bmatrix} \quad (8.48)$$

The transducer power gain of a commensurate distributed cascade network with  $N_v$  unit elements,  $N_h$  high-pass elements, and order  $N$  is given by an expression of the form [13]

$$s_{21}(S)s_{21}(-S) = K_0 \frac{S^{2N_h}[1-S^2]^{N_v}}{G_N(S^2)} \quad (8.49)$$

where  $G_N(S^2)$  is an  $N$ th degree polynomial in  $S^2$ . Each unit element, therefore, contributes a factor  $(1 - S^2)$  to the numerator of the transducer power gain function.

With the gain function chosen, the input impedance of the corresponding network can be determined by Darlington synthesis, as described previously for lumped impedance-matching networks. With the input impedance established, the network can be synthesized. This can be done as before except for the extraction of unit elements.

A unit element can be extracted from the impedance function when the even part of the input impedance at  $S = 1$  is equal to zero. The characteristic impedance of the unit element is given by

$$Z_0 = Z_{in}(S) \Big|_{S=1} \quad (8.50)$$

With the unit element extracted, the remaining input impedance can be determined by using the expression [12]

$$Z'_{in} = Z_{in}(1) \frac{S Z_{in}(1) - Z_{in}(S)}{S Z_{in}(S) - Z_{in}(1)} \quad (8.51)$$

This impedance function will always have a common factor  $S^2 - 1$  in its denominator and numerator which can be canceled.

With its lumped-element equivalent known, the design of the required distributed matching network is completed, that is, if impedance scaling is not required.

#### EXAMPLE 8.6 Extraction of a unit element.

The extraction procedure for a unit element will be illustrated by synthesizing the network with input impedance.

$$Z_{in}(S) = \frac{75S^2 + 125S}{1.5S^2 + 1.5S + 1.0}$$

$$= \frac{[75S^2] + 125S}{[1.5S^2 + 1.0] + 1.5S}$$

Because the numerator of the even part of  $Z_{in}(S)$  at  $S = 1$  is given by

$$NZ_{\text{even}} \Big|_{S=1} = [75S^2][1.5S^2 + 1.0] - [125S][1.5S] \Big|_{S=1} = 0$$

and

$$Z_{in}(1) = 50$$

a unit element of  $50\Omega$  can be extracted.

The input impedance with the unit element removed can be determined by applying (8.51):

$$\begin{aligned} Z'_{in} &= Z_{in}(1) \frac{S Z_{in}(1) - Z_{in}(S)}{S Z_{in}(S) - Z_{in}(1)} \\ &= 50 \frac{75S^3 - 75S^2}{75S^3 + 50S^2 - 75S - 50} \\ &= 50 \frac{[S^2 - 1]75S}{[S^2 - 1][75S + 50]} \\ &= \frac{1}{1/[75S] + 1/50} \end{aligned}$$

The synthesized network is shown in Figure 8.16.

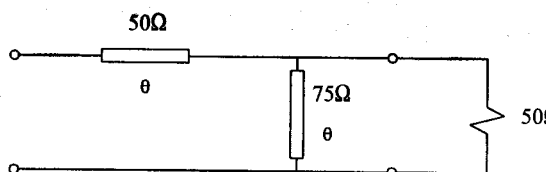
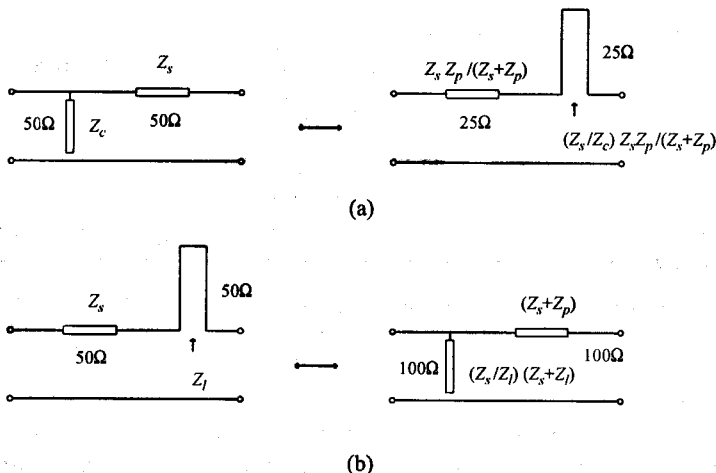


Figure 8.16 The network synthesized in Example 8.6.

### 8.3.6.2 Kuroda and Norton's Identities

Kuroda's low-pass identities are shown in Figure 8.17. These identities can sometimes be used to transform unrealistic impedances to more realistic levels, but they are more frequently used to remove unwanted series short-circuited stubs from planar designs.

Kuroda's high-pass identities are shown in Figure 8.18. These identities can be used to change the impedance level in a matching network, as illustrated. The impedance level



**Figure 8.17** Kuroda's low-pass identities for commensurate networks.

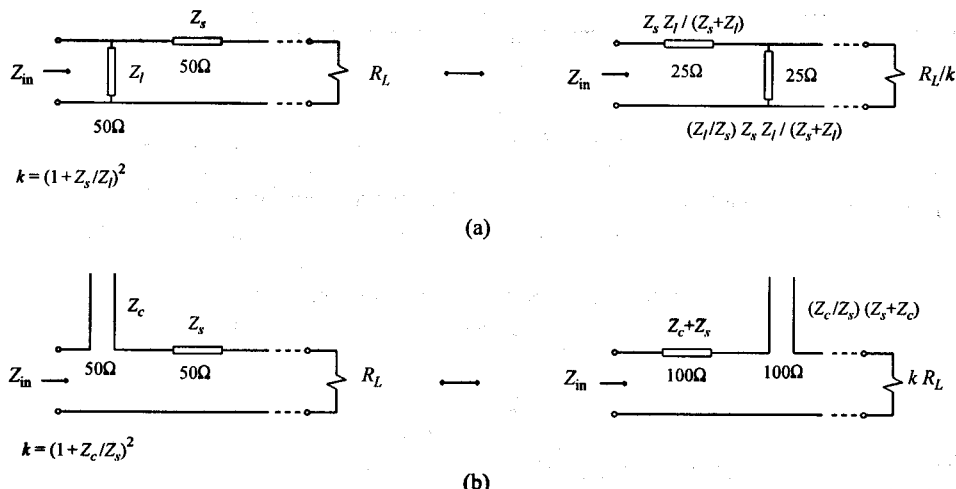


**Figure 8.18** Kuroda's high-pass identities for commensurate networks.

to the right of the transformed components is scaled with a factor  $k$ , while the input impedance ( $Z_{in}$ ) remains unchanged.

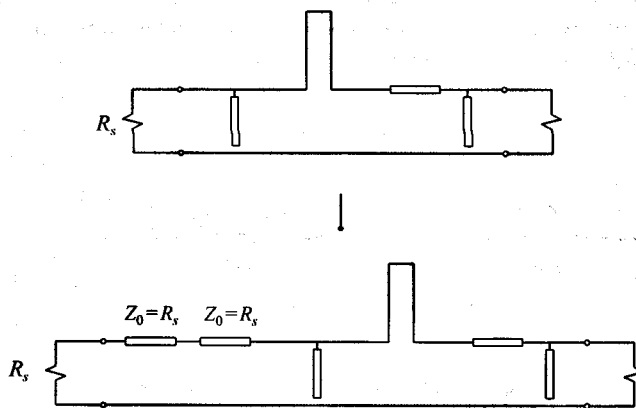


**Figure 8.19** Adding unit elements to a commensurate network with a resistive source.

In applying Kuroda's identities it is useful to know that when the load or source impedance is purely resistive, any number of unit elements (with  $Z_0 = R_s$  or  $Z_0 = R_L$ ) can be added in series with it without changing the amplitude response. This is illustrated in Figure 8.19.

The impedance level in a network can also be changed by using Norton's identities. Unlike Kuroda's identities in which unit elements are always involved, Norton's identities

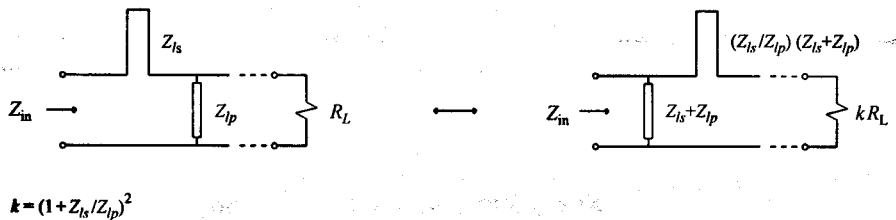


**Figure 8.20** Norton's band-pass identities for commensurate networks.

are applied to L-sections consisting only of open-ended or short-circuited stubs. These identities are shown in Figure 8.20.

## 8.4 THE ITERATIVE DESIGN OF IMPEDANCE-MATCHING NETWORKS

Instead of following the analytical approach, impedance-matching networks can also be designed iteratively. The "real-frequency" iterative techniques considered here have a major advantage over analytical and other techniques in that equivalent circuits for the load or source impedances, or an analytical expression for the transducer power gain versus frequency response, is not required. The networks synthesized by using iterative techniques are generally simpler in form with superior gain properties [6-8].

The first "real-frequency" technique was introduced by Carlin [3]. A complex load can be matched to a purely resistive source by using this technique. In this technique a piece-wise linear approximation of the output resistance or conductance of the network to be designed is optimized by using a least-square optimization routine.

The convergence properties of this technique are very good, and it can be used generally to estimate the gain-bandwidth constraints imposed by any complex load.

It has the disadvantage, however, that the response outside the passband is usually unnecessarily constrained, and occasionally it will not give the best results obtainable without considerable experimentation with the response outside the passband.

When band-pass networks are designed, the reactance of the network may not approximate the expected reactance well because of the difficulty of detecting and approximating the narrow spikes that can occur in the resistance function of a band-pass network. In these cases, the actual response will be poorer than that expected from the line-segment results [14].

Despite these disadvantages, the networks synthesized by using this technique are superior to those obtainable by direct application of analytical theory. This technique will be discussed in detail in Section 8.4.1.

Apart from matching a complex load to a purely resistive source, the "real-frequency" technique introduced by Yarman and Carlin in [7] can also be used to match a complex load to a complex source. In this technique, the numerator coefficients of the input reflection parameter ( $s_{11}$ ) of the network terminated in a purely resistive load are optimized.

Compared to the line-segment technique (where only one of the terminations is complex), the reflection coefficient technique has the advantage that it has no approximation step.

Initialization of the reflection coefficient procedure is not as simple as in the case of the line-segment technique where the unknown output impedance of the network to be synthesized is taken to be equal to the resistive part of the known reactive load. However, excellent results can usually be achieved if the results obtained from the line-segment technique are used for initialization.

Although the solution achieved may not necessarily be the best solution obtainable,

it is, as a rule, much better than anything obtainable by direct application of analytical theory.

The reflection coefficient technique will be discussed in detail in Section 8.4.2.

In another technique proposed by Yarman and Carlin to solve double-matching problems (i.e., problems in which the load and the source are complex) [6], the output resistance of the matching network terminated at the input in a purely resistive load is optimized. Because this procedure has no significant advantage over the reflection coefficient technique, it will not be covered here. The interested reader is referred to [6].

The double-matching problem can also be solved very effectively by doing a synthesis-based systematic search on the transformation  $Q$ -factors (introduced in Chapter 3) to obtain initial solutions, which can then be optimized. Instead of optimizing only the best solution obtained in the search, it is a good idea to store a number of the best solutions obtained (10–25 are usually adequate) and then optimize all of these.

This approach has the distinct advantage that initial solutions are generated by the software and are not required from the designer.

If the systematic search is done thoroughly enough and enough solutions are stored for optimization, the probability of finding the optimum solution to any impedance-matching problem is very high.

Other major advantages of this approach are that many solutions are obtained (not just one) and that transformers are never required in the solutions synthesized. This technique is also very robust and can easily be extended to incorporate a great variety of constraints (topology constraints, constraints on the element values, etc.).

Synthesis with this technique is over all topologies (if required), as is the case with the “real-frequency” techniques introduced by Carlin et al.

The transformation- $Q$  approach can also be extended to form the basis of a algorithm for the design of distributed matching networks. This can be done without resorting to Richards’ transformation, being restricted to commensurate solutions, and having to deal with any short-circuited stubs in the main line.

When commensurate networks are designed by following this approach, the variables are the characteristic impedances and the line lengths are fixed. The networks synthesized can also be generalized so that the same length is used for the different types of lines (main-line sections, open-ended stubs, and shorted stubs) and not all the lines are used [15]. In addition to its generality, this approach has the advantage that the line lengths used for stubs can be constrained to be short for replacement with lumped elements (mixed lumped/distributed solutions) or different stubs, if required [15].

If commensurate solutions are not required, the characteristic impedances to be used for the different line types can be fixed and the optimum lengths can be determined [15]. To approximate the results obtainable with lumped solutions, the characteristic impedance assigned to the main-line sections and any shorted stubs should be as high as possible, while that used for open-ended stubs should be as low as possible.

The lengths of the lines used can be reduced by using lumped elements, if space is a problem. Part of the line to be replaced should be retained as a pad for the lumped component. Again the transformation- $Q$  technique can be extended easily to achieve this [15].

The basic transformation- $Q$  technique will be considered in detail in Section 8.4.3.

**Table 8.6**  
Comparison of the different iterative impedance-matching techniques considered here

Line-segment technique	Reflection coefficient technique	Transformation- <i>Q</i> technique
Single-matching technique.	Double-matching technique.	Double-matching technique.
Topology independent, except for the number of transmission zeros at the origin which must be specified.	Topology independent, except for the number of transmission zeros at the origin which must be specified.	Topology independent.
Topology control only through the number of transmission zeros at the origin and the sign of the reflection coefficient.	Topology control only through the number of transmission zeros at the origin and the sign of the reflection coefficient.	Topology control can be implemented easily.
Initialization by setting the output resistance equal to the required load resistance.	Initialization by using the results of the line-segment technique.	Initialization by synthesis- based systematic searches.
The results obtained are usually degraded in the approximation step present in this procedure.	No approximation step. Can be used to optimize the solution obtained with the line-segment approach.	No approximation step.
Excellent convergence properties, for low-pass or high-pass solutions, but no guarantee of finding the global optimum.	Strongly dependent on initial solutions. No guarantee of finding the global optimum.	Dependent on the search range and density used. If the systematic search is done densely enough, it is highly likely that the global optimum will be obtained.
Ideal transformers may be required in band-pass solutions.	Ideal transformers may be required in band-pass solutions.	Ideal transformers are never required.
Single solution for each set of specifications.	Single solution for each set of specifications.	Many solutions to each matching problem.
Limited to lumped or commensurate distributed networks.	Limited to lumped or commensurate distributed networks.	Can be generalized easily to synthesize lumped solutions, commensurate solutions (without any series stubs), non-commensurate distributed solutions and mixed lumped/distributed solutions.
Easy to implement.	Easy to implement.	More involved.

The advantages and disadvantages of the three techniques considered in this section are compared in Table 8.6 above. The first two techniques were implemented in the programs LSM and RCDM supplied on the diskette accompanying this book, respectively. The third technique is implemented in [15].

### 8.4.1 The Line-Segment Approach to Matching a Complex Load to a Resistive Source

The gain-bandwidth constraints imposed by a reactive load (or source) can be determined iteratively by assuming that the output impedance (or admittance) of the network is a minimum-impedance (admittance) function (see Figure 8.21). When this is done, the output reactance of the network is known when the resistance is known. The optimum resistance can then be determined by minimizing the mean-square deviation between the desired and the actual transducer power gain.

If the resistance is approximated with line segments, the problem is well behaved and the optimization can be done with a simple least-square optimization routine.

A detailed description of the procedure [3, 16] and the mathematics involved follows. This technique is implemented in the program LSM FORTRAN, which can be found on the diskette accompanying this book. The source code is provided in directory “\lsm” with a Watcom [17] make file. The executable file is provided in the root directory of the diskette.

#### The Line-Segment Approach

1. Assume that the output impedance/admittance of the optimum network is a minimum-impedance/minimum-admittance function.
2. Assume as a first approximation that the resistive part ( $R(\omega)$ ) of the output impedance of the optimum network is equal to the resistive part of the measured load impedance ( $Z_L$ ); that is,

$$R(\omega_i) = R_L(\omega_i) \quad (8.52)$$

3. Approximate the rational output resistance of the network with a piece-wise linear function, as illustrated in Figure 8.22.

Enough increment frequencies (the frequencies at which the slope of the linear function changes) must be chosen to ensure a reasonable ap-

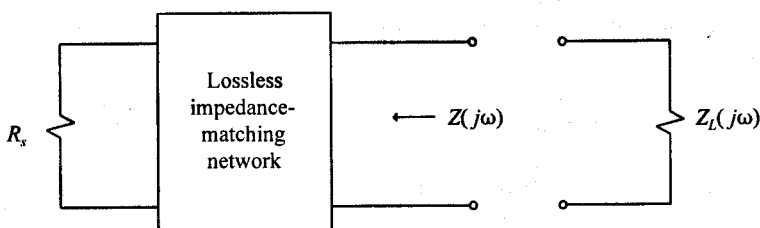


**Figure 8.21** The impedance-matching problem under consideration.

proximation of the unknown resistance. This can usually be done by choosing the frequencies to ensure a good approximation of the measured load resistance.

For the sake of simplicity, the resistance  $R(\omega)$  is assumed to equal zero at frequencies greater than the last increment frequency ( $\omega_n$ ).

The linear resistance function can be considered to be the sum of the semi-infinite functions  $a_1(\omega), a_2(\omega), \dots, a_n(\omega)$  shown in Figure 8.23, each with an appropriate weight factor  $r_k$ :

$$R(\omega) = r_0 + \sum_k r_k a_k(\omega) \quad (8.53)$$

where

$$a_k(\omega) = \begin{cases} 0 & \text{if } \omega < \omega_{k-1} \\ \frac{\omega - \omega_{k-1}}{\omega_k - \omega_{k-1}} & \text{if } \omega_{k-1} < \omega_k \\ 1 & \text{if } \omega_k < \omega \end{cases} \quad (8.54)$$

and

$$r_0 = Z_s(0) \quad (8.55)$$

When the optimum low-pass network is determined,

$$r_0 = R_s \quad (8.56)$$

where  $R_s$  is the source resistance as shown in Figure 8.21.

In all other cases,  $r_0$  is equal to zero.

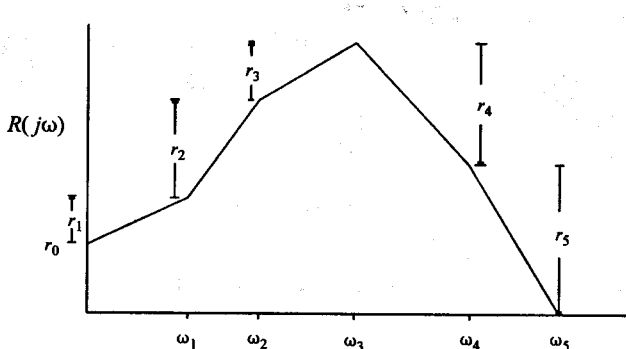


**Figure 8.22** Approximation of the output resistance of the matching network with a piece-wise linear function.

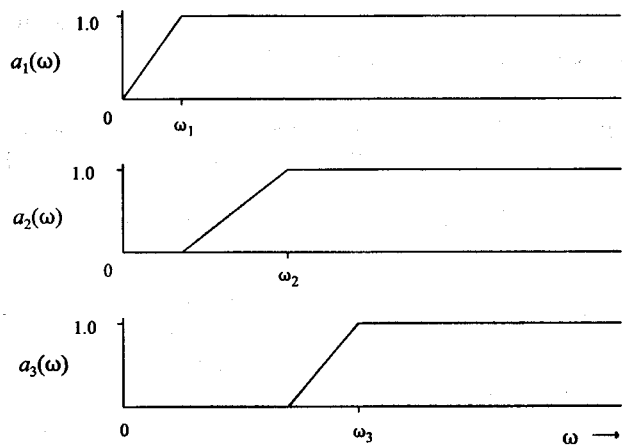


**Figure 8.23** Illustration of the semi-infinite functions used in the line-segment approach.

Since the resistance  $R(j\omega)$  is equal to zero when the frequency is greater than the last increment frequency ( $\omega_n$ ), the increment factor (weight factor)  $r_n$  is not independent of the other increment factors. The following equation applies:

$$r_n = -[r_0 + r_1 + r_2 + \dots + r_{n-1}] \quad (8.57)$$

When this value for  $r_n$  is substituted into (8.53), it changes to

$$R(\omega) = [1 - a_n(\omega)]r_0 + \sum_k r_k [a_k(\omega) - a_n(\omega)] \quad (8.58)$$

In vector form this becomes

$$R(\omega) = [1 - a_n(\omega)]r_0 + \bar{a}^T(\omega)\bar{r}' \quad (8.59)$$

where

$$\bar{a}^T(\omega) = [a_1(\omega) - a_n(\omega), a_2(\omega) - a_n(\omega), \dots, a_{n-1}(\omega) - a_n(\omega)] \quad (8.60)$$

and

$$\bar{r}' = \begin{bmatrix} r_1 \\ r_2 \\ \vdots \\ r_{n-1} \end{bmatrix} \quad (8.61)$$

The resistance value at any particular frequency can be calculated by using (8.59).

Because the impedance function was assumed to be a minimum-impedance function, the reactance associated with the resistance  $R(j\omega)$  is known. It can be determined by using the equation

$$X(\omega) = \bar{b}^T(\omega) \bar{r} \quad (8.62)$$

where

$$\bar{b}^T(\omega) = [b_1(\omega), b_2(\omega), \dots, b_n(\omega)] \quad (8.63)$$

and

$$b_k(\omega) = \frac{1}{\pi[\omega_k - \omega_{k-1}]} \int_{\omega_{k-1}}^{\omega_k} \ln \left| \frac{y + \omega}{y - \omega} \right| dy \quad (8.64)$$

The value of the integral in the last equation is high when the relevant increment frequencies are close to  $\omega$ , and the value decreases as the increment frequencies deviate from  $\omega$ . It follows from this and (8.62), that the reactance associated with the resistance at a particular frequency will be high when the resistance changes rapidly at nearby frequencies.

The integral in (8.64) has a simple closed form evaluation [9], which is useful in determining its value.

If the dependence of  $r_n$  on the other increment factors is taken into account, (8.62) becomes

$$X(\omega) = [0 - b_n(\omega)] r_0 + \bar{b}'^T(\omega) \bar{r}' \quad (8.65)$$

where

$$\bar{b}'(\omega) = \begin{bmatrix} b_1(\omega) - b_n(\omega) \\ b_2(\omega) - b_n(\omega) \\ \vdots \\ b_{n-1}(\omega) - b_n(\omega) \end{bmatrix} \quad (8.66)$$

The resistance and reactance corresponding to a particular increment vector  $\bar{r}'$ , can be determined at any particular frequency by using (8.59) and (8.66).

4. Calculate the transducer power gain associated with the initial value ( $\bar{r}'_0$ )

of the increment vector  $\bar{r}'$  at the various frequencies of interest. This can be done by using the equation

$$\begin{aligned}
 G_T(\omega) &= 1 - |s_{11}|^2 \\
 &= 1 - \left| \frac{Z_L(\omega) - Z^*(\omega)}{Z_L(\omega) + Z(\omega)} \right|^2 \\
 &= 1 - \left| \frac{[R_L(\omega) + jX_L(\omega)] - [R(\omega) + jX(\omega)]^*}{[R_L(\omega) + jX_L(\omega)] + [R(\omega) + jX(\omega)]} \right|^2 \\
 &= \frac{4 R_L(\omega) R(\omega)}{[R_L(\omega) + R(\omega)]^2 + [X_L(\omega) + X(\omega)]^2} \quad (8.67)
 \end{aligned}$$

where  $Z_L(\omega)$  is the measured load impedance.

5. Determine the optimum value of the increment vector  $\bar{r}'$  iteratively by minimizing the sum of the relative difference in the actual transducer power gain ( $G_T(\omega)$ ) and the desired transducer power gain ( $G_I(\omega)$ ) squared at the different frequencies of interest. This can be done by using a least-square optimization routine.

The relevant equations are as follows:

$$E = \sum_j e^2(\bar{r}', \omega_j) \quad (8.68)$$

$$= \sum_j \left[ \frac{G_T(\bar{r}', \omega_j)}{G_I(\omega_j)} - 1 \right]^2 \quad (8.69)$$

$$\bar{f}'(\omega) = \frac{\partial e(\bar{r}', \omega)}{\partial \bar{r}_0'} \quad (8.70)$$

$$= \frac{\partial e(R(\omega), X(\omega))}{\partial R(\omega)} \frac{\partial R(\omega)}{\partial \bar{r}_0'} + \frac{\partial e(R(\omega), X(\omega))}{\partial X(\omega)} \frac{\partial X(\omega)}{\partial \bar{r}_0'} \quad (8.71)$$

$$= \frac{\partial e(R(\omega), X(\omega))}{\partial R(\omega)} \bar{a}(\omega) + \frac{\partial e(R(\omega), X(\omega))}{\partial X(\omega)} \bar{b}(\omega) \quad (8.72)$$

where  $\bar{r}'_0$  is the current initial value of the increment vector, and  $\bar{f}'(\omega)$  is the gradient vector associated with the error function  $e(\bar{r}', \omega)$ , where

$$e(R(\omega), X(\omega)) = G_T(R(\omega), X(\omega)) / G_I(\omega) - 1 \quad (8.73)$$

with  $G_T(R(\omega), X(\omega))$  as defined in (8.67).

$$e(\bar{r}', \omega_j) = e(\bar{r}'_0, \omega_j) + \bar{f}'^T(\omega_j) \cdot \bar{\delta} \quad (8.74)$$

with  $\bar{\delta}$  defined by the equation

$$\bar{r}' = \bar{r}'_0 + \bar{\delta} \quad (8.75)$$

where  $\bar{r}'$  is the new initial value of the increment vector.

$$\frac{\partial \sum_j e(\bar{r}', \omega_j)}{\partial \delta} = 0 \quad (8.76)$$

→

$$\sum_j \bar{f}'(\omega_j) \bar{f}'^T(\omega_j) \bar{\delta} = -\sum_j e(\bar{r}'_0, \omega_j) \bar{f}'(\omega_j) \quad (8.77)$$

With the optimum increment vector known, the gain-bandwidth constraints imposed by the load, as well as the output impedance (admittance) of the optimum network, are known.

#### 6. The next step is to determine the optimum network.

Since the optimum increment vector is known, the output resistance of the network is known at any particular frequency. A rational approximation function and the corresponding minimum-impedance (admittance) function can be obtained by following the procedure outlined in Section 8.2.

The order of the network and the number of zeros at the origin are variables in the approximation stage.

With the minimum-impedance and minimum-admittance functions known, the optimum network can be synthesized easily.

Whether a minimum-impedance or minimum-admittance function will be the best solution to a particular problem is usually not known at the outset. If good results are not obtained by using one, the other can be tried.

When the load resistance is higher than the source resistance, a minimum-impedance solution often yields better results.

When the gain-bandwidth product in a problem is a limiting factor,

it will be found that the results are dependent on the position of the last increment frequency. Some experimentation with this frequency will then be necessary.

When band-pass networks are designed, both the first and the last increment frequencies have a significant influence on the results when the gain-bandwidth product is limited.

The line-segment technique is implemented in the program LSM FORTRAN. This program can be used to solve single matching problems (load complex, source purely resistive).

The optimum increment vector and the gain-bandwidth constraints associated with any reactive load are established by the program, after which the resistance function (conduction function) is fitted to the numerical data and a network is extracted from the associated minimum-impedance (or minimum-admittance) function.

The input data for the program must be specified in an ASCII data file. The file "lsm.dat" is provided on the diskette as an example, as well as a template file.

The input data for the program consist of the following:

1. A title line (79 characters maximum);
2. The load impedance (or admittance) and the required transducer power gain at the different frequencies of interest ( $f, R, X, G_T$ );
3. The number of increment frequencies and the output resistance (or conductance) of the network to be designed at  $\omega = 0$ ;
4. The initial values of the increments at each increment frequency ( $f_i, r_i$ );
5. The number of iterations to be done;
6. The amount by which the last increment frequency must be incremented (in Hertz) and the number of times this must be done.

The increment vector is first optimized by the program, after which the resistance function (or conductance function) is determined (the user is prompted for the number of zeros to be used at the origin before this is done). With the resistance (conductance) function known the associated minimum-impedance (minimum-admittance) function can be found. The final step is to extract the matching network by continued fractionation.

#### **EXAMPLE 8.7      The gain-bandwidth constraints of a matching problem.**

As an illustration of using the program LSM FORTRAN, the gain-bandwidth constraints imposed on a low-pass network by the input impedance of the transistor

**Table 8.7**

The optimum values of the highest increment frequency and the associated normalized least-square error and maximum deviation from the prescribed transducer power gain for the MRF406 as a function of the transducer power gain specified

Transducer power gain specified	Optimum value of the highest increment frequency (MHz)	Maximum deviation from the prescribed transducer power gain (%)
1.00	36	23
0.98	37	15
0.96	37	11
0.94	38	8
0.92	39	5
0.90	42	3
0.88	58	2
0.86	83	1
0.84	120	1

in Example 8.1 is established. The source resistance used is  $6.25\Omega$ . The goal is to achieve a flat response across the 2–30 MHz passband.

The data file "MRF406a.dat" in directory "\lsm" on the diskette is used to define the matching problem. In order to determine the constraints, the gain in this file is decreased progressively until the ripple in the passband becomes very small. The last increment frequency (which establishes the zero resistance or conductance point) is also adjusted in each case to minimize the ripple.

The results obtained are summarized in Table 8.7.

If the criterion of minimum insertion loss across the passband is used, the best results will be obtained if the gain is chosen to be approximately 0.90. The insertion loss will then be less than 0.6 dB ( $G_{T,\min} = 0.866$ ). The matching network associated with this gain level is shown in Figure 8.24.

Note that the source resistance in Figure 8.24 is not  $6.25\Omega$  as required. When a low-pass network is synthesized, it should be possible to solve this problem by adding extra data points at the lower frequencies.

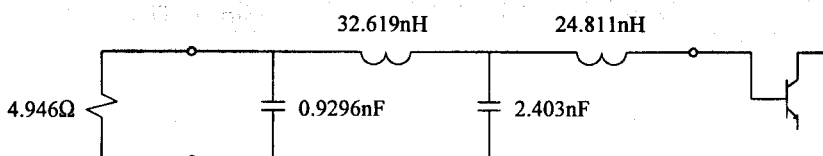


**Figure 8.24** The best solution obtained (highest minimum insertion gain) with the program LSM FORTRAN to the matching problem solved in Example 8.7.

### 8.4.2 The Reflection Coefficient Approach to Solving Double-Matching Problems

When both the load impedance and the source impedance are reactive, impedance-matching networks can be designed iteratively by using the algorithm developed by Yarman and Carlin [7].

In following this approach, the lossless matching network is modeled as a two-port network. When all the transmission zeros are at the origin or infinity, the scattering parameters (*S*-parameters) of the network are given by the following equations:

$$s_{11}(s) = h(s) / g(s) \quad (8.78)$$

$$s_{12}(s) = s_{21}(s) = \pm s^k / g(s) \quad (8.79)$$

$$s_{22}(s) = -(-1)^k [h(-s) / g(s)] \quad (8.80)$$

where  $k$  is an integer specifying the order of the zero of transmission at the origin, and  $h(s)$  and  $g(s)$  are polynomials.

Because the transfer and reflection parameters are related by the equation

$$s_{11}(s)s_{11}(-s) = 1 - s_{21}(s)s_{21}(-s) \quad (8.81)$$

it follows that

$$g(s)g(-s) = h(s)h(-s) + (-1)^k s^{2k} \quad (8.82)$$

It is clear from this equation, and the fact that the polynomial  $g(s)$  must be positive-real, that  $g(s)$  is a function of  $h(s)$  and the order of the zero of transmission at the origin only. Because the *S*-parameters of the network are completely determined by  $h(s)$ ,  $g(s)$ , and  $k$ , it follows that the network itself is defined when  $h(s)$  and  $k$  are defined. The optimum network, therefore, can be determined by finding the optimum coefficients of the numerator polynomial  $h(s)$  for a given value of  $k$ .

In order to optimize the coefficients of  $h(s)$ , an expression for calculating the transducer power gain at each relevant frequency is required. In terms of *S*-parameters, the gain is given by

$$G_T(\omega) = \frac{[1 - |S_G(\omega)|^2][1 - |S_L|^2]|s_{21}(\omega)|^2}{|1 - s_{11}(\omega)S_G(\omega)|^2 \left| 1 - \left[ s_{22}(\omega) + \frac{s_{21}^2(\omega)S_G(\omega)}{1 - s_{11}(\omega)S_G(\omega)} \right] S_L(\omega) \right|^2} \quad (8.83)$$

$$= \frac{[1 - |S_G(\omega)|^2][1 - |S_L|^2]|\omega^{2k}|}{\left| g(j\omega) - (-1)^k S_G S_L g(-j\omega) - S_G h(j\omega) + (-1)^k S_L h(-j\omega) \right|^2} \quad (8.84)$$

where

$$S_G(\omega) = \frac{Z_s(\omega) - R_0}{Z_s(\omega) + R_0} \quad (8.85)$$

$$S_L(\omega) = \frac{Z_L(\omega) - R_0}{Z_L(\omega) + R_0} \quad (8.86)$$

and  $R_0$  is the normalizing resistance of the  $S$ -parameters.

The coefficients of  $h(s)$  can be optimized by using a linear least-square routine. Because the gain is not a simple function of  $h(s)$ , the problem is more complex than before and the choice of the initial values can be critical.

Good results can be achieved if the results obtained by designing an impedance-matching network to match the more complex termination to a resistive source are used to determine the initial values.

The optimization can be done by using the program RCDM FORTRAN. The input data for this program are read from an ASCII data file. The example file "rcdm.dat" on the diskette can be used as a template for any new problem to be defined. Note that the relative spacings and the text strings in the file must remain as they are.

The source code and a Watcom [17] make file for this program are provided in directory "\rcdm" on the diskette. An executable file is provided in the root directory.

The input data of the program consist of the following:

1. A title line consisting of 79 characters or less;
2. The source and load impedances to be matched and the required transducer power gain at each frequency ( $f_i, R_s, X_s, R_L, X_L, G_T$ );
3. The degree of the numerator polynomial  $h(s)$  and the number of transmission zeros at the origin;
4. The initial values of the coefficients  $h_0, h_1, \dots, h_n$  in that sequence;
5. The normalization resistance to be used (usually  $50\Omega$ );
6. The number of iterations to be done.

When initial values are assigned to the coefficients of  $h(s)$ , it is important to realize that there are some constraints on the values of the coefficients.

In the case of low-pass networks, the value of the transmission parameter  $s_{21}(s)$  must be equal to 1 when  $\omega = 0$  and the same input and output normalizing resistance ( $R_0$ ) are used.

**Table 8.8**  
The constraints on the numerator ( $h(s)$ ) and the denominator ( $g(s)$ ) coefficients of  $\rho(s)$

Network	$h(s)$	$g(s)$
Low-pass	$h_0 = 0$	$g_0 = 1$
High-pass	$h_n = 0$	$g_n = 1$
Band-pass	scale factor $a$ for $h(s)$	—

Since

$$s_{21}(s) = \pm \frac{s^k}{g(s)} \quad (8.87)$$

$$= \frac{\pm s^k}{g_n s^n + g_{n-1} s^{n-1} + \dots + g_0} \quad (8.88)$$

and  $k = 0$  for a low-pass network, it is clear that  $g_0$  must equal 1 to ensure that  $s_{21}(0)$  will be equal to 1.

This restriction on the value of  $g_0$  imposes two constraints on the polynomial  $h(s)$ .

The first is that in determining initial values for  $h(s)$ , the numerator and denominator of the input reflection coefficient  $s_{11}(s)$  must be scaled to ensure that  $g_0$  will equal 1.

The second restriction follows from (8.82) by setting  $s = 0$ :

$$g_0^2 = h_0^2 + 1 \quad (8.89)$$

Since  $g_0 = 1$ , it implies that  $h_0$  must be equal to zero.

Following the reasoning above, it can be shown that for high-pass networks  $h_n$  must be equal to zero. The numerator and denominator of the input reflection coefficient must also be scaled to ensure that  $g_n = 1$  when initial values for the coefficients are determined.

When a band-pass problem is initialized, none of the coefficients needs to be equal to zero, but scaling is still required. It is obvious from (8.79) that if  $h(s)$  and  $g(s)$  are scaled by a factor  $a$ , the gain  $|s_{21}|^2$  will change by a factor  $a^2$ .

An appropriate scale factor can be determined by using (8.79) to calculate the gain at any frequency in the passband without a scaling factor. The required scaling factor can then be taken as  $\omega^k / (|g(j\omega)|^2 - |h(j\omega)|^2)^{1/2}$ .

The constraints on the numerator and denominator coefficients of  $\rho(s)$  are summarized in Table 8.8.

#### EXAMPLE 8.8 A double-matching example.

As an example of the application of the impedance-matching programs discussed,

a high-pass network will be designed to mismatch the source impedance in Table 8.9 to a  $50\Omega$  load, as indicated in the table. The problem will first be transformed to low-pass form in order to solve it with program LSM, after which the solution obtained will be used to initialize program RCDM.

**Table 8.9**

The source impedance, load impedance, and transducer power gain corresponding to the problem solved in Example 8.6

Frequency (MHz)	$R_s + jX_s$ ( $\Omega$ )	$R_L + jX_L$ ( $\Omega$ )	$G_T$ ( $\Omega$ )
100	$146.0 - j114.0$	$79.1 - j72.6$	0.224
110	$138.5 - j112.5$	$73.6 - j68.7$	0.262
120	$131.0 - j111.0$	$68.0 - j64.8$	0.299
140	$137.0 - j103.0$	$63.2 - j56.8$	0.400
160	$144.0 - j88.0$	$59.6 - j47.9$	0.559
180	$140.0 - j88.0$	$57.5 - j47.3$	0.709
190	$136.5 - j92.0$	$55.0 - j41.9$	0.764
200	$133.9 - j96.0$	$53.5 - j40.4$	0.818

### The Single-Matching Problem

In order to design the required high-pass network with program LSM FORTRAN, the specifications in Table 8.9 must be changed to those of the equivalent low-pass problem. This is done by using the transformation  $s \rightarrow 1/s$ . The new set of specifications is shown in Table 8.10. The frequencies in the table were obtained from the transformed frequencies ( $\omega' = 1/\omega \rightarrow f' = 1/(4\pi^2f)$ ) by using a scale factor of  $4\pi^2 \times 10^9$ .

Because of the transformation, the impedances to be matched are the conjugates of those in Table 8.9.

**Table 8.10**

The source impedance and transducer power gain corresponding to the equivalent low-pass problem in Example 8.6

Frequency (Hz)	$R_s$ ( $\Omega$ )	$X_s$ ( $\Omega$ )	$G_T$
5.00	133.0	96.0	0.818
5.56	140.0	88.0	0.709
6.25	144.0	88.0	0.559
7.14	137.0	103.0	0.400
8.33	131.0	111.0	0.299
10.00	146.0	114.0	0.224

**Table 8.11**  
The results obtained with the program LSM FORTRAN in Example 8.6

Frequency (Hz)	Input impedance of the network to be designed ( $\Omega$ )	Transducer power gain obtainable
5.00	$64.7 - j49.9$	0.835
5.56	$40.7 - j56.4$	0.677
6.25	$30.1 - j46.3$	0.541
7.14	$22.8 - j42.4$	0.427
8.33	$15.1 - j34.6$	0.291
10.00	$12.6 - j27.6$	0.225

A minimum-impedance matching network was designed. Note that as a rule, both options should be tried (the program can be modified to do this automatically).

The data file used is stored on the diskette as "lsm.dat". Note that while the impedance to be matched is the source impedance of the problem to be solved, it is taken to be the load impedance in program LSM.

The results obtained are summarized in Table 8.11. The gain-bandwidth limitations of the network were found to be insensitive to the value of the highest increment frequency. (This was not the case when a minimum-admittance solution was attempted.)

Because a low-pass solution is required, the number of transmission zeros at the origin was specified to be zero. The resistance function obtained is

$$R(\omega) = 1/T(\omega) = 1/(0.7730 \times 10^{-15} \omega^8 - 0.1004 \times 10^{-10} \omega^6 + 0.3965 \times 10^{-7} \omega^4 - 0.3238 \times 10^{-4} \omega^2 + 0.1974 \times 10^{-1})$$

The poles of this function are

$$\omega = \pm 78.854 \pm j11.837 \\ \pm 24.688 \pm j13.630$$

The minimum-impedance function obtained is

$$Z(j\omega) =$$

$$\frac{0.2562 \times 10^9 + j0.1308 \times 10^8 \omega - 0.1018 \times 10^6 \omega^2 - j0.1998 \times 10^4 \omega^3}{0.5057 \times 10^7 + j0.1922 \times 10^6 \omega - 0.7799 \times 10^4 \omega^2 - j0.5094 \cdot 10^2 \omega^3 + 1.000 \omega^4}$$

As a function of  $s$ , this becomes

$$Z(s) =$$

$$\frac{0.2562 \times 10^9 + 0.1307 \times 10^8 s + 0.10179 \times 10^6 s^2 + 0.1998 \times 10^4 s^3}{5.0565 \times 10^7 + 0.1922 \times 10^6 s + 0.7798 \times 10^4 s^2 + 0.5094 \times 10^2 s^3 + 1.000 s^4} \quad (8.90)$$

The network obtained from program LSM is shown in Figure 8.25. It was synthesized by continued fractionation of the impedance function.

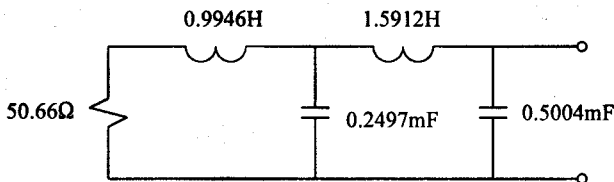


**Figure 8.25** The network associated with (8.90).

As a check on the results, the transducer power gain was calculated at the relevant frequencies. The results are compared to the specifications in Table 8.12.

The variation in gain is less than 0.24 dB over the frequency range of interest.

**Table 8.12**

Comparison of the gain obtained with the network in Figure 8.25 and the specified gain

Frequency (MHz)	Transducer power gain specified	Transducer power gain obtained
5.00	0.818	0.835
5.56	0.709	0.677
6.25	0.559	0.541
7.14	0.400	0.427
8.33	0.299	0.291
10.00	0.224	0.225

### The Double-Matching Problem

Initial values for the design of a double-matching network can be obtained by calculating the reflection coefficient for the network obtained from program LSM

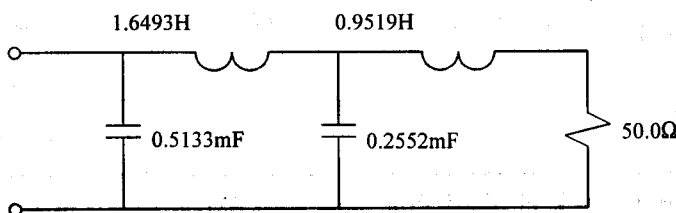


**Figure 8.26** The matching network designed by using the reflection coefficient technique.

(refer to Figure 8.25). The reflection coefficient obtained from LSM is

$$s_{22}(s) = \frac{0.6552 \times 10^{-2} - 0.6812 \times 10^{-2}s - 0.5661 \times 10^{-3}s^2 - 1.0773 \times 10^{-6}s^3 - 0.9823 \times 10^{-7}s^4}{1.0000 + 0.4456 \times 10^{-1}s + 0.9661 \times 10^{-3}s^2 + 0.8929 \times 10^{-5}s + 0.9823 \times 10^{-7}s^4}$$

The numerator coefficients were used as initial values in RCDM. Note that the network was synthesized from the load side towards the input side in LSM, while the reverse is done in RCDM.  $s_{22}(s)$  in LSM is therefore  $s_{11}(s)$  in RCDM.

The double-matching problem is defined in the data file "rcdm.dat" provided on the diskette. The source code for RCDM FORTRAN is provided in directory "\rcdm" with a make file. A Watcom [17] executable file is provided in the root directory of the diskette.

The matching network corresponding to the impedance function obtained is shown in Figure 8.26. The maximum deviation from the specified gain response is 0.24 dB. The results obtained are compared to the specifications in Table 8.13.

The final step in this example is to transform the results back to high-pass form under the transformation  $s \rightarrow 1/s$ . Because a scale factor of  $4\pi^2 \times 10^9$  was used to obtain the frequencies used in Table 8.10, the network obtained from RCDM

**Table 8.13**  
Comparison of the specifications and gain obtained with the network shown in Figure 8.26

Frequency (MHz)	Transducer power gain specified	Transducer power gain obtained
5.00	0.818	0.801
5.56	0.709	0.700
6.25	0.559	0.560
7.14	0.400	0.414
8.33	0.299	0.295
10.00	0.224	0.222

must be frequency scaled with the same factor in order to obtain the matching network required. The final network is shown in Figure 8.27.

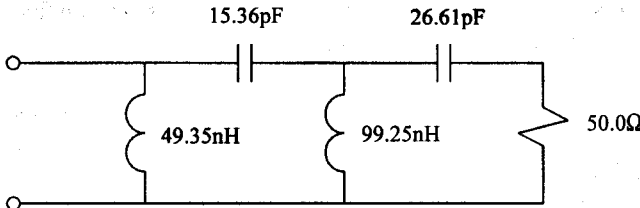


**Figure 8.27** The network associated with (8.90).

#### 8.4.3 The Transformation-*Q* Approach to the Design of Impedance-Matching Networks

The narrowband impedance-matching technique described in Chapter 4 can be extended to increase the number of elements to an arbitrary number and to mismatch any complex load to any complex source by any specified amount at any single frequency [15]. In order to do this, it will be shown in Section 8.4.3.1 that the locus of input impedances for which the source impedance of a network will be mismatched to the load by a specified amount is a circle in the linear admittance plane or the impedance plane. The parameters of these circles will be derived here.

The necessary extensions to the single-frequency technique will be made in Section 8.4.3.2.

The extended single-frequency matching technique forms an excellent basis for the iterative design of wideband impedance-matching networks. The main reason for this is that the range of each transformation *Q* is limited since high *Q*-factors will inevitably lead to a narrow bandwidth.

Because of this fact, it is feasible to do a systematic search on the transformation *Q*-factors in search of the optimum combination, thus eliminating the need for a good initial solution. Furthermore, if the search is done thoroughly enough, the probability of finding the optimum solution will be very high.

With the systematic search completed, a number of the best sets of *Q*-factors can be optimized. This can be done with a least-square optimization routine, but better results in less time are obtainable by using a simple gradient optimization technique.

The mean-square error from the specified gain response can be used in the systematic search and during the optimization phase, but a better alternative is to use the maximum relative deviation from the optimum as the error criterion. In doing so, the error value is determined by the worst performance in the passband and not the average response.

The topologies of the networks synthesized by following this approach can easily be limited to low-pass form, high-pass form, or to band-pass form with no series capacitors.

The last option is usually attractive in hybrid circuits at microwave frequencies.

The time required to solve a matching problem can be reduced significantly by constraining the gain at the frequency where the  $Q$ -factors are calculated to be higher than a specified minimum. The required run time is usually very short when networks with less than six elements are designed (a few minutes may be required when five-element solutions are synthesized for a difficult problem on a fast personal computer).

Major advantages of the transformation- $Q$  technique over the techniques described previously are that many solutions instead of only one are obtained, that transformers are never required in the solutions, and that the probability of finding the optimum solution to a matching problem is very high when the search is done thoroughly enough. This approach is also very robust and can be extended easily to design more complicated networks (like distributed or mixed lumped/distributed networks).

The first advantage is important when the best solution obtained is not physically realizable or when a different topology is required. The sensitivity to component changes will usually also be different for the solutions obtained.

#### 8.4.3.1 Constraints on the Input Admittance of a Lossless Impedance-Matching Network If the Gain Is to Remain Constant at a Specific Frequency

The locus of input admittances for which the gain of a lossless impedance-matching network will remain constant can be derived by using the expression

$$|S_s|^2 = \left| \frac{Z_{in} - Z_s^*}{Z_{in} + Z_s} \right|^2 \quad (8.91)$$

$$= \left| \frac{Y_{in} - Y_s^*}{Y_{in} + Y_s} \right|^2 \quad (8.92)$$

where  $S_s$  is the input reflection parameter with the actual source impedance ( $Z_s$ ) as normalizing impedance, and  $Z_{in}$  ( $Y_{in}$ ) is the input impedance (admittance) of the matching network.

By substituting

$$|S_s|^2 = 1 - G_T \quad (8.93)$$

$$Y_{in} = G_{in} + jB_{in} \quad (8.94)$$

and

$$Y_s = G_s + jB_s \quad (8.95)$$

into (8.92), it follows that the locus of the input admittance for which the transducer power

gain ( $G_T$ ) will remain constant is a circle in the admittance plane. The parameters (center and radius) of this circle are

$$G_0 + jB_0 = [2 / G_T - 1]G_s - jB_s \quad (8.96)$$

and

$$R_{Y_0} = 2[1 / G_T^2 - 1 / G_T]^{1/2} G_s \quad (8.97)$$

The gain of a lossless network will remain constant for all values of the input admittance that fall on the circumference of this circle. This is illustrated in Figure 8.28.

For all values of the input admittance that fall inside the constant gain circle, the gain will be higher than that on the circumference. The transducer power gain of a matching network, therefore, can be constrained to be higher than a specified minimum at any particular frequency by limiting its input admittance to the inside of the relevant constant transducer power gain circle.

Because (8.91) and (8.92) are of exactly the same form, the locus of input impedances for which the gain of a lossless network will remain constant is also a circle, and the parameters of this circle can also be obtained from (8.96) and (8.97) with  $G_s + jB_s$  replaced with  $R_s + jX_s$ , and  $G_0 + jB_0$  with  $R_0 + jX_0$ . The resulting equations are

$$R_0 + jX_0 = [2 / G_T - 1] R_s - jX_s \quad (8.98)$$

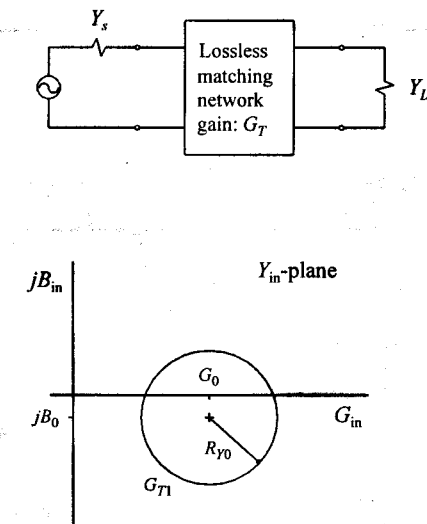


**Figure 8.28** The locus of the input admittance for which the gain of a lossless matching network will remain constant at a specified frequency.

and

$$R_{z0} = 2[1/G_T^2 - 1/G_T]^{1/2} R_s \quad (8.99)$$

### 8.4.3.2 Extension of the Transformation- $Q$ Impedance-Matching Technique

In an impedance-matching network, the resistance level is changed by each element except the last, which only serves to adjust the reactance or susceptance level. The change in the resistance of a four-element network with the first element a series element and no resonating sections is illustrated in Figure 8.29. The resistance is transformed in each transformation step by a factor of the form

$$D_n(\omega) = 1 + Q_n^2(\omega) \quad (8.100)$$

where

$$Q_n(\omega) = \frac{X_n(\omega) + X_m(\omega)}{R_m(\omega)} \quad (8.101)$$

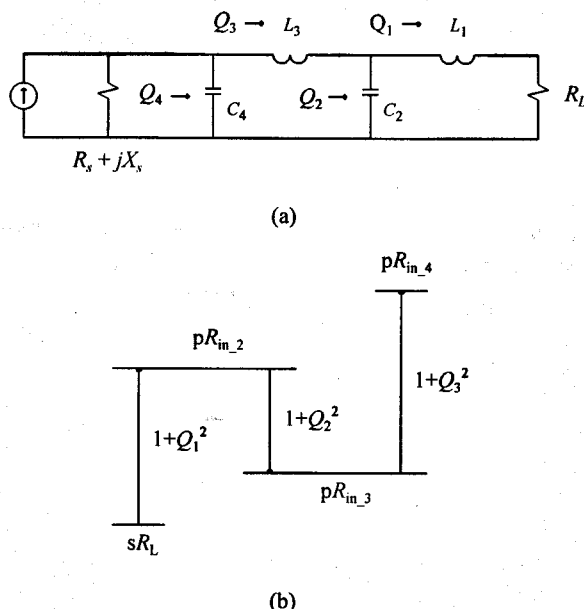


**Figure 8.29** (b) Schematic illustration of the change in the resistance level of (a) a matching network.

or

$$Q_n(\omega) = \frac{B_n(\omega) + B_m(\omega)}{G_m(\omega)} \quad (8.102)$$

depending on whether the transformation under consideration is series-to-parallel or parallel-to-series, respectively (see Figure 8.30).

The factor  $Q_n(\omega)$  is referred to as a transformation  $Q$ .

In (8.101),  $X_n(\omega)$  is the reactance of the  $n$ th component,  $X_m(\omega)$  the effective reactance to the right of it, and  $R_n(\omega)$  the effective resistance in series with it as illustrated in Figure 8.30(a).

Similarly,  $B_n(\omega)$  is the susceptance of the  $n$ th component,  $B_m(\omega)$  is the effective susceptance to the right of it, and  $G_m(\omega)$  the effective conductance in parallel with it. This is illustrated in Figure 8.30(b).

A series-to-parallel transformation will always transform the associated resistance upward, while downward transformations are effected with shunt elements.

It follows from (8.101) and (8.102) that the sign of a transformation  $Q$  is positive when the effective reactance in series with the effective resistance is inductive, or when the effective susceptance in parallel with the effective conductance is capacitive.

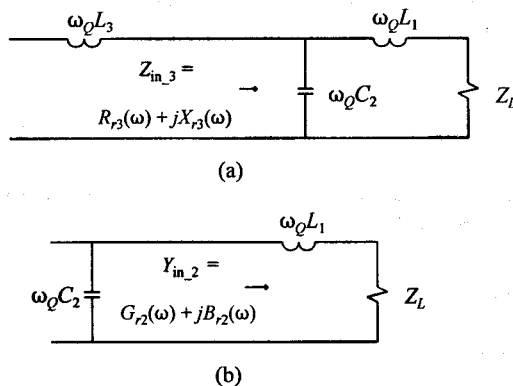


Figure 8.30 Definition of the symbols in (8.101) and (8.102).

When the first element of an  $N$ -element network is a series element, the input resistance is given after  $(N - 1)$  transformations by the expression [15; refer to Chapter 4]

$$R_{in,N} = R_L \frac{1+Q_1^2}{1+Q_2^2} \frac{1+Q_3^2}{1+Q_4^2} \cdots [1+Q_{N-1}^2] \quad (8.103)$$

or

$$R_{in,N} = R_L \frac{1+Q_1^2}{1+Q_2^2} \cdots \frac{1+Q_{N-2}^2}{1+Q_{N-1}^2} \quad (8.104)$$

depending on whether the last matching element is a shunt element or a series element, respectively.

When the first element is a shunt element, the input conductance is given by the expression

$$G_{in,N} = \frac{G_L}{1+Q_1^2} \frac{1+Q_2^2}{1+Q_3^2} \cdots [1+Q_{N-1}^2] \quad (8.105)$$

or

$$G_{in,N} = \frac{G_L}{1+Q_1^2} \frac{1+Q_2^2}{1+Q_3^2} \cdots \frac{1+Q_{N-2}^2}{1+Q_{N-1}^2} \quad (8.106)$$

Because (8.103) and (8.105), as well as (8.104) and (8.106), are of the same form except that the resistance and conductance must be interchanged, it is only necessary to consider the design of matching networks with a series element as the first element. Exactly the same procedure can then be followed to design networks in which the first element is a shunt element, after replacing all impedance specifications with the equivalent admittances.

In low-pass and high-pass designs the number of  $Q$ -factors is equal to the number of elements in the network. In a band-pass network with  $N$  elements, but  $M$  resonating sections (series of parallel LC combinations), the number of  $Q$ -factors increases to  $(N + M)$ . This is illustrated for a three-element network in Figure 8.31.

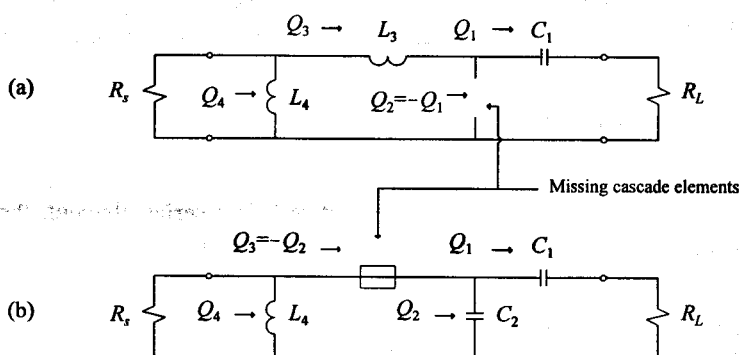


**Figure 8.31** The influence of (a) series and (b) parallel resonating sections on the transformation  $Q$ -factors in a matching network.

When an element is absent, the associated  $Q$  is equal to the negative of the previous  $Q$ .

By using (8.103) through (8.106), it is very easy to calculate the input resistance of any impedance-matching network when the  $Q$ -factors are known.

In order to design a matching network to have a specified transducer power gain ( $G_T$ ) at a particular frequency, it is only necessary to constrain the last two  $Q$ -factors to ensure that the input impedance (if the last element is a parallel element) will fall on the relevant gain circle as derived in the previous section.

When the last element is a series element (see Figure 8.32), the next to last  $Q$  should be constrained to ensure that the input resistance ( $R_{in}$ ) will fall in the range

$$R_{in,min} \leq R_{in} \leq R_{in,max} \quad (8.107)$$

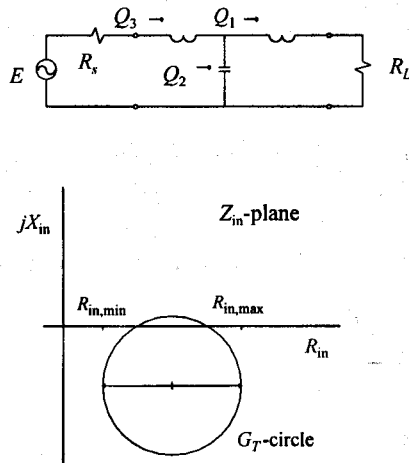


**Figure 8.32** The constraints on the input resistance of a matching network where the last element is a series element when the transducer power gain should be higher than or equal to a specified minimum at a particular frequency.

The bounds on the next to last  $Q$  follow easily from the values of the previous  $Q$ -factors by using (8.104) in conjunction with (8.107). The resulting constraints are

$$Q_{N-1}^2 \geq \frac{R_L}{R_{in,max}} \frac{1+Q_1^2}{1+Q_2^2} \dots [1+Q_{N-2}^2] - 1 \quad (8.108)$$

and

$$Q_{N-1}^2 \leq \frac{R_L}{R_{in,min}} \frac{1+Q_1^2}{1+Q_2^2} \dots [1+Q_{N-2}^2] - 1 \quad (8.109)$$

When the last element is a parallel element, the next to last  $Q$  should be constrained to ensure that the input conductance ( $G_{in}$ ) will be within the constraints imposed by the constant gain circle on the admittance plane.

The resulting constraints are

$$Q_{N-1}^2 \geq \frac{1}{R_L G_{in,max}} \frac{1+Q_2^2}{1+Q_1^2} \dots [1+Q_{N-2}^2] - 1 \quad (8.110)$$

and

$$Q_{N-1}^2 \leq \frac{1}{R_L G_{in,min}} \frac{1+Q_2^2}{1+Q_1^2} \dots [1+Q_{N-2}^2] - 1 \quad (8.111)$$

The constraints on the last transformation  $Q$  can be derived from Figure 8.33. With the resistance (if the last element is a series element) or conductance (if the last element is a parallel element) in range, the reactance or susceptance must be such that the resulting impedance of admittance falls on the circumference of the gain circle.

When the last element is a series element, the reactance is constrained to

$$X_{in} = X_0 \pm R_{z0} \sin \left[ \cos^{-1} \frac{R_{in} - R_0}{R_{z0}} \right] \quad (8.112)$$

The equivalent expression when the last element is a parallel element is

$$B_{in} = B_0 \pm R_{Y0} \sin \left[ \cos^{-1} \frac{G_{in} - G_0}{R_{Y0}} \right] \quad (8.113)$$

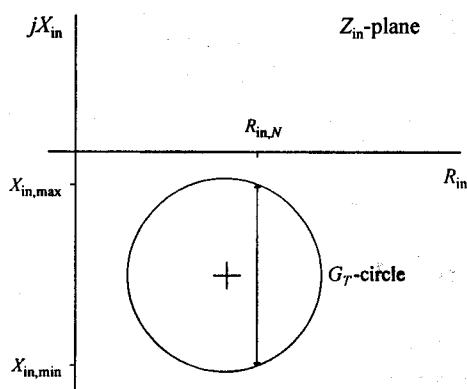


**Figure 8.33** The constraints on the last transformation  $Q$  of a network if the gain is to be higher than a specified minimum.

Because  $R_{in}$  or  $G_{in}$  is known, it is a simple matter to calculate the  $Q$  corresponding to these reactances or susceptances.

From a single-frequency matching viewpoint, there are no constraints on the first  $N - 2$  transformation  $Q$ . If the response is also of interest over a narrow passband, any change in the  $Q$ -factors should, as a first-order approximation, be constrained to be smaller than twice the  $Q$  required for the circuit. The change in  $Q$  from one transformation to the next is given by

$$\Delta Q = [Q_n + Q_{n-1}] \quad (8.114)$$

The reason for the positive sign is that the sign of a  $Q$  of transformation changes under a series-to-parallel or parallel-to-series transformation. As an example of this, if the  $Q$  of a series combination is +3 (inductive), the  $Q$  of the parallel equivalent will be -3 (again inductive).

In summary, the following procedure can be followed to design an  $N$ -element matching network to match or mismatch a complex load by a specified amount to a complex source at a particular frequency and to have a specified (approximate) quality factor.

### Design Procedure

**Specifications:** Load impedance  $Z_L$ , source impedance  $Z_s$ , transducer power gain  $G_T$  (at frequency  $f$ ), and quality factor  $Q$ .

1. If the first element of the network is to be a shunt element, change the source and load impedances to  $1/Z_s$  and  $1/Z_L$ , respectively, and assume that the first element is now a series element.
2. Choose any values for the first  $N - 2$  transformation  $Q$ -factors within the constraint that all the transformation  $Q$ s must be smaller than  $2Q$ , that is,

$$|Q_i| \leq 2Q \quad (8.115)$$

3. If the last element is to be a parallel element, calculate the parameters of the constant gain circle on the admittance plane by using (8.96) and (8.97).  
If the last element is a series element, use (8.98) and (8.99) to calculate the parameters of the constant gain circle on the impedance plane.
4. Calculate the minimum and maximum allowable values for the input conductance or resistance by using the following equations, as applicable:

$$G_{in,max} = G_0 + R_{Y0} \quad (8.116)$$

$$G_{in,min} = G_0 - R_{Y0} \quad (8.117)$$

$$R_{in,max} = R_0 + R_{Z0} \quad (8.118)$$

$$R_{in,min} = R_0 - R_{Z0} \quad (8.119)$$

5. Determine the constraints on the next to last transformation  $Q$  by using (8.108) and (8.109) when the last element is a series element. Otherwise use (8.110) and (8.111).

Choose a value for  $Q_{N-1}$  within these constraints and that imposed by (8.115).

6. When the last element is a series element, calculate the two possible reactance values corresponding to the last transformation  $Q$  ( $X_{in,min}$  and  $X_{in,max}$ ) by using (8.112). Otherwise, use (8.113) to calculate the allowable susceptance values ( $B_{in,min}$  and  $B_{in,max}$ ).

Calculate  $R_{in,N}$  or  $G_{in,N} = 1/R_{in,N}$  by using (8.103) or (8.104), as applicable. Calculate the two possible values for the last transformation  $Q$  by using the following equations:

$$Q_{N,max} = \frac{X_{in,max}}{R_{in,N}} \quad (8.120)$$

$$Q_{N,min} = \frac{X_{in,min}}{R_{in,N}} \quad (8.121)$$

or

$$Q_{N,max} = \frac{B_{in,max}}{G_{in,N}} \quad (8.122)$$

$$Q_{N,min} = \frac{B_{in,min}}{G_{in,N}} \quad (8.123)$$

Choose either of the two possible  $Q$  values within the constraint imposed by (8.115) on each transformation  $Q$ .

7. Calculate the element values corresponding to the set of  $Q$  values. The reactance or susceptance of each component at the frequency where the  $Q$  values are calculated is given by an expression of the form

$$X_n = (Q_n + Q_{n-1})R_m \quad (8.124)$$

or

$$B_n = (Q_n + Q_{n-1})G_m \quad (8.125)$$

depending on whether it is a series or parallel element.

In these equations  $R_m$  and  $G_m$  are the effective series resistance and effective parallel conductance to the right of the component whose value is to be determined, respectively (refer to Figure 8.30, if necessary).

8. If the first element of the final network should be a shunt element, consider all inductors to be capacitors (i.e., 5 pH is 5 pF) and all capacitors to be inductors, and assign these values in sequence to the actual network.

As an illustration of this step, if element values of 3 pH (series element), 9 nF (shunt element), and 7 pF (series element) were obtained by following the procedure outlined above, the element values in the final circuit are 3 pF (shunt element), 9 nH (series element), and 7 pH (shunt element), respectively.

#### EXAMPLE 8.9 A transformation- $Q$ example.

As an example of the application of the procedure outlined above, consider the design of a five-element matching network with the first element a series element, no resonating sections, and the following specifications:

$$Z_L = 50 + j50\Omega$$

$$Z_s = 20 - j20\Omega$$

$$G_T = 0.89$$

$$f_Q = 100\text{MHz}$$

$$Q = 5$$

1.  $Q_1 = 5 \ (\Delta Q = 4)$

$$Q_2 = 5 \ (\Delta Q = 10)$$

$$Q_3 = -3 \ (\Delta Q = 2)$$

7. With no resonating sections and specifications as above, the last element of the network will be a series element, and therefore the constant gain circle on the input impedance plane is of interest. Application of (8.98) and (8.99) yields that the parameters of this circle are

$$R_0 + jX_0 = [2 / 0.89 - 1]20 + j20 = 24.94 + j20.00\Omega$$

and

$$R_{Z_0} = 2\sqrt{1 / 0.89^2 - 1 / 0.89} \cdot 20 = 14.91$$

$$3. R_{in,max} = 24.94 + 14.91 = 39.85\Omega$$

$$R_{in,min} = 24.94 - 14.91 = 10.03\Omega$$

4. Application of (8.108) and (8.109) yields that

$$|Q_4| \geq \left[ \frac{50}{39.85} \frac{1+5^2}{1+5^2} (1+3^2) - 1 \right]^{1/2} = 3.398$$

$$|Q_4| \leq \left[ \frac{50}{10.03} \frac{1+5^2}{1+5^2} (1+3^2) - 1 \right]^{1/2} = 6.989$$

$$Q_{n-1} = 5 \quad (\Delta Q = 2)$$

5. The two allowable values for the input reactance are found by using (8.112):

$$X_{in} = 20 \pm 14.91 \sin \left[ \cos^{-1} \frac{19.23 - 24.94}{14.91} \right]$$

$$= 6.23\Omega; 33.77\Omega$$

In the equation above,  $R_{in}$  was found by applying (8.103):

$$R_{in} = 19.23\Omega \quad (10.03 \leq 19.23 \leq 39.85)$$

The last transformation  $Q$  is simply

$$Q_n = 6.23 / 19.23 - 0.32 \quad (\Delta Q = 5.32)$$

$$6. X_1 = Q_1 R_1 - X_L = 5(50) - 50 = 200\Omega \quad (318.3 \text{ nH})$$

$$Y_2 = [Q_2 + Q_1]G_{L2} = \frac{10(1)}{50(1+5^2)} = 7.69 \text{ mS} \quad (12.24 \text{ pF})$$

$$X_3 = [Q_3 + Q_2]R_{L3} = 2(50) \frac{1+5^2}{1+5^2} = 100\Omega \quad (1592 \text{ nH})$$

$$Y_4 = [Q_4 + Q_3]G_{L4} = 2 \frac{1}{50} \frac{1+5^2}{1+5^2} \frac{1}{1+3^2} = 4.0 \text{ mS} \quad (6.37 \text{ pF})$$

$$X_5 = [Q_5 + Q_4]R_{L5} = 5.32(50) \frac{1+5^2}{1+5^2} \frac{1+3^2}{1+5^2} = 102.3\Omega \quad (162.8 \text{ nH})$$

The designed network is shown in Figure 8.34. The gain at 100 MHz is equal to 0.889 and the  $Q$  of the circuit is equal to 6.0.

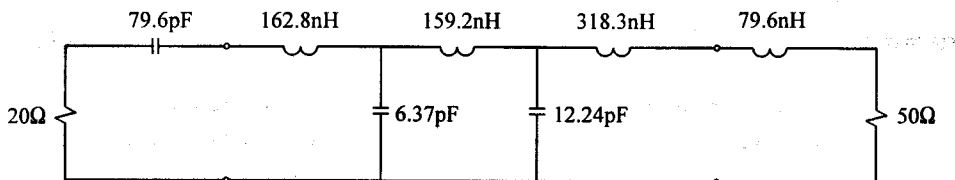


Figure 8.34 The network synthesized in Example 8.9.

#### 8.4.3.3 Optimization of the Transformation $Q$ s of a Network

The transformation  $Q$ -factors corresponding to an initial solution for a matching problem can be optimized by using a linear least-square optimization routine. Although good results can be obtained by doing this, better results are obtainable through a slightly different approach.

The first improvement is to use the maximum relative deviation (MRD)

$$\text{MRD} = \text{MAX} \left| \frac{G_T(\omega)}{G_{T_{\text{opt}}}(\omega)} - 1 \right| \quad (8.126)$$

as the error criterion instead of the mean-square error.

The main advantage of the MRD error criterion is that the maximum deviation from the optimum rather than the average deviation will be minimized. Because of this, the solution with the lowest insertion loss will be obtained when the ideal gain is set to unity.

The second improvement is to optimize the error by using the steepest-decent method. The results obtained in doing this were superior to those corresponding to the least-square method.

The gradient vector required for optimizing the  $Q$  values can be determined by calculating the change in MRD corresponding to a small increment in each  $Q$ .

The new set of  $Q$  values ( $Q_N$ ) can be obtained from the previous set ( $Q_{N-1}$ ) and the current MRD by using the equation

$$\bar{Q}_N = \bar{Q}_{N-1} - \frac{\alpha}{\sqrt{(\partial \text{MRD} / \partial Q_1)^2 + \dots + (\partial \text{MRD} / \partial Q_N)^2}} \begin{bmatrix} \partial \text{MRD} / \partial Q_1 \\ \vdots \\ \partial \text{MRD} / \partial Q_N \end{bmatrix} \quad (8.127)$$

where the optimum value of  $\alpha$  can be determined iteratively by using the following method [18].

Start with a small value of  $\alpha$  ( $\alpha_1$ ), and increase it during subsequent iterations ( $\alpha_i$ ) by using the expression

$$\alpha_i = \alpha_1 [1 + l + l^2 + \dots + l^{i-1}] \quad i = 1, 2, 3, \dots \quad l = 1.5 \quad (8.128)$$

until the error value increases. This will result in the situation depicted in Figure 8.35. A quadratic curve can now be fitted to the last three coordinates, and the value of  $\alpha$  ( $\alpha_m$ ), for which the error will be a minimum, can be estimated by using the expression

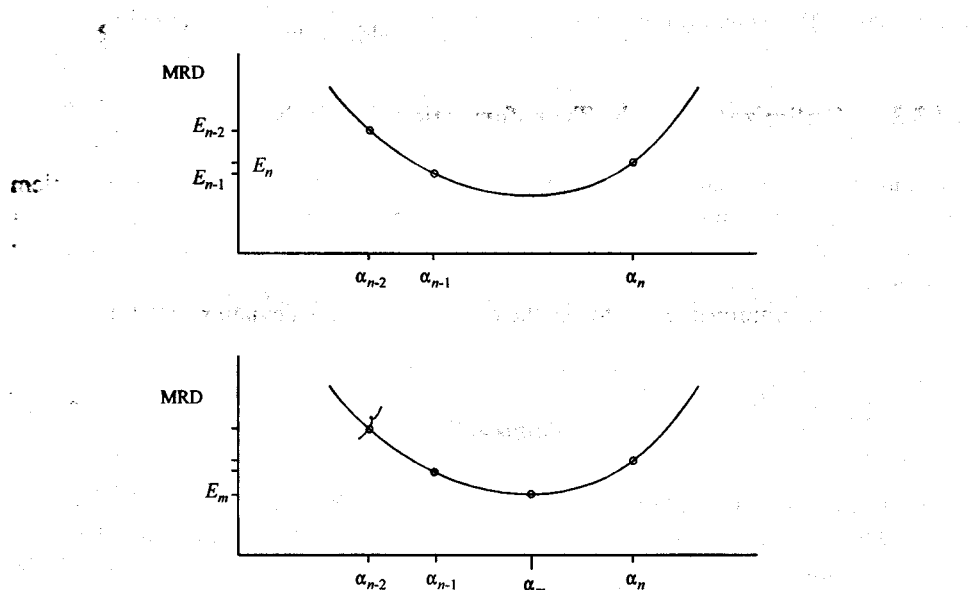


Figure 8.35 Estimation of the optimum scale factor in optimizing the MRD.

$$\alpha_M = \frac{1}{2}$$

$$[\alpha_{n-1}^2 - \alpha_n^2]MRD_{n-2} + [\alpha_n^2 - \alpha_{n-2}^2]MRD_{n-1} + [\alpha_{n-2}^2 - \alpha_{n-1}^2]MRD_n \\ [\alpha_{n-1} - \alpha_n]MRD_{n-2} + [\alpha_n - \alpha_{n-2}]MRD_{n-1} + [\alpha_{n-2} - \alpha_{n-1}]MRD_n \quad (8.129)$$

The actual value of the MRD at  $\alpha_M$  can now be calculated. Depending on which of the four errors is now the largest, one of the four coordinates can be eliminated and the procedure can be repeated on the remaining three points.

The optimum value of  $\alpha$  can be determined by continuing with this procedure until the improvement in the error value is negligible.

Excellent results were obtained by optimizing the  $Q$  values of transformation as outlined above.

#### 8.4.3.4 An Algorithm for the Design of Impedance-Matching Networks by Using the Transformation $Q$ -Factors of the Network

A procedure for designing a network to match a complex load to a complex source with a specified gain at a specified frequency was outlined in Section 8.4.3.2. By taking the transducer power gain to be the minimum expected gain at the frequency where the  $Q$  values are evaluated (usually the highest frequency in the passband or the frequency at which the gain required is a maximum), this narrowband technique forms the basis of an excellent approach to solving wideband impedance-matching problems.

It was shown that the first  $(N - 2)$   $Q$  values in the single-frequency design can take arbitrary values and the constraints imposed on the last two  $Q$  values were derived. Since the range of possible transformation- $Q$  values is limited in a wideband design, it is feasible to do a systematic search on these  $Q$  values in order to find solutions that yield good results over the whole passband. In this way, the dependence on a good initial solution is eliminated.

When the search is completed, a number of the best results obtained can be optimized as described in Section 8.4.3.3. If the search was done thoroughly enough, the optimum solution to any matching problem will be obtained. A further advantage is that the local minima corresponding to other initial solutions will also be obtained, and, consequently, a large choice between networks with different element values and topologies exist.

An idea of the required range of  $Q$  values can be obtained from the desired  $Q$  of the network when applicable, the maximum  $Q$  of the load and source impedances, and the analytically derived constraints on simple reactive loads as summarized in Table 8.5.

As a rule, a minimum value of -4.2 and a maximum value of 4.2 yield excellent results. When some of the  $Q$  values of solutions obtained exceed these values and the optimum solution is required, the bounds must be extended. This will seldom be necessary when a wideband network is designed. Increment values in the range from 0.4 to 0.6 are used.

The algorithm described below can be used when this approach is followed.

### Algorithm

1. Decide on the number of elements and the frequency at which the  $Q$  values are to be evaluated ( $f_Q$ ).  
Estimate the range of possible  $Q$  values of transformation and specify the incremental value to be used.  
Estimate the minimum gain expected at  $f_Q$ .  
Specify the number of transformation- $Q$  sets to be stored during the search ( $M$ ).
2. Generate an allowable set of  $Q$  values by using the theory outlined in Section 8.4.3.2.
3. Synthesize the equivalent network and calculate the gain error (MRD). Compare the results with the previous results obtained and store the solution if it is better than the  $M$  best solutions previously stored.
4. Optimize the best results obtained in the search as described in Section 8.4.3.3.

### EXAMPLE 8.10 A double-matching problem solved with the transformation- $Q$ technique [15].

As an example of the results obtainable with the transformation- $Q$  technique, consider the double-matching problem of Example 8.8.

With the gain set equal to the specified value of 0.818 at 200 MHz during the systematic search, and using minimum, increment, and maximum values of -4.4, 0.4, and 4.4, respectively, for the transformation- $Q$  values, the maximum deviation from the specified response was found to be 0.05 dB (MRD = 1.23%) for the best four-element solution synthesized. This network is shown in Figure 8.36(a).

The  $Q$  values corresponding to this solution are 2.399, -1.797, 1.039, and -0.148, respectively.

The second best solution obtained is the network shown in Figure 8.36(b). The maximum deviation from the specified gain response is 0.06 dB (MRD = 1.43%), and the  $Q$  values are -0.777, 3.422, 2.360, and -0.130, respectively.

The maximum deviations for the other solutions shown in Figure 8.36 are 0.09 dB (MRD = 2.08%), 0.11 dB (MRD = 2.58%), 0.13 dB (MRD = 3.02%), and 0.15 dB (MRD = 3.41%), respectively.

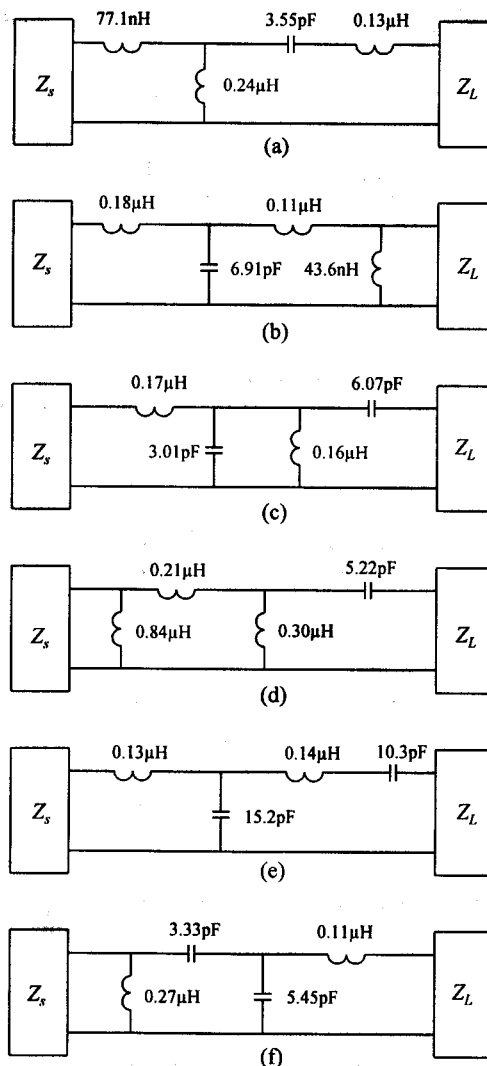


**Figure 8.36** Some of the solutions obtained with the transformation- $Q$  technique for the matching problem of Example 8.8.

The best three-element solution obtained under the constraint that the topology must be of high-pass form is shown in Figure 8.37. The maximum deviation from the specified gain is 0.15 dB (MRD = 3.4%) and the  $Q$  values are -0.185, -0.570, and -0.931, respectively. This solution is basically the same as that obtained with the reflection parameter technique.

Having several solutions to choose from is an advantage both from the viewpoint of topology and sensitivity.

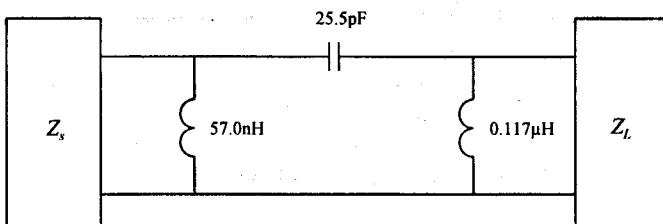


**Figure 8.37** The best three-element solution (high-pass topology) obtained with the transformation-*Q* technique for the matching problem of Example 8.8.

It is important to note that the solution with the best performance with the design values may not have the best worst-case performance too. It also does not necessarily follow that fewer elements will be better from a sensitivity viewpoint.

In this case, the MRD of the best four-element solution found is increased from 1.23% to 4.12% if the tolerance in all the lumped components is assumed to be 1%. A 1% change in the component values, therefore, leads to a 2.9% increase in the MRD in this case.

The MRD of the three-element solution shown increases from 3.4% to 5.5% with 1% tolerances in the component values.

The solutions shown so far are purely lumped. In practice, solder pads are also required for the lumped components. The transformation-*Q* approach can be extended to allow for this requirement too. A few of the best mixed lumped/distributed solutions obtained [15] are shown in Figure 8.38 with the pads used. The pads do not have a strong influence in this example, but will become a factor as the frequency is increased. The influence of the pads is also more severe when the dielectric constant of the substrate is high.

The MRD of the best solution is 1.09%. This value is increased to 4.32% when 1% tolerances are assumed for the lumped components.

The MRD values for the other three solutions shown in Figure 8.38 are 1.29% (4.29%), 3.0% (5.67%), and 3.18% (6.78%), respectively. Note that the worst-case performance of the second solution is fractionally better than that of the first solution (4.29% versus 4.32%).

The electrical parameters of the pads used for the shunt inductors are  $57\Omega$  and  $0.38^\circ$  (at 0.2 GHz), while those used for the shunt capacitor pads are  $36.4\Omega$  and  $0.38^\circ$ .  $57\Omega$  pads ( $0.23^\circ$  or  $0.36^\circ$  long) were also used for the series inductors, while  $71.2\Omega$  pads ( $0.23^\circ$  or  $0.36^\circ$  long) were used for the series capacitors.

A low dielectric constant substrate was used ( $\epsilon_r = 2.99$ ;  $h = 0.381$  mm). The width of these pads on the substrate used are 0.75 mm, 1.5 mm, 0.75 mm, and 0.5mm, respectively.

Note that the length used for the series pads should be long enough to ensure sufficient separation between the shunt components. This is essential to prevent overlap in the artwork and coupling between the shunt components.

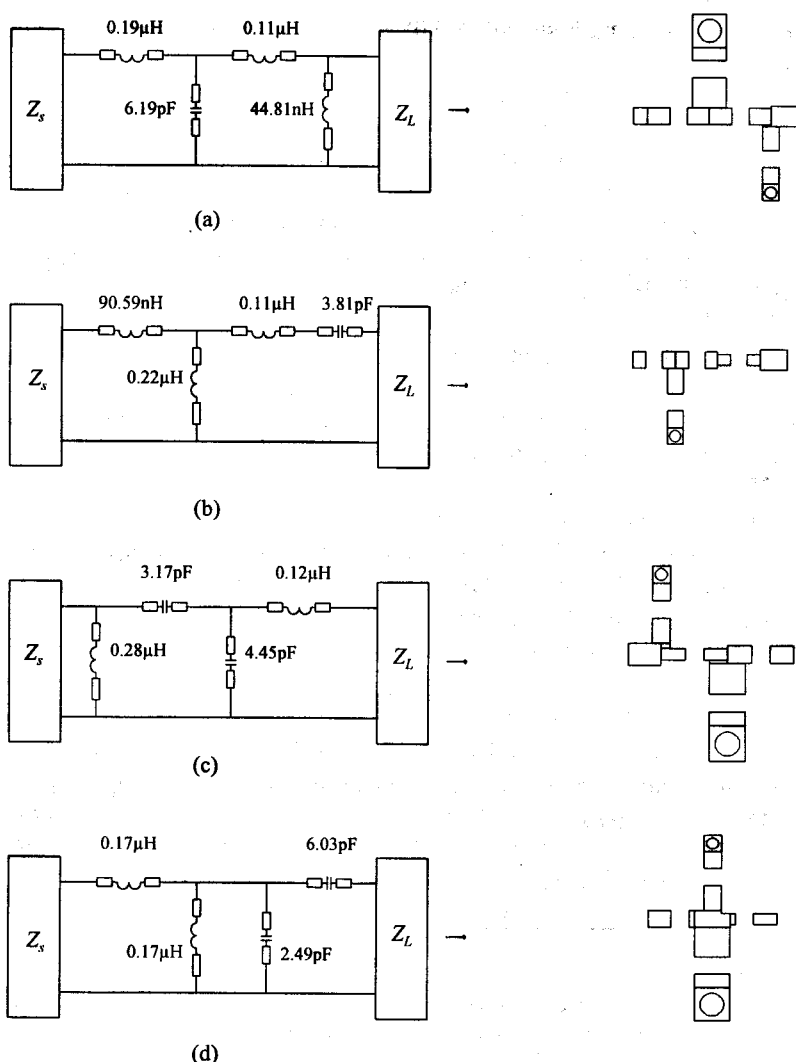


**Figure 8.38** The four best mixed lumped/distributed solutions obtained with the transformation- $Q$  technique for the matching problem of Example 8.8.

### EXAMPLE 8.11 Matching a $25\Omega$ source to a $100\Omega$ load (2–6 GHz).

A load resistance of  $100\Omega$  will be transformed to  $25\Omega$  over the passband 2–6 GHz in this example. The solutions were synthesized for a 10 mil microstrip substrate with  $\epsilon_r = 9.8$  by using [15].

The best solutions to a purely resistive matching problem are usually obtained with a commensurate distributed network. When the bandwidth required

is large, the line length should be  $90^\circ$  long at the center frequency (arithmetic mean).

The commensurate solution shown in Figure 8.39(a) was synthesized by setting the line length equal to  $90^\circ$  at 4 GHz. This solution was obtained by setting the search range for the transformation  $Q_s$  to the interval  $[-1.2, 1.2]$ , with a step size of 0.1. Note that a  $25\Omega$  pad was used to complete the input junction (the first element of the network synthesized was a shunt element).

The input VSWR of this solution is better than 1.06 over the passband ( $|s_{11}| < -30.58$  dB; MRD = 0.08%, MRD<sub>wc</sub> = 0.35%). The size of this solution is 11.63 mm by 6.41 mm.

The noncommensurate solution shown in Figure 8.39(b) was obtained by setting the characteristic impedance of the main-line sections and the short-circuited stubs to  $73\Omega$ . The characteristic impedance used for the open-ended stubs was  $33.5\Omega$ . The search range for the transformation  $Q_s$  was from -1.5 to 1.5, with steps of 0.25. The  $100\Omega$  line on the output side was used to complete the junction associated with the open-ended stub.

The input VSWR of this solution is better than 1.25 ( $|s_{11}| < -19.16$  dB; MRD = 1.2%, MRD<sub>wc</sub> = 1.78%). The outline size of this solution is 6.88 mm by 4.133 mm (a gap of 0.1 mm was used for the series capacitor).

The best six-element lumped-element solution obtained is shown in Figure 8.39(c). The input VSWR of this solution is better than 1.19 over the passband ( $|s_{11}| < -21.36$  dB, MRD = 0.71%, MRD<sub>wc</sub> = 1.24%).

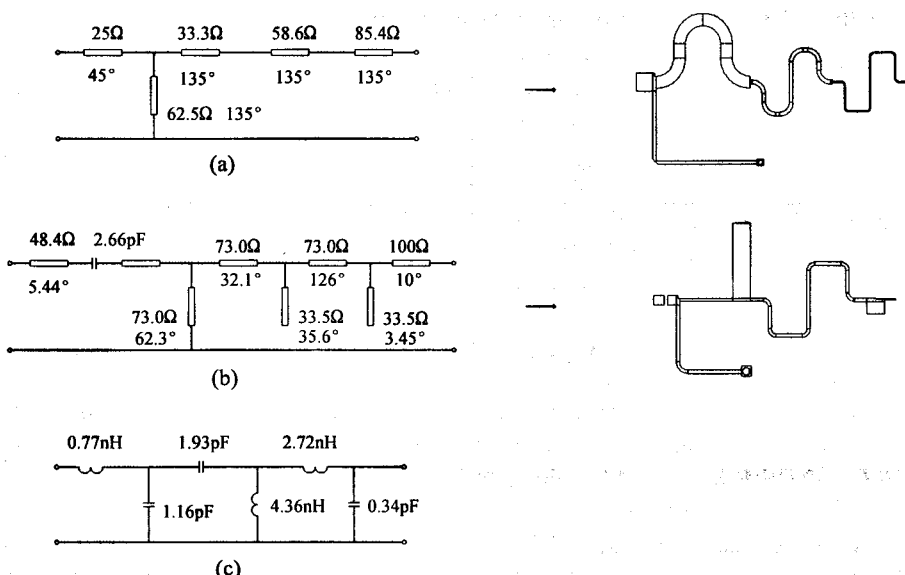


**Figure 8.39** The best (a) commensurate (four elements), (b) noncommensurate (six elements), and (c) lumped (six elements) solutions obtained for matching a  $25\Omega$  source to a  $100\Omega$  load (2–6 GHz).

## 8.5 THE DESIGN OF RLC IMPEDANCE-MATCHING NETWORKS

RLC impedance-matching networks are often used to compensate for the decrease in the gain of the transistors used with increasing frequencies. This can usually be done without reactive mismatching, which is an advantage of these networks over lossless networks.

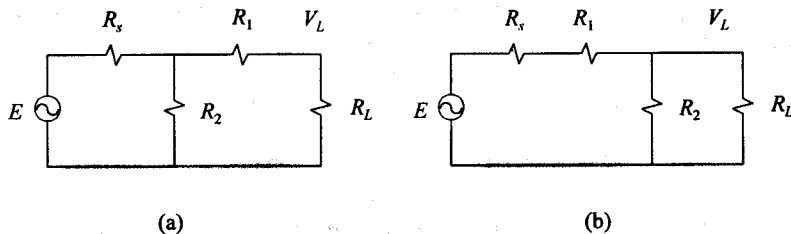


**Figure 8.40** Impedance matching with resistors.

RLC networks are usually designed by using a computer optimization program on a circuit with a suitable topology, after initial values have been assigned to its components.

The resistors in an RLC impedance-matching network have two functions: they provide the required attenuation at the lowest frequency in the passband, and they match the load impedance to the source impedance at this frequency. A minimum of one series and one parallel resistor are required in order to do this.

When only one series and one parallel resistor are used, initial values can be assigned to them by using the following set of equations:

$$A^2 = (E / V_L)^2 = \frac{4R_s}{G_T R_L} \quad (8.130)$$

$$G_1^2 \left[ 1 + \frac{G_{in}}{G_s} - A \right] + G_1 \left[ 2G_L \left( 1 + \frac{G_{in}}{G_s} - A/2 \right) \right] + G_L^2 \left[ 1 + \frac{G_{in}}{G_s} \right] = 0 \quad (8.131)$$

$$G_2 = G_{in} - \frac{G_1 G_L}{G_1 - G_L} \quad (8.132)$$

where  $G_T$  is the required transducer power gain at the lowest frequency in the passband,  $G_1=1/R_1$ ,  $G_2=1/R_2$ , and  $G_{in}$  is the required input admittance of the matching network at the lowest frequency (if a perfect match is required,  $G_{in} = G_s$ ).

Equations (8.130) to (8.132) apply to Figure 8.40(a). The equations relevant to Figure 8.40(b) can be obtained by replacing  $G_s$  with  $G_L$  and  $G_L$  with  $G_s$  in these equations.

In order to minimize the insertion loss at the higher frequencies in the passband,

the resistors in an RLC network should be used in parallel with capacitors and in series with inductors, depending on whether they are used in a series or a parallel branch, respectively.

Apart from reducing the insertion loss, the capacitors and inductors used in the network also serve to match the load to the source at the higher frequencies.

The network shown in Figure 8.41 is a typical example of an RLC network. Note that the elements that are not combined with resistors are used as low-pass elements.

Initial values can be assigned to the lossless elements of the network chosen by considering the different elements to be part of independent L-, T-, and PI-sections. As an example of this,  $C_2$  and  $L_2$  in the network shown in Figure 8.41 form a low-pass L-section that should be designed to match the load to the source at the highest frequency in the passband.  $L_1$  and  $C_1$  should be designed to ensure that the insertion loss at the highest frequency will be as low as possible.

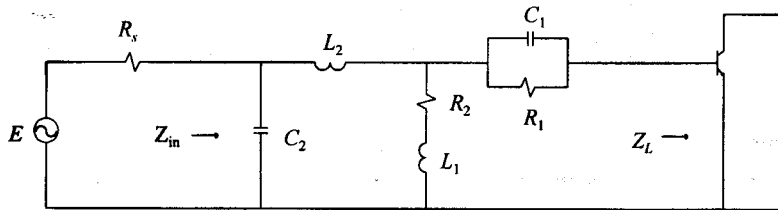


**Figure 8.41** An example of an RLC impedance-matching network.

An alternative way of assigning initial values to the lossless components of an RLC network is to follow the iterative approaches outlined earlier for designing a lossless bandpass network that will match the source to the load at the intermediate and higher frequencies in the passband.

With initial values assigned to the lossless components and the resistors, an optimization program can be used to optimize the network.

#### EXAMPLE 8.12 Example of a RLC matching network.

The use of (8.130) to (8.132) will be illustrated by applying them to the following problem:

$$R_L = 7.50\Omega$$

$$R_s = 6.25\Omega$$

$$G_T = 0.19$$

$$R_{in} = 6.25\Omega$$

$$A = \frac{4R_s}{R_L G_T} = \frac{4(6.25)}{0.19(7.5)} = 4.19$$

$$G_1^2[2.00 - 4.19] + G_1 \left[ 2 \frac{2 - 4.19/2}{7.5} \right] + 1 \frac{2}{7.5^2} = 0$$

$$G_1 = 0.1218; -0.1334S$$

$$G_2 = \frac{1}{6.25} - \frac{0.1218}{7.5[0.1218 + 1/75]} = 0.096S$$

The initial values of the resistors are therefore

$$R_1 = 8.2\Omega \text{ and } R_2 = 10.4\Omega$$

### EXAMPLE 8.13 Matching networks for an HF power amplifier

In this example a 5–20 MHz power amplifier will be designed with the Motorola MRF406 (20W peak envelope power (PEP)) by using [1]. The operating power gain will first be leveled by using an series-shunt RLC network on the input side of the transistor. Mixed lumped/distributed matching networks will then be designed to maximize the output power and to provide a good input match over the passband. It will be assumed that the terminations were transformed to  $12.5\Omega$  with transmission-line transformers.

The load impedance required to maximize the output power and the associated input impedance and operating power gain are provided in the data sheet for the transistor. The estimated values are shown in Table 8.14.

It is convenient to convert the impedance and gain specifications in Table 8.14 to an equivalent set of unilateral *S*-parameters. The input reflection coefficient is chosen to correspond to the input impedance of the transistor when the optimum

**Table 8.14**  
The optimum load impedance of the MRF406, with the associated operating power gain and input impedance

Frequency (MHz)	Input impedance ( $\Omega$ )	Load impedance ( $\Omega$ )	Operating power gain (dB)
2.0	$7.5 - j2.6$	$8.314 - j4.263$	20.93
5.0	$5.2 - j2.4$	$6.212 - j4.914$	20.14
10.0	$3.1 - j1.9$	$4.971 - j4.476$	18.44
15.0	$2.3 - j1.75$	$4.471 - j4.028$	16.99
20.0	$1.7 - j1.7$	$4.272 - j3.536$	16.01
30.0	$1.0 - j1.0$	$3.484 - j2.445$	14.30

load is in place, while the output impedance is taken to be the conjugate of the optimum load impedance. The forward transmission parameter ( $s_{21}$ ) is set to the value required to ensure that the maximum available gain (MAG) of this equivalent transistor is the same as the operating power gain of the transistor with the optimum load in place. The equivalent S-parameters for the MRF406 are shown in Table 8.15 in polar format (magnitude and angle).

**Table 8.15**  
The equivalent set of S-parameters of the MRF406

Frequency (MHz)	$s_{11}$ (-; °)	$s_{21}$ (-; °)	$s_{12}$ (-; °)	$s_{22}$ (-; °)
2.0	0.7398	186.1	5.224	327.6
3.0	0.7661	185.9	4.597	316.7
5.0	0.8120	185.6	3.707	299.1
7.0	0.8473	185.1	2.907	284.5
10.0	0.8834	184.4	2.238	264.7
15.0	0.9121	184.0	1.588	234.1
20.0	0.9343	183.9	1.210	206.0
30.0	0.9608	182.3	0.709	148.7

With the equivalent S-parameters in place, the original targets can be realized by leveling the MAG of the equivalent transistor (lossy sections on the input side; no feedback allowed) and designing matching networks to minimize the input and the output VSWRs.

The RLC network designed to level the MAG of the equivalent transistor is shown in Figure 8.42. With this network in place, the MAG varies between 10.94

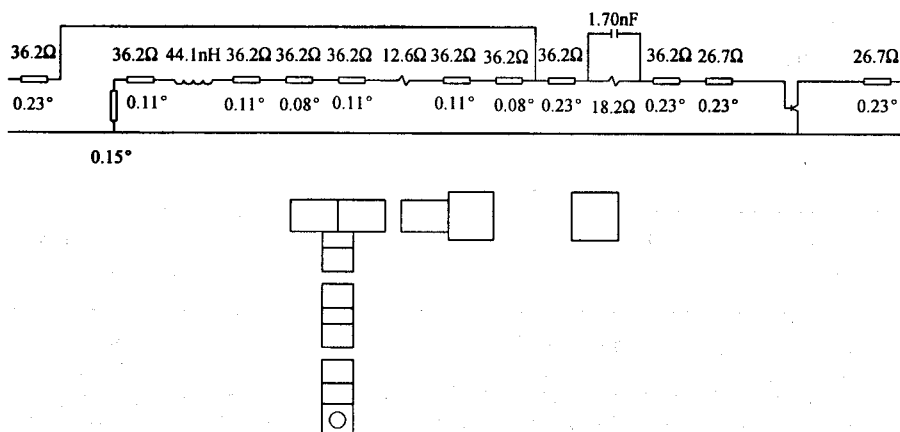


**Figure 8.42** The RLC network used to level the operating power gain of the MRF406.

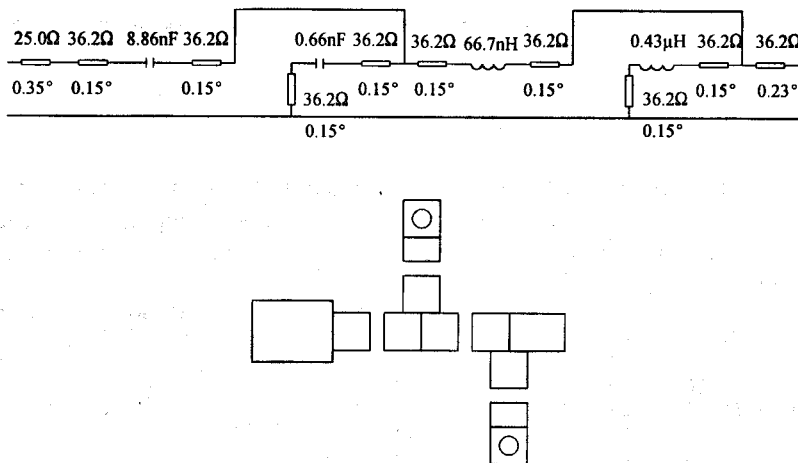


Figure 8.43 The mixed lumped/distributed input matching network synthesized for the MRF406.

and 11.14 dB, and the input VSWR (relative to the  $12.5\Omega$  source termination) varies between 1.61 and 3.06.

Leveling the MAG of the equivalent transistor corresponds to leveling the operating power gain of the actual transistor terminated in the optimum load impedance.

The mixed lumped/distributed input matching network is shown in Figure 8.43 (the electrical line lengths are specified at 20MHz). The input VSWR varies between 1.24 and 1.46 over the passband ( $|s_{11}| < -14.57$  dB).

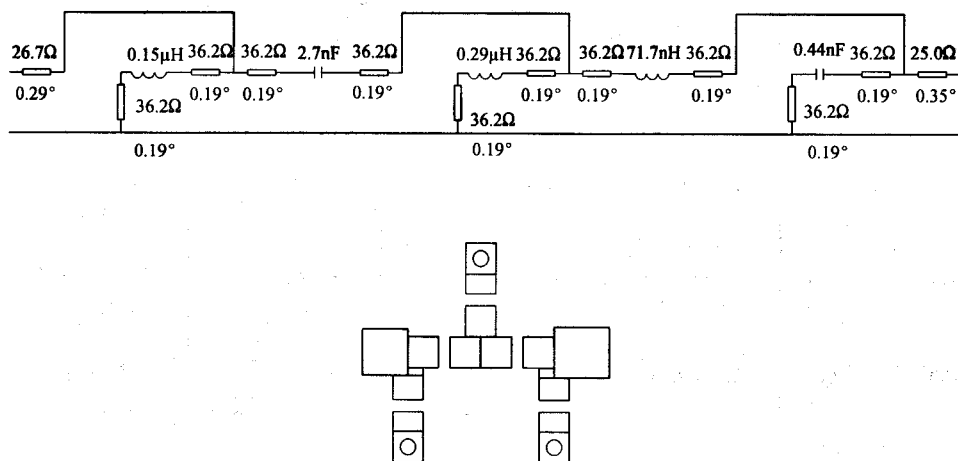
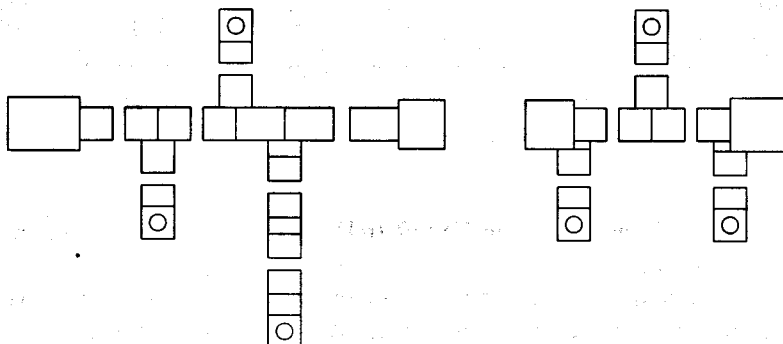


Figure 8.44 The mixed lumped/distributed load network synthesized for the MRF406.

The load network synthesized (five-element network) to match the output of the equivalent transistor (maximize the output power of the actual transistor) is shown in Figure 8.44 (the electrical line lengths are specified at 25 MHz). The output VSWR in the equivalent circuit varies between 1.16 and 1.32 over the passband ( $|s_{11}| < -17.03$  dB).

The artwork of the amplifier designed is shown in Figure 8.45 (the gap spacings must be adjusted to accommodate the lumped components to be used).

The final response associated with the equivalent transistor is shown in Figure 8.46 and tabulated in Table 8.16.



**Figure 8.45** The artwork of the amplifier synthesized.

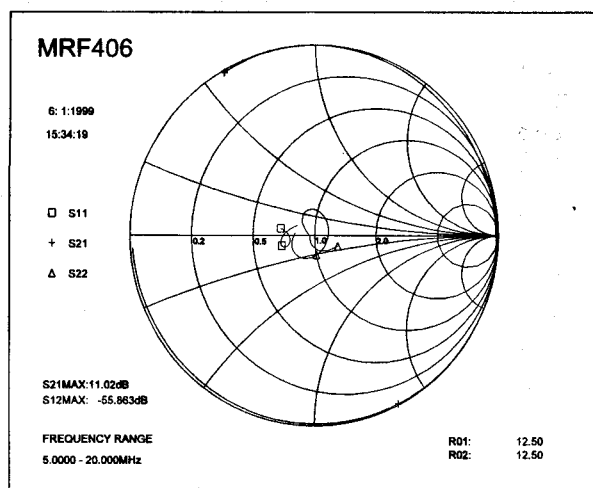


**Figure 8.46** The final response associated with the equivalent transistor. (Note that the highest frequency on each trace is not marked; the Smith Chart should be viewed as a polar plot only when the  $s_{21}$  trace is interpreted.)

**Table 8.16**  
The S-parameters of the final circuit (equivalent transistor)

Frequency (MHz)	$s_{11}$		$s_{12}$		$s_{21}$		$s_{22}$	
	(dB)	(°)	(dB)	(°)	(dB)	(°)	(dB)	(°)
2.0	-3.72	217.0	-110.56	10.0	-16.64	311.6	-0.01	133.9
5.0	-14.57	168.0	-76.96	237.0	10.91	120.0	-17.16	336.3
6.0	-16.67	174.8	-74.66	207.8	10.97	77.2	-20.15	133.2
7.0	-17.48	185.6	-72.59	189.3	10.84	47.1	-17.14	100.3
8.0	-17.23	194.4	-70.65	175.2	10.85	22.5	-18.16	72.5
9.0	-16.51	199.3	-68.87	163.0	10.91	0.9	-20.40	41.8
10.0	-15.76	200.8	-67.25	152.0	11.00	341.3	-22.41	3.9
11.0	-15.18	200.2	-65.75	142.0	11.00	323.0	-22.28	320.7
12.0	-14.78	198.2	-64.37	132.5	10.98	305.7	-20.64	288.6
13.0	-14.58	195.2	-63.10	123.4	10.95	289.3	-19.04	266.8
14.0	-14.58	191.7	-61.92	114.6	10.93	273.4	-17.91	250.5
15.0	-14.79	187.5	-60.81	106.0	10.91	257.9	-17.24	237.0
16.0	-15.12	182.9	-59.74	97.6	10.88	243.0	-17.03	224.8
17.0	-15.68	177.4	-58.71	89.2	10.87	228.2	-17.17	213.2
18.0	-16.52	170.9	-57.72	80.7	10.87	213.5	-17.64	201.2
19.0	-17.75	162.4	-56.78	72.1	10.88	198.8	-18.45	188.1
20.0	-19.49	150.4	-55.86	63.2	10.91	183.9	-19.58	172.4
25.0	-14.59	0.2	-51.95	12.2	10.80	103.7	-17.14	44.1
30.0	-4.19	306.9	-50.45	306.6	7.90	8.2	-8.24	352.0

## REFERENCES

1. Fano, R. M., "Theoretical Limitations on the Broadband Matching of Arbitrary Impedances," *Journal of the Franklin Inst.*, Vol. 249, January/ February 1950, pp. 57-83, 139-154.
2. Youla, D. C., "A New Theory of Broad-Band Matching," *IEEE Trans. Circuits Syst.*, Vol. CT-11, March 1964, pp. 30-50.
3. Carlin, H. J., "A New Approach to Gain-Bandwidth Problems," *IEEE Trans. Circuits Syst.*, Vol. CAS-24, April 1977, pp. 170-175.
4. Lev, J., "Calculator program finds Fano bandwidth," *Microwaves & RF*, September 1985.
5. Chen, W., and C. Satyanarayana, "General Theory of Broadband Matching," *IEE Proc. C (GB)*, Vol. 129, No. 3, June 1982, pp. 96-102.
6. Carlin, H. J., and B. S. Yarman, "The Double Matching Problem: Analytic and Real Frequency Solutions," *IEEE Trans. Circuits Syst.*, Vol. CAS-30, No. 1, January 1983, pp. 15-27.

7. Yarman, B. S., and H. J. Carlin, "A Simplified 'Real-Frequency' Technique Applied to Broad-Band Multistage Microwave Amplifiers," *IEEE Trans. Microwave Theory Tech.*, Vol. MTT-30, No. 12, December 1982, pp. 2216-2222.
8. Carlin, H. J., and P. Amstutz, "On Optimum Broad-Band Matching," *IEEE Trans. Circuits Syst.*, Vol. CAS-28, No. 5, May 1981, pp. 401-405.
9. Bode H. W., *Network Analysis and Feedback Amplifier Design*, New York: Van Nostrand, 1945, pp. 205-207, 319.
10. Chen, W. K., *The Theory and Design of Broadband Matching Networks*, London: Pergamon Press, 1976.
11. Levy, R., "Explicit Formulas for Chebyshev Impedance-Matching Networks, Filters and Interstages," *Proc. IEEE*, Vol. 111, No. 6, June 1964.
12. Richards, P. I., "Resistor-Transmission-Line Circuits," *Proc. IRE*, February 1948, pp. 217-219.
13. Baher H., *Synthesis of Electrical Networks*, New York: John Wiley & Sons, 1984.
14. Yarman, B. S., *Broad-Band Matching a Complex Generator to a Complex Load*, Doctoral Dissertation, Cornell University, 1982, pp. 117-120.
15. *MultiMatch RF and Microwave Impedance-Matching, Amplifier and Oscillator Synthesis Software*, Somerset West, RSA: Ampsa (PTY) Ltd; <http://www.ampsap.com>, 1998.
16. Carlin, H. J., and J. J. Komiak, "A New Method of Broadband Equalization Applied to Microwave Amplifiers," *IEEE Trans. Microwave Theory Tech.*, Vol. MTT-27, No. 2, February 1979, pp. 93-99.
17. *Watcom Fortran 77 User's Guide*, Ontario, Canada: Watcom International Corporation; <http://www.watcom.on.ca>, 1996.
18. Ha, T. T., *The Design of Microwave Solid State Amplifiers*, New York: John Wiley and Sons, 1981, pp. 178-179.

## SELECTED BIBLIOGRAPHY

Abrie, P. L. D., *Impedance Matching Networks and Bandwidth Limitations of Class B Power Amplifiers in the HF and VHF Ranges*, Master's Thesis, University of Pretoria, November 1982.

- Fletcher, R., and M. J. D. Powell, "A Rapidly Convergent Descent Method for Minimization," *Computer J.*, Vol. 6, 1963, pp. 163-168.
- Ku, W. H., and W. C. Peterson, "Optimum Gain-Bandwidth Limitations of Transistor Amplifiers as Reactively Constrained Two-Port Networks," *IEEE Trans. Circuits Syst.*, Vol. CAS-22, June 1975, pp. 523-533.
- Liu, L. C. T., and W. H. Ku, "Computer-Aided Synthesis of Lumped Lossy Matching Networks for Monolithic Microwave Integrated Circuits (MMICs)," *IEEE Trans. Microwave Theory Tech.*, Vol. MTT-32, No. 3, March 1984, pp. 282-290.
- Matthaei, G. L., "Tables of Chebyshev Impedance Transforming Networks of Low-pass Filter Form," *Proc. IEEE*, August 1964.
- Mellor, D. J., and J. G. Linvill, "Synthesis of Interstage Networks of Prescribed Gain versus Frequency Slopes," *IEEE Trans. Microwave Theory Tech.*, Vol. MTT-23, No. 12, December 1975.
- Pitzalis, O., and R. A. Gilson, "Tables of Impedance Matching Networks which Approximate Prescribed Attenuation versus Frequency Slopes," *IEEE Trans. Microwave Theory Tech.*, Vol. MTT-19, No. 14, April 1971.
- Schoeffler, J. D., "Impedance Transformation Using Lossless Networks," *IRE Trans. Circuit Theory*, CT-8, June 1961, pp. 131-137.
- Van Valkenburg, M. E., *Introduction to Modern Network Synthesis*, New York: John Wiley and Sons, 1960.

# CHAPTER 9

## MICROWAVE LUMPED ELEMENTS, DISTRIBUTED EQUIVALENTS, AND MICROSTRIP PARASITICS

### 9.1 INTRODUCTION

Impedance-matching networks can be realized in lumped form as long as the dimensions of the components used are small compared to a quarter-wavelength at the highest frequency of interest. The different types of inductors and capacitors used at microwave frequencies will be considered in this chapter. The design of microwave inductors will also be considered.

When the dimensions are on the order of 1/12 of a wavelength, the phase shift associated with the component can cause a significant deviation from the expected response. Furthermore, if the associated characteristic impedance is too low for inductors and too high for capacitors, the response will be degraded even more by the parasitic capacitance or inductance, respectively. Because it is often a problem when high impedance circuits are designed, the bounds imposed by the phase shift across and the finite characteristic impedance of practical inductors will be examined in this chapter. In order to do this, the transforming properties of a series transmission line will be examined first.

When the components cannot be realized with negligible phase shift and parasitics, matching networks should be realized in distributed form when possible. Fabrication of distributed networks using microstrip, on thin-film substrates or as microwave integrated circuits (MICs), is relatively easy. The design effort involved is also much less than that required when lumped elements are used and the parasitics cannot be ignored.

Excellent equations for the characteristic impedance and effective dielectric constant of microstrip lines have been developed by the many workers in the field [1] and were reviewed in Chapter 3. In MIC/MMIC layouts, transmission-line discontinuities such as open-ends, gaps, steps in width, right-angle bends, T-junctions and cross-junctions are encountered. At higher frequencies it becomes necessary to incorporate the effect of these discontinuities into designs in order to obtain good results. The magnitude of these effects at the lower microwave frequencies [2] will be considered here along with a compensation technique [3].

Prototype lumped-element designs are often transformed into distributed designs

by replacing the inductors and capacitors in the network with shorted stubs, open-circuited stubs, and cascade sections of transmission line. The range of series and shunt reactances, which can be transformed with negligible error, will be examined here. It will also be shown that significantly better results can be obtained by replacing low-pass T-sections and PI-sections with sections of series transmission lines.

## 9.2 MICROWAVE RESISTORS

**Thin-film techniques** are often used to manufacture resistors at microwave frequencies. By keeping the dimensions of a resistor small, the associated capacitance and inductance can be minimized. The capacitance can be reduced further by depositing the thin film on a low dielectric-constant substrate.

A thin-film resistor can be characterized as a lossy transmission line. The relevant equations were considered in Chapter 7.

Thin films with resistances of  $10\Omega$  to  $1000\Omega$  per square are available.

Adjustment of resistance values by laser trimming is only an option at microwave frequencies if a broad gap is used.

## 9.3 THE LIMITATIONS OF A SERIES TRANSMISSION LINE USED TO REPLACE A LUMPED ELEMENT

All lumped inductors of finite dimension have some capacitance to ground and as such can be considered transmission lines of high characteristic impedance. The characteristic impedance will not be uniform when bonding wire inductors or square or spiral inductors are used.

In order to get an idea of the bounds on the inductance that can be realized with lumped inductors, as well as the limits on the inductance that can be replaced with series transmission lines with negligible error, it is necessary to consider the transformation properties of a series transmission line.

Assuming a load impedance of  $Z_L = R_L + jQ \cdot R_L$ , the input resistance and reactance of a lossless series transmission line having a characteristic impedance of  $Z_0$  is given by

$$R_{in} = R_L [1 + \tan^2 \theta] / Z \quad (9.1)$$

and

$$X_{in} = j[QR_L(1 - \tan^2 \theta) + Z_0 \tan \theta - R_L^2 \tan \theta (1 + Q^2) / Z_0] / Z \quad (9.2)$$

where

$$Z = [1 - QR_L \tan \theta / Z_0]^2 + [R_L \tan \theta / Z_0]^2 \quad (9.3)$$

and

$$\theta = \beta l \quad (9.4)$$

In order to exhibit truly lumped behavior, the line length and characteristic impedance, respectively, must be short enough and high enough for the input impedance to be approximately

$$Z_{in} = R_L + jQ R_L + jZ_0 \tan \theta \quad (9.5)$$

For (9.5) to apply, the following inequalities must be satisfied:

$$R_{in} \approx R_L :$$

$$\tan^2 \theta \ll 1$$

$$Z_0 / R_L \gg 2Q \tan \theta$$

$$(Z_0 / R_L)^2 \gg \tan^2 \theta \quad (9.6)$$

$$X_{in} \approx jQ R_L + jZ_0 \tan \theta :$$

$$\tan^2 \theta \ll 1$$

$$Z_0 / R_L \gg 2Q \tan \theta$$

$$(Z_0 / R_L)^2 \gg \tan^2 \theta$$

$$(Z_0 / Z_L)^2 \gg 1 + Q^2 \quad (9.7)$$

It follows from (9.1) and (9.3) that, even if the characteristic impedance of the line was equal to infinity, the resistance would still be transformed to

$$R_{in} = R_L [1 + \tan^2 \theta] \quad (9.8)$$

that is, the influence of the phase shift does not become negligible with increasing characteristic impedance.

With  $Z_0$  approaching infinity, the input reactance of the line is given by

$$X_{in} = jQ R_L [1 - \tan^2 \theta] + jZ_0 \tan \theta \quad (9.9)$$

Equations (9.8) and (9.9) can be used to provide upper bounds on the line length for which

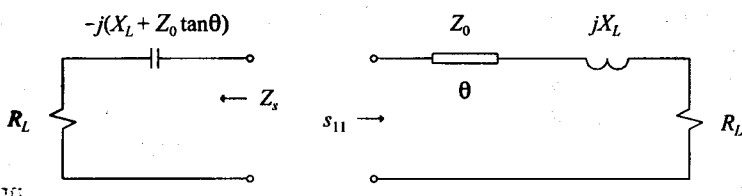


**Figure 9.1** The equivalent circuit used to derive (9.10).

input impedance of the line will be approximately equal to that given by (9.5). One way to do this is to evaluate the reflection coefficient of the circuit in Figure 9.1 for an infinite value of the characteristic impedance of the line. The input reflection coefficient of this circuit is then given by

$$\begin{aligned} s_{11} &= \frac{R_L(1 + \tan^2 \theta) - R_L + j[X_L(1 - \tan^2 \theta) - X_L]}{R_L(1 + \tan^2 \theta) + j[X_L(1 - \tan^2 \theta) - X_L]} \\ &= \frac{1 - jQ}{[2 / \tan^2 \theta + 1] - jQ} \end{aligned} \quad (9.10)$$

It follows from (9.10) that the deviation from lumped behavior is a strong function of the length of the line and the quality factor  $Q$  of the load impedance. This is clearly illustrated by the following results, which correspond to an insertion loss of 0.25 dB ( $G_T = 1 - |s_{11}|^2$ ):

$Q = 0:$	$\theta = 38^\circ$
$Q = 1:$	$\theta = 33^\circ$
$Q = 2:$	$\theta = 26^\circ$
$Q = 3:$	$\theta = 22^\circ$
$Q = 4:$	$\theta = 19^\circ$

Because of the finite characteristic impedance of any physical line, the exact deviation will always be greater than that predicted by (9.10). The exact reflection parameter for any particular case can be calculated by substituting  $R_{in}$  and  $X_{in}$ , as given by (9.1) to (9.4), into the equation

$$s_{11} = \frac{[R_{in} - R_L] + j[X_{in} - X_L - Z_0 \tan \theta]}{[R_{in} + R_L] + j[X_{in} - X_L - Z_0 \tan \theta]} \quad (9.11)$$

As an illustration of the combined influence of a reactive load and finite values for the characteristic impedance, the line lengths corresponding to an insertion loss of approximately 0.25 dB in the circuit shown in Figure 9.1 are tabulated in Table 9.1 as a

function of the ratio  $Z_0/R_L$  and the line length.

It is clear from the results in Table 9.1 that the range of characteristic impedances and line lengths over which a series transmission line can be considered to be a lumped inductor (and, inversely, over which the distributed nature of a series inductor can be ignored) is very limited, especially when the load  $Q$  is high.

**Table 9.1**

The line lengths corresponding to an insertion loss of 0.25 dB in Figure 9.1 as a function of the characteristic impedance of the line and the  $Q$ -factor of the load

$Z_0/R_L$	Line Length ( $^\circ$ )					
	$Q = 0$	$Q = 1$	$Q = 2$	$Q = 3$	$Q = 4$	$Q = 5$
1.0	26	13	5	3	2	1
2.0	35	20	10	5	3	2
3.0	37	24	13	7	4	3
4.0	37	26	15	9	6	4
5.0	38	27	17	11	7	5
7.5	38	29	20	14	9	7
10.0	38	30	21	15	11	9
15.0	38	31	23	17	13	10
20.0	38	31	24	18	15	12

## 9.4 LUMPED MICROWAVE INDUCTORS

Lumped microwave inductors can be fabricated in different forms. For low inductance values, strip inductors or bonding wire is frequently used, while larger inductance values are realizable with spiral or solenoidal inductors. The basic equations required to design these inductors will be considered here.

### Strip Inductors

The inductance of an isolated (no ground plane), flat, ribbon inductor (or strip inductor) is given approximately by [4]

$$L(\text{nH / mm}) = 0.2 \{ \ln[l/(w+t)] + 1.193 + 0.2235(w+t)/l \} \quad (9.12)$$

where  $w$  is the width of the ribbon,  $t$  its thickness, and  $l$  its length.

An approximate expression for the  $Q$  of a ribbon inductor is [5]

$$Q = 2.15 \times 10^3 \frac{L(\text{nH})}{K} \frac{\omega}{l} \left( \frac{\rho(\text{Cu})}{\rho} \right)^{1/2} \left( \frac{f(\text{GHz})}{2} \right)^{1/2} \quad (9.13)$$

where  $\rho$  is the resistivity of the material used, and  $K$  is a correction factor for the current crowding occurring at the corners of the strip [4].  $K$  is given approximately by the following expression:

$$K = 1.3565 - 0.2319 \ln(w/t) + 0.2386 [\ln(w/t)]^2 \\ - 0.0536 [\ln(w/t)]^3 + 0.0043 [\ln(w/t)]^4 \quad (9.14)$$

The inductance of a strip inductor is decreased by the presence of a ground plane. The effective inductance for this case is given in terms of the free-space value by [6, 7]

$$L_{\text{eff}} = [0.570 - 0.145 \ln(W/h)] \cdot L \quad (9.15)$$

### Single-Turn Circular Loop

Equations (9.12) and (9.15) can also be used to calculate the inductance of a single-turn circular loop in those cases where the width of the strip is much smaller than the diameter. When the ground plane can be ignored, the following expression [8] can also be used:

$$L(\text{nH/mm}) = 0.2[\ln(l/w+t) - 1.76] \quad (9.16)$$

For (9.16) to apply, the inequality  $l \gg 2(w+t)$  must be satisfied.

### Bond Wire Inductors

Bonding wire inductors have the advantage over strip inductors that higher  $Q$ -factors can be expected because of the larger surface area. Furthermore, touch-up tuning is possible with bonding wire inductors, while the inductance is fixed for strip inductors. The fixed inductance, however, is an advantage in a first-time-right design.

The inductance associated with a long ( $l/d \geq 100$ ) free-space bonding wire of diameter  $d$  and length  $l$  can be calculated by using the equation [4]

$$L(\text{nH/mm}) = 0.20[\ln(l/d) + 0.386] \quad (9.17)$$

The effect of a ground plane can be incorporated by using the equation [4, 6]

$$L(\text{nH/mm}) = 0.2 \left\{ \ln \frac{4h}{d} + \ln \frac{l + \sqrt{l^2 + d^2/4}}{l + \sqrt{l^2 + 4h^2}} \right. \\ \left. + \sqrt{1 + \frac{4h^2}{l^2}} - \sqrt{1 + \frac{d^2}{4l^2}} - 2 \frac{h}{l} + \frac{d}{2l} \right\} \quad (9.18)$$

An approximate expression for the  $Q$  of a round wire inductor is [5]

$$Q = 3.38 \times 10^3 L(\text{nH}) \frac{d}{l} \left( \frac{\rho(\text{Cu})}{\rho} \right)^{1/2} \left( \frac{f(\text{GHz})}{2} \right)^{1/2} \quad (9.19)$$

Equations (9.17) and (9.18) are only accurate when  $l/d \geq 100$  [9]. When short bond wires are used, the following equation is recommended for the free-space case [9]:

$$L(H) = [\mu_0 / (4\pi)] l \left\{ \ln \left[ (2l/d) + \sqrt{1 + (2l/d)^2} \right] + d/(2l) - \sqrt{1 + (d/(2l))^2} + \mu_r \delta \right\} \quad (9.20)$$

When the wire is manufactured with nonmagnetic material, as is usually the case,  $\mu_r = 1$ . The skin depth term ( $\delta$ ) in (9.20) represents the internal inductance of the wire.

The effect of the ground plane is similar to a current image reflection of the inductor. Because of this effect the inductance of the bond wire is decreased when a ground plane is present. The effective inductance is this case is given by [9]

$$L_{\text{eff}}(H) = L - [\mu_0 / (2\pi)] \cdot l \cdot \left\{ \ln \left[ l/(2h) + \sqrt{1 + (l/(2h))^2} \right] - \sqrt{1 + (2h/l)^2} + 2h/l \right\} \quad (9.21)$$

where  $2h$  is the center-to-center separation between the wire and its image, and  $h$  is the distance from the ground plane.

It is recommended in [9] that  $h$  in (9.21) should be replaced by

$$h' = h + 4.6 \delta \quad (9.22)$$

to account for the nonperfect ground (finite conductance).

### Square Spiral Inductors

For square spirals the inductance (in the absence of any ground plane) is given approximately by [10]

$$L(\text{nH}) = 0.85 \sqrt{A} N^{5/3} \quad (9.23)$$

where  $A$  is the area in square millimeters and  $N$  the number of turns.

The associated line length (in square millimeters) is approximately

$$l_e = N [8r_i + d(4N - 3)] \quad (9.24)$$

The parameters in this equation are defined in Figure 9.2.

Square spirals are often used as RF chokes in MICs.

### Circular Spiral Inductors

The inductance of a circular spiral inductor can be calculated by using the following equations:

$$L(\text{nH}) = 3.930a^2 N^2 / [0.8a + 1.1c] \quad (9.25)$$

$$a(\text{mm}) = (d_o + d_i) / 4.0 \quad (9.26)$$

$$c(\text{mm}) = (d_o - d_i) / 2.0 \quad (9.27)$$

where  $d_i$  and  $d_o$  are the inner and outer diameter of the spiral, respectively,  $s$  the spacing between two adjacent conductors, and  $N$  the number of turns.

For minimum losses, the outer diameter of a spiral inductor should be approximately five times the inner diameter [11]. Under this constraint, the  $Q$  is given approximately ( $\pm 20\%$ ) by [5]

$$Q = \frac{1.3 \times 10^2 w}{K'} \sqrt{\frac{L}{d_0}} \left( \frac{\rho(\text{Cu})}{\rho} \right)^{1/2} \left( \frac{f(\text{GHz})}{2} \right)^{1/2} \quad (9.28)$$

where  $K'$  is a function of the width of the conductor ( $w$ ) and the spacing between the conductors and is given by [4]

$$K' = 1.009 + 0.8584 e^{-(s+w)/w} + 0.6376 e^{-2(s+w)/w} + 1.843 e^{-3(s+w)/w} \quad (9.29)$$

In order for (9.28) to apply,  $d_o$  should be greater than  $1.2d_i$ ,  $N$  greater than 1, and the thickness ( $t$ ) greater than five skin depths [5].

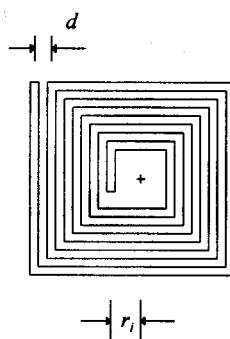


Figure 9.2 A square spiral inductor.

Typical values for the conducting strip width of a spiral inductor are 50–250  $\mu\text{m}$ . For close to optimum results, a width-to-spacing ratio of unity is recommended [5].

### Single-Layer Solenoidal Air-Cored Inductors

At microwave frequencies, solenoidal inductors are often used as RF chokes in hybrid circuits. When the size is not prohibitively small, they can also be used as inductors.

The inductance of a solenoidal coil is given by

$$L(\text{nH}) = 10.0r^2N^2 / [2.29l + 2.54r] \quad (9.30)$$

where  $r$  is the radius (in millimeters),  $l$  is the length (in millimeters), and  $N$  is the number of turns of the coil.

In order to remain essentially lumped, an inductor must be electrically short. Reasonable results can be expected with shunt inductors when the associated electrical length is shorter than  $30^\circ$  (the deviation from the expected linear increase in reactance will then be less than 10%). In the case of a series inductor, the restrictions are more severe because the resistance in series with the inductor will be transformed because of the transmission-line effect.

In order to provide an idea of the bounds on realizable series inductances, the inductances associated with a line of  $38^\circ$  ( $Q = 0$  and  $\epsilon_r = 1$ ) were calculated and are tabulated in Table 9.2 at different frequencies for each of the inductors discussed above. Because the inductive and capacitive coupling were ignored, the bounds on the inductance of square spiral and solenoidal coil inductors are only approximate.

The inductance values in Table 9.2 are optimistic in the sense that the  $Q$  of the load was assumed to be zero, the relative dielectric constant was assumed to be unity, and the influence of the finite incremental characteristic impedance associated with the lumped inductors was ignored. The influence of the effective relative dielectric constant is to increase the electrical length of the inductor by a factor  $\epsilon_r^{1/2}$ , and the  $Q$  and  $Z_0$  influences

**Table 9.2**  
Upper bounds on the series inductance realizable ( $\epsilon_r = 1$ ;  $\theta = 38^\circ$ ) with different inductors as a function of frequency

Frequency (GHz)	Inductance (nH)			
	Bonding wire ( $d = 25 \mu\text{m}$ )	Strip inductor ( $w = 50 \mu\text{m}$ )	Square spiral ( $r_i = 20 \mu\text{m}$ ( $25 \mu\text{m}$ )) ( $d_i = 10 \mu\text{m}$ ( $50 \mu\text{m}$ ))	Solenoidal coil ( $c = 25 \mu\text{m}$ )
1	48.0	48.0	109.0 (65.0)	144.0
2	22.0	22.0	41.0 (25.0)	50.0
4	9.7	9.9	15.0 (9.1)	17.0
6	6.1	6.2	8.2 (5.0)	9.4
8	4.3	4.4	5.3 (3.2)	6.1
10	3.3	3.4	3.8 (2.3)	4.3
12	2.7	2.7	2.9 (1.7)	3.1

Table 9.3

The inductance of different inductors as a function of the length of the conductor

Length (mm)	Inductance (nH)			
	Strip inductor $w = 50 \mu\text{m}$	Bonding wire $d = 25 \mu\text{m}$	Square spiral $r_i = 25 \mu\text{m} (20 \mu\text{m})$ $d_i = 50 \mu\text{m} (10 \mu\text{m})$	Solenoidal coil $c = 25 \mu\text{m}$
1.0	0.8	0.8	0.3 (0.6)	0.7
1.5	1.4	1.3	0.7 (1.2)	1.3
2.0	2.0	1.9	1.1 (1.9)	2.1
2.5	2.6	2.5	1.6 (2.6)	2.9
3.0	3.2	3.1	2.1 (3.5)	3.9
4.0	4.5	4.4	3.3 (5.4)	6.1
5.0	5.8	5.7	4.6 (7.6)	8.6
7.5	9.3	9.1	8.4 (14.0)	16.0
10.0	13.0	13.0	13.0 (21.0)	25.0
15.0	21.0	20.0	23.0 (38.0)	46.0
20.0	29.0	28.0	34.0 (57.0)	71.0
25.0	37.0	36.0	47.0 (78.0)	100.0

are tabulated in Table 9.1. An idea of the lowering in the inductance bounds caused by these factors can be obtained by using Table 9.3 in conjunction with Table 9.1. The inductance of the different inductors is tabulated in Table 9.3 as a function of the conductor length.

The inductance of the solenoidal coil in Tables 9.2 and 9.3 was calculated by using (9.30) and the following set of equations:

$$r_{\text{opt}} = 0.3788 \sqrt{l_e \cdot c} \quad (9.31)$$

$$l_{\text{opt}} = 0.4202 \sqrt{l_e \cdot c} + c \quad (9.32)$$

$$N = 0.4202 \sqrt{l_e / c} \quad (9.33)$$

where  $c$  is the wire thickness (in millimeters),  $r_{\text{opt}}$  the optimum radius,  $l_e$  the conductor length, and  $l_{\text{opt}}$  the optimum coil length.

The wire thickness of the solenoidal coil should be chosen to optimize the  $Q$  (refer to Section 3.3.6).

Equations (9.31) to (9.33) were derived by setting the derivative of the inductance, as given by (9.30), equal to zero in order to find the highest inductance corresponding to a specified conductor length.

#### EXAMPLE 9.1 Calculation of the inductance bounds for a matching network.

The matching network in Figure 9.3 was designed to match the output impedance

of a GaAs FET to a  $50\Omega$  load over the passband 2–6 GHz. As an example of the application of the material derived in the previous sections, the feasibility of realizing the inductors in the network in lumped form will be investigated.

Inspection of Table 9.2 yields that the maximum realizable inductance ( $\epsilon_r = 1$ ;  $Z_0 \rightarrow \infty$ ;  $Q_L = 0$ ;  $|S_{21}| = 0.25$  dB) at 6 GHz (solenoidal coils excluded) is approximately 8.2 nH, which is higher than the inductance values in Figure 9.3.

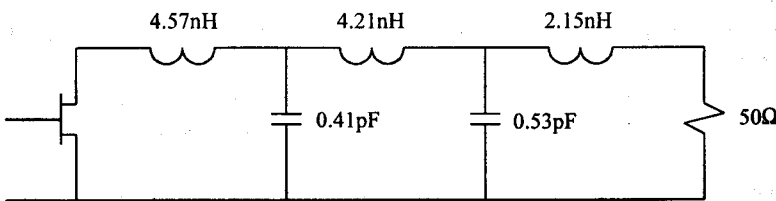


**Figure 9.3** The matching network considered in Example 9.1.

It follows from Table 9.3 that a conductor approximately 4 mm long will be required to realize the 4.58 nH inductor. Assuming the effective relative dielectric constant to be 2.17 (strip inductor), it follows that the required electrical length is approximately

$$\theta = 120 \times 10^{-11} l \sqrt{\epsilon_r} f = 120 \times 10^{-11} \times 4 \sqrt{2.17} \times 6 \times 10^9 = 42^\circ$$

Table 9.1 shows that even with an infinite value for the characteristic impedance, the 4.58-nH inductor cannot be realized without significantly degrading the match. The 4.21-nH inductor presents an even bigger problem because it is located at a higher  $Q$  point (2.01 compared to 1.37).

The electrical length of the 2.15-nH inductor is approximately  $22.8^\circ$ , and the load  $Q$  at that point is equal to zero. It follows from Table 9.1 that this inductor can be realized in lumped form even with an incremental characteristic impedance as low as  $100\Omega$ . Application of (9.11) yields an approximate value of  $-0.07$  dB for the error in gain with  $Z_0$  taken as  $100\Omega$ .

## 9.5 LUMPED MICROWAVE CAPACITORS

Lumped microwave chip capacitors can be used up to very high frequencies. The self-resonant frequencies for some capacitance values as specified by one manufacturer [12] are tabulated in Table 9.4. The dimensions of these capacitors are as small as 0.154 by 0.508 mm and 2.032 by 2.540 mm for capacitance values between 0.1 and 5.6 pF and 3.0 and 62 pF, respectively. The thicknesses vary between 0.076 and 0.254 mm. The

approximate series inductance is 0.05 nH. It should be noted that the power that can be dissipated in capacitors with such small dimensions is limited.

Instead of using discrete capacitors, capacitors can be integrated into a microstrip, thin film, or MIC design. These capacitors can be small plate capacitors, microstrip gap capacitors, or interdigital capacitors. Microstrip gap capacitors [13] are only used at the higher microwave frequencies.

**Table 9.4**

The self-resonant frequencies for some high quality microwave chip capacitors

Capacitance (pF)	Self-resonant frequency (GHz)
0.1	50
1	28
10	9
100	3
1000	1

Interdigital capacitors with capacitors ranging from 0.1–15 pF can be realized on MICs and thin film. The approximate capacitance of an interdigital capacitor is given by the equation

$$C(F) = [(\epsilon_r + 1) / W] l^2 [(N - 3) A_1 + A_2] \quad (9.34)$$

where  $N$  is the number of fingers,  $A_1$  and  $A_2$  are weighting factors associated with the inside and outside fingers, respectively, and  $l$  is the length of overlap, as illustrated in Figure 9.4. When the substrate is thick enough, these constants are  $8.85826 \times 10^{-3}$  pF/mm and  $9.92125 \times 10^{-3}$  pF/mm, respectively. For maximum capacitance, the line widths and spacings should be equal [14]. Spacing of 10–25  $\mu\text{m}$  between the fingers is typical [5].

The parasitics associated with interdigital capacitors can be ignored as long as the capacitance-frequency product is smaller than  $2.0 \times 10^{-3}$  [14].

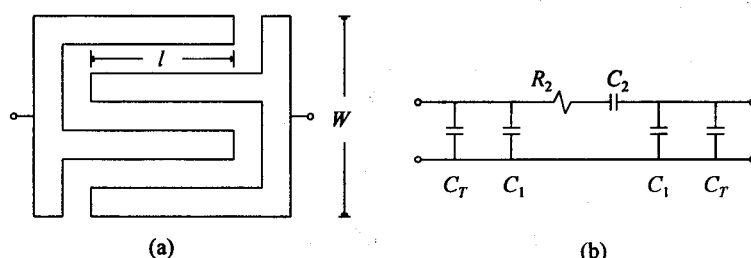


**Figure 9.4** (a) An example of the layout of an interdigital capacitor; (b) a low-frequency equivalent circuit for a series interdigital capacitor.

Interdigital capacitors are considered in detail in [14].

## 9.6 DISTRIBUTED EQUIVALENTS FOR SHUNT INDUCTORS AND CAPACITORS

If the required inductance is low enough, a shunt inductor can be replaced to good approximation by a shorted, high characteristic impedance, transmission line. Similarly, a shunt capacitor can be replaced with an open-ended stub having low characteristic impedance if the required capacitance is small enough. The accuracy with which these replacements can be made is dependent on the linearity of the tangent function. To give an indication of the frequency range over which this function can be considered linear, the value of  $(\tan \theta - \theta) / \theta$  is summarized for several values of  $\theta$  (radians) in Table 9.5. If a 10% deviation is acceptable, the maximum electrical length for an equivalent line is  $30^\circ$ . The maximum deviation across the passband can be reduced to less than 5% with the same line length by averaging the deviation across the passband.

The equations applying to replacing the lumped component exactly at a frequency  $f_H$  are

$$Z_{0L} \tan(\beta\ell) = X_{HL} \quad (\text{inductive}) \quad (9.35)$$

and

$$Z_{0C} / \tan(\beta\ell) = X_{HC} \quad (\text{capacitive}) \quad (9.36)$$

where  $X_{HL}$  and  $X_{HC}$  are the reactances to be replaced at frequency  $f_H$ , and  $Z_{0L}$  (short-circuited stub) and  $Z_{0C}$  (open-ended stub) are the characteristic impedances of the stubs.

**Table 9.5**

The value of  $(\tan \theta - \theta) / \theta$  (in radians) as a function of the angle  $\theta$  (in degrees)

$\theta$ (°)	$(\tan \theta - \theta) / \theta$ (%)	$\theta$ (°)	$(\tan \theta - \theta) / \theta$ (%)
5.0	0.3	35.0	14.6
7.5	0.6	37.5	17.2
10.0	1.0	40.0	20.2
12.5	1.6	42.5	23.5
15.0	2.3	45.0	27.3
17.5	3.2	47.5	31.6
20.0	4.3	50.0	36.0
22.5	5.5	52.5	42.2
25.0	6.9	55.0	48.8
27.5	8.5	57.5	56.4
30.0	10.3	60.0	65.4

**Table 9.6**  
Approximate values for the minimum capacitive and maximum inductive shunt reactance  
that can be replaced with shunt stubs

$\epsilon_r$		2.17	10.3
$Z_{0\text{-min}} (\Omega)$		21/2	10/2
$Z_{0\text{-max}} (\Omega)$		141	72
$X_{HC\text{-min}} (\Omega)$	(+10% deviation)	34/2	16/2
$X_{HL\text{-max}} (\Omega)$		85	43
$X_{HC\text{-min}} (\Omega)$	(+20% deviation)	24/2	12/2
$X_{HL\text{-max}} (\Omega)$		118	60
$X_{HC\text{-min}} (\Omega)$	( $\pm 4.4\%$ deviation; 2–6 GHz)	38/2	18/2
$X_{HL\text{-max}} (\Omega)$		78	40
$X_{HC\text{-min}} (\Omega)$		27/2	13/2
$X_{HL\text{-max}} (\Omega)$	( $\pm 8.3\%$ deviation; 2–6 GHz)	109	56

To give an idea of the range of reactance values that can be replaced in this way, the minimum capacitive reactance and the maximum inductive reactance corresponding to a perfect match at low frequencies, and a 10% and 20% deviation at the highest frequency in the passband are tabulated in Table 9.6. This is done for  $\epsilon_r = 2.17$  and  $\epsilon_r = 10.3$ . In deriving this table, the minimum and maximum width-to-height ratios were taken as 0.3 and 10.0, respectively. The minimum width is determined by the amount of (unpredictable) under-etching and the acceptable resistive losses. The maximum ratio is determined by the electrical width of the stub.

In calculating the minimum capacitive reactance entered into Table 9.6, the capacitor was replaced with two parallel stubs (cross-junction).

As an example of the improvement possible by averaging the deviation across the passband, the reactance corresponding to a passband of 2–6 GHz and maximum deviations of  $\pm 4.4\%$  ( $\theta = 29^\circ$ ) and  $\pm 8.3\%$  ( $\theta = 39.5^\circ$ ) are also given in Table 9.6. The equations used to calculate these reactances are

$$Z_{0L} = 1.808 X_{HL} \quad (9.37)$$

$$Z_{0C} = X_{HC} / 1.808 \quad (9.38)$$

and

$$Z_{0L} = 1.209 X_{HL} \quad (9.39)$$

$$Z_{0C} = X_{HC} / 1.209 \quad (9.40)$$

respectively.

Because a significant reduction in the deviation in reactance is possible in wide-band designs by averaging it across the passband, an equation for the optimum characteristic impedance (admittance) as a function of the inductance (capacitance) to be replaced and the line length will be derived here.

When an inductor is replaced with a short-circuited stub, the error in reactance is given by

$$\begin{aligned}\Delta X &= \frac{Z_0 \tan \theta - \omega L}{\omega L} \\ &= \frac{\tan \theta - \omega L / Z_0}{\omega L / Z_0}\end{aligned}\quad (9.41)$$

Under the equality

$$Z_0 = \frac{b}{\theta_{\max}} \omega_{\max} L \quad (9.42)$$

(9.41) can be changed to

$$\Delta X = \frac{\tan \theta - \theta / b}{\theta / b} \quad (9.43)$$

The optimum value for  $b$ , and therefore the characteristic impedance, can be calculated by setting the error at  $\theta_{\max}$  in the passband equal to the negative of the error at  $\theta_{\min} = \theta_{\max} / u$ , where  $u$  is the relative bandwidth. The result is

$$b = 2 / \left[ \frac{\tan \theta_{\max}}{\theta_{\max}} + \frac{\tan(\theta_{\max} / u)}{\theta_{\max} / u} \right] \quad (9.44)$$

The optimum value for the characteristic impedance can be obtained as a function of the phase shift at the highest frequency in the passband ( $\theta_{\max}$ ) and the reactance to be replaced by substituting the result of (9.44) into (9.42). These impedances are tabulated in Table 9.7 together with the corresponding errors in reactance. The error in reactance is small when the bandwidth is relatively narrow and the electrical line length at the highest frequency in the passband is short.

The characteristic impedance required is clearly a weak function of the relative bandwidth and a strong function of the stub length and reactance required at the highest frequency in the passband.

### EXAMPLE 9.2 Replacing lumped capacitors with open-ended stubs.

Consider the matching network in Figure 9.5 (passband 2–4 GHz). Assuming that the inductors can be realized in lumped form with negligible error, equivalent open-

Table 9.7

The optimum normalized characteristic impedance (admittance) and the corresponding error in reactance (susceptance) for a short-circuited (open-ended) stub as a function of the line length at the highest frequency in the passband and the relative bandwidth ( $u = f_H/f_L$ )

$\theta_{\max}$	$Z_{0\text{-opt}}/[\omega_H L]$ ; reactance error (%) $Y_{0\text{-opt}}/[\omega_H C]$ ; susceptance error (%)							
	(°)	$u = 1.5$	$u = 2.0$	$u = 3.0$	$u = 4.0$	$u = 5.0$		
10.0	5.687	$\pm 0.3$	5.693	$\pm 0.4$	5.697	$\pm 0.5$	5.698	$\pm 0.5$
11.0	5.162	$\pm 0.3$	5.169	$\pm 0.5$	5.173	$\pm 0.6$	5.174	$\pm 0.6$
12.0	4.724	$\pm 0.4$	4.731	$\pm 0.6$	4.736	$\pm 0.7$	4.737	$\pm 0.7$
13.0	4.353	$\pm 0.5$	4.360	$\pm 0.7$	4.365	$\pm 0.8$	4.367	$\pm 0.8$
14.0	4.033	$\pm 0.6$	4.041	$\pm 0.8$	4.407	$\pm 0.8$	4.049	$\pm 0.9$
15.0	3.756	$\pm 0.6$	3.765	$\pm 0.9$	3.771	$\pm 1.0$	3.773	$\pm 1.1$
16.0	3.513	$\pm 0.7$	3.522	$\pm 1.0$	3.529	$\pm 1.2$	3.531	$\pm 1.2$
17.0	3.298	$\pm 0.8$	3.308	$\pm 1.1$	3.315	$\pm 1.3$	3.317	$\pm 1.4$
18.0	3.107	$\pm 0.9$	3.117	$\pm 1.3$	3.124	$\pm 1.5$	3.126	$\pm 1.6$
19.0	2.935	$\pm 1.1$	2.945	$\pm 1.4$	2.953	$\pm 1.7$	2.956	$\pm 1.8$
20.0	2.780	$\pm 1.2$	2.791	$\pm 1.6$	2.799	$\pm 1.9$	2.801	$\pm 2.0$
21.0	2.639	$\pm 1.3$	2.651	$\pm 1.7$	2.659	$\pm 2.1$	2.662	$\pm 2.2$
22.0	2.511	$\pm 1.4$	2.523	$\pm 1.9$	2.531	$\pm 2.3$	2.534	$\pm 2.4$
23.0	2.393	$\pm 1.6$	2.406	$\pm 2.1$	2.415	$\pm 2.5$	2.410	$\pm 2.6$
24.0	2.285	$\pm 1.7$	2.298	$\pm 2.3$	2.310	$\pm 2.7$	2.310	$\pm 2.9$
25.0	2.185	$\pm 1.9$	2.199	$\pm 2.5$	2.208	$\pm 3.0$	2.211	$\pm 3.1$
26.0	2.092	$\pm 2.0$	2.106	$\pm 2.7$	2.116	$\pm 3.2$	2.120	$\pm 3.4$
27.0	2.006	$\pm 2.2$	2.021	$\pm 3.0$	2.031	$\pm 3.5$	2.035	$\pm 3.7$
28.0	1.926	$\pm 2.4$	1.941	$\pm 3.2$	1.952	$\pm 3.8$	1.955	$\pm 4.0$
29.0	1.851	$\pm 2.6$	1.866	$\pm 3.5$	1.877	$\pm 4.1$	1.881	$\pm 4.3$
30.0	1.780	$\pm 2.8$	1.797	$\pm 3.7$	1.808	$\pm 4.4$	1.812	$\pm 4.6$
31.0	1.714	$\pm 3.0$	1.731	$\pm 4.0$	1.742	$\pm 4.7$	1.746	$\pm 4.9$
32.0	1.652	$\pm 3.2$	1.669	$\pm 4.3$	1.681	$\pm 5.0$	1.685	$\pm 5.2$
33.0	1.593	$\pm 3.5$	1.611	$\pm 4.6$	1.623	$\pm 5.4$	1.627	$\pm 5.6$
34.0	1.537	$\pm 3.7$	1.555	$\pm 4.9$	1.568	$\pm 5.7$	1.572	$\pm 6.0$
35.0	1.485	$\pm 3.9$	1.503	$\pm 5.2$	1.516	$\pm 6.1$	1.520	$\pm 6.4$
36.0	1.434	$\pm 4.2$	1.466	$\pm 5.6$	1.471	$\pm 6.5$	1.471	$\pm 6.8$
37.0	1.387	$\pm 4.5$	1.406	$\pm 5.9$	1.419	$\pm 6.9$	1.423	$\pm 7.3$
38.0	1.341	$\pm 4.8$	1.361	$\pm 6.3$	1.374	$\pm 7.4$	1.379	$\pm 7.7$
39.0	1.298	$\pm 5.1$	1.318	$\pm 6.7$	1.331	$\pm 7.8$	1.336	$\pm 8.2$
40.0	1.256	$\pm 5.4$	1.276	$\pm 7.1$	1.290	$\pm 8.3$	1.295	$\pm 8.7$
41.0	1.216	$\pm 5.7$	1.237	$\pm 7.5$	1.251	$\pm 8.7$	1.256	$\pm 9.2$
42.0	1.178	$\pm 6.1$	1.199	$\pm 8.0$	1.213	$\pm 9.2$	1.219	$\pm 9.7$
43.0	1.141	$\pm 6.4$	1.163	$\pm 8.4$	1.177	$\pm 9.8$	1.182	$\pm 10.2$
44.0	1.106	$\pm 6.8$	1.128	$\pm 8.9$	1.142	$\pm 10.3$	1.147	$\pm 10.8$
45.0	1.072	$\pm 7.2$	1.094	$\pm 9.4$	1.109	$\pm 10.9$	1.113	$\pm 11.4$
46.0	1.039	$\pm 7.6$	1.061	$\pm 9.9$	1.076	$\pm 11.5$	1.081	$\pm 12.0$
47.0	1.007	$\pm 8.0$	1.030	$\pm 10.4$	1.045	$\pm 12.1$	1.050	$\pm 12.6$
48.0	0.977	$\pm 8.5$	0.999	$\pm 11.0$	1.015	$\pm 12.7$	1.020	$\pm 13.2$
49.0	0.947	$\pm 8.9$	0.970	$\pm 11.6$	0.985	$\pm 13.4$	0.991	$\pm 14.0$
50.0	0.918	$\pm 9.4$	0.941	$\pm 12.2$	0.957	$\pm 14.0$	0.962	$\pm 14.7$
51.0	0.890	$\pm 9.9$	0.914	$\pm 12.8$	0.929	$\pm 14.8$	0.935	$\pm 15.4$
52.0	0.863	$\pm 10.5$	0.887	$\pm 13.5$	0.902	$\pm 16.2$	0.908	$\pm 16.2$
53.0	0.837	$\pm 11.0$	0.861	$\pm 14.2$	0.876	$\pm 16.3$	0.881	$\pm 17.0$
54.0	0.811	$\pm 11.6$	0.835	$\pm 14.9$	0.851	$\pm 17.1$	0.856	$\pm 17.8$
55.0	0.786	$\pm 12.2$	0.810	$\pm 15.7$	0.826	$\pm 17.9$	0.831	$\pm 18.7$

ended stubs will be determined for the capacitors ( $\epsilon_r = 2.17$ ).

It follows from Table 9.6 that the lowest practical characteristic impedance on a substrate with  $\epsilon_r = 2.17$  is approximately  $25\Omega$ . The susceptance of the  $0.485 \text{ pF}$  capacitor is  $12.189 \text{ mS}$  at  $4 \text{ GHz}$ , which leads to a value of  $3.28$  for the  $Y_0 / (\omega_H C)$  ratio in Table 9.7. Inspection of this table for  $u = 2$  ( $4 \text{ GHz} / 2 \text{ GHz}$ ), yields that the required line length will be around  $17^\circ$  (at  $4 \text{ GHz}$ ) if the error values are the same at the passband edges. The error in the reactance values will be around  $1\%$ . The expected error for the  $0.477 \text{ pF}$  capacitor is more or less the same.

If the error is not averaged over the passband and the capacitors are transformed exactly at the highest frequency in the passband instead, the line lengths required for the two capacitors (at  $4 \text{ GHz}$ ) are, respectively,

$$\beta l = \tan^{-1} \frac{Z_{0C}}{X_{HC}} = \tan^{-1} (25 / 1000 / (2\pi \times 4 \times 0.485)) = \tan^{-1} [25 / 82.04] = 16.9^\circ$$

and

$$\beta l = 16.7^\circ \text{ (0.477 pF).}$$

The expected errors at  $2 \text{ GHz}$  are

$$[25 / \tan \theta_L - 1 / (\omega_L C)] / (1 / \omega_L C) = 2.6\%$$

and  $2.1\%$ , respectively.

While the error in the reactance is larger in this case, the performance obtained in a wide-band network by replacing the shunt capacitors exactly at the highest frequency in the passband is often better than that obtained when the error values at the passband edges are chosen to be the same. The main reason for this is that the effect of a shunt capacitor is significantly greater at the higher frequencies in the passband when the passband is wide.

It follows from the above, that if the error is not averaged, series capacitors and shunt inductors should be replaced exactly at the lowest frequency in the passband, while series inductors (and shunt capacitors) should be replaced exactly at the highest frequency in the passband.

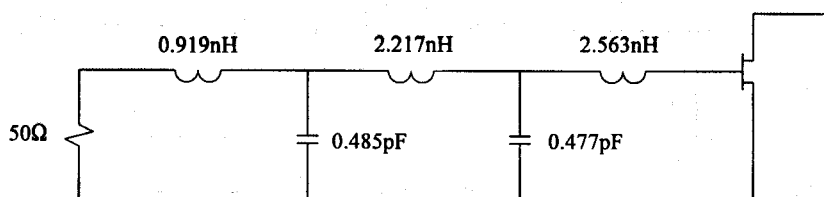


**Figure 9.5** The matching network considered in Example 9.2.

## 9.7 A TRANSMISSION LINE EQUIVALENT FOR A SYMMETRIC LOW-PASS T-SECTION OR PI-SECTION

Series inductors in lumped designs are often replaced with high characteristic impedance transmission lines. It was shown in Section 9.3 that the range of inductances that can be replaced in this way is limited. Where an inductor forms part of a low-pass PI-section, significantly better results can be obtained by replacing the inductance and some of the capacitance with a series line. Similarly, shunt capacitors forming part of a low-pass T-section can also be replaced with series lines. These two possibilities are illustrated in Figure 9.6.

An exact transmission line equivalent for any symmetric low-pass T- or PI-section can be obtained at any particular frequency by equating the transmission matrix of the section to be replaced to that of a transmission line.

The transmission matrix of the T-section shown in Figure 9.7(a) is

$$\begin{bmatrix} 1 - \omega^2 LC & j\omega L(2 - \omega^2 LC) / (1 - \omega^2 LC) \\ j\omega C & 1 - \omega^2 LC \end{bmatrix} \quad (9.45)$$

By equating this to

$$\begin{bmatrix} \cos(\beta l) & jZ_0 \sin(\beta l) \\ jY_0 \sin(\beta l) & \cos(\beta l) \end{bmatrix} \quad (9.46)$$

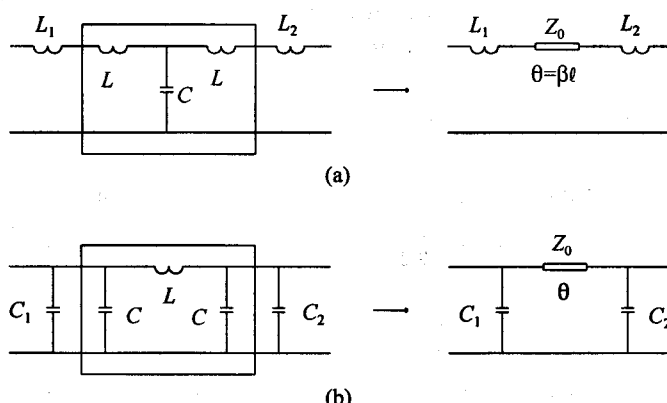


**Figure 9.6** The partial replacement of (a) a low-pass T-section and (b) a low-pass PI-section with a series line.

it follows that a transmission line with the following parameters will be exactly equivalent to the T-section at the frequency of interest ( $\omega$ ):

$$L' = \frac{L}{1 - \omega^2 LC} [2 - \omega^2 LC] \quad (9.47)$$

$$C' = \frac{C}{1 - \omega^2 LC} \quad (9.48)$$

$$Z_0 = \sqrt{\frac{L'}{C'}} \quad (9.49)$$

$$\beta l = \tan^{-1}(\omega \sqrt{L' C'}) \quad (9.50)$$

Excellent results can be expected when a T-section is replaced with a transmission line and the difference between the characteristic impedances and line lengths required for exact equivalents at the low and the high ends of the passband is negligible. Alternatively, the capacitance and inductance associated with a chosen line section at the lowest and at the highest frequency in the passband can be compared. The equations required for this purpose are

$$\omega L = Z_0 \frac{\sin(\beta l)}{1 + \cos(\beta l)} \quad (9.51)$$

$$\omega C = Y_0 \sin(\beta l) \quad (9.52)$$

where  $Y_0$  is the inverse of  $Z_0$ .

The equations associated with the PI-section equivalent of Figure 9.7(b) are

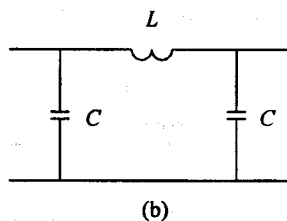
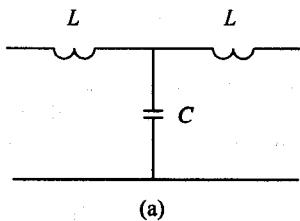


Figure 9.7 (a) A symmetrical low-pass T-section and (b) a symmetrical low-pass PI-section.

$$L' = \frac{L}{1 - \omega^2 LC} \quad (9.53)$$

$$C' = \frac{C}{1 - \omega^2 LC} [2 - \omega^2 LC] \quad (9.54)$$

and

$$Z_0 = \sqrt{\frac{L'}{C'}} \quad (9.55)$$

$$\beta l = \tan^{-1}(\omega \sqrt{L' C'}) \quad (9.56)$$

The inverse relationships are

$$\omega L = Z_0 \sin(\beta l) \quad (9.57)$$

and

$$\omega C = Y_0 \frac{\sin(\beta l)}{1 + \cos(\beta l)} \quad (9.58)$$

It follows from the equations given above that the length of the equivalent line for a T- or PI-section is only a function of the normalized reactance  $\omega L/Z_0$  and the normalized susceptance  $\omega C/Y_0$ , respectively. The following equations can be used to calculate the required normalized susceptance  $\omega C/Y_0$  and the line length corresponding to a specified normalized value for the reactance of the inductor in a PI-section:

$$\frac{\omega C}{Y_0} = \frac{Z_0}{\omega L} \left[ 1 - \sqrt{1 - \left( \frac{\omega L}{Z_0} \right)^2} \right] \quad (9.59)$$

and

$$\beta l = \tan^{-1} \frac{\omega L / Z_0}{\sqrt{1 - (\omega L / Z_0)^2}} \quad (9.60)$$

With  $\omega C$ ,  $\omega L$ , and  $Y_0$ ,  $Z_0$  interchanged, the same set of equations applies to a T-section.

The normalized reactance and susceptance corresponding to different line lengths are tabulated in Table 9.8. The deviations in the equivalent inductance and capacitance

**Table 9.8**

The normalized reactance/susceptance and susceptance/reactance of the components of the lumped PI-section/T-section equivalent of a series transmission line as a function of the line length and the percent deviation between these lumped components and those associated with a line length of  $10^\circ$

$\beta l$ (°)	$\omega L/Z_0   (\omega C/Y_0)$ (-; %)	$\omega C/Y_0   (\omega L/Z_0)$ (-; %)
10.0	0.1736 (0.0)	0.0875 (0.0)
12.5	0.2164 (-0.3)	0.1095 (0.1)
15.0	0.2588 (-0.6)	0.1317 (0.3)
17.5	0.3007 (-1.0)	0.1539 (0.5)
20.0	0.3420 (-1.5)	0.1763 (0.7)
22.5	0.3827 (-2.0)	0.1989 (1.0)
25.0	0.4226 (-2.6)	0.2217 (1.3)
27.5	0.4617 (-3.3)	0.2447 (1.7)
30.0	0.5000 (-4.0)	0.2679 (2.1)
32.5	0.5373 (-4.8)	0.2915 (2.5)
35.0	0.5736 (-5.6)	0.3153 (3.0)
37.5	0.6088 (-6.5)	0.3395 (3.5)
40.0	0.6428 (-7.4)	0.3640 (4.0)
42.5	0.6756 (-8.4)	0.3889 (4.6)
45.0	0.7071 (-9.5)	0.4142 (5.2)
47.5	0.7373 (-10.6)	0.4400 (5.9)
50.0	0.7660 (-11.8)	0.4663 (6.6)
52.5	0.7934 (-12.9)	0.4931 (7.3)
55.0	0.8192 (-14.2)	0.5206 (8.2)
57.5	0.8434 (-15.5)	0.5486 (9.0)
60.0	0.8660 (-16.9)	0.5774 (10.0)

compared to the values associated with a  $10^\circ$  line (same characteristic impedance) are also listed in the table. With the necessary changes, Table 9.8 also applies to T-sections.

Table 9.8 serves to provide an idea of how much the component values in the equivalent circuit change as the line length (and therefore the frequency) is increased. If the passband stretches from  $10^\circ$  up to  $20^\circ$  (octave bandwidth), the change in the equivalent inductance is less than 1.5%, while the capacitance changes by less than 0.7%.

Table 9.8 can also be used as a design aid when an inductor (or a capacitor) is to be replaced with an equivalent line. The change that can be tolerated in the inductance over the passband would determine the maximum electrical line length at the highest frequency in the passband. The reactance of the inductor at the highest frequency in the passband should be calculated next, after which the characteristic impedance required can be calculated by using the normalized reactance listed in the table. The parasitic capacitance is obtained similarly.

As an example of this, if the inductance variation should be less than 10%, the line length can be  $45^\circ$  at the highest passband frequency. It follows from this that the characteristic impedance required is  $70.7\Omega$ . The parasitic capacitive susceptance required is  $5.86 \text{ mS}$  ( $0.4142/70.7$ ).

**EXAMPLE 9.3** Replacing a lumped inductor with a line.

As an example of the application of the PI-section transformation, a transmission line equivalent for a series 2 nH inductor will be determined over the passband 2–8 GHz.

With  $Z_0 = 150\Omega$ , application of (9.59) and (9.60) yields that the required capacitance and the line length corresponding to an exact equivalent at 8 GHz are

$$C = 0.051 \text{ pF}$$

and

$$\beta l = 42.08^\circ$$

The PI-section equivalent for this line at 2 GHz ( $\beta l = 42.08/4 = 10.52^\circ$ ) can be found by using (9.57) and (9.58). The results are

$$L = 2.18 \text{ nH}$$

and

$$C = 0.049 \text{ pF}$$

which are close to the original values (within +9.0% and -7.3% respectively).

Better results can sometimes (narrowband cases) be obtained by minimizing the error across the passband. This can be done by lowering the frequency at which the transformation is exact iteratively. By selecting this frequency as 5.8 GHz, the line length becomes  $29.07^\circ$  (at 5.8 GHz) and the difference in inductance becomes 3.9% at 2 GHz and -3.9% at 8 GHz. The difference in the parasitic capacitance reduces to -1.9% and 2.0%, respectively.

**EXAMPLE 9.4** Distributed equivalents for a lumped-element network.

Consider the matching network shown in Figure 9.8. A distributed equivalent over the passband 2–6 GHz will be determined for it. This will be done by replacing the two series inductors and some of the shunt capacitance with two series transmission lines ( $Z_0 = 150\Omega$ ), after which the remaining capacitance will be replaced with open-ended stubs. The relative dielectric constant of the material is taken to be 2.17.

By applying (9.61) through (9.68) and changing the frequency of transformation iteratively, the optimum transformation frequency for both inductors is found to be approximately 5.74 GHz. The required line lengths and capacitance are

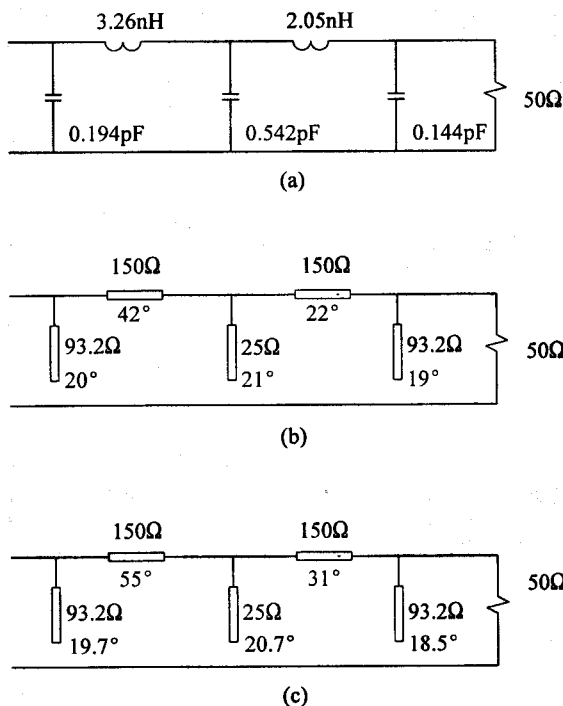


**Figure 9.8** (a) The matching network considered in Example 9.4, (b) a distributed equivalent obtained by minimizing the reactance errors, and (c) an alternative distributed equivalent (electrical lengths specified at 6 GHz).

42° and 0.03 pF for the 3.26 nH inductor and 22.2° and 0.047 pF for the 2.05 nH inductor. The maximum errors in the inductance over the passband are  $\pm 7.8\%$  and  $\pm 2.0\%$ , respectively.

After subtracting the capacitance required for the series lines, the new values for the shunt capacitance are found to be 0.102 pF (previously 0.194 pF), 0.402 pF (previously 0.542 pF), and 0.097 pF (previously 0.144 pF), respectively.

The reactances of the first and last capacitors are very high and the error resulting from transforming them to equivalent stubs will be very small. It follows by inspection of Table 9.7 that the error in susceptance will be less than 1.9% if  $X_{HC}/Z_0$  is equal to 2.799; that is,  $Z_0 = 93.2\Omega$ . With this value for the characteristic impedance, the required line lengths are approximately 20° for the 0.107-pF capacitor and 19° for the 0.097-pF capacitor.

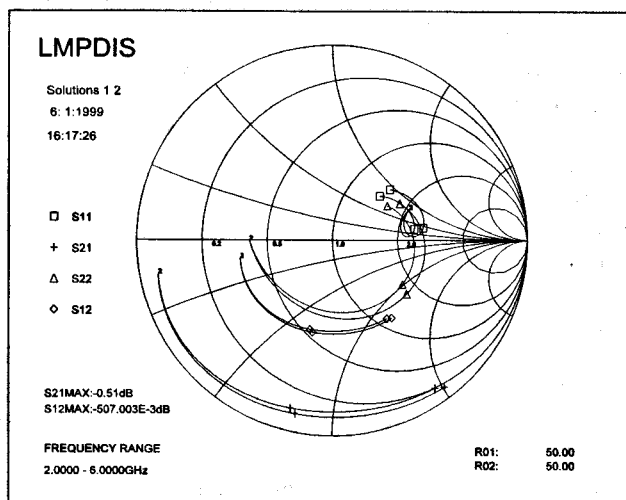
For minimum error, the 0.402-pF capacitor should be replaced with a low characteristic impedance line. A 25Ω line will be used in this case. The corresponding  $X_{HC}/Z_0$  ratio is then 2.647. Inspection of Table 9.7 yields that the error will be approximately 1.9%. The required line length is approximately 21°.

The transformed circuit is shown in Figure 9.8(b). The output voltage

**Table 9.9**  
Comparison of the input reflection coefficients ( $s_{11}$ ) of the three networks shown in Figure 9.8

Frequency (GHz)	$s_{11}$ (a) (dB, °)	$s_{11}$ (b) (dB, °)	$s_{11}$ (c) (dB, °)
2.00	-9.58 43.0	-11.13 53.1	-8.10 41.5
2.25	-8.91 37.7	-10.37 48.9	-7.51 36.3
2.50	-8.38 32.7	-9.75 44.9	-7.06 31.4
2.75	-7.97 27.9	-9.23 41.1	-6.73 26.8
3.00	-7.67 23.3	-8.81 37.4	-6.51 22.4
3.25	-7.48 18.9	-8.48 33.9	-6.38 18.2
3.50	-7.38 14.8	-8.22 30.5	-6.35 14.3
3.75	-7.37 11.1	-8.02 27.4	-6.41 10.8
4.00	-7.46 7.8	-7.89 24.6	-6.56 7.7
4.25	-7.65 5.1	-7.81 22.0	-6.81 5.1
4.50	-7.92 3.3	-7.78 19.8	-7.15 3.4
4.75	-8.28 2.7	-7.79 17.9	-7.57 2.7
5.00	-8.65 3.7	-7.84 16.5	-8.02 3.6
5.25	-8.93 6.8	-7.90 15.7	-8.40 6.5
5.50	-8.91 11.8	-7.96 15.5	-8.53 11.3
5.75	-8.42 17.5	-7.99 16.0	-8.22 17.0
6.00	-7.44 21.9	-7.94 17.1	-7.45 21.9

standing-wave ratio (VSWR) of the two-stage amplifier in which this network was used decreased from 1.72 to 1.65 with the transformation. The error in the input reflection coefficient of the network itself ( $s_{11}(b)$ ) is, however, not insignificant, as

**Figure 9.9**

Comparison of the  $S$ -parameters of the distributed equivalent shown in Figure 9.8(c) and the original lumped-element network (Figure 9.8(a)).

is illustrated in Table 9.9. The reflection coefficient of the original lumped-element network is listed as  $s_{11}(a)$  in this table.

Better results can be obtained by replacing the series inductors, and the capacitance remaining after this was done, exactly at the highest frequency in the passband (refer to Example 9.2). The distributed network obtained by doing this is shown in Figure 9.8(c). The input reflection coefficient of this network is also listed in Table 9.9. The S-parameters of this network are compared with those of the original lumped-element network in Figure 9.9. Note that the highest frequency on the different traces is not marked.

## 9.8 MICROSTRIP DISCONTINUITY EFFECTS AT THE LOWER MICROWAVE FREQUENCIES

Microstrip discontinuity effects associated with bends, curves, changes in the line width, T-junctions, crosses, and the open end of open-ended stubs add undesirable inductance and capacitance to designed circuits. The magnitude of these parasitics at the lower microwave frequencies (below X-band) [2] will be considered in this section. A compensation technique that can be used to reduce these effects [3] will also be considered.

### Open-Ended Stubs

The effect of the fringing capacitance associated with the open end of an open-ended stub is similar to extending the length of the line slightly.

The equivalent additional line length is given empirically by [13]. The expression for the phase shift (in degrees) is

$$\Delta\theta_{oc} = 4.944 \times 10^{-7} h f \sqrt{\epsilon_{r\_eff}} \frac{\epsilon_{r\_eff} + 0.300}{\epsilon_{r\_eff} - 0.258} \frac{W/h + 0.264}{W/h + 0.800} \quad (9.61)$$

where  $h$  is the thickness of the substrate (in meters) and  $f$  the frequency (in Hertz).

The maximum relative error in (9.61) as compared to the more accurate expression of Silvester and Benedek [15] is less than 4% for  $W/h \geq 0.2$  and  $2 \leq \epsilon_r \leq 50$  [13].

As an illustration of the magnitude of the open-end parasitic, the parasitic electrical line length (at 10 GHz) associated with different width-to-height ratios and dielectric constants ( $\epsilon_r = 2.5$  and  $\epsilon_r = 10.2$ ) are tabulated in Table 9.10 for a substrate with  $h = 0.635$  mm. It is clear from these results that the parasitic influence of an open end cannot be neglected at the higher frequencies and that this effect is more pronounced with higher dielectric constants and low impedance lines.

The simplest way to compensate for the increase in line length is to reduce the length of the designed line by the correct amount.

A distance of at least the equivalent line length should be allowed between the end of an open-ended stub and the substrate edge.

**Table 9.10**

The increase in electrical line length caused by an open end as a function of the dielectric constant and the width-to-height ratio of the line ( $f = 10$  GHz;  $h = 0.635$  mm)

$\epsilon_r$	$Z_0$ ( $\Omega$ )	$W/h$	$\theta$ ( $^\circ$ )
2.5	25	7.20	5.6
	50	2.80	5.0
	75	1.35	4.4
	100	0.70	3.7
	125	0.38	3.2
10.2	15	6.90	9.3
	25	3.35	8.4
	50	0.90	6.2
	75	0.30	4.5

### Steps in Width

The parasitic effect of a step junction is similar to that of an open end. The effect of the fringing capacitance associated with the wider line of the step discontinuity is similar to an increase in the length of that line. The change in the electrical length (in degrees) can be estimated by using the equation [16]

$$\Delta\theta_{\text{step}} = \Delta\theta_{\text{oc}} [1 - W_2 / W_1] \quad (9.62)$$

where  $\Delta\theta_{\text{oc}}$  can be calculated by using (9.61).

An alternative and more accurate approach to characterizing a step discontinuity is to use the equivalent circuit shown in Figure 9.10(b). An approximate expression for the inductance  $L_s = L_1 + L_2$  is ( $\pm 5\%$  for  $W_1 / W_2 \leq 5.0$  and  $W_2 / h = 1.0$ ) [13].

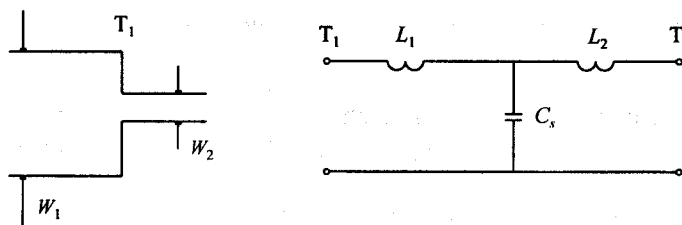


**Figure 9.10** The equivalent circuit of a step discontinuity.

$$L_s (\text{nH / m}) = 40.5 \left( \frac{W_1}{W_2} - 1.0 \right) - 75 \log \left( \frac{W_1}{W_2} \right) + 0.2 \left( \frac{W_1}{W_2} - 1 \right)^2 \quad (9.63)$$

The individual inductances are given by [13]

$$L_1 = L_{w1} / [L_{w1} + L_{w2}] \cdot L_s \quad (9.64)$$

and

$$L_2 = L_{w2} / [L_{w1} + L_{w2}] \cdot L_s \quad (9.65)$$

where  $L_{w1}$  and  $L_{w2}$  are the inductances associated with the characteristic impedances of the two lines.

An approximate closed form expression for the capacitance  $C_s$  in Figure 9.10(b) is ( $\pm 10\%$  for  $\epsilon_r \leq 10$  and  $1.5 \leq W_2 / W_1 \leq 3.5$ ) [13]

$$\frac{C_s}{\sqrt{W_1 W_2}} (\text{pF / m}) = [10.1 \log \epsilon_r + 2.33] \frac{W_1}{W_2} - 12.6 \log \epsilon_r - 3.17 \quad (9.66)$$

An idea of the magnitude of the parasitic effects associated with step discontinuities can be obtained from the extensions in line length resulting from an open-ended line as given in Table 9.10 and (9.62).

A first-order compensation technique for a step discontinuity would be to decrease the length of the wider line by the appropriate amount. The phase shift associated with a step discontinuity will always be less than that caused by an open end in a line with the lower characteristic impedance.

### Microstrip Bends

The equivalent circuit for a microstrip bend with lines of equal width is shown in Figure 9.11.

Closed-form expressions for the right-angled bend discontinuity capacitance and inductance are [2]

$$\frac{C_b}{W} (\text{pF / m}) = \begin{cases} \frac{(14\epsilon_r + 12.5)W/h - (1.83\epsilon_r - 2.25)}{\sqrt{W/h}} + \frac{0.02\epsilon_r}{W/h} & (W/h \leq 1) \\ (9.5\epsilon_r + 1.25)W/h + 5.2\epsilon_r + 7.0 & (W/h \geq 1) \end{cases} \quad (9.67)$$

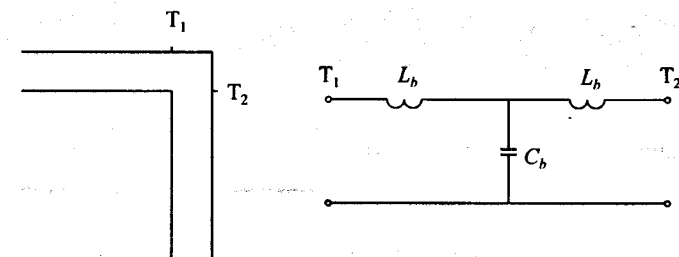


**Figure 9.11** Equivalent circuit for a microstrip bend.

$$L_b / h (\text{nH/m}) = 100[4\sqrt{W/h} - 4.21] \quad (9.68)$$

Equation (9.67) is accurate to within 5% for  $2.5 \leq \epsilon_r \leq 15$  and  $0.1 \leq W/h \leq 5$ . The accuracy of (9.68) is about 3% for  $0.5 \leq W/h \leq 2.0$  [13].

**Table 9.11**

The VSWR (theoretical) associated with an unchamfered  $90^\circ$  bend in a  $75 \Omega$  ( $\epsilon_r = 2.5$ ) and a  $50\Omega$  ( $\epsilon_r = 10.2$ ) line as a function of the frequency ( $h = 0.508 \text{ mm}$ )

$\epsilon_r$	$Z_0$ ( $\Omega$ )	$f$ (GHz)	VSWR
2.5	75	2	1.03
		4	1.06
		8	1.12
		10	1.15
10.2	50	2	1.06
		4	1.13
		8	1.28
		10	1.36

An idea of the magnitude of the parasitics associated with a bend discontinuity can be obtained from Table 9.11. The theoretical VSWRs associated with two bends are shown in this table as a function of the frequency.

Although the effect of a single bend may be small at the lower microwave frequencies, it should be kept in mind that it will increase with frequency, the number of bends used in cascade, and the line width.

The parasitic effects of bend discontinuities are usually reduced by mitering the bend as shown in Figure 9.12. The optimum value of  $L$  in this figure is about  $1.8 \text{ W}$  for  $50\Omega$  lines on alumina and rexolite substrates, and it seems to be independent of the bend angle [2].

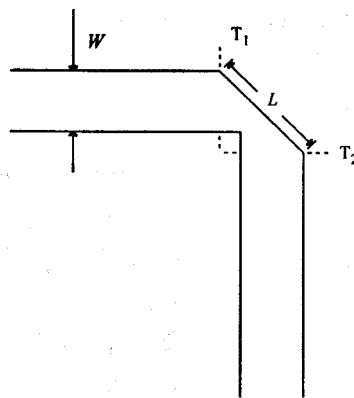


**Figure 9.12** Compensation of a microstrip bend.

When  $W/h \geq 0.25$  and  $\epsilon_r \leq 25$ , the length  $L$  can be calculated by using the following equation:

$$L/W = \sqrt{2} [1.04 + 1.3 e^{-1.35W/h}] \quad (9.69)$$

The equivalent electrical line length of the mitre ( $l$ ) can be estimated by using the equation

$$l = L/\sqrt{2} \quad (9.70)$$

When the line is too thin ( $W/h \leq 0.25$ ) the optimum miter cannot be used.

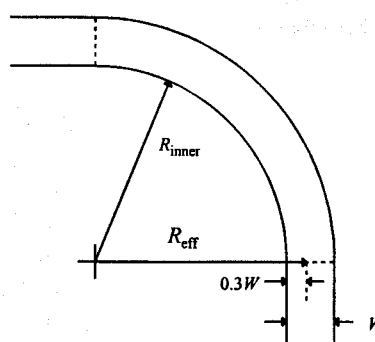


**Figure 9.13** The effective curving radius when a line is curved.

Curving a line is frequently a better option than mitering it. When the curving radius is larger than twice the width of the line, the main parasitic effect is a change in the effective line length. The effective length of the curve ( $3 < R/W < 7$ ) can be estimated by assuming the effective radius to be [17]

$$R_{\text{eff}} = R_{\text{inner}} + 0.3W \quad (9.71)$$

This is illustrated in Figure 9.13.

Curving a line also has the advantage that the direction of the line can be changed with any arbitrary angle.

### T-Junctions

Hammerstad's approach [16] to characterizing the parasitic effects of a T-junction with constant main-line width is illustrated in Figure 9.14. The different parameters are defined by the following equations:

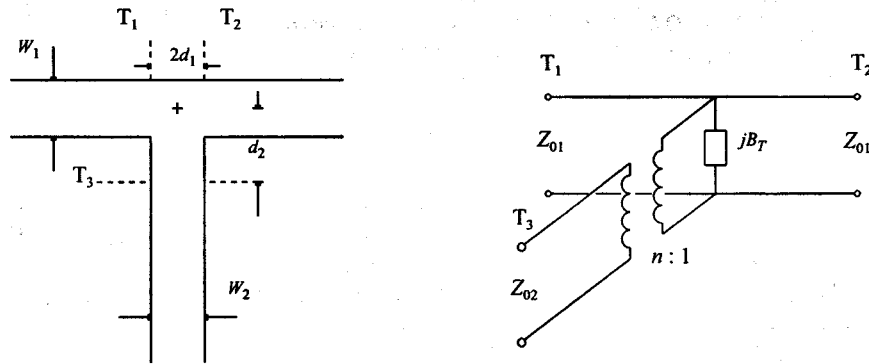


**Figure 9.14** The equivalent circuit for a microstrip T-junction.

$$D_1 = 120\pi h / Z_{01}(\text{air}) \quad D_2 = 120\pi h / Z_{02}(\text{air}) \quad (9.72)$$

$$d'_2 = \frac{D_1}{2} - d_2 \quad (9.73)$$

$$n^2 = \left\{ \frac{\sin\left(\frac{\pi}{2} \frac{2D_1}{\lambda_m} \frac{Z_{01}}{Z_{02}}\right)}{\frac{\pi}{2} \frac{2D_1}{\lambda_m} \frac{Z_{01}}{Z_{02}}} \right\}^2 \left\{ 1 - \left( \frac{\pi}{\lambda_m} \frac{2D_1}{D_1} \frac{d'_2}{D_1} \right)^2 \right\} \quad (9.74)$$

$$d_1 / D_2 = 0.05n^2 Z_{01} / Z_{02} \quad (9.75)$$

$$\begin{aligned} d_2' / D_1 = & \{0.076 + 0.2(2D_1 / \lambda_m)^2 + 0.663 e^{-1.71Z_{01}/Z_{02}} \\ & - 0.172 \ln(Z_{01} / Z_{02})\} Z_{01} / Z_{02} \end{aligned} \quad (9.76)$$

$$\frac{B_T \lambda_m}{Y_{01} D_1} = \begin{cases} -[1 - 2D_1 / \lambda_m] Z_{01} / Z_{02} & Z_{01} / Z_{02} \leq 0.5 \\ [1 - 2D_1 / \lambda_m][3Z_{01} / Z_{02} - 2] & Z_{01} / Z_{02} \geq 0.5 \end{cases} \quad (9.77)$$

$$\lambda_m = \lambda_0 / \sqrt{\epsilon_{r\_eff}} \quad (9.78)$$

When  $Z_{01} / Z_{02} \geq 2$ , the calculated value of  $d_2 / D_1$  is too high. In this range, a better value for  $d_2$  can be obtained by replacing  $Z_{01} / Z_{02}$  in (9.76) with its inverse [16].

T-junctions can be compensated easily for the reference plane offsets by simply adjusting the lengths of the different lines. The offset in the main line is usually very small, and the main effect is on the length of the stub.

The best solution to the transformer effect is to keep the width of the stub narrow enough for the transforming effect to be negligible ( $n$  should be close to unity).

Because of the approximate nature of the equation for the loading susceptance at the junction, no compensation for this effect is recommended. As with the transformer effect, the best option is again to limit the stub width to values for which the loading susceptance will be negligible. If this cannot be done, a better model for the junction should be obtained or physical compensation of the junction should be considered [18].

### Crosses

As a first order approximation, a cross can be considered to be two T-junctions in parallel.

### Via Holes

The best option when short circuits (connections to the ground plane) are required is to use via holes. The parasitic effect of a via hole is usually not severe and the same performance can be expected every time (repeatability).

Via holes are made by drilling holes in the substrate at the appropriate positions before the tracks are etched (a drill file is usually created for this purpose), after which the substrate is treated chemically and metal is deposited electrolytically or by sputtering on the cylindrical surface of these holes. Manufacturing reliable via holes in teflon substrates is not a simple matter and is best left to experts.

The main parasitic associated with the hole itself is the inductance to ground. Depending on the diameter and the substrate thickness, this inductance is usually very

small. The via hole inductance (cylindrical via hole) can be estimated by using the following equation [19]:

$$L_{\text{via}} = \frac{\mu_0}{2\pi} \left[ h \cdot \ln \left( \frac{h + \sqrt{r^2 + h^2}}{r} \right) + \frac{3}{2} (r - \sqrt{r^2 + h^2}) \right] \quad (9.79)$$

where  $h$  is the substrate height and  $r$  is the radius of the hole.

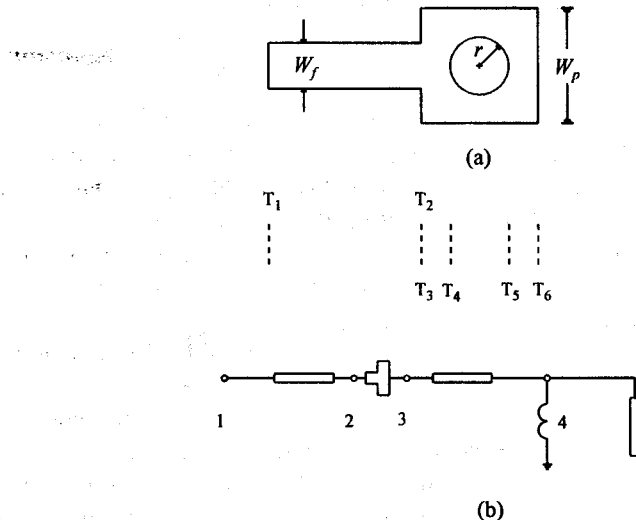


**Figure 9.15** (a) A single via hole and (b) an equivalent circuit for it.

The parasitics associated with the via hole pad and any step associated with the feeding line will often dominate the effect of the via and will usually increase the effective inductance of the via significantly. An equivalent circuit for the via hole is shown in Figure 9.15(b). Note that the length of the open stub used is determined by the pad section to the right of the via hole (T<sub>5</sub> to T<sub>6</sub>).

#### EXAMPLE 9.5     An artwork example.

Application of some of the material in this section is illustrated in Figure 9.16. The artwork of the synthesized [20] GSM (global mobile system) amplifier shown in Figure 9.16(b) was modified to that shown in Figure 9.16(c) by adding via holes to provide the ground connections required and by curving and bending (optimal mitre) some of the lines to reduce the size of the artwork. The lengths of the relevant lines were adjusted to compensate for the effect of the changes made.

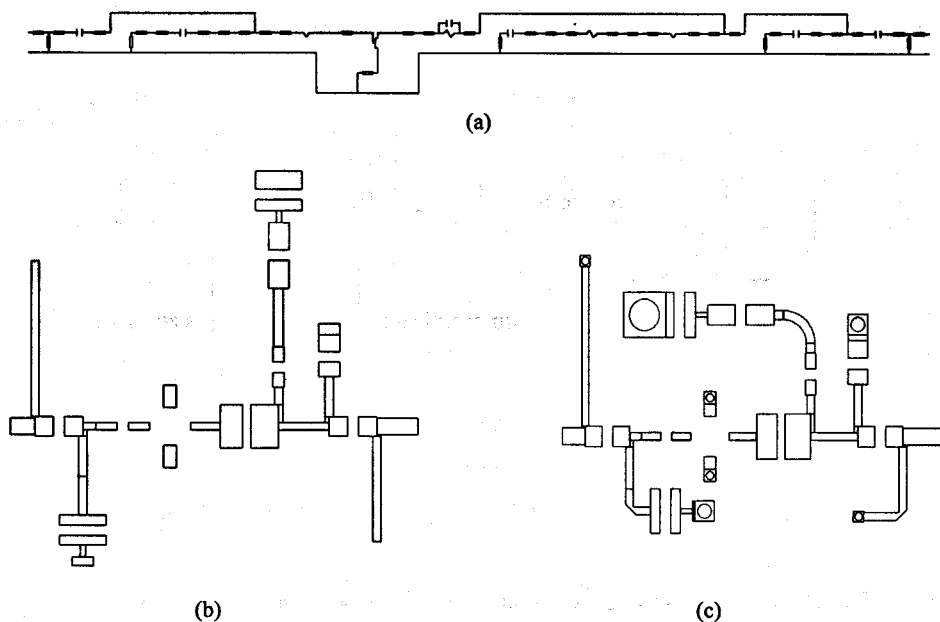


**Figure 9.16** (c) Modification of the artwork of a GSM amplifier (a, b) by adding via holes to provide the ground connections required and by bending and curving some lines to reduce its size (Courtesy of Grinaker Avtronics, Highveld Technopark, South Africa).

The performance of the amplifier before and after the modifications is essentially the same ( $G_T = 14$  dB;  $F = 0.5$  dB).

## 9.9 A COMPENSATION TECHNIQUE FOR MICROSTRIP DISCONTINUITIES

It is possible to reduce the parasitic effects associated with open ends, steps, bends, and T-junctions by using constant impedance tapers. The basic idea is illustrated in Figure 9.17. The characteristic impedance of an incremental section of the line is a function of the effective dielectric constant and the capacitance to ground. The capacitance consists of plate capacitance and fringing capacitance associated with the edge. If the line width is reduced smoothly, the plate capacitance is reduced, but the fringing capacitance is increased. If the line width is reduced fast enough, the total capacitance can be kept constant, while the line width is reduced.

In the case of a step, the width can be reduced until it is the same as that of the narrower line. The width should be reduced to approximate a point junction when an open-end or a T-junction is compensated (i.e., the width should be reduced to a predetermined limit that is mainly a function of the current density).

This compensation technique was introduced for striplines by Malherbe and Steyn [3]. The same approach can be followed with microstrip lines and the relevant equations will be derived here.

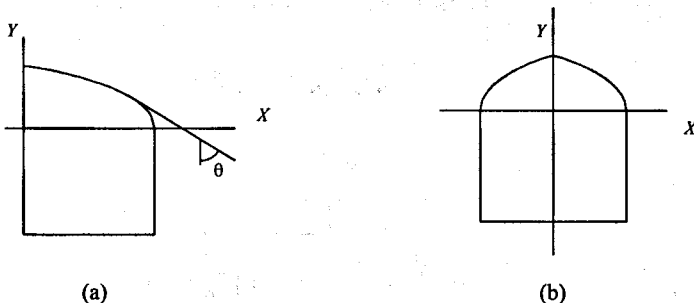


**Figure 9.17** (a) An asymmetrical and (b) a symmetrical constant impedance taper.

The characteristic impedance of an incremental section of the line is given by

$$Z_0 = 1 / [v_p C] \quad (9.80)$$

$$= \sqrt{\epsilon_r} / [cC] \quad (9.81)$$

where  $\epsilon_r$  is the relative effective dielectric constant of the line,  $c$  the speed of light, and  $C$  the capacitance per unit length. If the characteristic impedance is to remain constant with the narrowing width-to-height ratio, the quotient  $C / \sqrt{\epsilon_r}$  in (9.81) must remain constant.

The capacitance corresponding to a section with incremental length  $dy$  and the untapered width  $W$  is given by

$$C_w dy = \epsilon_0 \epsilon_r (W/h) dy + \epsilon_0 (W/H_2) dy + 2C_{fw} dy \quad (9.82)$$

where  $\epsilon_r$  is the effective dielectric constant of the material used,  $C_{fw}$  the fringing capacitance per unit length corresponding to the width  $W$ ,  $H_2$  the distance from the conductor to the cover, and  $h$  the substrate thickness.

The capacitance corresponding to an incremental section of an asymmetrical line with tapered width  $x$  is given by

$$C_x dy = [\epsilon_0 \epsilon_r (x/h) + \epsilon_0 (x/H_2) + C_{fx} + C_{fx} \sec \theta] dy \quad (9.83)$$

The fringing capacitance ( $C_{fx}$ ) is a function of the characteristic impedance and the effective relative dielectric constant of an untapered line with width  $x$ . It can be calculated as follows:

$$C_{fx} = 0.5 [\sqrt{\epsilon_{\infty}} / (cZ_{0x}) - \epsilon_0 \epsilon_r x / h - \epsilon_0 x / H_2] \quad (9.84)$$

$\epsilon_{rx}$  is the effective dielectric constant of the untapered line (width  $x$ ). This equation can be derived by combining (9.81) and (9.82) with  $W$  set equal to  $x$  in (9.82).

By equating the characteristic impedances at  $x$  and  $W$ , the following result is obtained:

$$1 + \sec \theta = \left\{ \sqrt{\frac{\epsilon_{rx}}{\epsilon_{rw}}} \left[ \frac{\epsilon_0 \epsilon_r W}{h} + \frac{\epsilon_0 W}{H_2} + 2C_{fw} \right] - \frac{\epsilon_0 \epsilon_r x}{h} - \frac{\epsilon_0 x}{H_2} - C_{fx} \right\} / C_{fx} \quad (9.85)$$

With  $\theta$  known as a function of  $x$ , it is a simple matter to construct the taper. Alternatively, the exact position  $y$  where the taper width is equal to  $X$  can be determined numerically by evaluating the integral

$$y = - \int_w^x \cot \theta dx \quad (9.86)$$

The length of the taper can be determined by setting the boundary  $X$  in (9.86) equal to the final value of  $x$ .

The electrical length of the tapered section can be obtained with the following equation:

$$\Delta\theta(\text{degrees}) = 306(f/c) \int_w^x -\sqrt{\epsilon_x} \cot \theta dx \quad (9.87)$$

where  $f$  is the frequency of interest and  $X$  is the final value of  $x$ .

When a symmetrical taper is required, (9.86) and (9.87) can be used in conjunction with the following equations:

$$C_{fx} = 0.5 [\sqrt{\epsilon_{rx}} / (cZ_{0x}) - \epsilon_0 \epsilon_r 2(x/h) - \epsilon_0 2(x/H_2)] \quad (9.88)$$

$$\sec \theta = \left\{ \sqrt{\frac{\epsilon_{rx}}{\epsilon_{rw}}} \left[ \frac{\epsilon_0 \epsilon_r W}{h} + \frac{\epsilon_0 W}{H_2} + 2C_{fw} \right] - \frac{\epsilon_0 \epsilon_r 2x}{h} - \frac{\epsilon_0 2x}{H_2} \right\} / [2C_{fx}] \quad (9.89)$$

Application of the tapering technique to reduce the effect of step junctions is illustrated in Figure 9.18.

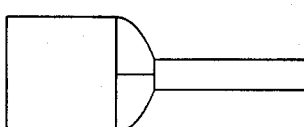


**Figure 9.18** The tapering technique applied to reduce the discontinuity effects associated with a step-junction.

## REFERENCES

1. March, S., "Microstrip Packaging: Watch The Last Step," *Microwaves*, December 1981.
2. Gupta, K. C., R. Garg, and I. J. Bahl, *Microstrip Lines and Slotlines*, Norwood, MA: Artech House, 1979.
3. Malherbe, J. A. G., and A. F. Steyn, "The Compensation of Step Discontinuities in TEM-Mode Transmission Lines," *IEEE Trans. Microwave Theory Tech.*, Vol. MTT-26, No. 11, November 1978.
4. Terman, F. E., *Radio Engineers Handbook*, New York: McGraw-Hill, 1943.
5. Young, L., *Advances in Microwaves*, New York: Academic Press, 1977.
6. Gupta, K. C., R. Garg, and R. Chadha, *Computer-Aided Design of Microwave Circuits*, Norwood, MA: Artech House, 1981.
7. Chaddock, R. E., "The Application of Lumped Element Techniques to High Frequency Hybrid Integrated Circuits," *Radio and Electronics Engg.* (GB), Vol. 44, 1974, pp. 414-420.
8. Dukes, J. M. C., *Printed Circuits, Their Design and Application*, London: MacDonald, 1961, pp. 120-135.
9. March, S. L., "Simple Equations Characterize Bond Wires," *Microwaves & RF*, November 1991, pp. 105-110.
10. Dill, H. G., "Designing Inductors for Thin-Film Applications," *Electron. Des.*, February 17, 1967, pp. 52-59.
11. Caulton, M., S. P. Knight, and D. A. Daly, "Hybrid Integrated Lumped-Element Microwave Amplifiers," *IEEE J. Solid-State Circ.*, Vol. SC-3, No. 2, June 1968.
12. "RF and Microwave Porcelain Capacitors," Cazenovia, NY: Dielectric Laboratories, Inc., 1998.
13. Garg, R., and I. J. Bahl, "Microstrip Discontinuities," *Int. J. Electronics*, Vol. 45, July 1978.
14. Alley, G. D., "Interdigital Capacitors and Their Application to Lumped-Element Microwave Integrated Circuits," *IEEE Trans. Microwave Theory Tech.*, Vol. MTT-18, No. 12, December 1970.

15. Silvester, P., and P. Benedek, "Equivalent Capacitance of Microstrip Open Circuits," *IEEE Trans. Microwave Theory Tech.*, Vol. MTT-20, 1972, pp. 511-516.
16. Hammerstad, E. O., "Equations for Microstrip Circuit Design," *Conference Proceedings*, 5<sup>th</sup> European Microwave Conference, September 1975, Hamburg.
17. Foundry Manual, GaAs Foundry Services, Texas Instruments, Inc., January 1991.
18. Chadha, R., and K. C. Gupta, "Compensation of Discontinuities in Planar Transmission Lines," *IEEE Trans. Microwave Theory Tech.*, Vol. MTT-30, No. 12, December 1982, pp. 2151-2156.
19. Goldfarb, M. E., and R. A. Pucel, "Modeling Via Hole Grounds in Microstrip," *IEEE Microwave and Guided Wave Letters*, Vol. 1, No. 6, June 1991.
20. *MultiMatch RF and Microwave Impedance-Matching, Amplifier and Oscillator Synthesis Software*, Somerset West, RSA: Ampsa (PTY) Ltd; <http://www.ampsap.com>.

## SELECTED BIBLIOGRAPHY

- De Brecht, R., and M. Caulton, "Lumped Elements in Microwave Integrated Circuits in the 1-12 GHz Range," *IEEE G-MTT Internat. Microwave Symp.*, May 1970, p. 14.
- Hammerstad, E. O., and F. Bekkadal, *Microstrip Handbook*, ELAB Report STF 44/A74 169, University of Trondheim, Norwegian Institute of Technology, 1975.
- Hammerstad, E. O., and O. Jensen, *IEEE MTT-S Symposium Digest*, June 1980, pp. 407-409.
- Pettenpaul E., H. Kapusta, A. Weisgerber, H. Mampe, J. Luginsland, and I. Wolff, "CAD Models of Lumped Elements on GaAs up to 18GHz," *IEEE Trans. Microwave Theory Tech.*, Vol. 36, No. 2, February 1988.
- Sobel, H., "Application of Integrated Circuit Technology to Microwave Frequencies," *Proc. IEEE*, Vol. 59, August 1971, pp. 1200-1211.

## **CHAPTER 10**

# **THE DESIGN OF RADIO-FREQUENCY AND MICROWAVE AMPLIFIERS AND OSCILLATORS**

### **10.1 INTRODUCTION**

In this chapter the design of radio-frequency and microwave amplifiers and oscillators will be considered. Many of the considerations applying to amplifiers also apply to oscillators and vice versa.

Basic considerations such as stability, tunability, and unilaterality will be introduced first. The dynamic range of an amplifier was considered in Chapter 2.

Stability is evaluated in terms of stability circles or in terms of the Rollette and the Sterne stability factors. The Linville stability factor will also be considered.

Experience has shown that the loop gain should also be evaluated when the stability of an amplifier is considered. The gain and phase margins associated with the loop gain should be calculated for each stage in which feedback is used.

It is important to understand that the stability factors normally used are “black-box” parameters and provide no information on the effect that component tolerances (sometimes very small changes) can have on the stability of the circuit. In contrast, the loop gain is applied at the source of the instability (the various feedback loops) and provides a much clearer picture of the stability situation.

By using and extending the material provided in Chapters 1 and 2, a wide range of amplifiers can be designed.

The basic procedure proposed here for the design of cascade amplifiers is summarized in the flow diagram shown in Figure 10.1 [1]. The procedure consists basically of designing the stages in the amplifier chain sequentially from one side to the other. Each stage is designed by first adding feedback and/or loading networks to the transistor selected, after which the performance targeted for that stage is realized with a lossless impedance-matching network.

The two amplifiers shown in Figure 10.2 are examples of cascade amplifiers designed by following this approach. The first amplifier is a switched amplifier module covering the frequency range 2–18 GHz, while the second is a GSM amplifier (905–915 MHz). Couplers were used in both amplifiers to improve the VSWRs.

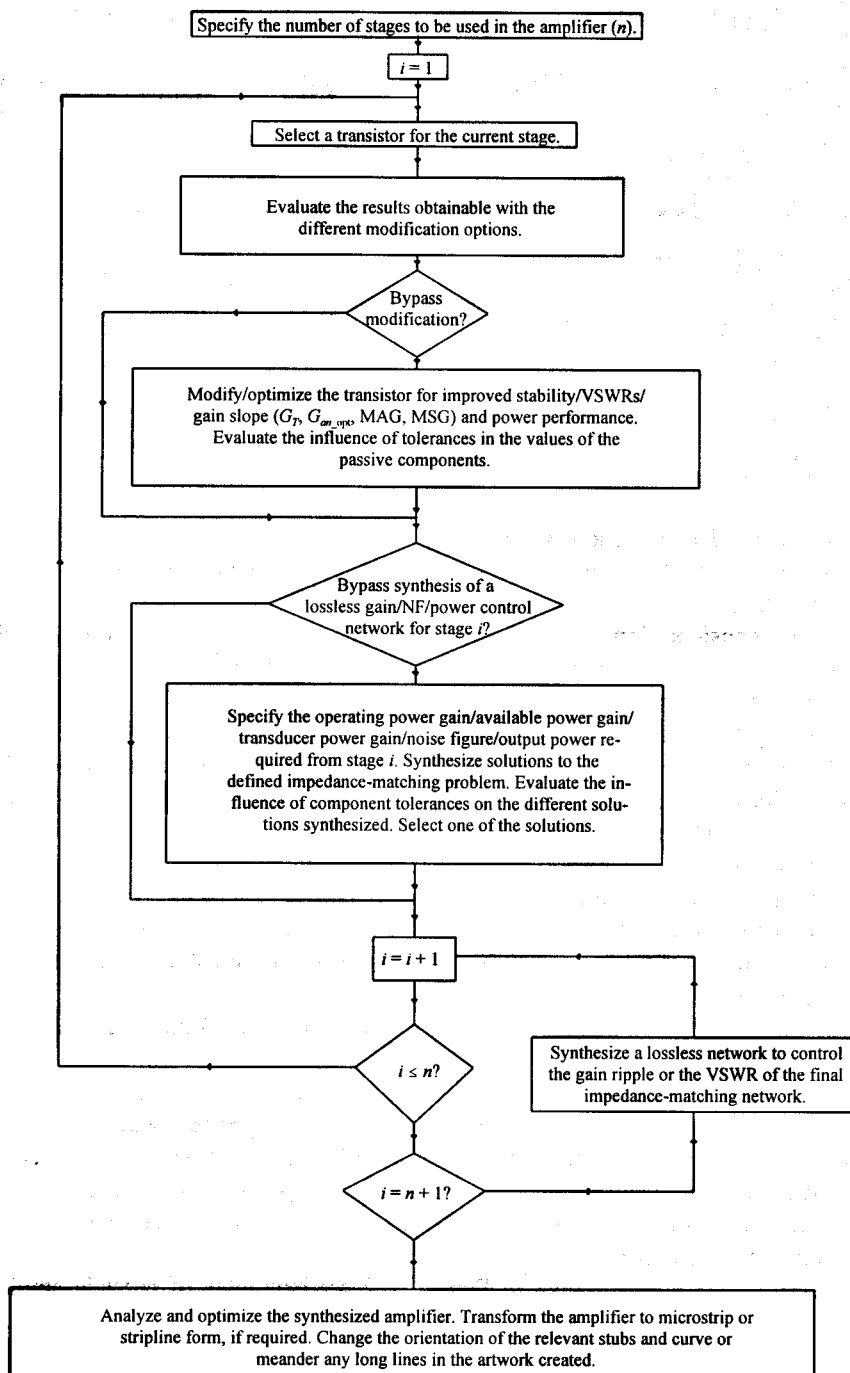
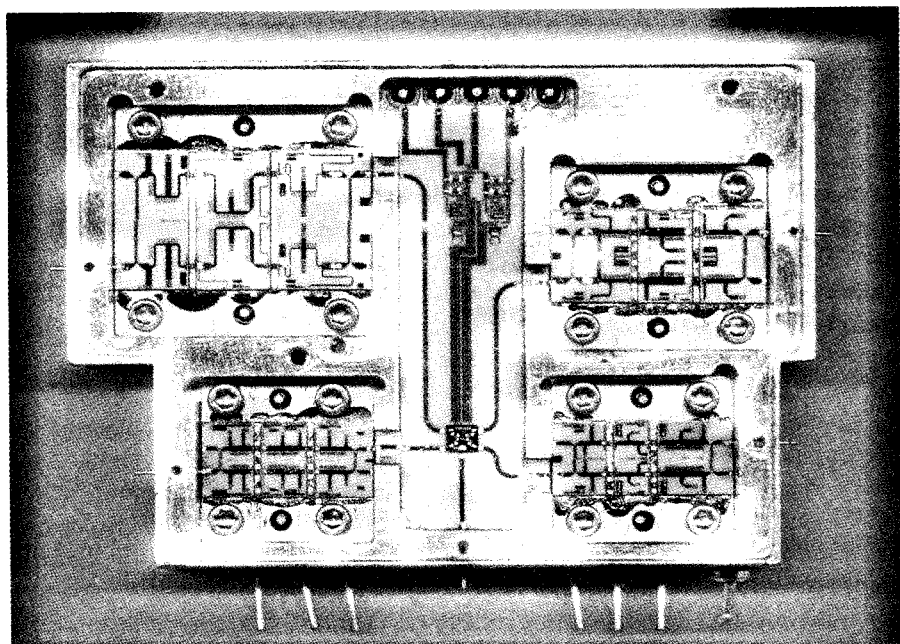
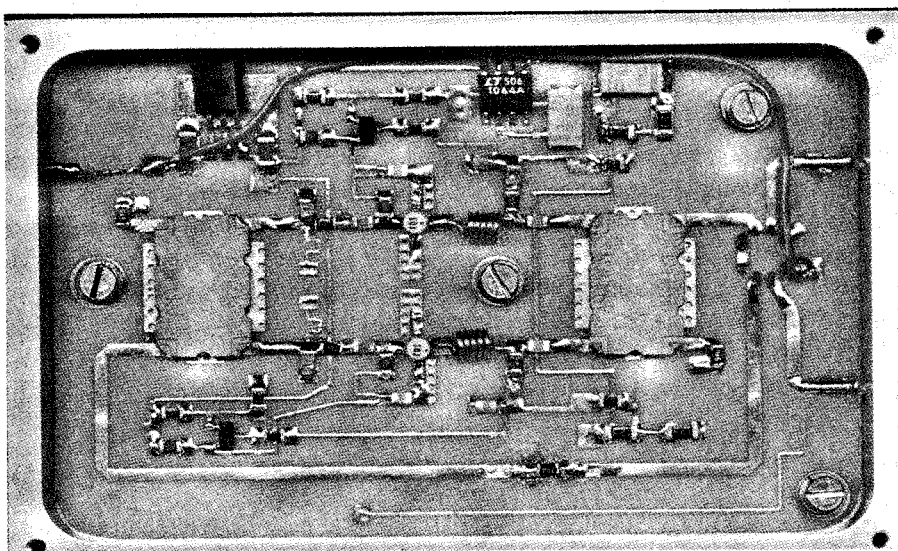


**Figure 10.1** A flow diagram of a typical amplifier synthesis cycle [1].



(a)



(b)

**Figure 10.2** (a) A switched amplifier module (2–18 GHz; the switching is done on the output sides of the different modules) and (b) a GSM amplifier (Courtesy of Grinaker Avitronics, Highveld Technopark, South Africa).

It will be shown here that when wideband amplifiers are designed, device-modification (adding resistive feedback and/or loading sections to the transistors used) is probably the most critical step in the design cycle. Device-modification serves to exchange the excess in gain and noise capabilities at the lower frequencies for more desirable characteristics (improved stability, gain leveling, lower VSWRs). It can also be used to bring the optimum noise or power match closer to a conjugate match.

Amplifiers with excellent noise performance and low input VSWRs are often required. If hybrid couplers or isolators cannot be used (losses, cost factor, etc.), the first step in realizing such an amplifier is device-modification. If the VSWR associated with the optimum noise match is still not satisfactory, the nonzero  $s_{12}$  of the modified transistor is often used to improved the input VSWR. The design of a high power stage with a good output match proceeds along similar lines.

The gain of each amplifier stage is controlled by its operating, available, or transducer power gain. In doing this, it is not necessary to ignore the effect of the reverse transfer gain ( $s_{12}$ ) as is often done.

The design of matching networks for passive problems was considered in Chapter 8. It will be shown here that, if the (modified) transistor is inherently stable, the active gain or noise figure control problems can be transformed exactly to equivalent passive problems. The impedance-matching techniques outlined can therefore also be used to solve active problems.

Note that inherent stability is not required when the noise figure is controlled.

It is important to realize that the correct choice for the transistor to be used in a particular stage can have a dramatic effect on both the performance and the sensitivity. The same can be said for using a suitable network to control the gain, the noise figure, or the output power of each stage. In order to find the right network, the capability of synthesizing over different topologies is essential.

When a high dynamic range amplifier is required at RF frequencies, a lossless feedback amplifier should be considered. The performance obtainable with these amplifiers is excellent. It should be noted, however, that with careful design and the right choice of the transistor, similar performance can often be obtained with a cascade amplifier. Lossless feedback amplifiers will be considered in Section 10.10.

The design of reflection and balanced amplifiers will be also considered. For an excellent treatment on the design of distributed amplifiers refer to [2].

Oscillator design will be considered in section 10.13.

## 10.2 STABILITY

In order to design an oscillator or to prevent an amplifier from oscillating, it is necessary to know more about the conditions under which oscillations can occur. These conditions will be established here.

It will be shown that steady-state oscillations will occur when the input and output admittance of an active circuit is equal to zero. Oscillation is not possible at any frequency at which the input conductance is positive or, equivalently, the magnitude of the input and

output reflection coefficients are smaller than unity. The boundary condition at which the input conductance is equal to zero or the magnitude of the reflection coefficient is equal to unity will be considered on the admittance plane and on the Smith Chart, respectively. It will be shown that the stable and potentially unstable areas are separated by circles in both planes. The area inside the relevant circle is usually the area of potential instability.

When oscillations cannot occur with any passive termination, a transistor is said to be inherently stable.

The stability of a two-port can be considered by establishing the positions of the stability circles on the plane of interest or by calculating various stability factors defined for this purpose. The Rollette, the Sterne, and the Linville stability factors are frequently used.

Although essential, the stability factors by themselves do not provide sufficient information on the stability of an amplifier. The main problem is that the stability of the two-port as a whole is considered without reference to the specific cause of the instability (the intrinsic and/or external feedback loops). Small changes in the component values can sometimes have a very pronounced effect on the stability factors. In order to get a clearer picture of the situation, the following should also be done:

1. The series or shunt stabilizing resistance required on either or both sides of the two-port should be calculated (see Figure 10.3). In the well-behaved case, the series resistance required will decrease with increasing frequency. Similarly, the shunt resistance will increase with increasing frequency.

Note that the use of stabilizing components is not necessarily intended. The resistance required, however, provides a good idea of how severe the potential instability is.

2. The loop gain for each transistor stage to which external feedback is applied should be calculated and the associated gain and phase margins should be established. If more than one loop is used, the gain for each loop should be calculated.

It is important to realize that the loop-gain is dependent on the ter-

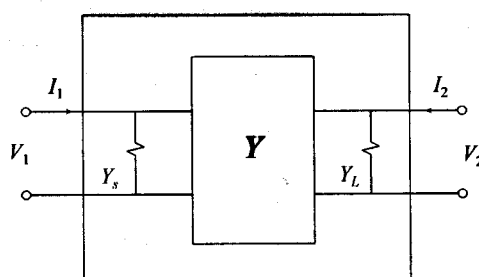


Figure 10.3 A two-port network augmented with its terminations.

minations used. The actual terminations of interest should be used (usually  $50\Omega$ ).

3. The reflection gain at the input and the output of each (modified) transistor should be calculated.

The reflection gain is also dependent on the terminations used.

It should be noted that oscillations will start up because of favorable loop gain conditions and may also start up because of favorable reflection conditions (negative resistance). At steady-state these conditions will apply simultaneously.

Calculation of the stability circles, the stability factors, the stabilizing resistance, and the loop and reflection gain will be considered in this section.

### 10.2.1 Stability Circles on the Admittance Plane

Consider the two-port network in Figure 10.3. The terminal currents of the two-port augmented with its terminations can be calculated by using the equation

$$\begin{bmatrix} I_1 \\ I_2 \end{bmatrix} = \begin{bmatrix} y_{11} + Y_s & y_{12} \\ y_{21} & y_{22} + Y_L \end{bmatrix} \begin{bmatrix} V_1 \\ V_2 \end{bmatrix} \quad (10.1)$$

If the circuit is oscillating, the terminal voltages will not be equal to zero, even though the terminal currents are equal to zero.

In order for the voltages in (10.1) not to be equal to zero while the currents are equal to zero, the determinant of the extended  $Y$ -parameter matrix must be equal to zero. Were this not the case, the  $Y$ -parameter matrix would have had an inverse, and the only solution corresponding to zero values for  $I_1$  and  $I_2$  would have been zero values for both  $V_1$  and  $V_2$  as well.

A zero value for the determinant implies that

$$[y_{11} + Y_s][y_{22} + Y_L] - y_{12}y_{21} = 0 \quad (10.2)$$

leading to

$$y_{11} + Y_s - \frac{y_{12}y_{21}}{y_{22} + Y_L} = 0 \quad (10.3)$$

and

$$y_{22} + Y_L - \frac{y_{12}y_{21}}{y_{11} + Y_s} = 0 \quad (10.4)$$

The last two equations are easily recognized as the equations for the input and output

admittances of the augmented two-port, respectively.

A necessary condition for any oscillation to occur, therefore, is that the input and output admittance of the augmented two-port must be equal to zero. This condition will apply at steady-state.

It is clear from (10.2) to (10.4) that if the input admittance of a network is equal to zero, the same will apply to its output admittance, that is, as long as the product  $y_{12} y_{21}$  is not equal to zero.

It is also clear from (10.3) and (10.4) that whenever the resistive part of the input or output admittance is greater than zero at any particular frequency, oscillations cannot occur at that frequency. Therefore, if care is taken to ensure that the input (or output) conductance of an amplifier is always greater than zero, oscillations will not be possible. The locus of load admittances (source admittances) for which the input (output) admittance will be purely reactive (zero conductance) is therefore of interest.

Considering only the input admittance for the moment, the locus of the load admittance for which the input conductance will be equal to zero can be derived easily by setting  $\text{REAL}[Y_{\text{in}}(Y_L)] = 0$ :

$$\Re(Y_{\text{in}}) = G_s = g_{11} - \Re\left(\frac{y_{12}y_{21}}{y_{22} + Y_L}\right) = 0$$

where

$$g_{11} + jb_{11} = y_{11} \quad (10.5)$$

With

$$g_{22} + jb_{22} = y_{22} \quad (10.6)$$

$$y_{12}y_{21} = P + jQ \quad (10.7)$$

and

$$G_L + jB_L = Y_L \quad (10.8)$$

it follows that

$$G_s + g_{11} - \Re\left\{\frac{(P + jQ)[(g_{22} + G_L) - j(b_{22} + B_L)]}{(g_{22} + G_L)^2 + (b_{22} + B_L)^2}\right\} = 0$$

This equation can be manipulated into the following form:

$$\left[ G_L + g_{22} - \frac{P}{2(G_s + g_{11})} \right]^2 + \left[ B_L + b_{22} - \frac{Q}{2(G_s + g_{11})} \right]^2 = \frac{|y_{12}y_{21}|^2}{4(G_s + g_{11})^2} \quad (10.9)$$

Equation (10.9) is the equation of a circle in the linear admittance plane. The center of the circle is given by

$$G_L + jB_L = \left[ \frac{P}{2(G_s + g_{11})} - g_{22} \right] + j \left[ \frac{Q}{2(G_s + g_{11})} - b_{22} \right] \quad (10.10)$$

while the radius is given by

$$R = \left| \frac{y_{12}y_{21}}{2(G_s + g_{11})} \right| \quad (10.11)$$

For all load admittances on the circumference of this circle, the input conductance will be equal to zero, and if the input susceptance is also equal to zero, the amplifier will oscillate. The input conductance is usually negative for all load admittances falling inside the stability circle. The exception occurs when  $g_{11} < 0$ .

If only passive loads are considered, the worst-case condition will clearly be when  $G_s = 0$ . Under this condition (10.10) and (10.11) simplify to

$$G_L^* + jB_L^* = \left[ \frac{P}{2g_{11}} - g_{22} \right] + j \left[ \frac{Q}{2g_{11}} - b_{22} \right] \quad (10.12)$$

and

$$R_L^* = \left| \frac{y_{12}y_{21}}{2g_{11}} \right| \quad (10.13)$$

Whenever this stability circle lies to the left of the imaginary axis of the admittance plane, it will not be possible for an amplifier to oscillate at that particular frequency as long as its terminations are passive. Such an amplifier is said to be inherently stable.

Proceeding as above, the parameters of the stability circle in the source plane can be determined easily. The resulting equations are

$$G_s + jB_s = \left[ \frac{P}{2(G_L + g_{22})} - g_{11} \right] + j \left[ \frac{Q}{2(G_L + g_{22})} - b_{11} \right] \quad (10.14)$$

$$R = \left| \frac{y_{12}y_{21}}{2(G_L + g_{22})} \right| \quad (10.15)$$

The stable area will be outside this circle as long as  $g_{22} \geq 0$ . The worst-case condition is again associated with  $G_L = 0$ .

The Linville stability factor can be defined in terms of the parameters of the stability circle in the following way:

$$C = -\frac{R_L^*}{G_L^*} \quad (10.16)$$

$$= -\frac{\left| \frac{y_{12}y_{21}}{2g_{11}} \right|}{\frac{P}{2g_{11}} - g_{22}} \quad (10.17)$$

Whenever  $0 \leq C < 1$ , the stability circle will lie to the left of the imaginary axis of the admittance plane. If  $g_{11}$  is positive, the inside of the circle will represent the unstable area ( $Y_{in} = y_{11}$  when  $Y_L \rightarrow \infty$ ) and the device under consideration will be inherently stable.

The stability circle is plotted for different values of  $C$  in Figure 10.4.

The Linville stability factor is independent of the two-port terminations and is only a function of the parameters of the device used.

Another useful measure of stability is the Sterne stability factor. The Sterne stability factor takes the influence of the resistive loading by the load and source admittance into account:

$$K = \frac{g_{22} + G_L}{\frac{y_{12}y_{21}}{2(g_{11} + G_s)} + \frac{P}{2(g_{11} + G_s)}} \quad (10.18)$$

An amplifier will be stable at any frequency for which  $K \geq 1$ , that is, as long as the terminations used are in place.

Equation (10.18) is based on the fact that for inherent stability, it is required that

$$R_L^* + G_L^* \leq 0 \quad (10.19)$$

that is, if  $g_{11} > 0$ .

Whenever either or both of the terminations can change, it is advisable to set  $G_L$  and/or  $G_s$  in (10.18) equal to zero.

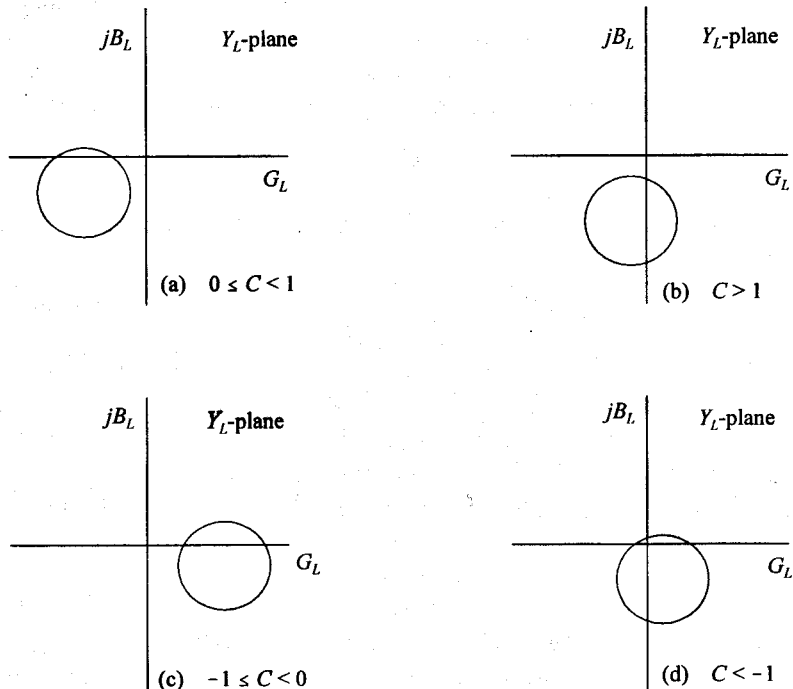


**Figure 10.4** The relationship between the Linville stability factor and the position of a stability circle relative to the imaginary axis of the admittance plane. (The stable area is on the outside of each circle as long as  $g_{11} > 0$ .)

### 10.2.2 Stability Circles on the Smith Chart

The locus of load and source reflection coefficients for which the input or output conductance or resistance of an amplifier will be equal to zero are also circles on a Smith Chart.

The equations for the stability circles on the Smith Chart can be derived by using the expressions derived for  $s_{11\omega}$  and  $s_{22\omega}$  in Chapter 1 ((1.86) and (1.87)). For inherent stability it is required that

$$|s_{11\omega}| < 1 \quad (10.20)$$

and

$$|s_{22a}| < 1 \quad (10.21)$$

for any passive termination (i.e., for  $|\Gamma_L| \leq 1$  and  $|\Gamma_s| \leq 1$ ).

It follows from these equations that [3]

$$|s_{11} - \Delta S_L| < |1 - s_{22} S_L| \quad (10.22)$$

and

$$|s_{22} - \Delta S_s| < |1 - s_{11} S_s| \quad (10.23)$$

where

$$\Delta = s_{11} s_{22} - s_{12} s_{21} \quad (10.24)$$

The parameters for the load stability circle (the values of  $S_L$  for which  $|s_{11\omega}| = 1$ , that is, the load terminations for which the input impedance will be purely reactive) follow from (10.22) and are given by

$$C_L = \frac{(s_{22} - \Delta s_{11}^*)^*}{|s_{22}|^2 - |\Delta|^2} \quad (10.25)$$

$$R_L = \frac{|s_{12} s_{21}|}{|s_{22}|^2 - |\Delta|^2} \quad (10.26)$$

where  $C_L$  is the center of the circle and  $R_L$  its radius.

Similarly, the parameters for the source stability circle (the values of  $S_s$  for which  $|s_{22\omega}| = 1$ , that is, the source terminations for which the output impedance will be purely reactive) are given by

$$C_s = \frac{(s_{11} - \Delta s_{22}^*)^*}{|s_{11}|^2 - |\Delta|^2} \quad (10.27)$$

$$R_s = \frac{|s_{12}s_{21}|}{|s_{11}|^2 - |\Delta|^2} \quad (10.28)$$

The stable area could be outside or inside the circle. The specific case can be established by observing the magnitudes of  $s_{11}$  and  $s_{22}$ , respectively. If, for example,  $|s_{11}| < 1$ , the input resistance is positive with a  $50\Omega$  load; and if the  $50\Omega$  load falls outside the load stability circle, the area inside the circle is the unstable area.

It follows that the following conditions must be satisfied for a transistor to be inherently stable:

$$|C_s| - |R_s| > 1 \quad (10.29)$$

$$|C_L| - |R_L| > 1 \quad (10.30)$$

$$|s_{11}| \leq 1 \quad (10.31)$$

and

$$|s_{22}| \leq 1 \quad (10.32)$$

that is, the stability circles must lie outside the Smith Chart and the input and output reflection coefficients associated with  $50\Omega$  terminations must be passive.

Instead of formulating the inherent stability conditions in terms of stability circles, the Rollette stability factor ( $k$ ) can be used. Inherent stability is then established by the following conditions:

$$k = \frac{1 - |s_{11}|^2 - |s_{22}|^2 + |\Delta|^2}{2|s_{12}||s_{21}|} \geq 1 \quad (10.33)$$

$$|s_{12}s_{21}| < 1 - |s_{11}|^2 \quad (10.34)$$

$$|s_{12}s_{21}| < 1 - |s_{22}|^2 \quad (10.35)$$

These conditions can be derived by establishing the conditions under which  $s_{11\omega}$  or  $s_{22\omega}$  will be passive for passive  $S_L$  or  $S_s$ , respectively [3]. This can be done by considering  $|s_{11\omega}|$  or  $|s_{22\omega}|$  when  $|S_L| \leq 1$  or  $|S_s| \leq 1$  (passive terminations), respectively.

An example of a Smith Chart stability circle is provided in Figure 10.5.

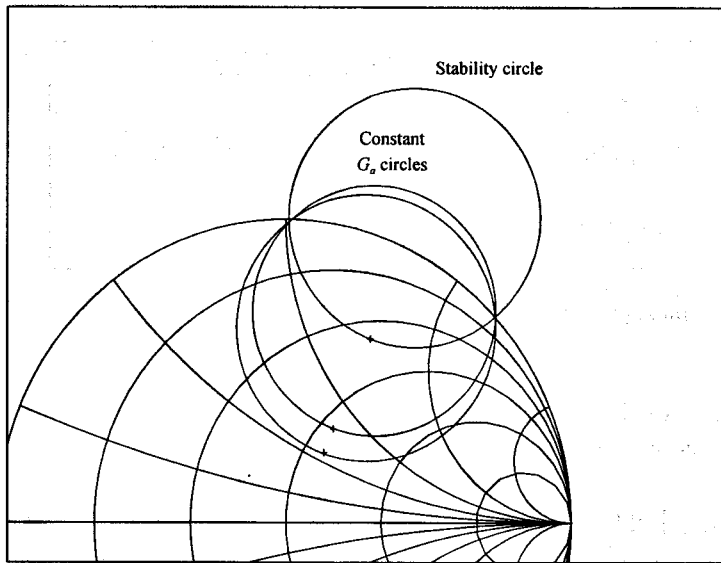


**Figure 10.5** An example of a stability circle displayed with some constant gain circles ( $G_a$  circles) on a Smith Chart (source plane). Note that a stability circle can be considered as the gain circle with infinite gain.

### 10.2.3 The Reflection Gain Approach

Steady-state oscillations will occur in a circuit when [4]

$$|\Gamma_{rhs} \Gamma_{lhs}| = 1 \quad (10.36)$$

and

$$\text{ANGLE} [\Gamma_{rhs}] = -\text{ANGLE} [\Gamma_{lhs}] \quad (10.37)$$

where  $\Gamma_{rhs}$  is the reflection coefficient to the right of the point of interest, and  $\Gamma_{lhs}$  is the reflection coefficient to the left.

These conditions follow easily from Figure 10.6. If  $a_L$  is the signal incident on the load (RHS), it will be reflected as  $b_L = \Gamma_{rhs} a_L$ . Considering the conditions at steady-state, this reflected signal will be the incident signal on the LHS and, assuming no external signal to be present, will be reflected as  $b_s = \Gamma_{lhs} \Gamma_{rhs} a_L$ . This signal is in turn the incident signal on the load, which implies that  $b_s = a_L$  (steady-state). This can only be the case for nonzero  $a_L$  if  $\Gamma_{lhs} \Gamma_{rhs} = 1$ . This condition is equivalent to the zero admittance oscillation condition at the common node.

This result can also be obtained from the expression for the transducer power gain

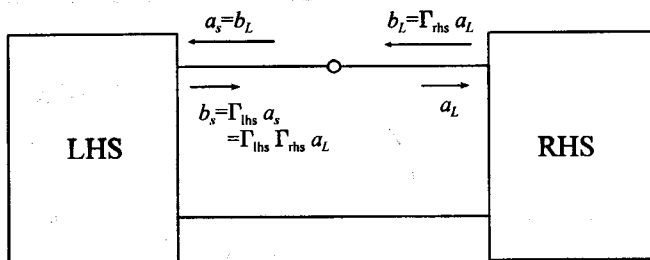


**Figure 10.6** Illustration of calculating the reflection gain at a given point in a circuit.

of a one-port. By using the equation derived for the power available from a source and the constraint imposed by the load ((1.101) and (1.79)), it follows that

$$G_T = \frac{[1 - |\Gamma_{rhs}|^2][1 - |\Gamma_{lhs}|^2]}{|1 - \Gamma_{lhs}\Gamma_{rhs}|^2} \quad (10.38)$$

Oscillation will occur when the gain approaches infinity, which will be the case when  $\Gamma_{lhs}\Gamma_{rhs} = 1$ , as was shown above.

At start-up, the magnitude of  $\Gamma_{lhs}\Gamma_{rhs}$  must be higher than unity.

Assuming the one side to be passive and the other to be active, (10.36) and (10.37) can be modified to

$$|\Gamma_{\text{passive}}| \geq \left| \frac{1}{\Gamma_{\text{active}}} \right| \quad (10.39)$$

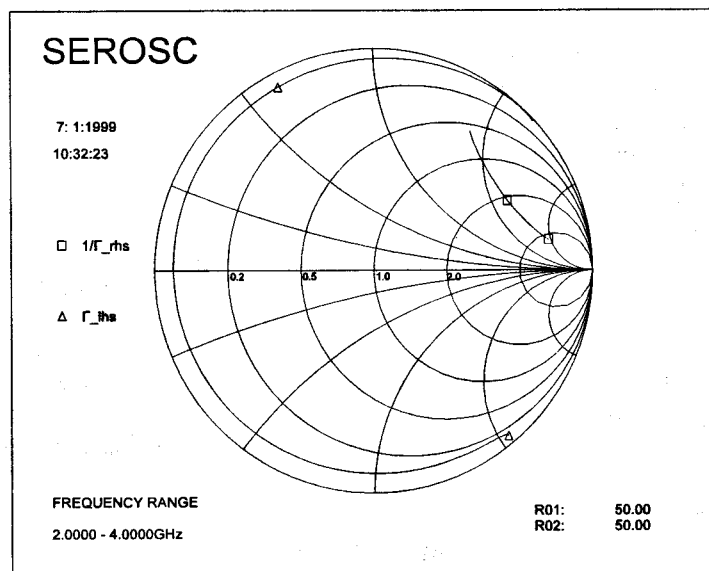
and

$$\text{ANGLE} [\Gamma_{\text{passive}}] = \text{ANGLE} [1/\Gamma_{\text{active}}] \quad (10.40)$$

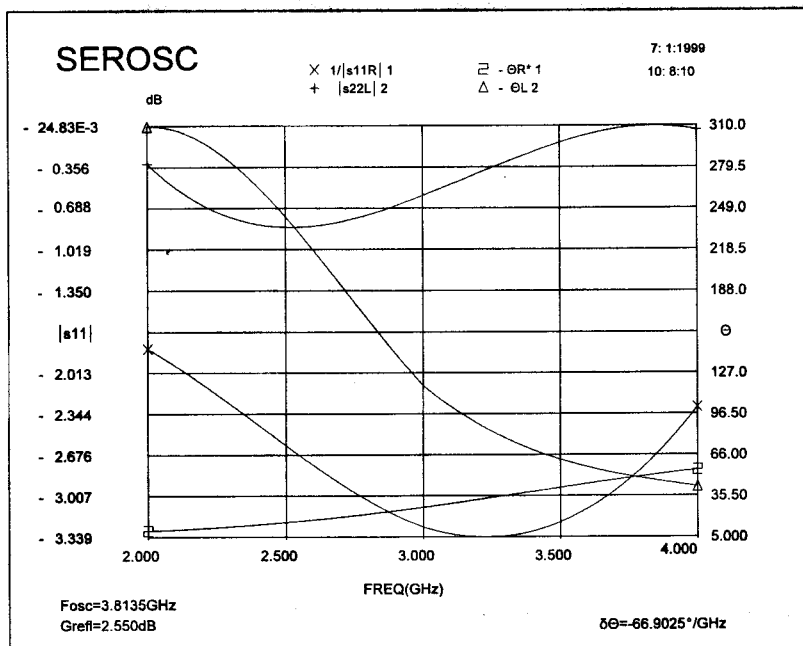
Note that (10.39) and (10.40) are essentially steady-state conditions. If the magnitude of  $\Gamma_{lhs}\Gamma_{rhs}$  is significantly larger than unity, start-up cannot be guaranteed, but the two-port will certainly be potentially unstable.

Conditions (10.39) and (10.40) can be detected easily if the inverted reflection coefficient of the active side is compared to the reflection coefficient of the other side (usually the resonator side) on a rectangular plot as a function of the frequency. The magnitude of the inverted reflection coefficient of the active side should be smaller than that of the passive side at the point where the phase traces cross (resonance point for the reflection coefficients).

Because no explicit frequency information is available when it is done, the common practice of considering only these quantities on a Smith Chart is not recommended. The absence of explicit frequency information can be misleading and can lead to wrong conclusions.



(a)



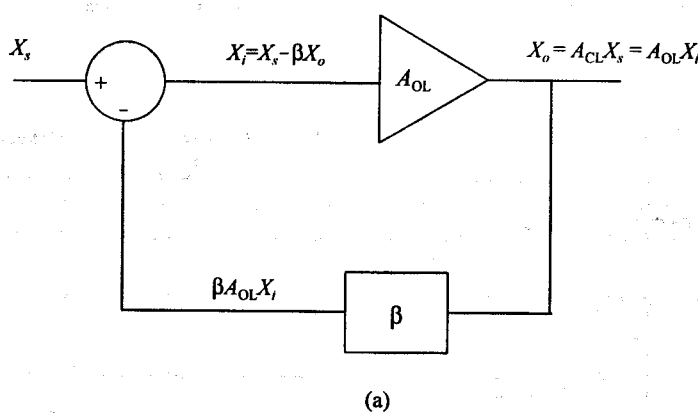
(b)

**Figure 10.7** The start-up reflection performance of an oscillator displayed on (a) a Smith Chart and (b) a rectangular plot [1].

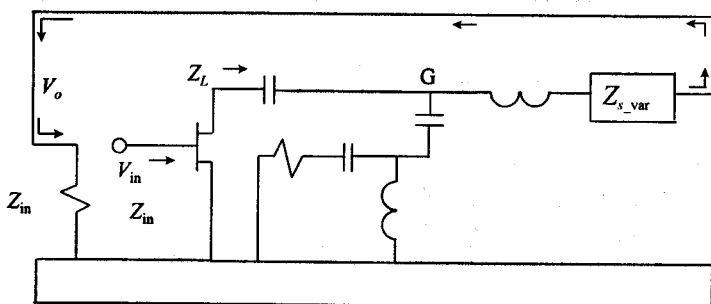
The reflection performance of an oscillator is displayed in Figure 10.7(b) on a rectangular plot. The reflection gain ( $|\Gamma_{\text{rhs}} \Gamma_{\text{lhs}}|$ ) and the rate at which the phase changes (in degrees per gigahertz) at the oscillation frequency were calculated and are also displayed. Note that the phase traces cross at 3.8135 GHz and that the trace for the inverted magnitude of the reflection coefficient of the active side (RHS) is below that of the passive side (LHS). The reflection gain is 2.55 dB at 3.8135 GHz and the rate of the change in the phase ( $\partial (\text{ANGLE} [\Gamma_{\text{passive}}] - \text{ANGLE} [1 / \Gamma_{\text{active}}]) / \partial f$ ) is  $-66.9^\circ/\text{GHz}$ .

The reflection coefficients are displayed on the Smith Chart in Figure 10.7(a). Note that the magnitude of the inverted reflection coefficient of the active side is again smaller than that of the passive side.

#### 10.2.4 The Loop Gain Approach



(a)



(b)

**Figure 10.8** (a) Calculation of the loop gain of a feedback amplifier. (b) The circuit used to calculate the loop gain ( $-\beta A$ ) of a series feedback oscillator [1]. (The actual ground of the circuit is at the point marked "G".)

The loop gain of an oscillator or an amplifier stage can be calculated by using feedback theory (see Figure 10.8). The closed loop gain ( $A_{CL}$ ) is given by

$$A_{CL} = \frac{A_{OL}}{1 + \beta A_{OL}} \quad (10.41)$$

where  $A_{OL}$  is the open-loop gain and  $-\beta A_{OL}$  is the loop gain (that is, the gain around the loop).

The loading effect of the feedback network on the relevant loops (at the relevant nodes) should be taken into account when the open-loop gain is calculated. The feedforward effect associated with the sampling network should also be taken into account.

When an oscillator with series feedback is designed, the effective impedance in the input loop ( $Z_{in\_eff} = R_{in\_eff} + jX_{in\_eff}$ ) is equal to the sum of the open-loop impedance ( $Z_{in\_ol}$ ) and the impedance resulting from the feedback applied ( $Z_{in\_fb}$ ). The feedback impedance is a function of the loop gain, which implies that the negative resistance in the input loop is a function of the loop gain too. The loop gain ( $G_{loop} = -\beta A_{OL}$ ) and the negative resistance are linked by the simple equation shown below:

$$Z_{in\_fb} = -G_{loop} Z_{in\_ol} \quad (10.42)$$

The negative resistance in the input loop, therefore, is proportional to the loop gain.

When an oscillator with shunt feedback is designed, the admittances at the input node are of interest, and the loop impedances in (10.42) must be replaced with the relevant admittances.

If the open-loop resistance in the input loop (series feedback case; open-loop conductance at the input node in the shunt feedback case) is positive, oscillations will start at any frequency at which:

1. The loop gain (gain around the loop) is greater or equal to 0 dB;
2. The phase shift around the loop is  $0^\circ$  or a multiple of  $360^\circ$ .

Oscillations are always possible if the sum of the open-loop resistance in the input loop and the resistance resulting from the feedback is negative (series feedback case). Suitable reactance in series or parallel with this negative resistance (conductance) may inhibit oscillations and may even result in a Rollette factor bigger than unity.

The open-loop and feedback impedances of an oscillator are displayed in Table 10.1. The effective impedance in the input loop is given by  $Z_{in\_eff} = Z_{in\_ol} + Z_{in\_fb}$ .

It is important to realize that the reactance in the input loop will not necessarily resonate when the loop gain is in-phase (oscillations will start up around 11.5 GHz in the oscillator considered in Table 10.1). Resonance of the reactance (susceptance) in the relevant loop (at the relevant node) is only a necessary condition at steady-state (loop gain compressed to 0 dB).

It should also be realized that the gain will be different around different loops. This

**Table 10.1**

The open-loop impedance of an oscillator is displayed with the impedance resulting from the feedback and the associated loop gain [1]

Frequency (GHz)	$Z_{in\_ol}$ ( $\Omega$ )	$Z_{in\_fb}$ ( $\Omega$ )	Loop gain (dB; $^\circ$ )
9.0000	9.01	-j37.75	-3.76 51.45
10.0000	8.30	-j23.70	-1.60 41.82
11.0000	7.62	-j11.16	2.36 22.45
11.5000	7.31	-j5.27	5.23 0.36
11.5500	7.28	-j4.72	5.50 357.31
11.6000	7.26	-j4.17	5.76 353.94
11.6500	7.23	-j3.62	6.00 350.46
11.7000	7.20	-j3.02	6.24 346.36
11.7500	7.17	-j2.42	6.45 342.02
11.8000	7.14	-j1.88	6.60 337.88
11.8500	7.11	-j1.34	6.72 333.58
11.9000	7.09	-j0.80	6.78 329.14
11.9500	7.06	-j0.26	6.80 324.61
12.0000	7.03	j0.33	6.77 319.55
13.0000	6.61	j11.15	0.32 258.99
14.0000	6.29	j21.05	-5.29 240.68

can be appreciated easily by considering a transistor with both current-series and voltage-shunt feedback loops (consider the case with significant voltage-shunt feedback and negligible current-series feedback).

The loop of interest is usually the loop associated with the gain compression. With a well-behaved load-line, the main reason for gain compression will be compression of the transconductance caused by the voltage swing across the input junction (nonlinear transfer function).

The loop gain for an amplifier stage is shown in Figure 10.9. Note that the resonance frequency is listed with the loop gain and the slope in the phase response at this frequency. The loop gain at the resonance frequency is also the gain margin of the amplifier stage. The gain margin is 20.5 dB. In this case, there is clearly no chance of oscillations at all.

The loop gain for two oscillators are shown in Figure 10.10. The oscillation frequency is listed with the loop gain and the slope in the phase response at this frequency below each plot.

The effective loop resistance (sum of the open-loop resistance and the feedback resistance) for these oscillators is negative when the 0-dB loop gain level is marked (horizontal line segments) on the plots. Oscillation is not possible when this level is not marked.

The first oscillator is a dielectric resonator oscillator (DRO) (series feedback oscillator; puck on the gate side). Oscillations will start up at 15.6435 GHz with a loop gain of 6.961 dB. The slope in the phase response is  $-895^\circ/\text{GHz}$  at this point. The loop phase

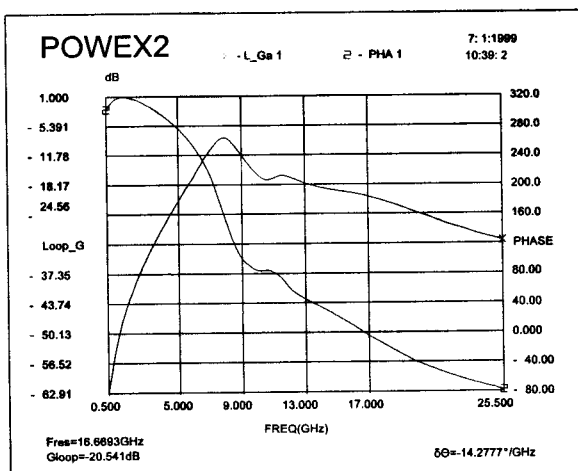


**Figure 10.9** The loop gain calculated for an amplifier stage with some current-series and voltage-shunt feedback [1].

again approaches zero at a higher frequency but the loop gain is too low for oscillation when this happens.

The second oscillator will start up at 4.4819 GHz with a loop gain of 4.474 dB. The slope in the phase response is  $-399^\circ/\text{GHz}$  at this point.

The loop gain performance of the oscillator considered previously in Figure 10.7 is displayed in Figure 10.11 on a rectangular plot as well as on a Smith Chart. Note that the start-up frequency predicted with the loop gain approach is 3.7873 GHz instead of 3.8135 GHz as predicted with the reflection gain approach. The loop gain at start-up is 5.225 dB and the slope in the phase response is  $-114^\circ/\text{GHz}$ .

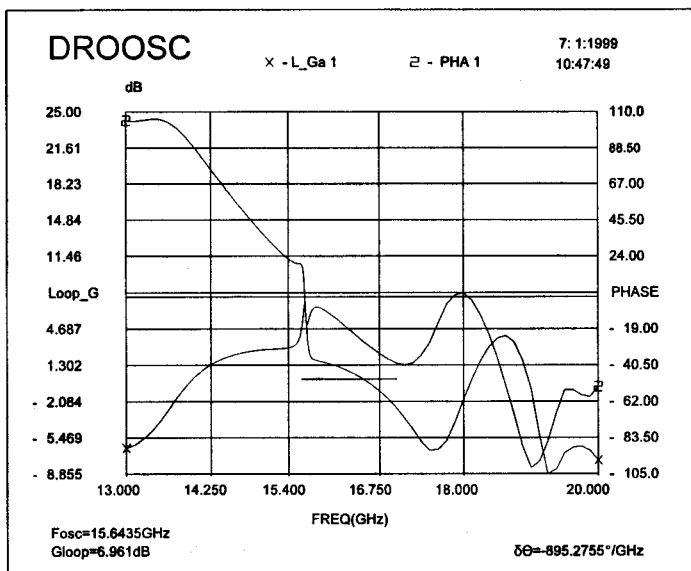
Note that the phase response of this oscillator is well-behaved and that oscillations are not possible at the higher frequencies.

The loop gain of the oscillator is displayed on a Smith Chart in Figure 10.11(b). The gain was scaled so that its maximum would fall on the edge of the Smith Chart (the Smith Chart should be viewed as a polar plot when the gain is considered).

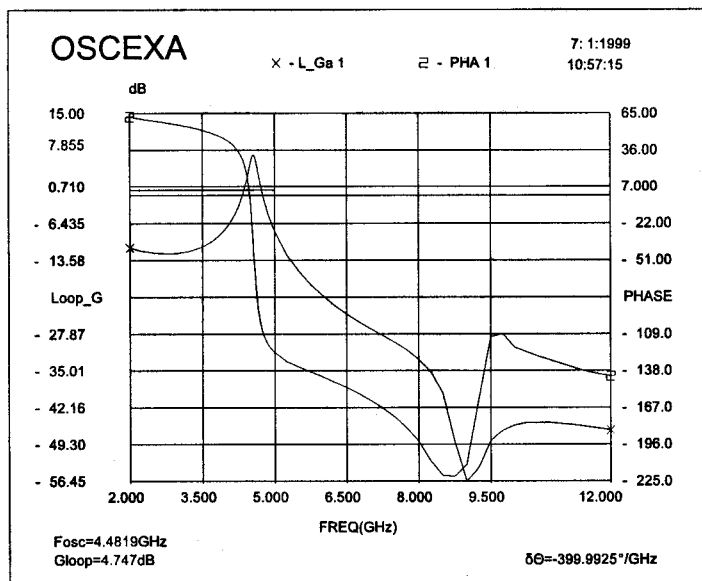
Note that the unity loop gain circle is also displayed on the Smith Chart (Figure 10.11(b)). Start-up will occur if the loop gain trace is outside this circle at the point where the phase passes through zero. Multiple crossings should not be allowed on the horizontal axis on the right-hand side of the unity gain circle.

The load termination presented to the transistor ( $T_{r,LL}$ ) at start-up is also displayed in Figure 10.11(b).

Note that the termination used on the left-hand side (unconnected side) of the oscillator ( $R_{01}$ ) was chosen to be  $10\text{k}\Omega$  (choosing a higher value may be safer) and that the  $s_{11}$  displayed is meaningless. The load presented to the oscillator is  $50\Omega$  ( $R_{02}$ ).  $s_{22}$  in Figure 10.11(b) was calculated with the input side of the two-port terminated in  $R_{01}$  ( $10\text{k}\Omega$  in this case).

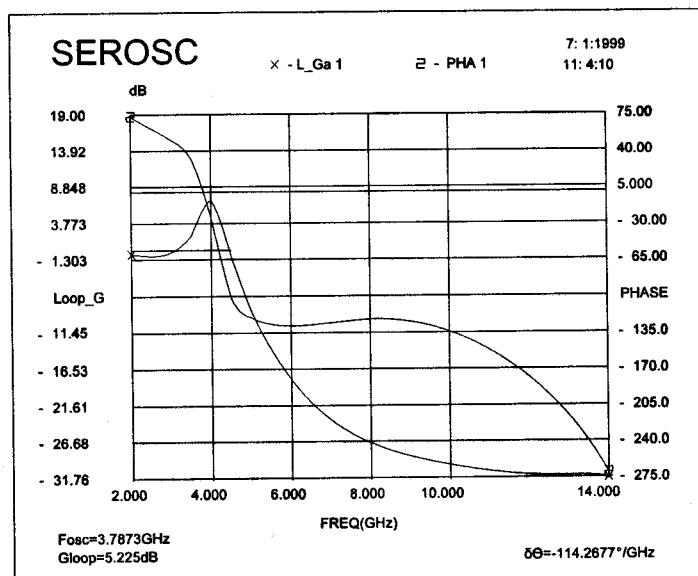


(a)

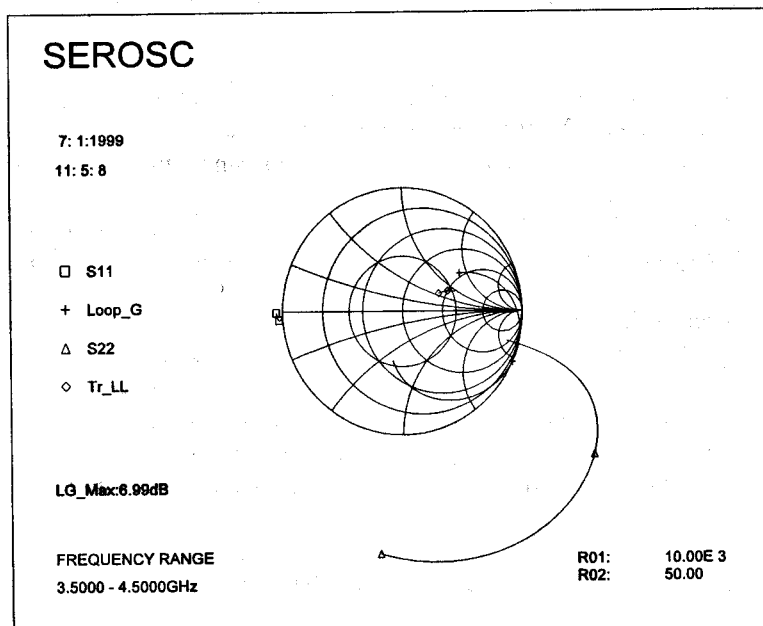


(b)

**Figure 10.10** The loop gain calculated for (a) a dielectric resonator oscillator and (b) a varactor-tuned oscillator [1].



(a)



(b)

**Figure 10.11** The loop gain and phase of the oscillator in Figure 10.7 displayed (a) on a rectangular plot and (b) on a Smith Chart [1].

The rate at which the phase is changing at the oscillation frequency is an indication of the loaded  $Q$  of the circuit. In the special case when a single-tuned response can be assumed and when the oscillation frequency is also the resonance frequency or a frequency close to it, the  $Q$  can be estimated by using the following equations for a parallel resonant circuit [3]:

$$\begin{aligned}
 Z_{in} &= \frac{1}{G + j\omega C + 1/(j\omega L)} \\
 &= \frac{1}{G + j(\omega_0 + \Delta\omega)C + 1/(j(\omega_0 + \Delta\omega)L)} \\
 &= \frac{1}{G + j\omega_0 C + j\Delta\omega C + 1/(j(\omega_0(1 + \Delta\omega/\omega_0))L)} \\
 &\approx \frac{1}{G + j\omega_0 C + j\Delta\omega C + (1 - \Delta\omega/\omega_0)/(j\omega_0 L)} \\
 &= \frac{R}{1 + j2Q(\Delta\omega/\omega_0)}
 \end{aligned} \tag{10.43}$$

where the approximation applies at frequencies close to the resonant frequency. (This equation explains why the phase of a resonant circuit is linear close to the resonant frequency.)

Note that at start-up the oscillation frequency may not also be the resonance frequency. However, this will always be the case at steady-state.

It follows from (10.43) that the  $Q$  of an oscillator (single-tuned response) can be estimated as

$$Q = \frac{\pi}{360} (\Delta\theta/\Delta f) f_0 \tag{10.44}$$

where the phase slope ( $\Delta\theta/\Delta f$ ) is specified in degree per gigahertz and the resonant frequency in gigahertz.

By using this equation, the  $Q$  for the oscillator considered in Figure 10.10(b) ( $F_{osc} = 4.4819$  GHz;  $399^\circ/\text{GHz}$ ) is estimated to be 15.6 at start-up.

Note that the loaded  $Q$  will decrease as the transistor is driven into compression.

### 10.2.5 Stabilization of a Two-Port with Shunt or Series Resistance

Any transistor (two-port) can be stabilized by adding shunt or series resistance to it. It is sometimes necessary to add resistance on both sides of the transistor. This may be the case when the real part of  $y_{11}$ ,  $y_{22}$ ,  $z_{11}$ , or  $z_{22}$  is negative.

The shunt conductance required can be calculated by using the equations derived

for the stability circles in terms of the  $Y$ -parameters (Section 10.2.1):

$$G_{11\text{sta}} = G_L^* + R_L^* \quad (10.45)$$

and

$$G_{22\text{sta}} = G_s^* + R_s^* \quad (10.46)$$

where  $G_{11\text{sta}}$  is the shunt conductance required on the input side,  $G_{22\text{sta}}$  the conductance required on the output side,  $G_L^*$  the real part of the center of the stability circle on the load plane (admittance plane),  $R_L^*$  the radius of this circle,  $G_s^*$  the real part of the center on the source plane, and  $R_s^*$  the radius of this circle.

The equations for the series resistance can be derived by deriving equations for the stability circles in the impedance plane first. The equations are identical in form to those for the shunt admittance. The only differences are that each  $Y$ -parameter should be replaced with the corresponding  $Z$ -parameter. The reason for this is clear if the expressions for the input/output admittance and impedance are compared:

$$Y_{\text{in}} = y_{11} - \frac{y_{12} y_{21}}{y_{22} + Y_L} \quad (10.47)$$

and

$$Z_{\text{in}} = z_{11} - \frac{z_{12} z_{21}}{z_{22} + Z_L} \quad (10.48)$$

The form of these two equations is identical and, because the input conductance and the input resistance are calculated by taking the real part of the two equations, respectively, the equations for the stability circles will also have the same form.

An example of the series and shunt resistance required to stabilize a Fujitsu FHX35LG transistor is provided in Table 10.2. If series loading is considered, the transistor can be stabilized by adding resistance in series with the input or the output side.

$177\Omega$  is required on the input side to stabilize the transistor at 100 MHz, while only  $0.82\Omega$  is required at 11 GHz. A parallel combination of a  $200\Omega$  resistor and a  $1.07\text{-pF}$  capacitor in series with the input terminal will provide the required series resistance at 0.1 GHz and 11 GHz. Some adjustment in the capacitance may be required for inherent stability over the complete frequency range.

Note that the series resistance required is well-behaved and only a small amount of loading is required at the higher frequencies.

In contrast with the series case, stabilization by using shunt loading is simply not an option. The (shunt) resistance decreases with increasing frequency (greater loading is required at the higher frequencies), and loading is also required on the other side of the transistor in order to remove the negative conductance associated with  $y_{11}$  or  $y_{22}$ . The value

**Table 10.2**  
The series (top) and the shunt (bottom) resistance required to stabilize a transistor [1]

Frequency (GHz)	Source loading ( $\Omega$ )		Load loading ( $\Omega$ )	
	$R_i$	$(R_o)$	$(R_i)$	$R_o$
0.10	177.0			166.0
0.50	118.0	200Ω	262.0	186Ω
1.00	58.4	//	145.0	//
2.00	28.4	1.07 pF	70.8	0.87 pF
3.00	17.6		44.2	
4.00	11.7		28.7	
5.00	7.95		18.8	
6.00	5.69		12.8	
7.00	4.11		8.84	
8.00	3.03		6.18	
9.00	2.52		4.87	
10.0	1.92		3.43	
11.0	0.82		1.32	

Frequency (GHz)	Source loading ( $\Omega$ )		Load loading ( $\Omega$ )	
	$R_i$	$(R_o)$	$(R_i)$	$R_o$
0.10	12.7k			64.5
0.50	1.46k	9.240	3.50	0.46
1.00	770.0	+	7.31	+
2.00	399.0	4.89 pF	4.86	0.31nF
3.00	265.0		3.16	
4.00	191.0		2.79	
5.00	145.0		3.90	
6.00	104.0		3.88	
7.00	74.0		2.14	
8.00	44.5		6.03k	0.10
9.00	11.8		279	1.09
10.0	0.8	111.0	66.6	1.38
11.0	0.48	7.38	6.88	0.51

required on the other side is listed under the headings ( $R_o$ ) for the input side and ( $R_i$ ) for the output side.

Note again that in general, the intention is not necessarily to actually stabilize the transistor in this way, but rather to evaluate the degree of instability by getting an idea of the resistance required for inherent stability. Furthermore, even if the goal is inherent stability, better results can usually be obtained by using two modification sections instead of one.

### 10.3 TUNABILITY

When a designed amplifier is realized, it may be necessary to tune it to obtain the exact results predicted. When the influence of the reverse transfer gain of a transistor ( $s_{12}$ ) is not negligible, its input impedance will be a function of the load termination, and, if the load changes, whether because of tuning, temperature drift, or a change in load, the input impedance will also change. The consequent dependence of the input match on the changes in the output circuit (and vice versa) is usually undesirable.

The tunability factor [5]

$$\delta = \left| \frac{\partial Y_{in} / Y_{in}}{\partial Y_L / Y_L} \right| \quad (10.49)$$

$$= \frac{|y_{12}y_{21}Y_L|}{|y_{22} + Y_L|^2 |Y_{in}|}$$

$$= \left| \frac{y_{12}}{y_{21}} \right| G_\omega \sec \theta_L / \sec \theta_{in} \quad (10.50)$$

where

$$\theta_{in} = \tan^{-1}[B_{in} / G_{in}] \quad (10.51)$$

and

$$\theta_L = \tan^{-1}[B_L / G_L] \quad (10.52)$$

is a measure of the relative dependence of the input match on changes in the output circuit.

It is obvious from (10.49) that the tunability factor is a strong function of the operating power gain. If the gain is decreased enough, the output circuit will usually have very little influence on the input circuit and vice versa.

A tunability factor of less than 0.3 is usually advisable [5]. When the two sides of a transistor are completely isolated ( $s_{12} = 0$ ), the tunability factor will be equal to zero.

The relative change in the output admittance as a function of the relative change in the source admittance is given by

$$\delta' = \left| \frac{\partial Y_{out} / Y_{out}}{\partial Y_s / Y_s} \right| \quad (10.53)$$

$$= \frac{|y_{12}y_{21}Y_s|}{|y_{11} + Y_s|^2 |Y_{\text{out}}|} \quad (10.54)$$

The order of magnitude of the two tunability factors are usually the same.

An expression for the tunability expressed in terms of the reflection coefficients is given by [2]

$$\begin{aligned} \delta_{\Gamma} &= \left| \frac{\partial \Gamma_{\text{in}} / \Gamma_{\text{in}}}{\partial \Gamma_L / \Gamma_L} \right| \\ &= \frac{|s_{12}s_{21}\Gamma_L|}{|1 - s_{22}\Gamma_L| |s_{11} - \Delta\Gamma_L|} \end{aligned} \quad (10.55)$$

Because of tunability difficulties, the MAG or MSG of a transistor often cannot be realized. The maximum tunable gain (MTG) usually provides a more realistic idea of the gain obtainable with a transistor. The MTG can be established iteratively by decreasing the gain from its MSG or MAG value until the associated tunability factor is acceptable.

It should be noted that poor tunability is not always undesirable. When a low noise stage is designed, the dependence of the input admittance on the load admittance can be used to improve the input VSWR associated with an optimum noise match by changing the load admittance appropriately. This effect can also be used to improve the output VSWR associated with an optimum power match.

## 10.4 CONTROLLING THE GAIN OF AN AMPLIFIER

The best way to control the gain of an amplifier is to control the operating power gain ( $G_o$ ) and/or the available power gain ( $G_a$ ) of each stage (refer to Figure 10.12).

If the noise figure is critical, the design should be started at the input side, and if the power performance is more important, the design should be started at the load side. The design can also be done from both sides and linked up at some point. This would be done when the dynamic range required is high.

If the operating power gain or the available power gain of the last stage in the cascade is controlled, it is implicitly assumed that the other side of the (modified) transistor will be conjugately matched (in practice, a good match will suffice: if the relevant VSWR is below 2.0, the gain will be within 0.5 dB of that targeted). The mismatch associated with the last matching network is incorporated in  $G_{\text{net},3}$ , as shown in Figure 10.12.

The requirement of a conjugate match may be too restrictive when the last stage of a high dynamic range amplifier is designed, and in this case a better option could be to control the transducer power gain of this stage with the current load or source termination for the stage in place (refer to Figure 10.13). If this approach is followed to design a single-stage amplifier, the load termination can be designed for optimum power, after which the

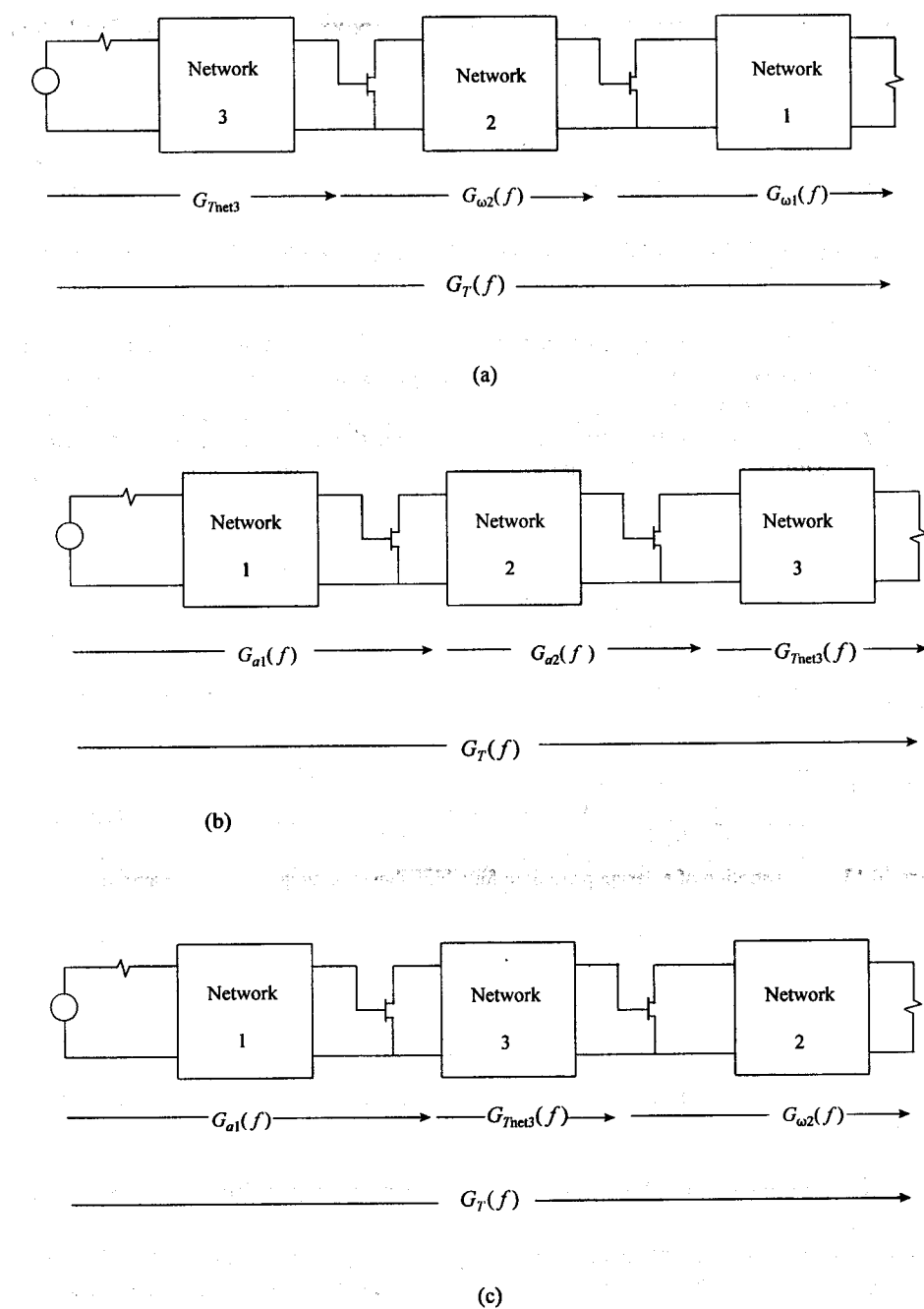


**Figure 10.12** Calculation of the power gain of a multistage amplifier when the design is done by starting (a) at the load, (b) at the source, and (c) from both sides (high dynamic range case).

input network can be designed to control the transducer power gain of the amplifier. In this case, the source terminations associated with the best noise performance can then be selected on the different gain circles.

If the operating power gain, the available power gain, or the transducer power gain is controlled, the gain is controlled exactly and no approximations are made as is the case when the transistors used are assumed to be unilateral. It has been shown in [6] that the errors made by assuming a transistor to be unilateral are seldom negligible.

Before controlling the gain of a transistor with a lossless network, it is a good idea to first level its gain by using resistive modification sections (feedback or loading sections). The gain to be leveled is usually the MAG. Leveling the available power gain associated with the best noise figure ( $G_{an,opt}$ ) is usually a better choice when a low-noise stage is designed. Similarly, leveling the operating power gain associated with the highest output power is usually a good idea.

Instead of using lossy modification sections, the gain can also be leveled by designing the impedance-matching networks (gain control networks) to have positive gain slopes, but this route usually leads to sensitive designs and should be avoided if the goal is to design a first-time-right amplifier.

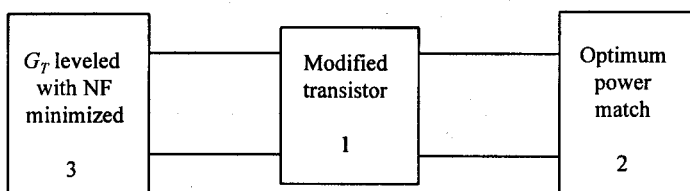


**Figure 10.13** Illustration of a design procedure for a high dynamic range single stage amplifier.

In order to control the operating or the available power gain of a stage, it is necessary to establish what the source terminations or the load terminations should be to provide the required gain. The actual source or load impedance can then be transformed to that required by designing an impedance-matching network for this purpose.

It will be shown here that the contours of interest are circles on the admittance plane or on the Smith Chart. The center and radius of the constant gain circles will be derived here.

When a transistor is inherently stable, the gain circles will be inside the Smith Chart (passive terminations). It will be shown that in this case, it is always possible to transform the active gain problem exactly to an equivalent passive impedance-matching problem. The equivalent passive problem can be solved by using standard impedance-matching techniques. As long as these problems are solved accurately, the solutions synthesized will also solve the original active problem.

If a wideband problem is solved by transforming the active problem to the equivalent passive problem, the deviation between the gain targeted and that obtained may

not be insignificant. In this case an extra step should be introduced in which the solutions obtained from the equivalent passive problem are optimized for the best active performance.

At those frequencies at which the transistor is potentially unstable, the best point on each constant gain circle can be selected as targets. It should be noted that while the relevant gain will remain constant on the circumference of a constant gain circle, the other parameters of interest may change significantly. These parameters may include the noise figure, the power gain, the stability, the associated VSWRs, and various sensitivity factors.

#### 10.4.1 Circles of Constant Mismatch for a Passive Problem

It was shown in Section 8.4.3.1 that the locus of load admittances for which the transducer power gain  $G_T$  of a passive source with internal admittance  $Y_s = G_s + jB_s$  terminated in a passive load  $Y_L = G_L + jB_L$  will remain constant is a circle in the linear admittance plane with center

$$G_0 + jB_0 = [2 / G_T - 1]G_s - jB_s \quad (10.56)$$

and radius

$$R_{Y_0} = 2 G_s \sqrt{1 / G_T^2 - 1 / G_T} \quad (10.57)$$

Similarly, the locus of constant transducer power gain is also a circle on the Smith Chart

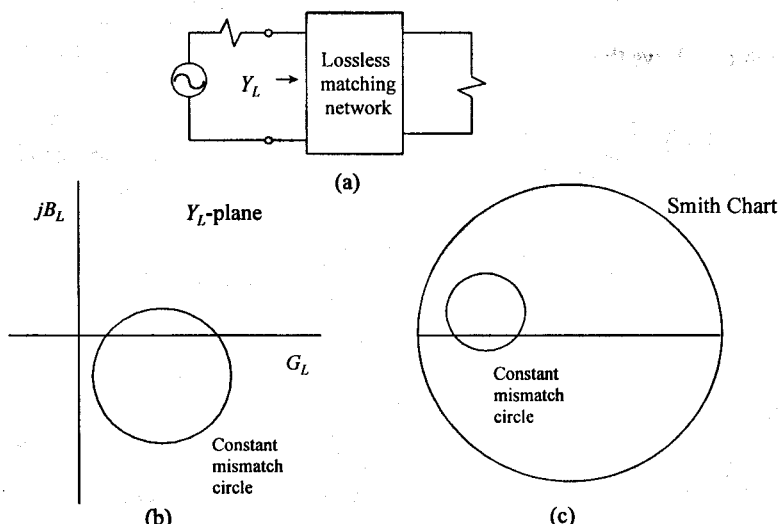


**Figure 10.14** (a) The equivalent circuit relevant to the derivation of the constant mismatch circles and an example of these loci on (b) the admittance plane and (c) a Smith Chart.

(see Figure 10.14). The parameters of this circle are given by

$$C_p = \frac{\Gamma_s^* G_T}{1 - |\Gamma_s|^2 (1 - G_T)} \quad (10.58)$$

$$R_p = \frac{(1 - |\Gamma_s|^2) \sqrt{1 - G_T}}{1 - |\Gamma_s|^2 (1 - G_T)} \quad (10.59)$$

where  $C_p$  is the center of the circle and  $R_p$  its radius.

Equations (10.58) and (10.59) can be derived from the expression for the transducer power gain of a one-port:

$$G_T = \frac{(1 - |\Gamma_L|^2)(1 - |\Gamma_s|^2)}{|1 - \Gamma_s \Gamma_L|^2} \quad (10.60)$$

where  $\Gamma_L$  is the reflection coefficient of the load termination, and  $\Gamma_s$  is the reflection coefficient of the source termination. The derivation is repeated here for convenience.

It follows from (10.60) that

$$G_T |1 - \Gamma_s \Gamma_L|^2 = (1 - |\Gamma_L|^2)(1 - |\Gamma_s|^2)$$

from which it follows that

$$|1 - \Gamma_s \Gamma_L|^2 + \frac{1 - |\Gamma_s|^2}{G_T} |\Gamma_L|^2 = \frac{1 - |\Gamma_s|^2}{G_T}$$

that is,

$$|1 - \Gamma_s \Gamma_L|^2 + \alpha |\Gamma_L|^2 = \alpha$$

which can be written as

$$(1 - \Gamma_s \Gamma_L)(1 - \Gamma_s^* \Gamma_L^*) + \alpha \Gamma_L \Gamma_L^* = \alpha$$

This expression can be written as

$$\left( \Gamma_L - \frac{\Gamma_s^*}{\alpha + |\Gamma_s|^2} \right) \left( \Gamma_L^* - \frac{\Gamma_s}{\alpha + |\Gamma_s|^2} \right) = \frac{\alpha - 1}{\alpha + |\Gamma_s|^2} + \frac{|\Gamma_s|^2}{(\alpha + |\Gamma_s|^2)^2} \quad (10.61)$$

which is the equation for a circle on the Smith Chart.

The center and radius of the circle can be obtained from this equation, and, after some simplification, the expressions given here are obtained.

The important point to grasp at this point is that while the problem of a conjugate match implies transforming a given load (source) termination into a specific input (output) impedance, the problem of getting a specified amount of mismatch is a circle problem. The load (source) termination can then be transformed to any point on the circumference of the relevant gain circle, and the gain of the passive network will be as specified.

#### 10.4.2 Constant Operating Power Gain Circles

It will be shown here that the contours of constant operating power gain are circles on the admittance plane, as well as on the Smith Chart. The equations for both cases will be derived here. The admittance plane case will be considered first.

The operating power gain of a transistor (see Figure 10.15) is given in terms of its  $Y$ -parameters by

$$G_{\omega} = P_L / P_{in}$$

$$= \left| \frac{y_{21}}{y_{22} + Y_L} \right|^2 \frac{G_L}{\operatorname{Re} \left( y_{11} - \frac{y_{12}y_{21}}{y_{22} + Y_L} \right)} \quad (10.62)$$

where  $P_L$  is the power dissipated in the load, and  $P_{in}$  is the power entering the input terminals of the amplifier.

With

$$y_{12}y_{21} = P + jQ$$

as defined before, and

$$y_{22} + Y_L = (G_L + g_{22}) + j(B_L + b_{22}) = G'_L + jB'_L$$

(10.62) becomes

$$G_{\omega} = \frac{|y_{21}|^2 G_L}{g_{11}G'^2_L + g_{11}B'^2_L - PG'_L - QB'_L} \quad (10.63)$$

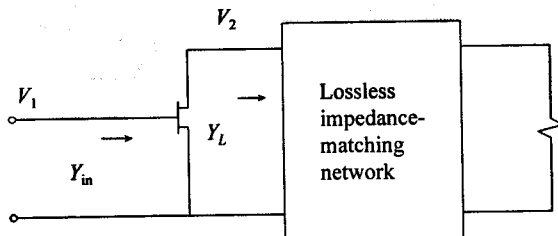


Figure 10.15 The circuit relevant to calculating the operating power gain of an amplifier stage.

By multiplying both sides of this equation with the denominator of the right-hand side and dividing them by  $g_{11}G_\omega$ , the following equation is obtained:

$$G_L'^2 - \frac{PG'_L}{g_{11}} + B_L'^2 - \frac{QB'_L}{g_{11}} = \frac{|y_{21}|^2(G'_L - g_{22})}{g_{11}G_\omega} \quad (10.64)$$

This equation can be manipulated into the explicit form of the equation for a circle. The center of this circle is found to be

$$G_{L\omega} + jB_{L\omega} = \left[ \left( \frac{P}{2g_{11}} - g_{22} \right) + \frac{|y_{21}|^2}{2g_{11}G_\omega} \right] + j \left( \frac{Q}{2g_{11}} - b_{22} \right) \quad (10.65)$$

and its radius ( $R_{L\omega}$ ) can be obtained from the equation

$$R_{L\omega}^2 = G_{L\omega}^2 - \left\{ \left( \frac{P}{2g_{11}} - g_{22} \right)^2 - \left| \frac{y_{12}y_{21}}{2g_{11}} \right|^2 \right\} \quad (10.66)$$

When the transistor is inherently stable [ $0 < C < 1$ ;  $g_{11} > 0$ ;  $g_{22} > 0$ ], the operating power gain circles lie entirely in the right-hand side of the admittance plane. When the transistor is potentially unstable, these circles cross over into the left-hand side of the plane, as is illustrated in Figure 10.16. Note that the gain circles cross the imaginary axis at the same two points, and that the gain circle corresponding to an infinite value for the gain is also the stability circle on the admittance plane, as derived in Section 10.2.

When a transistor is inherently stable, an expression for the maximum realizable power gain can be derived by calculating the operating power gain corresponding to the gain circle with radius equal to zero. With  $R_{L\omega}$  set equal to zero in (10.66), the maximum

realizable power gain is found to be

$$G_{\omega-\max} = \frac{|y_{21}|^2 / (2g_{11})}{G_{L\omega-\text{opt}} - G_L^*} \quad (10.67)$$

where  $G_{L\omega-\text{opt}}$  is the real part of the load termination corresponding to the maximum realizable gain, and  $G_L^*$  is defined by (10.12). Equation (10.67) can be simplified to

$$G_{\omega-\max} = \left| \frac{y_{21}}{y_{12}} \right| \left| 1/C - \sqrt{1/C^2 - 1} \right| \quad (10.68)$$

The load termination corresponding to the maximum realizable gain is given by

$$Y_{L\text{opt}} = \sqrt{G_L^{*2} - R_L^{*2}} + jB_L^* \quad (10.69)$$

with  $B_L^*$  as defined in (10.12).

When a transistor is potentially unstable, the maximum operating power gain obtainable is, theoretically, equal to infinity. The parameters of the constant operating power gain circles displayed on a Smith Chart can be derived by using the expression for the operating power gain in terms of the load reflection coefficient (1.89):

$$G_\omega = \frac{|s_{21}|^2 [1 - |S_L|^2]}{|1 - s_{22}S_L|^2 - |s_{11}(1 - s_{22}S_L) + s_{12}s_{21}S_L|^2} \quad (10.70)$$

The center of each constant operating power gain circle is given by

$$C_\omega = \frac{g_\omega (s_{22}^* - \Delta^* s_{11})}{1 + g_\omega (|s_{22}|^2 - |\Delta|^2)} \quad (10.71)$$

and its radius by

$$R_\omega = \frac{(1 - 2k|s_{12}s_{21}|g_\omega + |s_{12}s_{21}|^2 g_\omega^2)^{1/2}}{\left| 1 + g_\omega (|s_{22}|^2 - |\Delta|^2) \right|} \quad (10.72)$$

The normalized gain,  $g_\omega$ , is given by

$$g_\omega = G_\omega / |s_{21}|^2 \quad (10.73)$$

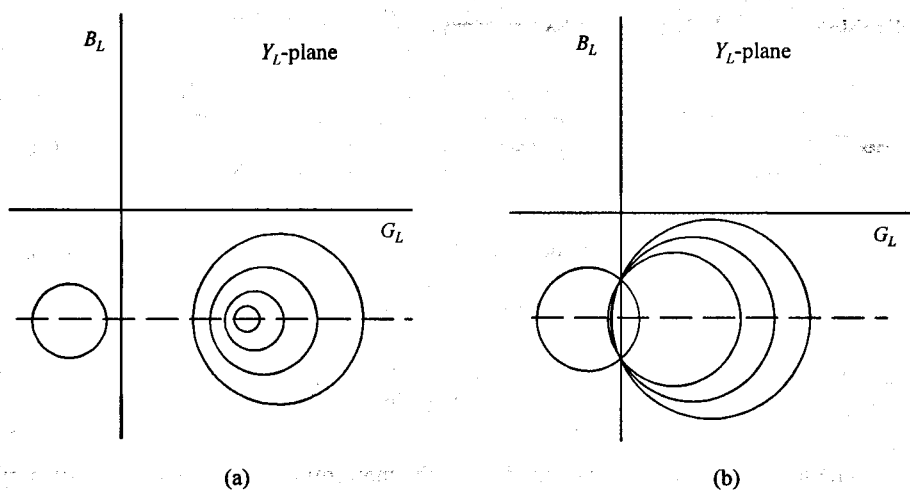


**Figure 10.16** The position of the constant operating power gain circles relative to the imaginary axis of the admittance plane, illustrated for (a) an inherently stable transistor and (b) a transistor for which  $C > 1$ .

### 10.4.3 Constant Available Power Gain Circles

The contours of constant available power gain are also circles on the admittance plane or on the Smith Chart. The equations for both cases will be presented here. The admittance plane case will be considered first.

The available power gain of an amplifier (see Figure 10.17) is given by

$$\begin{aligned}
 G_A &= \frac{P_{av-O}}{P_{av-E}} \\
 &= \left| \frac{y_{21}}{y_{11} + Y_s} \right|^2 \frac{\Re(Y_s)}{\Re(Y_o)} \quad (10.74)
 \end{aligned}$$

where  $P_{av-O}$  is the maximum power available at the output of the amplifier, and  $P_{av-E}$  is the maximum power available from the source.

Comparison of (10.74) and the expression for the operating power gain of an amplifier yields that if  $y_{11}$  is replaced with  $y_{22}$ ,  $Y_s$  with  $Y_L$ , and  $Y_{out}$  with  $Y_{in}$ , the two expressions are identical. Because  $y_{21}$ ,  $y_{11}$ , and  $y_{22}$  are constants, and the relationship between  $Y_s$  and  $Y_{out}$  is identical to that between  $Y_L$  and  $Y_{in}$ , it is possible to determine the locus of source admittances for which the available power gain of a transistor will be equal to a specified value by using the results obtained for the operating power gain. By following this approach, the center of a constant available power gain circle is found to be located at

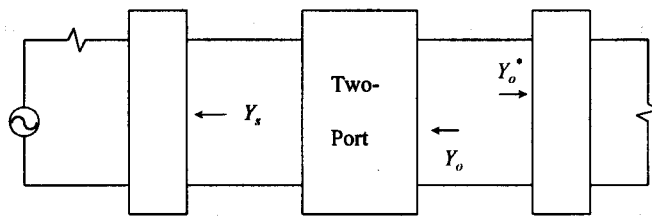


**Figure 10.17** The equivalent circuit relevant to determining the available power gain of an amplifier.

$$G_{sa} + jB_{sa} = \left[ \left( \frac{P}{2g_{22}} - g_{11} \right) + \frac{|y_{21}|^2}{G_a} \right] + j \left( \frac{Q}{2g_{22}} - b_{11} \right) \quad (10.75)$$

and its radius ( $R_{sa}$ ) can be obtained from the equation

$$R_{sa}^2 = G_{sa}^2 - \left\{ \left( \frac{P}{2g_{22}} - g_{11} \right)^2 - \left| \frac{y_{12}y_{21}}{2g_{22}} \right|^2 \right\} \quad (10.76)$$

When displayed on a Smith Chart, the center of each constant available power gain circle is given by

$$C_a = \frac{g_a(s_{11}^* - \Delta^* s_{22})}{1 + g_a(|s_{11}|^2 - |\Delta|^2)} \quad (10.77)$$

and the radius by

$$R_a = \frac{(1 - 2k|s_{12}s_{21}|g_a + |s_{12}s_{21}|^2 g_a^2)^{1/2}}{|1 + g_a(|s_{11}|^2 - |\Delta|^2)|} \quad (10.78)$$

The normalized gain,  $g_a$ , is given by

$$g_a = G_a / |s_{21}|^2 \quad (10.79)$$

These equations are also identical in form to the operating power gain equations. This follows from the fact that the expressions for  $G_a$  and  $G_\omega$  are identical in form too. An expression for  $G_a$  is shown below:

$$G_a = \frac{|s_{21}|^2 [1 - |S_s|^2]}{|1 - s_{11}S_s|^2 - |s_{22}(1 - s_{11}S_s) + s_{12}s_{21}S_s|^2} \quad (10.80)$$

#### 10.4.4 Constant Transducer Power Gain Circles

The set of source admittances or reflection coefficients associated with a specified value of the transducer power gain is again a circle on the admittance plane or on the Smith Chart. The same applies if the load admittance or reflection coefficient is considered.

The derivation of the relevant equations for the admittance plane is based on the  $Y$ -parameter expression for the transducer power gain (refer to (1.11)):

$$G_T = \frac{4|y_{21}|^2 G_L G_s}{|(y_{22} + Y_L)(y_{11} + Y_s) - y_{12}y_{21}|^2} \quad (10.81)$$

If the admittance  $Y_s$  is considered to be fixed, this equation can be used to find the constraints on  $Y_L$  to ensure that  $G_T$  will remain constant.

It follows, after some manipulation, that the center of the circle is given by

$$G_{LT} + jB_{LT} = -Y_{\text{out}} + \left| \frac{y_{21}}{y_{11} + Y_s} \right|^2 \frac{2G_s}{G_T} \quad (10.82)$$

and the radius by

$$R_{LT}^2 = G_{LT}^2 - G_{\text{out}}^2 \quad (10.83)$$

where  $Y_{\text{out}} = G_{\text{out}} + jB_{\text{out}}$  is the output admittance of the (modified) transistor terminated in the source admittance  $Y_s$ .

If the source admittance is taken to be the independent variable (fixed  $Y_L$ ), the center of the circle is given by

$$G_{sT} + jB_{sT} = -Y_{\text{in}} + \left| \frac{y_{21}}{y_{22} + Y_L} \right|^2 \frac{2G_L}{G_T} \quad (10.84)$$

and the radius ( $R_{sT}$ ) by

$$R_{sT}^2 = G_{sT}^2 - G_{\text{in}}^2 \quad (10.85)$$

where  $Y_{in} = G_{in} + jB_{in}$  is the input admittance of the (modified) transistor terminated in the load admittance  $Y_L$ .

The parameters for the circles on the Smith Chart can be derived by using the  $S$ -parameter expression for  $G_T$  (refer to (1.90)):

$$G_T = \frac{|s_{21}|^2 (1 - |S_L|^2)(1 - |S_s|^2)}{|(1 - s_{11}S_s)(1 - s_{22}S_L) - s_{12}s_{21}S_sS_L|^2} \quad (10.86)$$

The center of the relevant circle on the load plane ( $S_s$  fixed) is given by

$$C_{LT} = \frac{1}{S_{out} \left( 1 + \frac{|s_{21}|^2 (1 - |S_s|^2)}{G_T |1 - s_{11}S_s|^2} \frac{1}{|S_{out}|^2} \right)} \quad (10.87)$$

and its radius by

$$R_{LT} = \frac{\sqrt{X_L \left( 1 + X_L - \frac{1}{S_{out} S_{out}^*} \right)}}{1 + X_L} \quad (10.88)$$

where

$$X_L = \frac{|s_{21}|^2 (1 - |S_s|^2)}{G_T |1 - s_{11}S_s|^2 |S_{out}|^2} \quad (10.89)$$

The equations for the circles on the source plane ( $S_L$  fixed) are

$$C_{st} = \frac{1}{S_{in} \left( 1 + \frac{|s_{21}|^2 (1 - |S_L|^2)}{G_T |1 - s_{22}S_L|^2} \frac{1}{|S_{in}|^2} \right)} \quad (10.90)$$

and

$$R_{sT} = \frac{\sqrt{X_s \left( 1 + X_s - \frac{1}{S_{in} S_{in}^*} \right)}}{1 + X_s} \quad (10.91)$$

where

$$X_s = \frac{|s_{21}|^2 (1 - |S_L|^2)}{G_T |1 - s_{22} S_L|^2 |S_{in}|^2} \quad (10.92)$$

The transducer power gain circles can be used to control the transducer power gain and the noise figure of an amplifier when the load network has already been designed to optimize the power performance, and vice versa.

## 10.5 CONTROLLING THE NOISE FIGURE OF AN AMPLIFIER

It was shown in Chapter 2 (Section 2.2) that the noise figure of a (modified) transistor is determined by the source impedance presented at its input terminals by the circuit. It was also shown that the contours of constant noise figure are circles in the source plane.

It follows from

$$F = F_{\min} + \frac{R_{nv}}{G_s} [(G_s - G_{s\_opt})^2 + (B_s - B_{s\_opt})^2] \quad (10.93)$$

(refer to (1.174a)) that the center of each constant noise figure circle is given by

$$G_F + jB_F = \left( G_{s\_opt} + \frac{F - F_{\min}}{2R_{nv}} \right) + jB_{s\_opt} \quad (10.94)$$

while its radius ( $R_F$ ) is given by

$$R_F^2 = G_F^2 - G_{s\_opt}^2 \quad (10.95)$$

An expression for the noise figure in terms of the reflection coefficient presented at the input terminals of the transistor can be derived by first modifying (10.93) to

$$F = F_{\min} + \frac{R_{nv}}{G_s} |Y_s - Y_{s\_opt}|^2 \quad (10.96)$$

$G_s$  in (10.96) can be replaced by using the following result:

$$\frac{G_s}{Y_0} = \frac{1 - |\Gamma_s|^2}{|1 + \Gamma_s|^2} \quad (10.97)$$

$|Y_s - Y_{s\_opt}|$  can be replaced by using the equality

$$\frac{Y_s - Y_{s\_opt}}{Y_0} = -\frac{2(\Gamma_s - \Gamma_{s\_opt})}{(1 + \Gamma_s)(1 + \Gamma_{s\_opt})} \quad (10.98)$$

Substitution in (10.96) yields the following expression for the noise figure:

$$F = F_{min} + \frac{4r_{nv}|\Gamma_s - \Gamma_{s\_opt}|^2}{(1 - |\Gamma_s|^2)|1 + \Gamma_{s\_opt}|^2} \quad (10.99)$$

where

$$r_{nv} = \frac{R_{nv}}{Z_0} \quad (10.100)$$

Straightforward manipulation of (10.99) yields that the center of each constant noise figure circle is given on the Smith Chart by

$$C_F = \frac{\Gamma_{s\_opt}}{1 + \alpha} \quad (10.101)$$

where

$$\alpha = \frac{F - F_{min}}{4r_{nv}} |1 + \Gamma_{s\_opt}|^2 \quad (10.102)$$

The radius ( $R_F$ ) of each circle is given by

$$R_F^2 = \frac{\alpha(1 - \alpha - \Gamma_{s\_opt}\Gamma_{s\_opt}^*)}{(1 + \alpha)^2} \quad (10.103)$$

If the available power gain associated with the optimum noise figure is too low or the associated VSWRs are unacceptable, the noise performance must be sacrificed to some extent.

The point with the highest gain on a constant noise figure circle is usually of interest. This point can be determined graphically by finding the noise figure circle that just touches the gain circle of interest. A better alternative is to tabulate the noise figure with

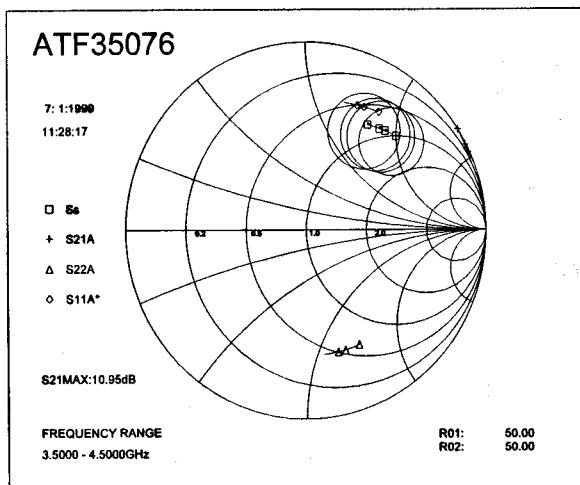


**Figure 10.18** The optimum noise source terminations for a modified transistor ( $S_o$ ) and the noise circles associated with a degradation of 0.1 dB in the noise figure.

the other parameters of interest at different positions around the constant gain circle (or vice versa).

Constant noise figure circles for a modified (series and shunt loading were used on the output side) Avantek ATF35076 transistor are displayed graphically in Figure 10.18, as an example. The optimum points ( $S_o$ ) and the contours corresponding to a 0.1dB degradation in the noise figure are displayed for a number of frequencies in the passband (3.5–4.5 GHz). The output reflection coefficients associated with the optimum source terminations ( $s_{22A}$ ), and the reflection coefficients associated with a conjugate match on the output side ( $s_{11A^*}$ ) are also displayed. Because the  $s_{11A^*}$  and the  $S_o$  traces are close to each other, the input VSWR associated with the optimum noise match will be good (around 2.5 in this case). The square of the magnitude of  $s_{21A}$  is also the available power gain of the modified transistor; note that the gain is constant over the passband of interest.

## 10.6 CONTROLLING THE OUTPUT POWER OR THE EFFECTIVE OUTPUT POWER OF A TRANSISTOR

It was shown in Chapter 2 (Section 2.2) that the power performance (1-dB compression point) of a linear two-port (class A and class B) can be controlled by using the power parameter approach. An accurate small-signal model and the boundary lines to be used to constrain the load line on the  $I/V$ -plane (intrinsic) are required for this purpose.

The power parameter approach can be used to generate power contours for any transistor, with or without modification networks. When an amplifier stage is designed, the actual output power ( $P_{out}$ ) is usually of interest, while the effective output power ( $P_{out} - P_{in}$ ) is of interest when an oscillator is designed.

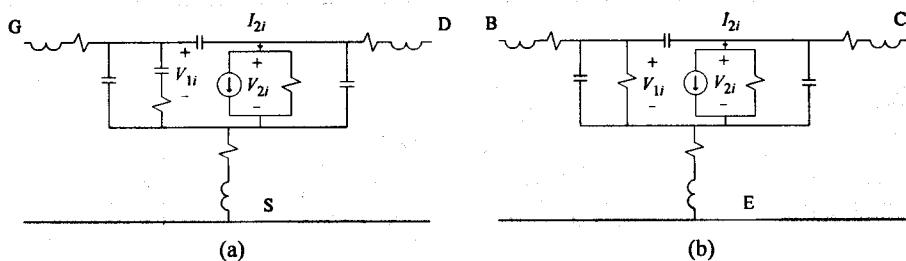


Figure 10.19 Typical small-signal models for (a) FETs and (b) bipolar transistors.

A small-signal model (see Figure 10.19) can be fitted to the measured  $S$ -parameters by optimizing initial values estimated for the components in the model to be used. Any information available on the physical transistor or its model (package parasitics, lines, etc.) should be used to ensure that the model fitted accurately represents the actual device. The parameters used should be those associated with the operating current and voltage at the power level of interest (the bias point usually shifts when the amplifier is driven hard).

If a model is fitted to a packaged transistor and no information is available on the package parasitics, the process is usually simplified by first fitting an intrinsic model only (no parasitics used) to the parameters at the lower end of the frequency range over which  $S$ -parameter data are available. The package parasitics can then be introduced during the second phase.

It is usually a good idea to optimize the fit to the  $Y$ -parameters of the device first. When a reasonable fit is obtained, the  $S$ -parameters can be targeted.

The least-square deviation from the actual parameters is usually a good choice. During the final stages of the optimization process, the  $L_1$  error (sum of the absolute values of the relative deviation from the target parameters at the different frequencies) is usually a good choice.

If accurate nonlinear models are available for the transistors used, the results obtained with the power parameter approach can be refined with a nonlinear simulator.

Constant output power contours for the modified transistor used in Figure 10.18 are displayed in Figure 10.20, as an example. The load terminations at which the output power will be a maximum ( $S_L$ ) are displayed, with the contours associated with a 1-dBm decrease in the output power, for a number of frequencies in the passband. The input reflection coefficients associated with the optimum power terminations ( $s_{11\omega}$ ) are also displayed. Note that  $|s_{21\omega}|^2$  is also the operating power gain of the modified transistor. The maximum output power and the associated termination are listed with the gain in Table 10.3.

## 10.7 THE EQUIVALENT PASSIVE IMPEDANCE-MATCHING PROBLEM

It was shown in Section 10.4.1 that the locus of load impedances for which the transducer power gain of a voltage or current source terminated in a passive load remain constant

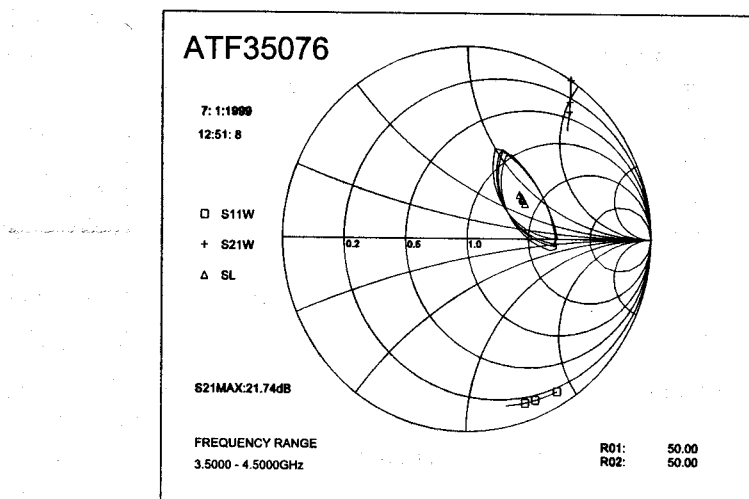


**Figure 10.20** The constant output power contours generated for a transistor (pads added;  $V_{sat} = 0.4V$ ;  $R_{sat} = 0.0$ ;  $R_{ds\_max} = 100k\Omega$ ;  $R_{ds\_min} = 100k\Omega$ ) by using the power parameter approach. ( $S_{11\omega}$  is the input reflection parameter associated with the optimum power load  $S_L$ , and  $|S_{21\omega}|^2$  is the operating power gain associated with this load.)

is a circle in the admittance plane or on the Smith Chart. These constant transducer power gain circles always lie in the right-hand side of the admittance plane or inside the Smith Chart. Similarly, it was shown that the constant operating, available, or transducer power gain contours for an active two-port are also circles, and, if the two-port is inherently stable, these circles will also be located inside the Smith Chart or in the RHS of the admittance plane. The constant noise figure circles are always located inside the Smith Chart.

**Table 10.3**

The maximum output power and the associated load impedance and operating power gain for the transistor used in Figure 10.20 (bias point: 1.5V, 10 mA)

Frequency (GHz)	Load termination ( $\Omega$ )	Output power (dBm)	Power gain (dB)
3.5	$86.0 + j36.5$	7.2	21.74
3.6	$85.4 + j37.1$	7.2	21.49
3.7	$84.3 + j37.5$	7.2	21.28
3.8	$83.5 + j38.2$	7.2	21.07
3.9	$82.5 + j38.4$	7.2	20.87
4.0	$81.8 + j39.0$	7.2	20.67
4.1	$80.6 + j39.3$	7.2	20.46
4.2	$79.4 + j39.4$	7.2	20.26
4.3	$78.8 + j39.9$	7.2	20.03
4.4	$77.6 + j40.0$	7.2	19.82
4.5	$76.9 + j40.6$	7.2	19.62

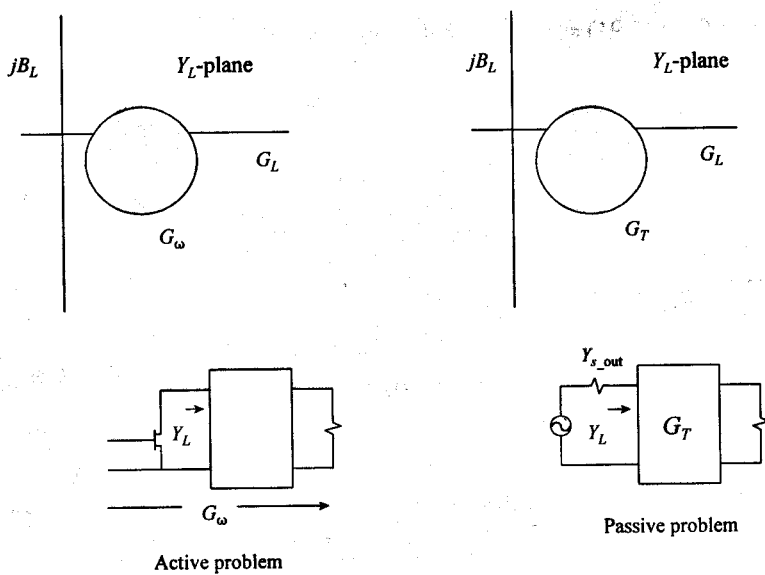


**Figure 10.21** Illustration of the equivalence between a constant operating power gain circle and the circle corresponding to mismatching a voltage source to a passive load.

By considering the active constant power gain or constant noise figure circles to be the gain circles of a passive source terminated in a passive load, the problem of finding a network to transform a given load or source to fall on the circumferences of the relevant active circles can be transformed to that of matching a complex source to a complex load with a specified transducer power gain. This can be done at each of the frequencies of interest whenever the transistor used is inherently stable inside the passband.

The equivalence between a constant operating power gain circle and a passive constant transducer power gain circle is illustrated in Figure 10.21.

### 10.7.1 Constant Operating Power Gain Case

The equations relevant to finding the output admittance and transducer power gain equivalent to a given operating power gain circle can be derived by setting

$$G_{L\omega} + jB_{L\omega} = G_0 + jB_0 \quad (10.104)$$

$$R_{L\omega} = R_{Y_0} \quad (10.105)$$

where  $G_{L\omega}$ ,  $B_{L\omega}$ , and  $R_{L\omega}$ , and  $G_0$ ,  $B_0$ , and  $R_{Y_0}$  are the parameters of the constant operating power gain and the constant transducer power gain circles, respectively.

It follows from (8.91) and (8.92) that

$$G_s \left( \frac{2}{G_T} - 1 \right) = G_0 \quad (10.106)$$

and

$$G_s \frac{2}{G_T} \sqrt{1 - G_T} = R_{Y0} \quad (10.107)$$

$G_s$  is eliminated if (10.106) is divided by (10.107):

$$\frac{\frac{2}{G_T} - 1}{\frac{2}{G_T} \sqrt{1 - G_T}} = \frac{G_0}{R_{Y0}} = g_0 \quad (10.108)$$

After simplification of (10.108), it follows that

$$G_T^2 + 4(g_0^2 - 1)G_T - 4(g_0^2 - 1) = 0 \quad (10.109)$$

It follows from (10.109) that

$$G_T = \frac{-b \pm \sqrt{b^2 - 4(1)(-b)}}{2(1)} \quad (10.110)$$

$$= -\frac{b}{2} \left( 1 \pm \sqrt{1 + \frac{4}{b}} \right)$$

$$= \frac{4(g_0^2 - 1)}{2} \left( 1 \pm \sqrt{1 + \frac{4}{4(g_0^2 - 1)}} \right)$$

$$= -2(g_0^2 - 1) \pm 2(g_0^2 - 1) \sqrt{\frac{g_0^2}{g_0^2 - 1}}$$

$$= -2(g_0^2 - 1) \pm 2g_0 \sqrt{g_0^2 - 1}$$

$$= 2 - 2g_0^2 + 2g_0 \sqrt{g_0^2 - 1} \quad (10.111)$$

Because  $g_0$  is bigger than one, only the positive sign in (10.111) will yield a value of  $G_T$  that is bigger than zero.

Equation (10.111) can also be written as

$$G_T = 1 - \left[ g_0 - \sqrt{g_0^2 - 1} \right]^2 \quad (10.112)$$

from which it follows that

$$G_{s\_out} = R_{L\omega} G_{T\_out} / (2 \sqrt{1 - G_{T\_out}}) \quad (10.113)$$

$$B_{s\_out} = -B_{L\omega} \quad (10.114)$$

$$G_{T\_out} = 1 - \left( \frac{G_{L\omega}}{R_{L\omega}} - \sqrt{\frac{G_{L\omega}^2}{R_{L\omega}^2} - 1} \right)^2 \quad (10.115)$$

While  $G_{s\_out}$  appears to be a function of  $G_{T\_out}$ , it can be shown that (10.113) reduces to the output conductance associated with the highest value of the operating power gain and a conjugate match at the input ( $Y_{s\_out} = Y_{L\_opt}^*$ ).

If the Smith Chart circles are considered, the equivalent passive problem is given by

$$\Gamma_{s\_out} = \Gamma_{L\_opt}^* \quad (10.116)$$

$$G_T = \frac{A_\omega}{2} (\sqrt{1 + 4/A_\omega} - 1) \quad (10.117)$$

$$A_\omega = \frac{|C_\omega|^2}{R_\omega^2 |\Gamma_{s\_out}|^2} \left[ 1 - |\Gamma_{s\_out}|^2 \right]^2 \quad (10.118)$$

where  $\Gamma_{L\_opt}$  is the load termination associated with the highest operating power gain.

### 10.7.2 Constant Available Power Gain Case

The equations necessary for transforming an available power gain circle to an equivalent load admittance (equivalent input admittance of the transistor) and transducer power gain

are

$$G_{L\_in} = R_{sa} G_{T\_in} / (2\sqrt{1 - G_{T\_in}}) \quad (10.119)$$

$$B_{L\_in} = -B_{sa} \quad (10.120)$$

$$G_{T\_in} = 1 - \left( \frac{G_{sa}}{R_{sa}} - \sqrt{\left( \frac{G_{sa}}{R_{sa}} \right)^2 - 1} \right)^2 \quad (10.121)$$

If the Smith Chart circles are considered, the equivalent passive problem is given by

$$\Gamma_{L\_in} = \Gamma_{s\_opt}^* \quad (10.122)$$

$$G_T = \frac{A_{av}}{2} (\sqrt{1 + 4/A_{av}} - 1) \quad (10.123)$$

$$A_{av} = \frac{|C_{av}|^2}{R_{av}^2 |\Gamma_{L\_in}|^2} \left[ 1 - |\Gamma_{L\_in}|^2 \right]^2 \quad (10.124)$$

where  $\Gamma_{s\_opt}$  is the source termination associated with the highest available power gain.

### 10.7.3 Constant Noise Figure Case

The equations necessary for transforming a constant noise figure to an equivalent load admittance (equivalent input admittance of the transistor) and transducer power gain are

$$G_L = R_{yF} G_{Tn} / (2\sqrt{1 - G_{Tn}}) \quad (10.125)$$

$$B_L = -B_{sf} \quad (10.126)$$

$$G_{Tn} = 1 - \left( \frac{G_{sf}}{R_{sf}} - \sqrt{\left( \frac{G_{sf}}{R_{sf}} \right)^2 - 1} \right)^2 \quad (10.127)$$

and

$$\Gamma_{L\_in} = \Gamma_{sn\_opt}^* \quad (10.128)$$

$$G_T = \frac{A_F}{2} (\sqrt{1 + 4 / A_F} - 1) \quad (10.129)$$

$$A_F = \frac{|C_F|^2}{R_F |\Gamma_{L\_in}|^2} \left[ 1 - |\Gamma_{L\_in}|^2 \right]^2 \quad (10.130)$$

where  $\Gamma_{sn\_opt}$  is the source termination associated with the optimum noise figure.

## 10.8 DEVICE-MODIFICATION

The main problem during amplifier synthesis is often not the impedance-matching networks to be designed, but rather the feedback and loading sections that should be added to the transistor before the matching is done, that is, device-modification [1,7]. The resistive sections used usually strongly modify the transistor at the lower frequencies and have little influence at the higher frequencies where the gain is low and the noise figure is high.

Device-modification has the following advantages:

1. The stability of the transistor can be improved. Inherent stability over the complete working frequency range of the transistor can often be obtained without degrading the potential performance significantly.
2. The inherent gain slope of the transistor can be reduced or, ideally, removed over the passband of interest (frequency selective feedback and/or loading).
3. The gain-bandwidth constraints associated with the impedance-matching problems to be solved can be reduced.
4. The optimum gain point can be forced to be closer to the optimum noise point. This is usually essential if low noise figures with low VSWRs are required without using hybrid couplers or isolators.
5. The optimum gain point can be forced to be closer to the optimum power point.

With reference to point 3 above, the difference between the actual impedance in

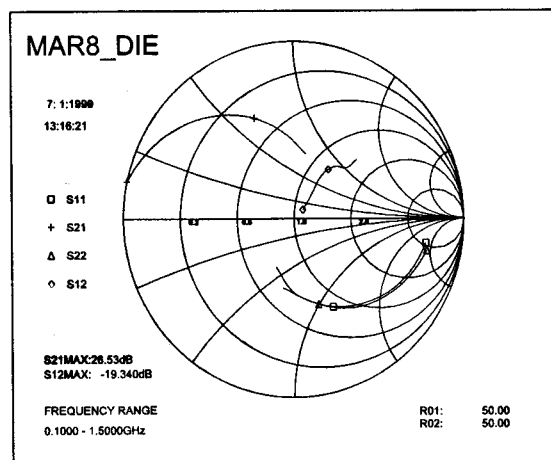


Figure 10.22 The S-parameters of the MAR8 die before modification.

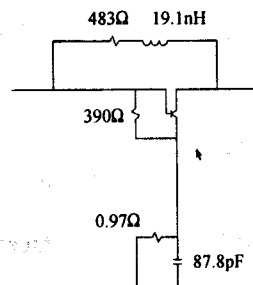


Figure 10.23 A lumped-element modification network for the transistor in Figure 10.22 [1].

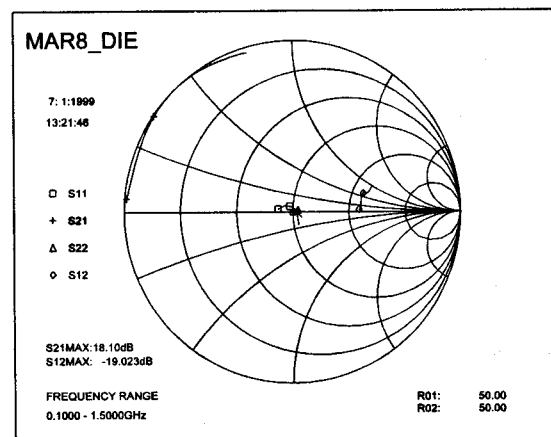


Figure 10.24 The S-parameters of the modified transistor.

place and that required to get the specified performance from the transistor can be expressed as a reflection coefficient or a VSWR. Either of these parameters can be used as a first-order indication of the severity of the matching problem to be solved.

These points will be illustrated with three examples. In the first example a transistor will be modified for improved VSWRs, level gain, and inherent stability. In the second example a low-noise transistor will be modified to get the optimum gain match closer to the optimum noise match with simultaneous flat gain and inherent stability. In the third example a transistor will be modified to get the optimum power load closer to the optimum gain match, again with simultaneous flat gain and inherent stability.

#### **EXAMPLE 10.1** Modifying a transistor for flat gain and low input and output VSWRs.

The *S*-parameters for a transistor (MAR8 die) are shown in Figure 10.22. The input and output VSWRs are poor and the gain is sloping downward over the passband (0.1–1.5 GHz). The transistor is also potentially unstable ( $k \geq 0.53$ ).

The performance with the lumped-element modification network shown in Figure 10.23 is displayed in Figure 10.24. The  $390\Omega$  resistor shown was used to remove the negative  $g_{11}$  of the transistor. The gain of the modified transistor is  $17.96 \pm 0.14$  dB. The input VSWR is lower than 1.19 and the output VSWR is lower than 1.14. The modified transistor is just inherently stable.

#### **EXAMPLE 10.2** Modifying a transistor to get the optimum noise match closer to the optimum gain match.

The transistor to be modified (ATF35076) was used as the first stage in a low-noise amplifier. The goal was to level the available power gain associated with the

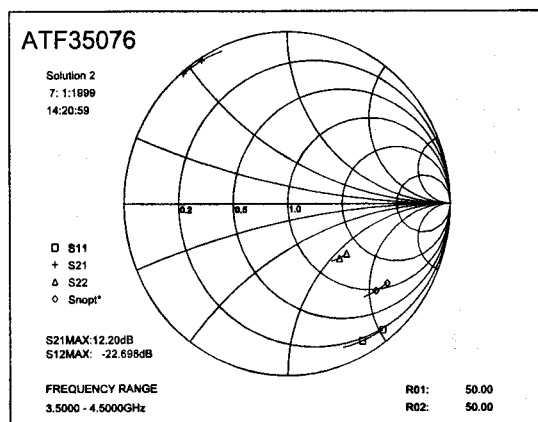


**Figure 10.25** The *S*-parameters and the optimum noise impedance of the ATF35076 transistor before modification (passband 3.5–4.5GHz).

Table 10.4

The characteristics of an ATF35076 transistor before modification over the passband 3.5–4.5 GHz

Frequency (GHz)	<i>k</i>	MAG (dB)	MSG (dB)	$G_a$ (dB)	$G_\omega$ (dB)	$G_T$ (dB)	NF (dB)
2.00	0.17	infinity	20.69	13.45	26.28	12.26	0.88
3.00	0.27	infinity	18.99	13.21	22.24	12.13	0.88
3.50	0.30	infinity	18.33	13.14	21.14	12.10	0.87
3.60	0.30	infinity	18.21	13.12	20.95	12.10	0.87
3.70	0.31	infinity	18.09	13.11	20.76	12.05	0.86
3.80	0.31	infinity	17.99	13.09	20.57	12.08	0.86
3.90	0.32	infinity	17.07	13.07	20.39	12.07	0.85
4.00	0.33	infinity	17.77	13.05	20.20	12.06	0.85
4.10	0.33	infinity	17.67	13.01	20.01	12.05	0.85
4.20	0.34	infinity	17.58	12.98	19.81	12.03	0.85
4.30	0.35	infinity	17.48	12.94	19.61	12.01	0.85
4.40	0.36	infinity	17.39	12.90	19.42	11.99	0.85
4.50	0.37	infinity	17.30	12.86	19.24	11.97	0.84
5.00	0.42	infinity	16.89	12.64	18.31	11.84	0.83
6.00	0.51	infinity	16.16	12.18	16.5?	11.50	0.79
7.00	0.57	infinity	15.61	11.79	15.47	11.22	0.82
8.00	0.62	infinity	15.14	11.42	14.70	10.96	0.86

Frequency (GHz)	$F_{opt}$ (dB)	$G_a(Z_{sn\_opt})$ (dB)	$M(Z_{sn\_opt})$	$F_m$ (dB)	$\delta(Z_{ns\_opt})$
			—		—
2.00	0.130	21.07	0.03	0.13	1.58
3.00	0.190	19.22	0.05	0.19	1.70
3.50	0.220	18.17	0.05	0.22	1.70
3.60	0.230	17.95	0.06	0.23	1.70
3.70	0.230	17.78	0.06	0.23	1.69
3.80	0.240	17.58	0.06	0.24	1.69
3.90	0.240	17.43	0.06	0.24	1.69
4.00	0.250	17.25	0.06	0.25	1.68
4.10	0.260	17.13	0.06	0.26	1.68
4.20	0.260	17.01	0.06	0.27	1.69
4.30	0.270	16.87	0.07	0.28	1.67
4.40	0.280	16.75	0.07	0.29	1.68
4.50	0.280	16.64	0.07	0.29	1.67
5.00	0.320	16.10	0.08	0.33	1.63
6.00	0.380	14.95	0.09	0.39	1.39
7.00	0.440	13.89	0.11	0.46	1.26
8.00	0.500	13.28	0.13	0.52	1.22

optimum noise figure and to get the optimum noise match condition closer to that for optimum gain. Inherent stability was also required.

The performance before modification is listed in Table 10.4. Note that  $k$  is less than 1 and  $G_a(Z_{sn\_opt})$  varies from 17.95 to 16.64 dB over the passband. Also note the large tunability factor before modification (around 1.70 in the passband).

The S-parameters and the optimum noise impedance before modification are

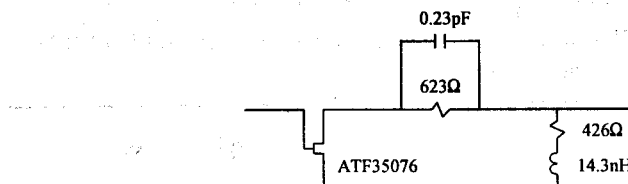


**Figure 10.26** The lumped-element modification network used [1].

shown in Figure 10.25. It is clear from this figure that the input reflection with a  $50\Omega$  load is severe and that the traces for the optimum noise match and the input reflection coefficient are far apart.

It is important to realize that the terminations for the transistor are taken to be  $50\Omega$  in Figure 10.25 and that the actual terminations will be different.

The performance associated with the lumped-element modification network displayed in Figure 10.26 is listed in Table 10.5. Note that  $G_a(Z_{m, \text{opt}})$  has been leveled (in this case the gain is level over a very wide band). The noise figure has been degraded slightly (better than 0.5 dB; previously better than 0.28 dB), and the modified transistor is inherently stable at all frequencies. Also note the improvement in the tunability factor (down to 0.35).

The  $S$ -parameters and the optimum noise impedance for the modified transistor are shown in Figure 10.27. Note from the  $s_{11}$  and  $S_{n,\text{opt}}$  traces ( $50\Omega$  load termination) that the optimum noise match is now much closer to the optimum gain match.

Pads and connecting lines are required in a real modification network. The performance associated with a more realistic network (Figure 10.28) is listed in Table 10.6 and Figure 10.28. Note that the gain is now around 12 dB and the noise figure around 0.44 dB. The stability has also improved.

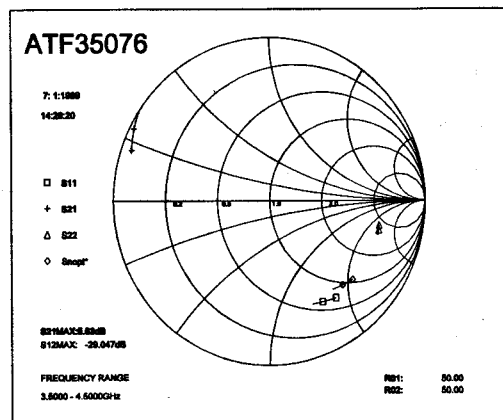


**Figure 10.27** The  $S$ -parameters and the optimum noise impedance of the ATF35076 transistor after modification with lumped elements (passband 3.5–4.5 GHz).

Table 10.5

The characteristics of an ATF35076 transistor after modification over the passband 3.5–4.5 GHz (lumped-element circuit) [1]

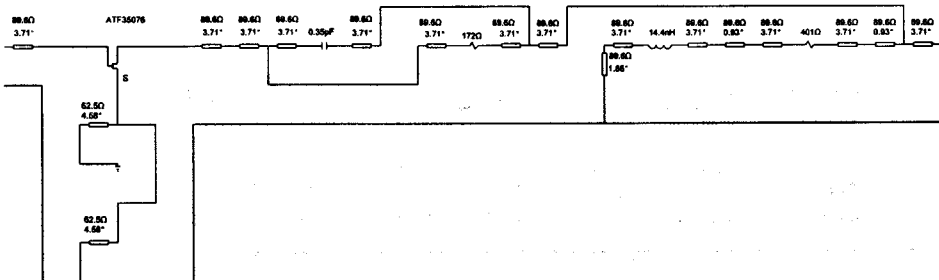
Frequency (GHz)	<i>k</i> —	MAG (dB)	MSG (dB)	$G_a$ (dB)	$G_\omega$ (dB)	$G_T$ (dB)	NF (dB)
2.00	3.62	12.17	12.17	6.18	8.66	3.23	1.52
3.00	2.47	12.24	12.24	7.69	8.40	4.63	1.30
3.50	2.08	12.41	12.41	8.21	8.39	5.09	1.22
3.60	2.02	12.45	12.45	8.30	8.39	5.17	1.21
3.70	1.96	12.49	12.49	8.39	8.40	5.24	1.19
3.80	1.90	12.52	12.52	8.47	8.40	5.31	1.18
3.90	1.84	12.57	12.57	8.55	8.41	5.38	1.17
4.00	1.80	12.60	12.60	8.62	8.41	5.44	1.16
4.10	1.75	12.63	12.63	8.68	8.41	5.49	1.15
4.20	1.71	12.65	12.65	8.74	8.41	5.54	1.13
4.30	1.68	12.68	12.68	8.79	8.42	5.59	1.13
4.40	1.64	12.70	12.70	8.85	8.42	5.64	1.12
4.50	1.61	12.73	12.73	8.89	8.43	5.68	1.11
5.00	1.47	12.82	12.82	9.09	8.46	5.88	1.07
6.00	1.30	12.90	12.90	9.34	8.44	6.16	0.99
7.00	1.17	13.14	13.14	9.49	8.56	6.42	0.98
8.00	1.07	13.58	13.58	9.63	8.82	6.78	0.99
10.00	1.01	13.62	13.62	9.42	9.11	7.03	1.05
12.00	1.05	12.44	12.44	9.13	9.29	7.33	1.09
16.00	1.12	11.07	11.07	8.58	9.94	7.81	1.01
18.00	1.14	10.65	10.65	8.53	10.26	8.07	1.04

Frequency (GHz)	$F_{opt}$ (dB)	$G_a(Z_{sn\_opt})$ (dB)	$M(Z_{sn\_opt})$ —	$F_m$ (dB)	$\delta(Z_{sn\_opt})$ —
2.00	0.442	11.27	0.12	0.48	0.24
3.00	0.466	11.35	0.12	0.50	0.30
3.50	0.478	11.39	0.13	0.51	0.32
3.60	0.484	11.39	0.13	0.52	0.32
3.70	0.480	11.40	0.13	0.52	0.33
3.80	0.486	11.41	0.13	0.52	0.33
3.00	0.482	11.42	0.13	0.52	0.34
4.00	0.488	11.43	0.13	0.52	0.34
4.10	0.493	11.44	0.13	0.53	0.34
4.20	0.489	11.46	0.13	0.52	0.35
4.30	0.495	11.47	0.13	0.53	0.35
4.40	0.500	11.48	0.13	0.54	0.35
4.50	0.496	11.50	0.13	0.53	0.35
5.00	0.514	11.56	0.14	0.55	0.36
6.00	0.543	11.48	0.14	0.58	0.35
7.00	0.579	11.29	0.15	0.62	0.35
8.00	0.614	11.26	0.16	0.66	0.37

OPTIMIZATION RESULTS		OPTIMIZATION ERROR	
GmPMin:	12.24dB		1.58791
GmPMax:	12.36dB		
VswrI_Mi:	2.57		
VswrI_Ma:	2.66		
VsNro_Mi:	4.00		
VsNro_Ma:	4.10		
F_Mi:	0.40dB		
F_Ma:	0.42dB		
UsNMa_Mi:	4.74		
UsNMa_Ma:	5.89		
k_min:	1.20		

VARIABLES AND GRADIENTS			
SIn_Bo	1	496.576	-1.477E-3
SIn_Lo	2	14.437	1.216E-3
SI_Ro	3	171.528	-6.949E-3
SI_Co	4	6.347	0.136
CSF_B	5	18.387	-0.991



**Figure 10.28** The topology of a more realistic modification network for the transistor in Example 10.2 with the associated performance (electrical line lengths specified at 4.5GHz).

The S-parameters and the optimum noise impedance associated with the distributed modification network are displayed in Figure 10.29.

It is important to realize that a distorted picture can be obtained only if the Smith Chart results are interpreted. As mentioned above, the actual terminations of the modified transistor will not be  $50\Omega$  and the impedances associated with the actual terminations will be different. The performance associated with the actual termination should be evaluated and targeted during the optimization process. The optimization results listed in Figure 10.28 correspond to the actual terminations of interest.

Note that the “VswrI” values listed in Figure 10.28 define the range of the input VSWR values associated with the optimum noise match and a conjugate match on the output side of the transistor. The input VSWR will vary between 2.57 and 2.66 over the passband if the relevant matching problems can be solved perfectly. Similarly, the output VSWR (with the optimum noise matching network in place and before matching the output side) will vary between 4.00 and 4.10. The output VSWRs were calculated for a  $50\Omega$  load. The “VsNMa” values are the VSWR values calculated for the optimum noise impedances relative to the physical termination for the stage ( $50\Omega$  in this case). These VSWRs serve as a measure of the degree of difficulty of the noise matching problem.

**Table 10.6**  
The performance associated with the distributed modification network [1]

Frequency (GHz)	<i>k</i>	MAG (dB)	MSG (dB)	$G_a$ (dB)	$G_\omega$ (dB)	$G_T$ (dB)	NF (50Ω) (dB)
2.00	2.18	14.55	14.55	8.15	12.51	6.30	1.23
3.00	1.92	13.46	13.46	8.97	11.09	6.88	1.12
3.50	1.74	13.35	13.35	9.41	10.78	7.19	1.04
3.60	1.71	13.34	13.34	9.49	10.74	7.25	1.03
3.70	1.68	13.34	13.34	9.58	10.70	7.31	1.02
3.80	1.65	13.35	13.35	9.66	10.68	7.37	1.01
3.90	1.62	13.35	13.35	9.74	10.65	7.43	1.00
4.00	1.59	13.36	13.36	9.82	10.64	7.49	0.98
4.10	1.56	13.37	13.37	9.88	10.63	7.55	0.96
4.20	1.54	13.37	13.37	9.94	10.62	7.60	0.95
4.30	1.52	13.38	13.38	9.99	10.62	7.65	0.93
4.40	1.50	13.37	13.37	10.04	10.62	7.70	0.92
4.50	1.49	13.37	13.37	10.08	10.62	7.75	0.91
5.00	1.45	13.18	13.18	10.19	10.53	7.94	0.87
6.00	1.39	12.72	12.72	10.14	10.34	8.22	0.81
7.00	1.37	12.38	12.38	9.98	10.36	8.51	0.80
8.00	1.27	12.38	12.38	9.94	10.60	8.84	0.81

Frequency (GHz)	$F_{opt}$ (dB)	$G_a(Z_{sn\_opt})$ (dB)	$M(Z_{sn\_opt})$	$F_m$ (dB)	$\delta(Z_{sn\_opt})$
			—	(dB)	—
2.00	0.305	13.31	0.08	0.32	0.35
3.00	0.386	12.50	0.10	0.41	0.35
3.50	0.398	12.30	0.10	0.42	0.34
3.60	0.405	12.27	0.10	0.43	0.34
3.70	0.412	12.26	0.11	0.44	0.34
3.80	0.409	12.25	0.10	0.43	0.34
3.90	0.415	12.24	0.11	0.44	0.34
4.00	0.412	12.24	0.11	0.44	0.34
4.10	0.407	12.25	0.10	0.43	0.34
4.20	0.413	12.27	0.11	0.44	0.34
4.30	0.408	12.28	0.10	0.43	0.34
4.40	0.414	12.29	0.11	0.44	0.34
4.50	0.410	12.30	0.11	0.43	0.34
5.00	0.443	12.22	0.11	0.47	0.33
6.00	0.483	11.87	0.13	0.51	0.32
7.00	0.527	11.51	0.14	0.56	0.36
8.00	0.565	11.47	0.15	0.60	0.45

Note that while the output VSWR in this case is a measure of the mismatch between the output impedance of the transistor ( $Z_{out}$ ) and a  $50\Omega$  load, it can also be used as a measure of the difference between the actual load ( $50\Omega$  in this case) and

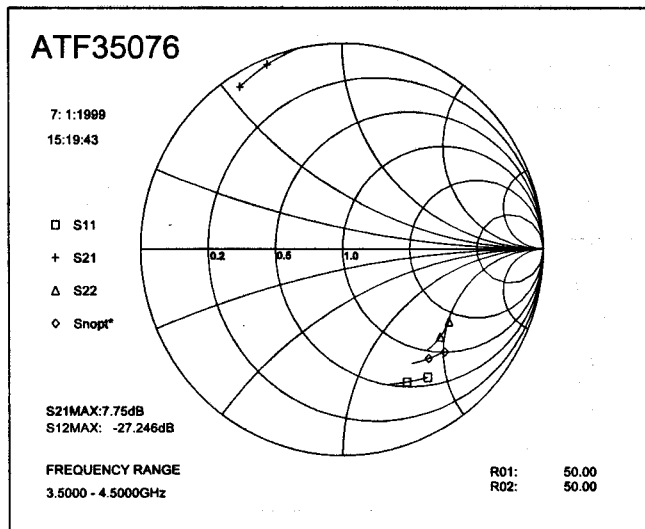


**Figure 10.29** The *S*-parameters and optimum noise impedance associated with the distributed modification network [1].

the load required by the modified transistor ( $Z_{out}^*$  in this case). If interpreted in this way, the VSWR becomes a measure of how difficult the associated matching problem will be. With a predefined passband, this approach usually yields good results. The alternative is to calculate the exact gain-bandwidth constraints associated with the matching problem.

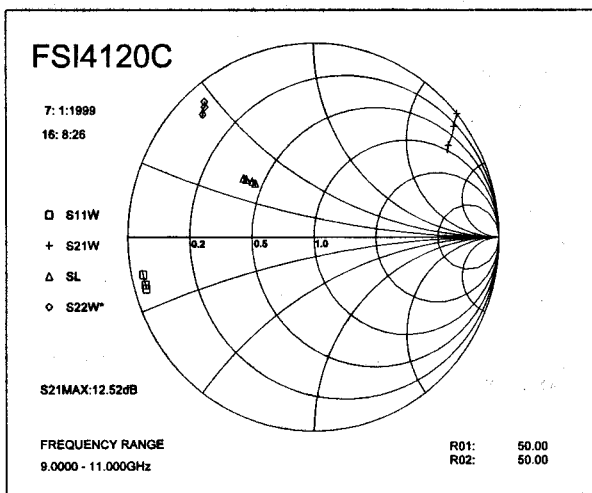


**Figure 10.30** The optimum power termination and small-signal gain for a Texas Instruments foundry FET [1] ( $V_{sat} = 0.55V$ ;  $R_{sat} = 1.86\Omega$ ;  $R_{ds\_max} = 100\text{ k}\Omega = R_{ds\_min}$ ; Bias point: 8V, 180 mA).

Table 10.7

The estimated optimum power termination of the foundry FET with the associated output power and small-signal operating gain [1]

Frequency (GHz)	Load termination (Ω)	Output power (dBm)	Power gain (dB)
9.00	$22.61 + j15.52$	27.910	12.541
9.25	$22.17 + j15.54$	27.918	12.300
9.50	$21.71 + j15.55$	27.925	12.059
9.75	$21.25 + j15.54$	27.933	11.903
10.00	$20.80 + j15.52$	27.941	11.750
10.25	$20.37 + j15.50$	27.949	11.530
10.50	$19.94 + j15.46$	27.957	11.303
10.75	$19.53 + j15.41$	27.965	11.163
11.00	$19.12 + j15.35$	27.974	11.041

### EXAMPLE 10.3 Modifying a power transistor to improve its stability and the VSWRs associated with an optimum power match.

The optimum power termination and the associated small-signal operating power gain for a Texas Instruments foundry FET (without modification) are shown in Figure 10.30 and listed in Table 10.7. Note that the traces corresponding to the optimum power match ( $S_o$ ) and the optimum gain match ( $s_{22\omega}^*$ ) are far apart. The operating power gain ( $s_{21\omega}$  trace) is also decreasing with increasing frequency. The transistor is also potentially unstable (refer to the top panel of Table 10.8).

The modification network used is shown in Figure 10.31. The electrical line lengths of the pads used are specified at 11GHz. The optimum power termination and the gain after modification are shown in Figure 10.32. The numerical values are listed in Table 10.9.

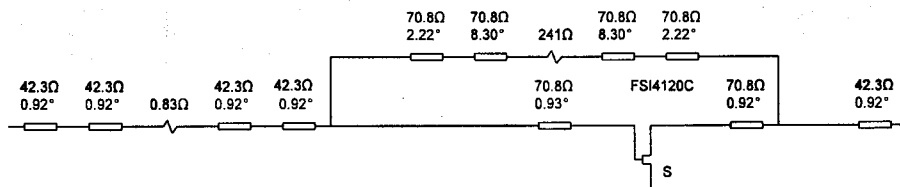


Figure 10.31 The modification circuit designed for the foundry FET [1].

Table 10.8

The stability and gain of the foundry FET before (top) and after (bottom) modification [1]

Frequency (GHz)	<i>k</i> —	MAG (dB)	MSG (dB)	$G_a$ (dB)	$G_\omega$ (dB)	$G_T$ (dB)
2.00	0.21	infinity	19.47	13.96	21.42	13.48
3.00	0.26	infinity	17.75	11.65	18.54	11.21
4.00	0.34	infinity	16.54	9.68	16.19	9.21
5.00	0.40	infinity	15.59	8.05	14.41	7.52
6.00	0.47	infinity	14.85	6.67	12.93	6.06
7.00	0.52	infinity	14.23	5.49	11.68	4.78
8.00	0.58	infinity	13.68	4.45	10.61	3.61
8.50	0.61	infinity	13.44	3.99	10.06	3.08
9.00	0.64	infinity	13.22	3.54	9.59	2.57
9.25	0.66	infinity	13.11	3.34	9.34	2.33
9.50	0.68	infinity	13.01	3.15	9.09	2.10
9.75	0.69	infinity	12.90	2.94	8.88	1.85
10.00	0.69	infinity	12.80	2.75	8.68	1.62
10.25	0.71	infinity	12.71	2.57	8.45	1.40
10.50	0.73	infinity	12.62	2.40	8.21	1.18
10.75	0.74	infinity	12.53	2.22	8.03	0.97
11.00	0.75	infinity	12.44	2.05	7.86	0.76
15.00	0.96	infinity	11.33	-0.11	5.05	-2.17
20.00	1.04	9.03	9.03	-1.80	2.42	-5.16
25.50	1.26	6.28	6.28	-3.09	-0.79	-7.98

Frequency (GHz)	<i>k</i> —	MAG (dB)	MSG (dB)	$G_a$ (dB)	$G_\omega$ (dB)	$G_T$ (dB)
6.00	1.43	9.63	9.63	5.03	8.69	4.87
7.00	1.44	9.38	9.38	4.12	8.23	3.85
8.00	1.45	9.15	9.15	3.29	7.74	2.87
8.50	1.45	9.04	9.04	2.94	7.50	2.43
9.00	1.45	8.88	8.88	2.56	7.20	1.96
9.25	1.46	8.77	8.77	2.39	7.04	1.74
9.50	1.47	8.66	8.66	2.23	6.87	1.53
9.75	1.46	8.63	8.63	2.07	6.75	1.32
10.00	1.46	8.59	8.59	1.91	6.62	1.10
10.25	1.46	8.50	8.50	1.76	6.46	0.90
10.50	1.47	8.41	8.41	1.61	6.30	0.71
10.75	1.45	8.39	8.39	1.48	6.19	0.52
11.00	1.44	8.36	8.36	1.35	6.07	0.33
11.50	1.46	8.16	8.16	1.06	5.73	-0.07
12.00	1.41	8.21	8.21	0.83	5.55	-0.42
13.00	1.40	7.97	7.97	0.38	4.97	-1.11
14.00	1.41	7.60	7.60	-0.01	4.31	-1.75

**Table 10.9**

The optimum power terminations of the modified foundry FET with the associated output power and small-signal gain [1]

Frequency (GHz)	Load termination ( $\Omega$ )	Output power (dBm)	Power gain (dB)
9.00	$22.8 + j18.3$	27.2	8.69
9.25	$22.0 + j18.2$	27.2	8.59
9.50	$21.5 + j18.0$	27.2	8.48
9.75	$21.0 + j17.8$	27.2	8.44
10.00	$20.6 + j17.6$	27.2	8.38
10.25	$19.7 + j17.4$	27.3	8.30
10.50	$19.3 + j17.2$	27.3	8.20
10.75	$18.9 + j16.9$	27.3	8.16
11.00	$18.3 + j16.7$	27.3	8.13

The optimum power match is now much closer to the optimum gain match. Note that the gain is now very flat (although it is on the low side). The maximum power obtainable has decreased by 1 dBm. The modified transistor is inherently stable (refer to the bottom panel of Table 10.8).

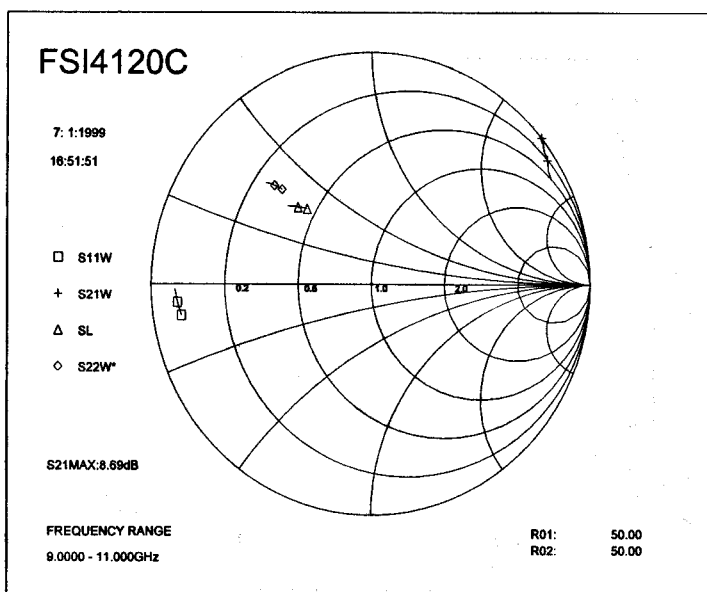


**Figure 10.32** The optimum power termination and small-signal gain for a foundry FET (Texas Instruments FSI4120C) after modification [1].

## 10.9 DESIGNING CASCADE AMPLIFIERS

At this point the basic knowledge required to design single or multistage cascade type amplifiers are in place. A typical design cycle is outlined in the flow diagram shown in Figure 10.1. When this approach is followed, the design cycle proceeds from the load side toward the source, or vice versa. A low-noise design is usually done by starting the design at the input side. When the output power is more important, the design is usually started at the load side.

When a multistage high dynamic range amplifier is synthesized, the design can be started at both sides and the two sections can then be linked up with an interstage matching network (refer to Figure 10.12(c)). In the single-stage case, the load network can first be designed for maximum output power after which the input network can be designed to level the gain with the noise figure as low as possible (this can be done by choosing the optimum noise figure points on the relevant constant gain circles).

The design of each stage consists of selecting a transistor for the stage, modifying it appropriately, and synthesizing a lossless gain, noise figure, or power control network for it. If the associated matching problem is too difficult to be solved properly, the transistor should be modified more strongly or a different transistor should be used.

When the control network for each stage is designed, the performance around the relevant constant gain, noise figure, or output power circle should be evaluated. The options to match to a specific point on each circle (a point match) or to any arbitrary point on the circle (circle match) exist. If the performance is only acceptable in a narrow region on the circle circumference, a point-match should be enforced.

The performance of a transistor around a constant noise figure circle is displayed in Table 10.10. The following values are listed as a function of the angle around the constant noise figure circle (Smith Chart case) in this table:

1. The reflection coefficient at the point of interest ( $\Gamma_{L\_mag}$ ,  $\Gamma_{L\_ang}$ );
2. The available power gain ( $G_a$ );
3. The output power if the output side is conjugately matched;
4. The difference between the actual source termination ( $50\Omega$  in this case) and the source termination required expressed as a VSWR;
5. The sensitivity of the noise figure to changes in the admittance presented at the input of the modified transistor ( $\delta_n$ );
6. The sensitivity of the available power gain to changes in the source admittance ( $\delta_a$ );
7. The sensitivity of the output match to changes in the source admittance ( $\delta_{vs}$ ).

**Table 10.10**  
The performance of a modified transistor around a constant noise figure circle [1]

$\theta$ (°)	$G_a$ (dB)	Power (dBm)	VSWR	$\delta_n$ (%)	$\delta_g$ (%)	$\delta_{nr}$	$\Gamma_{L\_mag}$	$\Gamma_{L\_ang}$ (°)
0.0	10.54	1.63	9.05	0.17	1.85	0.02	0.80	36.35
25.0	10.86	1.58	10.96	0.22	2.30	0.02	0.83	40.90
50.0	11.56	1.59	11.51	0.25	2.26	0.03	0.84	45.82
75.0	12.37	1.71	10.26	0.24	1.55	0.03	0.82	50.65
100.0	12.87	1.90	8.14	0.20	0.73	0.03	0.78	54.89
125.0	12.94	2.01	6.18	0.16	0.47	0.03	0.72	57.97
150.0	12.73	1.98	4.72	0.13	0.58	0.03	0.65	59.12
175.0	12.42	1.99	3.77	0.10	0.64	0.02	0.58	57.47
200.0	12.07	2.02	3.23	0.09	0.67	0.02	0.53	52.42
225.0	11.73	2.03	3.06	0.08	0.69	0.02	0.51	44.72
250.0	11.40	1.97	3.24	0.08	0.73	0.02	0.53	37.05
275.0	11.09	1.90	3.70	0.08	0.81	0.01	0.58	32.05
300.0	10.81	1.83	4.74	0.09	0.95	0.01	0.65	30.46
325.0	10.59	1.75	6.20	0.11	1.21	0.01	0.72	31.65
350.0	10.50	1.66	8.18	0.15	1.64	0.02	0.78	34.75

Note: The highlighting is used to indicate the optimum point on the circle

If matching to any point on a circle is acceptable (circle match), the equivalent passive problem can be defined for the circle as described in Section 10.7. Matching to a specific point may also be required. The highlighting in Table 10.10 is used to indicate the optimum point on the circle circumference for both cases.

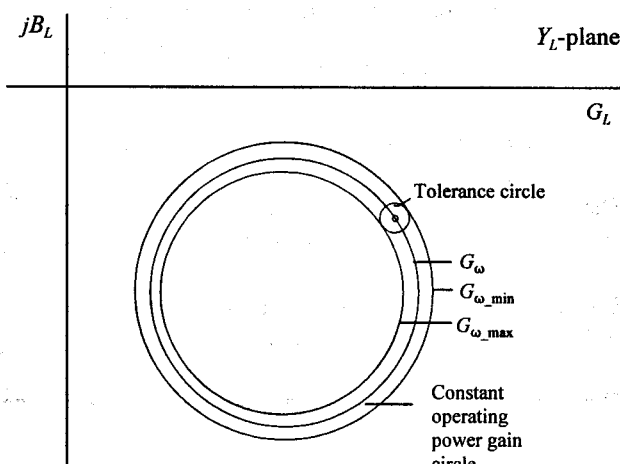


**Figure 10.33** Calculation of the sensitivity factor associated with the operating power gain ( $\delta_\omega$ ) [1].

The sensitivity factor is calculated by considering the change in the parameter of interest when the controlling admittance changes by 1%. Calculation of the operating power gain sensitivity factor ( $\delta_{\omega}$ ) is demonstrated in Figure 10.33. The lowest and highest gain associated with the tolerance circle are  $G_{\omega_{\min}}$  and  $G_{\omega_{\max}}$ , respectively. The sensitivity factor ( $\delta_{\omega}$ ) is calculated as the maximum of

$$\delta_{\omega_1} = \text{ABS} [(G_{\omega_{\max}} - G_{\omega}) / G_{\omega}] \quad (10.131)$$

and

$$\delta_{\omega_2} = \text{ABS} [(G_{\omega_{\min}} - G_{\omega}) / G_{\omega}] \quad (10.132)$$

High values for any of the sensitivity factors are undesirable. Note that the sensitivity factors calculated are indications of the sensitivity of the problem to be solved.

#### **EXAMPLE 10.4** An example of a single-stage LNA (passband 3.3–4.4 GHz) [1].

As an example of a single-stage design, consider the amplifier shown in Figures 10.34, 10.35, and 10.36.

The transistor (NE32484A; optimum noise bias point) was modified by using series and shunt loading networks on the output side (0.7 pF in parallel with  $165\Omega$  and  $102\Omega$  in series with a line). The structure to the right of the transistor position in Figure 10.35 was designed to accommodate the parallel capacitor/resistor combination (a gap capacitor and a chip resistor).

The modification was done to level the available power gain associated with an optimum noise match and to improve the associated VSWRs. The target for the input VSWR was around 2.5, and that for the output was around 8.0. Note that the input VSWR target was the actual VSWR expected if the defined noise matching problem could be solved exactly. The output VSWR calculated is a measure of the degree of difficulty of the output match, as discussed above (the actual output VSWR will be 1.0 if the output matching problem could be solved perfectly).

The modification network was also used to improve the stability. However, inherent stability is not obtained at all frequencies with the network designed. The  $2.9k\Omega$  resistor in the output circuit was used to obtain inherent stability at all frequencies.

The step after device-modification was to design the input matching network for the optimum noise figure. The input matching network designed is shown in Figure 10.36(a).

With the input network designed, the output impedance of the modified transistor is known. The output matching network was used to match this impe-

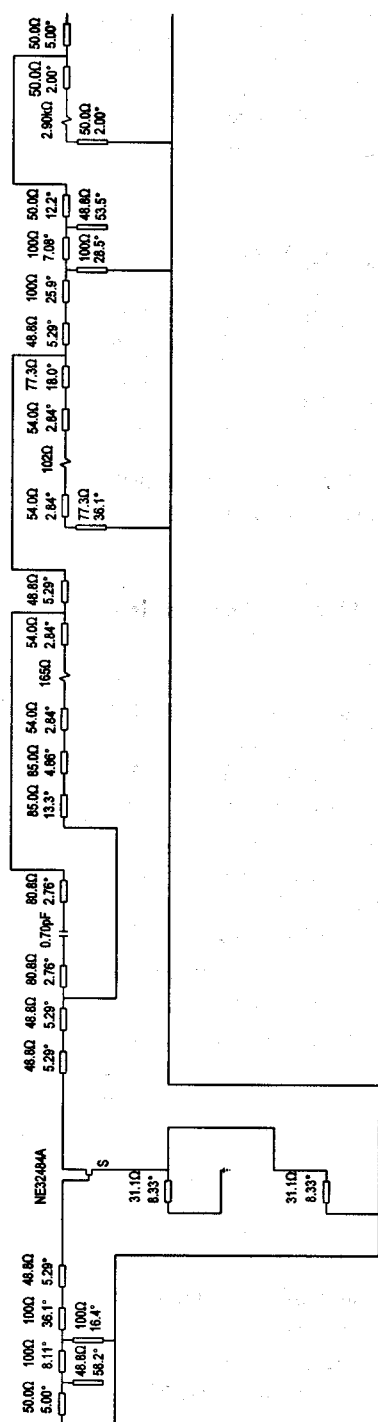


**Figure 10.34** The schematic diagram of the single-stage amplifier of Example 10.4 [1].

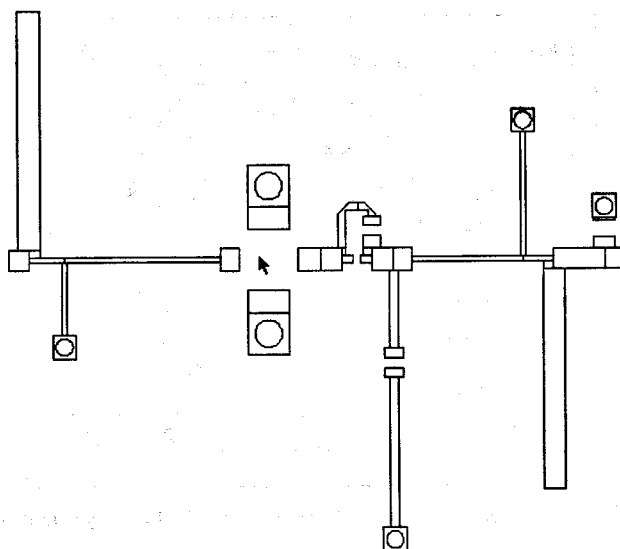
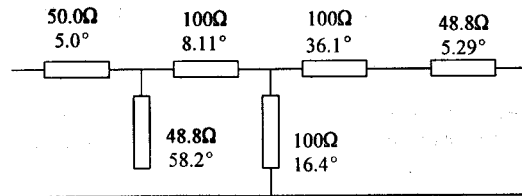
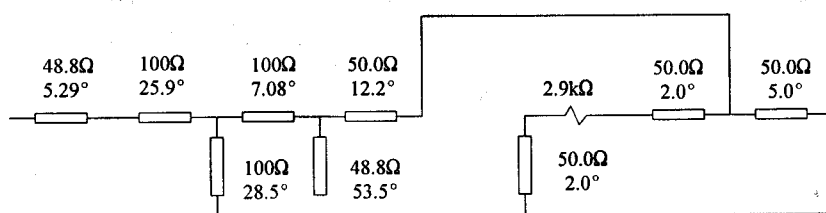


**Figure 10.35** The artwork of the single-stage LNA of Example 10.4 [1]. The transistor is located at the position indicated with the mouse cursor.



(a)



(b)

**Figure 10.36** (a) The input matching network used in Example 10.4. (b) The output matching network used in Example 10.4 [1]. The electrical line lengths are specified at 4.4 GHz.

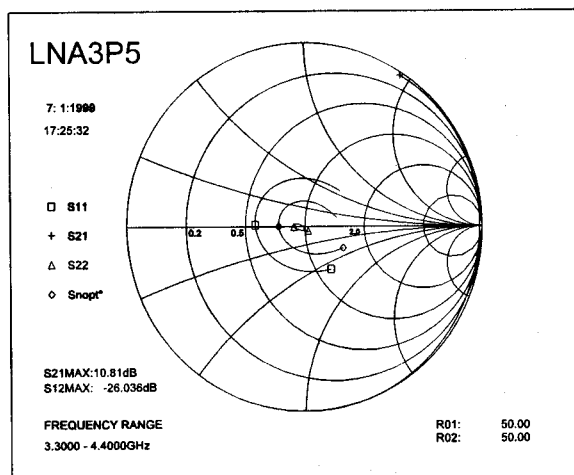


**Figure 10.37** The  $S$ -parameters of the amplifier in Example 10.4 displayed graphically [1].

dance to the  $50\Omega$  load. The output matching network designed is shown in Figure 10.36(b).

The final step in the design was to remove the input network and to redesign it for the best input match instead of the best noise figure. The noise figure increased slightly when this was done.

The artwork of the amplifier is shown in Figure 10.35.

**Table 10.11**  
The  $S$ -parameters of the amplifier in Example 10.4 [1]

Frequency (GHz)	$S_{11}$		$S_{12}$		$S_{21}$		$S_{22}$	
	(dB)	(°)	(dB)	(°)	(dB)	(°)	(dB)	(°)
3.20	-9.52	329.7	-28.95	11.8	10.48	71.3	-24.99	339.2
3.30	-11.25	302.4	-28.50	357.8	10.66	56.6	-30.29	311.3
3.40	-12.25	273.1	-28.16	344.6	10.72	42.6	-32.83	255.2
3.50	-12.45	244.0	-27.89	331.8	10.73	29.0	-29.87	215.6
3.60	-12.05	218.7	-27.67	319.7	10.71	15.8	-27.06	198.5
3.70	-11.53	196.7	-27.49	307.9	10.68	2.9	-25.30	189.1
3.80	-11.12	178.2	-27.29	296.6	10.66	350.3	-24.27	181.8
3.90	-10.92	160.7	-27.08	285.3	10.66	337.8	-23.93	175.3
4.00	-10.93	143.1	-26.86	273.8	10.69	325.1	-24.35	169.2
4.10	-11.20	124.3	-26.63	262.1	10.73	312.1	-25.84	163.4
4.20	-11.53	101.6	-26.39	249.8	10.77	298.5	-29.65	158.1
4.30	-11.69	75.0	-26.18	236.7	10.81	284.4	-45.40	179.4
4.40	-11.19	44.4	-26.04	222.8	10.79	269.2	-28.92	311.5
4.50	-9.84	13.4	-25.99	207.7	10.67	253.2	-21.02	304.9

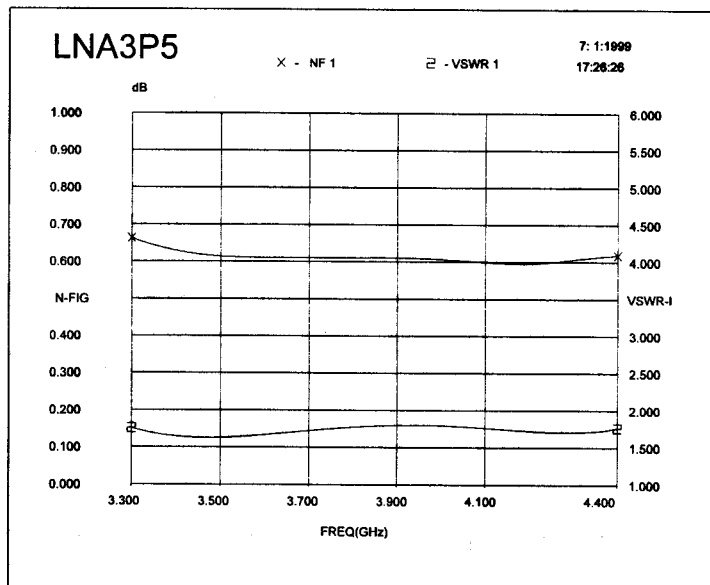


**Figure 10.38** The noise figure and the input VSWR of the amplifier considered in Example 10.4.

The  $S$ -parameters of the final amplifier are listed in Table 10.11 and are displayed graphically in Figure 10.37. The noise figure and the input VSWR are displayed graphically in Figure 10.38.

The gain of the amplifier is close to 10.7 dB over the whole passband. The noise figure is lower than 0.7 dB. The input VSWR is below 1.8 and the output VSWR below 1.15. The Rollette stability factor is larger than 1.1 over the complete frequency range. The expected 1-dB compression point varies between -2.8 dBm and -1.2 dBm over the passband.

#### EXAMPLE 10.5 Designing a two-stage amplifier.

As an example of designing a multistage amplifier, a distributed two-stage amplifier will be designed over the passband 2–6 GHz by designing a lumped-element network and using the PI-section transformation technique described in Chapter 9 to convert the matching networks to distributed form. In order to use this technique, the impedance-matching networks designed will be constrained to contain low-pass PI-sections whenever possible. The  $S$ -parameters of the transistor used are repeated in Table 10.12.

Because the gain-bandwidth constraints resulting from the input and output impedances of the transistor are too severe, it was decided to use a voltage-shunt feedback modification network in order to reduce these constraints. More feedback was used on the transistor of the first stage because a low input VSWR is required

and the constraints associated with the input impedances of the FET are more severe than those associated with its output impedance (this is usually the case). The feedback components are shown in Figure 10.39(a).

**Table 10.12**  
The S-parameters of the Dexcel 1503A GaAs transistor (chip)

Frequency (GHz)	$s_{11}$		$s_{12}$		$s_{21}$		$s_{22}$	
	(dB)	(°)	(dB)	(°)	(dB)	(°)	(dB)	(°)
2.0	-0.265	-22	-30.5	78	9.99	159	-2.270	-10
3.0	-0.630	-31	-28.0	76	9.48	150	-2.384	-13
4.0	-1.012	-42	-24.4	69	9.40	143	-2.734	-16
5.0	-1.412	-53	-23.1	66	9.48	134	-2.975	-19
6.0	-1.938	-68	-21.9	56	9.25	122	-4.013	-22

The specifications of the output matching network are shown in Table 10.13. Because a good output match is required, the operating power gain was chosen to be as high as possible. The minimum gain of the five-element output matching network designed is 0.955 and the deviation from the desired response is therefore very small.

The specifications of the interstage matching network are shown in Table 10.14. The designed network is shown in Figure 10.39(a). The maximum deviation from the specified gain response was 0.25 dB.

The specifications of the input matching network are shown in Table 10.15. The designed network is shown in Figure 10.39(a). The calculated transducer power gain of the amplifier is  $18.65 \pm 0.35$  dB, and the input and output VSWRs are

**Table 10.13**  
The specifications for the initial output matching network of the two-stage amplifier designed

Frequency (GHz)	Source impedance (Ω)	Load impedance (Ω)	Transducer power gain
2	$86.98 - j22.13$	$50.0 + j0.00$	1.000
3	$95.97 - j28.85$	$50.0 + j0.00$	1.000
4	$88.90 - j44.97$	$50.0 + j0.00$	1.000
5	$88.33 - j52.29$	$50.0 + j0.00$	1.000
6	$79.85 - j48.70$	$50.0 + j0.00$	1.000

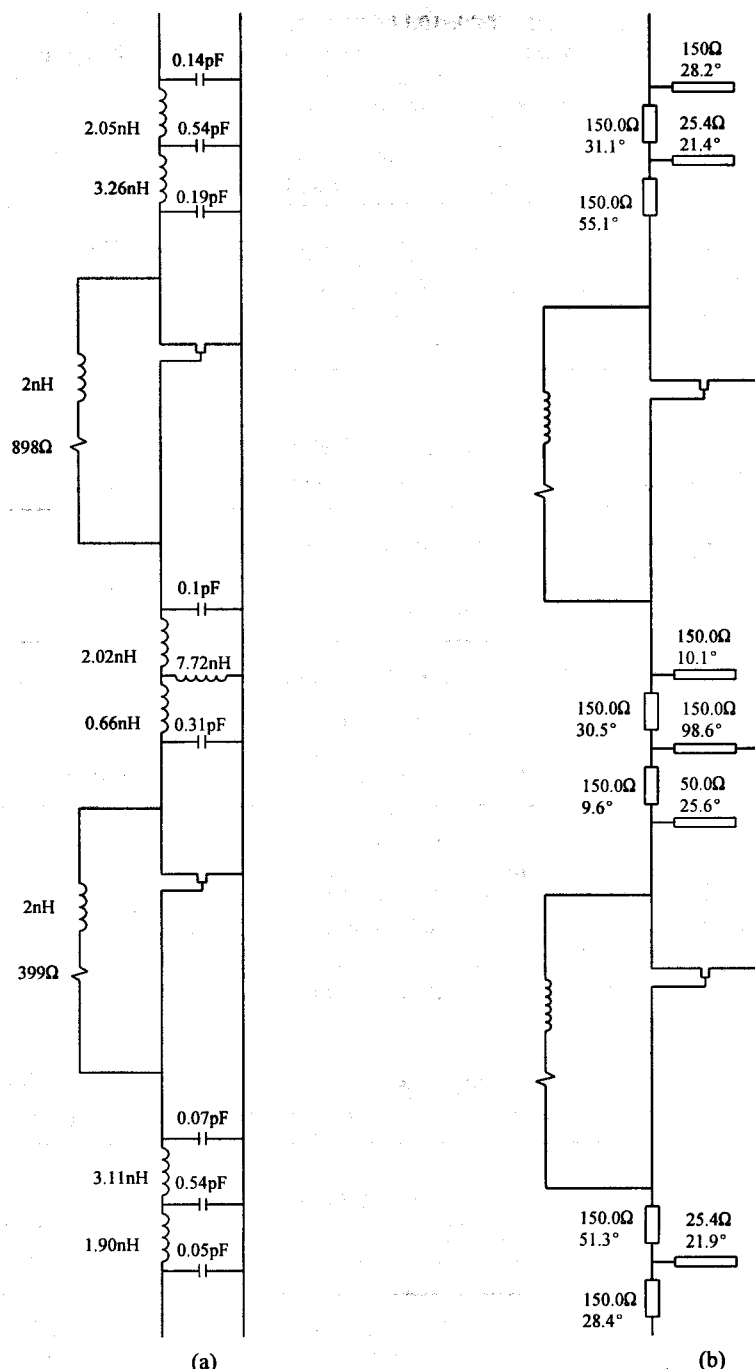


**Figure 10.39** (a) The lumped-element two-stage amplifier designed in Example 10.5 [ $G_T = 18.59 \pm 0.34$  dB; input VSWR  $\leq 1.81$ , output VSWR  $\leq 1.73$ ] and (b) a distributed equivalent [ $G_T = 18.65 \pm 0.19$  dB; input VSWR  $\leq 1.81$ ; output VSWR  $\leq 1.86$ ].

**Table 10.14**

The specifications of the interstage matching network of the two-stage amplifier designed

Frequency (GHz)	Source impedance ( $\Omega$ )	Load impedance ( $\Omega$ )	Transducer power gain
2.0	$75.08 + j0.84$	$83.16 - j135.9$	0.7462
3.0	$81.22 + j2.98$	$53.02 - j102.9$	0.8874
4.0	$81.94 - j1.52$	$35.56 - j77.55$	0.8802
5.0	$85.15 - j1.40$	$39.93 - j68.64$	1.0000
6.0	$81.44 - j1.19$	$22.69 - j46.11$	0.8605

**Table 10.15**

The specifications for the input matching network of the two-stage amplifier designed

Frequency (GHz)	Source impedance ( $\Omega$ )	Load impedance ( $\Omega$ )	Transducer power gain
2.0	$49.95 - j1.57$	$80.13 - j13.83$	0.9383
3.0	$49.89 - j2.35$	$139.00 - j21.11$	0.9685
4.0	$49.80 - j3.13$	$102.50 - j79.36$	0.9672
5.0	$46.69 - j3.90$	$68.13 - j64.62$	1.0000
6.0	$49.56 - j4.67$	$41.80 - j37.01$	0.9783

smaller than 1.81 and 2.24, respectively. Because the output VSWR is too high, the specifications in Table 10.16 were used to redesign the output matching network.

The source impedance shown is the actual output impedance of the designed two-stage amplifier. The designed output matching network is shown in Figure

**Table 10.16**

The specifications for the final output matching network of the two-stage amplifier designed

Frequency (GHz)	Source impedance ( $\Omega$ )	Load impedance ( $\Omega$ )	Transducer power gain
2.0	$122.6 - j42.09$	$50.0 + j0.00$	0.944
3.0	$131.6 - j36.89$	$50.0 + j0.00$	1.000
4.0	$120.4 - j35.73$	$50.0 + j0.00$	1.000
5.0	$117.0 - j34.32$	$50.0 + j0.00$	1.000
6.0	$93.1 - j16.88$	$50.0 + j0.00$	1.000

10.39(a). The transducer power gain of the final amplifier is  $18.6 \pm 0.34$  dB, the input VSWR is smaller than 1.69, and the output VSWR is smaller than 1.72.

At this stage a distributed equivalent can be found by using the techniques outlined in Chapter 9. The distributed amplifier is shown in Figure 10.39(b). The electrical line lengths are specified at 6 GHz. The transducer power gain of the amplifier is  $18.60 \pm 0.34$  dB, and the input and output VSWRs are smaller than 1.80 and 1.86, respectively.

The high impedance capacitance stubs in the designed amplifier can be neglected without significantly degrading the performance.

#### **EXAMPLE 10.6      A three-stage LNA (3.7–4.2 GHz; NF = 0.65 dB)**

A three-stage amplifier designed for the passband 3.7–4.2 GHz will be considered in this example [1].

Note that it is usually a good idea to overdesign an amplifier in bandwidth. In this case the passband was extended to 3.5–4.5 GHz. Adding 100 MHz on each side is usually adequate.

The artwork (soft substrate; biasing details not shown) of the amplifier is shown in Figure 10.40 and the schematic is shown in Figure 10.41. The transistor used was the NEC NE32484A (optimum noise figure bias point). In Figure 10.41, the input stage is shown first, followed by the other stages. The same device-modification topology was used in all three stages (different components). The initial input matching network was designed for optimum noise. The other control (matching) networks were designed to level the overall gain (MAG). The final (output) matching network was designed to minimize the output VSWR.

Note that the device-modification in the second and third stages was only done when the design of the previous stage(s) was completed. The actual source impedance presented to the relevant stage and the performance of the stage(s) already designed were therefore taken into account when the modification network was designed.

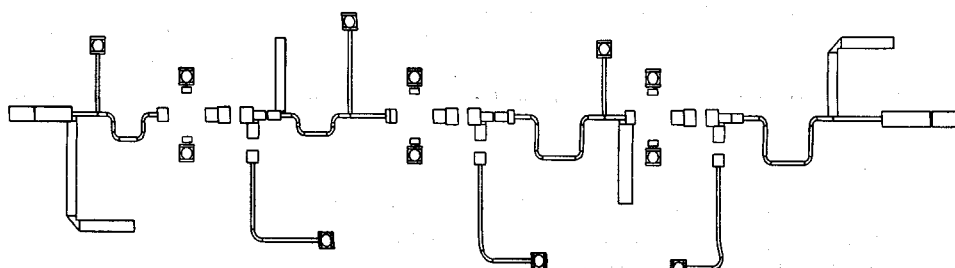


**Figure 10.40** The microstrip artwork of the LNA considered in Example 10.6 (biasing details not shown).

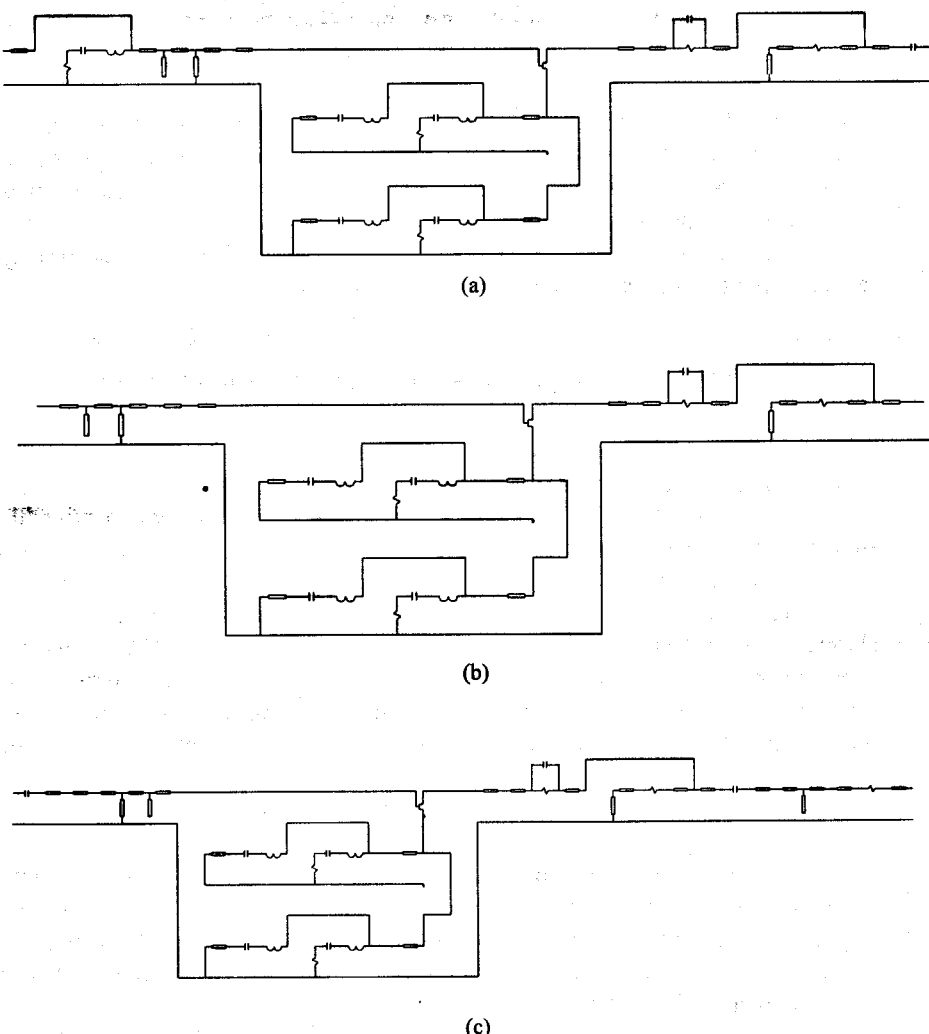


**Figure 10.41** The schematics of (a) the input stage, (b) the second stage, and (c) the output stage of the amplifier considered in Example 10.6.

With the basic design completed, the interstage matching network on the input side was resynthesized to level the overall gain and to improve the input VSWR.

The *S*-parameters of the LNA are displayed graphically in Figure 10.42 and numerically in Table 10.17. The gain and the output VSWR are displayed in Figure 10.43, and the noise figure is displayed in Figure 10.44 with the input VSWR. The Rollette factor for this amplifier is greater than 31 over the complete frequency range.

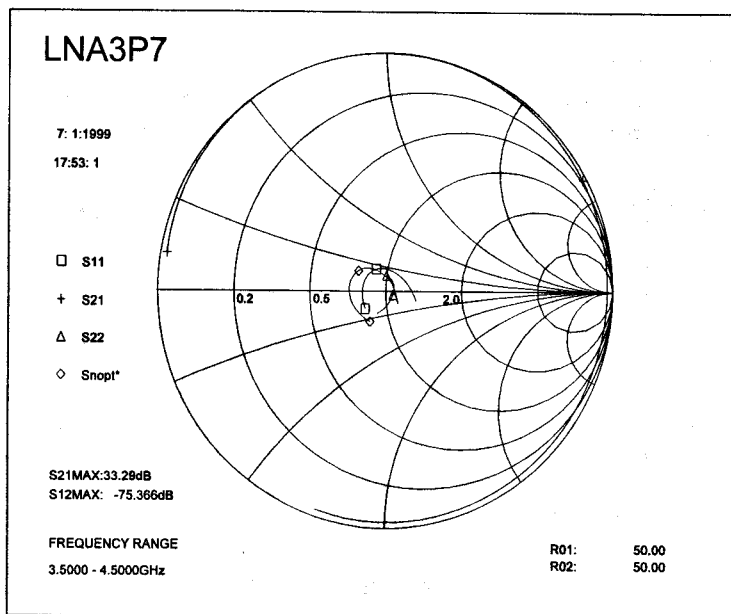


**Figure 10.42** The  $S$ -parameters and the optimum noise impedance of the LNA considered in Example 10.6 displayed graphically.

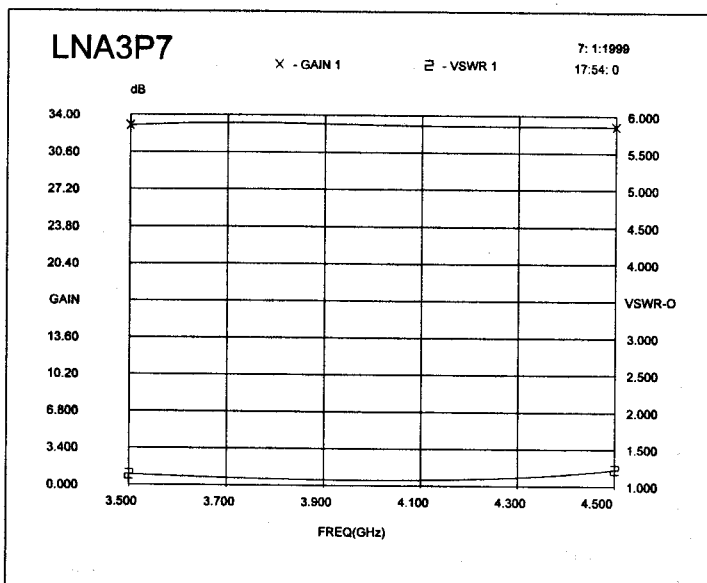


**Figure 10.43** The gain and the output VSWR of the LNA considered in Example 10.6.

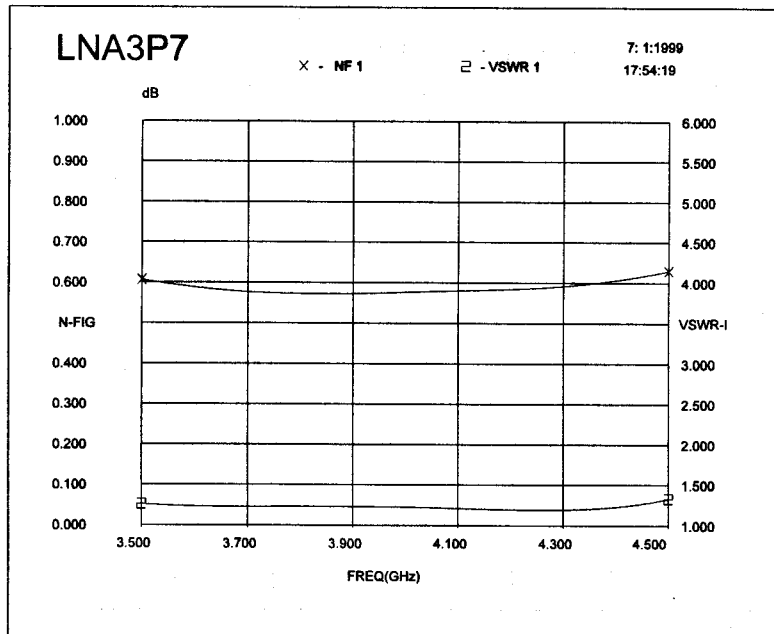


**Figure 10.44** The noise figure and the input VSWR of the amplifier considered in Example 10.6.

**Table 10.17**  
The S-parameters of the LNA considered in Example 10.6 [1]

Frequency (GHz)	$s_{11}$ (dB)	$s_{12}$ (°)	$s_{21}$ (dB)	$s_{22}$ (°)
3.30	-14.05	265.7	-85.07	87.5
3.40	-16.83	243.6	-83.75	59.6
3.50	-18.80	218.8	-82.62	33.1
3.60	-19.70	192.3	-81.67	8.1
3.70	-19.84	168.4	-80.85	344.3
3.80	-19.75	148.2	-80.12	321.4
3.90	-19.76	130.7	-79.46	299.4
4.00	-19.95	114.0	-78.80	278.2
4.10	-20.46	96.3	-78.17	257.1
4.20	-21.01	74.6	-77.49	236.0
4.30	-21.04	46.2	-76.78	214.6
4.40	-19.72	13.3	-76.05	192.2
4.50	-17.03	342.8	-75.36	168.6
4.60	-13.84	317.8	-74.79	143.2

## 10.10 LOSSLESS FEEDBACK AMPLIFIERS

Lossless feedback networks implemented with transformers or directional couplers [2] can be used to remove the gain slope of a transistor in the place of using resistive feedback or loading networks. When this is done, no (or very little) power is dissipated in the feedback networks; most of the power generated by the transistor ends up in the load. At the same time, any distortion in the output voltage and/or the output current is reduced by the feedback.

Low input and output VSWRs can be obtained by choosing the correct turns ratios for the transformers. Most lossless feedback circuits are designed to minimize the VSWRs. It should be noted that the noise figure and the output power, and, therefore, the dynamic range, are not necessarily optimized when this is done.

A circuit using the principle of lossless feedback (Figure 10.45) was patented in November 1971 by D. Norton (Anzac Corporation) in the United States of America [8]. Two transformers are used and configured so that the load voltage is sampled by one and fed back as a voltage in series with the input of the amplifier, while the other one samples the load current and feeds it back as a current to the input of the amplifier (voltage-series and current-shunt feedback). The turns ratios of the transformers were chosen to create a directional coupler arrangement, the main purpose of which was to provide excellent VSWRs and to control the gain. Because of the directional coupler arrangement, any power entering the input port is directed to the input of the transistor and to the output port, and any power generated by the transistor is directed back to its own input as (negative) feedback and to the load as external power.

The main advantage of this circuit is that gain leveling at very low gain values can be obtained without a degradation in performance relative to that associated with the highest gain obtainable with this configuration. It has the disadvantage that any power incident on the output port ( $s_{12}$ ) will be directed toward the input port and the output port

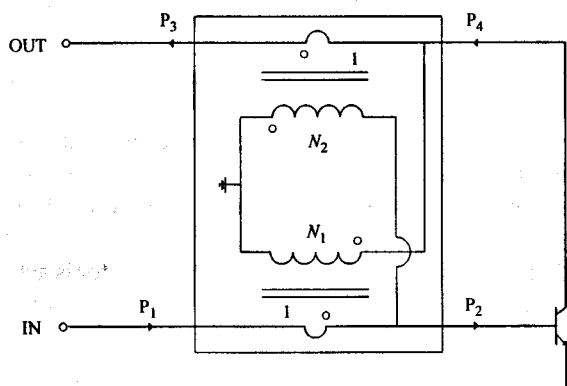


**Figure 10.45** The lossless feedback amplifier patented by David E. Norton in 1971 [8].

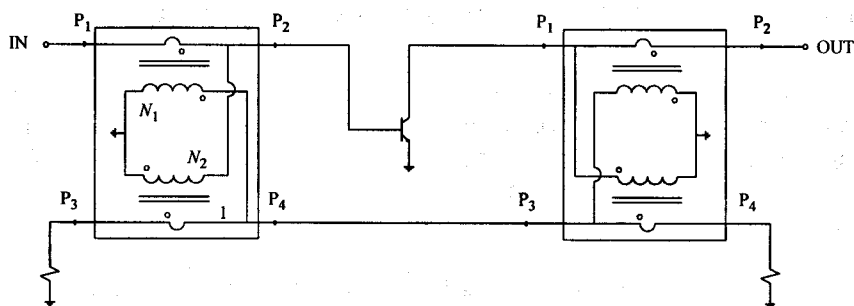


**Figure 10.46** The lossless feedback circuit (Power Feedback Technology™) patented by Q-bit [9].

of the transistor. The isolation of this amplifier, therefore, is usually poor, especially when an amplifier with low gain is designed.

The isolation problem was solved by Q-bit [9] by using two couplers instead of only one (Power Feedback Technology™). In this arrangement (refer to Figure 10.46), the power incident on the output side is directed at the transistor and the termination of the input coupler, instead of the input port. The isolation, therefore, tends to be that of the transistor only plus the through losses of the two couplers (which should be small). However, some (most) of the power fed back is dissipated in the termination of the input coupler. This actually violates the principle of lossless feedback.

The input power in this Q-bit circuit is directed at the input of the transistor and the termination of the input coupler, which degrades the noise figure (slightly) and dissipates some of the input power.

An alternative circuit (Figure 10.47) was introduced in [10]. The output voltage across the load and the output current are sampled with two of the windings of an impedance-matching transformer with three windings, and both the current and the voltage are fed back to the third winding, which is in series with the input terminal of the transistor (the winding that samples the current determines the current through the input winding, and the winding that samples the voltage determines the voltage across the input winding). The impedance associated with the third winding, therefore, is completely determined by the voltage and current sampled (alternatively, the input impedance required would determine the ratio between the voltage and the current feedback).

Ideally, the input impedance of the transistor used should approximate a short-circuit in this arrangement, while its output impedance should look like an open-circuit (a bipolar transistor used in the common-base configuration can usually be used to present such impedances).

It should be noted that while the output current of the transistor is actually sampled in this circuit, the transformer arrangement and the fact that the input current is very low compared to the output current ( $i_b = i_c/\beta$ ) force the load current to be directly proportional to the transistor current.

With a correct choice of the turns ratio of the transformer, a two-way impedance match can be obtained easily with this arrangement.

This circuit is frequently used. It has the advantages that no power is dissipated in

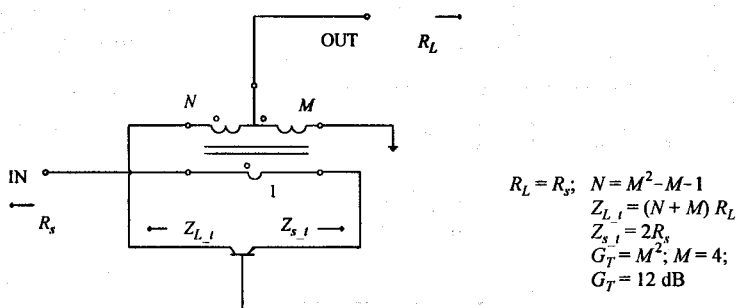


**Figure 10.47** The impedance-matching transformer configuration patented by Norton and Podell [10].

the terminations of directional couplers and that the impedances presented by the circuit to the transistor tend to approximate those required for optimum output power in a common-emitter or a common-base configuration at low currents and at the lower frequencies.

The high load impedance at the collector ( $15R_L$  when the terminations are equal and when the transformer is designed for an amplifier gain of 12 dB) tends to limit the bandwidth obtainable with this arrangement. The isolation is also not as good as that obtainable with the Q-bit circuit, but a two-stage design can be used to improve this (refer to Figure 10.48).

A higher gain cascade version of this type of amplifier is shown in Figure 10.48. The gain claimed for this amplifier is 19 dB over the bandwidth 70–570 MHz.

The single transistor version of this amplifier (see Figure 10.49) can also be used with the transistor in a common-emitter configuration instead of a common-base configuration (the correct configuration is obtained by simply rotating the emitter/winding combination to be the common branch). A transformer will be required on the input to transform the high input impedance downward as shown by Rohde in [11]. However, the input impedance will be a stronger function of the transistor parameters ( $r_{be'} = r_{bb'} + \beta g_m$ ) than was the case with the common-base configuration with its low (negligible) input impedance.

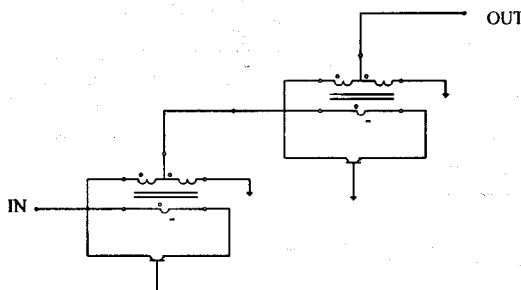


**Figure 10.48** A cascade example of a high dynamic range amplifier using lossless feedback based on the impedance-matching transformer principle [2].

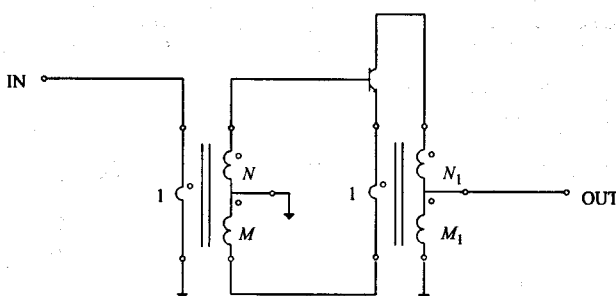


**Figure 10.49** A different variation of the impedance-matching transformer lossless feedback amplifier [8].

A better alternative would probably be to use the original configuration with an input transformer to provide an additional degree of freedom on the design parameters, if required.

An interesting variation on lossless feedback with transformers was also introduced by Rohde in [12]. In this variation the load current is sampled and fed back as a current, and the output voltage (actually the voltage across the transistor) is sampled and fed back as a voltage in series with the input (current-shunt and voltage-series feedback). The circuit is shown in Figure 10.50.

If wideband performance is required, the best choice seems to be a modified version of the Norton coupler circuit (see Figure 10.51). The Norton coupler circuit was originally investigated for bipolar transistors only and was considered to be a good solution only if the transistor to be used had input and output impedances that were closely matched to the terminations presented to the coupler circuit. However, excellent results can be obtained by using FETs (capacitive input impedance; resistive output impedance) in this circuit. While the original coupler circuit used two identical transformers, it was found that better results could be obtained by increasing the turns ratio for the input transformer, that is, when a FET is used (an alternative is to increase the source impedance). This circuit is also not very sensitive to reduction of the coupling factor by leakage flux, and a simple shunt capacitor can be used to compensate for the effect as long as the coupling factor remains

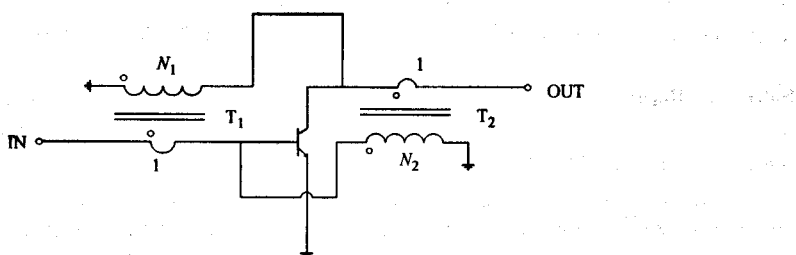


**Figure 10.50** Another lossless feedback amplifier configuration introduced by Rohde [12].

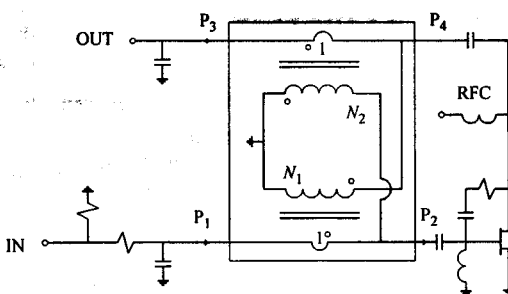


Figure 10.51 A modified version of the Norton coupler amplifier [1].

fairly good ( $k > 0.9$ ). The isolation of the modified Norton coupler circuit also turns out to be much better than expected.

It should be noted that the magnetizing inductance required in a modified Norton coupler amplifier is not only a function of the terminations and the lowest frequency at which acceptable performance is required, but is also a function of the transconductance and the input and output impedances of the transistor to be used. The transconductance also determines the isolation (reverse gain) of the amplifier. Lower transconductance values are associated with better isolation.

The performance obtainable with the modified Norton coupler circuit is impressive. Assuming a coupling factor of unity and no interwinding capacitance, an amplifier was designed over the passband 10 MHz to 1 GHz. The expected power gain was approximately 10.49 dB, the 1-dB compression point was close to 23 dBm, and the isolation was better than 19.7 dB. The expected efficiency was around 39%. The expected input VSWR was smaller than 1.81 over the whole band and less than 1.5 up to 625 MHz. The expected output VSWR was smaller than 1.5 over the whole band.

The performance of a manufactured prototype turned out to be close to that predicted except for the upper end of the passband, which was reduced to around 500 MHz. A modification to the circuit was also required to eliminate oscillations above 2 GHz.

The transistor was biased with an active biasing circuit. An active biasing circuit suitable for FETs is shown in Figure 10.52.

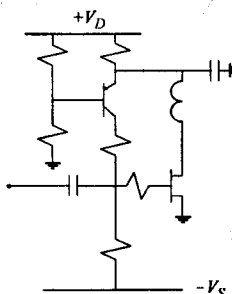


Figure 10.52 An active biasing circuit suitable for FETs.

## 10.11 REFLECTION AMPLIFIERS

At very high frequencies, Impatt, Gunn, and tunnel diodes are also used to provide amplification. These negative resistance single-port devices are usually used in combination with circulators and occasionally with 3-dB hybrid couplers. Only the circulator-type will be considered here.

The S-parameter matrix of an ideal circulator is given by

$$\mathbf{S} = \begin{bmatrix} 0 & 0 & 1 \\ 1 & 0 & 0 \\ 0 & 1 & 0 \end{bmatrix} \quad (10.133)$$

This implies that

$$\begin{bmatrix} b_1 \\ b_2 \\ b_3 \end{bmatrix} = \begin{bmatrix} a_3 \\ a_1 \\ a_2 \end{bmatrix} \quad (10.134)$$

and, therefore, the energy incident at port 1 is always delivered to the load connected to port 2, the energy incident at port 2 to the load connected to port 3, and the energy incident at port 3 to the load connected to port 1. Consequently, the energy is propagated in a circular fashion around the circulator; hence the name circulator. These relationships are illustrated in Figure 10.53. The configuration of a circulator-type reflection amplifier is shown in Figure 10.54.

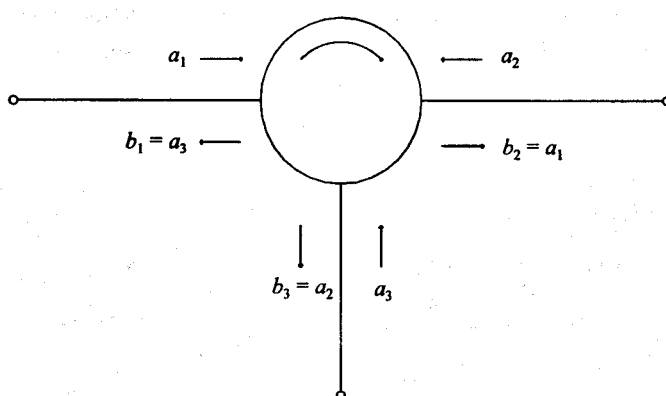


**Figure 10.53** The relationships between the normalized incident and reflected components of an ideal circulator.

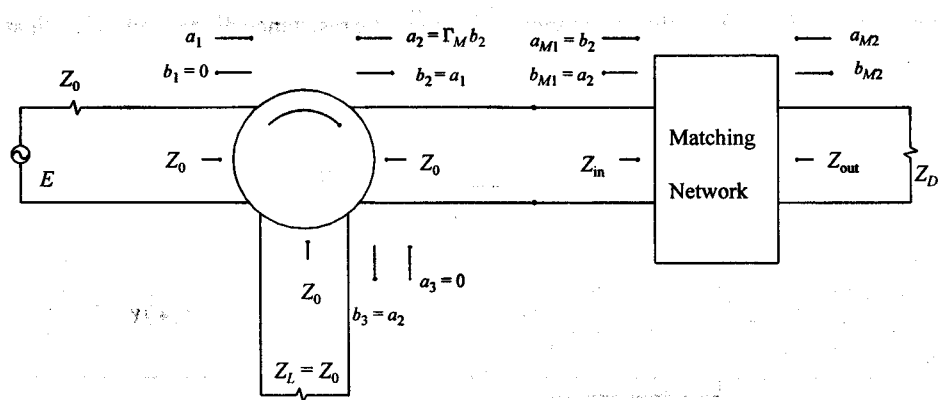


**Figure 10.54** The configuration of a circulator-type reflection amplifier.

The transducer power gain of the amplifier is defined by

$$G_T = \frac{P_L}{P_{av-E}} \quad (10.135)$$

where \$P\_{av-E}\$ is the power available from the source. By using the relationships shown in Figure 10.54, it follows that

$$\begin{aligned} G_T &= \frac{|b_3|^2}{|a_1|^2} \\ &= \frac{|a_2|^2}{|b_2|^2} \\ &= \frac{|b_{M1}|^2}{|a_{M1}|^2} \\ &= \frac{|b_{M2}|^2}{|a_{M2}|^2} \\ &= \left| \frac{Z_{out} - Z_D^*}{Z_{out} + Z_D} \right|^2 \end{aligned} \quad (10.136)$$

where  $Z_D = -R_D + jX_D$  is the impedance of the negative resistance diode, and  $Z_D^*$  indicates its conjugate.

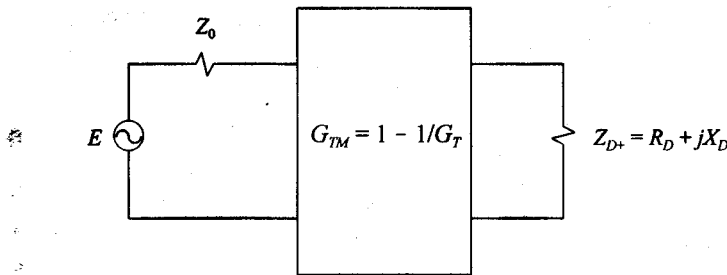


**Figure 10.55** The matching problem to be solved when the amplifier in Figure 10.54 is designed.

Equation (10.136) can be manipulated in the following way:

$$\begin{aligned}
 G_T &= \left| \frac{Z_{\text{out}} - (-R_D - jX_D)^*}{Z_{\text{out}} + (-R_D + jX_D)} \right|^2 \\
 &= \left| \frac{Z_{\text{out}} + (R_D + jX_D)}{Z_{\text{out}} - (R_D + jX_D)^*} \right|^2 \\
 &= 1 / \left| \frac{Z_{\text{out}} - (R_D + jX_D)^*}{Z_{\text{out}} + (R_D + jX_D)} \right|^2 \\
 &= 1 / |\Gamma_{D+}|^2
 \end{aligned} \tag{10.137}$$

where  $\Gamma_{D+}$  is the reflection parameter of the network shown in Figure 10.55 with the source and load impedances shown as normalizing impedances. The problem of maximizing the gain of a circulator-type reflection amplifier, therefore, is equivalent to minimizing the mismatch between the source and the load shown in Figure 10.55.

When the amplifier is designed to have a specified gain versus frequency response, the gain of the equivalent matching network should be

$$G_{TM} = 1 - 1/G_T \tag{10.138}$$

where  $G_T$  is the transducer power gain specification for the reflection amplifier.

**Table 10.18**  
The specifications for the output matching network of the reflection amplifier

Frequency (GHz)	Source impedance (Ω)	Load impedance (Ω)	Transducer power gain
7.0	$50.0 + j0.00$	$10.0 + j3.0$	0.900
7.5	$50.0 + j0.00$	$12.0 + j7.0$	0.900
8.0	$50.0 + j0.00$	$15.0 + j10.0$	0.900
8.5	$50.0 + j0.00$	$19.0 + j13.0$	0.900
9.0	$50.0 + j0.00$	$25.0 + j15.0$	0.900

### EXAMPLE 10.7 Designing a matching network for a reflection amplifier.

As an example of designing the matching network of a reflection amplifier, a matching network will be designed for a Gunn diode (M/A-COM, MA-49110) with input impedance corresponding to the load impedance of the corresponding equivalent matching problem (as given in Table 10.18) and a gain of 10 dB across the pass band 7–9 GHz.

With the required transducer power gain equal to 10 dB, the transducer power gain of the equivalent matching problem is found to be

$$G_{TM} = 1 - 1/G_T$$

$$= 1 - 1/10.0$$

$$= 0.90$$

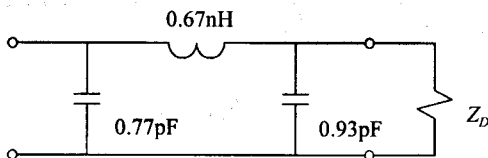


**Figure 10.56** The designed matching network for the reflection amplifier of Example 10.7.

The specifications of the equivalent matching problem is shown in Table 10.18.

The designed matching network is shown in Figure 10.56. The maximum deviation from the specified gain response is 0.16 dB, and the transformation *Q*-factors corresponding to the solution are 1.183, 1.506, and 0.511, respectively.

## 10.12 BALANCED AMPLIFIERS

In a balanced amplifier, the input signal is split into two or more amplifiers, and the output signals of these amplifiers are combined to a single load, with isolation between the individual amplifier ports in both cases. The most commonly used configuration is shown in Figure 10.57.

The *S*-parameter matrix of a 3-dB, 90° hybrid divider is given by [13], with the ports numbered as in Figure 10.57.

For the divider, the energy incident at port 1, therefore, is delivered to the loads connected to ports 2 and 3 with a 90° phase shift between the two components. The energy incident at ports 2 and 3 in the combiner is routed to port 1, again with a 90° phase shift between the two components.

$$S_{Hd} = 0.707 \begin{bmatrix} 0 & j & 1 \\ j & 0 & 0 \\ 1 & 0 & 0 \end{bmatrix} \quad (10.139)$$

and that for a 3-dB, 90° hybrid combiner by

$$S_{Hc} = 0.707 \begin{bmatrix} 0 & 0 & j \\ 0 & 0 & 1 \\ j & 1 & 0 \end{bmatrix} \quad (10.140)$$

The *S*-parameter matrix of the amplifier is given in terms of the *S*-parameters of the two individual amplifiers by [13]

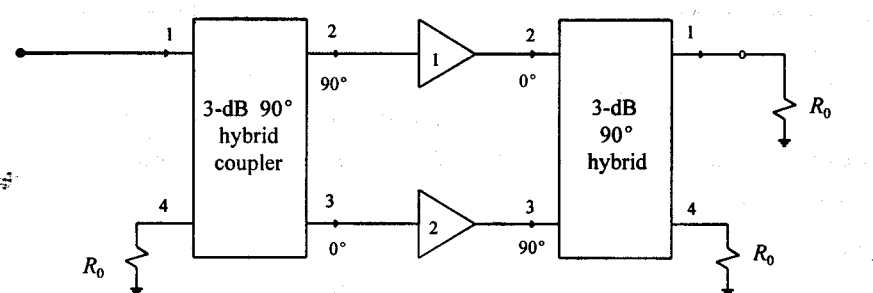


Figure 10.57 The most commonly used balanced amplifier configuration.

$$S_T = 0.5 \begin{bmatrix} s_{11,1} - s_{11,2} & j(s_{12,1} + s_{12,2}) \\ j(s_{21,1} + s_{21,2}) & -s_{22,1} + s_{22,2} \end{bmatrix} \quad (10.141)$$

It is clear from this equation that if amplifiers 1 and 2 are identical, the input and output reflection parameters of the balanced amplifier will be equal to zero, even when the reflection parameters of the individual amplifiers are not equal to zero. As long as the individual amplifiers are almost identical, the input and output VSWRs of a balanced amplifier will therefore be very low, independent of the VSWRs of the individual amplifiers.

The transducer power gain of the balanced amplifier is given by

$$G_T = 0.25 |s_{21,1} + s_{21,2}|^2 \quad (10.142)$$

When the individual amplifiers are identical, this reduces to

$$G_T = |s_{21,1}|^2 \quad (10.143)$$

which is identical to the gain of a single amplifier.

Although the gain of the balanced amplifier is therefore identical to that of each individual amplifier in the ideal case, the output power is twice that obtainable by using only a single-ended stage.

Should one of the amplifiers comprising the balanced amplifier fail, the gain will be reduced to one-fourth of its original value. This can be proved easily by setting  $s_{21,1}$  in (10.142) equal to zero. In some applications this advantage can be an important factor when deciding whether a balanced or single-ended amplifier should be used.

## 10.13 OSCILLATOR DESIGN

Oscillators can be designed by controlling the reflection coefficient (negative resistance) or the loop gain of the transistor [1–4]. The better alternative usually is to control the loop gain. At steady-state, both conditions will be satisfied, but this does not necessarily follow at start-up. Independent of how the design was done, both conditions should be checked to ensure that spurious oscillations will not occur.

The two basic oscillator configurations are shown in Figure 10.58. Voltage-shunt feedback is used in Figure 10.58(a), while current-series feedback is used in Figure 10.58(b).

In order to control the output power of an oscillator, the load termination presented to the transistor should be controlled too. The load termination can be controlled easily by first modifying the basic configurations to those shown in Figure 10.59 [14]. In the case of the series feedback, the original ground connection was floated and a virtual ground was

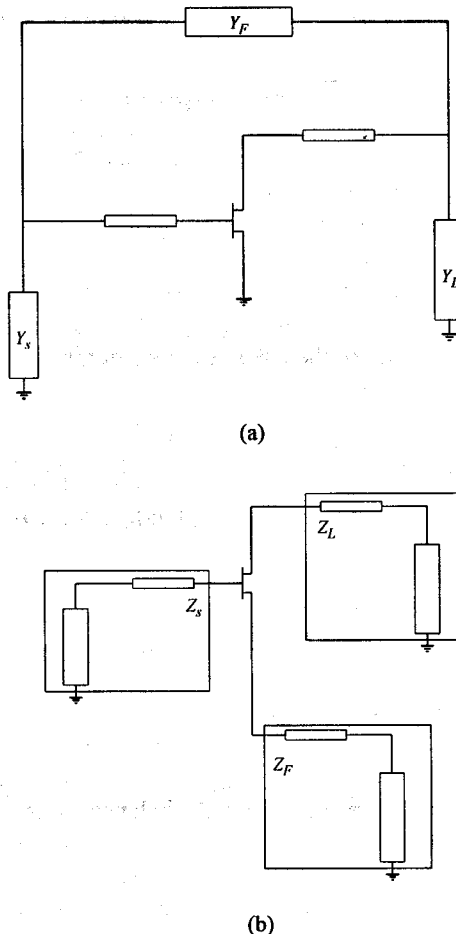


**Figure 10.58** The basic configurations for oscillators with (a) shunt feedback and (b) series feedback.

introduced. No physical change is required in the shunt feedback circuit.

In the series feedback case, any transmission lines used should first be converted to lumped T- or PI-section equivalents before the ground connection is changed.

Any extension lines should be kept as short as possible. The extra phase shift around the loop will reduce the frequency range over which oscillation is possible and will also increase the start-up time.

A simplified flow diagram of the oscillator design process is shown in Figure 10.60.

In order to control the output power, power contours can be generated for the transistor by using the power parameter approach described in Chapter 2 or by using a nonlinear simulator. A suitable load line can then be selected, after which a feedback network can be designed to provide this load termination to the transistor with the loop gain required. Ideally, the load line at steady-state should be controlled, but excellent results can also be obtained with the small-signal parameters if the loop gain required is low.

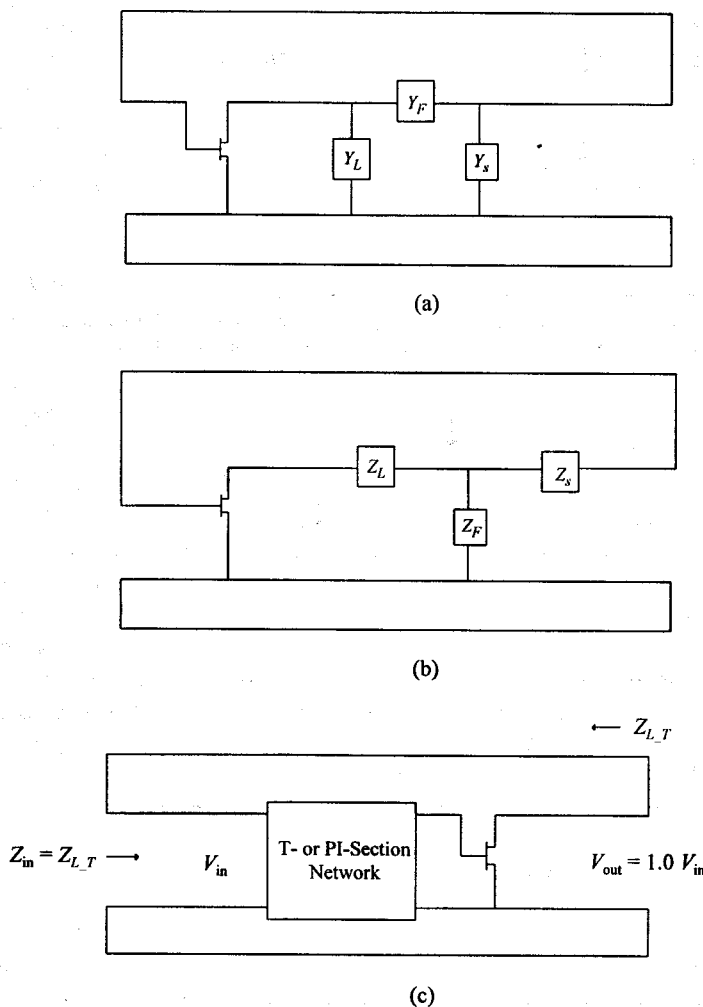


**Figure 10.59** (a), (b) The two oscillator topologies shown in Figure 10.58 modified for the purpose of calculating the transistor load-termination and the loop gain [1]. (c) The voltage and impedance at steady-state.

The output power of an oscillator will increase initially as it is driven harder into compression, after which it will decrease. The transistor will be driven harder into compression as the loop gain or the negative resistance in the input loop (series feedback case) is increased.

The gain compression associated with the maximum effective output power can be estimated by assuming the power saturation characteristic to be governed by an exponential law function [15]. Under the assumptions made, this point is only a function of the small-signal gain associated with the load termination chosen. The relevant equations are derived in Section 10.13.1.

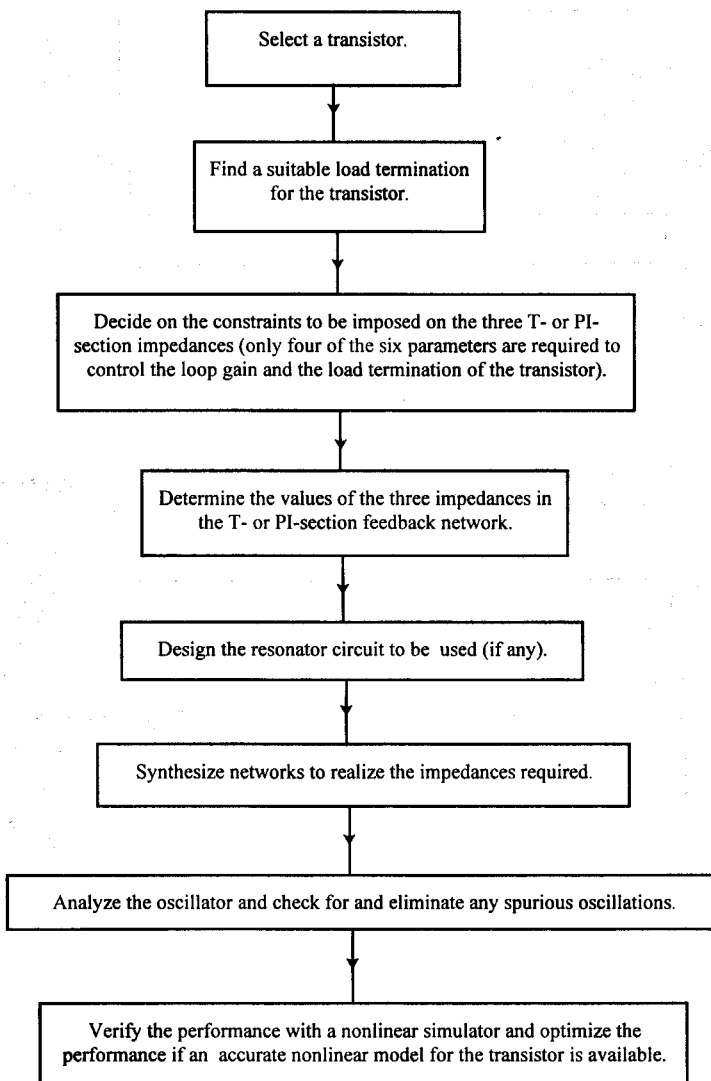


**Figure 10.60** A simplified flow diagram of the oscillator design process outlined [1].

If the compression required is relatively low (a few decibels), the compression at steady-state will be approximately the same as the loop gain at start-up. In this case the loop gain at start-up can be used directly to force the transistor to its peak power point.

Substantial compression is frequently required to extract the maximum output power from an oscillator. It is important to realize that in these cases the load termination presented to the transistor and the oscillator frequency will change as the transistor is driven into compression. In order for this change and the change in the oscillation

frequency to be small, the conditions listed in Section 10.13.1 must apply.

If these conditions do not apply, a better approach would be to make use of the fact that, with a well-behaved load line, the main nonlinear effect in the transistor would be the compression of the transconductance ( $G_m$ ). The transconductance in the small-signal model can therefore be reduced until the large-signal operating gain is compressed as required. The feedback network can then be designed with the associated set of  $S$ -parameters instead of the small-signal parameters. In this case the steady-state load line is controlled instead of the load line at start-up.

When the goal is low phase-noise and not power, the steady-state compression should be kept low. If this is done, the conversion efficiency (mixing effects) will be low, with a corresponding effect on the up-conversion of the flicker noise. A well-behaved load line for the transistor is still desirable as it will prevent running into nonlinear effects associated with a poor choice of the load line.

If low phase-noise is required, extra care should be taken to maximize the loaded  $Q$  (or equivalently the slope in the phase of the loop gain response) of the oscillator. This will reflect on the choice of the resonator to be used, as well as the load line chosen (higher parallel or lower series resistance will be associated with higher  $Q$ s). In simple cases the loaded  $Q$  at start-up can be estimated from the loop gain response by using (10.44). Instead of trying to estimate the loaded  $Q$ , a better option seems to be to control the slope in the loop phase directly.

The feedback network (refer to Figure 10.58) must be designed to provide the required load line and loop gain at start-up or at steady-state (or an approximation of

**Table 10.19**

An example of a table of the T-section impedances required at a specific frequency (3.5 GHz) as a function of the loop gain [1]

Loop gain (dB)	$R_L$ ( $\Omega$ )	$X_L$ ( $\Omega$ )	$L_F, C_F$ (nH, pF)	$X_F$ ( $\Omega$ )	$L_s, C_s$ (nH, pF)	$X_s$ ( $\Omega$ )
-0.0927	49.620	1.808	23.300 pF	-1.952	4.651 nH	102.356
0.9073	49.573	2.029	20.765 pF	-2.190	4.665 nH	102.594
1.9073	49.521	2.277	18.508 pF	-2.457	4.677 nH	102.861
2.9073	49.463	2.555	16.495 pF	-2.757	4.691 nH	103.161
3.9073	49.397	2.866	14.701 pF	-3.093	4.706 nH	103.494
4.9073	49.324	3.216	13.103 pF	-3.471	4.723 nH	103.875
5.9073	49.241	3.608	11.678 pF	-3.894	4.743 nH	104.298
6.9073	49.149	4.049	10.408 pF	-4.369	4.764 nH	104.773
7.9073	49.015	4.543	9.276 pF	-4.902	4.789 nH	105.306
8.9073	48.928	5.097	8.267 pF	-5.500	4.816 nH	105.905
9.9073	48.798	5.719	7.368 pF	-6.172	4.846 nH	106.576
10.9073	48.651	6.417	6.567 pF	-6.925	4.881 nH	107.329
11.9073	48.486	7.200	5.853 pF	-7.770	4.919 nH	108.174
12.9073	48.301	8.078	5.216 pF	-8.718	4.962 nH	109.122

Note: The highlighted loop gain is equal to the estimated compression required to maximize the output power.

steady-state). Two of the three impedances (series case) or admittances (shunt feedback case) are usually assumed to be purely reactive (i.e., at least during the initial stages of the design), while the output power is extracted from the third impedance or admittance.

Because the load line is known, the input impedance of the transistor is also known, and it follows that the terminations for the T- or PI-section feedback are known. With the terminations and the gain of the transistor known, equations can be derived for the components that will provide the required loop gain, as well as the required load termination. This is done in Section 10.13.2 [1].

An example of a table of the  $Z_L$ ,  $Z_F$ , and  $Z_s$  values required (series feedback case) at 3.5 GHz to realize different values of the loop gain and a specified load termination is given in Table 10.19. In this case,  $Z_F$  and  $Z_s$  were chosen to be purely reactive. The highlighted loop gain is equal to the estimated compression required to maximize the output power.

Table 10.20 gives the  $Z_L$ ,  $Z_F$ , and  $Z_s$  values generated for this oscillator from 3.5 to 4.5 GHz after selecting the loop gain estimated for peak power. The required terminations are displayed on a Smith Chart in Figure 10.61. Table 10.19 shows the T-section impedances required at a specific frequency as a function of the loop gain.

Note that the trace for at least one of the sets of impedances to be used must rotate counterclockwise around the Smith Chart in order to ensure frequency stability (i.e., the oscillator must lock at the frequency of interest and not drift around in frequency). Such impedances will be referred to as of varactor type.

The equivalent statement in terms of the loop phase versus frequency response (displayed on a rectangular plot) is that the phase trace must pass through zero without any jitter and must not cross the zero-degree line again before the loop gain is too low for oscillation.

With the T- or PI-section impedances known over the frequency range of interest, networks must be synthesized to approximate each of the impedances over the frequency range of interest. One would generally select a combination that would result in one fixed-valued component, a varactor, or a resonator circuit and a complex impedance (to be realized with an impedance-matching network).

When a voltage-controlled oscillator (VCO) is designed, better results can usually be obtained with two varactors and one impedance-matching network.

The impedance associated with the load termination is often taken to be the actual load ( $50\Omega$ ), but this is clearly not optimum. In general, an impedance-matching network is required to realize the impedance required.

The reactances required can be realized with capacitors, inductors, transmission lines, varactor diodes, or resonators, depending on the requirements. The design of high  $Q$  resonator networks is considered in Section 10.13.3, while that of varactor networks is considered in Section 10.13.5.

If a resonator is used, the resonator impedance must be transformed to present the impedance required at the relevant position. This can often be done by simply using a transmission line with the correct characteristic impedance and length. This is illustrated in Section 10.13.4.

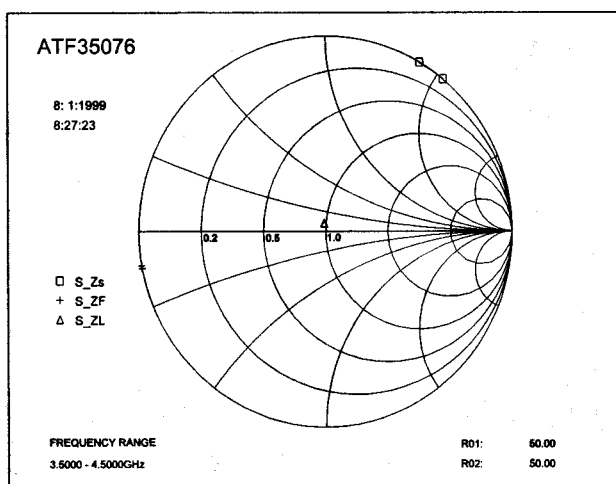
One would generally use series tuned varactor networks in a series feedback oscil-

**Table 10.20**

An example of a table of the T-section impedances required to provide the specified load termination and the specified loop gain over the oscillation band (VCO with two varactors) [1]

Frequency (GHz)	$R_L$ (Ω)	$X_L$ (Ω)	$L_f, C_f$ (nH, pF)	$X_F$ (Ω)	$L_s, C_s$ (nH, pF)	$X_s$ (Ω)
3.50	49.149	4.049	10.408 pF	-4.369	4.764 nH	104.773
3.60	49.114	4.085	9.979 pF	-4.430	4.452 nH	100.707
3.70	49.078	4.126	9.565 pF	-4.497	4.177 nH	97.097
3.80	49.041	4.165	9.178 pF	-4.564	3.916 nH	93.492
3.90	49.004	4.212	8.797 pF	-4.639	3.684 nH	90.275
4.00	48.965	4.257	8.438 pF	-4.715	3.464 nH	87.051
4.10	48.923	4.327	8.053 pF	-4.820	3.273 nH	84.305
4.20	48.878	4.403	7.679 pF	-4.935	3.095 nH	81.683
4.30	48.832	4.475	7.335 pF	-5.046	2.925 nH	79.038
4.40	48.786	4.552	7.002 pF	-5.166	2.772 nH	76.645
4.50	48.738	4.632	6.685 pF	-5.290	2.630 nH	74.352

lator and parallel tuned networks in a shunt feedback oscillator. The particular choice would depend on the component values and the behavior outside the oscillation band. When a series tuned network is used in a shunt feedback oscillator, and vice versa, losses in the varactor network could have a serious stabilizing effect on the circuit. If such a choice was made, be sure to check the effect of such losses on the performance of the circuit.

**Figure 10.61**

The T-section impedances in Table 10.20 displayed on a Smith Chart [1]. Note that at least one of the sets of impedances should rotate counterclockwise around the Smith Chart to ensure frequency stability ( $Z_F$  in this case).

Care should be taken when deciding on the impedance to be approximated with a fixed capacitor or inductor. Ideally, the choice made should result in a topology that cannot sustain oscillations at very low or very high frequencies.

When suitable networks have been fitted to the target impedances, the oscillator should be analyzed to confirm its performance and to check for any spurious oscillations. Because loops may be present, the analysis should be done fairly densely. Both the loop gain and the reflection gain performance should be checked.

If an accurate nonlinear model for the transistor used is available, the oscillator performance should be verified and optimized with a nonlinear simulator.

An example of a dielectric resonator oscillator (DRO) designed as described here is shown in Figure 10.62 (Courtesy of Plessey Avionics, Retreat, South Africa). The topology is shown in Figure 10.63. The oscillator was designed to oscillate at 15.65 GHz with the output power higher than 10 dBm (Bias point: 2V, 20 mA). The performance was realized with slight adjustments in the supply voltage and the puck position.

Note that because a nonlinear model for the transistor used was not available, a nonlinear simulator was not used.

The loop gain performance of the oscillator is shown in Figure 10.64. Oscillations seem to be possible around 6 GHz too. However, a modification was made to the basic oscillator circuit (a gap capacitor was inserted between the transistor and the resonator circuit) to delay the change in the loop phase in this area, and the gain margin in this case

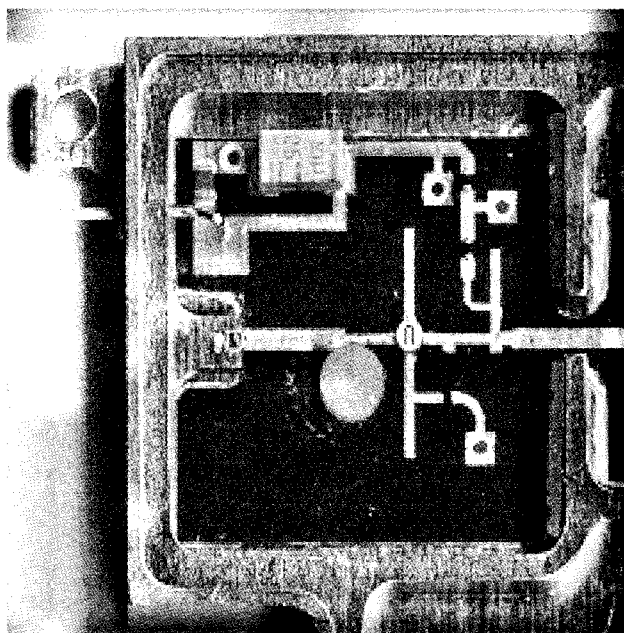


Figure 10.62

An example of a DRO oscillator (Courtesy of Plessey Avionics, Retreat, South Africa). The oscillation frequency is 15.65 GHz and the output power is around 11.6 dBm. The puck is coupled to a line connected to the gate of the transistor.

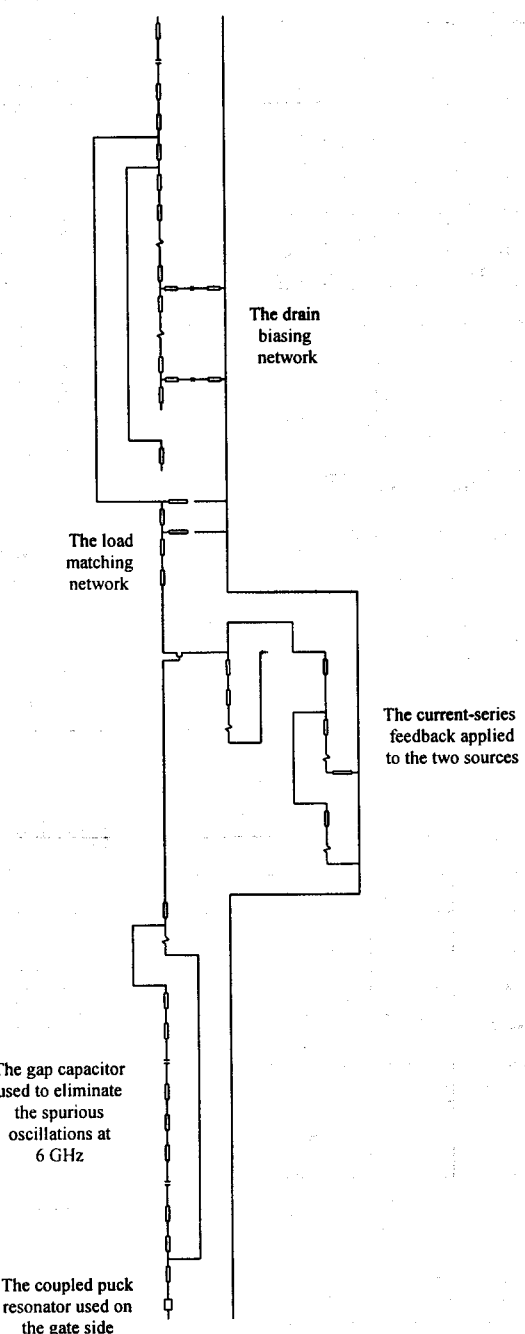
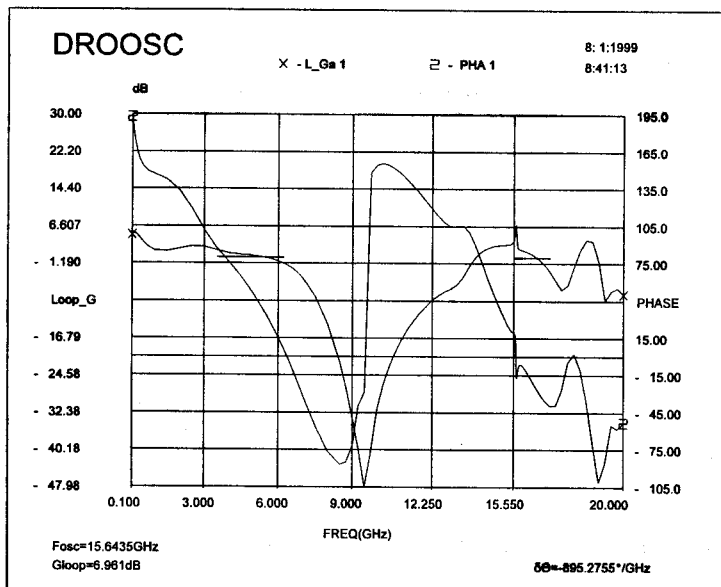
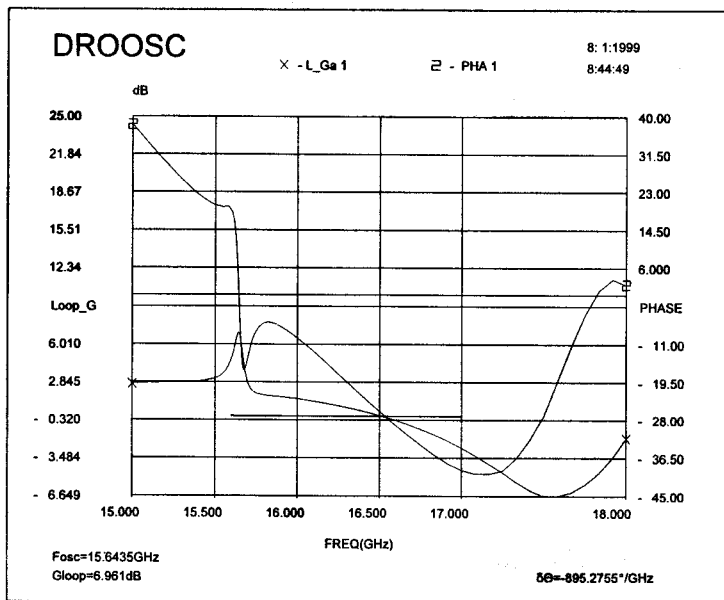


Figure 10.63 The schematic of the oscillator shown in Figure 10.62 [1].



(a)



(b)

**Figure 10.64** (a), (b) The theoretical loop gain and phase of the oscillator shown in Figure 10.62 [1].

is actually quite large. Interestingly enough, the circuit does oscillate around 6 GHz if the change introduced is not made. While the spurious oscillation is undesirable, the fact that it can be predicted with such accuracy and can be eliminated with relative ease serves as a validation for the loop gain approach.

The spurious oscillation can also be eliminated by using a different (more expensive) transistor.

### 10.13.1 Estimation of the Compression Associated with the Maximum Effective Output Power

If the power gain of a transistor is considered as a function of the drive level, it is clear that the gain is equal to the small-signal operating power gain ( $G_{\text{ox}}$ ) when the input power is low and the output power will approach the saturation limit when the input power is high (see Figure 10.65). Assuming the transition to be exponential, the output power could be described by the following equation [15]:

$$P_{\text{out}} = P_{\text{sat}} \left[ 1 - e^{-G_{\text{ox}} P_{\text{in}} / P_{\text{sat}}} \right] \quad (10.144)$$

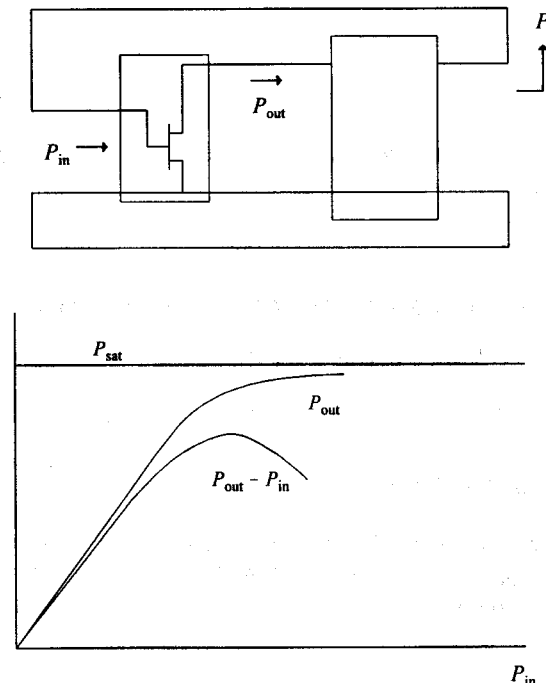


Figure 10.65 Typical saturation characteristics for a transistor.

The maximum effective output power ( $P_{\text{out}} - P_{\text{in}}$ ) is delivered by the transistor when

$$\frac{\partial(P_{\text{out}} - P_{\text{in}})}{\partial P_{\text{in}}} = 0$$

that is, when

$$\frac{\partial P_{\text{out}}}{\partial P_{\text{in}}} = 1$$

Applying this to the equation above yields

$$P_{\text{in}} = P_{\text{sat}} [\ln(G_{\omega s}) / G_{\omega s}] \quad (10.145)$$

and

$$P_{\text{out\_max}} = P_{\text{sat}} (1 - 1 / G_{\omega s}) \quad (10.146)$$

from which it follows that

$$\begin{aligned} P_{\text{osc\_max}} &= P_{\text{out\_max}} - P_{\text{in}} \\ &= P_{\text{sat}} [1 - 1 / G_{\omega s} - \ln(G_{\omega s}) / G_{\omega s}] \end{aligned} \quad (10.147)$$

The corresponding value of the large-signal operating power gain ( $G_{\omega l}$ ) at this maximum effective output power point is given by

$$\begin{aligned} G_{\omega l} &= P_{\text{out\_max}} / P_{\text{in}} \\ &= (G_{\omega s} - 1) / \ln(G_{\omega s}) \end{aligned} \quad (10.148)$$

The ratio of the small-signal and the large-signal operating power gain is therefore

$$G_{\omega s} / G_{\omega l} = [G_{\omega s} / (G_{\omega s} - 1)] \ln(G_{\omega s}) \quad (10.149)$$

If an oscillator is synthesized with a set of small-signal S-parameters, a first order approximation for the loop gain that will result in the maximum possible output power is the square root of this ratio, that is,

$$G_{\text{loop\_opt}} = \sqrt{\frac{G_{\omega s}}{G_{\omega l}}}$$

$$= \sqrt{\ln(G_{\omega s})[G_{\omega s} / (G_{\omega s} - 1)]} \quad (10.150)$$

This approximation would apply to the degree that the following conditions [1] apply.

### Series Feedback Case

$$|Z_{o\_loop}| = |Z_s + Z_F + z_{11}| \gg |Z_F| \quad (10.151)$$

and

$$|Z_F / G_{loop\_opt}| \gg |z_{12}| \quad (10.152)$$

### Shunt Feedback Case

$$|Y_{o\_loop}| = |Y_s + Y_F + y_{11}| \gg |Y_F| \quad (10.153)$$

and

$$|Y_F / G_{loop\_opt}| \gg |y_{12}| \quad (10.154)$$

### 10.13.2 Derivation of the Equations for the T- and PI-Section Feedback Components Required

With the transmission parameters of the transistor in Figure 10.66 assumed to be

$$\begin{bmatrix} A_t & B_t \\ C_t & D_t \end{bmatrix}$$

it follows that [1]

$$Z_{in} = \frac{A_t Z_{LL} + B_t}{C_t Z_{LL} + D_t} \quad (10.155)$$

and

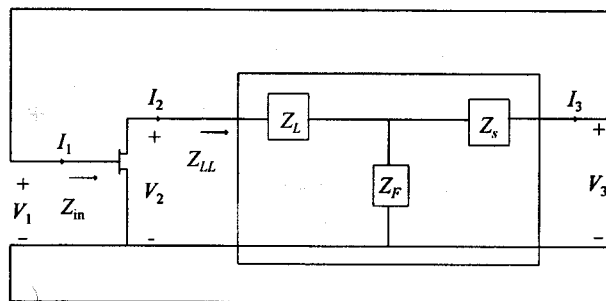


**Figure 10.66** The T-section network in an oscillator with series feedback.

$$A_I = \frac{Z_{21t}}{Z_{22t} + Z_{LL}} \quad (10.156)$$

where  $Z_{LL}$  is the specified load termination for the transistor.

$Z_{LL}$  is given in terms of  $Z_{in}$  and the T-section impedances by

$$\begin{aligned} Z_{LL} &= Z_L + \frac{1}{Y_F + \frac{1}{Z_s + Z_{in}}} \\ &= Z_L + \frac{Z_s + Z_{in}}{1 + Y_F(Z_s + Z_{in})} \end{aligned} \quad (10.157)$$

while the loop gain ( $G_{loop}$ ) is given by

$$\begin{aligned} G_{loop} I_1 = I_3 &= \frac{Z_F}{Z_F + (Z_s + Z_{in})} I_2 \\ &= \frac{A_I I_1}{1 + Y_F(Z_s + Z_{in})} \end{aligned} \quad (10.158)$$

from which it follows that

$$Z_F = -\frac{Z_s + Z_{in}}{\frac{A_I}{G_{loop}} + 1} \quad (10.159)$$

This expression can be written as

$$Z_F = -\frac{Z_s}{\frac{A_I}{G_{\text{loop}}} + 1} - \frac{Z_{\text{in}}}{\frac{A_I}{G_{\text{loop}}} + 1} \quad (10.160)$$

Equation (10.159) can be used to simplify (10.157):

$$\begin{aligned} Z_{LL} &= Z_L + \frac{Z_s + Z_{\text{in}}}{1 - \left( \frac{A_I}{G_{\text{loop}}} + 1 \right)} \\ &= Z_L - \frac{G_{\text{loop}}}{A_I} (Z_s + Z_{\text{in}}) \end{aligned} \quad (10.161)$$

which can be rearranged to give an expression for  $Z_L$  in terms of  $Z_s$ :

$$Z_L = \frac{G_{\text{loop}}}{A_I} Z_s + \left( Z_{LL} + \frac{G_{\text{loop}}}{A_I} Z_{\text{in}} \right) \quad (10.162)$$

Equations (10.162) and (10.160) can be combined to eliminate  $Z_s$  and give an expression for  $Z_L$  in terms of  $Z_F$ :

$$Z_F = -\frac{1}{\frac{A_I}{G_{\text{loop}}} + 1} \frac{Z_L - \left( Z_{LL} + \frac{G_{\text{loop}}}{A_I} Z_{\text{in}} \right)}{\frac{G_{\text{loop}}}{A_I}} - \frac{Z_{\text{in}}}{\frac{A_I}{G_{\text{loop}}} + 1} \quad (10.163)$$

which can be simplified to

$$Z_L = -\left[ 1 + \frac{G_{\text{loop}}}{A_I} \right] Z_F + Z_{LL} \quad (10.164)$$

Equations (10.160), (10.162), and (10.164) can be used to solve for the required components once the relevant constraints on  $Z_L$ ,  $Z_s$ , or  $Z_F$  have been established. The real parts of two of these impedances are usually assumed to be zero or to be fixed, after which these equations can be solved for the remaining values.

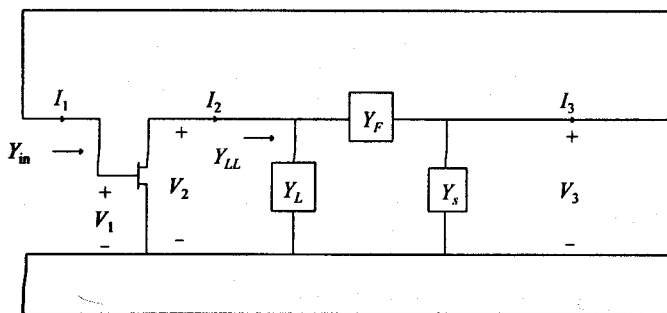


**Figure 10.67** The PI-section network in an oscillator with parallel feedback.

The derivation of the equations for the PI-section components proceeds similarly to that for the T-section components.

With the transmission parameters of the transistor in Figure 10.67 assumed to be

$$\begin{bmatrix} A_t & B_t \\ C_t & D_t \end{bmatrix}$$

it follows that

$$Y_{\text{in}} = \frac{C_t Z_{LL} + D_t}{A_t Z_{LL} + B_t} \quad (10.165)$$

and

$$A_v = \frac{1}{A_t + B_t Y_{LL}} \quad (10.166)$$

where  $Y_{LL}$  is the specified load termination for the transistor.

$Y_{LL}$  is given in terms of  $Y_{\text{in}}$ , and the PI-section impedances by

$$\begin{aligned} Y_{LL} &= Y_L + \frac{1}{Z_F + \frac{1}{Y_s + Y_{\text{in}}}} \\ &= Y_L + \frac{Y_s + Y_{\text{in}}}{Z_F (Y_s + Y_{\text{in}}) + 1} \end{aligned} \quad (10.167)$$

while the loop gain ( $G_{\text{loop}}$ ) is given by

$$G_{\text{loop}} V_1 = V_3 = \frac{\frac{V_2}{Y_s + Y_{\text{in}}}}{\frac{1}{Y_s + Y_{\text{in}}} + Z_F} = \frac{A_v V_1}{1 + Z_F (Y_s + Y_{\text{in}})} \quad (10.168)$$

from which it follows that

$$Y_F = \frac{Y_s + Y_{\text{in}}}{\frac{A_v}{G_{\text{loop}}} - 1} \quad (10.169)$$

Equation (10.169) can be written as

$$Y_F = \frac{1}{\frac{A_v}{G_{\text{loop}}} - 1} Y_s + \frac{Y_{\text{in}}}{\frac{A_v}{G_{\text{loop}}} - 1} \quad (10.170)$$

which provides a simple expression for  $Y_F$  in terms of  $Y_s$ .

Equation (10.169) can also be used to simplify (10.167):

$$\begin{aligned} Y_{LL} &= Y_L + \frac{Y_s + Y_{\text{in}}}{Z_F (Y_s + Y_{\text{in}}) + 1} \\ &= Y_L + \frac{Y_s + Y_{\text{in}}}{\left( \frac{A_v}{G_{\text{loop}}} - 1 \right) + 1} \\ &= Y_L + \frac{G_{\text{loop}}}{A_v} Y_s + \frac{G_{\text{loop}}}{A_v} Y_{\text{in}} \end{aligned} \quad (10.171)$$

which can be rearranged to provide an expression for  $Y_L$  in terms of  $Y_s$ :

$$Y_L = -\frac{G_{\text{loop}}}{A_v} Y_s + \left( Y_{LL} - \frac{G_{\text{loop}}}{A_v} Y_{\text{in}} \right) \quad (10.172)$$

Equations (10.170) and (10.172) can be combined to eliminate  $Y_s$ , which will give an expression for  $Y_L$  in terms of  $Y_F$  too:

$$Y_L = \left( \frac{G_{\text{loop}}}{A_v} - 1 \right) Y_F + Y_{LL} \quad (10.173)$$

Equations (10.170), (10.172), and (10.173) can be used to solve for the required components once the relevant constraints on  $Y_L$ ,  $Y_s$ , or  $Y_F$  have been established. The real parts of two of these impedances are usually assumed to be zero or to be fixed, after which these equations can be solved for the remaining values.

### 10.13.3 High $Q$ Resonator Circuits

High  $Q$  resonator circuits can be realized by using dielectric resonators, cavity resonators or a magnetically biased yttrium iron garnet (YIG) sphere.

The YIG resonator is a high  $Q$ , ferrite sphere of yttrium iron garnet ( $\text{Y}_2\text{Fe}_2(\text{FeO}_4)_3$ ) that can be tuned over a wide band by varying the biasing dc field. In a YIG-tuned oscillator, a YIG sphere is normally used to control the inductance of a coil in the resonant circuit. Because YIG is a ferri-magnetic material, its effective permeability can be controlled with an external dc magnetic field, thus controlling the oscillator frequency. YIG oscillators can be made to tune over more than a decade of bandwidth, while varactor-tuned oscillators are limited to a tuning range of about an octave [3].

Cavity resonators are usually realized with low-loss coaxial line or waveguide. The simplest coaxial cavity is a quarter wavelength ( $\lambda/4$ ) shorted stub. The signal is coupled into the cavity with a shorted loop or an open probe. The resonant frequency is usually adjusted with a tuning screw near the open end. It can be shown [3] that the impedance near the resonance frequency and the  $Q$  of the resonator are given by

$$Z_{\text{in}} \approx \frac{1}{\frac{\alpha l}{Z_0} + j\pi \frac{\Delta\omega}{2\omega_0} Y_0} \quad (10.174)$$

$$Q \approx \frac{\pi}{4\alpha l} = \frac{\beta}{2\alpha} \quad (10.175)$$

Equations (10.174) and (10.175) are derived by starting with the expression

$$Z_{\text{in}} = Z_0 \tanh[(\alpha + j\beta)l] \quad (10.176)$$

Open-circuited  $\lambda/2$  resonators are often used on microstrip. The input impedance and  $Q$  in this case are given by [3]

$$Z_{in} \approx \frac{1}{\frac{\alpha l}{Z_0} + j\pi \frac{\Delta\omega}{\omega_0} Y_0} \quad (10.177)$$

$$Q \approx \frac{\pi}{2\alpha l} = \frac{\beta}{2\alpha} \quad (10.178)$$

The width and length of the smallest rectangular waveguide cavity is  $\lambda/2$  ( $TE_{101}$  mode). The rectangular cavity is a waveguide version of a short-circuited  $\lambda/2$  transmission-line resonator [3].

Because of the small size and low cost, dielectric resonators are frequently used at microwave frequencies. The high dielectric constant of the resonator puck ensures that most of the fields are contained within the dielectric, but there is some fringing from the sides and ends of the puck. The fringing fields provide a convenient means of coupling to a microstrip line. The spacing between the puck and the microstrip conductor determines the amount of coupling.

Only dielectric losses are present in the puck, and  $Q$ s of several thousand can be realized. Metallic shielding is required to minimize radiation losses. The  $Q$  can be increased by with a dielectric spacer under the puck.

The resonant frequency of the puck can be adjusted by using an adjustable metal plate above it.

The lowest order resonant mode for a dielectric puck is the  $TE_{018}$  mode. This mode couples easily to a microstrip line. The resonant frequency for a puck can be estimated by solving the following transcendental equation iteratively [3]:

$$\tan \frac{\beta L}{2} = \frac{\alpha}{\beta} \quad (10.179)$$

where

$$\alpha = \sqrt{\left(\frac{2.405}{a}\right)^2 - k_0^2} \quad (10.180)$$

$$\beta = \sqrt{\epsilon_r k_0^2 - \left(\frac{2.405}{a}\right)^2} \quad (10.181)$$

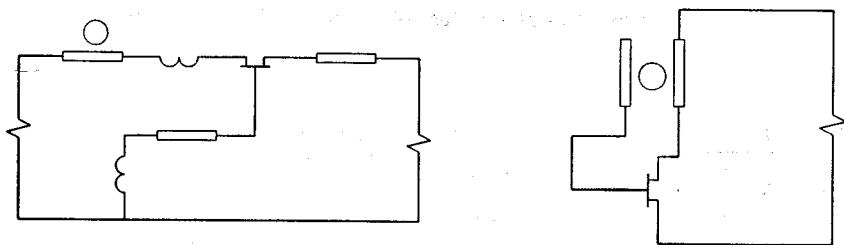


**Figure 10.68** Two commonly used dielectric resonator oscillator configurations.

$$k_0 = \frac{2\pi f}{c} \quad (10.182)$$

In these equations,  $f$  is the required resonant frequency,  $\epsilon_r$  is the dielectric constant of the puck material,  $L$  the height of the puck, and  $a$  its radius.

The resonant frequency must lie in the interval  $[f_1, f_2]$ , where [3]

$$f_1 = \frac{2.405 c}{2\pi\sqrt{\epsilon_r} a} \quad (10.183)$$

and

$$f_2 = \frac{2.405 c}{2\pi a} \quad (10.184)$$

Equations (10.183) and (10.184) are necessary conditions to ensure that the roots in (10.180) and (10.181) can be taken.

The unloaded  $Q$  of a dielectric puck can be estimated as [3]

$$Q = \frac{1}{\tan \delta} \quad (10.185)$$

Two commonly used DRO configurations are shown in Figure 10.68. The equivalent circuits associated with the coupled sections are shown in Figure 10.69.

#### 10.13.4 Transforming the Impedance Presented by a Resonator Network to That Required in the T- or PI-Section Feedback Network

When a resonator is used, the impedance presented by the resonator must usually be transformed to present the target impedance in the T- or PI-section feedback network. This

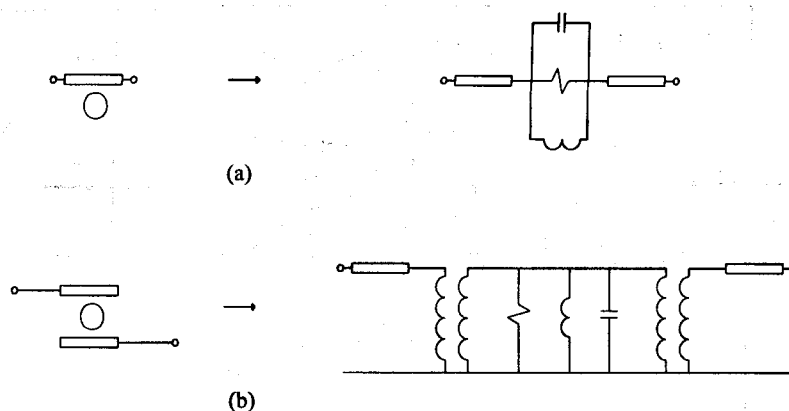


**Figure 10.69** The equivalent circuits associated with (a) a dielectric puck coupled to a microstrip line and (b) a puck used to couple two microstrip lines.

can often be done by simply using a transmission line with the correct characteristic impedance and length.

The principle is illustrated in Figures 10.70 and 10.71 below. The trace on the right-hand side of Figure 10.71 (trace *A*; the smaller arc) is the measured impedance of a dielectric resonator puck coupled to a microstrip line (15.6–15.7 GHz). The impedance at the oscillation frequency (15.65 GHz) is in the area of a second marker shown on this trace (point *a*). The target impedance in the T-section feedback network designed is in the area of the cursor displayed on the left-hand side of this figure (trace *B*, point *b*). The measured impedance was transformed to this point by cascading a transmission line with suitable characteristic impedance and length to the resonator circuit as shown in Figure 10.70.

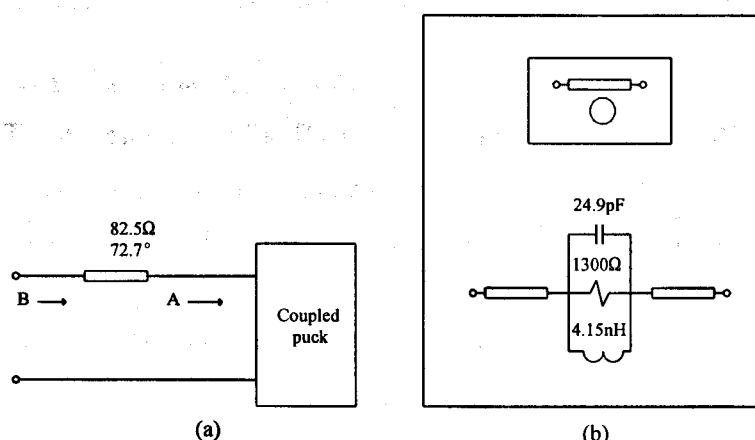


**Figure 10.70** (a) The transmission line used to transform the impedance presented by a dielectric resonator puck coupled to a microstrip line as shown in Figure 10.69 (electrical line length specified at 15.65 GHz). (b) The equivalent circuit fitted to resonator circuit.

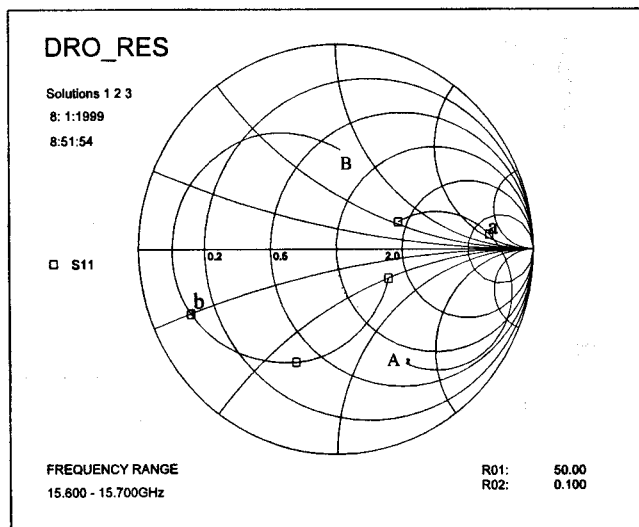


**Figure 10.71** An example of transforming the impedance presented by a resonator circuit to the target impedance in the T-section feedback network at the oscillation frequency [1].

The equivalent circuit fitted to the resonator circuit is shown in Figure 10.70(b). If wideband measurements are not available, an equivalent circuit can be used to check for spurious oscillations.

The size of the modified resonator loop is a function of the characteristic impedance chosen.

Note that if the characteristic impedance used was  $50\Omega$ , the original loop will simply be rotated around the origin as the line length is increased. This follows because the electrical length of the line added is basically constant over the narrow frequency range considered.

### 10.13.5 Designing Varactor Circuits to Realize the Varactor-Type Reactance Required

The varactor-type reactances (impedance rotating counterclockwise on the Smith Chart) required in the T- or PI-section feedback network must be realized with varactor networks. The design of the varactor network usually consists of finding a varactor with a tuning range bigger than the minimum required and calculating the loading capacitance or inductance required.

The loading inductance or capacitance required is usually realized with lumped elements.

The effect of the parasitic inductance of the varactor diode should be included when the tuning circuit is designed.

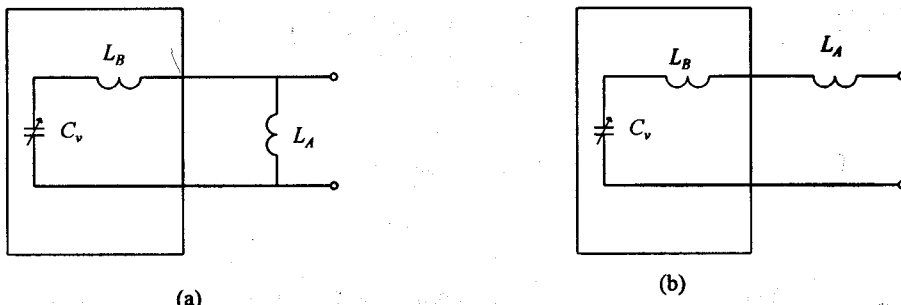


**Figure 10.72** Loading a varactor with (a) a parallel inductor and (b) a series inductor to obtain the series reactance required at the passband edges.

The basic varactor networks are shown in Figure 10.72.

With a maximum achievable varactor capacitance ratio of

$$\rho_{v_{\max}} = C_{v_{\max}} / C_{v_{\min}} \quad (10.186)$$

and specified limiting values of the series reactance required at the passband edges ( $X(\omega_H)$  and  $X(\omega_L)$ ), the loading capacitance or inductance required can be calculated.

Considering the series loading circuit (Figure 10.72(b)), it follows that

$$X(\omega_H) = X_A(\omega_H) + \omega_H L_B - \frac{1}{\omega_H C_{y_{\min}}} \quad (10.187)$$

and

$$X(\omega_L) = X_A(\omega_L) + \omega_L L_B - \frac{1}{\omega_L C_{v_{\max}}} \quad (10.188)$$

where  $L_B$  is the package inductance of the varactor.

These equations can be manipulated to give expressions for the minimum and maximum values of the varactor capacitance. Substitution of these expressions in (10.186) yields an expression that can be solved to obtain the value of  $X_4$ .

It follows from this equation that

$$L_A = \frac{\alpha X(\omega_L) - X(\omega_H)}{\alpha \omega_L - \omega_H} - L_B \quad (10.189)$$

with

$$\alpha = \frac{\omega_L C_{v\_max}}{\omega_H C_{v\_min}} = \frac{\omega_L}{\omega_H} \rho_{v\_max} \quad (10.190)$$

If  $L_A$  is found to be negative, a series capacitor is required instead. The value of the capacitor is given by

$$C_A = \frac{\frac{1}{\omega_H} - \frac{\alpha}{\omega_L}}{\omega_H L_B - \alpha \omega_L L_B - X(\omega_H) + \alpha X(\omega_L)} \quad (10.191)$$

The value of  $C_A$  or  $L_A$  required in the parallel case can be found by starting with the equations

$$-B(\omega_H) = \frac{1}{\omega_H L_A} + \frac{1}{\omega_H L_B - \frac{1}{\omega_H C_{v\_min}}} \quad (10.192)$$

and

$$-B(\omega_L) = \frac{1}{\omega_L L_A} + \frac{1}{\omega_L L_B - \frac{1}{\omega_L C_{v\_max}}} \quad (10.193)$$

These equations can be manipulated to give expressions for the minimum and maximum values of the varactor capacitance. Substitution of these expressions in (10.186) yields a quadratic expression that can be solved to obtain the value of the loading component ( $L_A$  or  $C_A$ ).

If an inductor is required, its value is given by [14]

$$L_A = \frac{1}{P \pm \sqrt{P^2 - Q}} \geq 0 \quad (10.194)$$

where

$$P = \frac{1}{2} \left\{ \frac{\omega_L}{X(\omega_L)} + \frac{\omega_H}{X(\omega_H)} - \frac{1}{L_B} \right\} \quad (10.195)$$

and

$$Q = \frac{\omega_L \omega_H}{X(\omega_L) X(\omega_H)} - \frac{1}{L_B} \frac{(\omega_H / X(\omega_L)) - \omega_L \rho_{v\_max} / X(\omega_H))}{(\omega_H / \omega_L) - \omega_L \rho_{v\_max} / \omega_H} \quad (10.196)$$

### 10.13.6 Considerations Applying to Oscillators with Low Phase Noise

The phase noise of an oscillator can be minimized by doing the following:

1. Select a transistor with a low noise figure and low flicker noise;
2. Bias the transistor correctly;
3. Maximize the loaded  $Q$  or the rate at which the loop phase passes through zero;
4. Keep the conversion gain of the oscillator low.

The conversion gain can be kept low by keeping the output power well below saturation (limiting the loop gain) and/or by linearizing the transconductance with resistive feedback (a small series resistor can be used in the source or the emitter). The conversion gain will also be low if the loop gain at start-up is kept low.

If the amplitude of the oscillation tends to be unstable because of these measures, a linear automatic gain control (AGC) loop can be designed to stabilize it. A pin diode circuit is probably the best option.

It is also possible to reduce the level of the up-converted flicker noise by designing suitable low-frequency circuitry for the oscillator [16]. The aim of such circuitry is to reduce the level of the flicker noise across the nonlinear junctions.

When a fixed frequency oscillator is designed and large-signal information is available, AM to PM conversion can be minimized if a network is designed to ensure rectangular crossing of the impedance versus frequency and impedance versus amplitude traces displayed on a Smith Chart.

## REFERENCES

1. *MultiMatch RF and Microwave Impedance-Matching, Amplifier and Oscillator Synthesis Software*, Somerset West, RSA: Ampsa (PTY) Ltd; <http://www.amps.com.>, 1998.
2. Vendelin, G. D., A. M. Pavio, and U. L. Rohde, *Microwave Circuit Design Using Linear and Nonlinear Techniques*, New York: John Wiley and Sons, 1990.

3. Pozar, D. M., *Microwave Engineering*, Reading, MA: Addison-Wesley Publishing Company, 1990.
4. Boyles, J. W., "The Oscillator as a Reflection Amplifier: An Intuitive Approach to Oscillator Design," *Microwave Journal*, June 1986.
5. Carson, R. S., *High Frequency Amplifiers*, New York: John Wiley and Sons, 1979.
6. Abrie, P. L. D., and P. Rademeyer, "A Method for Evaluating and the Evaluation of the Influence of the Reverse Transfer Gain on the Transducer Power Gain of Some Microwave Transistors," *IEEE Trans. Microwave Theory Tech.*, Vol. MTT-33, No. 8, August 1985, pp. 711-713.
7. Abrie, P. L. D., "A Series of CAD Techniques for Designing Microwave Feedback Amplifiers and Simplifying the Design of Reactively Matched Single-Ended Amplifiers," *IEEE MTT-S Digest*, 1990.
8. Norton, D., U.S. Patent No. 3,426,298, 1969, "High Dynamic Range Amplifier," U.S. Patent No. 3,624,536, November 1971, Anzac Corporation.
9. Mead, H. B., and G. R. Callaway: "Broadband Amplifier," U.S. Patent No. 4,042,887, August 1977, Q-bit Corporation.
10. Norton, D. E., and A. F. Podell, "Transistor Amplifier with Impedance-Matching Transformer," US Patent No. 3,891,934, June 1975, Anzac Corporation.
11. Rohde, U. L., "Wideband Amplifier Summary," *Ham Radio*, November 1979.
12. Rohde, U. L., "The Design of a Wide-Band Amplifier with Large Dynamic Range and Low Noise Figure Using CAD Tools," *IEEE Long Island MTT Symposium Digest*, April 28, 1987, pp. 47-55.
13. Russel, K. J., "Microwave Power Combining Techniques," *IEEE Trans. Microwave Theory Tech.*, MTT-27, No. 5, 1979, pp. 472-478.
14. Rauscher, C., "Large-Signal Technique for Designing Single-Frequency and Voltage-Controlled GaAs FET Oscillators," *IEEE Trans. Microwave Theory Tech.*, Vol. MTT-29, No. 4, April 1981.
15. Johnson, K. M., "Large Signal GaAs MESFET Oscillator Design," *IEEE Trans. Microwave Theory Tech.*, Vol. MTT-27, No. 3, March 1979.
16. Prigent, M., and J. Obregon, "Phase Noise Reduction in FET Oscillators by Low-Frequency Loading and Feedback Circuitry Optimization," *IEEE Trans. Microwave Theory Tech.*, Vol. MTT-35, No. 3, March 1987.

## SELECTED BIBLIOGRAPHY

- Bodway, G. E., "Two Port Power Flow Analysis Using Generalized Scattering Parameters," *Microwave Journal*, May 1967, pp. 61-69.
- Ha, T. T., *Solid-State Microwave Amplifier Design*, New York: John Wiley and Sons, 1981.
- Krauss, H. L., W. B. Bostian, and F. H. Raab, *Solid-State Radio Engineering*, New York: John Wiley and Sons, 1980.
- Kurokawa, K., "Design Theory of Balanced Transistor Amplifiers," *Bell Syst. Tech. J.*, Vol. 44, No. 10, 1965, pp. 1675-1698.
- Roddy, D., and J. Coolen, *Electronic Communications*, Reston, VA: Reston Publishing Company, 1981.
- Tajima, Y., and P. D. Miller, "Design of Broad-Band Power GaAs Fet Amplifiers," *IEEE Trans. Microwave Theory Tech.*, Vol. MTT-32, No. 3, March 1984.

## APPENDIX A

### THE UNBALANCED TRANSMISSION LINE

The basic equations associated with a transmission line when the currents are unbalanced [1] will be derived here. For the sake of simplicity, it will be assumed that there is no magnetic coupling between the two conductors of the line. The equivalent circuit shown in Figure A.1 applies.

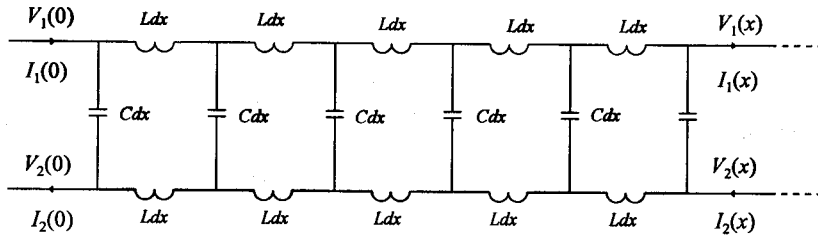


Figure A.1 The equivalent circuit of an unbalanced transmission line.

The current at position  $x$  on the line will be considered first. The current can be expressed in terms of balanced and unbalanced components as follows:

$$I_1(x) = I_b(x) - I_u(x) \quad (\text{A.1})$$

and

$$I_2(x) = I_b(x) + I_u(x) \quad (\text{A.2})$$

$I_b(x)$  in these equations is the balanced component of the current, while  $I_u(x)$  is the unbalanced component.

It follows from these two equations that

$$I_2(x) = [I_b(x) - I_u(x)] + 2I_u(x) = I_1(x) + 2I_u(x) \quad (\text{A.3})$$

$$= I_1(x) + I_0(x) \quad (\text{A.4})$$

where  $I_0(x)$  is the difference between the two currents.

Because there is no ground path on the line itself, the difference current ( $I_0(x)$ ) must be the same at all positions along the line (refer to Figure 6.17, if necessary), and (A.4) can therefore be simplified to

$$I_2(x) = I_1(x) + I_0 \quad (\text{A.5})$$

With the currents defined, it follows that

$$D_x \cdot I_1(x) = -sCV_{12}(x) \quad (\text{A.6})$$

$$D_x \cdot I_2(x) = -sCV_{12}(x) \quad (\text{A.7})$$

$$D_x \cdot V_1(x) = -sLI_1(x) \quad (\text{A.8})$$

$$D_x \cdot V_2(x) = sLI_2(x) = sLI_1(x) + sLI_0 \quad (\text{A.9})$$

$$V_{12}(x) = V_1(x) - V_2(x) \quad (\text{A.10})$$

Differentiation of (A.6) yields that

$$\begin{aligned} D_x^2 \cdot I_1(x) &= -sC [D_x \cdot V_{12}(x)] \\ &= -sC [D_x \cdot V_1(x) - D_x \cdot V_2(x)] \\ &= -sC [-sLI_1(x) - sLI_1(x) - sLI_0] \\ &= 2s^2 LC I_1(x) + s^2 LC I_0 \end{aligned}$$

that is,

$$(D_x^2 - 2s^2 LC) \cdot I_1(x) = s^2 LC I_0 \quad (\text{A.11})$$

The solution to the equation is

$$I_1(x) = A e^{-\sqrt{2LC} \cdot sx} + B e^{\sqrt{2LC} \cdot sx} - I_0 / 2 \quad (\text{A.12})$$

$$= -I_0 / 2 + Ae^{-\Gamma x} + Be^{+\Gamma x} \quad (A.13)$$

where

$$\Gamma = \sqrt{2LC} \cdot s = j\omega \cdot \sqrt{2LC} \quad (A.14)$$

The equation for  $I_2(x)$  can be derived similarly and is given by

$$I_2(x) = I_0 / 2 + Ae^{-\Gamma x} + Be^{+\Gamma x} \quad (A.15)$$

An expression for  $V_1(x)$  can now be obtained by integrating (A.8) after substitution of  $I_1(x)$  and by using (A.13):

$$V_1(x) = V_1(0) - Z_0 / 2 \cdot (A - B) + Z_0 / 2 \cdot [Ae^{-\Gamma x} - Be^{\Gamma x}] + sLx \cdot I_0 / 2 \quad (A.16)$$

where

$$Z_0 = \sqrt{\frac{2L}{C}} \quad (A.17)$$

The required expression for  $V_2(x)$  follows similarly:

$$V_2(x) = V_2(0) + Z_0 / 2 \cdot (A - B) - Z_0 / 2 \cdot [Ae^{-\Gamma x} - Be^{\Gamma x}] + sLx \cdot I_0 / 2 \quad (A.18)$$

An expression for  $V_{12}(x)$  can be obtained by using (A.6):

$$V_{12}(x) = V_1(x) - V_2(x) = Z_0 [Ae^{-\Gamma x} - Be^{\Gamma x}] \quad (A.19)$$

The equations derived are summarized below:

$$I_1(x) = -I_0 / 2 + Ae^{-\Gamma x} + Be^{+\Gamma x} \quad (A.13)$$

$$I_2(x) = I_0 / 2 + Ae^{-\Gamma x} + Be^{+\Gamma x} \quad (A.15)$$

$$V_1(x) = V_1(0) - Z_0 / 2 \cdot (A - B) + Z_0 / 2 \cdot [Ae^{-\Gamma x} - Be^{\Gamma x}] + sLx \cdot I_0 / 2 \quad (A.16)$$

$$V_2(x) = V_2(0) + Z_0 / 2 \cdot (A - B) - Z_0 / 2 \cdot [Ae^{-\Gamma x} - Be^{\Gamma x}] + sLx \cdot I_0 / 2 \quad (\text{A.18})$$

$$V_{12}(x) = V_1(x) - V_2(x) = Z_0 [Ae^{-\Gamma x} - Be^{\Gamma x}] \quad (\text{A.19})$$

## REFERENCES

1. Abrie, P. L. D., *Impedance-Matching Networks and Bandwidth Limitations of Class B Power Amplifiers in the HF and VHF Ranges*, Master's Thesis, University of Pretoria, 1982.

# INDEX

1:4 transmission line transformer, 180

1-dB compression point, 62, 67, 78

Active biasing, 435

Admittance, 161

Admittance plane, 53, 366, 387

AI-product, 114–116

All-pass function, 259

American wire gauge, 100

Amplifier

chain, 72

synthesis, 360

Attenuation, 117–118, 226

constant, 121

Auto-transformer, 179

Available

power, 5, 20

gain, 386, 397

circle, 403

Balanced amplifier, 440–441

Balun, 113–114, 213

core, 113, 151

Band-pass identities, 272

Bandwidth, 125, 127, 139, 146, 149, 156, 180, 196, 208, 266

Bias point, 399

Bipolar transistor, 78, 399

Bond wire, 223

Bonding-wire inductor, 326

Boundary, 66

lines, 77

Branch, 16, 31

multipliers, 31

Building block, 188, 191–192

Capacitance, 99, 179, 190, 234

ratio, 463

Capacitor, 93–94, 331

Cascade, 72, 77, 82

network, 11, 59, 82, 84

representation, 55, 57

Center frequency, 127

Ceramics, 96

Chamfer, 348

Characteristic impedance, 117–118, 121–122, 179, 185, 196–197, 226–227, 323

Chebyshev function, 257

Chip

capacitor, 95

coil, 100

Circle, 53, 366, 386–387, 390

Circuit Q, 135

Circular

loop, 326

spiral, 328

Circulator, 436

Class

A, 62–63, 67, 78, 212

AB, 62

B, 62, 65–67, 78, 185, 212, 215

C, 212

Clipping, 64, 80

Coaxial

cable, 117–118, 179, 197

line, 117

Coil, 99, 107, 109–110

Combiner, 187

Common-base, 7

Common-collector, 8

Common-drain, 90, 91

Common-emitter, 8

Common-gate, 88–90

Common-source, 88–89, 91

Compensation, 203–207, 210, 354

Complex

impedance, 446

termination, 144

Compression, 444

point, 73

Conduction angle, 62

Conductor, 101

Configuration, 88, 133, 181, 183–184, 186, 433, 442, 460

Conjugate match, 384

- Connection, 93**
- Constant**
  - impedance taper, 354
  - noise figure circle, 396
  - operating power
    - gain, 389, 392
    - circle, 391
- Constraints, 21, 256, 286, 297–298**
- Contour, 67**
- Control network, 417**
- Conversion, 44**
- Copper losses, 122, 154**
- Core, 113, 179, 189, 196**
  - dimensions, 104, 114–115
- Correlation matrix, 55, 57, 59**
- Coupled coils, 175**
- Coupling, 179, 190, 227, 233, 459**
  - factor, 154, 156, 158, 161, 166, 173, 175
- Current, 76, 180, 188–189**
- Current-representation, 55**
- Curving radius, 349**
- Cut-off frequency, 157, 196, 205**
- Darlington synthesis, 249, 258**
- DC**
  - component, 69
  - dissipation, 66
  - power, 64, 66
- Decoupling, 93, 221**
- Device-modification, 405**
- Diagram, 16**
- Dielectric**
  - constant, 118, 121
  - resonator, 458
  - puck, 460, 461
- Diode, 438**
- Discontinuity effect, 345**
- Dispersion, 121**
- Dissipation factor, 95–96, 122**
- Distortion, 72**
- Double-tuned transformer, 166**
- DRO, 448**
- Dualism, 131**
- Dynamic range, 67–68, 386, 433**
- Edge capacitance, 223**
- Effective output power, 398**
- Efficiency, 66, 212**
- Electrical field, 101**
- Equivalent**
  - circuit, 2–3, 9, 4, 14, 75, 94, 97, 151, 155–156, 162, 167–168, 198, 223, 226, 228–229, 232, 241, 387, 461
- noise source, 48**
- passive problem, 386, 403**
- External load, 47, 79**
- Feedback, 75, 442**
  - network, 375
- Ferrite materials, 104**
- FET, 78, 399**
- Field, 101**
- Field strength, 102**
- Film resistor, 219**
- Fixed-valued component, 446**
- Flicker noise, 465**
- Flow**
  - diagram, 360, 444
  - graph, 32
- Flux, 181**
  - coupling, 152
  - density, 105–106, 114, 116, 201, 209
- Fourier series, 65**
- Free space, 226, 229**
- Frequency response, 126**
- Friiss' formula, 60**
- Fringing capacitance, 354**
- Fundamental tone, 65, 66–67, 71**
- Gain**
  - circle, 371, 390, 392, 399, 401
  - compression, 69–70, 443
  - leveling, 431
  - slope, 405
  - tapering, 212
- Gain-bandwidth constraints, 239, 405**
- Gap capacitor, 217**
- Gap-capacitor, 220, 236**
- Gm, 78**
- Gradient vector, 304**
- Ground plane, 93, 223, 326, 327**
- Half-sinusoid, 65**
- Harmonic**
  - components, 69
  - currents, 78
- High-pass identities, 271**
- Hybrid**
  - combiner, 440
  - divider, 207, 440
  - transformer, 187
- I/V constraints, 67**
- I/V-plane, 66, 76**
- Ideal transformer, 151**
- Image reflection, 327**

- Impedance**, 153, 193, 220  
function, 240, 250  
matrix, 15
- Incident current**, 18
- Increment frequency**, 276, 278
- Indefinite**  
admittance matrix, 7  
*S*-matrix, 35
- Inductance**, 94, 105, 107, 114, 116, 181, 190
- Inductor**, 93, 97, 113, 322, 330
- Infinite chain**, 60, 73
- Inherently stable**, 390
- Input**  
admittance, 6, 292–293, 365  
impedance, 270
- Input loop**, 375
- Insertion loss**, 60, 126, 147–148, 172, 224–225
- Intercept point**, 70–73, 77
- Interdigital capacitor**, 332
- Intrinsic**  
load, 47, 64, 79  
line, 74  
termination, 66
- Isolation**, 187–188, 432
- L-section**, 125, 133, 135, 214
- L1 error**, 399
- Large-signal**, 452
- LC transformers**, 253–254
- Leakage**, 155  
flux, 153  
inductance, 151
- Line segments**, 64, 273
- Linearity**, 62, 67
- Linville stability factor**, 367
- Load**  
impedance, 154  
line, 64, 67, 442  
area, 77
- Load-pull contours**, 81
- Loaded Q**, 380
- Loop**  
gain, 363, 374–379, 441, 446, 448, 450, 457  
product, 31
- Loops**, 33–34
- Loss tangent**, 95, 122
- Losses**, 75, 94, 98, 100, 104, 106, 121, 152–153
- Lossless**  
feedback, 431–432, 434  
network, 12, 386  
two-port, 43
- Lossy transmission-line**, 322
- Low-pass identities**, 271
- MAG**, 5, 386
- Magnetic**  
core, 113, 180  
field, 101, 189  
flux, 151  
material, 93, 98, 113, 189, 196
- Magnetizing inductance**, 151, 153, 181, 196, 198, 200, 210
- Matching network**, 214–215, 315
- Matrix**, 2
- Maximum**  
relative deviation, 303  
tunable gain, 384
- Microstrip**, 118, 121, 218–220, 233–235, 345  
bend, 347  
line, 117
- MIM capacitor**, 236
- Minimum detectable signal**, 67, 68
- Minimum-admittance function**, 241
- Minimum-impedance function**, 240, 279
- Miter**, 349
- Model**, 48, 78, 153, 218, 235, 236, 399, 445
- Modification**  
circuit, 414  
network, 411  
section, 386
- MSG**, 5
- Multi-stage**, 417
- Negative resistance**, 375
- Node**, 31, 131
- Noise**  
figure, 6, 49, 53, 59–60, 386, 396, 404  
circle, 54, 387  
floor, 68  
match, 6  
measure, 60, 73  
parameters, 47, 48  
power, 50  
source, 48, 57
- Normalizing impedance**, 16, 25–26, 29, 38
- One-port**, 25–26
- Open-ended stub**, 333, 345
- Open-loop impedance**, 375
- Operating power gain**, 384, 386, 451–452
- Optimum termination**, 211
- Order**, 31
- Oscillation**, 362, 371–372, 376  
frequency, 444
- Oscillator**, 373, 378–379, 441, 456, 460

- configuration, 441
- design, 444
- Output**
  - current, 65, 67
  - impedance, 252, 260
  - power, 47, 61, 65, 210, 398, 441, 443, 451
  - voltage, 67
- Package parasitics, 399
- Parallel double-tuned transformer, 166
- Parallel-plate capacitor, 217–218, 226, 235
- Parasitic**
  - inductance, 462
  - absorption, 248–249
  - capacitance, 97, 107
- Parasitics, 93
- Passive**
  - cascade, 60
  - network, 59–60, 82
- Path, 33–34
- Peak envelope power, 313
- PEP, 313
- Phase**
  - noise, 445, 465
  - shift, 442
- Phase velocity, 120
- PI-section, 125, 138–139, 140–142, 144, 338–339, 442, 446, 456
- Planar transmission lines, 94
- Point junction, 94
- Polarity, 181**
- Poles, 38, 241, 249–250, 252, 259
- Potentially unstable, 391
- Power, 19, 40, 147, 152, 398, 446
  - amplifier, 210–211, 213–215, 313
  - contour, 67, 73–75, 80, 125, 400
  - gain, 4, 194, 385
  - parameters, 47, 62, 76, 80–81, 85–86, 88–90, 442
  - splitter, 187
  - termination, 413, 416
- Primary**
  - current, 152
  - inductance, 156
- Propagation constant, 101
- Proximity effect, 103, 123
- Puck, 448, 459
- Push-pull, 185
- Q, 107**
- Q-factor, 96, 98, 110, 127–128**
- Q-value, 100**
- Quality factor, 95**
- Ratings, 210
- Ratios, 181
- Reactive**
  - loading, 463
  - load line, 67
- Real-frequency, 273
- Reference temperature, 50
- Reflected**
  - component, 18
  - power, 20
- Reflection**
  - amplifier, 437, 439
  - coefficient, 12, 22, 259, 324, 368, 438, 441
  - gain, 364, 372, 374
  - parameter, 20, 23, 25, 27, 29
- Rejection, 128–129, 166
- Representation, 48**
- Residue, 241
- Resistance, 98, 102, 181
  - level, 294
- Resistive load line, 67
- Resistor, 311, 322
- Resonance, 93
- Resonant
  - circuit, 78, 126, 132, 458
  - frequency, 93, 95, 98–99, 109, 221–222, 225–226
- Resonating section, 296
- Resonator, 446, 461
- Ribbon, 223
  - inductor, 325
- Richards' transformation, 267
- Ripple, 166, 168
- RLC
  - network, 311
  - matching network, 212
- Rod core, 113
- Rollette stability factor, 370, 376
- Route, 33
- S-parameters, 11, 14, 22, 30, 42, 44, 175–176, 284, 440**
- Saturation, 451
  - resistance, 62, 211
  - voltage, 62, 211
- Scale factor, 286, 304
- Scattering
  - matrix, 20, 40
  - parameters, 27
- Search, 291
- Secondary**
  - inductance, 156
  - winding, 175

- Self-capacitance, 99, 111–112  
Self-resonant frequency, 332  
Semi-infinite function, 277–278  
Sensitivity, 417–419  
    factor, 419
- Series  
    double-tuned transformer, 172  
    feedback, 86, 375, 454–456  
    resistance, 96  
    resonant circuit, 131
- Shunt  
    feedback, 376  
    inductor, 333
- Signal flow graph, 31
- Single-tuned transformer, 158
- Size, 114, 221
- Skin  
    depth, 101–102  
    effect, 117, 123, 220
- Small-signal model, 78, 80, 399
- Smith Chart, 54, 368, 370–371, 373, 379, 387, 389, 391, 394, 397, 403, 447
- Solenoidal coil, 99, 107, 329
- Spiral inductor, 328
- Spurious free dynamic range, 68
- Square spiral, 327
- Stability, 362, 405  
    circle, 368–369, 371  
    factor, 363
- Stabilizing resistance, 363
- Stacked core, 113, 201
- Stacked toroids, 113
- Standard wire gauge, 100
- Step, 355  
    discontinuity, 346  
    junction, 346
- Sterne stability factor, 367
- Stub, 224
- Superposition, 50
- T-junction, 350
- T-section, 138, 142–145, 338, 447, 454
- Tapped coil, 159–160, 162
- Temperature, 106
- Termination, 23
- Thermal runaway, 96
- Thin film, 322  
    resistor, 94
- TOI, 67
- Topology, 33, 138, 443
- Toroid, 113, 151
- Toroidal core, 114–116, 156, 201
- Transconductance, 445
- Transducer  
    power gain, 68, 148, 279–280, 284, 311, 371, 387–388, 437–438, 441  
    circle, 396
- Transformation, 133, 135, 138, 140, 239, 247  
    diagram, 137, 145  
    distance, 255  
    factor, 163  
    matrix, 56  
     $Q$ , 134–135, 274, 291  
    ratio, 182  
    step, 134
- Transformer, 151, 179, 182, 191–192, 195–196, 248
- Transistor, 399
- Transmission  
    line, 13, 117, 122, 179, 188–189, 197, 219, 333, 338  
    matrix, 10, 57, 220  
    parameters, 10, 23  
    zero, 284
- Transmission-line transformer, 179, 182, 212
- Tunability factor, 383
- Turns, 109, 114  
    ratio, 154
- Twisted pairs, 117, 122
- Two-port, 3, 9, 11, 25–26, 31–32, 42, 48, 53
- Two-tone  
    intercept point, 62  
    products, 67  
    signal, 70
- Unbalanced current, 180
- Unit element, 268–269, 272
- Unitary matrix, 40
- Unloaded Q, 113–114, 132, 147, 164, 460
- Varactor, 446, 463  
    network, 462
- Varactor-type, 446, 462
- Variable, 31
- Via hole, 351
- Voltage, 76, 97, 131, 180  
    gain, 176
- Voltage-controlled oscillator, 446
- Voltage-representation, 55
- Waveforms, 62
- Weight factor, 277
- Winding, 179
- Wire thickness, 109
- $Y$ -parameter matrix, 364

**Y-parameters**, 1, 44, 231–232, 389

**Z-parameters**, 8, 154, 175–176

**Zero**, 38, 244, 250, 252

MICROWAVE

ISBN 0-89006-797-X



9 780890 067970



Artech House Publishers

BOSTON • LONDON